DELFT PLANING MODELS 2

DELFT	Planning		Model																															
Model	**Lpx**		**Lwl**		**Bpx**		**Dep**		**βχ**	**βτχ**	**Centroid**	**Lcg aft**	**Lcg from**		**Lcg/Lpx**	**Centerline**	**Ap**		**Twisted**	**Lpx/Bpx**	**Ap/Vol**	**Lpx/Ap**	**Lpx/Vol**	**Cv**	**Vcg/Lpx**	**Shaft**	**Lce**								
							488,50	N				of Centroid	Transom			angle			angle							Angle	Transom								
241-243	**4,101**	ft	**4,000**	ft	**1,203**	ft	**109,814**	Lb	**30,50**	**30,00**	**47,879**	**0,0**	**1,964**	ft	**0,479**	**0,00**	5,733	ft^2	**0,50**	**3,41**	**4,000**	**2,934**	**3,434**	**0,986**	----------	----------	**0,000**	ft							
	1,250	m	1,219	m	0,367	m	49,812	kg					0,599	m			0,533	m^2									0,0000	m							
	4,101	ft	**4,000**	ft	**1,203**	ft	**109,814**	Lb	**30,50**	**30,00**	**47,879**	**-2,0**	**1,882**	ft	**0,459**	**0,00**	5,733	ft^2	**0,50**	**3,41**	**4,000**	**2,934**	**3,434**	**0,986**	----------	----------	**0,000**	ft							
	1,250	m	1,219	m	0,367	m	49,812	kg					0,574	m			0,533	m^2									0,0000	m							
	4,101	ft	**4,000**	ft	**1,203**	ft	**109,814**	Lb	**30,50**	**30,00**	**47,879**	**-4,0**	**1,800**	ft	**0,439**	**0,00**	5,733	ft^2	**0,50**	**3,41**	**4,000**	**2,934**	**3,434**	**0,986**	----------	----------	**0,000**	ft							
	1,250	m	1,219	m	0,367	m	49,812	kg					0,549	m			0,533	m^2									0,0000	m							
	4,101	ft	**4,000**	ft	**1,203**	ft	**109,814**	Lb	**30,50**	**30,00**	**47,879**	**-8,0**	**1,636**	ft	**0,399**	**0,00**	5,733	ft^2	**0,50**	**3,41**	**4,000**	**2,934**	**3,434**	**0,986**	----------	----------	**0,000**	ft							
	1,250	m	1,219	m	0,367	m	49,812	kg					0,499	m			0,533	m^2									0,0000	m							
230-233	**4,101**	ft	**4,000**	ft	**1,203**	ft	**68,136**	Lb	**30,50**	**30,00**	**47,879**	**0,0**	**1,964**	ft	**0,479**	**0,00**	5,733	ft^2	**0,50**	**3,41**	**5,500**	**2,934**	**4,026**	**0,612**	----------	----------	**0,000**	ft							
	1,250	m	1,219	m	0,367	m	30,907	kg					0,599	m			0,533	m^2									0,0000	m							
	4,101	ft	**4,000**	ft	**1,203**	ft	**68,136**	Lb	**30,50**	**30,00**	**47,879**	**-2,0**	**1,882**	ft	**0,459**	**0,00**	5,733	ft^2	**0,50**	**3,41**	**5,500**	**2,934**	**4,026**	**0,612**	----------	----------	**0,000**	ft							
	1,250	m	1,219	m	0,367	m	30,907	kg					0,574	m			0,533	m^2									0,0000	m							
	4,101	ft	**4,000**	ft	**1,203**	ft	**68,136**	Lb	**30,50**	**30,00**	**47,879**	**-4,0**	**1,800**	ft	**0,439**	**0,00**	5,733	ft^2	**0,50**	**3,41**	**5,500**	**2,934**	**4,026**	**0,612**	----------	----------	**0,000**	ft							
	1,250	m	1,219	m	0,367	m	30,907	kg					0,549	m			0,533	m^2									0,0000	m							
	4,101	ft	**4,000**	ft	**1,203**	ft	**68,136**	Lb	**30,50**	**30,00**	**47,879**	**-8,0**	**1,636**	ft	**0,399**	**0,00**	5,733	ft^2	**0,50**	**3,41**	**5,500**	**2,934**	**4,026**	**0,612**	----------	----------	**0,000**	ft							
	1,250	m	1,219	m	0,367	m	30,907	kg					0,499	m			0,533	m^2									0,0000	m							
220-223	**4,101**	ft	**4,000**	ft	**1,203**	ft	**47,410**	Lb	**30,50**	**30,00**	**47,879**	**0,0**	**1,964**	ft	**0,479**	**0,00**	5,733	ft^2	**0,50**	**3,41**	**7,000**	**2,934**	**4,543**	**0,426**	----------	----------	**0,000**	ft							
	1,250	m	1,219	m	0,367	m	21,505	kg					0,599	m			0,533	m^2									0,0000	m							
	4,101	ft	**4,000**	ft	**1,203**	ft	**47,410**	Lb	**30,50**	**30,00**	**47,879**	**-2,0**	**1,882**	ft	**0,459**	**0,00**	5,733	ft^2	**0,50**	**3,41**	**7,000**	**2,934**	**4,543**	**0,426**	----------	----------	**0,000**	ft							
	1,250	m	1,219	m	0,367	m	21,505	kg					0,574	m			0,533	m^2									0,0000	m							
	4,101	ft	**4,000**	ft	**1,203**	ft	**47,410**	Lb	**30,50**	**30,00**	**47,879**	**-4,0**	**1,800**	ft	**0,439**	**0,00**	5,733	ft^2	**0,50**	**3,41**	**7,000**	**2,934**	**4,543**	**0,426**	----------	----------	**0,000**	ft							
	1,250	m	1,219	m	0,367	m	21,505	kg					0,549	m			0,533	m^2									0,0000	m							
	4,101	ft	**4,000**	ft	**1,203**	ft	**47,410**	Lb	**30,50**	**30,00**	**47,879**	**-8,0**	**1,636**	ft	**0,399**	**0,00**	5,733	ft^2	**0,50**	**3,41**	**7,000**	**2,934**	**4,543**	**0,426**	----------	----------	**0,000**	ft							
	1,250	m	1,219	m	0,367	m	21,505	kg					0,499	m			0,533	m^2									0,0000	m							
210-213	**4,101**	ft	**4,000**	ft	**1,203**	ft	**35,496**	Lb	**30,50**	**30,00**	**47,879**	**0,0**	**1,964**	ft	**0,479**	**0,00**	5,733	ft^2	**0,50**	**3,41**	**8,500**	**2,934**	**5,003**	**0,319**	----------	----------	**0,000**	ft							
	1,250	m	1,219	m	0,367	m	16,101	kg					0,599	m			0,533	m^2									0,0000	m							
	4,101	ft	**4,000**	ft	**1,203**	ft	**35,496**	Lb	**30,50**	**30,00**	**47,879**	**-2,0**	**1,882**	ft	**0,459**	**0,00**	5,733	ft^2	**0,50**	**3,41**	**8,500**	**2,934**	**5,003**	**0,319**	----------	----------	**0,000**	ft							
	1,250	m	1,219	m	0,367	m	16,101	kg					0,574	m			0,533	m^2									0,0000	m							
	4,101	ft	**4,000**	ft	**1,203**	ft	**35,496**	Lb	**30,50**	**30,00**	**47,879**	**-4,0**	**1,800**	ft	**0,439**	**0,00**	5,733	ft^2	**0,50**	**3,41**	**8,500**	**2,934**	**5,003**	**0,319**	----------	----------	**0,000**	ft							
	1,250	m	1,219	m	0,367	m	16,101	kg					0,549	m			0,533	m^2									0,0000	m							
	4,101	ft	**4,000**	ft	**1,203**	ft	**35,496**	Lb	**30,50**	**30,00**	**47,879**	**-8,0**	**1,636**	ft	**0,399**	**0,00**	5,733	ft^2	**0,50**	**3,41**	**8,500**	**2,934**	**5,003**	**0,319**	----------	----------	**0,000**	ft							
	1,250	m	1,219	m	0,367	m	16,101	kg					0,499	m			0,533	m^2									0,0000	m							

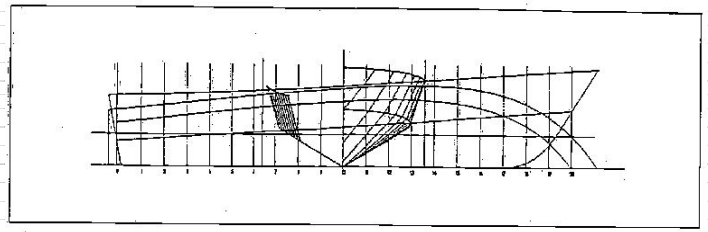

*** Fresh Water

ITTC
Fv 0.75-3.00

LİTERATURE = Resistance tests of a Series Planing Hull Forms with 30 degree deadrise angle and a calculation model based on this and similar systematic series
J.A.Keuning,J.Gerritsma,and P.F.Van Terwisga
Report No : 959
Resistance tests of a Series Planing Hull Forms with 30 degree deadrise angle, and a calculation model based on this and similar systematic series
J.A.Keuning,J.Gerritsma,and P.F.Van Terwisga
ISP 40,No:424

DELFT	Planning		Model																													
Model	**Lpx**		**Lwl**		**Bpx**		**Dep**		**βχ**	**βτχ**	**Centroid**	**Lcg aft**	**Lcg from**		**Lcg/Lpx**	**Centerline**	**Ap**		**Twisted**	**Lpx/Bpx**	**Ap/Vol**	**Lpx/Ap**	**Lpx/Vol**	**Cv**	**Vcg/Lpx**	**Shaft**	**Lce**	
							369,90	N				of Centroid	Transom			angle			angle							Angle	Transom	
341-343	**4,922**	ft	**4,800**	ft	**1,003**	ft	**83,153**	Lb	**30,50**	**30,00**	**48,800**	**0,0**	**2,402**	ft	**0,488**	**0,00**	4,763	ft^2	**0,50**	**4,09**	**4,000**	**5,085**	**4,521**	**1,288**	----------	**10,00**	**0,000**	ft
	1,500	m	1,463	m	0,306	m	37,718	kg					0,732	m			0,442	m^2									0,0000	m
	4,922	ft	**4,800**	ft	**1,003**	ft	**83,153**	Lb	**30,50**	**30,00**	**48,800**	**-2,0**	**2,303**	ft	**0,468**	**0,00**	4,763	ft^2	**0,50**	**4,09**	**4,000**	**5,085**	**4,521**	**1,288**	----------	**10,00**	**0,000**	ft
	1,500	m	1,463	m	0,306	m	37,718	kg					0,702	m			0,442	m^2									0,0000	m
	4,922	ft	**4,800**	ft	**1,003**	ft	**83,153**	Lb	**30,50**	**30,00**	**48,800**	**-4,0**	**2,205**	ft	**0,448**	**0,00**	4,763	ft^2	**0,50**	**4,09**	**4,000**	**5,085**	**4,521**	**1,288**	----------	**10,00**	**0,000**	ft
	1,500	m	1,463	m	0,306	m	37,718	kg					0,672	m			0,442	m^2									0,0000	m
	4,922	ft	**4,800**	ft	**1,003**	ft	**83,153**	Lb	**30,50**	**30,00**	**48,800**	**-8,0**	**2,008**	ft	**0,408**	**0,00**	4,763	ft^2	**0,50**	**4,09**	**4,000**	**5,085**	**4,521**	**1,288**	----------	**10,00**	**0,000**	ft
	1,500	m	1,463	m	0,306	m	37,718	kg					0,612	m			0,442	m^2									0,0000	m
330-333	**4,922**	ft	**4,800**	ft	**1,003**	ft	**51,591**	Lb	**30,50**	**30,00**	**48,800**	**0,0**	**2,402**	ft	**0,488**	**0,00**	4,763	ft^2	**0,50**	**4,09**	**5,500**	**5,085**	**5,300**	**0,799**	----------	**10,00**	**0,000**	ft
	1,500	m	1,463	m	0,306	m	23,402	kg					0,732	m			0,443	m^2									0,0000	m
	4,922	ft	**4,800**	ft	**1,003**	ft	**51,591**	Lb	**30,50**	**30,00**	**48,800**	**-2,0**	**2,303**	ft	**0,468**	**0,00**	4,763	ft^2	**0,50**	**4,09**	**5,500**	**5,085**	**5,300**	**0,799**	----------	**10,00**	**0,000**	ft
	1,500	m	1,463	m	0,306	m	23,402	kg					0,702	m			0,443	m^2									0,0000	m
	4,922	ft	**4,800**	ft	**1,003**	ft	**51,591**	Lb	**30,50**	**30,00**	**48,800**	**-4,0**	**2,205**	ft	**0,448**	**0,00**	4,763	ft^2	**0,50**	**4,09**	**5,500**	**5,085**	**5,300**	**0,799**	----------	**10,00**	**0,000**	ft
	1,500	m	1,463	m	0,306	m	23,402	kg					0,672	m			0,443	m^2									0,0000	m
	4,922	ft	**4,800**	ft	**1,003**	ft	**51,591**	Lb	**30,50**	**30,00**	**48,800**	**-8,0**	**2,008**	ft	**0,408**	**0,00**	4,763	ft^2	**0,50**	**4,09**	**5,500**	**5,085**	**5,300**	**0,799**	----------	**10,00**	**0,000**	ft
	1,500	m	1,463	m	0,306	m	23,402	kg					0,612	m			0,443	m^2									0,0000	m
320-323	**4,922**	ft	**4,800**	ft	**1,003**	ft	**35,923**	Lb	**30,50**	**30,00**	**48,800**	**0,0**	**2,402**	ft	**0,488**	**0,00**	4,763	ft^2	**0,50**	**4,09**	**7,000**	**5,085**	**5,980**	**0,556**	----------	**10,00**	**0,000**	ft
	1,500	m	1,463	m	0,306	m	16,295	kg					0,732	m			0,443	m^2									0,0000	m
	4,922	ft	**4,800**	ft	**1,003**	ft	**35,923**	Lb	**30,50**	**30,00**	**48,800**	**-2,0**	**2,303**	ft	**0,468**	**0,00**	4,763	ft^2	**0,50**	**4,09**	**7,000**	**5,085**	**5,980**	**0,556**	----------	**10,00**	**0,000**	ft
	1,500	m	1,463	m	0,306	m	16,295	kg					0,702	m			0,443	m^2									0,0000	m
	4,922	ft	**4,800**	ft	**1,003**	ft	**35,923**	Lb	**30,50**	**30,00**	**48,800**	**-4,0**	**2,205**	ft	**0,448**	**0,00**	4,763	ft^2	**0,50**	**4,09**	**7,000**	**5,085**	**5,980**	**0,556**	----------	**10,00**	**0,000**	ft
	1,500	m	1,463	m	0,306	m	16,295	kg					0,672	m			0,443	m^2									0,0000	m
	4,922	ft	**4,800**	ft	**1,003**	ft	**35,923**	Lb	**30,50**	**30,00**	**48,800**	**-8,0**	**2,008**	ft	**0,408**	**0,00**	4,763	ft^2	**0,50**	**4,09**	**7,000**	**5,085**	**5,980**	**0,556**	----------	**10,00**	**0,000**	ft
	1,500	m	1,463	m	0,306	m	16,295	kg					0,612	m			0,443	m^2									0,0000	m
310-313	**4,922**	ft	**4,800**	ft	**1,003**	ft	**26,863**	Lb	**30,50**	**30,00**	**48,800**	**0,0**	**2,402**	ft	**0,488**	**0,00**	4,763	ft^2	**0,50**	**4,09**	**8,500**	**5,085**	**6,588**	**0,416**	----------	**10,00**	**0,000**	ft
	1,500	m	1,463	m	0,306	m	12,185	kg					0,732	m			0,443	m^2									0,0000	m
	4,922	ft	**4,800**	ft	**1,003**	ft	**26,863**	Lb	**30,50**	**30,00**	**48,800**	**-2,0**	**2,303**	ft	**0,468**	**0,00**	4,763	ft^2	**0,50**	**4,09**	**8,500**	**5,085**	**6,588**	**0,416**	----------	**10,00**	**0,000**	ft
	1,500	m	1,463	m	0,306	m	12,185	kg					0,702	m			0,443	m^2									0,0000	m
	4,922	ft	**4,800**	ft	**1,003**	ft	**26,863**	Lb	**30,50**	**30,00**	**48,800**	**-4,0**	**2,205**	ft	**0,448**	**0,00**	4,763	ft^2	**0,50**	**4,09**	**8,500**	**5,085**	**6,588**	**0,416**	----------	**10,00**	**0,000**	ft
	1,500	m	1,463	m	0,306	m	12,185	kg					0,672	m			0,443	m^2									0,0000	m
	4,922	ft	**4,800**	ft	**1,003**	ft	**26,863**	Lb	**30,50**	**30,00**	**48,800**	**-8,0**	**2,008**	ft	**0,408**	**0,00**	4,763	ft^2	**0,50**	**4,09**	**8,500**	**5,085**	**6,588**	**0,416**	----------	**10,00**	**0,000**	ft
	1,500	m	1,463	m	0,306	m	12,185	kg					0,612	m			0,443	m^2									0,0000	m

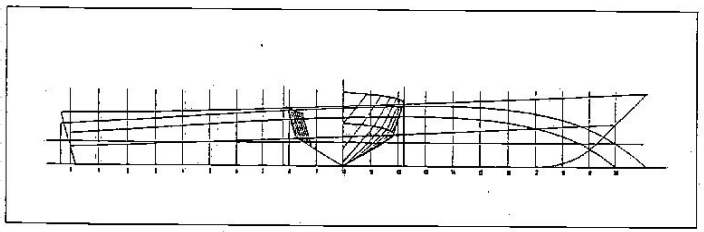

*** Fresh Water

ITTC
Fv 0.75-3.00

LİTERATURE = Resistance tests of a Series Planing Hull Forms with 30 degree deadrise angle and a calculation model based on this and similar systematic series
J.A.Keuning,J.Gerritsma,and P.F.Van Terwisga
Report No : 959
Resistance tests of a Series Planing Hull Forms with 30 degree deadrise angle, and a calculation model based on this and similar systematic series
J.A.Keuning,J.Gerritsma,and P.F.Van Terwisga
ISP 40,No:424

DELFT | Planning | Model

Model	Lpx	Lwl	Bpx	Dep (237,40 N)	βχ	βτχ	Centroid	Lcg aft of Centroid	Lcg from Transom	Lcg/Lpx	Centerline angle	Ap	Twisted angle	Lpx/Bpx	Ap/Vol	Lpx/Ap	Lpx/Vol	Cv	Vcg/Lpx	Shaft Angle	Lce Transom
441-443	4,922 ft	4,837 ft	0,746 ft	53,367 Lb	30,50	30,00	48,600	0,0	2,392 ft	0,486	0,00	3,544 ft^2	0,50	5,50	4,000	6,834	5,241	2,010	----------	7,30	0,104 ft
	1,500 m	1,474 m	0,227 m	24,207 kg					0,729 m			0,329 m^2									0,0097 m
	4,922 ft	4,837 ft	0,746 ft	53,367 Lb	30,50	30,00	48,600	-2,0	2,293 ft	0,466	0,00	3,544 ft^2	0,50	5,50	4,000	6,834	5,241	2,010	----------	7,30	0,000 ft
	1,500 m	1,474 m	0,227 m	24,207 kg					0,699 m			0,329 m^2									0,0000 m
	4,922 ft	4,837 ft	0,746 ft	53,367 Lb	30,50	30,00	48,600	-4,0	2,195 ft	0,446	0,00	3,544 ft^2	0,50	5,50	4,000	6,834	5,241	2,010	----------	7,30	0,000 ft
	1,500 m	1,474 m	0,227 m	24,207 kg					0,669 m			0,329 m^2									0,0000 m
	4,922 ft	4,880 ft	0,746 ft	53,367 Lb	30,50	30,00	48,600	-8,0	1,998 ft	0,406	0,00	3,544 ft^2	0,50	5,50	4,000	6,834	5,241	2,010	----------	7,30	0,000 ft
	1,500 m	1,487 m	0,227 m	24,207 kg					0,609 m			0,329 m^2									0,0000 m
430-433	4,922 ft	4,837 ft	0,746 ft	33,113 Lb	30,50	30,00	48,600	0,0	2,392 ft	0,486	0,00	3,544 ft^2	0,50	5,50	5,500	6,834	6,145	1,247	----------	7,30	0,000 ft
	1,500 m	1,474 m	0,227 m	15,020 kg					0,729 m			0,329 m^2									0,0000 m
	4,922 ft	4,837 ft	0,746 ft	33,113 Lb	30,50	30,00	48,600	-4,0	2,195 ft	0,446	0,00	3,544 ft^2	0,50	5,50	5,500	6,834	6,145	1,247	----------	7,30	0,000 ft
	1,500 m	1,474 m	0,227 m	15,020 kg					0,669 m			0,329 m^2									0,0000 m
	4,922 ft	4,837 ft	0,746 ft	33,113 Lb	30,50	30,00	48,600	-8,0	1,998 ft	0,406	0,00	3,544 ft^2	0,50	5,50	5,500	6,834	6,145	1,247	----------	7,30	0,000 ft
	1,500 m	1,474 m	0,227 m	15,020 kg					0,609 m			0,329 m^2									0,0000 m
420-423	4,922 ft	4,837 ft	0,746 ft	23,064 Lb	30,50	30,00	48,600	0,0	2,392 ft	0,486	0,00	3,544 ft^2	0,50	5,50	7,000	6,834	6,932	0,869	----------	7,30	0,000 ft
	1,500 m	1,474 m	0,227 m	10,462 kg					0,729 m			0,329 m^2									0,0000 m
	4,922 ft	4,837 ft	0,746 ft	23,064 Lb	30,50	30,00	48,600	-2,0	2,293 ft	0,466	0,00	3,544 ft^2	0,50	5,50	7,000	6,834	6,932	0,869	----------	7,30	0,000 ft
	1,500 m	1,474 m	0,227 m	10,462 kg					0,699 m			0,329 m^2									0,0000 m
	4,922 ft	4,837 ft	0,746 ft	23,064 Lb	30,50	30,00	48,600	-4,0	2,195 ft	0,446	0,00	3,544 ft^2	0,50	5,50	7,000	6,834	6,932	0,869	----------	7,30	0,000 ft
	1,500 m	1,474 m	0,227 m	10,462 kg					0,669 m			0,329 m^2									0,0000 m
	4,922 ft	4,837 ft	0,746 ft	23,064 Lb	30,50	30,00	48,600	-8,0	1,998 ft	0,406	0,00	3,544 ft^2	0,50	5,50	7,000	6,834	6,932	0,869	----------	7,30	0,000 ft
	1,500 m	1,474 m	0,227 m	10,462 kg					0,609 m			0,329 m^2									0,0000 m
410-413	4,922 ft	4,837 ft	0,746 ft	17,220 Lb	30,50	30,00	48,600	0,0	2,392 ft	0,486	0,00	3,544 ft^2	0,50	5,50	8,500	6,834	7,641	0,649	----------	7,30	0,000 ft
	1,500 m	1,474 m	0,227 m	7,811 kg					0,729 m			0,329 m^2									0,0000 m
	4,922 ft	4,837 ft	0,746 ft	17,220 Lb	30,50	30,00	48,600	-2,0	2,293 ft	0,466	0,00	3,544 ft^2	0,50	5,50	8,500	6,834	7,641	0,649	----------	7,30	0,000 ft
	1,500 m	1,474 m	0,227 m	7,811 kg					0,699 m			0,329 m^2									0,0000 m
	4,922 ft	4,837 ft	0,746 ft	17,220 Lb	30,50	30,00	48,600	-4,0	2,195 ft	0,446	0,00	3,544 ft^2	0,50	5,50	8,500	6,834	7,641	0,649	----------	7,30	0,000 ft
	1,500 m	1,474 m	0,227 m	7,811 kg					0,669 m			0,329 m^2									0,0000 m
	4,922 ft	4,837 ft	0,746 ft	17,220 Lb	30,50	30,00	48,600	-8,0	1,998 ft	0,406	0,00	3,544 ft^2	0,50	5,50	8,500	6,834	7,641	0,649	----------	7,30	0,000 ft
	1,500 m	1,474 m	0,227 m	7,811 kg					0,609 m			0,329 m^2									0,0000 m

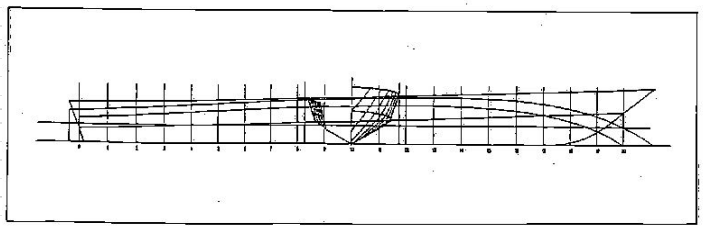

*** Fresh Water

ITTC
Fv 0.75-3.00

LİTERATURE = Resistance tests of a Series Planing Hull Forms with 30 degree deadrise angle and a calculation model based on this and similar systematic series
J.A.Keuning,J.Gerritsma,and P.F.Van Terwisga
Report No : 959
Resistance tests of a Series Planing Hull Forms with 30 degree deadrise angle, and a calculation model based on this and similar systematic series
J.A.Keuning,J.Gerritsma,and P.F.Van Terwisga
ISP 40,No:424

DELFT | Planning | Model

Model	Lpx	Lwl	Bpx	Dep (165,20 N)	βχ	βτχ	Centroid	Lcg aft of Centroid	Lcg from Transom	Lcg/Lpx	Centerline angle	Ap	Twisted angle	Lpx/Bpx	Ap/Vol	Lpx/Ap	Lpx/Vol	Cv	Vcg/Lpx	Shaft Angle	Lce Transom
541-543	4,922 ft	4,880 ft	0,586 ft	37,137 Lb	30,50	30,00	48,600	0,0	2,392 ft	0,486	0,00	2,783 ft^2	0,50	7,00	4,000	8,703	5,914	2,884	----------	5,75	0,000 ft
	1,500 m	1,487 m	0,179 m	16,845 kg					0,729 m			0,259 m^2									0,0000 m
	4,922 ft	4,880 ft	0,586 ft	37,137 Lb	30,50	30,00	48,600	-2,0	2,293 ft	0,466	0,00	2,783 ft^2	0,50	7,00	4,000	8,703	5,914	2,884	----------	5,75	0,000 ft
	1,500 m	1,487 m	0,179 m	16,845 kg					0,699 m			0,259 m^2									0,0000 m
	4,922 ft	4,880 ft	0,586 ft	37,137 Lb	30,50	30,00	48,600	-4,0	2,195 ft	0,446	0,00	2,783 ft^2	0,50	7,00	4,000	8,703	5,914	2,884	----------	5,75	0,000 ft
	1,500 m	1,487 m	0,179 m	16,845 kg					0,669 m			0,259 m^2									0,0000 m
	4,922 ft	4,880 ft	0,586 ft	37,137 Lb	30,50	30,00	48,600	-8,0	1,998 ft	0,406	0,00	2,783 ft^2	0,50	7,00	4,000	8,703	5,914	2,884	----------	5,75	0,000 ft
	1,500 m	1,487 m	0,179 m	16,845 kg					0,609 m			0,259 m^2									0,0000 m
530-533	4,922 ft	4,880 ft	0,586 ft	23,019 Lb	30,50	30,00	48,600	0,0	2,392 ft	0,486	0,00	2,783 ft^2	0,50	7,00	5,500	8,703	6,936	1,788	----------	5,75	0,000 ft
	1,500 m	1,487 m	0,179 m	10,442 kg					0,729 m			0,259 m^2									0,0000 m
	4,922 ft	4,880 ft	0,586 ft	23,019 Lb	30,50	30,00	48,600	-2,0	2,293 ft	0,466	0,00	2,783 ft^2	0,50	7,00	5,500	8,703	6,936	1,788	----------	5,75	0,000 ft
	1,500 m	1,487 m	0,179 m	10,442 kg					0,699 m			0,259 m^2									0,0000 m
	4,922 ft	4,880 ft	0,586 ft	23,019 Lb	30,50	30,00	48,600	-4,0	2,195 ft	0,446	0,00	2,783 ft^2	0,50	7,00	5,500	8,703	6,936	1,788	----------	5,75	0,000 ft
	1,500 m	1,487 m	0,179 m	10,442 kg					0,669 m			0,259 m^2									0,0000 m
	4,922 ft	4,880 ft	0,586 ft	23,019 Lb	30,50	30,00	48,600	-8,0	1,998 ft	0,406	0,00	2,783 ft^2	0,50	7,00	5,500	8,703	6,936	1,788	----------	5,75	0,000 ft
	1,500 m	1,487 m	0,179 m	10,442 kg					0,609 m			0,259 m^2									0,0000 m
520-523	4,922 ft	4,880 ft	0,586 ft	16,028 Lb	30,50	30,00	48,600	0,0	2,392 ft	0,486	0,00	2,783 ft^2	0,50	7,00	7,000	8,703	7,826	1,245	----------	5,75	0,000 ft
	1,500 m	1,487 m	0,179 m	7,270 kg					0,729 m			0,259 m^2									0,0000 m
	4,922 ft	4,880 ft	0,586 ft	16,028 Lb	30,50	30,00	48,600	-2,0	2,293 ft	0,466	0,00	2,783 ft^2	0,50	7,00	7,000	8,703	7,826	1,245	----------	5,75	0,000 ft
	1,500 m	1,487 m	0,179 m	7,270 kg					0,699 m			0,259 m^2									0,0000 m
	4,922 ft	4,880 ft	0,586 ft	16,028 Lb	30,50	30,00	48,600	-4,0	2,195 ft	0,446	0,00	2,783 ft^2	0,50	7,00	7,000	8,703	7,826	1,245	----------	5,75	0,000 ft
	1,500 m	1,487 m	0,179 m	7,270 kg					0,669 m			0,259 m^2									0,0000 m
	4,922 ft	4,880 ft	0,586 ft	16,028 Lb	30,50	30,00	48,600	-8,0	1,998 ft	0,406	0,00	2,783 ft^2	0,50	7,00	7,000	8,703	7,826	1,245	----------	5,75	0,000 ft
	1,500 m	1,487 m	0,179 m	7,270 kg					0,609 m			0,259 m^2									0,0000 m
510-513	4,922 ft	4,880 ft	0,586 ft	12,004 Lb	30,50	30,00	48,600	0,0	2,392 ft	0,486	0,00	2,783 ft^2	0,50	7,00	8,500	8,703	8,617	0,932	----------	5,75	0,000 ft
	1,500 m	1,487 m	0,179 m	5,445 kg					0,729 m			0,259 m^2									0,0000 m
	4,922 ft	4,880 ft	0,586 ft	12,004 Lb	30,50	30,00	48,600	-2,0	2,293 ft	0,466	0,00	2,783 ft^2	0,50	7,00	8,500	8,703	8,617	0,932	----------	5,75	0,000 ft
	1,500 m	1,487 m	0,179 m	5,445 kg					0,699 m			0,259 m^2									0,0000 m
	4,922 ft	4,880 ft	0,586 ft	12,004 Lb	30,50	30,00	48,600	-4,0	2,195 ft	0,446	0,00	2,783 ft^2	0,50	7,00	8,500	8,703	8,617	0,932	----------	5,75	0,000 ft
	1,500 m	1,487 m	0,179 m	5,445 kg					0,669 m			0,259 m^2									0,0000 m
	4,922 ft	4,880 ft	0,586 ft	12,004 Lb	30,50	30,00	48,600	-8,0	1,998 ft	0,406	0,00	2,783 ft^2	0,50	7,00	8,500	8,703	8,617	0,932	----------	5,75	0,000 ft
	1,500 m	1,487 m	0,179 m	5,445 kg					0,609 m			0,259 m^2									0,0000 m

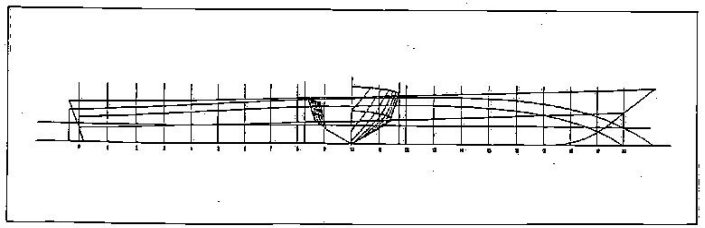

*** Fresh Water

ITTC
Fv 0.75-3.00

LİTERATURE = Resistance tests of a Series Planing Hull Forms with 30 degree deadrise angle and a calculation model based on this and similar systematic series
J.A.Keuning,J.Gerritsma,and P.F.Van Terwisga
Report No : 959
Resistance tests of a Series Planing Hull Forms with 30 degree deadrise angle, and a calculation model based on this and similar systematic series
J.A.Keuning,J.Gerritsma,and P.F.Van Terwisga
ISP 40,No:424

DELFT	Planing	Model																												
Model	**Lpx**		**Lwl**		**Bpx**		**Dep**		**βx**	**βτχ**	**centroid**	**Lcg aft**	**Lcg from**	**Lcg/Lpx**	**centerline**	**Ap**		**Twisted**	**Lpx/Bpx**	**Ap/Vol**	**Lpx/Ap**	**Lpx/Vol**	**Cv**	**Vcg/Lpx**	**Shaft**	**Lce**	
232A	**4,922**	ft	**4,800**	ft	**1,003**	ft	**37,027**	Lb	**25,00**	**10,00**	**48,800**	**0,0**	**2,402**	ft **0,488**	**-4,90**	**4,860**	ft^2	**15,00**	**4,09**	**7,000**	**4,983**	**5,920**	**0,574**	----------	**10,00**	**0,000**	ft
	1,500	m	1,463	m	0,306	m	16,795	kg					0,732	m		0,452	m^2									0,0000	m
	4,922	ft	**4,800**	ft	**1,003**	ft	**37,027**	Lb	**25,00**	**10,00**	**48,800**	**-4,0**	**2,205**	ft **0,448**	**-4,90**	**4,860**	ft^2	**15,00**	**4,09**	**7,000**	**4,983**	**5,920**	**0,574**	----------	**10,00**	**0,000**	ft
	1,500	m	1,463	m	0,306	m	16,795	kg					0,672	m		0,452	m^2									0,0000	m
	4,922	ft	**4,800**	ft	**1,003**	ft	**37,027**	Lb	**25,00**	**10,00**	**48,800**	**-8,0**	**2,008**	ft **0,408**	**-4,90**	**4,860**	ft^2	**15,00**	**4,09**	**7,000**	**4,983**	**5,920**	**0,574**	----------	**10,00**	**0,000**	ft
	1,500	m	1,463	m	0,306	m	16,795	kg					0,612	m		0,452	m^2									0,0000	m
	4,922	ft	**4,800**	ft	**1,003**	ft	**37,027**	Lb	**25,00**	**10,00**	**48,800**	**-12,0**	**1,811**	ft **0,368**	**-4,90**	**4,860**	ft^2	**15,00**	**4,09**	**7,000**	**4,983**	**5,920**	**0,574**	----------	**10,00**	**0,000**	ft
	1,500	m	1,463	m	0,306	m	16,795	kg					0,552	m		0,452	m^2									0,0000	m
232A	**4,922**	ft	**4,800**	ft	**1,003**	ft	**53,147**	Lb	**25,00**	**10,00**	**48,800**	**0,0**	**2,402**	ft **0,488**	**-4,90**	**4,860**	ft^2	**15,00**	**4,09**	**5,500**	**4,983**	**5,248**	**0,823**	----------	**10,00**	**0,000**	ft
	1,500	m	1,463	m	0,306	m	24,107	kg					0,732	m		0,452	m^2									0,0000	m
	4,922	ft	**4,800**	ft	**1,003**	ft	**53,147**	Lb	**25,00**	**10,00**	**48,800**	**-4,0**	**2,205**	ft **0,448**	**-4,90**	**4,860**	ft^2	**15,00**	**4,09**	**5,500**	**4,983**	**5,248**	**0,823**	----------	**10,00**	**0,000**	ft
	1,500	m	1,463	m	0,306	m	24,107	kg					0,672	m		0,452	m^2									0,0000	m
	4,922	ft	**4,800**	ft	**1,003**	ft	**53,147**	Lb	**25,00**	**10,00**	**48,800**	**-8,0**	**2,008**	ft **0,408**	**-4,90**	**4,860**	ft^2	**15,00**	**4,09**	**5,500**	**4,983**	**5,248**	**0,823**	----------	**10,00**	**0,000**	ft
	1,500	m	1,463	m	0,306	m	24,107	kg					0,612	m		0,452	m^2									0,0000	m
	4,922	ft	**4,800**	ft	**1,003**	ft	**53,147**	Lb	**25,00**	**10,00**	**48,800**	**-12,0**	**1,811**	ft **0,368**	**-4,90**	**4,860**	ft^2	**15,00**	**4,09**	**5,500**	**4,983**	**5,248**	**0,823**	----------	**10,00**	**0,000**	ft
	1,500	m	1,463	m	0,306	m	24,107	kg					0,552	m		0,452	m^2									0,0000	m
232A	**4,922**	ft	**4,800**	ft	**1,003**	ft	**85,698**	Lb	**25,00**	**10,00**	**48,800**	**0,0**	**2,402**	ft **0,488**	**-4,90**	**4,860**	ft^2	**15,00**	**4,09**	**4,000**	**4,983**	**4,476**	**1,327**	----------	**10,00**	**0,000**	ft
	1,500	m	1,463	m	0,306	m	38,872	kg					0,732	m		0,452	m^2									0,0000	m
	4,922	ft	**4,800**	ft	**1,003**	ft	**85,698**	Lb	**25,00**	**10,00**	**48,800**	**-4,0**	**2,205**	ft **0,448**	**-4,90**	**4,860**	ft^2	**15,00**	**4,09**	**4,000**	**4,983**	**4,476**	**1,327**	----------	**10,00**	**0,000**	ft
	1,500	m	1,463	m	0,306	m	38,872	kg					0,672	m		0,452	m^2									0,0000	m
	4,922	ft	**4,800**	ft	**1,003**	ft	**85,698**	Lb	**25,00**	**10,00**	**48,800**	**-8,0**	**2,008**	ft **0,408**	**-4,90**	**4,860**	ft^2	**15,00**	**4,09**	**4,000**	**4,983**	**4,476**	**1,327**	----------	**10,00**	**0,000**	ft
	1,500	m	1,463	m	0,306	m	38,872	kg					0,612	m		0,452	m^2									0,0000	m
	4,922	ft	**4,800**	ft	**1,003**	ft	**85,698**	Lb	**25,00**	**10,00**	**48,800**	**-12,0**	**1,811**	ft **0,368**	**-4,90**	**4,860**	ft^2	**15,00**	**4,09**	**4,000**	**4,983**	**4,476**	**1,327**	----------	**10,00**	**0,000**	ft
	1,500	m	1,463	m	0,306	m	38,872	kg					0,552	m		0,452	m^2									0,0000	m
232B	**4,922**	ft	**4,800**	ft	**1,003**	ft	**27,655**	Lb	**25,00**	**5,00**	**48,800**	**0,0**	**2,402**	ft **0,488**	**-2,60**	**4,860**	ft^2	**20,00**	**4,09**	**8,500**	**4,983**	**6,525**	**0,428**	----------	**10,00**	**0,000**	ft
	1,500	m	1,463	m	0,306	m	12,544	kg					0,732	m		0,452	m^2									0,0000	m
	4,922	ft	**4,800**	ft	**1,003**	ft	**27,655**	Lb	**25,00**	**5,00**	**48,800**	**-4,0**	**2,205**	ft **0,448**	**-2,60**	**4,860**	ft^2	**20,00**	**4,09**	**8,500**	**4,983**	**6,525**	**0,428**	----------	**10,00**	**0,000**	ft
	1,500	m	1,463	m	0,306	m	12,544	kg					0,672	m		0,452	m^2									0,0000	m
	4,922	ft	**4,800**	ft	**1,003**	ft	**27,655**	Lb	**25,00**	**5,00**	**48,800**	**-8,0**	**2,008**	ft **0,408**	**-2,60**	**4,860**	ft^2	**20,00**	**4,09**	**8,500**	**4,983**	**6,525**	**0,428**	----------	**10,00**	**0,000**	ft
	1,500	m	1,463	m	0,306	m	12,544	kg					0,612	m		0,452	m^2									0,0000	m
	4,922	ft	**4,800**	ft	**1,003**	ft	**27,655**	Lb	**25,00**	**5,00**	**48,800**	**-12,0**	**1,811**	ft **0,368**	**-2,60**	**4,860**	ft^2	**20,00**	**4,09**	**8,500**	**4,983**	**6,525**	**0,428**	----------	**10,00**	**0,000**	ft
	1,500	m	1,463	m	0,306	m	12,544	kg					0,552	m		0,452	m^2									0,0000	m
232B	**4,922**	ft	**4,800**	ft	**1,003**	ft	**37,027**	Lb	**25,00**	**5,00**	**48,800**	**0,0**	**2,402**	ft **0,488**	**-2,60**	**4,860**	ft^2	**20,00**	**4,09**	**7,000**	**4,983**	**5,920**	**0,574**	----------	**10,00**	**0,000**	ft
	1,500	m	1,463	m	0,306	m	16,795	kg					0,732	m		0,452	m^2									0,0000	m
	4,922	ft	**4,800**	ft	**1,003**	ft	**37,027**	Lb	**25,00**	**5,00**	**48,800**	**-4,0**	**2,205**	ft **0,448**	**-2,60**	**4,860**	ft^2	**20,00**	**4,09**	**7,000**	**4,983**	**5,920**	**0,574**	----------	**10,00**	**0,000**	ft
	1,500	m	1,463	m	0,306	m	16,795	kg					0,672	m		0,452	m^2									0,0000	m
	4,922	ft	**4,800**	ft	**1,003**	ft	**37,027**	Lb	**25,00**	**5,00**	**48,800**	**-8,0**	**2,008**	ft **0,408**	**-2,60**	**4,860**	ft^2	**20,00**	**4,09**	**7,000**	**4,983**	**5,920**	**0,574**	----------	**10,00**	**0,000**	ft
	1,500	m	1,463	m	0,306	m	16,795	kg					0,612	m		0,452	m^2									0,0000	m
	4,922	ft	**4,800**	ft	**1,003**	ft	**37,027**	Lb	**25,00**	**5,00**	**48,800**	**-12,0**	**1,811**	ft **0,368**	**-2,60**	**4,860**	ft^2	**20,00**	**4,09**	**7,000**	**4,983**	**5,920**	**0,574**	----------	**10,00**	**0,000**	ft
	1,500	m	1,463	m	0,306	m	16,795	kg					0,552	m		0,452	m^2									0,0000	m
232B	**4,922**	ft	**4,800**	ft	**1,003**	ft	**53,147**	Lb	**25,00**	**5,00**	**48,800**	**0,0**	**2,402**	ft **0,488**	**-2,60**	**4,860**	ft^2	**20,00**	**4,09**	**5,500**	**4,983**	**5,248**	**0,823**	----------	**10,00**	**0,000**	ft
	1,500	m	1,463	m	0,306	m	24,107	kg					0,732	m		0,452	m^2									0,0000	m
	4,922	ft	**4,800**	ft	**1,003**	ft	**53,147**	Lb	**25,00**	**5,00**	**48,800**	**-4,0**	**2,205**	ft **0,448**	**-2,60**	**4,860**	ft^2	**20,00**	**4,09**	**5,500**	**4,983**	**5,248**	**0,823**	----------	**10,00**	**0,000**	ft
	1,500	m	1,463	m	0,306	m	24,107	kg					0,672	m		0,452	m^2									0,0000	m
	4,922	ft	**4,800**	ft	**1,003**	ft	**53,147**	Lb	**25,00**	**5,00**	**48,800**	**-8,0**	**2,008**	ft **0,408**	**-2,60**	**4,860**	ft^2	**20,00**	**4,09**	**5,500**	**4,983**	**5,248**	**0,823**	----------	**10,00**	**0,000**	ft
	1,500	m	1,463	m	0,306	m	24,107	kg					0,612	m		0,452	m^2									0,0000	m
	4,922	ft	**4,800**	ft	**1,003**	ft	**53,147**	Lb	**25,00**	**5,00**	**48,800**	**-12,0**	**1,811**	ft **0,368**	**-2,60**	**4,860**	ft^2	**20,00**	**4,09**	**5,500**	**4,983**	**5,248**	**0,823**	----------	**10,00**	**0,000**	ft
	1,500	m	1,463	m	0,306	m	24,107	kg					0,552	m		0,452	m^2									0,0000	m
232B	**4,922**	ft	**4,800**	ft	**1,003**	ft	**85,698**	Lb	**25,00**	**5,00**	**48,800**	**0,0**	**2,402**	ft **0,488**	**-2,60**	**4,860**	ft^2	**20,00**	**4,09**	**4,000**	**4,983**	**4,476**	**1,327**	----------	**10,00**	**0,000**	ft
	1,500	m	1,463	m	0,306	m	38,872	kg					0,732	m		0,452	m^2									0,0000	m
	4,922	ft	**4,800**	ft	**1,003**	ft	**85,698**	Lb	**25,00**	**5,00**	**48,800**	**-4,0**	**2,205**	ft **0,448**	**-2,60**	**4,860**	ft^2	**20,00**	**4,09**	**4,000**	**4,983**	**4,476**	**1,327**	----------	**10,00**	**0,000**	ft
	1,500	m	1,463	m	0,306	m	38,872	kg					0,672	m		0,452	m^2									0,0000	m
	4,922	ft	**4,800**	ft	**1,003**	ft	**85,698**	Lb	**25,00**	**5,00**	**48,800**	**-8,0**	**2,008**	ft **0,408**	**-2,60**	**4,860**	ft^2	**20,00**	**4,09**	**4,000**	**4,983**	**4,476**	**1,327**	----------	**10,00**	**0,000**	ft
	1,500	m	1,463	m	0,306	m	38,872	kg					0,612	m		0,452	m^2									0,0000	m
	4,922	ft	**4,800**	ft	**1,003**	ft	**85,698**	Lb	**25,00**	**5,00**	**48,800**	**-12,0**	**1,811**	ft **0,368**	**-2,60**	**4,860**	ft^2	**20,00**	**4,09**	**4,000**	**4,983**	**4,476**	**1,327**	----------	**10,00**	**0,000**	ft
	1,500	m	1,463	m	0,306	m	38,872	kg					0,552	m		0,452	m^2									0,0000	m

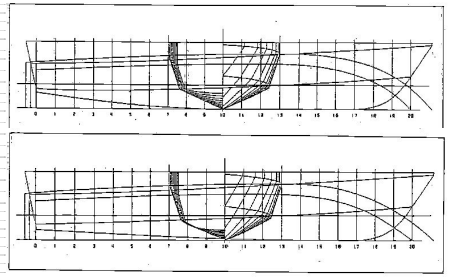

twisted bottom model 232 B

***	Fresh Water
	ITTC
Fv	0.75-3.00

LITERATURE = Resistance tests of a Series Planing Hull Forms with 30 degree deadrise angle and a calculation model based on this and similar systematic series
J.A.Keuning,J.Gerritsma,and P.F.Van Terwisga
Report No.: 959
Resistance tests of a Series Planing Hull Forms with 30 degree deadrise angle, and a calculation model based on this and similar systematic series
J.A.Keuning,J.Gerritsma,and P.F.Van Terwisga
ISP 40,No:424

REPORTS

FACULTY OF MECHANICAL ENGINEERING AND
MARINE TECHNOLOGY
Delft University of Technology
The Netherlands

RESISTANCE TESTS OF A SERIES PLANING HULL FORMS WITH 30 DEGREES DEADRISE ANGLE, AND A CALCULATION MODEL BASED ON THIS AND SIMILAR SYSTEMATIC SERIES

by

J. A. Keuning, J. Gerritsma and P. F. van Terwisga

MEMT 25

1993

REPORT No. 959

Ship Hydromechanics Laboratory.
Mekelweg 2, 2628 CD Delft, The Netherlands.

CIP-DATA KONINKLIJKE BIBLIOTHEEK, DEN HAAG

Keuning, J. A.
Resistance tests of a series planing hull forms with 30 degrees deadrise angle, and a calculation model based on this and similar systematic series / J. A. Keuning, J. Gerritsma and P. F. Terwisga – Delft: Delft University of Technology, Ship Hydromechanics Laboratory. – Ill. (MEMT, ISSN 0925-6555 ; 25).
First publ.: Delft University of Technology, Ship Hydromechanics Laboratory, 1992 - (Report ; no 959). With ref.
ISBN 90-370-0085-1
Subject headings: planing Hull forms ; resistance tests.

Resistance tests of a series planing hull forms with 30 degrees deadrise angle, and a calculation model based on this and similar systematic series

J.A. Keuning* J. Gerritsma** P.F. van Terwisga*

December 23, 1992

Abstract

In addition to the well known systematic series planing hull forms with a deadrise angle of 12.5 degrees as presented by Clement and Blount (DTMB), and a similar series by Keuning and Gerritsma, in this paper the results of the tests on a 30 degrees deadrise series are presented.

The combined data of these three series are fitted to a regression model for total resistance, trim and rise of center of gravity. This regression model is verified by a comparison with existing model data. Although in general the calculations show good agreement with experiments, the need for additional data for a deadrise angle between 12.5 and 25 degrees became obvious.

Additional resistance test results of two models with varying deadrise and rising buttock lines in the aft part of the hull are presented. Regression of these data results in simple expressions to take these effects into account.

Contents

*Delft University of Technology, Ship Hydromechanics Laboratory
**Professor, emeritus, Delft University of Technology, Ship Hydromechanics Laboratory

Nomenclature

A_p	projected planing bottom area [m^2]
B_{pa}	breadth over chines [m]
B_{pt}	breadth over chines at transom [m]
B_{px}	maximum breadth over chines [m]
C_{Ap}	center of A_p [$\%L_p$]
Fn_∇	volumetric Froude number $\frac{v}{\sqrt{g\nabla^{1/3}}}$
g	gravity acceleration [m/s^2]
LCG	longitudinal center of gravity [$\%L_p$]
L_c	wetted length over the chines [m]
L_k	wetted length over the keel [m]
L_p	length of the projected planing bottom area [m]
R_t	total resistance (in towing tank conditions)[N]
RCG	rise of center of gravity relative to its position at zero speed [m]
v	speed [m/s]
β	deadrise angle [deg]
γ	average centerline angle from ordinate 0 to 10 with respect to the baseline positive for a draft at ordinate 0 greater than draft at ordinate 10 [deg]
ϵ	twist angle, i.e. deadrise at ordinate 10 minus the deadrise at ordinate 0 [deg]
Δ	weight of displacement [N]
$\Delta R_t/\Delta$	difference in R_t/Δ of twisted bottom model and 25 deg. parent model for equal loading coefficient and LCG values
$\Delta\theta$	difference in trim angle of twisted bottom model and 25 deg. parent model for equal loading coefficient and LCG values
$\Delta RCG/\nabla^{1/3}$	difference in $RCG/\nabla^{1/3}$ of twisted bottom model and 25 deg. parent model for equal loading coefficient and LCG values
θ	trim angle relative to its value at zero speed, positive for an upward displaced bow [deg]
∇	volume of displacement [m^3]

1 Introduction

In 1963 E.P. Clement and D.L. Blount presented the results of resistance tests of a systematically varied series of planing hull forms, generally known as the TMB Series 62 or the Clement series [1]. The models in this series all had a deadrise of 12.5 degrees. The need for better seakeeping characteristics lead to increasing deadrise angles, although this also lead to an increase of the resistance of the planing ship. To give more insight into this trade off between resistance and seakeeping quality of a particular design, in 1982, Keuning and Gerritsma published the results of a series of planing hull forms, similar to those of Clement and Blount, with higher deadrise, i.e. 25 degrees [2]. These results showed that the increase in resistance is highest for low L_p/B_{px} ratios and independent of the loading coefficient, defined as the ratio of projected chine area and the volume of displacement to the power 2/3. The loading coefficient does have a marked influence on the hump resistance, i.e. is highest for low loading coefficients.

Apart from the resistance data, the trim and rise of center of gravity appeared to be of great importance for the assesment of seakeeping characteristics. In [3] Keuning shows that the still water reference position of the craft at speed may not be neglected in the calculations of the motions of these craft in waves.

The models of the 25 deg deadrise series were varied in their main parameters in the same way as the Clement and Blount series to obtain a systematic experimental set of data. The parent model for this series was similar to the parent model of the 12.5 deg series as much as possible.

In addition to these tests a new parent model with a deadrise of 30 deg. was developed and tested in a similar way. This new parent model and the L_p/B_{px} variations derived herefrom are described in subsequent

sections. Experimental data on resistance, trim and rise of center of gravity are listed.

The data ranging from a Froude coefficient based on volume of displacement 0.75 to 3.0 and a deadrise of 12.5 to 30 degrees, are represented by polynomials. These offer a quick and easy method of interpolating the resistance, trim and sinkage of any arbitrary planing hull form.

The polynomial representation of the Planing Hull Form series is verified by comparison with some model test results of the series and model test results of three arbitrary hull forms tested in the Delft University of Technology facilities, i.e. the towing tank of the shiphydromechanics laboratory.

To account for non prismatic hull forms, two models with twisted bottoms have been derived from the 25 deg parent hull. For both models, the deadrise varied from 25 deg at ordinate 10 to 5 deg. at the transom. The slope of the buttock lines in the aft bodies varies with respect to the 25 deg. parent hull. Results of these tests are listed. The difference in resistance, trim, and rise of center of gravity of the constant deadrise hullform and the twisted bottom hull form is expressed in simple polynomials.

2 Setup of the series

For the 25 deg and 30 deg. deadrise angle a parent model has been developed based on the parent model of Clement and Blount. To keep the design as much the same as possible the following parameters have been kept the same :

- the length over the chine
- the maximum breadth over the chine and the vertical projection of the chine
- the vertical projection of the deck line
- the keel line, except from ordinate 16 forwards where the contour has been lifted upwards to obtain the proper length over the chine.
- the transom slope
- the length of the prismatic part of the hull

Also, all models consisted entirely of developable surfaces, just as the Clement parent hull form. The main particulars of the parent models are listed in table 1. The body plan of the 30 degrees deadrise parent model is presented in fig 1.

β	30	25	12.5	degrees
L_p	1.5	1.5	2.436	m
B_{pa}	0.3	0.3	0.487	m
B_{px}	0.367	0.367	0.596	m
B_{pt}	0.235	0.235	0.381	m
L_p/B_{pa}	5.0	5.0	5.0	-
L_p/B_{px}	4.087	4.087	4.09	-
B_{px}/B_{pa}	1.22	1.22	1.22	-
B_{pt}/B_{px}	0.64	0.64	0.46	-
C_{AP} rel to ord 0	48.8	48.8	48.8	$\%L_p$

Table 1: Main particulars of parent models

From these parent models, for each deadrise, several other models, with different L_p/B_{px} ratios have been derived. For the 25 deg. deadrise and 30 deg. deadrise models this was done using the affine transformation technique as described a.o. by Versluis [5]. The total series comprised the deadrise - L_p/B_{px} ratio combinations listed in table 2.

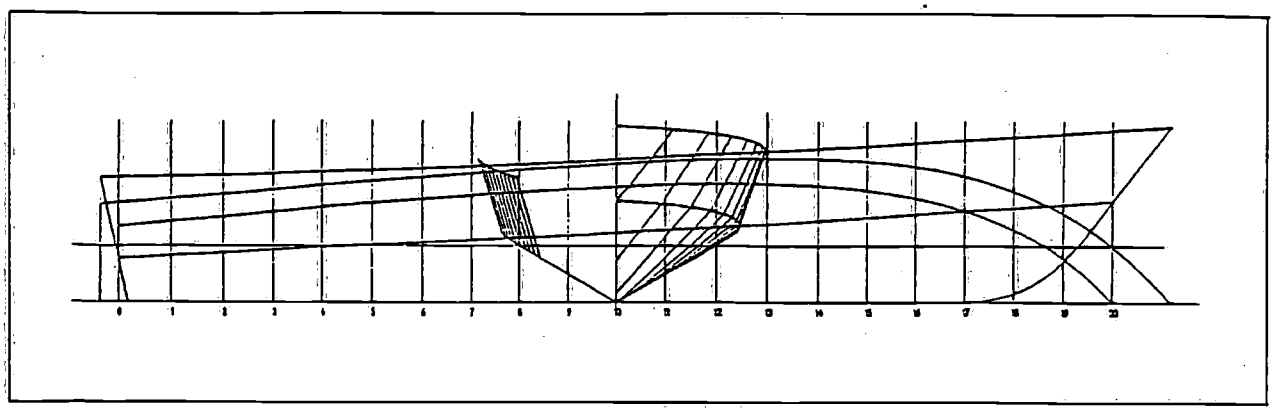

Figure 1: Body plan of the 30 degrees deadrise parent model

β	L_p/B_{px}				
30		3.41	4.09	5.5	7.0
25	2.0	3.06	4.09	5.5	7.0
12.5	2.0	3.06	4.09	5.5	7.0

Table 2: L_p/B_{px} ratios for separate series

The model with L_p/B_{px} ratio 3.41 and deadrise 30 deg. was modified in the same way as had been done by Clement for the 12.5 deg deadrise series. This was done to generate a design which is more alike an actual craft with a low L_p/B_{px} ratio (usually small pleasure crafts, which are propelled by either the outboard engine on the transom or the inboard-outboard type of engine) and which needs more volume of displacement aft than would result from the linear transformation of the parent model.

The body plans of the three L_p/B_{px} variants of the 30 deg. series parent model are shown in figures 2 to 4. The main particulars are listed in table 3. The shaft center lines are shown in the body plans. The same shaft rakes and clearances as described by Clement and Blount have been used here.

L_p/B_{px}	3.41	4.09	5.5	7.0	-
L_p	1.25	1.5	1.5	1.5	m
A_p	0.3843	0.4499	0.3346	0.2627	m^2
B_{pa}	0.3	0.3	0.223	0.175	m
B_{px}	0.367	0.367	0.273	0.214	m
B_{pt}	0.26	0.235	0.175	0.137	m
L_p/B_{pa}	4.17	5.0	6.726	8.571	-
B_{px}/B_{pa}	1.22	1.22	1.22	1.22	-
B_{pt}/B_{px}	0.71	0.64	0.64	0.64	-
C_{AP} rel to ord 0	47.9	48.8	48.6	48.6	$\%L_p$

Table 3: Main particulars of L_p/B_{px} variations

The models had spray strips attached over the entire length of the chine. The bottom of the spray strip followed the line of bottom of the model from ordinate zero (transom) to ordinate 10 and was horizontal from ordinate 12 to ordinate 20 (the stem) with a transition region from ordinate 10 to ordinate 12. The

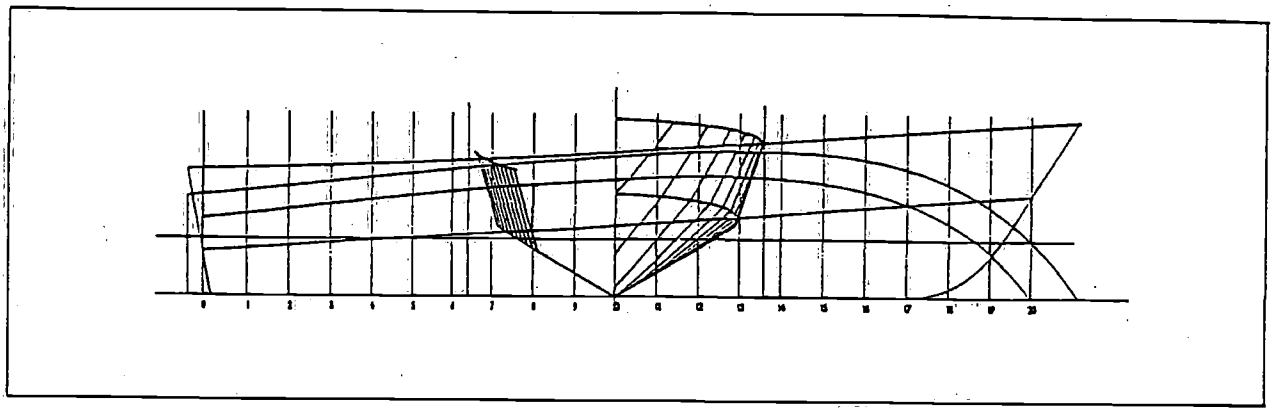

Figure 2: Body plan for $L_p/B_{px} = 3.41$

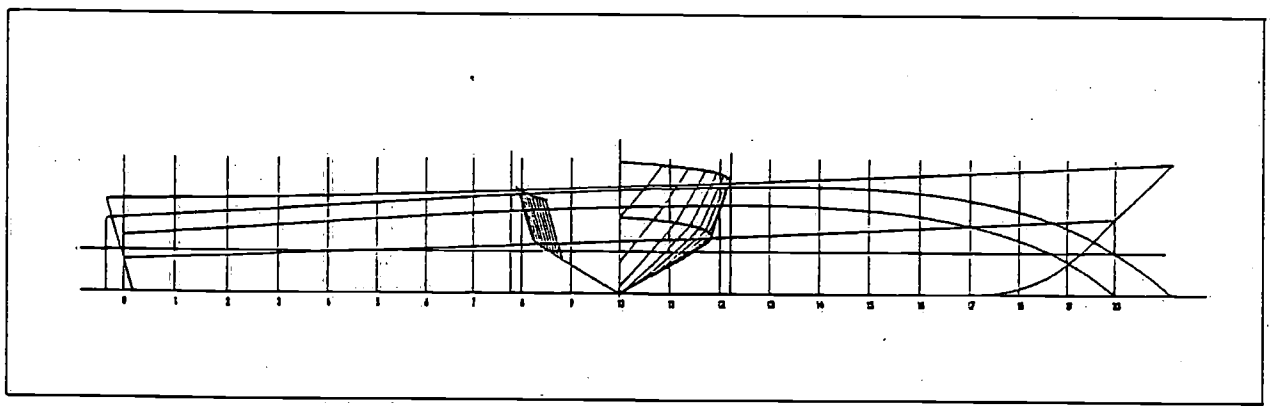

Figure 3: Body plan for $L_p/B_{px} = 5.5$

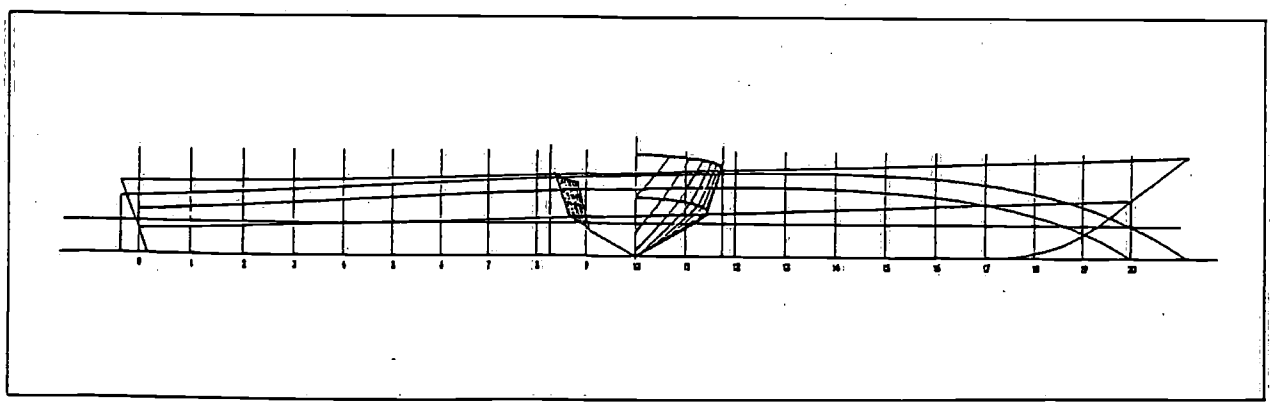

Figure 4: Body plan for $L_p/B_{px} = 7$

width of the spray strips was aproximately 4 mm. and they had non-radiused edges.

The models have been constructed of GRP, which enabled through-hull photography, used for the determination of the wetted surface and wetted length of the keel and chine of the craft at speed.

3 Experimental setup

The tests have been carried out in the no. 1 towing tank of the Ship Hydromechanics Laboratory of the Delft University of Technology. The dimensions of this tank are: length 142 m., breadth 4.22 m., and waterdepth 2.5 m.

The models have been connected to the towing tank carriage in such a way that they were free to heave and pitch but restrained in all other modes of motion. The pivot of the construction was located at the intersection of the assumed centerline of the shaft and the cross section at the LCG. The resistance was measured by means of a strain gauge dynamometer. Pitch and heave have been measured by means of 2 wire over potentiometers on the stern and the bow of the model. The values of resistance, sinkage and trim are the integrated mean values over the duration of the test run, typically 10 sec.

During each run a photo has been taken through the transparant bottom of the hull, for the determination of the wetted length and wetted area.

No turbulence stimulators have been used since the model scale and speed were considered to be large enough to yield reliable results. No towing speeds below 1.0 m/s were used.

4 Measurement scheme

For the 30 deg. deadrise series, 4 L_p/B_{px} ratios have been developed including the parent model. For each of these L_p/B_{px} ratios each possible combination of the loading coefficients $A_p/\nabla^{2/3}$ (4, 5.5 , 7, and 8.5) and the longitudinal position of the center of gravity (0, 2, 4, and 8 % of Lp aft of the Centroid of Ap) were tested in the speed range of Fn_∇ 0.75 to 3.0. The total number of test runs of the 30 deg. deadrise series was approximately 570.

5 Results of the 30 deg. deadrise tests

The results of the experiments are presented in Appendix 1. For every L_p/B_{px}, $A_p/\nabla^{2/3}$, and LCG combination as a function of modelspeed are listed :

- the total resistance of the model R_{tm}
- the wetted length over the keel L_k
- the wetted length over the chines L_c
- the trim angle, positive for an upward displaced bow, relative to the position at $v_m = 0$
- the rise of the center of gravity (positive for upward displacement) relative to its position at $v_m = 0$

Some combinations of small values of $A_p/\nabla^{2/3}$ and LCG 8% aft of Centroid Ap have been omitted due to the fact that the aft deck was submerged at rest. These situations were considered to be impractical.

6 Polynomial model of experimental data

Based on the experimental results, polynomial expressions have been formulated to approximate the total resistance, the trim angle and the rise of center of gravity of the planing hull. The expressions are dependent of the L_p/B_{px} ratio, the loading coefficient $A_p/\nabla^{2/3}$, and the longitudinal center of gravity LCG and fitted to separate datasets for every deadrise-Fn_∇ combination. Describing the (non-dimensional) resistance, trim

and (non-dimensional) sinkage for a number of discrete values of Fn_∇ proved to give a better fit than the description of these parameters by means of one polynomial for the entire speed range.

The total resistance of the planing hull can be predicted by interpolating the Rt/Δ fitted to separate datasets, each containing the total model resistance scaled to a different volume of displacement. Separating the total model resistance into a residuary resistance coefficient and a wetted length and wetted surface would have reduced the number of fitted coefficients, but also reduces the accuracy of the resistance prediction. Sets of coefficients have been determined for a volume of displacement ranging from 2.5 m^3 to 5000 m^3. For the expansion of the resistance data, use has been made of the I.T.T.C. '57 friction line.

The polynomials have the following form :

$$\left.\begin{array}{r} Rt/\Delta \\ \theta \\ RCG/\nabla^{1/3} \end{array}\right\} = a_0 + a_1\ L_p/B_{px} + a_2\ L_p/{B_{px}}^2 + a_3\ L_p/{B_{px}}^3 + a_4\ A_p/\nabla^{2/3} + a_5\ A_p/{\nabla^{2/3}}^2 + a_6\ A_p/{\nabla^{2/3}}^3 + a_7\ LCG + a_8\ LCG^2 + a_9\ LCG^3 + a_{10}\ LCG\ A_p/\nabla^{2/3} + a_{11}\ L_p/B_{px}\ A_p/\nabla^{2/3} + a_{12}\ LCG\ L_p/B_{px} \quad (1)$$

Appendix 2 contains 120 sets of coefficients $a_0 \ldots a_{12}$, i.e. for every deadrise, volumetric froudenumber combination, two sets for Rt/Δ for a volumes of displacement of 5 m^3 and 50 m^3 [1], a set for trim angle, and a set for $RCG/\nabla^{1/3}$

7 Verification of the polynomial model

The goodness of fit of the polynomial expressions is demonstrated in the figures 10 to 18 for three respective models of the systematic series. The deadrise, L_p/B_{px}, $A_p/\nabla^{2/3}$, and LCG parameters of these models, based on a medium, light and heavy weight of displacement, are listed in table 4

model	β	L_p/B_{px}	$A_p/\nabla^{2/3}$	LCG
PHF1	25	5.5	5.5	-4
PHF2	25	5.5	8.5	-12
PHF3	25	2.0	4.0	0

Table 4: Models used to validate polynomial results

The largest discrepancies occur for the heavy model with low L_p/B_{px} value. The total resistance is underpredicted in the speed region below Fn_∇ 1.75 and overpredicted for higher speeds. Also for this model, the trim calculation underpredicts the measured values for speeds higher than Fn_∇ 1.25. The RCG values agree satisfactory for these three models.

To validate the polynomials for the use in predicting the resistance trim and sinkage of arbitrary planing ships, three models tested at the Delft University of Technology Ship Hydromechanics Laboratory were used for a comparison with the polynomial results. In figure 5 to 7 the body plans of a coastal patrol vessel, a planing motor yacht (R410) and a coastal rescue boat are shown. The main dimensions of these craft are listed in table 5 to 7

In figures 19 to 27 both measured and calculated results are presented for these three vessels. Also in these cases the prediction is reasonably accurate.

It appeared however that the interpolation of the 12.5 and 25 degrees deadrise for the patrol boat, as well as for the motoryacht resulted in a better fit to experiments when a linear interpolation with respect to deadrise angle β was used instead of a quadratic interpolation over all available data. Since many planing

[1] To minimize the amount of listed coefficients, the Rt/Δ coefficients are given for two volumes of displacement. The complete set of coefficients for Rt/Δ ranging from 2.5 m^3 to 5000m^3 are obtainable at the Delft University of Technology, Ship Hydromechanics Laboratory

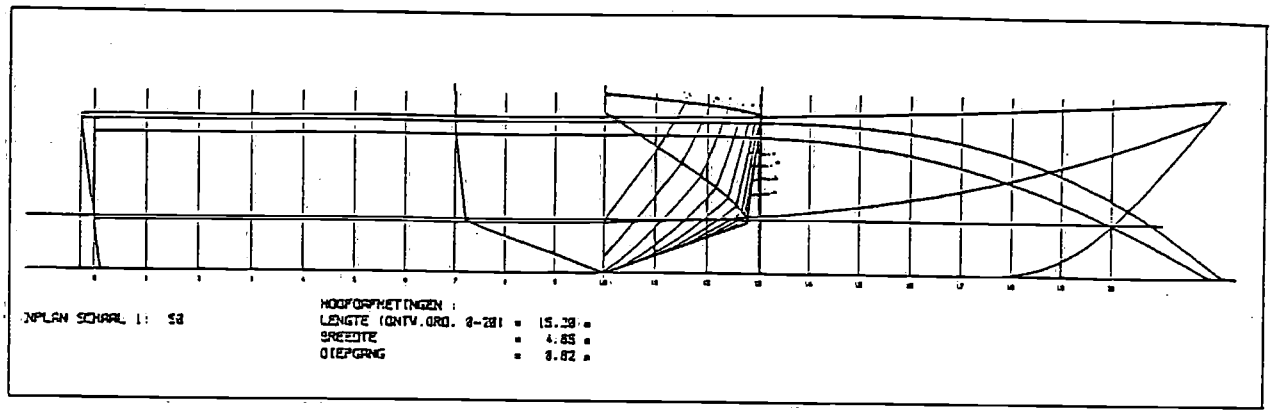

Figure 5: Body plan of coastal patrol vessel

L_p	16.8	m
B_{px}	4.22	m
A_p	60.5	m^2
∇	23.7	m^3
C_{A_p} rel to ord 0	39.3	$\%L_p$
β	20	deg.
L_p/B_{px}	4.0	-
$A_p/\nabla^{2/3}$	7.36	-
LCG rel to C_{A_p}	-3.9	$\%L_p$

Table 5: Main dimensions Patrol Vessel

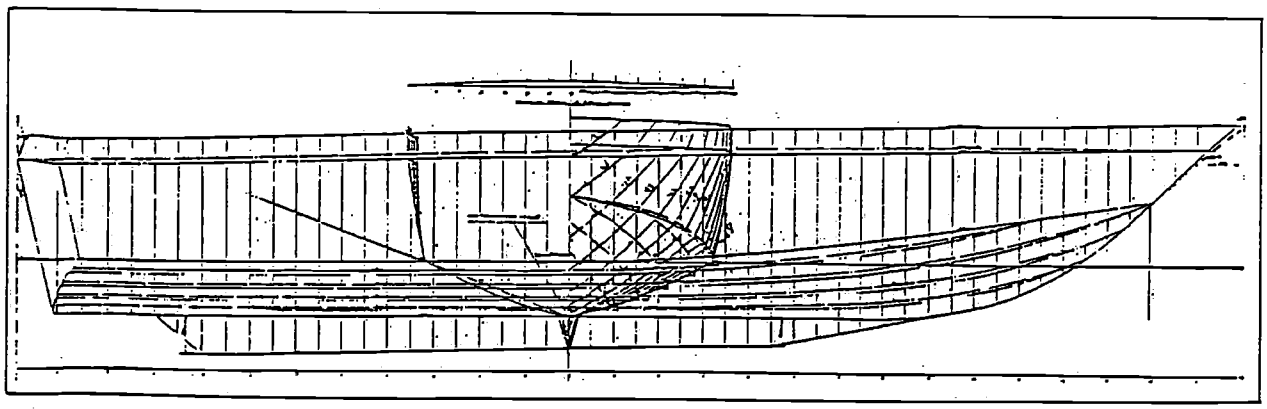

Figure 6: Body plan of motor yacht R410

L_p	19.2	m
B_{px}	5.05	m
A_p	84.3	m^2
∇	44.9	m^3
C_{A_p} rel to ord 0	45.8	$\%L_p$
β	21	deg.
L_p/B_{px}	3.8	-
$A_p/\nabla^{2/3}$	6.67	-
LCG rel to C_{A_p}	-5.31	$\%L_p$

Table 6: Main dimensions Motor Yacht R410

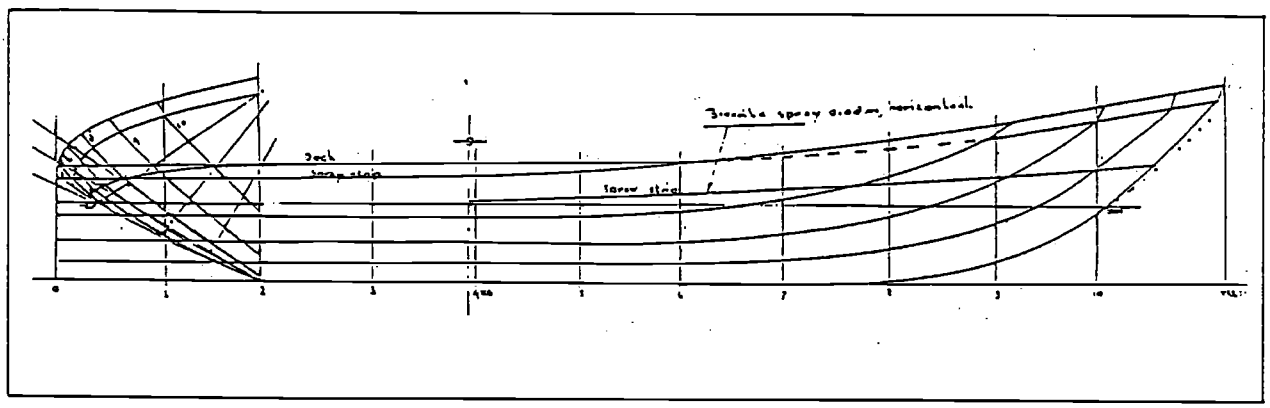

Figure 7: Body plan of coastal rescue boat

L_p	11.21	m
B_{px}	3.30	m
A_p	35.3	m^2
∇	13.3	m^3
C_{A_p} rel to ord 0	36.9	$\%L_p$
β	26	deg.
L_p/B_{px}	3.3	-
$A_p/\nabla^{2/3}$	6.3	-
LCG rel to C_{A_p}	-4.8	$\%L_p$

Table 7: Main dimensions coastal rescue boat

vessels designed for operation in coastal areas have deadrise angles close to 20 degrees, the influence of deadrise on resistance trim and sinkage in the range of 12.5 degrees to 25 degrees needs to be investigated more extensively. Therefore it was decided to test an additional 19 degrees deadrise series in the Delft towing tank facilities in the near future.

8 Twisted bottom models

Many planing hull form designs do not have the prismatic aft body of the parent models of the previously described series, but show a variation in deadrise angle over the length and rising center line in the aft part of the hull, which allows the propeller shaft to have a lower inclination angle. To investigate the possible influence of these effects on resistance, trim and sinkage, two models with a strong resemblance to the 25 degrees deadrise parent model have been tested in the speed range Fn_∇ 0.75 .. 3. [4]

Both models have a twisted bottom, i.e. a deadrise variation of 25 degrees at ordinate 10 to 5 degrees deadrise at ordinate 0. The two models had a different center line however. For model 232-A the average inclination angle of the center line is −4.9 degrees, whereas this angle for model 232-B equals −2.6 degrees. In order to maintain sufficient bouyancy in the aft body, the width of the chines had to be increased. Although this parameter clearly influences the characteristics of a planing hull and hereby the validity of a comparison of characteristics between the twisted bottom models and the prismatic hull forms, this was accepted to obtain realistic models. The sections forward of ordinate 10 are equal to those of the parent model of the 25 deg. deadrise series. The body plans of the two models are shown in fig 8 and 9. Propeller clearances and shaft inclination were equal to those used for the prismatic hull forms. The main particulars of the models are listed in table 8

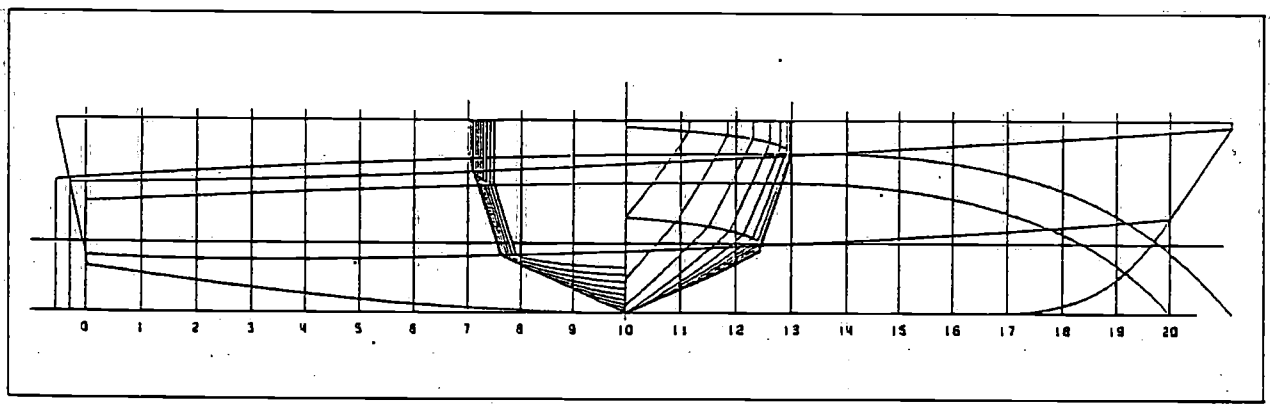

Figure 8: Body plan of twisted bottom model 232 A

The experimental setup was equal to the setup used in the 25 and 30 degrees deadrise series and described in section 3.

The measurement scheme was equal to the scheme used for the previously described series, i.e. $A_p/\nabla^{2/3}$ values of 4.0, 5.5, 7.0, 8.5 and LCG values of 0, 4, 8, and 12 % L_p aft of the C_{Ap}.

Some combinations of heavy weight of displacement and position of the center of gravity were not tested due to excessive trim which caused flooding of the model at rest.

The results of the tests are listed in appendix 3.

8.1 Polynomial model of the twisted bottom results

The effect of twist and rising center line can be described by the difference in resistance, trim and sinkage of the twisted bottom models and the parent model of the 25 degrees deadrise series. To ease the work

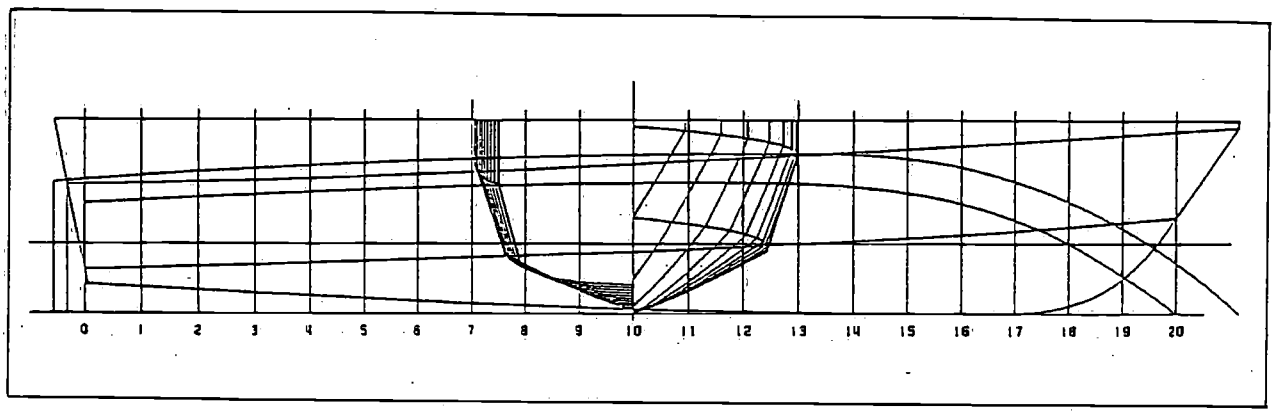

Figure 9: Body plan of twisted bottom model 232 B

	Model		
	232-A	232-B	
L_p/B_{px}	4.09	4.09	-
L_p	1.5	1.5	m
A_p	0.4589	0.4540	m^2
B_{pa}	0.306	0.303	m
B_{px}	0.367	0.367	m
B_{pt}	0.32	0.31	m
L_p/B_{pa}	4.9	4.9	-
B_{px}/B_{pa}	1.2	1.2	-
B_{pt}/B_{px}	0.872	0.844	-
C_{AP} rel to ord 0	48.8	48.8	$\%L_p$

Table 8: Main particulars of twisted bottom models

of interpolating the experimental results, these terms are represented by polynomials, in which a linear dependency on the centerline inclination angle γ and the twist angle ϵ, as well as coupling between these angles and the loading coefficient and LCG is assumed. The polynomials have the following form :

$$\left.\begin{array}{r} \Delta Rt/\Delta \\ \Delta\theta \\ \Delta RCG/\nabla^{1/3} \end{array}\right\} = a_0\,\gamma + a_1\,\epsilon + a_2\,\gamma\,A_p/\nabla^{2/3} + a_3\,\gamma\,LCG + a_4\,\epsilon\,A_p/\nabla^{2/3} + a_5\,\epsilon\,LCG + a_6\,\gamma\,A_p/\nabla^{2/3^2} + a_7\,\gamma\,LCG^2 \quad (2)$$

Also in this case, the regression analysis has been been performed for separate datasets for each Fn_∇. The experimental $\Delta R_t/\Delta$ values have been scaled to the same weights of displacement as used in section 6. The polynomial coefficients are listed in Appendix 4 [2].

8.2 Verification of the twisted bottom polynomial model

The results of the polynomial approximations are validated by a comparison of calculated and measured values of $\Delta R_t/\Delta$, $\Delta\theta$, and $\Delta RCG/\nabla^{1/3}$. The selected twisted bottom models for this comparison are listed in table 9

model	$A_p/\nabla^{2/3}$	LCG
232A-1	5.5	0
232A-2	5.5	-8
232B-1	7.0	-4

Table 9: Twisted bottom models used to validate polynomials

In figures 28 to 36 the results of the experiments of the twisted bottom and the 25 degrees deadrise parent model as well as the experimental difference and its polynomial values are presented. In these figures; *PHF exp* denotes the experimental value of the 25 degree deadrise model, *TB exp* denotes the experimental value of a twisted bottom model, *TB - PHF exp* denotes the difference between these two values, and *TB - PHF polyn* denotes the polynomial approximation of *TB - PHF exp*. The agreement is in all cases satisfactory for the resistance as well as for the trim and rise of center of gravity.

9 Conclusions

The experimental data presented in this paper provides resistance information necessary in the design trade off between seakeeping characteristics (high deadrise) and low resistance (small deadrise angles).

The trim and rise of center of gravity data give the still water position of the vessel at speed, which are shown to have a significant effect on seakeeping calculations [3].

The combined series data represented in a polynomial model provide an easy way to interpolate over a wide range of planing hull forms. It appeared however that additional experimental data is needed in the deadrise range from 12.5 to 25 degrees.

The experimental data and polynomial representation of the twisted bottom models give insight into the influence of a varying deadrise and inclined buttock lines in the aft body of the planing craft. The results obtained with the polynomial expressions for the difference in resistance, trim and rise of center of gravity due to change of deadrise and center line inclination show a good fit with the measured data. The use of this correction for arbitrary designs however should be considered with care because they are based only on a limited amount of experimental data.

[2] To minimize the amount of listed coefficients, the $\Delta Rt/\Delta$ coefficients are given for two volumes of displacement. The complete set of coefficients for $\Delta Rt/\Delta$ ranging from 2.5 m^3 to 5000m^3 are obtainable at the Delft University of Technology, Ship Hydromechanics Laboratory

References

[1] E.P. Clement, D.L. Blount
Resistance Tests of a Systematic Series of Planing Hull Forms
Transactions SNAME 1963

[2] J.A. Keuning, J. Gerritsma
Resistance Tests of a Systematic Series of Planing Hull Forms with 25 Degrees Deadrise Angle
International Shipbuilding Progress Vol.29, No. 337, 1982

[3] J.A. Keuning
Non Linear Heave and Pitch Motions of Fast Ships in Irregular Head Seas
Intersociety High Performance Marine Vehicle Conference and Exhibit, HPMV 1992, Arlington

[4] J.A. Keuning
Resistance Tests of Two Planing Boats with Twisted Bottom
Report no. 731, Ship Hydromechanics Laboratory, Delft University of Technology

[5] A. Versluis
Computer Aided Design of Shipform by Afine Transformation
Report no. 438-P, Ship Hydromechanics Laboratory, Delft University of Technology

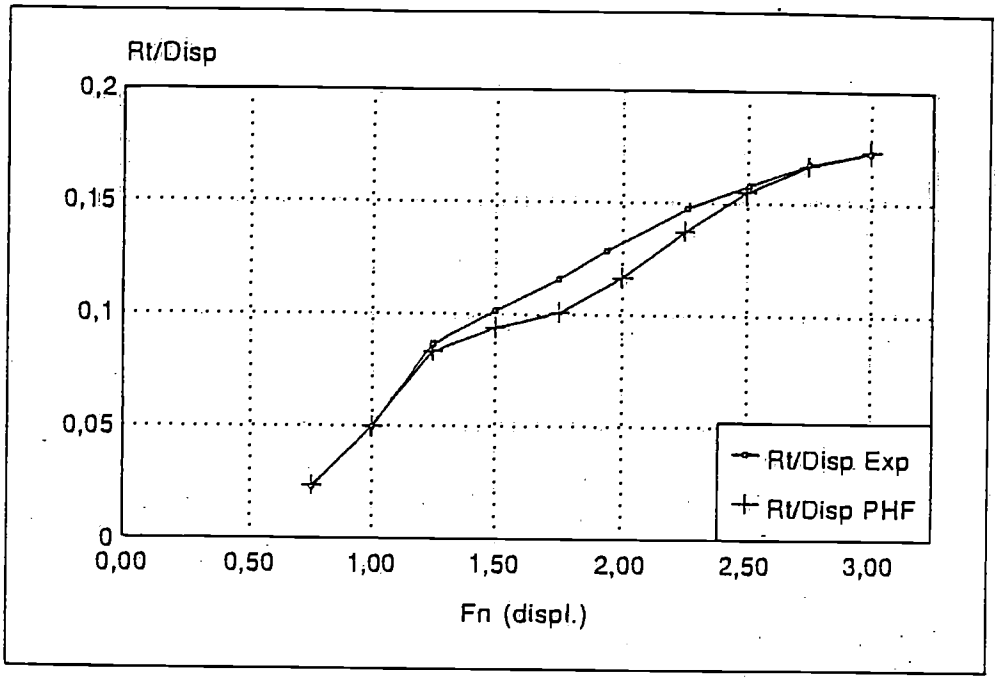

Figure 10: PHF 1 Experimental and calculated Rt/Δ

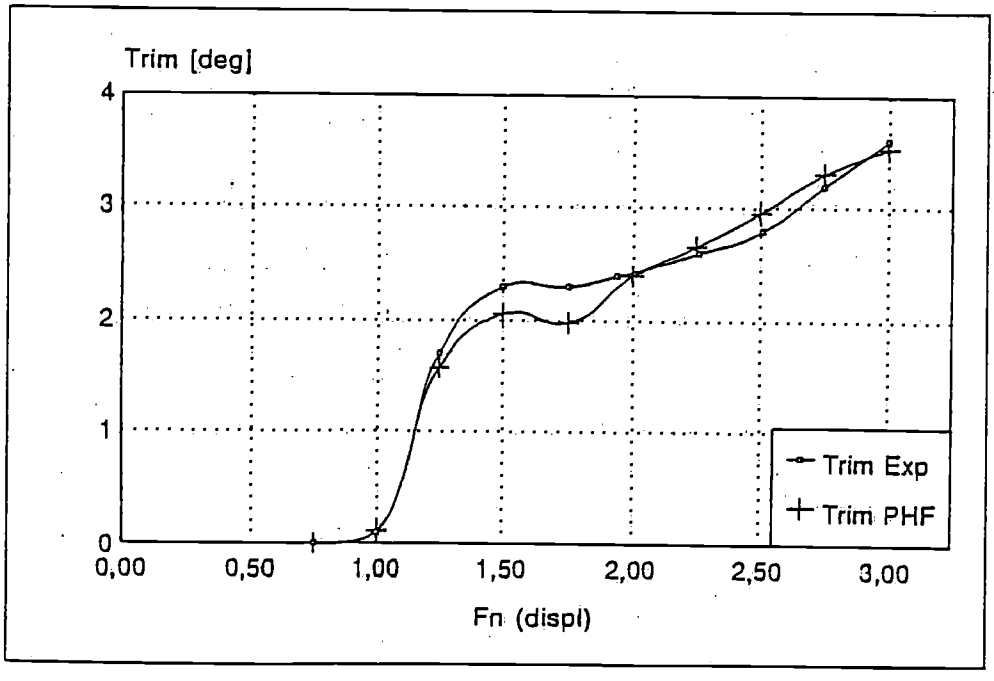

Figure 11: PHF 1 Experimental and calculated trim

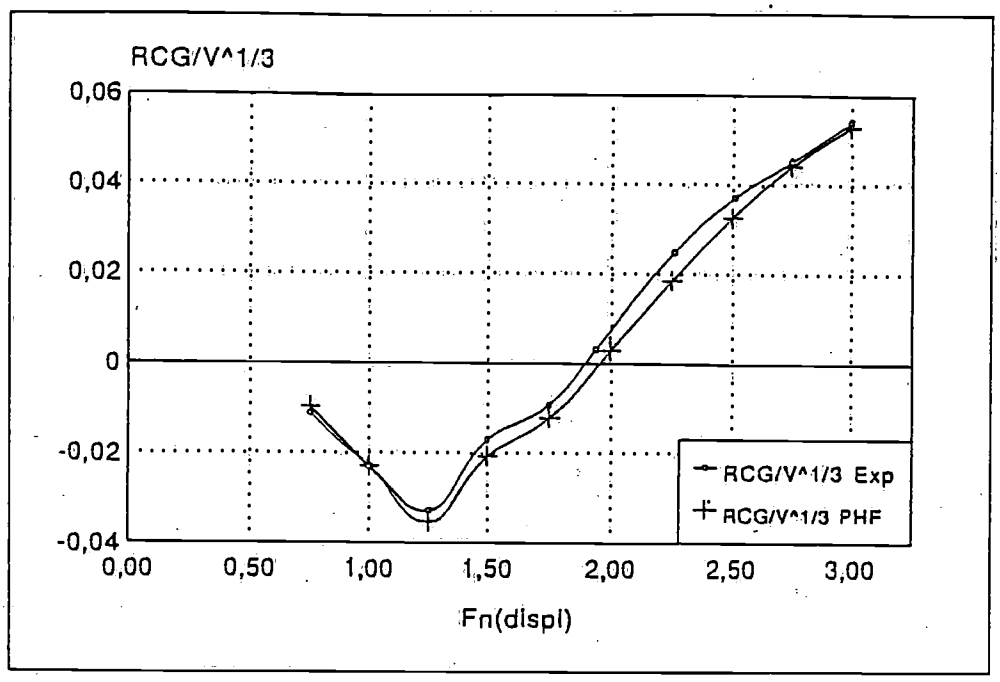

Figure 12: PHF 1 Experimental and calculated $RCG/\nabla^{1/3}$

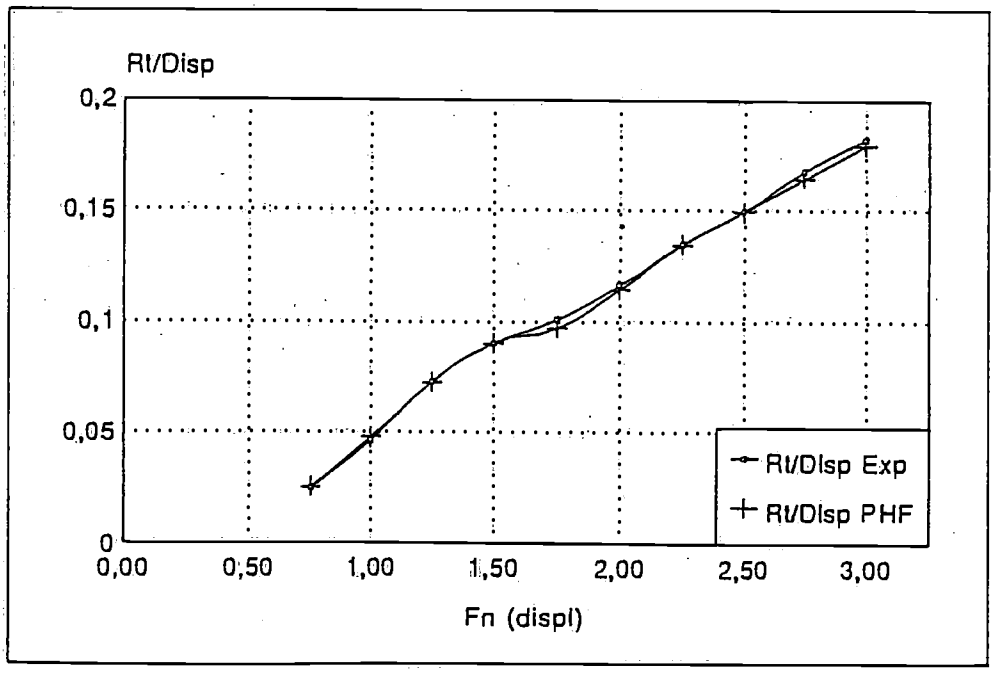

Figure 13: PHF 2 Experimental and calculated Rt/Δ

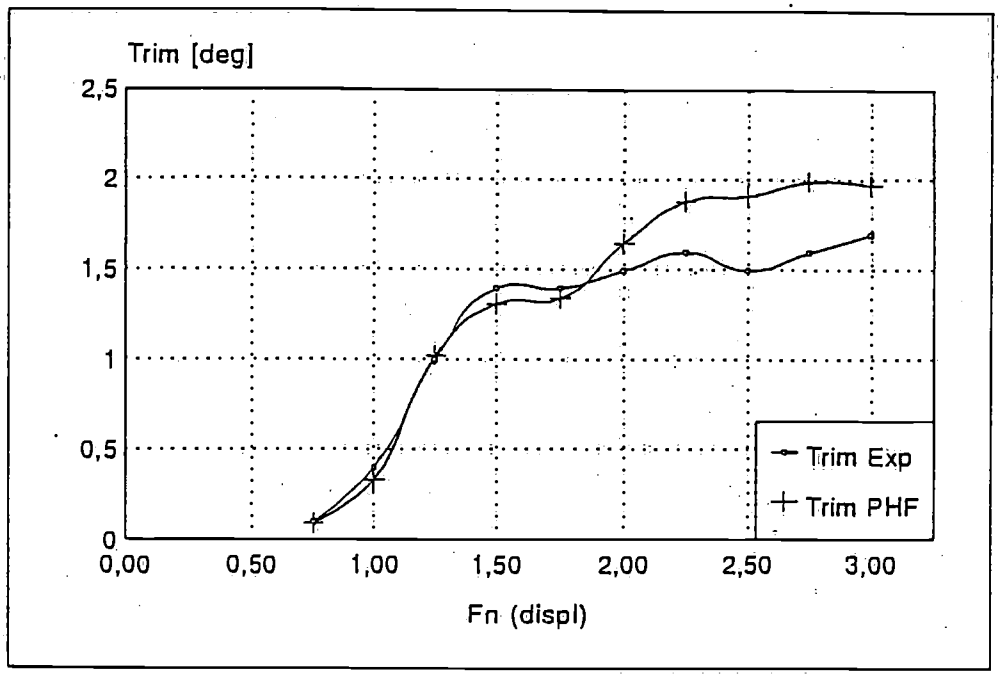

Figure 14: PHF 2 Experimental and calculated trim

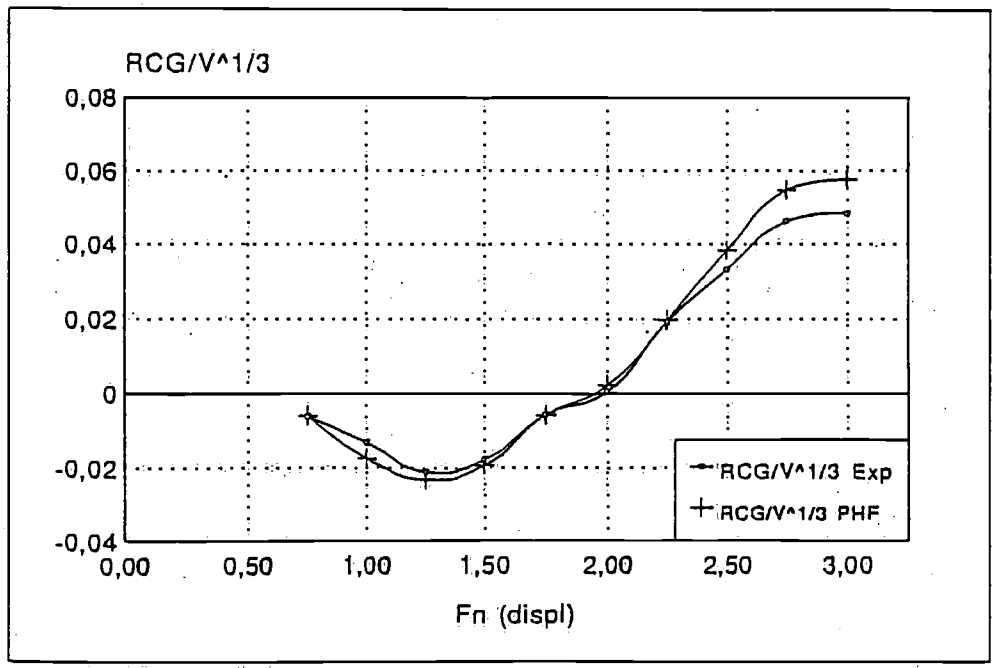

Figure 15: PHF 2 Experimental and calculated $RCG/\nabla^{1/3}$

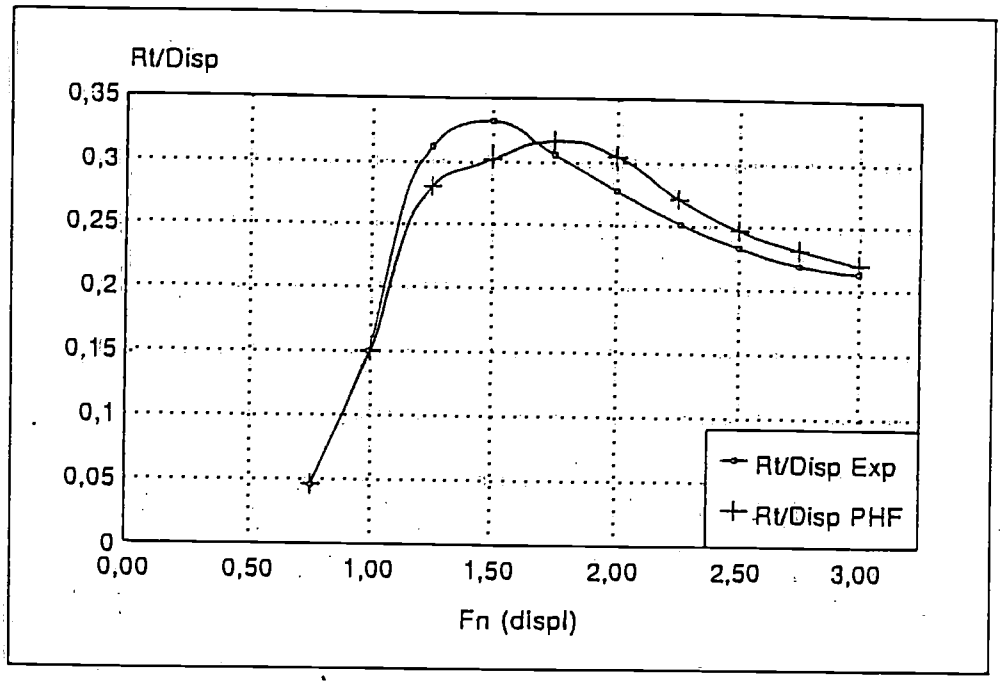

Figure 16: PHF 3 Experimental and calculated Rt/Δ

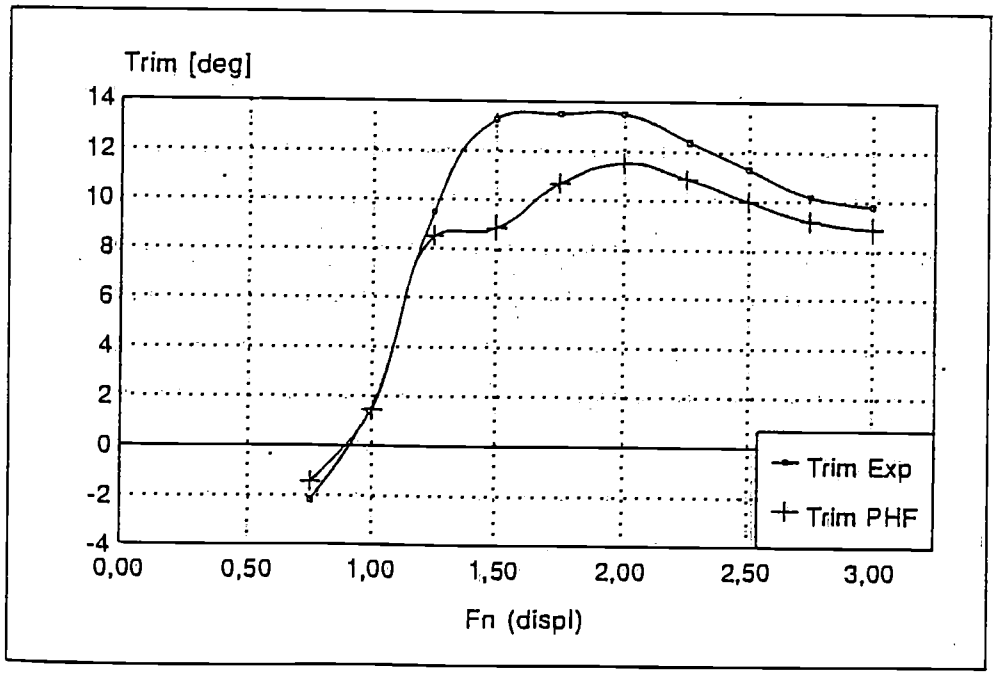

Figure 17: PHF 3 Experimental and calculated trim

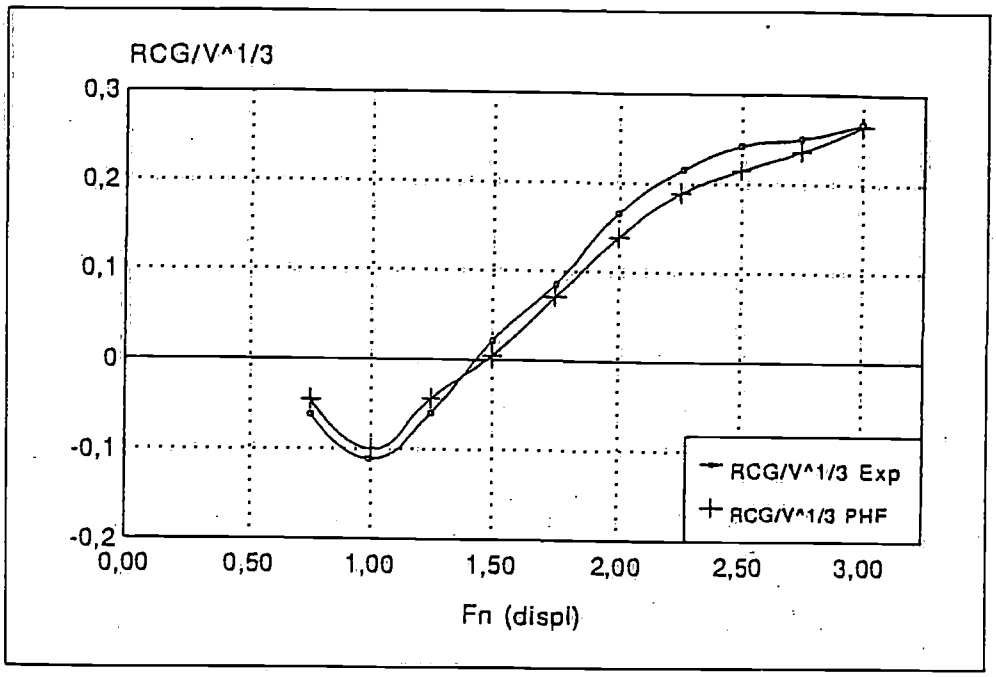

Figure 18: PHF 3 Experimental and calculated $RCG/\nabla^{1/3}$

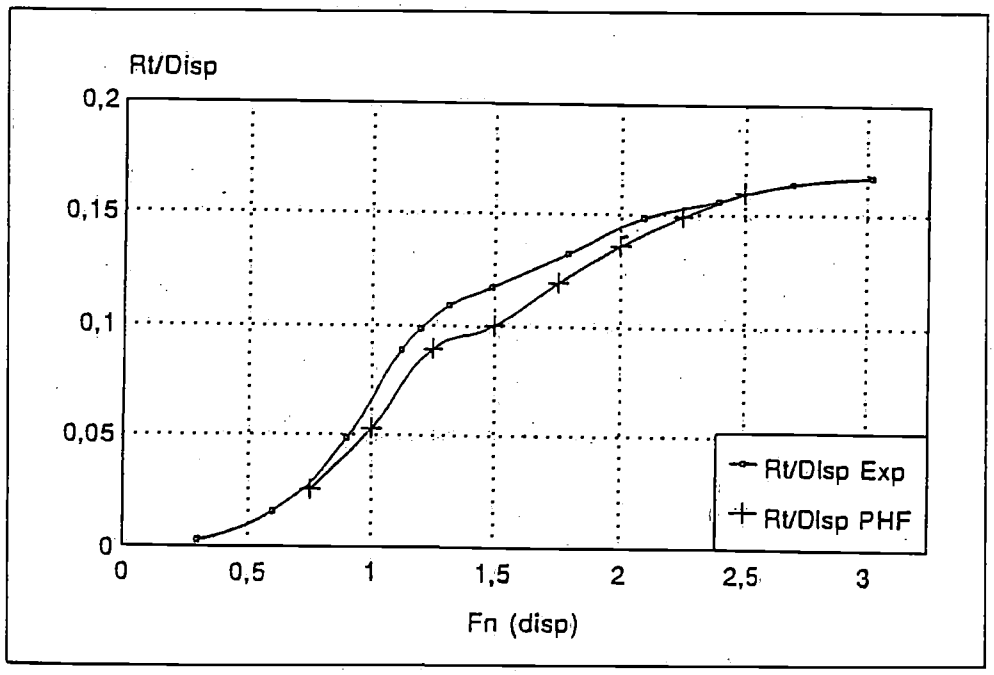

Figure 19: Coastal Patrol Vessel Experimental and calculated Rt/Δ

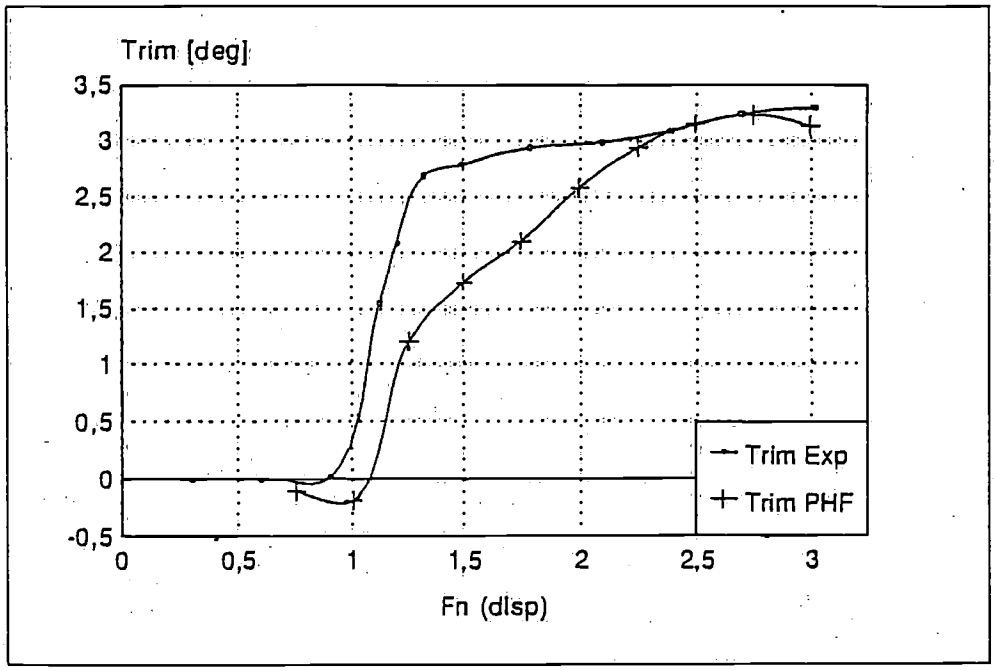

Figure 20: Coastal Patrol Vessel Experimental and calculated trim

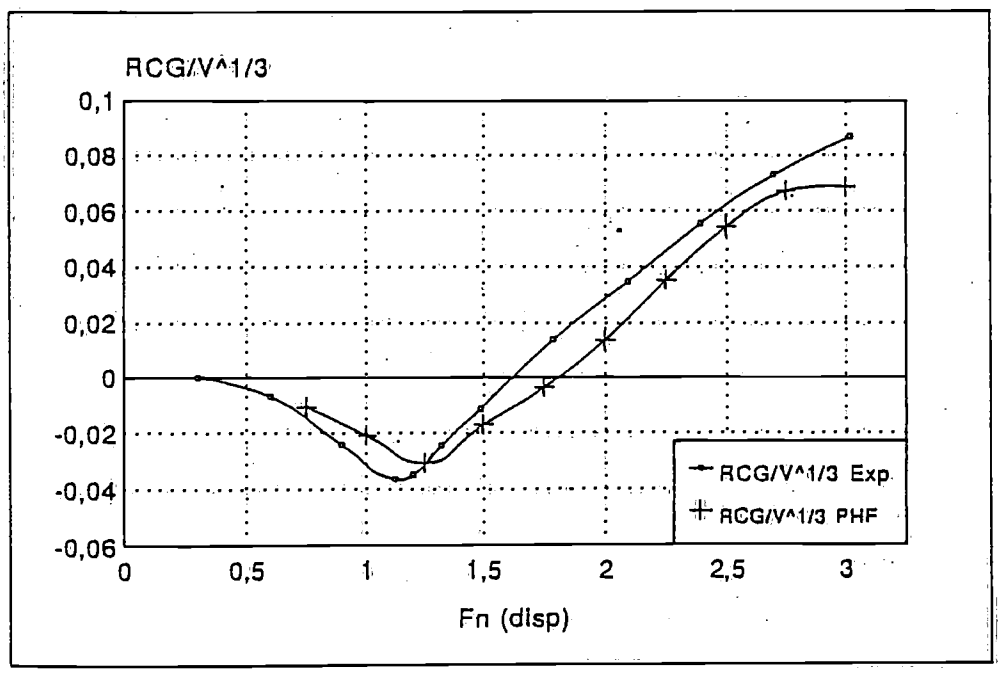

Figure 21: Coastal Patrol Vessel Experimental and calculated $RCG/\nabla^{1/3}$

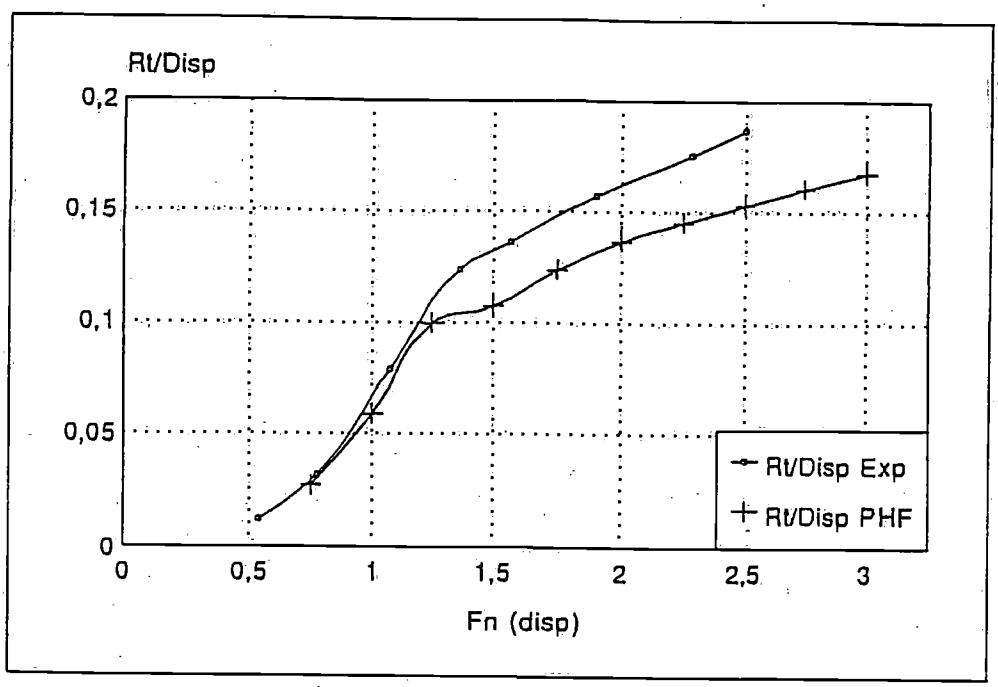

Figure 22: Motor Yacht R410 Experimental and calculated Rt/Δ

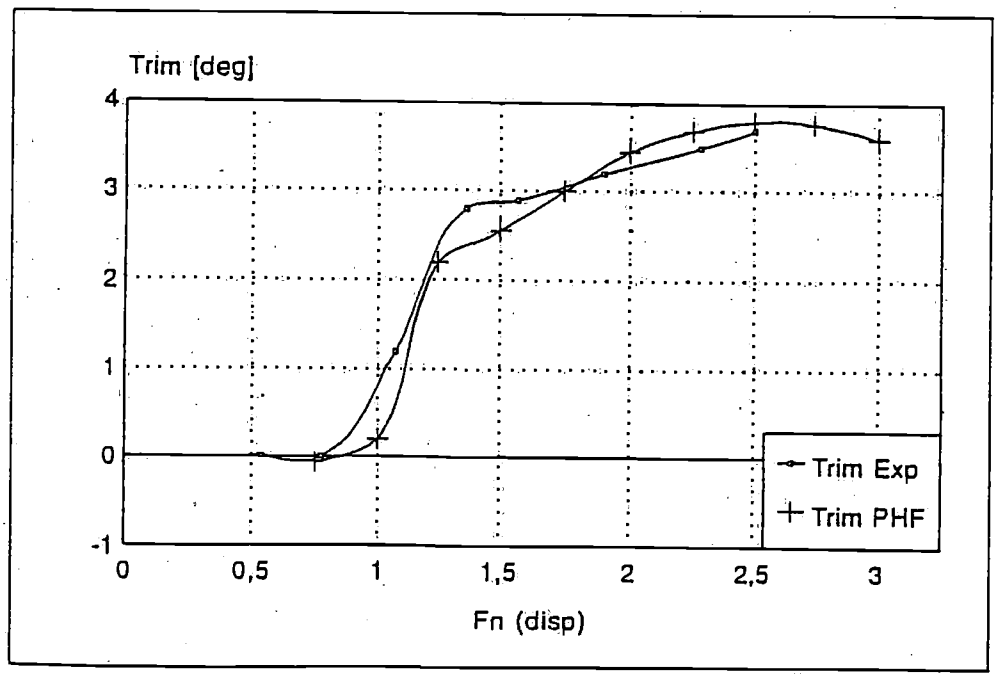

Figure 23: Motor Yacht R410 Experimental and calculated trim

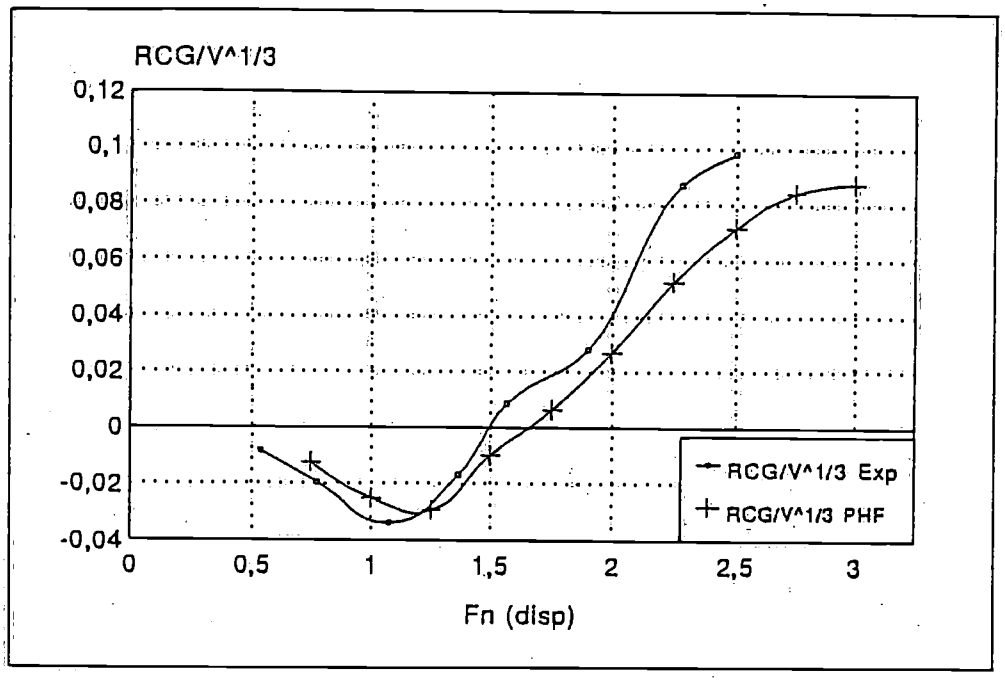

Figure 24: Motor Yacht R410 Experimental and calculated $RCG/\nabla^{1/3}$

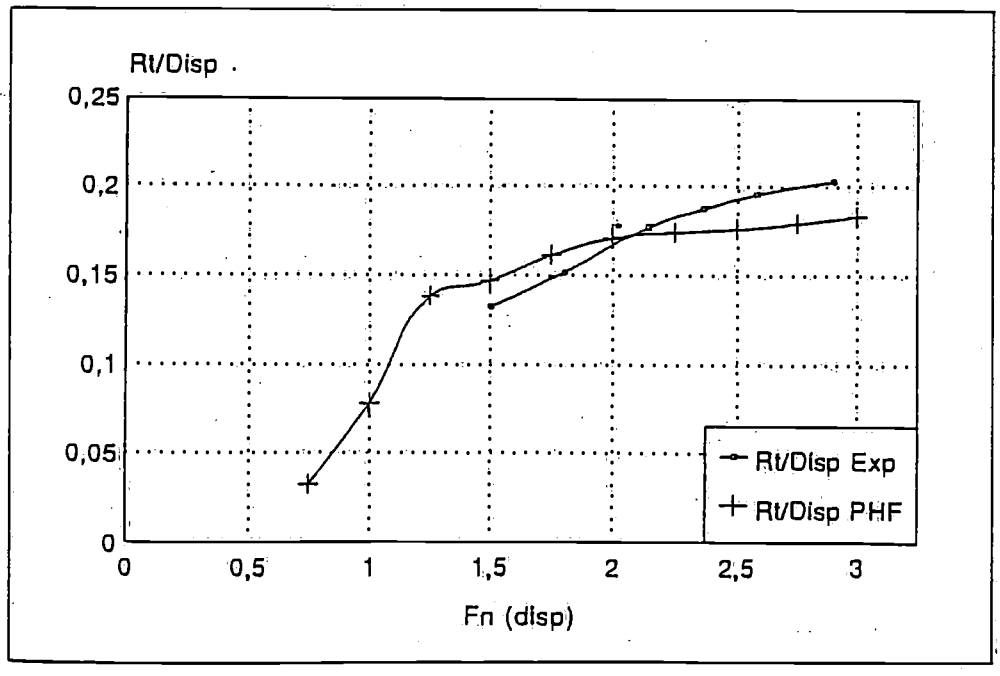

Figure 25: Coastal rescue boat Experimental and calculated Rt/Δ

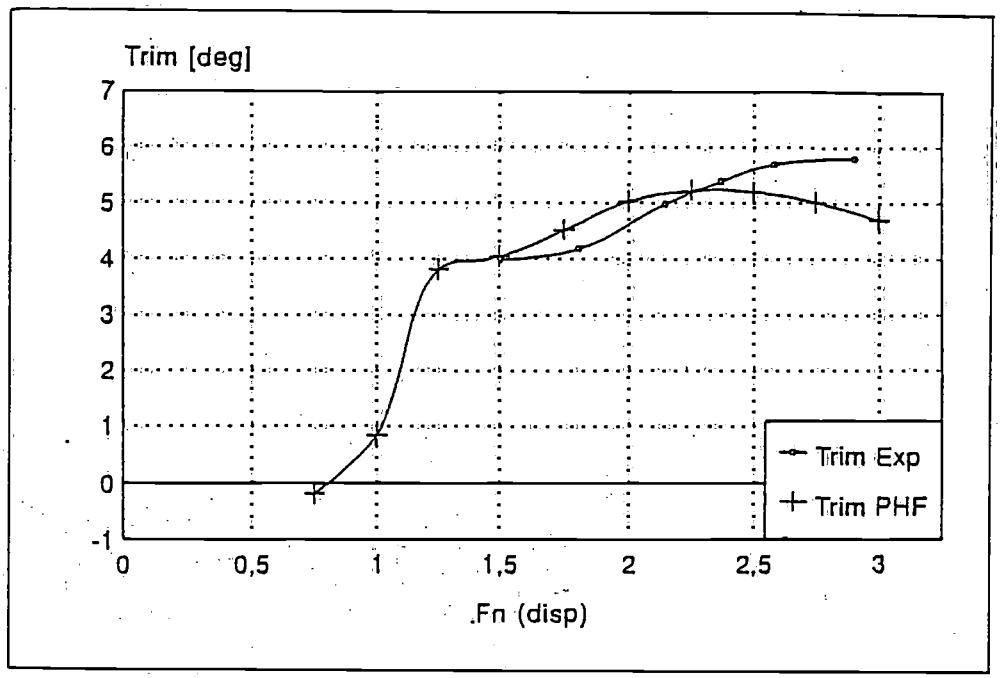

Figure 26: Coastal rescue boat Experimental and calculated trim

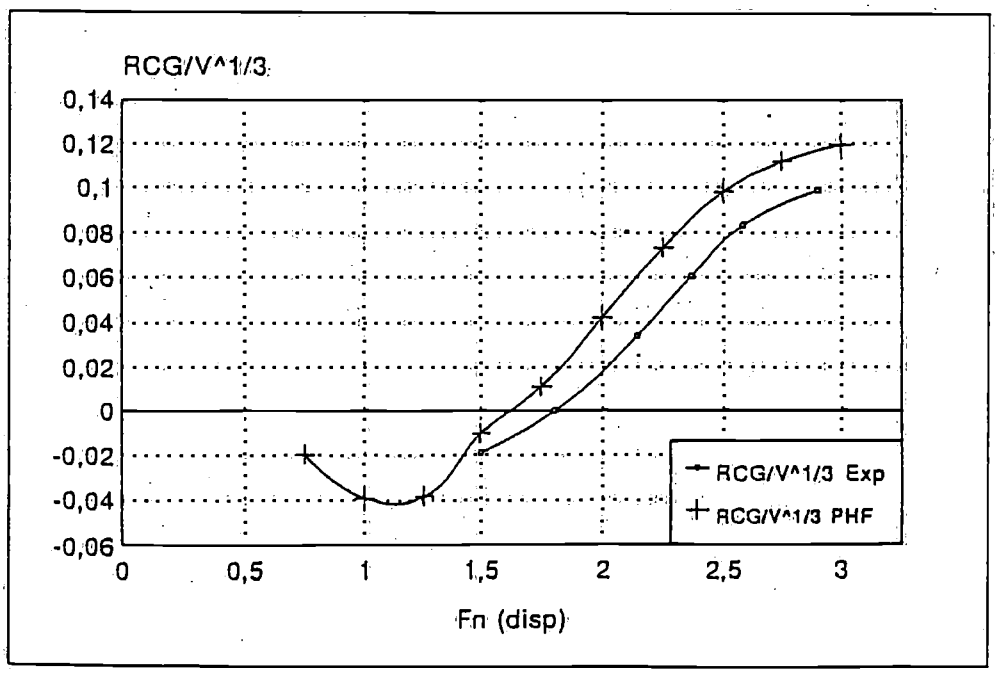

Figure 27: Coastal rescue boat Experimental and calculated $RCG/\nabla^{1/3}$

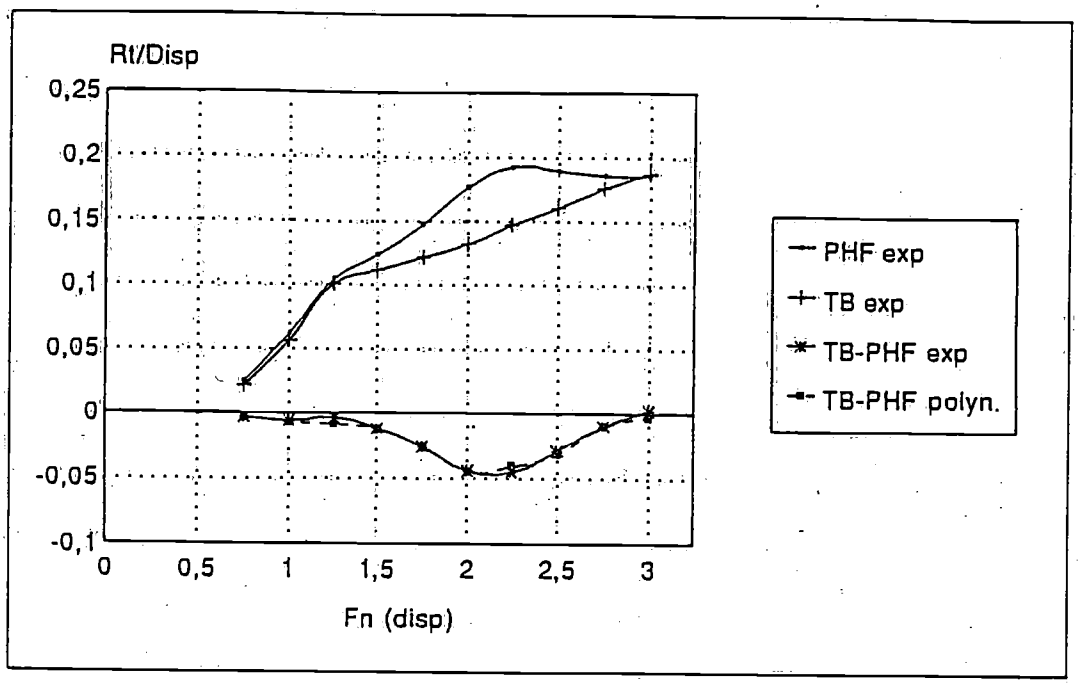

Figure 28: Model 232A-1 Experimental and calculated $\Delta Rt/\Delta$

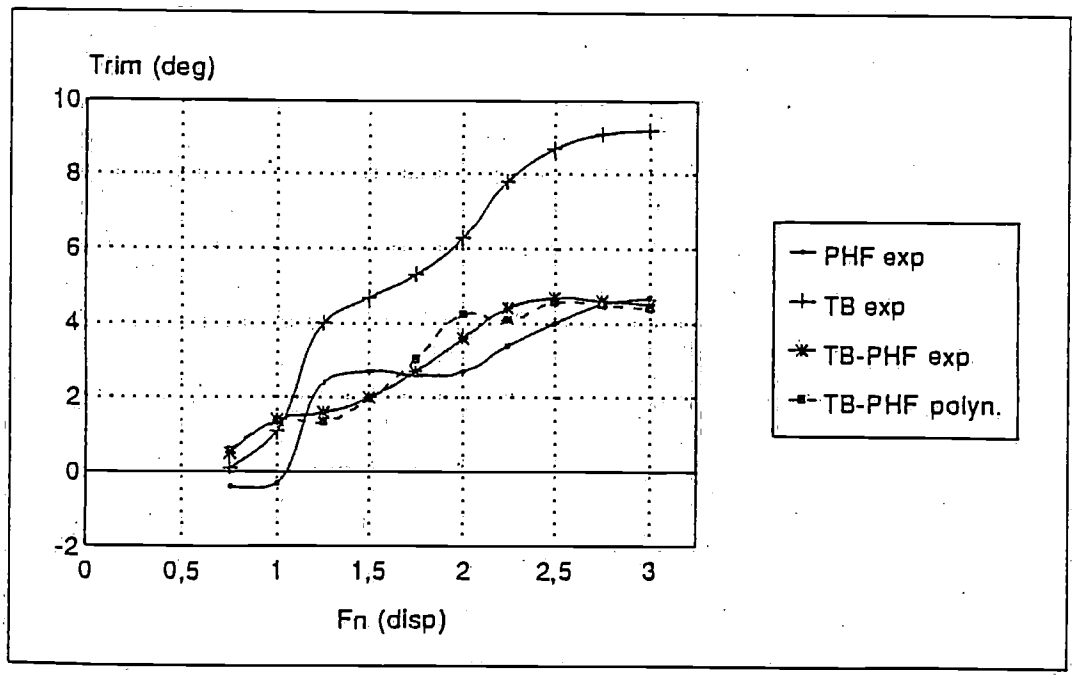

Figure 29: Model 232A-1 Experimental and calculated $\Delta\theta$

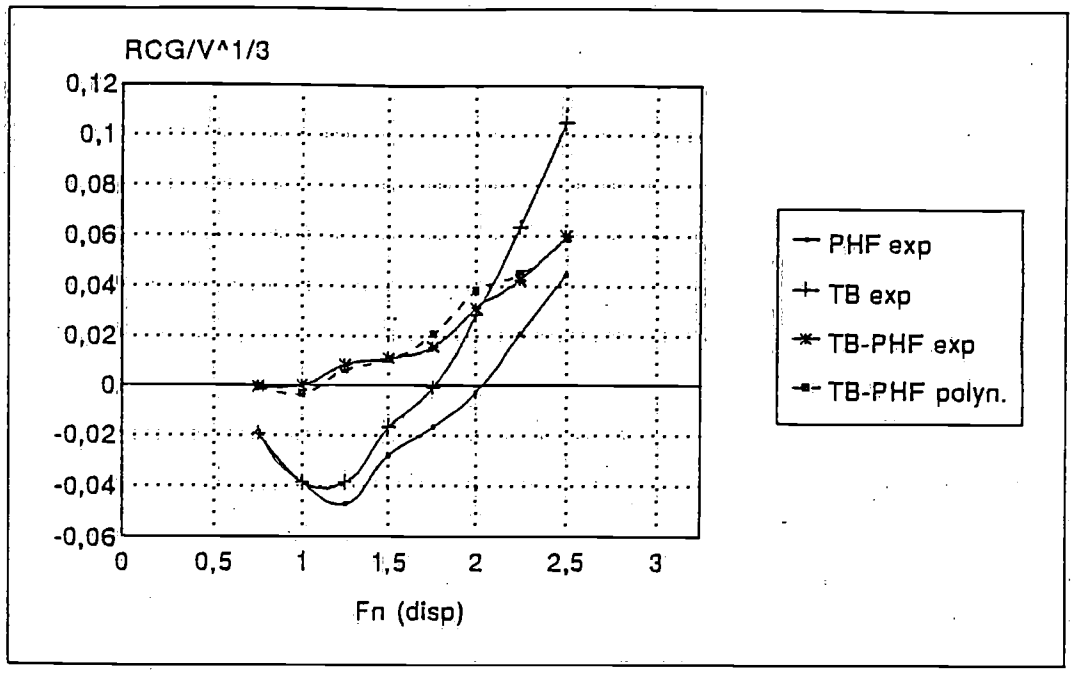

Figure 30: Model 232A-1 Experimental and calculated $\Delta RCG/\nabla^{1/3}$

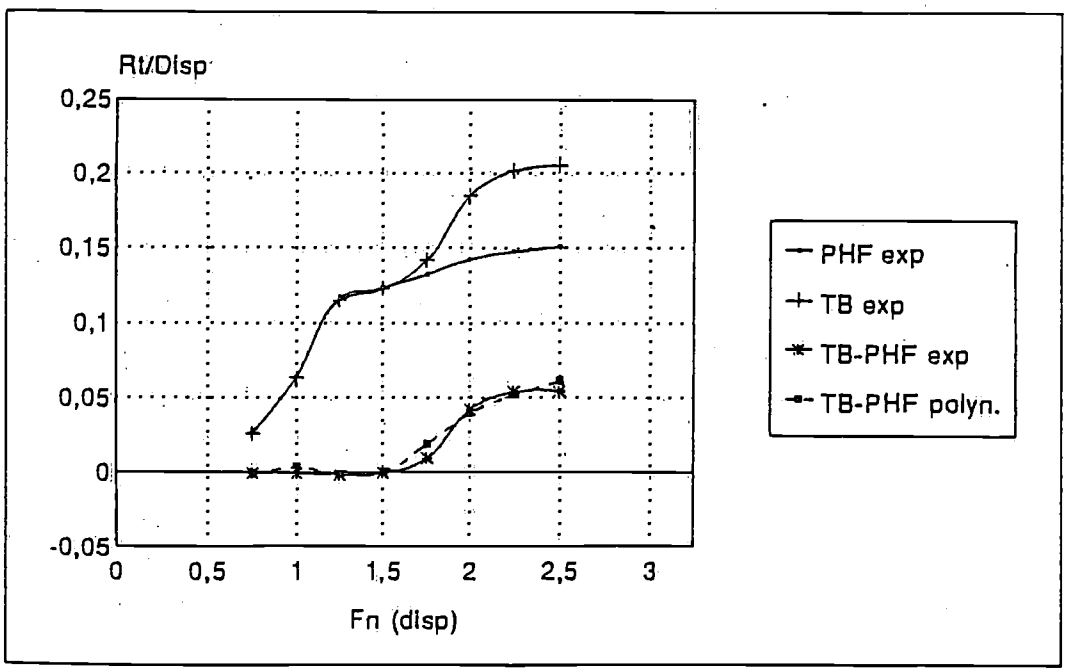

Figure 31: Model 232A-2 Experimental and calculated $\Delta Rt/\Delta$

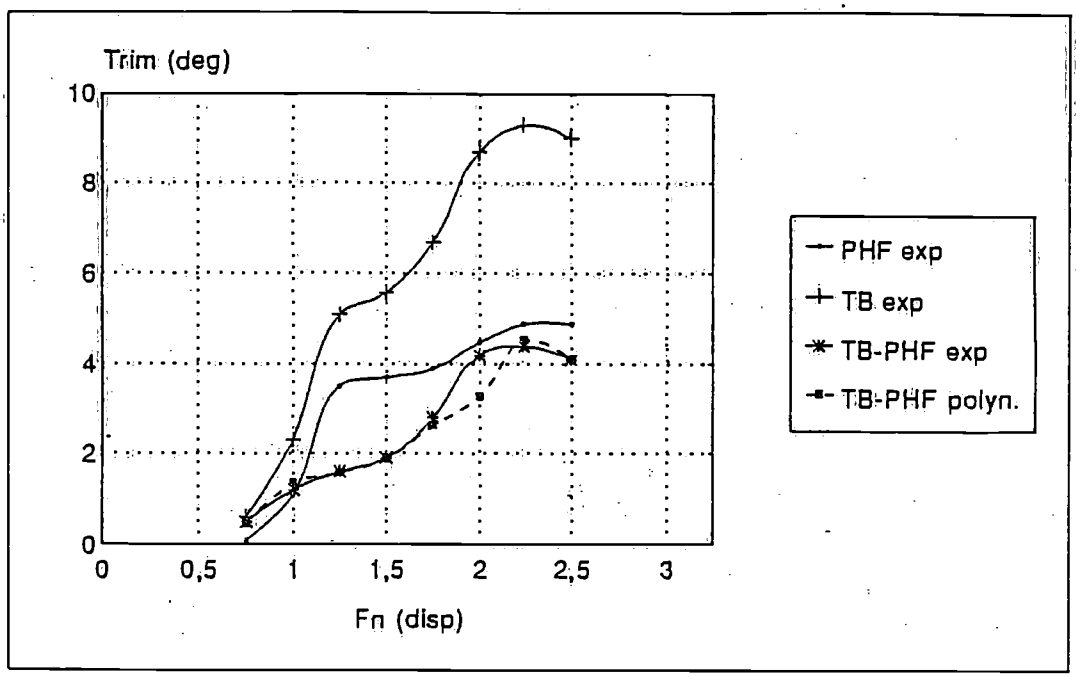

Figure 32: Model 232A-2 Experimental and calculated $\Delta\theta$

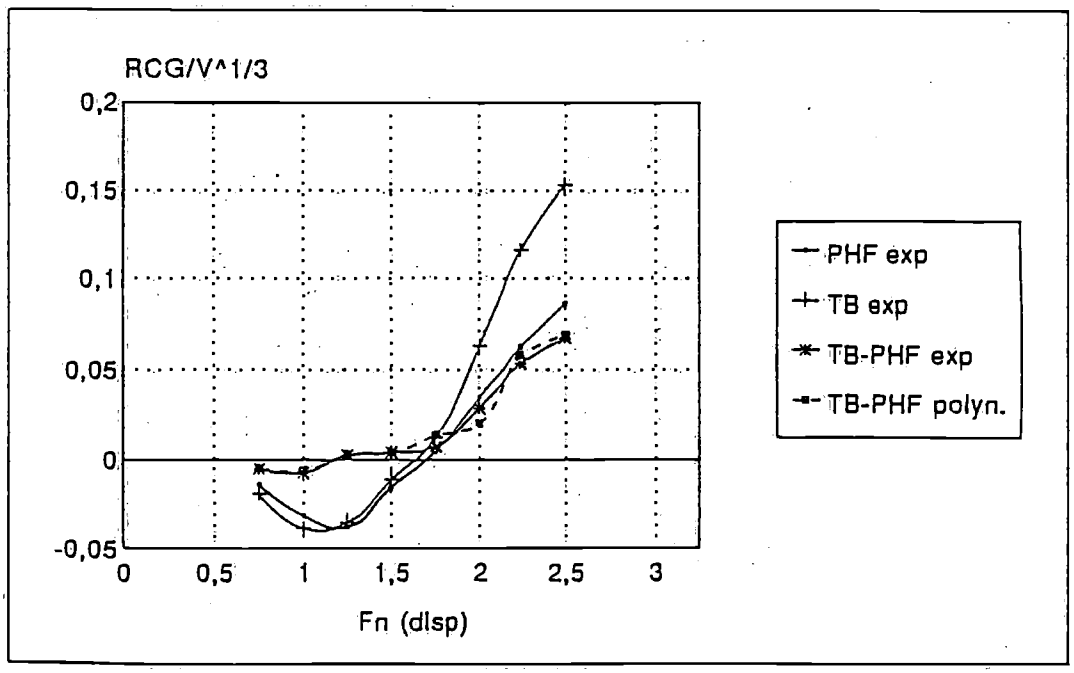

Figure 33: Model 232A-2 Experimental and calculated $\Delta RCG/\nabla^{1/3}$

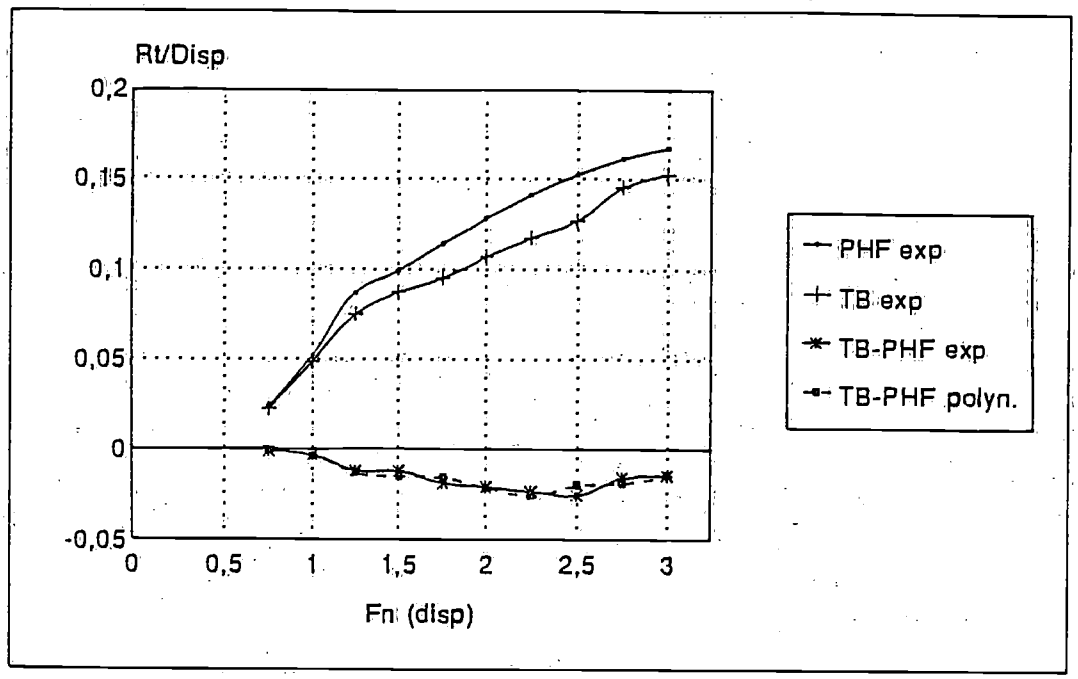

Figure 34: Model 232B-1 Experimental and calculated $\Delta Rt/\Delta$

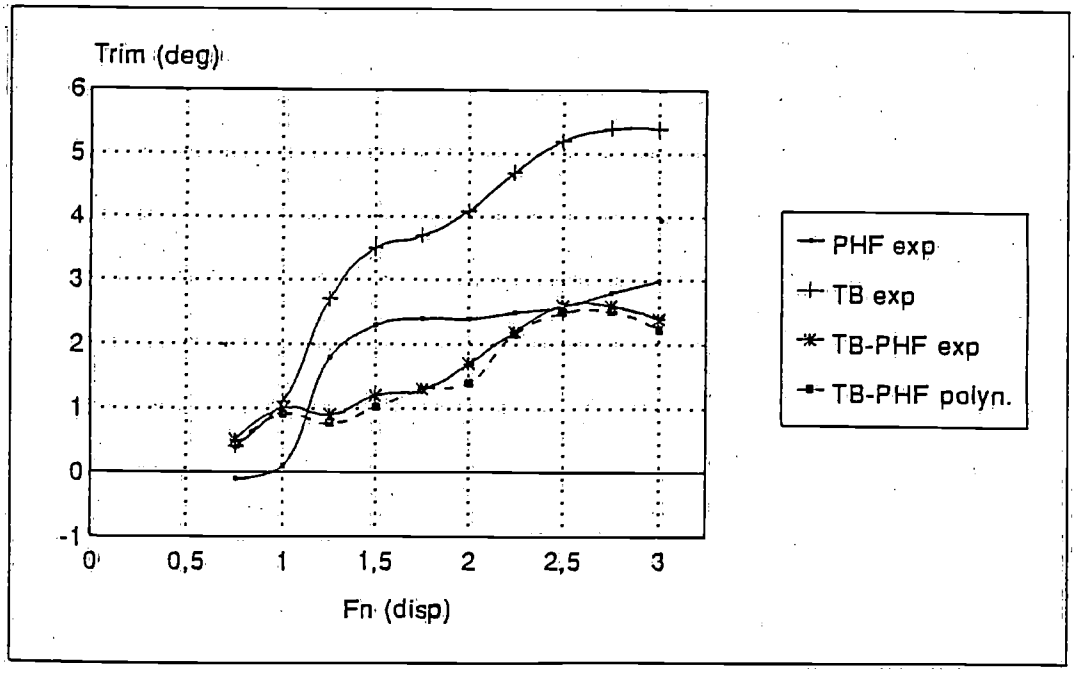

Figure 35: Model 232B-1 Experimental and calculated $\Delta\theta$

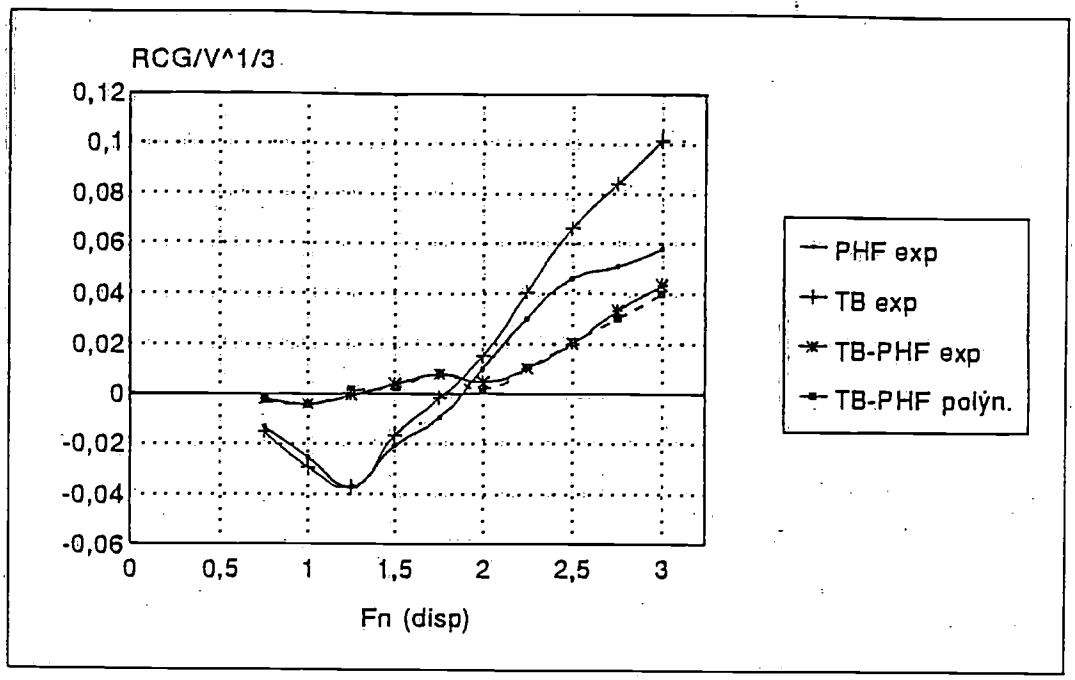

Figure 36: Model 232B-1 Experimental and calculated $\Delta RCG/\nabla^{1/3}$

Appendix 1 :Experimental results 30 degrees deadrise series

model 241

L/B [−]	Depl [N]	LCG [%Lp]	Ap/V [−]
3.41	488.500	0.000	4.00

run	Vm [m/s]	Rtm [N]	Lk [m]	Lc [m]	S [m2]	Trim [deg]	RCG [mm]
794	1.425	18.210	1.25	1.25	0.456	−0.75	−15.0
795	1.900	57.540	1.25	1.25	0.456	3.25	−27.0
796	2.375	105.930	1.25	1.25	0.456	6.90	−20.0
797	2.850	115.140	1.25	1.25	0.456	6.00	−15.0

model 231

L/B [−]	Depl [N]	LCG [%Lp]	Ap/V [−]
3.41	303.100	0.000	5.50

run	Vm [m/s]	Rtm [N]	Lk [m]	Lc [m]	S [m2]	Trim [deg]	RCG [mm]
743	1.333	10.349	1.25	1.25	0.456	−0.85	−10.0
744	1.790	29.053	1.25	1.25	0.456	1.25	−20.0
745	2.193	51.729	1.25	1.25	0.456	5.20	−16.0
746	2.632	54.902	1.25	1.25	0.456	4.32	−8.5

model 240

L/B [−]	Depl [N]	LCG [%Lp]	Ap/V [−]
3.41	488.500	−2.000	4.00

run	Vm [m/s]	Rtm [N]	Lk [m]	Lc [m]	S [m2]	Trim [deg]	RCG [mm]
789	1.425	18.950	1.25	1.25	0.456	−0.35	−14.0
790	1.900	56.200	1.25	1.25	0.456	3.70	−24.0
791	2.375	108.680	1.25	1.25	0.456	7.40	−17.0
792	2.850	115.720	1.25	1.25	0.456	7.20	−12.0
793	3.344	132.050	1.25	1.25	0.456	7.60	−6.5

model 230

L/B [−]	Depl [N]	LCG [%Lp]	Ap/V [−]
3.41	303.100	−2.000	5.50

run	Vm [m/s]	Rtm [N]	Lk [m]	Lc [m]	S [m2]	Trim [deg]	RCG [mm]
747	1.316	10.660	1.25	1.25	0.456	−0.55	−8.5
748	1.755	28.530	1.25	1.25	0.456	1.70	−18.0
749	2.211	53.850	1.25	1.25	0.456	5.60	−13.0
750	2.649	59.370	1.25	1.25	0.456	5.30	−5.5
751	3.070	68.740	0.88	1.16	0.402	6.50	1.0
753	3.527	68.910	0.81	1.16	0.388	8.45	14.5
752	3.948	65.750	0.75	1.16	0.373	8.85	31.0
754	4.404	62.880	0.75	1.16	0.373	8.90	42.5
755	4.842	61.660	0.63	1.16	0.345	8.40	48.0
756	5.264	61.130	0.59	1.16	0.335	8.00	53.5
757	5.702	63.500	0.55	1.16	0.325	7.65	57.0

model 242

L/B [−]	Depl [N]	LCG [%Lp]	Ap/V [−]
3.41	488.500	−4.000	4.00

run	Vm [m/s]	Rtm [N]	Lk [m]	Lc [m]	S [m2]	Trim [deg]	RCG [mm]
784	1.425	19.430	1.25	1.25	0.456	−0.15	−13.0
785	1.900	57.070	1.25	1.25	0.456	4.20	−22.0
786	2.375	110.400	1.25	1.25	0.456	7.90	−15.5
787	2.850	121.930	1.25	1.25	0.456	8.40	−8.0
788	3.325	144.770	1.25	1.25	0.456	13.20	17.0

model 232

L/B [−]	Depl [N]	LCG [%Lp]	Ap/V [−]
3.41	303.100	−4.000	5.50

run	Vm [m/s]	Rtm [N]	Lk [m]	Lc [m]	S [m2]	Trim [deg]	RCG [mm]
758	1.316	10.620	1.25	1.25	0.456	−0.35	−8.5
759	1.772	29.890	1.25	1.25	0.456	2.35	−16.5
760	2.211	56.590	1.19	1.25	0.461	5.95	−11.5
761	2.632	60.480	0.94	1.19	0.421	6.10	−3.5
762	3.070	65.470	0.84	1.16	0.394	7.40	5.5
763	3.527	65.590	0.75	1.16	0.373	9.10	20.5
764	3.983	63.530	0.69	1.16	0.359	9.10	36.5
765	4.386	61.760	0.63	1.13	0.338	8.60	44.5
766	4.825	59.850	0.56	1.09	0.313	8.10	51.5
767	5.264	59.650	0.56	1.09	0.313	7.45	56.5
768	5.702	60.000	0.56	1.09	0.313	6.75	60.0

model 243

L/B [−]	Depl [N]	LCG [%Lp]	Ap/V [−]
3.41	488.500	−8.000	4.00

run	Vm [m/s]	Rtm [N]	Lk [m]	Lc [m]	S [m2]	Trim [deg]	RCG [mm]
780	1.425	21.200	1.25	1.25	0.456	0.85	−12.0
781	1.900	61.860	1.25	1.25	0.456	5.55	−17.0
782	2.375	116.010	0.94	1.19	0.421	9.00	−8.0
783	2.869	139.900	0.88	1.19	0.409	12.10	5.5

model 233

L/B [−]	Depl [N]	LCG [%Lp]	Ap/V [−]
3.41	303.100	−8.000	5.50

run	Vm [m/s]	Rtm [N]	Lk [m]	Lc [m]	S [m2]	Trim [deg]	RCG [mm]
769	1.316	11.640	1.25	1.25	0.456	0.20	−7.5
770	1.755	31.680	1.25	1.25	0.456	3.25	−14.0
771	2.193	61.630	0.91	1.22	0.421	7.00	−10.0
772	2.632	65.030	0.75	1.16	0.373	7.85	1.0
773	3.070	69.950	0.69	1.13	0.352	9.80	14.5
774	3.509	70.390	0.59	0.94	0.289	9.80	29.5
775	3.948	68.800	0.53	0.93	0.273	9.20	44.5
776	4.369	65.140	0.53	0.91	0.269	8.30	54.0
777	4.825	62.010	0.50	0.91	0.262	7.30	60.5
778	5.264	61.520	0.47	0.91	0.255	6.45	64.0
779	5.702	60.280	0.44	0.88	0.243	5.60	67.5

model 221

L/B [-]	Depl [N]	LCG [%Lp]	Ap/V [-]
3.41	210.900	0.000	7.00

run	Vm [m/s]	Rtm [N]	Lk [m]	Lc [m]	S [m2]	Trim [deg]	RCG [mm]
705	1.222	6.280	1.25	1.25	0.456	−0.60	−5.5
706	1.652	17.700	1.25	1.25	0.456	0.10	−14.0
707	2.064	30.870	1.25	1.25	0.456	3.65	−13.5
708	2.477	35.640	1.19	1.25	0.461	3.55	−7.0
709	2.890	42.810	1.13	1.25	0.462	3.40	−5.5
710	3.287	50.400	1.06	1.25	0.456	4.15	0.0
711	3.716	51.730	0.97	1.22	0.433	5.15	9.0
712	4.129	50.390	0.88	1.19	0.409	5.80	18.5
713	4.558	50.020	0.79	1.17	0.384	6.05	23.5
714	4.971	50.140	0.69	1.16	0.359	6.10	29.0
715	5.368	52.000	0.69	1.16	0.359	6.00	33.0
716	5.781	53.700	0.69	1.16	0.359	5.90	36.0

model 211

L/B [-]	Depl [N]	LCG [%Lp]	Ap/V [-]
3.41	157.9	0.0	8.5

run	Vm [m/s]	Rtm [N]	Lk [m]	Lc [m]	S [m2]	Trim [deg]	RCG [mm]
630	1.180	4.572	1.25	1.25	0.456	−0.40	−5.5
631	1.590	12.310	1.25	1.25	0.456	−0.10	−10.2
632	1.999	21.399	1.06	1.25	0.456	2.60	−11.0
633	2.408	25.263	0.97	1.25	0.440	2.75	−6.0
634	2.754	29.413	0.94	1.25	0.434	2.70	−4.5
635	3.148	34.500	0.89	1.22	0.418	2.85	−0.5
636	3.541	38.800	0.83	1.22	0.405	3.30	4.0
637	3.982	41.531	0.78	1.19	0.386	3.50	10.0
638	4.344	42.758	0.72	1.19	0.372	3.60	12.0
639	4.721	43.655	0.69	1.17	0.361	4.10	17.0
640	5.115	44.945	0.63	1.16	0.345	4.25	20.0
641	5.508	46.800	0.57	1.16	0.330	4.30	24.0
642	5.902	48.000	0.50	1.16	0.313	4.40	29.0

model 220

L/B [-]	Depl [N]	LCG [%Lp]	Ap/V [-]
3.41	210.900	−2.000	7.00

run	Vm [m/s]	Rtm [N]	Lk [m]	Lc [m]	S [m2]	Trim [deg]	RCG [mm]
718	1.222	6.670	1.25	1.25	0.456	−0.35	−5.5
719	1.652	17.400	1.25	1.25	0.456	0.55	−13.5
720	2.064	31.730	1.25	1.25	0.456	4.05	−12.0
721	2.477	35.440	1.00	1.25	0.446	4.10	−5.0
722	2.890	40.510	0.88	1.25	0.422	4.30	−1.0
723	3.303	44.020	0.81	1.19	0.393	4.95	6.5
724	3.716	43.480	0.75	1.19	0.379	5.70	15.5
725	4.129	43.420	0.69	1.19	0.365	6.00	22.5
726	4.558	43.480	0.63	1.19	0.351	6.00	28.0
727	4.971	43.850	0.59	1.16	0.335	5.90	32.0
728	5.368	45.800	0.56	1.16	0.327	5.70	36.0
729	5.781	47.600	0.53	1.16	0.320	5.60	40.5

model 210

L/B [-]	Depl [N]	LCG [%Lp]	Ap/V [-]
3.41	157.9	−2.0	8.5

run	Vm [m/s]	Rtm [N]	Lk [m]	Lc [m]	S [m2]	Trim [deg]	RCG [mm]
644	1.180	5.068	1.25	1.25	0.456	−0.25	−5.0
645	1.590	12.055	1.25	1.25	0.456	0.20	−10.0
646	1.967	20.699	1.06	1.25	0.456	2.90	−11.0
647	2.376	23.650	0.94	1.25	0.434	3.10	−4.5
648	2.723	26.716	0.88	1.22	0.415	3.00	−1.8
649	3.148	30.695	0.81	1.19	0.393	3.15	2.0
650	3.541	33.613	0.75	1.19	0.379	3.50	7.0
651	3.935	35.000	0.70	1.17	0.360	3.80	13.0
652	4.359	36.095	0.59	1.16	0.335	4.05	18.0
653	4.769	37.406	0.56	1.16	0.327	4.25	21.0
654	5.115	39.481	0.53	1.16	0.320	4.25	23.0
655	5.508	41.000	0.51	1.16	0.315	4.25	26.5

model 222

L/B [-]	Depl [N]	LCG [%Lp]	Ap/V [-]
3.41	210.900	−4.000	7.00

run	Vm [m/s]	Rtm [N]	Lk [m]	Lc [m]	S [m2]	Trim [deg]	RCG [mm]
730	1.222	6.960	1.25	1.25	0.456	−0.25	−5.5
731	1.652	17.390	1.25	1.25	0.456	1.05	−12.5
733	2.064	31.890	1.06	1.22	0.450	4.40	−11.0
734	2.477	34.330	1.00	1.22	0.439	4.40	−3.5
735	2.890	37.800	0.88	1.19	0.409	4.80	2.0
736	3.303	39.430	0.69	1.19	0.365	5.65	10.0
737	3.716	39.270	0.63	1.19	0.351	6.15	20.5
738	4.129	39.210	0.63	1.19	0.351	6.15	27.0
739	4.558	38.790	0.59	1.16	0.335	6.00	32.0
740	4.971	39.410	0.56	1.16	0.327	5.80	37.0
741	5.368	40.200	0.51	1.16	0.315	5.50	40.5
742	5.781	43.000	0.50	1.16	0.313	5.25	44.0

model 212

L/B [-]	Depl [N]	LCG [%Lp]	Ap/V [-]
3.41	157.9	−4.0	8.5

run	Vm [m/s]	Rtm [N]	Lk [m]	Lc [m]	S [m2]	Trim [deg]	RCG [mm]
666	1.180	5.122	1.25	1.25	0.456	−0.15	−4.0
667	1.590	11.895	1.25	1.25	0.456	0.50	−9.0
668	1.967	20.069	1.00	1.19	0.433	3.05	−10.0
669	2.376	22.606	0.81	1.19	0.393	3.40	−3.5
670	2.723	24.940	0.75	1.19	0.379	3.32	−0.5
671	3.148	27.892	0.69	1.25	0.378	3.60	5.0
679	3.573	29.529	0.66	1.25	0.371	4.00	10.5
672	3.935	30.900	0.63	1.17	0.347	4.20	16.5
673	4.297	31.293	0.59	1.16	0.335	4.25	20.0
674	4.721	32.400	0.56	1.16	0.327	4.30	23.0
675	5.115	33.695	0.50	1.16	0.313	4.25	26.5
676	5.461	35.955	0.47	1.16	0.305	4.15	29.0
677	5.902	38.800	0.45	1.16	0.300	4.00	32.0

model 223

L/B [-]	Depl [N]	LCG [%Lp]	Ap/V [-]
3.41	210.900	−8.000	7.00

run	Vm [m/s]	Rtm [N]	Lk [m]	Lc [m]	S [m2]	Trim [deg]	RCG [mm]
693	1.239	7.500	0.88	1.25	0.422	0.30	−5.0
694	1.652	17.440	0.88	1.25	0.422	1.85	−11.0
695	2.064	32.860	0.88	1.19	0.409	5.10	−9.0
696	2.477	33.880	0.78	1.16	0.380	5.25	0.0
697	2.890	34.950	0.72	1.16	0.368	5.90	7.0
698	3.303	35.650	0.63	1.13	0.338	6.60	17.0
699	3.716	36.400	0.56	1.06	0.307	6.55	26.5
700	4.145	36.750	0.53	1.06	0.300	6.10	34.0
701	4.542	36.700	0.50	1.03	0.286	5.70	39.0
702	4.971	37.240	0.47	1.03	0.279	5.20	42.0
703	5.368	38.400	0.44	1.00	0.266	4.75	45.0
704	5.781	40.000	0.44	1.00	0.266	4.35	49.0

model 213

L/B [-]	Depl [N]	LCG [%Lp]	Ap/V [-]
3.41	157.900	−8.000	8.50

run	Vm [m/s]	Rtm [N]	Lk [m]	Lc [m]	S [m2]	Trim [deg]	RCG [mm]
680	1.180	5.518	0.69	1.25	0.378	0.15	−4.0
681	1.590	12.024	0.69	1.25	0.378	1.20	−8.0
682	1.967	20.722	0.81	1.16	0.388	3.70	−8.7
683	2.345	21.538	0.69	1.16	0.359	3.75	−1.0
684	2.738	22.606	0.66	1.16	0.352	3.90	3.0
685	3.148	23.857	0.63	1.16	0.345	4.30	9.5
686	3.557	25.036	0.58	1.16	0.332	4.50	17.0
687	3.950	25.548	0.52	1.16	0.318	4.45	25.5
688	4.312	26.355	0.47	1.11	0.295	4.25	26.0
689	4.721	27.200	0.44	1.10	0.285	4.10	28.5
690	5.115	28.959	0.41	1.09	0.277	3.80	31.5
691	5.508	31.310	0.39	1.09	0.272	3.50	32.5

model 341

L/B [−]	Depl [N]	LCG [%Lp]	Ap/V [−]
4.09	369.900	0.000	4.00

run	Vm [m/s]	Rtm [N]	Lk [m]	Lc [m]	S [m2]	Trim [deg]	RCG [mm]
138	1.360	11.229	1.50	1.50	0.536	−0.45	−9.0
139	1.814	27.874	1.50	1.50	0.536	0.75	−19.0
140	2.267	52.604	1.50	1.50	0.536	4.30	−18.0
141	2.775	57.931	1.50	1.50	0.536	4.05	−11.0
142	3.174	65.541	1.50	1.50	0.536	3.65	−8.5

model 331

L/B [−]	Depl [N]	LCG [%Lp]	Ap/V [−]
4.09	229.500	0.000	5.50

run	Vm [m/s]	Rtm [N]	Lk [m]	Lc [m]	S [m2]	Trim [deg]	RCG [mm]
126	1.256	6.116	1.28	1.50	0.534	−0.30	−5.5
127	1.692	14.769	1.13	1.50	0.511	−0.05	−11.0
128	2.094	27.300	1.05	1.50	0.496	2.30	−14.0
129	2.546	31.662	1.13	1.46	0.502	2.75	−8.5
130	2.948	37.381	1.13	1.46	0.502	2.84	−5.0
131	3.350	43.515	1.13	0.46	0.502	2.85	−1.4
132	3.769	47.936	1.05	1.46	0.487	3.55	4.0
133	4.188	49.810	1.01	1.46	0.478	4.10	10.0
134	4.606	49.828	0.98	1.43	0.464	4.60	16.5
135	5.075	49.963	0.86	1.43	0.436	5.00	21.0
136	5.444	51.000	0.79	1.43	0.419	5.20	25.5

model 340

L/B [−]	Depl [N]	LCG [%Lp]	Ap/V [−]
4.09	369.900	−2.000	4.00

run	Vm [m/s]	Rtm [N]	Lk [m]	Lc [m]	S [m2]	Trim [deg]	RCG [mm]
171	1.360	11.175	1.50	1.50	0.536	−0.33	−8.0
172	1.814	27.457	1.50	1.50	0.536	1.10	−18.0
173	2.285	54.013	1.50	1.50	0.536	4.40	−16.2
174	2.739	59.712	1.50	1.50	0.536	4.35	−9.5
175	3.156	68.247	1.35	1.43	0.533	4.65	−4.0
176	3.646	75.767	1.20	1.43	0.510	6.05	5.5
178	4.081	75.000	1.09	1.43	0.488	7.65	22.0
177	4.534	72.000	0.94	1.35	0.437	8.00	38.0
179	4.988	71.000	0.88	1.31	0.415	7.80	43.0

model 330

L/B [−]	Depl [N]	LCG [%Lp]	Ap/V [−]
4.09	229.500	−2.000	5.50

run	Vm [m/s]	Rtm [N]	Lk [m]	Lc [m]	S [m2]	Trim [deg]	RCG [mm]
114	1.256	6.373	1.20	1.50	0.525	−0.15	−5.2
115	1.675	14.730	1.16	1.50	0.517	0.25	−10.5
116	2.094	26.300	1.09	1.50	0.503	2.60	−13.0
117	2.529	30.525	1.13	1.43	0.496	2.98	−7.0
118	2.948	35.249	1.13	1.43	0.496	3.10	−3.5
119	3.350	39.483	1.09	1.43	0.488	3.50	2.0
120	3.769	42.411	1.05	1.43	0.480	3.95	8.0
121	4.188	42.927	0.98	1.43	0.464	4.50	14.5
122	4.606	43.225	0.86	1.43	0.436	4.80	19.0
123	5.075	44.624	0.79	1.43	0.419	5.00	24.0
124	5.444	46.200	0.75	1.39	0.401	5.10	29.0

model 342

L/B [−]	Depl [N]	LCG [%Lp]	Ap/V [−]
4.09	369.900	−4.000	4.00

run	Vm [m/s]	Rtm [N]	Lk [m]	Lc [m]	S [m2]	Trim [deg]	RCG [mm]
160	1.360	11.282	1.50	1.50	0.536	−0.15	−7.5
161	1.814	27.254	1.50	1.50	0.536	1.35	−16.5
162	2.267	55.000	1.43	1.50	0.535	4.80	−13.5
163	2.775	61.816	1.28	1.50	0.534	4.95	−6.5
164	3.192	66.974	1.13	1.43	0.496	5.50	0.0
165	3.664	71.485	1.09	1.35	0.470	7.00	12.0
166	4.081	73.000	0.98	1.35	0.447	8.05	26.5
167	4.607	69.549	0.90	1.31	0.420	8.00	38.0
168	5.006	70.247	0.79	1.20	0.370	7.75	46.0
169	5.568	71.693	0.79	1.20	0.370	7.40	54.0

model 332

L/B [−]	Depl [N]	LCG [%Lp]	Ap/V [−]
4.09	229.500	−4.000	5.50

run	Vm [m/s]	Rtm [N]	Lk [m]	Lc [m]	S [m2]	Trim [deg]	RCG [mm]
102	1.256	6.646	1.31	1.50	0.539	0.00	−4.8
103	1.692	15.124	1.28	1.50	0.534	0.55	−9.8
104	2.094	26.587	1.20	1.50	0.525	2.88	−12.5
105	2.529	29.507	1.16	1.46	0.508	3.18	−5.5
106	2.948	33.353	1.13	1.46	0.502	3.40	−1.5
107	3.350	36.583	1.01	1.43	0.471	3.70	4.0
108	3.769	38.206	0.98	1.43	0.464	4.25	11.0
109	4.238	39.049	0.86	1.43	0.436	4.75	18.0
110	4.623	40.162	0.79	1.39	0.410	5.00	22.5
111	5.075	41.870	0.71	1.35	0.382	5.00	27.0
112	5.444	43.700	0.71	1.35	0.382	5.00	30.5
113	5.863	44.250	0.71	1.33	0.378	5.05	32.5

model 343

L/B [−]	Depl [N]	LCG [%Lp]	Ap/V [−]
4.09	369.900	−8.000	4.00

run	Vm [m/s]	Rtm [N]	Lk [m]	Lc [m]	S [m2]	Trim [deg]	RCG [mm]
144	1.360	12.445	1.50	1.50	0.536	0.32	−7.5
145	1.868	33.331	1.35	1.50	0.530	2.80	−15.5
146	2.285	61.430	1.20	1.50	0.525	5.70	−13.0
147	2.721	64.671	1.09	1.43	0.488	6.20	−5.0
148	3.192	70.978	1.01	1.38	0.460	7.55	6.0
149	3.700	77.471	0.90	1.28	0.413	8.80	22.0
150	4.045	77.858	0.75	1.24	0.369	8.65	34.5
151	4.571	77.305	0.75	1.24	0.369	8.10	46.5
153	4.988	76.000	0.71	1.20	0.351	7.55	56.0
154	5.441	75.000	0.71	1.20	0.351	6.90	63.0

model 333

L/B [−]	Depl [N]	LCG [%Lp]	Ap/V [−]
4.09	229.500	−8.000	5.50

run	Vm [m/s]	Rtm [N]	Lk [m]	Lc [m]	S [m2]	Trim [deg]	RCG [mm]
88	1.256	6.886	1.13	1.50	0.511	0.15	−4.5
89	1.675	14.810	1.13	1.50	0.511	1.00	−9.0
90	2.094	27.632	1.09	1.43	0.488	3.40	−11.2
91	2.513	29.900	1.05	1.43	0.480	3.75	−4.5
92	2.948	31.891	0.98	1.43	0.464	4.00	1.5
93	3.367	34.066	0.86	1.43	0.436	4.55	8.5
94	3.786	36.053	0.83	1.39	0.420	5.10	16.3
95	4.204	37.819	0.75	1.35	0.392	5.20	23.0
96	4.640	39.316	0.71	1.35	0.382	5.15	28.0
97	5.059	40.452	0.68	1.35	0.374	5.05	32.5
101	5.444	42.000	0.66	1.35	0.369	4.90	38.5
98	5.863	44.400	0.64	1.31	0.356	4.80	41.5

model 321

L/B [−]	Depl [N]	LCG [%Lp]	Ap/V [−]
4.09	159.600	0.000	7.00

run	Vm [m/s]	Rtm [N]	Lk [m]	Lc [m]	S [m2]	Trim [deg]	RCG [mm]
44	1.183	3.997	1.13	1.50	0.511	−0.18	−4.0
45	1.577	9.937	1.13	1.50	0.511	−0.16	−7.0
46	1.987	16.177	1.13	1.50	0.511	1.55	−10.5
47	2.365	19.238	1.13	1.46	0.502	2.10	−7.5
48	2.775	23.308	1.05	1.46	0.487	2.20	−4.5
49	3.170	27.675	1.05	1.46	0.487	2.25	−2.0
50	3.580	32.426	1.01	1.46	0.478	2.25	2.0
51	3.974	36.939	0.94	1.46	0.461	2.46	4.9
52	4.384	40.499	0.94	1.44	0.457	2.70	6.0
53	4.794	42.553	0.90	1.44	0.448	3.05	8.0
184	5.125	43.000	0.83	1.43	0.429	3.35	10.5
186	5.519	44.300	0.75	1.43	0.409	3.70	16.0

model 311

L/B [−]	Depl [N]	LCG [%Lp]	Ap/V [−]
4.09	119.500	0.000	8.50

run	Vm [m/s]	Rtm [N]	Lk [m]	Lc [m]	S [m2]	Trim [deg]	RCG [mm]
3	1.127	2.799	0.98	1.46	0.471	−0.15	−2.9
4	1.517	6.359	0.98	1.46	0.471	−0.28	−5.4
5	1.878	10.243	0.98	1.46	0.471	0.75	−6.8
6	2.254	12.708	0.98	1.46	0.471	1.55	−0.7
9	2.629	15.612	0.98	1.46	0.471	1.80	−5.5
8	3.020	19.113	0.94	1.46	0.461	1.75	−3.0
1	3.380	22.429	0.98	1.46	0.471	1.79	−1.0
2	3.771	26.869	0.98	1.46	0.471	1.70	1.8
7	4.132	29.843	0.98	1.46	0.471	1.75	2.3
10	4.507	35.252	0.94	1.46	0.461	1.85	1.5
200	4.883	38.250	0.75	1.43	0.409	2.10	2.5
183	5.258	40.750	0.68	1.39	0.382	2.50	6.0
182	5.634	42.500	0.62	1.39	0.362	2.85	9.0

model 320

L/B [−]	Depl [N]	LCG [%Lp]	Ap/V [−]
4.09	159.600	−2.000	7.00

run	Vm [m/s]	Rtm [N]	Lk [m]	Lc [m]	S [m2]	Trim [deg]	RCG [mm]
54	1.183	4.217	1.05	1.50	0.498	−0.15	−3.8
55	1.577	9.390	1.05	1.50	0.496	0.00	−7.0
56	1.971	15.649	1.05	1.50	0.496	1.65	−10.5
57	2.365	18.153	1.05	1.46	0.487	2.12	−7.2
58	2.775	21.457	1.05	1.46	0.487	2.20	−4.2
59	3.154	25.110	1.01	1.46	0.478	2.30	−5.0
60	3.564	28.957	0.94	1.46	0.461	2.40	3.5
61	3.958	32.153	0.86	1.44	0.438	2.52	7.0
62	4.337	34.500	0.79	1.44	0.421	2.85	8.5
63	4.731	36.300	0.79	1.44	0.421	3.20	10.5
187	5.125	38.200	0.71	1.35	0.382	3.50	13.0
188	5.519	39.400	0.64	1.35	0.384	3.75	18.0

model 310

L/B [−]	Depl [N]	LCG [%Lp]	Ap/V [−]
4.09	119.500	−2.000	8.50

run	Vm [m/s]	Rtm [N]	Lk [m]	Lc [m]	S [m2]	Trim [deg]	RCG [mm]
11	1.127	2.923	1.05	1.46	0.487	−0.08	−3.0
12	1.502	6.270	1.05	1.46	0.487	−0.01	−5.0
13	1.878	10.006	1.05	1.46	0.487	0.88	−8.0
14	2.269	12.790	1.05	1.46	0.487	1.75	−6.0
15	2.644	15.989	1.05	1.46	0.487	1.73	−4.3
16	3.035	17.867	1.01	1.46	0.478	1.88	−1.5
17	3.410	20.847	0.98	1.46	0.471	1.90	1.4
18	3.771	23.972	0.94	1.46	0.461	1.92	4.0
19	4.132	27.300	0.90	1.46	0.452	1.95	5.0
20	4.492	30.802	0.86	1.46	0.442	2.06	4.5
190	4.883	33.200	0.64	1.31	0.356	2.25	5.5
191	5.258	34.600	0.60	1.31	0.349	2.60	9.0
192	5.634	36.676	0.60	1.35	0.354	2.95	11.0

model 322

L/B [−]	Depl [N]	LCG [%Lp]	Ap/V [−]
4.09	159.600	−4.000	7.00

run	Vm [m/s]	Rtm [N]	Lk [m]	Lc [m]	S [m2]	Trim [deg]	RCG [mm]
64	1.183	4.381	0.98	1.50	0.480	0.00	−3.4
65	1.593	9.125	0.98	1.50	0.480	0.18	−6.1
66	1.987	15.494	0.98	1.50	0.480	1.85	−9.5
67	2.365	17.828	0.98	1.46	0.471	2.30	−6.5
68	2.760	20.461	0.94	1.46	0.461	2.35	−3.0
69	3.170	23.557	0.90	1.46	0.452	2.50	1.6
70	3.564	26.283	0.83	1.46	0.435	2.60	5.0
71	3.942	28.515	0.79	1.46	0.425	2.75	9.0
72	4.352	30.522	0.75	1.43	0.409	3.10	11.0
73	4.778	31.984	0.71	1.43	0.399	3.45	14.0
197	5.125	33.200	0.56	1.37	0.347	3.65	17.0
196	5.519	35.700	0.56	1.35	0.343	3.70	20.0

model 312

L/B [−]	Depl [N]	LCG [%Lp]	Ap/V [−]
4.09	119.500	−4.000	8.50

run	Vm [m/s]	Rtm [N]	Lk [m]	Lc [m]	S [m2]	Trim [deg]	RCG [mm]
21	1.127	3.043	1.05	1.46	0.487	0.00	−2.5
22	1.502	6.124	1.05	1.46	0.487	0.00	−4.5
23	1.878	9.837	1.05	1.46	0.487	0.98	−8.0
24	2.254	12.250	1.05	1.46	0.487	1.74	−6.0
25	2.629	14.378	1.05	1.46	0.487	1.80	−3.0
26	3.005	16.821	1.05	1.46	0.487	1.93	−1.0
27	3.380	19.286	0.90	1.46	0.452	2.00	2.2
29	3.756	21.955	0.77	1.46	0.420	2.00	5.8
28	4.132	24.800	0.79	1.46	0.425	2.00	6.0
30	4.522	27.388	0.75	1.46	0.415	2.25	7.0
31	4.883	29.800	0.75	1.46	0.415	2.50	8.5
193	5.258	31.400	0.54	1.35	0.338	2.80	10.5
195	5.634	32.200	0.53	1.31	0.327	2.90	13.0

model 323

L/B [−]	Depl [N]	LCG [%Lp]	Ap/V [−]
4.09	159.600	−8.000	7.00

run	Vm [m/s]	Rtm [N]	Lk [m]	Lc [m]	S [m2]	Trim [deg]	RCG [mm]
74	1.183	4.550	0.98	1.46	0.471	0.17	−2.8
75	1.577	9.210	0.90	1.46	0.452	0.60	−5.5
76	1.987	15.867	0.75	1.46	0.416	2.25	−9.5
77	2.365	17.842	0.75	1.46	0.416	2.62	−5.5
78	2.760	19.498	0.75	1.43	0.409	2.75	−1.5
79	3.170	21.328	0.79	1.43	0.419	2.85	4.0
80	3.564	22.933	0.79	1.43	0.419	3.05	9.0
81	3.942	24.404	0.79	1.39	0.410	3.30	13.0
82	4.368	26.373	0.68	1.39	0.382	3.50	16.5
83	4.810	30.220	0.64	1.39	0.372	3.55	19.0
84	5.125	32.200	0.60	1.35	0.354	3.55	21.0
86	5.519	34.000	0.56	1.35	0.338	3.55	24.0
87	5.914	35.700	0.53	1.28	0.323	3.60	28.0

model 313

L/B [−]	Depl [N]	LCG [%Lp]	Ap/V [−]
4.09	119.500	−8.000	8.50

run	Vm [m/s]	Rtm [N]	Lk [m]	Lc [m]	S [m2]	Trim [deg]	RCG [mm]
32	1.127	3.213	0.90	1.43	0.446	0.14	−2.5
33	1.502	6.300	0.83	1.43	0.429	0.31	−5.0
34	1.878	10.284	0.83	1.43	0.429	1.40	−7.5
35	2.254	12.099	0.83	1.43	0.429	1.98	−5.0
36	2.644	13.714	0.79	1.43	0.419	2.05	−2.5
37	3.020	15.382	0.75	1.43	0.409	2.10	1.0
38	3.380	17.145	0.68	1.43	0.391	2.20	5.4
39	3.756	18.784	0.60	1.43	0.370	2.20	8.2
40	4.102	20.639	0.56	1.43	0.359	2.38	10.0
41	4.522	22.823	0.53	1.43	0.340	2.60	11.3
42	4.883	25.200	0.53	1.31	0.327	2.75	12.5
199	5.258	27.320	0.49	1.35	0.347	2.70	16.0
198	5.634	30.300	0.49	1.31	0.317	2.75	18.0

model 441

L/B [−]	Depl [N]	LCG [%Lp]	Ap/V [−]
5.5	237.400	0.000	4.00

run	Vm [m/s]	Rtm [N]	Lk [m]	Lc [m]	S [m2]	Trim [deg]	RCG [mm]
380	1.263	5.972	1.50	1.50	0.400	−0.20	−5.0
381	1.684	12.800	1.50	1.50	0.400	0.70	−11.0
382	2.089	24.520	1.50	1.50	0.400	2.43	−13.0
383	2.527	27.856	1.50	1.50	0.400	2.85	−10.0
384	2.948	31.629	1.50	1.50	0.400	2.63	−6.0
385	3.369	36.923	1.50	1.50	0.400	2.15	−4.5
386	3.790	43.796	1.50	1.50	0.400	1.70	−6.0

model 431

L/B [−]	Depl [N]	LCG [%Lp]	Ap/V [−]
5.5	147.300	0.000	5.50

run	Vm [m/s]	Rtm [N]	Lk [m]	Lc [m]	S [m2]	Trim [deg]	RCG [mm]
314	1.151	3.228	1.50	1.50	0.389	−0.12	−3.5
315	1.556	7.155	1.50	1.50	0.389	−0.20	−6.5
316	1.945	12.144	1.50	1.50	0.394	1.20	−10.0
317	2.349	15.085	1.50	1.50	0.400	1.95	−6.5
318	2.738	17.479	1.50	1.50	0.400	1.95	−4.5

model 440

L/B [−]	Depl [N]	LCG [%Lp]	Ap/V [−]
5.5	237.400	−2.000	4.00

run	Vm [m/s]	Rtm [N]	Lk [m]	Lc [m]	S [m2]	Trim [deg]	RCG [mm]
387	1.263	6.075	1.50	1.50	0.400	−0.10	−6.0
388	1.684	13.410	1.50	1.50	0.400	0.45	−10.0
389	2.106	24.453	1.50	1.50	0.400	2.65	−12.5
390	2.527	28.368	1.43	1.50	0.400	3.20	−9.0
391	2.948	32.604	1.43	1.46	0.398	3.20	−4.0
392	3.369	37.158	1.43	1.46	0.398	3.00	0.0
393	3.790	43.527	1.43	1.46	0.398	2.65	2.0
394	4.211	49.860	1.50	1.50	0.400	2.60	5.0
395	4.616	58.412	1.50	1.50	0.400	2.40	0.0

model 442

L/B [−]	Depl [N]	LCG [%Lp]	Ap/V [−]
5.5	237.400	−4.000	4.00

run	Vm [m/s]	Rtm [N]	Lk [m]	Lc [m]	S [m2]	Trim [deg]	RCG [mm]
396	1.247	6.220	1.50	1.50	0.400	0.00	−4.0
397	1.668	13.357	1.50	1.50	0.400	0.60	−10.0
398	2.106	25.733	1.50	1.50	0.400	2.90	−11.5
399	2.510	29.209	1.39	1.44	0.398	3.40	−8.0
400	2.914	32.536	1.35	1.43	0.393	3.35	−3.5
401	3.369	36.414	1.31	1.43	0.390	3.45	1.0
402	3.807	40.832	1.24	1.43	0.383	3.90	6.0
403	4.228	42.301	1.13	1.39	0.362	4.70	11.0
404	4.649	43.440	1.01	1.33	0.337	5.75	16.0
405	5.053	42.047	0.94	1.29	0.319	5.85	23.0
406	5.475	42.191	0.90	1.28	0.310	5.70	34.0

model 432

L/B [−]	Depl [N]	LCG [%Lp]	Ap/V [−]
5.5	147.300	−4.000	5.50

run	Vm [m/s]	Rtm [N]	Lk [m]	Lc [m]	S [m2]	Trim [deg]	RCG [mm]
338	1.167	3.474	1.50	1.50	0.400	0.00	−3.8
339	1.556	7.558	1.50	1.50	0.400	0.30	−6.5
340	1.945	12.938	1.35	1.43	0.393	1.75	−8.2
341	2.349	15.045	1.24	1.43	0.383	2.31	−4.1
342	2.738	16.803	1.16	1.41	0.370	2.25	−2.0
343	3.142	19.228	1.13	1.39	0.362	2.36	1.0
344	3.516	21.416	1.09	1.39	0.357	2.45	5.0
345	3.920	23.514	1.05	1.39	0.353	2.60	8.5
346	4.278	25.000	0.98	1.37	0.338	2.75	9.5
347	4.667	26.364	0.96	1.37	0.334	3.13	10.5
348	5.056	27.420	0.94	1.37	0.331	3.25	13.2
350	5.445	29.000	0.86	1.35	0.315	3.35	15.0
351	5.834	31.700	0.83	1.35	0.308	3.80	16.5

model 443

L/B [−]	Depl [N]	LCG [%Lp]	Ap/V [−]
5.5	237.400	−8.000	4.00

run	Vm [m/s]	Rtm [N]	Lk [m]	Lc [m]	S [m2]	Trim [deg]	RCG [mm]
368	1.247	6.209	1.50	1.50	0.400	0.20	−4.0
369	1.684	14.453	1.43	1.46	0.398	1.20	−9.0
370	2.106	25.320	1.28	1.43	0.388	3.15	−11.0
371	2.510	26.628	1.24	1.37	0.375	3.45	−6.0
372	2.948	29.118	1.18	1.39	0.370	3.60	−2.0
373	3.369	30.740	1.13	1.37	0.359	3.80	4.0
374	3.807	30.934	1.11	1.33	0.350	4.30	9.0
375	4.228	29.999	0.99	1.31	0.332	4.70	15.0
376	4.649	27.326	0.88	1.22	0.297	5.25	20.0
377	5.037	28.423	0.83	1.20	0.284	5.25	26.0
378	5.475	31.300	0.79	1.18	0.274	5.10	31.5
379	5.896	35.500	0.77	1.14	0.265	4.80	38.5

model 433

L/B [−]	Depl [N]	LCG [%Lp]	Ap/V [−]
5.5	147.300	−8.000	5.50

run	Vm [m/s]	Rtm [N]	Lk [m]	Lc [m]	S [m2]	Trim [deg]	RCG [mm]
352	1.167	3.550	1.50	1.50	0.400	0.00	−2.5
353	1.556	7.799	1.35	1.46	0.398	0.20	−6.0
354	1.945	13.354	1.20	1.43	0.378	1.90	−9.5
355	2.349	15.197	1.13	1.39	0.362	2.50	−5.0
356	2.738	16.815	1.05	1.39	0.353	2.53	−2.0
357	3.158	18.655	1.01	1.37	0.344	2.60	1.0
359	3.516	20.033	0.94	1.37	0.331	2.60	5.0
360	3.869	21.567	0.92	1.37	0.328	2.80	8.0
361	4.294	22.719	0.86	1.35	0.315	3.25	11.0
362	4.683	23.959	0.83	1.33	0.304	3.40	14.0
363	5.040	25.407	0.79	1.31	0.295	3.40	16.0
366	5.445	27.000	0.75	1.31	0.289	3.35	19.5
367	5.834	29.000	0.69	1.29	0.276	3.20	25.0

model 421

L/B [-]	Depl [N]	LCG [%Lp]	Ap/V [-]
5.5	102.600	0.000	7.00

run	Vm [m/s]	Rtm [N]	Lk [m]	Lc [m]	S [m2]	Trim [deg]	RCG [mm]
287	1.084	2.156	1.50	1.50	0.383	-0.10	-2.5
288	1.465	4.759	1.50	1.50	0.380	-0.13	-4.0
289	1.831	7.539	1.50	1.50	0.380	0.60	-6.5
290	2.197	9.744	1.35	1.50	0.394	1.30	-5.5
291	2.563	11.654	1.20	1.46	0.378	1.35	-4.6
292	2.929	14.043	1.16	1.46	0.378	1.42	-2.5
293	3.281	16.777	1.13	1.43	0.369	1.42	0.0
294	3.676	19.843	1.09	1.43	0.364	1.40	1.0
295	4.043	23.126	1.05	1.43	0.359	1.35	1.5
296	4.336	26.609	1.01	1.43	0.352	1.35	0.0
297	4.775	30.032	0.98	1.43	0.347	1.50	-1.0
298	5.126	33.200	0.94	1.43	0.341	1.60	-0.5
299	5.493	36.000	0.90	1.43	0.334	1.75	1.0

model 411

L/B [-]	Depl [N]	LCG [%Lp]	Ap/V [-]
5.5	76.600	0.000	8.50

run	Vm [m/s]	Rtm [N]	Lk [m]	Lc [m]	S [m2]	Trim [deg]	RCG [mm]
201	1.046	1.607	1.35	1.50	0.357	-0.10	-1.8
202	1.395	3.371	1.28	1.50	0.343	-0.08	-3.0
203	1.758	5.035	1.20	1.50	0.340	0.25	-4.3
204	2.107	6.816	1.20	1.50	0.340	0.95	-4.8
205	2.455	7.999	1.05	1.50	0.331	0.95	-3.5
206	2.804	9.723	0.98	1.43	0.319	0.95	-3.0
207	3.139	12.000	0.98	1.43	0.319	1.00	-2.5
208	3.486	14.008	0.98	1.43	0.333	1.05	0.0
209	3.836	16.619	0.98	1.43	0.339	1.00	2.5
210	4.213	20.582	0.98	1.43	0.347	0.90	3.0
211	4.534	23.000	0.98	1.43	0.347	0.90	-1.0
212	4.883	26.300	0.98	1.43	0.347	0.65	-2.0
213	5.231	31.200	0.98	1.43	0.347	0.90	-2.0
214	5.580	35.200	0.98	1.43	0.347	0.90	-2.2

model 420

L/B [-]	Depl [N]	LCG [%Lp]	Ap/V [-]
5.5	102.600	-2.000	7.00

run	Vm [m/s]	Rtm [N]	Lk [m]	Lc [m]	S [m2]	Trim [deg]	RCG [mm]
300	1.099	2.272	1.50	1.50	0.380	-0.05	-3.0
301	1.450	4.725	1.50	1.50	0.377	-0.02	-4.3
302	1.831	7.554	1.43	1.50	0.380	0.72	-6.5
303	2.197	9.546	1.43	1.50	0.389	1.40	-5.0
304	2.563	11.104	1.35	1.46	0.392	1.45	-4.0
306	2.929	13.040	1.28	1.46	0.393	1.52	-2.5
307	3.296	15.557	1.16	1.46	0.378	1.52	0.0
308	3.662	18.066	1.05	1.43	0.359	1.50	3.5
309	4.043	20.633	0.98	1.43	0.347	1.45	4.0
310	4.423	23.491	0.90	1.43	0.334	1.50	3.0
311	4.760	26.207	0.86	1.43	0.326	1.65	2.5
312	5.126	29.400	0.83	1.43	0.320	1.70	2.5
312	5.493	30.826	0.80	1.43	0.317	1.80	4.0
313	5.873	34.251	0.79	1.43	0.313	1.95	7.0

model 410

L/B [-]	Depl [N]	LCG [%Lp]	Ap/V [-]
5.5	76.600	-2.000	8.50

run	Vm [m/s]	Rtm [N]	Lk [m]	Lc [m]	S [m2]	Trim [deg]	RCG [mm]
215	1.046	1.835	1.35	1.50	0.357	-0.05	-1.4
216	1.395	3.300	1.24	1.46	0.346	-0.05	-2.7
217	1.744	5.442	1.20	1.46	0.350	0.20	-4.5
219	2.093	6.700	1.05	1.44	0.338	1.00	-4.8
220	2.427	7.683	0.98	1.43	0.330	1.00	-3.0
221	2.804	9.416	0.94	1.43	0.327	1.05	-2.6
222	3.139	11.282	0.94	1.43	0.330	1.10	-1.5
223	3.502	13.348	0.94	1.43	0.333	1.10	-1.5
224	3.850	15.664	0.94	1.43	0.341	1.00	2.5
225	4.199	18.407	0.94	1.43	0.341	0.95	2.0
226	4.548	21.519	0.90	1.43	0.334	0.80	0.0
227	4.697	24.665	0.83	1.43	0.320	0.80	-1.0
0	0.000	0.000	0.00	0.00	0.000	0.00	0.0
228	5.580	31.400	0.79	1.43	0.313	0.85	0.0

model 422

L/B [-]	Depl [N]	LCG [%Lp]	Ap/V [-]
5.5	102.600	-4.000	7.00

run	Vm [m/s]	Rtm [N]	Lk [m]	Lc [m]	S [m2]	Trim [deg]	RCG [mm]
274	1.084	2.340	1.35	1.50	0.388	0.00	-2.0
275	1.465	4.767	1.43	1.50	0.386	0.10	-3.5
276	1.831	7.503	1.35	1.50	0.394	0.90	-6.0
273	2.197	9.400	1.35	1.50	0.382	1.25	-6.0
277	2.563	10.400	1.28	1.43	0.383	1.50	-3.5
278	2.929	12.559	1.05	1.43	0.559	1.60	-1.5
279	3.296	14.650	1.01	1.43	0.352	1.65	1.5
280	3.662	16.800	1.01	1.43	0.352	1.60	4.5
281	4.043	18.914	0.98	1.43	0.347	1.60	5.0
282	4.423	21.594	0.96	1.43	0.344	1.60	4.0
283	4.760	23.800	0.94	1.43	0.341	1.70	4.0
286	5.126	26.317	0.90	1.43	0.334	1.85	5.0
284	5.493	28.800	0.86	1.43	0.326	2.00	6.5
285	5.859	31.000	0.79	1.41	0.310	2.10	10.5

model 412

L/B [-]	Depl [N]	LCG [%Lp]	Ap/V [-]
5.5	76.600	-4.000	8.50

run	Vm [m/s]	Rtm [N]	Lk [m]	Lc [m]	S [m2]	Trim [deg]	RCG [mm]
230	1.046	1.711	1.35	1.50	0.354	-0.05	-1.5
231	1.381	3.371	1.31	1.50	0.366	0.05	-2.5
232	1.744	4.890	1.28	1.50	0.371	0.05	-4.2
233	2.093	6.546	1.20	1.43	0.359	1.05	-5.0
234	2.441	7.488	1.13	1.43	0.355	1.05	-2.5
235	2.804	9.059	1.13	1.43	0.358	1.05	-2.5
236	3.153	10.750	1.05	1.43	0.359	1.10	0.0
237	3.516	12.629	0.98	1.43	0.347	1.10	2.2
238	3.864	14.592	0.98	1.43	0.347	1.05	4.5
239	4.213	17.114	0.98	1.43	0.347	0.95	3.5
240	4.562	19.852	0.98	1.43	0.347	0.90	1.5
241	4.883	22.600	0.98	1.43	0.347	0.90	0.5
243	5.231	25.200	0.90	1.43	0.334	1.00	1.5
242	5.580	28.000	0.90	1.43	0.334	1.05	2.5
244	5.929	30.600	0.90	1.43	0.334	1.10	3.5

model 423

L/B [-]	Depl [N]	LCG [%Lp]	Ap/V [-]
5.5	102.600	-8.000	7.00

run	Vm [m/s]	Rtm [N]	Lk [m]	Lc [m]	S [m2]	Trim [deg]	RCG [mm]
259	1.084	2.414	1.35	1.50	0.374	0.10	-2.5
260	1.450	4.774	1.28	1.50	0.377	0.28	-5.0
261	1.831	7.804	1.16	1.43	0.353	1.20	-7.0
262	2.197	9.461	1.05	1.43	0.353	1.70	-5.0
263	2.563	10.535	0.98	1.43	0.347	1.75	-3.0
264	2.915	11.961	0.90	1.43	0.334	1.80	0.0
265	3.310	13.564	0.83	1.43	0.320	1.80	2.5
266	3.676	15.177	0.79	1.41	0.310	1.80	6.0
267	4.028	16.805	0.75	1.39	0.301	1.75	7.0
268	4.394	18.500	0.75	1.35	0.295	1.90	7.0
269	4.760	20.330	0.75	1.35	0.295	2.00	7.0
270	5.126	22.000	0.68	1.35	0.281	2.05	9.5
272	5.493	24.000	0.64	1.35	0.273	2.15	11.0
271	5.859	25.800	0.64	1.35	0.273	2.20	13.0

model 413

L/B [-]	Depl [N]	LCG [%Lp]	Ap/V [-]
5.5	76.600	-8.000	8.50

run	Vm [m/s]	Rtm [N]	Lk [m]	Lc [m]	S [m2]	Trim [deg]	RCG [mm]
245	1.046	1.847	1.35	1.50	0.354	0.05	-1.5
246	1.395	3.563	1.35	1.50	0.360	0.20	-2.5
247	1.744	5.254	1.20	1.43	0.362	0.70	-5.0
249	2.107	6.587	1.13	1.43	0.352	1.20	-4.5
250	2.441	7.517	0.98	1.43	0.336	1.25	-2.0
248	2.790	8.719	0.98	1.43	0.336	1.25	-1.0
251	3.139	9.981	0.43	1.43	0.320	1.30	1.0
252	3.486	11.515	0.71	1.43	0.300	1.21	3.5
253	3.836	13.118	0.71	1.41	0.300	1.10	5.5
254	4.213	15.049	0.71	1.41	0.296	1.05	5.5
256	4.534	17.000	0.68	1.43	0.291	1.05	4.5
255	4.883	19.000	0.68	1.41	0.291	1.05	5.0
257	5.231	21.300	0.68	1.41	0.291	1.10	6.0
258	5.580	23.500	0.68	1.41	0.291	1.20	7.5

model 541

L/B [-]	Depl [N]	LCG [%Lp]	Ap/V [-]
7	165.200	0.000	4.00

run	Vm [m/s]	Rtm [N]	Lk [m]	Lc [m]	S [m2]	Trim [deg]	RCG [mm]
596	1.173	3.484	1.50	1.50	0.324	-0.05	-4.0
597	1.570	7.558	1.50	1.50	0.324	0.00	-7.0
598	1.966	13.169	1.50	1.50	0.324	1.40	-10.0
599	2.363	16.603	1.50	1.50	0.324	2.30	-6.0
600	2.759	18.964	1.50	1.50	0.324	2.40	-5.0
601	3.045	20.753	1.50	1.50	0.324	2.35	-4.0
602	3.568	25.110	1.50	1.50	0.324	2.15	0.0
603	3.980	29.310	1.50	1.50	0.324	1.80	0.0

model 531

L/B [-]	Depl [N]	LCG [%Lp]	Ap/V [-]
7	102.400	0.000	5.50

run	Vm [m/s]	Rtm [N]	Lk [m]	Lc [m]	S [m2]	Trim [deg]	RCG [mm]
530	1.084	2.005	1.50	1.50	0.323	0.00	0.0
531	1.464	4.348	1.50	1.50	0.323	-0.10	-4.0
532	1.816	6.892	1.50	1.50	0.323	0.70	-8.0
533	2.182	9.086	1.50	1.50	0.323	1.40	-6.0
534	2.548	10.796	1.50	1.50	0.323	1.55	-4.0
535	2.958	12.844	1.50	1.50	0.323	1.65	-3.5
536	3.280	14.846	1.50	1.50	0.323	1.60	-1.8
537	3.661	18.239	1.50	1.50	0.323	1.50	0.3
538	4.041	21.667	1.50	1.50	0.323	1.30	1.0

model 540

L/B [-]	Depl [N]	LCG [%Lp]	Ap/V [-]
7	165.200	-2.000	4.00

run	Vm [m/s]	Rtm [N]	Lk [m]	Lc [m]	S [m2]	Trim [deg]	RCG [mm]
604	1.173	3.364	1.50	1.50	0.324	0.00	-3.0
605	1.570	7.560	1.50	1.50	0.324	0.10	-6.0
606	1.966	13.536	1.50	1.50	0.324	1.50	-10.0
607	2.363	16.892	1.50	1.50	0.324	2.30	-7.0
608	2.775	19.277	1.50	1.50	0.324	2.50	-5.0
609	3.171	22.473	1.50	1.50	0.324	2.50	-1.0
610	3.568	25.759	1.50	1.50	0.324	2.40	1.0
611	3.980	29.450	1.50	1.50	0.324	2.30	3.0
612	4.361	33.773	1.50	1.50	0.324	2.55	3.0

model 530

L/B [-]	Depl [N]	LCG [%Lp]	Ap/V [-]
7	102.400	-2.000	5.50

run	Vm [m/s]	Rtm [N]	Lk [m]	Lc [m]	S [m2]	Trim [deg]	RCG [mm]
541	1.084	2.015	1.50	1.50	0.323	-0.05	-2.0
540	1.450	4.267	1.50	1.50	0.323	0.00	-4.0
542	1.830	7.200	1.50	1.50	0.323	0.80	-7.0
543	2.196	9.523	1.50	1.50	0.323	1.70	-6.0
544	2.548	10.774	1.50	1.50	0.323	1.75	-4.0
545	2.928	12.491	1.35	1.46	0.318	1.80	-2.0
546	3.294	14.248	1.35	1.46	0.318	1.75	0.0
547	3.675	16.473	1.31	1.46	0.315	1.80	2.0
548	4.056	18.654	1.28	1.46	0.314	1.90	4.0
554	4.437	20.998	1.24	1.46	0.310	2.10	3.0
550	4.788	22.270	1.13	1.43	0.296	2.40	5.0
0	0.000	0.000	0.00	0.00	0.000	0.00	0.0
551	5.491	24.700	0.98	1.43	0.278	3.00	9.0

model 542

L/B [-]	Depl [N]	LCG [%Lp]	Ap/V [-]
7	165.200	-4.000	4.00

run	Vm [m/s]	Rtm [N]	Lk [m]	Lc [m]	S [m2]	Trim [deg]	RCG [mm]
613	1.158	3.612	1.50	1.50	0.324	0.00	-3.0
614	1.602	8.079	1.50	1.50	0.324	0.30	-7.0
615	1.966	14.013	1.50	1.50	0.324	1.80	-10.0
616	2.379	17.781	1.50	1.50	0.324	2.70	-7.0
617	2.775	19.584	1.50	1.50	0.324	2.65	-4.0
618	3.171	22.090	1.50	1.50	0.324	2.70	-1.0
619	3.568	24.790	1.50	1.50	0.324	2.70	2.0
620	3.996	27.236	1.35	1.43	0.307	2.95	6.0
622	4.377	29.406	1.13	1.39	0.290	3.70	9.0
623	4.757	30.500	1.07	1.39	0.283	4.35	12.0
625	5.154	31.000	0.91	1.36	0.257	5.00	16.0
624	5.550	31.400	0.90	1.33	0.253	5.30	22.0
626	5.946	33.000	0.88	1.30	0.247	5.10	27.0

model 532

L/B [-]	Depl [N]	LCG [%Lp]	Ap/V [-]
7	102.400	-4.000	5.50

run	Vm [m/s]	Rtm [N]	Lk [m]	Lc [m]	S [m2]	Trim [deg]	RCG [mm]
555	1.098	2.417	1.50	1.50	0.323	0.00	-2.5
556	1.450	4.492	1.50	1.50	0.323	0.05	-4.0
557	1.816	7.285	1.50	1.50	0.323	1.05	-7.5
558	2.182	9.155	1.50	1.50	0.323	1.70	-6.0
559	2.548	10.436	1.28	1.46	0.316	1.80	-3.8
560	2.928	12.090	1.26	1.43	0.310	1.85	-2.0
562	3.280	13.739	1.20	1.43	0.303	1.90	1.0
563	3.646	15.431	1.16	1.43	0.299	2.00	4.0
564	4.027	17.056	1.13	1.43	0.296	2.10	6.0
565	4.407	18.912	1.09	1.43	0.291	2.30	5.8
566	4.759	20.151	1.05	1.43	0.286	2.60	5.7
567	5.227	21.201	0.94	1.39	0.267	2.90	8.0
568	5.491	22.100	0.86	1.39	0.255	3.00	10.0
569	5.901	24.641	0.83	1.39	0.251	3.00	12.0

model 543

L/B [-]	Depl [N]	LCG [%Lp]	Ap/V [-]
7	165.200	-8.000	4.00

run	Vm [m/s]	Rtm [N]	Lk [m]	Lc [m]	S [m2]	Trim [deg]	RCG [mm]
584	1.158	3.679	1.50	1.50	0.323	0.20	-4.0
585	1.586	8.611	1.50	1.50	0.323	0.70	-8.0
586	1.982	15.021	1.35	1.46	0.318	2.15	-10.0
587	2.363	19.299	1.28	1.43	0.310	3.05	-6.0
588	2.759	20.483	1.24	1.43	0.300	3.05	-4.0
589	3.156	22.526	1.16	1.43	0.299	3.30	0.0
590	3.566	24.929	1.13	1.43	0.296	3.60	4.0
591	3.964	27.383	1.01	1.43	0.281	4.20	9.0
592	4.377	29.276	0.94	1.35	0.261	4.85	13.0
593	4.741	31.001	0.90	1.28	0.247	5.50	17.0
594	5.154	30.945	0.84	1.24	0.233	5.45	21.5

model 533

L/B [-]	Depl [N]	LCG [%Lp]	Ap/V [-]
7	102.400	-8.000	5.50

run	Vm [m/s]	Rtm [N]	Lk [m]	Lc [m]	S [m2]	Trim [deg]	RCG [mm]
570	1.098	2.316	1.35	1.46	0.318	0.05	-2.0
571	1.464	4.859	1.35	1.46	0.318	0.04	-4.0
572	1.830	8.052	1.28	1.43	0.310	1.35	-6.0
573	2.182	9.541	1.16	1.43	0.299	1.65	-5.0
574	2.562	10.530	1.09	1.41	0.288	2.00	-2.0
575	2.928	12.027	1.09	1.41	0.286	2.05	-1.0
576	3.280	13.522	1.01	1.41	0.278	2.20	1.0
577	3.646	15.030	0.98	1.39	0.272	2.30	4.0
578	4.041	16.348	0.94	1.39	0.267	2.50	8.0
579	4.407	17.945	0.86	1.39	0.255	2.80	7.0
580	4.773	18.756	0.83	1.39	0.251	3.10	9.0
581	5.169	20.153	0.79	1.35	0.240	3.15	12.0
582	5.491	21.600	0.75	1.35	0.234	3.20	14.5
583	5.857	23.400	0.71	1.31	0.223	3.10	16.5

model 521

L/B [−]	Depl [N]	LCG [%Lp]	Ap/V [−]
7	71.300	0.000	7.00

run	Vm [m/s]	Rtm [N]	Lk [m]	Lc [m]	S [m2]	Trim [deg]	RCG [mm]
468	1.034	1.357	1.28	1.46	0.306	−0.05	−1.5
469	1.378	2.757	1.28	1.46	0.306	−0.02	−3.0
470	1.723	4.220	1.28	1.46	0.306	0.30	−4.2
471	2.068	5.745	1.28	1.46	0.311	0.90	−5.0
472	2.399	6.717	1.28	1.43	0.310	1.10	−3.8
473	2.757	8.133	1.28	1.43	0.310	1.20	−2.0
474	3.102	9.600	1.24	1.43	0.306	1.20	−1.5
475	3.446	11.625	1.24	1.43	0.306	1.20	0.5
476	3.816	13.649	1.24	1.43	0.306	1.15	2.0
477	4.135	15.537	1.24	1.43	0.306	1.20	2.0
478	4.494	17.614	1.24	1.43	0.306	1.30	0.0
479	4.852	19.619	1.20	1.43	0.303	1.40	0.0
480	5.169	21.600	1.20	1.43	0.303	1.50	0.0
482	5.514	23.600	1.13	1.40	0.292	1.70	2.5
484	5.859	25.600	1.05	1.40	0.282	1.85	5.0

model 520

L/B [−]	Depl [N]	LCG [%Lp]	Ap/V [−]
7	71.300	−2.000	7.00

run	Vm [m/s]	Rtm [N]	Lk [m]	Lc [m]	S [m2]	Trim [deg]	RCG [mm]
485	1.034	1.448	1.38	1.46	0.306	−0.03	−2.0
486	1.378	2.800	1.38	1.46	0.306	0.03	−2.5
487	1.723	4.300	1.38	1.46	0.306	0.40	−4.0
488	2.068	5.661	1.31	1.44	0.305	0.92	−5.0
489	2.412	6.714	1.28	1.44	0.306	1.15	−2.2
490	2.771	8.070	1.26	1.43	0.306	1.20	−2.0
491	3.102	9.400	1.23	1.43	0.306	1.22	−1.2
492	3.460	11.053	1.20	1.43	0.303	1.30	1.8
493	3.791	12.462	1.16	1.43	0.299	1.30	4.0
494	4.204	14.587	1.13	1.43	0.296	1.30	4.0
495	4.508	16.331	1.09	1.43	0.291	1.35	1.0
496	4.825	18.437	1.05	1.41	0.284	1.45	2.0
497	5.169	19.900	1.05	1.39	0.281	1.50	2.0
499	5.542	21.890	0.98	1.39	0.272	1.70	4.0
498	5.859	23.200	0.90	1.39	0.261	1.80	5.5

model 522

L/B [−]	Depl [N]	LCG [%Lp]	Ap/V [−]
7	71.300	−4.000	7.00

run	Vm [m/s]	Rtm [N]	Lk [m]	Lc [m]	S [m2]	Trim [deg]	RCG [mm]
500	1.034	1.517	1.28	1.46	0.303	0.00	−2.5
501	1.378	2.600	1.28	1.46	0.303	0.10	−4.0
502	1.709	4.394	1.28	1.46	0.303	0.60	−5.0
503	2.054	5.549	1.28	1.43	0.306	1.00	−6.0
504	2.412	6.519	1.20	1.43	0.300	1.20	−3.0
505	2.757	7.853	1.18	1.43	0.301	1.25	−2.0
506	3.102	9.000	1.16	1.43	0.299	1.30	0.0
507	3.446	10.328	1.09	1.41	0.288	1.35	2.0
508	3.791	11.886	1.09	1.41	0.288	1.35	4.0
509	4.149	13.507	1.05	1.41	0.284	1.35	4.0
510	4.508	15.401	1.04	1.39	0.280	1.35	2.0
511	4.825	16.991	1.04	1.39	0.280	1.55	3.0
514	5.183	18.806	1.04	1.39	0.280	1.65	4.0
513	5.610	20.112	1.60	1.39	0.260	1.80	6.0

model 523

L/B [−]	Depl [N]	LCG [%Lp]	Ap/V [−]
7	71.300	−8.000	7.00

run	Vm [m/s]	Rtm [N]	Lk [m]	Lc [m]	S [m2]	Trim [deg]	RCG [mm]
515	1.034	1.612	1.28	1.43	0.299	0.08	−1.0
516	1.378	3.056	1.28	1.43	0.299	0.20	−2.0
517	1.709	4.717	1.24	1.43	0.295	0.60	−5.0
518	2.068	5.751	1.16	1.41	0.288	1.20	−5.0
519	2.412	6.566	1.05	1.41	0.281	1.30	−2.2
520	2.743	7.523	1.05	1.39	0.284	1.30	−2.0
522	3.102	9.000	0.98	1.39	0.272	1.45	0.5
523	3.432	10.366	0.90	1.39	0.261	1.50	2.0
521	3.763	11.366	0.90	1.37	0.258	1.50	5.7
524	4.122	12.680	0.83	1.39	0.251	1.50	6.0
525	4.494	14.166	0.83	1.37	0.249	1.60	4.0
526	4.839	15.634	0.79	1.35	0.240	1.80	6.0
527	5.169	17.000	0.75	1.35	0.234	1.90	6.5
529	5.528	18.643	0.79	1.35	0.240	1.95	8.0
528	5.859	20.600	0.75	1.33	0.232	2.00	10.5

model 511

L/B [−]	Depl [N]	LCG [%Lp]	Ap/V [−]
7	53.400	0.000	8.50

run	Vm [m/s]	Rtm [N]	Lk [m]	Lc [m]	S [m2]	Trim [deg]	RCG [mm]
407	0.985	1.117	1.38	1.50	0.299	−0.05	−1.0
409	1.340	2.106	1.31	1.50	0.303	0.00	−2.0
410	1.642	3.101	1.31	1.50	0.297	0.14	−3.0
411	1.970	4.026	1.29	1.50	0.304	0.50	−4.0
413	2.312	4.926	1.20	1.43	0.295	0.83	−2.2
414	2.627	5.924	1.13	1.43	0.288	0.85	−3.0
412	2.956	7.100	1.20	1.50	0.301	0.90	−2.0
415	3.284	8.389	1.13	1.43	0.290	0.95	0.0
416	3.626	10.038	1.09	1.43	0.291	0.93	2.0
417	3.954	11.804	1.05	1.43	0.286	0.90	2.2
418	4.283	13.725	1.01	1.43	0.281	0.85	0.0
419	4.611	15.932	1.01	1.43	0.281	0.90	−2.0
420	4.926	18.000	1.01	1.43	0.281	0.90	−2.0
422	5.294	20.523	1.01	1.43	0.281	0.90	−1.0

model 510

L/B [−]	Depl [N]	LCG [%Lp]	Ap/V [−]
7	53.400	−2.000	8.50

run	Vm [m/s]	Rtm [N]	Lk [m]	Lc [m]	S [m2]	Trim [deg]	RCG [mm]
423	0.985	1.120	1.38	1.46	0.291	0.00	−1.5
425	1.327	2.195	1.38	1.46	0.297	0.00	−2.0
426	1.642	3.085	1.38	1.46	0.299	0.20	−2.0
427	1.970	4.105	1.31	1.43	0.298	0.58	−4.0
430	2.378	5.111	1.28	1.43	0.310	0.80	−3.0
431	2.627	5.825	1.20	1.43	0.303	0.80	−3.0
429	2.982	7.405	1.13	1.43	0.296	0.90	−1.5
432	3.297	8.556	1.05	1.43	0.286	0.95	0.0
433	3.626	9.727	1.01	1.43	0.281	0.95	2.0
434	3.967	11.522	0.98	1.43	0.278	0.90	2.5
435	4.283	13.330	0.90	1.43	0.266	0.90	1.0
436	4.611	15.242	0.86	1.43	0.260	0.90	−0.5
437	4.926	16.860	0.84	1.42	0.256	1.00	0.0
439	5.255	19.000	0.84	1.41	0.256	1.00	0.0
438	5.583	21.000	0.84	1.41	0.256	1.05	1.0

model 512

L/B [−]	Depl [N]	LCG [%Lp]	Ap/V [−]
7	53.400	−4.000	8.50

run	Vm [m/s]	Rtm [N]	Lk [m]	Lc [m]	S [m2]	Trim [deg]	RCG [mm]
441	0.985	1.131	1.28	1.43	0.282	0.00	−1.0
440	1.314	2.169	1.28	1.43	0.282	0.10	−2.0
442	1.642	3.067	1.20	1.43	0.280	0.32	−3.5
443	1.970	3.901	1.20	1.43	0.283	0.60	−4.0
444	2.299	4.829	1.13	1.43	0.282	0.85	−2.5
445	2.640	5.892	1.13	1.43	0.282	0.85	−2.5
446	2.969	6.811	1.01	1.43	0.281	1.00	−1.0
447	3.284	7.791	1.01	1.43	0.281	1.00	0.0
448	3.613	9.353	0.98	1.43	0.278	1.00	1.8
449	3.941	11.023	0.94	1.43	0.272	0.98	3.0
450	4.296	12.842	0.90	1.43	0.266	0.95	2.0
451	4.624	14.564	0.90	1.41	0.263	0.95	1.0
452	4.926	16.000	0.83	1.41	0.254	1.00	1.0
453	5.255	17.850	0.83	1.39	0.251	1.05	2.0

model 513

L/B [−]	Depl [N]	LCG [%Lp]	Ap/V [−]
7	53.400	−8.000	8.50

run	Vm [m/s]	Rtm [N]	Lk [m]	Lc [m]	S [m2]	Trim [deg]	RCG [mm]
454	0.985	1.191	1.16	1.43	0.271	0.05	−1.0
455	1.314	2.290	1.16	1.43	0.279	0.20	−2.0
456	1.642	3.231	1.13	1.37	0.277	0.45	−3.0
457	1.970	4.052	0.98	1.37	0.262	0.72	−4.0
458	2.286	4.952	0.98	1.37	0.270	0.95	−2.0
459	2.627	5.826	0.94	1.37	0.264	0.95	−2.0
460	2.956	6.620	0.87	1.37	0.254	1.00	−1.0
461	3.284	7.748	0.83	1.37	0.249	1.05	2.0
462	3.626	8.921	0.83	1.37	0.249	1.02	4.0
463	3.954	10.121	0.83	1.37	0.249	1.00	5.0
464	4.269	11.477	0.83	1.37	0.249	1.00	5.0
465	4.624	13.271	0.79	1.37	0.243	1.00	3.0
466	4.926	14.688	0.75	1.37	0.237	1.10	3.0
467	5.294	16.509	0.71	1.37	0.230	1.20	4.0

Appendix 2 :Coefficients of polynomial model

β	Fn_∇		a_0	a_1	a_2	a_3	a_4	a_5	a_6
			a_7	a_8	a_9	a_{10}	a_{11}	a_{12}	
12.5	.75	R_t/Δ, ∇=5	.1120E+00	-.1289E-01	.1197E-02	-.3479E-04	-.2297E-01	.2924E-02	-.1347E-03
			-.7272E-03	.9765E-04	.4226E-05	.1256E-04	.2713E-03	.1774E-03	
		R_t/Δ, ∇=50	.1115E+00	-.1290E-01	.1199E-02	-.3510E-04	-.2300E-01	.2917E-02	-.1344E-03
			-.7217E-03	.9901E-04	.4318E-05	.1130E-04	.2728E-03	.1786E-03	
		θ	.1129E+01	.1696E+01	-.3130E+00	.2169E-01	-.2760E+01	.4720E+00	-.2433E-01
			-.3112E+00	.1163E-01	.5206E-03	.2458E-01	-.3180E-02	.3304E-01	
		$RCG/\nabla^{1/3}$	-.4074E+00	.9876E-01	-.2147E-01	.1515E-02	.9922E-01	-.1388E-01	.7181E-03
			-.6410E-02	.2775E-03	.1503E-04	.1030E-02	-.4586E-03	.1524E-04	
	1.00	R_t/Δ, ∇=5	.3996E+00	-.9231E-01	.1192E-01	-.6086E-03	-.4127E-01	.2720E-02	-.5832E-04
			.1094E-02	.3815E-03	.9987E-05	.2345E-03	.1766E-02	.5378E-04	
		R_t/Δ, ∇=50	.4002E+00	-.9267E-01	.1201E-01	-.6158E-03	-.4170E-01	.2753E-02	-.5955E-04
			.1136E-02	.3879E-03	.1025E-04	.2308E-03	.1773E-02	.5885E-04	
		θ	.1515E+02	-.9005E+00	.1166E+00	-.4535E-02	-.6366E+01	.8357E+00	-.3731E-01
			-.7934E+00	.1718E-01	.4324E-03	.5055E-01	.9474E-01	.9864E-01	
		$RCG/\nabla^{1/3}$	-.3261E+00	.9289E-01	-.2020E-01	.1426E-02	.2227E-01	.1884E-03	-.3914E-04
			-.1948E-01	.2537E-03	.1417E-04	.2314E-02	.3813E-03	.7281E-03	
	1.25	R_t/Δ, ∇=5	.8393E+00	-.1246E+00	.1461E-01	-.6615E-03	-.1753E+00	.2255E-01	-.1016E-02
			.4165E-02	.6591E-03	.1478E-04	.8072E-03	.1433E-02	-.7895E-03	
		R_t/Δ, ∇=50	.8375E+00	-.1248E+00	.1466E-01	-.6656E-03	-.1748E+00	.2243E-01	-.1009E-02
			.4036E-02	.6488E-03	.1417E-04	.8146E-03	.1445E-02	-.7806E-03	
		θ	.9889E+01	-.7061E+01	.9620E+00	-.5360E-01	.5572E+01	-.1291E+01	.7367E-01
			-.3946E+00	.3410E-01	.1764E-02	.1420E-01	.2198E+00	.7282E-01	
		$RCG/\nabla^{1/3}$	-.1057E+01	.6355E-01	-.2372E-01	.1890E-02	.4602E+00	-.7229E-01	.3700E-02
			-.1873E-01	.4248E-03	.2053E-04	.2296E-02	.3490E-02	.1174E-02	
	1.50	R_t/Δ, ∇=5	.7786E+00	-.1016E+00	.9022E-02	-.2943E-03	-.1539E+00	.1795E-01	-.7779E-03
			.3499E-02	.1219E-02	.3137E-04	.1069E-02	.3079E-02	.1622E-04	
		R_t/Δ, ∇=50	.7830E+00	-.1028E+00	.9261E-02	-.3111E-03	-.1560E+00	.1823E-01	-.7923E-03
			.3454E-02	.1226E-02	.3162E-04	.1069E-02	.3087E-02	.3045E-04	
		θ	.4786E+02	-.9164E+01	.1350E+01	-.7826E-01	-.9693E+01	.1005E+01	-.3806E-01
			-.3616E+00	.1714E-01	.6256E-03	.3080E-01	.2011E+00	.3556E-01	
		$RCG/\nabla^{1/3}$	-.5638E+00	-.2403E-01	-.1195E-01	.1194E-02	.3355E+00	-.5715E-01	.3043E-02
			-.2849E-01	-.8738E-03	-.4271E-04	.2585E-02	.5695E-02	.8498E-03	
	1.75	R_t/Δ, ∇=5	.5817E+00	.2683E-01	-.1742E-01	.1476E-02	-.1538E+00	.1827E-01	-.7977E-03
			.9107E-03	.1048E-02	.2881E-04	.1050E-02	.2770E-02	.1664E-03	
		R_t/Δ, ∇=50	.5824E+00	.2586E-01	-.1725E-01	.1465E-02	-.1542E+00	.1826E-01	-.7975E-03
			.8446E-03	.1059E-02	.2918E-04	.1052E-02	.2781E-02	.1844E-03	
		θ	.3161E+02	-.6006E+01	.6319E+00	-.2905E-01	-.2892E+01	-.7939E-01	.1623E-01
			-.4067E-01	.1568E-01	.6076E-03	-.1308E-02	.1856E+00	.1581E-01	
		$RCG/\nabla^{1/3}$	.7918E-01	.3672E-01	-.2361E-01	.2115E-02	.5393E-01	-.1695E-01	.1139E-02
			-.1168E-01	-.1828E-03	-.2390E-04	.5145E-03	.3081E-02	.1509E-02	

β	Fn_∇		a_0	a_1	a_2	a_3	a_4	a_5	a_6
			a_7	a_8	a_9	a_{10}	a_{11}	a_{12}	
12.5	2.00	R_t/Δ, ∇=5	.4372E+00	.6303E-01	-.2146E-01	.1633E-02	-.1229E+00	.1416E-01	-.6035E-03
			.1789E-02	.9401E-03	.2507E-04	.7046E-03	.2017E-02	.3221E-03	
		R_t/Δ, ∇=50	.4373E+00	.6227E-01	-.2136E-01	.1627E-02	-.1232E+00	.1413E-01	-.6023E-03
			.1758E-02	.9548E-03	.2561E-04	.6993E-03	.2028E-02	.3424E-03	
		θ	.1322E+02	-.2002E+01	-.1887E+00	.2538E-01	.3508E+01	-.1046E+01	.6417E-01
			.1978E+00	.3248E-02	-.2820E-03	-.2124E-01	.1421E+00	-.5899E-02	
		$RCG/\nabla^{1/3}$	.3061E+00	.5434E-01	-.2893E-01	.2561E-02	-.3087E-01	-.5601E-02	.6545E-03
			-.1355E-01	-.8926E-03	-.6666E-04	.5779E-03	.2339E-02	.1237E-02	
	2.25	R_t/Δ, ∇=5	.4683E+00	.4320E-01	-.1361E-01	.1000E-02	-.1418E+00	.1779E-01	-.7790E-03
			.9081E-03	.9836E-03	.3078E-04	.8248E-03	.1317E-02	.3086E-03	
		R_t/Δ, ∇=50	.4695E+00	.4205E-01	-.1342E-01	.9850E-03	-.1423E+00	.1773E-01	-.7758E-03
			.9280E-03	.1002E-02	.3148E-04	.8095E-03	.1326E-02	.3277E-03	
		θ	.2005E+02	-.8878E+00	-.2429E+00	.2151E-01	-.1223E+01	-.2412E+00	.2287E-01
			.4608E+00	.3414E-01	.1530E-02	-.1894E-01	.8043E-01	-.3643E-01	
		$RCG/\nabla^{1/3}$	.9376E-01	-.7904E-02	-.1772E-01	.1632E-02	.1013E+00	-.2329E-01	.1340E-02
			-.1703E-01	-.1087E-02	-.5905E-04	.1185E-02	.4634E-02	.2907E-03	
	2.50	R_t/Δ, ∇=5	.3276E+00	.2996E-01	-.7670E-02	.5118E-03	-.7863E-01	.8623E-02	-.3192E-03
			.1414E-02	.7821E-03	.2343E-04	.6311E-03	.5793E-03	.1716E-03	
		R_t/Δ, ∇=50	.3278E+00	.2871E-01	-.7447E-02	.4925E-03	-.7886E-01	.8539E-02	-.3161E-03
			.1371E-02	.7906E-03	.2369E-04	.6169E-03	.5856E-03	.1842E-03	
		θ	.5497E+01	-.1505E+00	-.2074E+00	.1448E-01	.4538E+01	-.1070E+01	.6381E-01
			.5650E+00	.1284E-01	.2049E-03	-.2930E-01	.1067E-01	-.5021E-01	
		$RCG/\nabla^{1/3}$	.5347E+00	.2676E-01	-.2602E-01	.2249E-02	-.1207E+00	.1309E-01	-.5889E-03
			.2506E-02	.1169E-02	.5121E-04	.4842E-03	.4146E-02	.1570E-04	
	2.75	R_t/Δ, ∇=5	.2864E+00	.2157E-01	-.4537E-02	.2855E-03	-.6463E-01	.7329E-02	-.2793E-03
			.2635E-02	.8383E-03	.2825E-04	.5046E-03	.3729E-03	.1657E-03	
		R_t/Δ, ∇=50	.2891E+00	.1934E-01	-.4014E-02	.2408E-03	-.6574E-01	.7390E-02	-.2841E-03
			.2672E-02	.8536E-03	.2874E-04	.4875E-03	.3528E-03	.1661E-03	
		θ	.5251E+01	-.2136E+00	-.4981E-01	-.2390E-03	.3763E+01	-.8703E+00	.5193E-01
			.7439E+00	.3604E-01	.1549E-02	-.2963E-01	-.3124E-01	-.6563E-01	
		$RCG/\nabla^{1/3}$	.4987E+00	-.2149E-01	-.8807E-02	.8621E-03	-.6185E-01	.3117E-02	-.3261E-04
			.7517E-02	.8079E-03	.3312E-04	-.3072E-03	.2070E-02	-.2094E-03	
	3.00	R_t/Δ, ∇=5	.2041E+00	.2262E-01	-.4611E-02	.3277E-03	-.3360E-01	.3327E-02	-.9487E-04
			.2499E-02	.6954E-03	.2360E-04	.4707E-03	.1737E-03	.8781E-04	
		R_t/Δ, ∇=50	.2085E+00	.1942E-01	-.3751E-02	.2557E-03	-.3523E-01	.3475E-02	-.1039E-03
			.2569E-02	.7122E-03	.2412E-04	.4573E-03	.9270E-04	.6799E-04	
		θ	.2750E+01	-.6138E+00	.1493E+00	-.1441E-01	.4592E+01	-.9479E+00	.5502E-01
			.8403E+00	.3900E-01	.1814E-02	-.3527E-01	-.7550E-01	-.7209E-01	
		$RCG/\nabla^{1/3}$	.5527E+00	-.8569E-01	.6848E-02	-.2166E-03	-.4469E-01	.5517E-03	.9890E-04
			.7751E-02	.3866E-03	.2107E-04	-.6350E-03	.1068E-02	-.7190E-03	

β	Fn_∇		a_0	a_1	a_2	a_3	a_4	a_5	a_6
			a_7	a_8	a_9	a_{10}	a_{11}	a_{12}	
25	.75	R_t/Δ, ∇=5	.1268E+00	-.2424E-01	.3491E-02	-.1893E-03	-.2136E-01	.2706E-02	-.1283E-03
			-.1462E-02	-.4897E-05	-.4912E-06	.3145E-05	.2632E-03	.2009E-03	
		R_t/Δ, ∇=50	.1260E+00	-.2365E-01	.3359E-02	-.1802E-03	-.2152E-01	.2711E-02	-.1285E-03
			-.1457E-02	-.5151E-05	-.5195E-06	.2379E-05	.2653E-03	.2007E-03	
		θ	-.2791E+01	.6060E+00	-.1479E-01	-.8580E-03	.4449E-01	.1737E-01	-.3669E-03
			-.3048E+00	-.2215E-02	-.6126E-04	.1374E-01	-.2986E-01	.2900E-01	
		$RCG/\nabla^{1/3}$	-.5631E-01	.1358E-01	.1978E-03	-.9157E-04	-.1305E-01	.3252E-02	-.1867E-03
			-.2090E-02	.6262E-04	.5807E-05	.3741E-04	-.5312E-03	.3005E-03	
	1.00	R_t/Δ, ∇=5	.3665E+00	-.1043E+00	.1400E-01	-.7408E-03	-.1955E-01	-.6496E-03	.1031E-03
			-.1763E-02	.3776E-04	-.5533E-05	.2222E-03	.2048E-02	.2132E-03	
		R_t/Δ, ∇=50	.3659E+00	-.1036E+00	.1385E-01	-.7299E-03	-.2000E-01	-.6113E-03	.1012E-03
			-.1767E-02	.3688E-04	-.5624E-05	.2198E-03	.2048E-02	.2160E-03	
		θ	.1064E+02	-.2476E+01	.2907E+00	-.1443E-01	-.1992E+01	.9811E-01	-.2754E-03
			-.6578E+00	.2138E-03	.3172E-05	.2929E-01	.1417E+00	.7013E-01	
		$RCG/\nabla^{1/3}$	-.2468E+00	.5017E-01	-.5742E-02	.2944E-03	.2368E-01	-.1508E-02	.4642E-04
			-.7365E-02	-.8799E-04	.3699E-06	.2715E-03	-.8045E-03	.7947E-03	
	1.25	R_t/Δ, ∇=5	.7346E+00	-.1753E+00	.2059E-01	-.1003E-02	-.6923E-01	.3296E-02	-.3195E-04
			-.2975E-02	.1928E-03	-.4883E-05	.7575E-03	.4465E-02	.1095E-04	
		R_t/Δ, ∇=50	.7331E+00	-.1744E+00	.2037E-01	-.9872E-03	-.6949E-01	.3290E-02	-.3134E-04
			-.2984E-02	.1955E-03	-.4780E-05	.7530E-03	.4459E-02	.1806E-04	
		θ	.2407E+02	-.6571E+01	.7093E+00	-.3195E-01	-.1193E+01	-.1873E+00	.1544E-01
			-.3438E+00	.7800E-02	.4234E-03	.1579E-01	.2244E+00	.3405E-01	
		$RCG/\nabla^{1/3}$	-.2845E-01	-.4699E-01	.7296E-02	-.3960E-03	.2604E-01	-.5517E-02	.3090E-03
			-.8058E-02	-.1553E-03	-.4078E-05	.2832E-03	.2089E-02	.8162E-03	
	1.50	R_t/Δ, ∇=5	.8278E+00	-.1938E+00	.2319E-01	-.1139E-02	-.8763E-01	.4455E-02	-.1599E-05
			-.6563E-02	.2575E-03	-.1677E-04	.1527E-02	.5371E-02	.2796E-03	
		R_t/Δ, ∇=50	.8263E+00	-.1927E+00	.2293E-01	-.1119E-02	-.8797E-01	.4460E-02	-.1314E-05
			-.6591E-02	.2606E-03	-.1666E-04	.1521E-02	.5364E-02	.2897E-03	
		θ	.2532E+02	-.8269E+01	.1002E+01	-.4986E-01	-.3671E+00	-.3866E+00	.2851E-01
			-.7646E+00	-.2883E-02	-.2796E-03	.5567E-01	.2880E+00	.6108E-01	
		$RCG/\nabla^{1/3}$	.5694E-01	-.1061E+00	.1742E-01	-.9896E-03	.4806E-01	-.8546E-02	.4183E-03
			-.1034E-01	-.1755E-03	-.7328E-05	.3267E-03	.2052E-02	.1164E-02	
	1.75	R_t/Δ, ∇=5	.9566E+00	-.1196E+00	.7891E-02	-.1443E-03	-.1932E+00	.2134E-01	-.8377E-03
			-.3208E-02	.7299E-03	-.3397E-06	.1896E-02	.4743E-02	-.6219E-04	
		R_t/Δ, ∇=50	.9550E+00	-.1183E+00	.7563E-02	-.1185E-03	-.1938E+00	.2133E-01	-.8361E-03
			-.3264E-02	.7311E-03	-.3583E-06	.1890E-02	.4738E-02	-.4953E-04	
		θ	.3901E+02	-.6757E+01	.5287E+00	-.1651E-01	-.6611E+01	.4903E+00	-.1453E-01
			-.6147E+00	-.5014E-02	-.4529E-03	.4609E-01	.3434E+00	.4319E-01	
		$RCG/\nabla^{1/3}$	.3378E+00	-.1661E+00	.2435E-01	-.1350E-02	.8538E-04	-.4868E-02	.3050E-03
			-.1249E-01	-.1158E-03	-.5414E-05	.3944E-03	.4640E-02	.1473E-02	

β	Fn_∇		a_0	a_1	a_2	a_3	a_4	a_5	a_6
			a_7	a_8	a_9	a_{10}	a_{11}	a_{12}	
25	2.00	R_t/Δ, ∇=5	.9093E+00	-.6004E-01	-.2084E-03	.2698E-03	-.2244E+00	.2790E-01	-.1173E-02
			.1494E-02	.1223E-02	.2299E-04	.1875E-02	.2861E-02	-.3119E-03	
		R_t/Δ, ∇=50	.9074E+00	-.5865E-01	-.5893E-03	.3005E-03	-.2249E+00	.2787E-01	-.1171E-02
			.1423E-02	.1228E-02	.2317E-04	.1868E-02	.2848E-02	-.2987E-03	
		θ	.4651E+02	-.5594E+01	.4061E+00	-.1428E-01	-.1074E+02	.1163E+01	-.4941E-01
			-.3024E+00	-.1047E-01	-.6648E-03	.2291E-01	.2767E+00	.4257E-02	
		$RCG/\nabla^{1/3}$	.6440E+00	-.2007E+00	.2825E-01	-.1576E-02	-.8261E-01	.6147E-02	-.2399E-03
			-.1344E-01	-.3522E-03	-.1875E-04	.3414E-03	.5541E-02	.1394E-02	
	2.25	R_t/Δ, ∇=5	.7267E+00	-.3065E-01	-.4856E-03	.1254E-03	-.1832E+00	.2340E-01	-.9550E-03
			.1759E-02	.1136E-02	.1964E-04	.1832E-02	.1057E-02	-.3018E-03	
		R_t/Δ, ∇=50	.7238E+00	-.2946E-01	-.8423E-03	.1554E-03	-.1830E+00	.2322E-01	-.9432E-03
			.1652E-02	.1129E-02	.1914E-04	.1825E-02	.1035E-02	-.2923E-03	
		θ	.3930E+02	-.3838E+01	.1671E+00	-.1504E-02	-.9002E+01	.9844E+00	-.4198E-01
			-.5436E-01	-.5073E-02	-.2881E-03	.1382E-01	.1938E+00	-.3012E-01	
		$RCG/\nabla^{1/3}$	.7810E+00	-.2062E+00	.2691E-01	-.1457E-02	-.1138E+00	.9881E-02	-.4012E-03
			-.1288E-01	-.2335E-03	-.1484E-04	.4903E-03	.5972E-02	.1138E-02	
	2.50	R_t/Δ, ∇=5	.5911E+00	-.1332E-02	-.2723E-02	.1880E-03	-.1582E+00	.2103E-01	-.8556E-03
			.2990E-02	.1367E-02	.3447E-04	.1735E-02	-.2485E-04	-.8911E-04	
		R_t/Δ, ∇=50	.5896E+00	.5678E-03	-.3241E-02	.2295E-03	-.1594E+00	.2106E-01	-.8555E-03
			.2934E-02	.1372E-02	.3467E-04	.1722E-02	-.6421E-04	-.8239E-04	
		θ	.3457E+02	-.2448E+01	.3596E-01	.3139E-02	-.8405E+01	.9749E+00	-.4280E-01
			.4796E-01	-.1524E-01	-.5625E-03	.6950E-02	.1132E+00	-.5600E-01	
		$RCG/\nabla^{1/3}$	.9096E+00	-.1932E+00	.2314E-01	-.1211E-02	-.1710E+00	.1877E-01	-.8557E-03
			-.1322E-01	-.1999E-03	-.1303E-04	.6159E-03	.6142E-02	.9184E-03	
	2.75	R_t/Δ, ∇=5	.5063E+00	.3047E-01	-.7043E-02	.4750E-03	-.1525E+00	.2178E-01	-.9195E-03
			.5580E-02	.1404E-02	.4042E-04	.1406E-02	-.1424E-02	-.1939E-03	
		R_t/Δ, ∇=50	.5042E+00	.3293E-01	-.7703E-02	.5276E-03	-.1538E+00	.2182E-01	-.9199E-03
			.5526E-02	.1411E-02	.4076E-04	.1391E-02	-.1479E-02	-.1887E-03	
		θ	.2718E+02	-.1949E+01	.7036E-01	-.2685E-02	-.5753E+01	.6084E+00	-.2452E-01
			.1545E+00	-.1495E-01	-.5452E-03	.5244E-02	.6356E-01	-.6772E-01	
		$RCG/\nabla^{1/3}$	.1010E+01	-.1952E+00	.2321E-01	-.1272E-02	-.2037E+00	.2262E-01	-.1013E-02
			-.1367E-01	-.3822E-03	-.2246E-04	.6646E-03	.6673E-02	.6786E-03	
	3.00	R_t/Δ, ∇=5	.4725E+00	.2993E-01	-.7451E-02	.5195E-03	-.1502E+00	.2257E-01	-.9848E-03
			.4185E-02	.1587E-02	.5345E-04	.1713E-02	-.7806E-03	-.1318E-03	
		R_t/Δ, ∇=50	.4693E+00	.3357E-01	-.8372E-02	.5913E-03	-.1520E+00	.2269E-01	-.9906E-03
			.4146E-02	.1587E-02	.5357E-04	.1687E-02	-.8693E-03	-.1363E-03	
		θ	.2337E+02	.1400E+00	-.1892E+00	.1559E-01	-.5536E+01	.6424E+00	-.2701E-01
			.6203E+00	.8787E-02	.4819E-03	-.3054E-01	-.6558E-01	-.7799E-01	
		$RCG/\nabla^{1/3}$	.1152E+01	-.1663E+00	.1819E-01	-.9180E-03	-.2701E+00	.3175E-01	-.1428E-02
			-.7406E-02	.1002E-03	-.2626E-05	.2663E-03	.5604E-02	.6099E-03	

β	Fn_∇		a_0	a_1	a_2	a_3	a_4	a_5	a_6
			a_7	a_8	a_9	a_{10}	a_{11}	a_{12}	
30	.75	R_t/Δ, ∇=5	.2375E+00	-.1031E+00	.1772E-01	-.1041E-02	-.5205E-02	-.2773E-04	.1531E-04
			-.1068E-02	-.6608E-04	-.4816E-05	-.7651E-05	.4227E-03	.9094E-04	
		R_t/Δ, ∇=50	.2441E+00	-.1069E+00	.1843E-01	-.1084E-02	-.5458E-02	-.9167E-05	.1467E-04
			-.1061E-02	-.6654E-04	-.4901E-05	-.9439E-05	.4219E-03	.9157E-04	
		θ	-.3308E+01	.2550E+01	-.4395E+00	.2636E-01	-.1037E+01	.1771E+00	-.8958E-02
			-.2613E+00	-.3974E-02	-.4585E-03	.1186E-01	-.7422E-02	.2557E-01	
		$RCG/\nabla^{1/3}$	-.3177E+00	.1208E+00	-.2063E-01	.1227E-02	.2717E-01	-.3003E-02	.1355E-03
			-.6540E-03	.3208E-03	.2741E-04	.5574E-05	-.7108E-03	.2287E-03	
	1.00	R_t/Δ, ∇=5	.9682E+00	-.4393E+00	.7588E-01	-.4470E-02	-.2704E-01	.1049E-02	-.5175E-05
			-.9952E-03	.1588E-03	.2220E-05	.2921E-03	.1925E-02	-.4311E-04	
		R_t/Δ, ∇=50	.9787E+00	-.4453E+00	.7700E-01	-.4538E-02	-.2747E-01	.1085E-02	-.6608E-05
			-.9873E-03	.1573E-03	.1994E-05	.2893E-03	.1921E-02	-.4144E-04	
		θ	.5441E+02	-.2288E+02	.3988E+01	-.2386E+00	-.5056E+01	.5340E+00	-.2318E-01
			-.4847E+00	.9449E-02	.5464E-03	.2527E-01	.1910E+00	.4970E-01	
		$RCG/\nabla^{1/3}$	-.4817E+00	.1940E+00	-.3240E-01	.1881E-02	.1884E-01	-.9944E-03	.2894E-04
			-.5076E-02	-.1482E-03	-.1146E-04	.2403E-03	-.8347E-03	.4546E-03	
	1.25	R_t/Δ, ∇=5	.1893E+01	-.8457E+00	.1457E+00	-.8577E-02	-.6406E-01	.3342E-02	-.7825E-04
			-.5532E-02	-.2505E-03	-.3509E-04	.5791E-03	.3928E-02	.1844E-03	
		R_t/Δ, ∇=50	.1908E+01	-.8539E+00	.1472E+00	-.8671E-02	-.6465E-01	.3390E-02	-.8027E-04
			-.5525E-02	-.2523E-03	-.3551E-04	.5756E-03	.3924E-02	.1879E-03	
		θ	.8265E+02	-.3612E+02	.6187E+01	-.3627E+00	-.4466E+01	.3828E+00	-.1584E-01
			-.3732E+00	.8297E-02	.4187E-03	.2140E-01	.1987E+00	.3160E-01	
		$RCG/\nabla^{1/3}$	.1322E+00	-.9430E-01	.1822E-01	-.1159E-02	-.2056E-01	.2794E-02	-.1375E-03
			-.7445E-02	-.3535E-03	-.2478E-04	.3577E-03	.1312E-02	.6003E-03	
	1.50	R_t/Δ, ∇=5	.1858E+01	-.8280E+00	.1431E+00	-.8422E-02	-.5704E-01	.2596E-02	-.2847E-04
			-.5175E-02	-.4050E-03	-.4045E-04	.7328E-03	.3278E-02	-.1106E-03	
		R_t/Δ, ∇=50	.1879E+01	-.8404E+00	.1454E+00	-.8563E-02	-.5732E-01	.2571E-02	-.2619E-04
			-.5174E-02	-.4052E-03	-.4082E-04	.7281E-03	.3271E-02	-.1054E-03	
		θ	.6978E+02	-.3135E+02	.5460E+01	-.3225E+00	-.2889E+01	.1742E+00	-.4266E-02
			-.6324E+00	.1348E-02	.1646E-03	.3824E-01	.1397E+00	.5171E-01	
		$RCG/\nabla^{1/3}$	.2261E-01	-.1064E+00	.2000E-01	-.1204E-02	.6209E-01	-.9628E-02	.5027E-03
			-.5670E-02	.4477E-03	.3335E-04	.4417E-03	-.1045E-03	.6196E-03	
	1.75	R_t/Δ, ∇=5	.1702E+01	-.7709E+00	.1305E+00	-.7581E-02	-.6966E-02	-.5282E-02	.3696E-03
			-.1824E-02	-.1237E-02	-.1262E-03	.6829E-03	.3235E-02	-.6792E-03	
		R_t/Δ, ∇=50	.1733E+01	-.7893E+00	.1339E+00	-.7791E-02	-.7524E-02	-.5292E-02	.3716E-03
			-.1813E-02	-.1224E-02	-.1256E-03	.6794E-03	.3231E-02	-.6722E-03	
		θ	.7224E+02	-.3582E+02	.6161E+01	-.3609E+00	.3320E+00	-.3882E+00	.2447E-01
			-.9607E+00	-.2280E-01	-.2228E-02	.5705E-01	.2030E+00	.7807E-01	
		$RCG/\nabla^{1/3}$	.4322E+00	-.2972E+00	.5325E-01	-.3187E-02	.4307E-01	-.8474E-02	.4483E-03
			-.1120E-01	.1239E-04	.5205E-05	.4255E-03	.1557E-02	.1150E-02	

β	Fn_∇		a_0	a_1	a_2	a_3	a_4	a_5	a_6
			a_7	a_8	a_9	a_{10}	a_{11}	a_{12}	
30	2.00	R_t/Δ, ∇=5	.1656E+01	-.6805E+00	.1134E+00	-.6550E-02	-.4770E-01	.1274E-02	.4691E-04
			.6126E-02	-.3168E-03	-.6683E-04	.7238E-03	.2907E-02	-.1289E-02	
		R_t/Δ, ∇=50	.1694E+01	-.7038E+00	.1177E+00	-.6804E-02	-.4649E-01	.9008E-03	.7014E-04
			.5933E-02	-.3613E-03	-.7191E-04	.7270E-03	.2913E-02	-.1273E-02	
		θ	.8804E+02	-.3982E+02	.6620E+01	-.3810E+00	-.2136E+01	-.1155E+00	.1139E-01
			-.1008E+01	-.3554E-01	-.2607E-02	.5899E-01	.3045E+00	.6854E-01	
		$RCG/\nabla^{1/3}$	.8667E+00	-.4740E+00	.8228E-01	-.4842E-02	.1408E-01	-.5696E-02	.3229E-03
			-.1656E-01	.1728E-03	.2300E-04	.7306E-03	.2799E-02	.1625E-02	
	2.25	R_t/Δ, ∇=5	.1453E+01	-.5376E+00	.9138E-01	-.5364E-02	-.8717E-01	.9157E-02	-.3582E-03
			.1024E-01	.2689E-03	-.3268E-04	.7508E-03	.1368E-02	-.1379E-02	
		R_t/Δ, ∇=50	.1506E+01	-.5676E+00	.9695E-01	-.5702E-02	-.8862E-01	.9234E-02	-.3604E-03
			.1017E-01	.2831E-03	-.3217E-04	.7504E-03	.1373E-02	-.1365E-02	
		θ	.9557E+02	-.3926E+02	.6365E+01	-.3630E+00	-.4819E+01	.2255E+00	-.4879E-02
			-.5270E+00	.1015E-01	.1224E-02	.3807E-01	.3517E+00	.3215E-01	
		$RCG/\nabla^{1/3}$	.1353E+01	-.6515E+00	.1099E+00	-.6388E-02	-.2494E-01	-.2037E-02	.1454E-03
			-.1627E-01	.1617E-03	.2885E-04	.5353E-03	.4753E-02	.1634E-02	
	2.50	R_t/Δ, ∇=5	.9319E+00	-.2954E+00	.5024E-01	-.2921E-02	-.6361E-01	.8261E-02	-.3369E-03
			.1184E-01	.8303E-03	.5622E-06	.9069E-03	-.7135E-03	-.1244E-02	
		R_t/Δ, ∇=50	.9948E+00	-.3296E+00	.5657E-01	-.3304E-02	-.6611E-01	.8461E-02	-.3445E-03
			.1181E-01	.8371E-03	.5183E-06	.8959E-03	-.7075E-03	-.1236E-02	
		θ	.9824E+02	-.3926E+02	.6440E+01	-.3724E+00	-.5970E+01	.3969E+00	-.1310E-01
			-.4028E+00	-.5026E-01	-.3700E-02	.2618E-01	.3341E+00	-.4590E-02	
		$RCG/\nabla^{1/3}$	.1842E+01	-.8079E+00	.1355E+00	-.7899E-02	-.9085E-01	.5616E-02	-.1970E-03
			-.1795E-01	-.1024E-02	-.7721E-04	.4877E-03	.6345E-02	.1413E-02	
	2.75	R_t/Δ, ∇=5	.6313E+00	-.1312E+00	.2362E-01	-.1399E-02	-.7721E-01	.1184E-01	-.5199E-03
			.1186E-01	.9825E-03	.2873E-05	.8766E-03	-.1911E-02	-.7917E-03	
		R_t/Δ, ∇=50	.7086E+00	-.1717E+00	.3109E-01	-.1850E-02	-.8123E-01	.1225E-01	-.5382E-03
			.1182E-01	.9787E-03	.2031E-05	.8611E-03	-.1907E-02	-.7870E-03	
		θ	.9068E+02	-.3365E+02	.5499E+01	-.3163E+00	-.7182E+01	.6379E+00	-.2509E-01
			-.4376E-01	.5334E-02	.1064E-02	.1525E-01	.2526E+00	-.2757E-01	
		$RCG/\nabla^{1/3}$	.2129E+01	-.9369E+00	.1570E+00	-.9168E-02	-.9685E-01	.4548E-02	-.1089E-03
			-.1769E-01	-.9548E-03	-.7379E-04	.6547E-03	.7718E-02	.1153E-02	
	3.00	R_t/Δ, ∇=5	.3244E+00	.3275E-01	-.5660E-02	.2629E-03	-.8965E-01	.1499E-01	-.6978E-03
			.3986E-02	.7377E-04	-.6592E-04	.1683E-02	-.1222E-02	-.8664E-03	
		R_t/Δ, ∇=50	.4106E+00	-.1235E-01	.2636E-02	-.2355E-03	-.9399E-01	.1542E-01	-.7167E-03
			.4036E-02	.5876E-04	-.6810E-04	.1653E-02	-.1243E-02	-.8652E-03	
		θ	.7509E+02	-.2554E+02	.4114E+01	-.2306E+00	-.6603E+01	.6169E+00	-.2355E-01
			.1718E+00	-.1843E-01	-.1362E-02	-.9041E-02	.1298E+00	-.3701E-01	
		$RCG/\nabla^{1/3}$	.2406E+01	-.9778E+00	.1612E+00	-.9288E-02	-.1598E+00	.1235E-01	-.4494E-03
			-.1356E-01	-.3565E-03	-.2769E-04	.4475E-03	.8148E-02	.1005E-02	

Appendix 3 :Experimental results of twisted bottom models

model 232-A

Disp [N]	LCG [%Lp]	Ap/V [-]
164.71	0	7.0

run [-]	vm [m/s]	Rtm [N]	Lk [m]	Lc [m]	S [m^2]	Trim [deg]	RCG [mm]
225	0.795	0.990	0.68	1.49	0.446	0.0	-1.0
226	1.199	3.750	1.32	1.51	0.460	0.1	-4.0
227	1.585	8.490	1.20	1.51	0.490	0.8	-8.3
228	1.979	14.240	1.13	1.48	0.487	2.6	-12.4
229	2.378	16.710	0.98	1.45	0.478	3.6	-4.9
230	2.785	19.080	0.98	1.42	0.463	4.0	-1.1
231	3.183	21.120	0.90	1.40	0.444	4.7	4.6
232	3.572	23.560	0.87	1.38	0.421	5.5	11.1
233	3.971	26.480	0.75	1.26	0.389	6.7	20.9
234	4.378	30.270	0.72	1.14	0.349	7.3	29.5
235	4.787	33.820	0.65	1.05	0.320	7.5	35.2

model 232-A

Disp [N]	LCG [%Lp]	Ap/V [-]
236.42	0	5.5

run [-]	vm [m/s]	Rtm [N]	Lk [m]	Lc [m]	S [m^2]	Trim [deg]	RCG [mm]
236	0.847	1.430	1.05	1.52	0.495	0.0	-2.0
237	1.273	5.600	1.26	1.54	0.528	0.1	-5.6
238	1.688	14.200	1.56	1.56	0.555	1.1	-11.2
239	2.124	25.160	1.32	1.48	0.529	4.0	-11.2
240	2.531	28.130	1.10	1.47	0.493	4.7	-4.9
241	2.942	30.990	1.09	1.43	0.482	5.3	-0.3
242	3.361	33.930	1.00	1.40	0.460	6.3	8.3
243	3.790	37.890	0.91	1.33	0.425	7.8	18.4
244	4.233	41.370	0.79	1.22	0.382	8.7	30.4
248	4.688	45.390	0.74	1.12	0.346	9.1	40.1
247	5.103	48.470	0.70	1.08	0.323	9.2	48.1

model 232-A

Disp [N]	LCG [%Lp]	Ap/V [-]
164.71	-4	7.0

run [-]	vm [m/s]	Rtm [N]	Lk [m]	Lc [m]	S [m^2]	Trim [deg]	RCG [mm]
213	0.798	1.150	0.65	1.48	0.412	0.1	-1.6
214	1.201	3.830	0.79	1.49	0.432	0.3	-4.4
215	1.598	8.600	0.75	1.47	0.447	1.2	-9.0
216	1.993	13.810	0.97	1.43	0.454	2.9	-10.8
217	2.390	18.110	0.91	1.41	0.449	3.7	-4.5
218	2.786	18.110	0.89	1.36	0.434	4.2	-0.9
219	3.158	21.100	0.87	1.33	0.414	5.3	4.7
220	3.572	24.560	0.87	1.18	0.388	6.7	14.4
221	3.972	29.080	0.69	1.09	0.355	7.4	25.7
222	4.371	31.400	0.64	1.02	0.320	7.7	32.3
223	4.798	34.330	0.59	0.97	0.280	7.7	37.8

model 232-A

Disp [N]	LCG [%Lp]	Ap/V [-]
236.42	-4	5.5

run [-]	vm [m/s]	Rtm [N]	Lk [m]	Lc [m]	S [m^2]	Trim [deg]	RCG [mm]
249	0.847	1.660	0.91	1.51	0.463	0.1	-2.0
250	1.262	5.940	1.56	1.54	0.555	0.3	-6.0
252	1.687	14.520	1.32	1.56	0.542	1.7	-11.4
253	2.123	25.290	1.13	1.44	0.482	4.4	-11.1
254	2.539	27.900	1.02	1.29	0.452	5.1	-4.5
255	2.958	30.220	0.98	1.37	0.434	5.6	1.2
256	3.377	35.630	0.87	1.28	0.403	6.9	10.1
257	3.785	42.200	0.79	1.15	0.387	8.4	27.2
258	4.228	46.640	0.75	1.04	0.332	8.8	38.8
259	4.666	49.060	0.68	0.98	0.307	8.8	44.8
260	5.059	50.470	0.64	0.93	0.294	8.6	50.1

model 232-A

Disp [N]	LCG [%Lp]	Ap/V [-]
164.71	-8	7.0

run [-]	vm [m/s]	Rtm [N]	Lk [m]	Lc [m]	S [m^2]	Trim [deg]	RCG [mm]
201	0.794	1.310	0.74	1.46	0.420	0.1	-1.5
202	1.198	4.190	0.78	1.44	0.424	0.5	-4.6
203	1.593	9.320	0.87	1.42	0.426	1.6	-9.4
204	1.990	15.190	0.95	1.37	0.425	3.3	-10.5
205	2.386	17.310	0.86	1.32	0.415	3.7	-4.3
206	2.783	20.280	0.79	1.25	0.393	4.8	0.5
207	3.182	24.540	0.75	1.12	0.362	5.9	8.7
208	3.569	28.760	0.87	1.31	0.325	7.0	21.2
209	3.971	32.330	0.62	0.90	0.279	7.2	31.4

model 232-A

Disp [N]	LCG [%Lp]	Ap/V [-]
236.42	-8	5.5

run [-]	vm [m/s]	Rtm [N]	Lk [m]	Lc [m]	S [m^2]	Trim [deg]	RCG [mm]
262	0.844	2.040	0.87	1.48	0.495	0.2	-1.8
263	1.269	6.570	0.91	1.47	0.457	0.6	-5.5
264	1.684	15.780	1.13	1.43	0.491	2.3	-11.2
265	2.118	28.270	0.99	1.35	0.446	5.1	-10.1
266	2.536	30.590	0.90	1.30	0.424	5.8	-3.2
267	2.955	35.430	0.87	1.24	0.398	6.7	3.8
268	3.374	45.910	0.79	1.06	0.356	8.7	18.3
269	3.601	50.160	0.70	0.98	0.315	9.3	33.8
270	4.235	51.310	0.61	0.91	0.283	9.0	44.4

model 232-A

Disp [N]	LCG [%Lp]	Ap/V [-]
164.71	-12	7.0

run [-]	vm [m/s]	Rtm [N]	Lk [m]	Lc [m]	S [m^2]	Trim [deg]	RCG [mm]
188	0.794	1.530	0.68	1.43	0.400	0.2	-1.5
189	1.199	4.530	0.68	1.41	0.397	0.7	-4.6
190	1.583	11.250	0.71	1.37	0.396	2.1	-10.0
192	1.978	18.310	0.83	1.25	0.395	4.3	-9.2
193	2.384	20.900	0.79	1.15	0.378	4.9	-1.9
194	2.781	24.810	0.71	1.04	0.351	6.1	5.3
195	3.190	31.660	0.67	1.03	0.313	7.8	13.7

model 232-A

Disp [N]	LCG [%Lp]	Ap/V [-]
236.42	-12	5.5

run [-]	vm [m/s]	Rtm [N]	Lk [m]	Lc [m]	S [m^2]	Trim [deg]	RCG [mm]
274	0.847	2.420	0.83	1.46	0.437	0.3	-2.1
275	1.262	7.090	0.83	1.44	0.440	0.9	-6.0
276	1.687	19.030	0.95	1.38	0.437	3.1	-11.9
277	2.102	34.720	0.90	1.25	0.410	6.1	-10.0
278	2.528	38.490	0.83	1.13	0.368	6.7	-0.7
280	2.938	46.920	0.75	1.03	0.330	8.8	10.4
279	3.364	56.900	0.68	0.89	0.295	10.0	28.8

model 232-A

Disp [N]	LCG [%Lp]	Ap/V [-]
381.22	0	4.0

run [-]	vm [m/s]	Rtm [N]	Lk [m]	Lc [m]	S [m^2]	Trim [deg]	RCG [mm]
307	0.917	2.360	1.56	1.56	0.555	0.0	-3.1
308	1.372	11.110	1.56	1.56	0.555	0.2	-8.8
309	1.828	26.300	1.56	1.56	0.555	2.3	-17.0
310	2.284	52.660	1.56	1.56	0.555	8.3	-13.1
311	2.741	58.390	1.32	1.53	0.530	6.9	-5.5
312	3.199	64.200	1.20	1.44	0.498	8.2	4.5
313	3.671	69.480	1.05	1.36	0.462	10.0	19.8

model 232-B

Disp [N]	LCG [%Lp]	Ap/V [-]
123.02	0	8.5

run [-]	vm [m/s]	Rtm [N]	Lk [m]	Lc [m]	S [m^2]	Trim [deg]	RCG [mm]
140	0.753	0.670	0.60	1.48	0.396	0.0	-1.9
141	1.138	2.730	1.32	1.51	0.535	0.1	-4.3
142	1.510	5.460	1.56	1.50	0.550	0.5	-7.0
143	1.885	8.760	1.28	1.47	0.523	1.5	-9.4
145	2.639	13.040	0.89	1.43	0.444	2.9	-1.4
146	3.020	15.110	0.87	1.42	0.437	3.2	2.4
147	3.405	17.090	0.83	1.41	0.426	3.5	7.0
148	3.773	16.590	0.83	1.37	0.412	3.9	8.9
149	4.156	21.440	0.75	1.33	0.393	4.4	13.5
150	4.553	22.370	0.68	1.27	0.373	4.8	16.0

model 232-A

Disp [N]	LCG [%Lp]	Ap/V [-]
381.22	-4	4.0

run [-]	vm [m/s]	Rtm [N]	Lk [m]	Lc [m]	S [m^2]	Trim [deg]	RCG [mm]
298	0.918	3.040	1.56	1.56	0.555	0.1	-3.4
299	1.370	11.760	1.56	1.56	0.555	0.5	-8.8
300	1.693	22.650	1.56	1.56	0.555	1.9	-13.9
301	1.837	31.050	1.56	1.56	0.555	3.4	-15.8
302	2.292	58.290	1.20	1.44	0.517	7.1	-12.0
303	2.750	59.630	1.13	1.40	0.475	7.9	-2.8
304	3.198	67.880	1.02	1.33	0.435	9.7	8.1
305	3.666	88.300	0.87	1.15	0.392	10.0	28.1

model 232-B

Disp [N]	LCG [%Lp]	Ap/V [-]
123.02	-4	8.5

run [-]	vm [m/s]	Rtm [N]	Lk [m]	Lc [m]	S [m^2]	Trim [deg]	RCG [mm]
151	0.754	0.990	0.55	1.47	0.385	0.1	-1.3
152	1.127	2.900	0.60	1.48	0.396	0.3	-3.0
154	1.511	5.740	1.13	1.50	0.504	0.8	-5.7
155	1.883	8.520	1.05	1.49	0.488	1.9	-8.2
156	2.268	10.550	0.90	1.42	0.444	2.8	-4.5
157	2.654	12.220	0.79	1.40	0.418	3.0	-1.8
158	3.032	13.960	0.79	1.38	0.413	3.2	1.4
159	3.388	15.820	0.75	1.37	0.403	3.7	6.1
160	3.768	17.340	0.72	1.31	0.385	4.2	11.7
161	4.159	20.780	0.67	1.25	0.363	4.6	16.0
162	4.548	22.700	0.62	1.17	0.337	4.8	18.6

model 232-A

Disp [N]	LCG [%Lp]	Ap/V [-]
381.22	-8	4.0

run [-]	vm [m/s]	Rtm [N]	Lk [m]	Lc [m]	S [m^2]	Trim [deg]	RCG [mm]
291	0.917	3.540	1.13	1.52	0.508	0.3	-2.0
292	1.373	12.400	1.56	1.50	0.550	0.9	-7.6
293	1.828	35.710	1.32	1.46	0.513	4.1	-14.6
294	2.285	64.280	1.05	1.36	0.468	7.6	-10.4
295	2.752	71.980	0.98	1.27	0.423	9.0	0.1
296	3.200	92.150	0.87	1.09	0.378	10.0	15.3

model 232-B

Disp [N]	LCG [%Lp]	Ap/V [-]
123.02	-8	8.5

run [-]	vm [m/s]	Rtm [N]	Lk [m]	Lc [m]	S [m^2]	Trim [deg]	RCG [mm]
164	0.752	1.110	0.53	1.45	0.374	0.1	-0.9
165	1.134	3.120	0.55	1.44	0.378	0.4	-3.1
166	1.509	6.430	0.72	1.44	0.411	1.1	-5.9
167	1.883	9.340	0.78	1.37	0.413	2.2	-8.0
168	2.258	11.000	0.83	1.35	0.411	2.9	-3.9
169	2.644	12.410	0.78	1.34	0.402	3.0	-0.6
170	3.033	14.280	0.73	1.29	0.386	3.4	4.8
171	3.391	15.890	0.70	1.23	0.367	3.9	11.8
172	3.777	17.580	0.63	1.13	0.342	4.2	15.6
173	4.169	19.570	0.59	1.05	0.315	4.4	19.9
174	4.549	21.510	0.56	1.04	0.288	4.5	22.9

model 232-A

Disp [N]	LCG [%Lp]	Ap/V [-]
381.22	-12	4.0

run [-]	vm [m/s]	Rtm [N]	Lk [m]	Lc [m]	S [m^2]	Trim [deg]	RCG [mm]
286	0.917	4.260	1.02	1.46	0.475	0.4	-2.8
287	1.372	12.540	1.20	1.44	0.478	1.3	-7.8
288	1.827	41.260	1.09	1.40	0.460	4.9	-14.9
289	2.293	81.550	0.98	1.24	0.424	9.0	-10.2

model 232-B

Disp [N]	LCG [%Lp]	Ap/V [-]
123.02	-12	8.5

run [-]	vm [m/s]	Rtm [N]	Lk [m]	Lc [m]	S [m^2]	Trim [deg]	RCG [mm]
176	0.754	1.260	0.53	1.43	0.382	0.3	-1.3
177	1.128	3.390	0.60	1.38	0.359	0.6	-3.7
178	1.512	7.680	0.55	1.36	0.362	1.6	-6.9
179	1.887	10.970	0.83	1.28	0.400	2.8	-7.0
160	2.272	12.200	0.75	1.23	0.378	3.3	-2.5
181	2.638	13.670	0.71	1.20	0.350	3.6	1.8
182	3.035	15.960	0.64	1.05	0.324	4.4	8.0
183	3.390	17.460	0.59	1.00	0.303	4.7	15.2
184	3.647	18.560	0.60	0.97	0.289	4.8	20.4
185	3.774	19.060	0.60	0.89	0.283	4.7	22.9
186	4.158	20.870	0.56	0.88	0.263	4.6	28.6

model 232-B

Disp [N]	LCG [%Lp]	Ap/V [-]
164.71	0	7.0

run [-]	vm [m/s]	Rtm [N]	Lk [m]	Lc [m]	S [m^2]	Trim [deg]	RCG [mm]
36	0.795	1.140	0.79	1.50	0.445	0.0	-1.5
39	1.189	3.900	1.58	1.51	0.551	0.1	-4.3
40	1.584	8.610	1.56	1.49	0.550	0.7	-7.9
41	1.980	13.920	1.32	1.51	0.532	2.3	-10.1
42	2.377	16.600	1.13	1.48	0.501	3.2	-4.9
43	2.783	19.010	1.05	1.46	0.478	3.5	-1.6
44	3.180	21.670	0.95	1.44	0.458	3.9	2.5
45	3.580	23.430	0.90	1.42	0.439	4.3	8.3
46	3.980	26.050	0.83	1.38	0.421	4.9	13.7
47	4.383	26.720	0.79	1.34	0.404	5.4	18.3
48	4.789	29.860	0.75	1.29	0.388	5.8	22.5

model 232-B

Disp [N]	LCG [%Lp]	Ap/V [-]
236.42	0	5.5

run [-]	vm [m/s]	Rtm [N]	Lk [m]	Lc [m]	S [m^2]	Trim [deg]	RCG [mm]
49	0.794	1.380	1.13	1.54	0.512	0.0	-1.6
50	1.187	4.740	1.56	1.55	0.552	0.1	-4.9
51	1.683	14.600	1.56	1.55	0.552	1.0	-11.1
61	1.847	19.370	1.45	1.53	0.552	2.1	-13.7
52	2.068	24.630	1.40	1.52	0.547	3.5	-12.2
53	2.526	28.330	1.23	1.46	0.523	4.2	-5.5
54	2.943	31.630	1.15	1.45	0.500	4.7	-0.5
55	3.373	34.520	1.05	1.43	0.475	5.3	6.0
56	3.794	36.150	0.98	1.41	0.451	6.1	13.7
57	4.234	38.680	0.89	1.36	0.426	6.9	22.6
59	4.652	40.570	0.83	1.31	0.406	7.2	28.7
60	5.094	42.300	0.79	1.25	0.386	7.3	34.7

model 232-B

Disp [N]	LCG [%Lp]	Ap/V [-]
164.71	-4	7.0

run [-]	vm [m/s]	Rtm [N]	Lk [m]	Lc [m]	S [m^2]	Trim [deg]	RCG [mm]
26	0.795	1.310	0.75	1.48	0.429	0.1	-1.4
27	1.189	4.180	1.26	1.50	0.626	0.4	-3.9
28	1.584	8.820	1.16	1.48	0.507	1.1	-7.6
29	1.981	13.570	1.05	1.46	0.481	2.7	-9.6
30	2.386	15.980	0.94	1.41	0.457	3.5	-4.3
31	2.783	17.730	0.90	1.40	0.439	3.7	-0.4
32	3.180	20.110	0.90	1.36	0.426	4.1	3.9
33	3.576	22.370	0.83	1.35	0.416	4.7	10.4
34	3.980	24.410	0.76	1.26	0.403	5.2	17.0
35	4.366	27.780	0.75	1.22	0.377	5.4	21.6
36	4.792	29.330	0.63	1.11	0.338	5.4	26.0

model 232-B

Disp [N]	LCG [%Lp]	Ap/V [-]
236.42	-4	5.5

run [-]	vm [m/s]	Rtm [N]	Lk [m]	Lc [m]	S [m^2]	Trim [deg]	RCG [mm]
63	0.846	1.970	1.05	1.50	0.490	0.2	-1.9
64	1.264	6.470	1.49	1.51	0.546	0.4	-5.4
65	1.676	14.750	1.56	1.58	0.552	1.6	-10.5
67	2.001	23.640	1.23	1.47	0.516	3.6	-12.5
68	2.121	25.090	1.16	1.44	0.505	4.0	-10.6
69	2.525	27.580	1.05	1.43	0.476	4.4	-4.7
70	2.954	30.270	0.98	1.40	0.452	5.0	1.9
71	3.384	33.180	0.90	1.35	0.426	5.6	8.9
72	3.807	35.930	0.87	1.31	0.406	6.5	18.5
73	4.247	40.240	0.79	1.23	0.384	7.0	27.6
74	4.663	39.930	0.75	1.15	0.364	6.9	34.0
75	5.001	41.510	0.72	1.12	0.347	6.7	38.1

model 232-B

Disp [N]	LCG [%Lp]	Ap/V [-]
164.71	-8	7.0

run [-]	vm [m/s]	Rtm [N]	Lk [m]	Lc [m]	S [m^2]	Trim [deg]	RCG [mm]
14	0.791	1.540	0.68	1.46	0.406	0.2	-1.0
15	1.189	4.490	0.79	1.50	0.436	0.5	-3.7
17	1.584	9.500	1.09	1.45	0.500	1.5	-7.9
25	1.828	13.520	1.05	1.42	0.468	3.0	-10.1
18	1.991	14.830	0.94	1.43	0.451	3.4	-9.3
19	2.386	16.670	0.87	1.38	0.426	4.0	-3.3
20	2.792	18.630	0.83	1.33	0.409	4.1	0.9
21	3.190	21.210	0.79	1.30	0.396	4.6	6.6
22	3.580	23.230	0.75	1.17	0.370	5.3	14.0
23	3.970	25.190	0.68	1.10	0.335	5.5	22.0
24	4.375	27.690	0.65	1.05	0.320	5.5	27.1

model 232-B

Disp [N]	LCG [%Lp]	Ap/V [-]
236.42	-8	5.5

run [-]	vm [m/s]	Rtm [N]	Lk [m]	Lc [m]	S [m^2]	Trim [deg]	RCG [mm]
77	0.845	2.310	0.83	1.48	0.445	0.2	-1.8
78	1.269	7.220	1.26	1.49	0.521	0.8	-5.0
80	1.674	15.370	1.13	1.46	0.497	2.0	-10.1
81	2.000	26.140	1.05	1.42	0.473	4.0	-11.8
82	2.141	27.650	1.02	1.40	0.483	4.5	-9.7
83	2.537	29.490	0.94	1.37	0.441	5.0	-2.8
84	2.966	32.810	0.90	1.30	0.418	5.5	3.6
85	3.386	36.300	0.83	1.21	0.387	6.4	12.6
86	3.805	40.110	0.75	1.10	0.354	7.3	24.7
87	4.234	41.720	0.72	1.05	0.331	6.9	34.4
88	4.660	41.830	0.68	1.02	0.314	6.6	39.6
89	5.048	41.340	0.80	1.00	0.301	6.0	43.6

model 232-B

Disp [N]	LCG [%Lp]	Ap/V [-]
164.71	-12	7.0

run [-]	vm [m/s]	Rtm [N]	Lk [m]	Lc [m]	S [m^2]	Trim [deg]	RCG [mm]
3	0.795	1.790	0.68	1.45	0.400	0.1	-1.0
9	1.189	4.910	0.75	1.42	0.415	1.1	-4.0
4	1.585	11.060	0.98	1.41	0.452	1.7	-8.3
13	1.827	16.170	0.90	1.37	0.437	3.2	-10.5
2	2.021	17.570	0.87	1.35	0.423	3.6	-8.1
5	2.388	19.230	0.79	1.26	0.394	3.8	-1.9
10	2.791	21.650	0.75	1.17	0.360	4.7	3.8
6	3.183	24.620	0.68	1.05	0.325	5.5	11.6
11	3.597	26.630	0.60	0.97	0.295	5.8	22.8
7	3.995	28.550	0.60	0.94	0.283	5.8	30.3
12	4.411	29.190	0.60	0.90	0.284	5.5	34.1
8	4.812	29.000	0.53	0.89	0.306	4.7	36.7

model 232-B

Disp [N]	LCG [%Lp]	Ap/V [-]
236.42	-12	5.5

run [-]	vm [m/s]	Rtm [N]	Lk [m]	Lc [m]	S [m^2]	Trim [deg]	RCG [mm]
91	0.846	2.610	0.87	1.45	0.443	0.3	-1.8
92	1.262	7.460	0.98	1.40	0.454	0.8	-5.2
102	1.677	18.500	0.96	1.29	0.452	2.6	-10.8
97	1.886	28.630	0.98	1.36	0.442	4.3	-12.6
93	2.123	32.830	0.91	1.28	0.426	5.1	-9.3
94	2.529	34.970	0.87	1.21	0.390	5.7	-0.4
95	2.948	39.820	0.79	1.10	0.354	6.8	7.8
96	3.366	47.340	0.72	0.99	0.322	8.0	22.3
98	3.787	47.270	0.65	0.92	0.298	7.8	35.7
99	4.236	43.740	0.64	0.87	0.278	7.1	42.6
100	4.655	43.950	0.60	0.86	0.269	6.6	49.6
101	5.095	43.150	0.60	0.81	0.264	5.9	53.2

model 232-B

Disp [N]	LCG [%Lp]	Ap/V [-]
381.22	0	4.0

run [-]	vm [m/s]	Rtm [N]	Lk [m]	Lc [m]	S [m^2]	Trim [deg]	RCG [mm]
128	0.915	2.690	1.56	1.56	0.555	0.1	-3.3
129	1.370	11.660	1.56	1.56	0.555	0.1	-9.2
130	1.815	28.220	1.56	1.56	0.555	1.9	-18.8
138	2.038	42.120	1.56	1.56	0.555	4.2	17.9
131	2.261	52.090	1.56	1.56	0.555	5.8	-14.3
132	2.728	56.210	1.45	1.52	0.555	6.3	-6.9
133	3.185	64.800	1.28	1.47	0.525	7.0	2.0
134	3.644	68.850	1.13	1.44	0.492	8.5	14.2
135	4.110	70.590	1.00	1.34	0.449	10.0	30.8
136	4.591	71.940	0.85	1.26	0.402	10.0	43.2
137	5.161	71.260	0.85	1.19	0.388	10.0	54.0

model 232-B

Disp [N]	LCG [%Lp]	Ap/V [-]
381.22	-4	4.0

run [-]	vm [m/s]	Rtm [N]	Lk [m]	Lc [m]	S [m^2]	Trim [deg]	RCG [mm]
118	0.917	3.210	1.56	1.56	0.555	0.3	-2.8
119	1.373	12.630	1.56	1.56	0.555	0.7	-7.7
120	1.818	31.180	1.56	1.56	0.555	2.8	-14.0
128	2.021	47.290	1.56	1.56	0.555	5.3	-15.4
121	2.265	55.530	1.26	1.47	0.524	6.6	-12.0
122	2.731	59.820	1.13	1.43	0.491	7.0	-3.3
123	3.190	85.390	1.05	1.37	0.461	8.2	6.8
124	3.848	72.580	0.98	1.29	0.432	9.5	21.3
125	4.111	78.440	0.91	1.24	0.205	10.0	39.5

model 232-B

Disp [N]	LCG [%Lp]	Ap/V [-]
381.22	-8	4.0

run [-]	vm [m/s]	Rtm [N]	Lk [m]	Lc [m]	S [m^2]	Trim [deg]	RCG [mm]
110	0.916	3.880	1.13	1.51	0.506	0.4	-2.8
111	1.372	12.720	1.56	1.56	0.555	1.0	-7.1
112	1.817	34.920	1.32	1.47	0.528	3.8	-13.6
113	2.273	62.940	1.13	1.39	0.484	7.4	-10.3
114	2.731	88.970	1.05	1.32	0.444	8.1	0.4
115	3.187	75.990	0.94	1.23	0.405	9.3	12.7
116	3.649	91.870	0.83	1.05	0.367	10.0	34.0

model 232-B

Disp [N]	LCG [%Lp]	Ap/V [-]
381.22	-12	4.0

run [-]	vm [m/s]	Rtm [N]	Lk [m]	Lc [m]	S [m^2]	Trim [deg]	RCG [mm]
104	0.917	4.750	1.05	1.46	0.485	0.5	-2.4
105	1.363	13.020	1.20	1.47	0.514	1.3	-7.2
106	1.829	40.620	1.13	1.41	0.467	4.6	-14.2
107	2.284	78.600	0.98	1.26	0.424	8.3	-9.8
108	2.732	88.770	0.91	1.16	0.393	9.5	2.8
109	3.201	79.320	0.91	1.13	0.386	10.0	-0.3

Appendix 4 :Coefficients of twisted bottom polynomial model

Fn_∇		a_0	a_1	a_2	a_3	a_4	a_5
		a_6	a_7				
.75	$\Delta R_t/\Delta$, ∇=5	.4983E-03	-.1485E-03	-.1233E-03	.2533E-05	.1277E-04	-.1850E-04
		.1597E-04	.4245E-05				
	$\Delta R_t/\Delta$, ∇=50	.4209E-03	-.1563E-03	-.9512E-04	.1984E-05	.1354E-04	-.1906E-04
		.1309E-04	.4288E-05				
	$\Delta\theta$	-.4610E-01	.4631E-01	.1214E-01	-.1037E-01	-.3454E-02	-.6250E-03
		-.8404E-03	-.6243E-03				
	$\Delta RCG/\nabla^{1/3}$	.3776E-02	-.9268E-04	-.1424E-02	-.1246E-03	.9463E-05	.1850E-06
		.1331E-03	-.3086E-05				
1.00	$\Delta R_t/\Delta$, ∇=5	-.7109E-02	.4784E-03	.2702E-02	-.7780E-05	-.1321E-03	-.5580E-04
		-.2408E-03	-.6455E-05				
	$\Delta R_t/\Delta$, ∇=50	-.7171E-02	.4771E-03	.2730E-02	-.8632E-05	-.1333E-03	-.5657E-04
		-.2446E-03	-.6400E-05				
	$\Delta\theta$	-.7175E+00	.9020E-01	.2028E+00	.1298E-03	-.7746E-02	.5703E-03
		-.1607E-01	-.1538E-03				
	$\Delta RCG/\nabla^{1/3}$	-.3234E-02	.5587E-03	.1200E-02	.3996E-04	-.7873E-04	.4558E-06
		-.7148E-04	.1229E-04				
1.25	$\Delta R_t/\Delta$, ∇=5	-.1611E-01	.6872E-03	.5469E-02	-.3476E-03	-.2235E-03	-.3902E-04
		-.4749E-03	-.4774E-04				
	$\Delta R_t/\Delta$, ∇=50	-.1611E-01	.6947E-03	.5484E-02	-.3426E-03	-.2256E-03	-.3927E-04
		-.4779E-03	-.4737E-04				
	$\Delta\theta$	-.1492E+01	.1383E+00	.4799E+00	-.5107E-02	-.1694E-01	-.8203E-04
		-.4096E-01	-.1271E-02				
	$\Delta RCG/\nabla^{1/3}$	-.2576E-02	.2884E-03	-.6448E-04	-.1077E-03	.1450E-05	-.1085E-04
		.9325E-04	.3125E-05				
1.50	$\Delta R_t/\Delta$, ∇=5	-.1156E-01	.1010E-02	.4347E-02	-.7582E-04	-.2816E-03	-.2185E-04
		-.3944E-03	-.4035E-04				
	$\Delta R_t/\Delta$, ∇=50	-.1153E-01	.1002E-02	.4325E-02	-.7148E-04	-.2804E-03	-.2218E-04
		-.3924E-03	-.3996E-04				
	$\Delta\theta$	-.1747E+01	.1264E+00	.5078E+00	-.8632E-02	-.1203E-01	.2301E-02
		-.3979E-01	-.1961E-02				
	$\Delta RCG/\nabla^{1/3}$	-.1265E-01	.1279E-02	.4050E-02	-.3522E-03	-.1449E-03	.9500E-05
		-.3254E-03	-.2848E-04				
1.75	$\Delta R_t/\Delta$, ∇=5	-.1781E-01	-.2777E-02	.3988E-02	.1913E-02	.3926E-03	.1714E-03
		-.4276E-04	.6918E-05				
	$\Delta R_t/\Delta$, ∇=50	-.1781E-01	-.2802E-02	.3962E-02	.1923E-02	.3985E-03	.1724E-03
		-.3853E-04	.7212E-05				
	$\Delta\theta$	-.2105E+01	.8404E-01	.5106E+00	-.1442E-01	-.6604E-03	.9035E-02
		-.3282E-01	-.5075E-02				
	$\Delta RCG/\nabla^{1/3}$	-.1976E-01	-.3741E-03	.4480E-02	.1019E-03	.2446E-03	.1656E-03
		-.1706E-03	-.4848E-04				

Fn_∇		a_0	a_1	a_2	a_3	a_4	a_5
		a_6	a_7				
2.00	$\Delta R_t/\Delta$, ∇=5	-.1896E-01	-.1133E-02	.5922E-02	.2811E-02	-.8412E-04	.9948E-05
		-.3640E-03	.7771E-04				
	$\Delta R_t/\Delta$, ∇=50	-.1891E-01	-.1142E-02	.5881E-02	.2814E-02	-.8078E-04	.1088E-04
		-.3603E-03	.7762E-04				
	$\Delta\theta$	-.2695E+01	.1853E+00	.6910E+00	-.6575E-01	-.1953E-01	.8210E-02
		-.5452E-01	-.9311E-02				
	$\Delta RCG/\nabla^{1/3}$	-.5989E-01	.2930E-02	.1785E-01	-.1535E-02	-.3801E-03	.6120E-04
		-.1412E-02	-.1650E-03				
2.25	$\Delta R_t/\Delta$, ∇=5	-.3588E-01	.1388E-03	.1107E-01	.3152E-02	-.3984E-03	-.1834E-04
		-.8323E-03	.1092E-03				
	$\Delta R_t/\Delta$, ∇=50	-.3725E-01	.3245E-03	.1161E-01	.3158E-02	-.4257E-03	-.1554E-04
		-.8867E-03	.1081E-03				
	$\Delta\theta$	-.1525E+01	-.1723E-01	.1660E+00	.2115E-01	.5883E-02	.1806E-02
		-.5244E-02	.3020E-03				
	$\Delta RCG/\nabla^{1/3}$	-.6100E-01	.9271E-03	.1565E-01	-.2120E-03	-.1254E-03	.8236E-04
		-.1101E-02	-.1095E-03				
2.50	$\Delta R_t/\Delta$, ∇=5	-.5260E-02	-.3146E-02	-.2567E-02	.3263E-02	.1492E-04	-.1185E-03
		.4338E-03	.1739E-03				
	$\Delta R_t/\Delta$, ∇=50	-.5245E-02	-.3185E-02	-.2639E-02	.3267E-02	.2341E-04	-.1145E-03
		.4400E-03	.1723E-03				
	$\Delta\theta$	-.2302E+00	.3193E-01	-.1812E+00	-.1211E-01	-.1979E-02	.2759E-03
		.1277E-01	-.2276E-03				
	$\Delta RCG/\nabla^{1/3}$	-.1935E-01	.1547E-02	.2596E-02	-.3649E-03	-.3085E-03	.1805E-04
		-.2492E-03	-.8810E-04				
2.75	$\Delta R_t/\Delta$, ∇=5	-.3454E-01	-.6475E-02	.1387E-02	.1848E-02	.3588E-03	-.3693E-03
		.3447E-03	.2075E-03				
	$\Delta R_t/\Delta$, ∇=50	-.3502E-01	-.6477E-02	.1490E-02	.1836E-02	.3595E-03	-.3669E-03
		.3317E-03	.2062E-03				
	$\Delta\theta$	.4111E-01	.7245E-01	-.1804E+00	.7383E-02	-.6458E-02	.7109E-02
		.6386E-02	-.2195E-02				
	$\Delta RCG/\nabla^{1/3}$	-.1573E-01	.1805E-02	.8777E-03	-.2462E-03	-.3616E-03	.6562E-04
		-.1874E-03	-.8928E-04				
3.00	$\Delta R_t/\Delta$, ∇=5	.1001E-01	-.5544E-02	-.1342E-01	.1636E-02	.1327E-03	-.5689E-03
		.1475E-02	.3445E-03				
	$\Delta R_t/\Delta$, ∇=50	.8563E-02	-.5354E-02	-.1287E-01	.1634E-02	.1020E-03	-.5691E-03
		.1413E-02	.3475E-03				
	$\Delta\theta$	-.1607E+01	.1098E+00	.3775E+00	.1483E-01	-.1283E-01	.1036E-01
		-.3977E-01	-.2998E-02				
	$\Delta RCG/\nabla^{1/3}$	-.7659E-02	.1821E-02	-.9599E-03	-.2954E-03	-.3330E-03	.7094E-04
		-.1434E-03	-.7165E-04				

A CALCUL[illegible]
SIMILAR SYSTEMATIC SERIES

J.A. Keuning*, J. Gerritsma**, and P.F. van Terwisga*

* *Delft University of Technology, Ship Hydromechanics Laboratory, Delft, The Netherlands*
** *Professor, emeritus, Delft University of Technology, Ship Hydromechanics Laboratory, Delft, The Netherlands*

Int. Shipbuild. Progr., **40**, no. 424 (1993) pp. 333–385

Received: December 1992
Accepted: February 1993

In addition to the well-known systematic series planing hull forms with a deadrise angle of 12.5° as presented by Clement and Blount (DTMB), and a similar series by Keuning and Gerritsma, in this paper the results of the tests on a 30° deadrise series are presented.

The combined data of these three series are fitted to a regression model for total resistance, trim and rise of centre of gravity. This regression model is verified by a comparison with existing model data. Although in general the calculations show good agreement with experiments, the need for additional data for a deadrise angle between 12.5 and 25° became obvious.

Additional resistance test results of two models with varying deadrise and rising buttock lines in the aft part of the hull are presented. Regression of these data results in simple expressions to take these effects into account.

Nomenclature

A_p	projected planing bottom area [m^2]
B_{pa}	breadth over chines [m]
B_{pt}	breadth over chines at transom [m]
B_{px}	maximum breadth over chines [m]
C_{Ap}	centre of A_p [% L_p]
Fn_∇	volumetric Froude number $v/\sqrt{g\nabla^{1/3}}$
g	gravity acceleration [m/s^2]
LCG	longitudinal centre of gravity [%L_p]

L_c	wetted length over the chines [m]
L_k	wettend length over the keel [m]
L_p	length of the projected planing bottom area [m]
R_t	total resistance (in towing tank conditions) [N]
RCG	rise of centre of gravity relative to its position at zero speed [m]
v	speed [m/s]
β	deadrise angle [deg]
γ	average centreline angle from ordinate 0 to 10 with respect to the baseline positive for a draft at ordinate 0 greater than draft at ordinate 10 [deg]
ϵ	twist angle, i.e., deadrise at ordinate 10 minus the deadrise at ordinate 0 [deg]
Δ	weight of displacement [N]
$\Delta R_t/\Delta$	difference in R_t/Δ of twisted bottom model and 25^o parent model for equal loading coefficient and LCG values
$\Delta\theta$	difference in trim angle of twisted bottom model and 25^o parent model for equal loading coefficient and LCG values
$\Delta RCG/\nabla^{1/3}$	difference in $RCG/\nabla^{1/3}$ of twisted bottom model and 25^o parent model for equal loading coefficient and LCG values
θ	trim angle relative to its value at zero speed, positive for an upward displaced bow [deg]
∇	volume of displacement [m^3]

1. Introduction

In 1963 E.P. Clement and D.L. Blount presented the results of resistance tests of a systematically varied series of planing hull forms, generally known as the TMB Series 62 or the Clement series [1]. The models in this series all had a deadrise of 12.5^o. The need for better seakeeping characteristics lead to increasing deadrise angles, although this also lead to an increase of the resistance of the planing ship. To give more insight into this trade off between resistance and seakeeping quality of a particular design, in 1982, Keuning and Gerritsma published the results of a series of planing hull forms, similar to those of Clement and Blount, with higher deadrise, i.e., 25^o [2]. These results showed that the increase in resistance is highest for low L_p/B_{px} ratios and independent of the loading coefficient, defined as the ratio of projected chine area and the volume of displacement to the power 2/3. The loading coefficient does have a marked influence on the hump resistance, i.e., is highest for low loading coefficients.

Apart from the resistance data, the trim and rise of centre of gravity appeared to be of great importance for the assessment of seakeeping characteristics. In [3]

Keuning shows that the still water resistance [illegible] be neglected in the calculations of the motions of these craft in waves.

The models of the 25^o deadrise series were varied in their main parameters in the same way as the Clement and Blount series to obtain a systematic experimental set of data. The parent model for this series was similar to the parent model of the 12.5^o series as much as possible.

In addition to these tests a new parent model with a deadrise of 30^o was developed and tested in a similar way. This new parent model and the L_p/B_{px} variations derived herefrom are described in subsequent sections. Experimental data on resistance, trim and rise of centre of gravity are listed.

The data ranging from a Froude coefficient based on volume of displacement 0.75 to 3.0 and a deadrise of 12.5 to 30^o, are represented by polynomials. These offer a quick and easy method of interpolating the resistance, trim and sinkage of any arbitrary planing hull form.

The polynomial representation of the Planing Hull Form series is verified by comparison with some model test results of the series and model test results of three arbitrary hull forms tested in the Delft University of Technology facilities, i.e., the towing tank of the Ship Hydromechanics Laboratory.

To account for non-prismatic hull forms, two models with twisted bottoms have been derived from the 25^o parent hull. For both models, the deadrise varied from 25^o at ordinate 10 to 5^o at the transom. The slope of the buttock lines in the aft bodies varies with respect to the 25^o parent hull. Results of these tests are listed. The difference in resistance, trim, and rise of centre of gravity of the constant deadrise hull form and the twisted bottom hull form is expressed in simple polynomials.

2. SET-UP OF THE SERIES

For the 25^o and 30^o deadrise angle a parent model has been developed based on the parent model of Clement and Blount. To keep the design as much the same as possible the following parameters have been kept the same:

- the length over the chine
- the maximum breadth over the chine and the vertical projection of the chine
- the vertical projection of the deck line
- the keel line, except from ordinate 16 forwards where the contour has been lifted upwards to obtain the proper length over the chine
- the transom slope
- the length of the prismatic part of the hull.

Also, all models consisted entirely of developable surfaces, just as the Clement parent hull form. The main particulars of the parent models are listed in Table 1. The body plan of the 30^o deadrise parent model is presented in Figure 1.

Table 1. Main particulars of parent models.

β	30	25	12.5	degrees
L_p	1.5	1.5	2.436	m
B_{pa}	0.3	0.3	0.487	m
B_{px}	0.367	0.367	0.596	m
B_{pt}	0.235	0.235	0.381	m
L_p/B_{pa}	5.0	5.0	5.0	-
L_p/B_{px}	4.087	4.087	4.09	-
B_{px}/B_{pa}	1.22	1.22	1.22	-
B_{pt}/B_{px}	0.64	0.64	0.46	-
C_{A_p} rel to ord 0	48.8	48.8	48.8	$\%L_p$

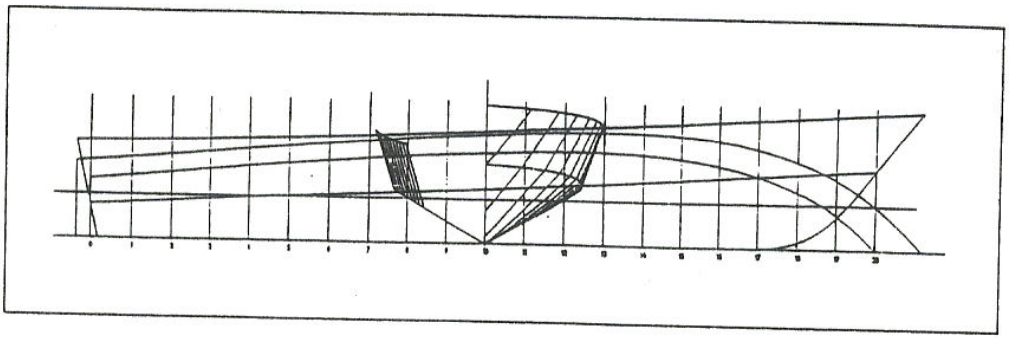

Figure 1. Body plan of the 30° deadrise parent model.

From these parent models, for each deadrise, several other models, with different L_p/B_{px} ratios have been derived. For the 25° deadrise and 30° deadrise models this was done using the affine transformation technique as described a.o. by Versluis [5]. The total series comprised the deadrise – L_p/B_{px} ratio combinations listed in Table 2.

Table 2. L_p/B_{px} ratios for separate series.

β	L_p/B_{px}				
30		3.41	4.09	5.5	7.0
25	2.0	3.06	4.09	5.5	7.0
12.5	2.0	3.06	4.09	5.5	7.0

way as had been done by Clement for the 12.5° deadrise series model to generate a design which is more alike an actual craft with a low L_p/B_{px} ratio (usually small pleasure crafts, which are propelled by either the outboard engine on the transom or the inboard-outboard type of engine) and which needs more volume of displacement aft than would result from the linear transformation of the parent model.

The body plans of the three L_p/B_{px} variants of the 30^o series parent model are shown in Figures 2 to 4. The main particulars are listed in Table 3.

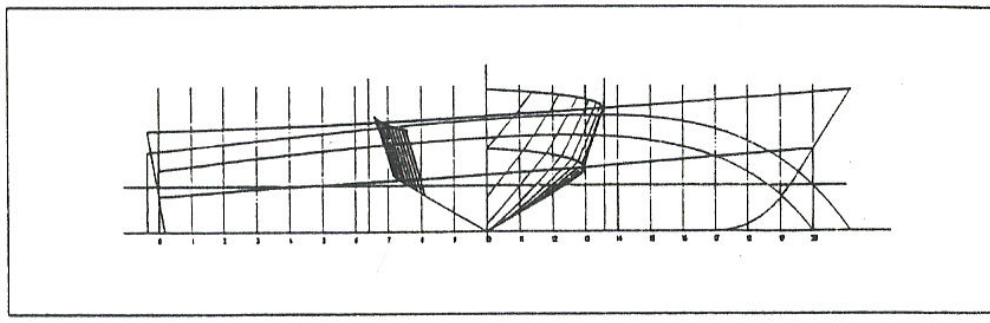

Figure 2. Body plan for $L_p/B_{px} = 3.41$.

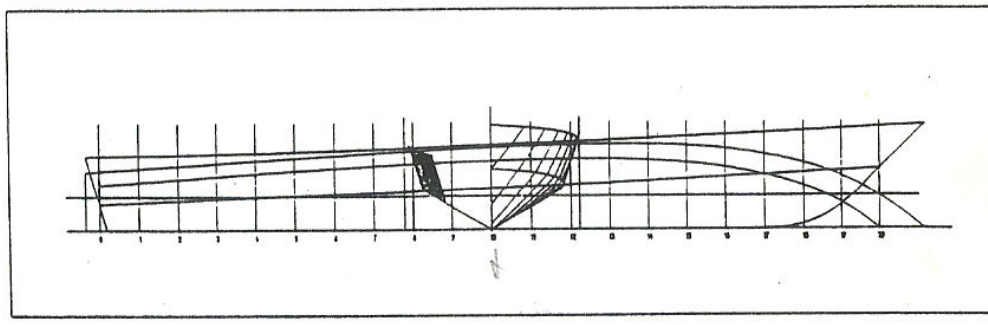

Figure 3. Body plan for $L_p/B_{px} = 5.5$.

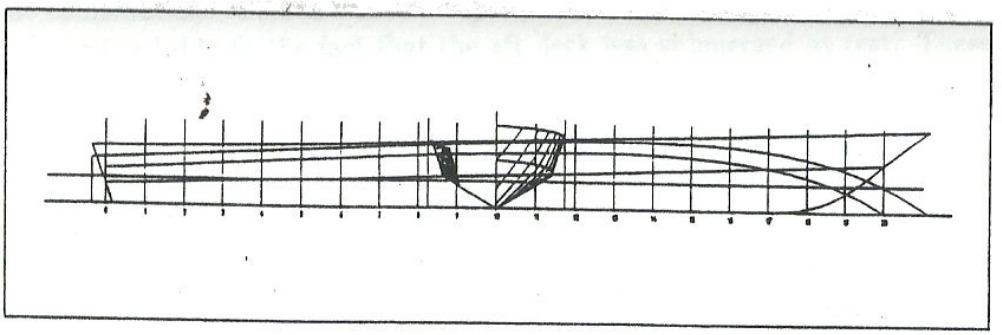

Figure 4. Body plan for $L_p/B_{px} = 7$.

Table 3. Main particulars of L_p/B_{px} variations.

L_p/B_{px}	3.41	4.09	5.5	7.0	-
L_p	1.25	1.5	1.5	1.5	m
A_p	0.3843	0.4499	0.3346	0.2627	m^2
B_{pa}	0.3	0.3	0.223	0.175	m
B_{px}	0.367	0.367	0.273	0.214	m
B_{pt}	0.26	0.235	0.175	0.137	m
L_p/B_{pa}	4.17	5.0	6.726	8.571	-
B_{px}/B_{pa}	1.22	1.22	1.22	1.22	-
B_{pt}/B_{px}	0.71	0.64	0.64	0.64	-
C_{A_p} rel to ord 0	47.9	48.8	48.6	48.6	$\%L_p$

The shaft centrelines are shown in the body plans. The same shaft rakes and clearances as described by Clement and Blount have been used here.

The models had spray strips attached over the entire length of the chine. The bottom of the spray strip followed the line of bottom of the model from ordinate zero (transom) to ordinate 10 and was horizontal from ordinate 12 to ordinate 20 (the stern) with a transition region from ordinate 10 to ordinate 12. The width of the spray strips are approximately 4 mm and they had non-radiused edges.

The models have been constructed of GRP, which enabled through-hull photography, used for the determination of the wetted surface and wetted length of the keel and chine of the craft at speed.

3. EXPERIMENTAL SET-UP

The tests have been carried out in the no. 1 towing tank of the Ship Hydromechanics Laboratory of the Delft University of Technology. The dimensions of this tank are: length 142 m, breadth 4.22 m, and waterdepth 2.5 m.

The models have been connected to the towing tank carriage in such a way that they were free to heave and pitch but restrained in all other modes of motion. The pivot of the construction was located at the intersection of the assumed centreline of the shaft and the cross-section at the LCG. The resistance was measured by means of a strain gauge dynamometer. Pitch and heave have been measured by means of 2 wire over potentiometers on the stern and the bow of the model. The values of resistance, sinkage and trim are the integrated mean values over the duration of the test run, typically 10 sec.

During each run a photo has been taken through the transparent bottom of the hull, for the determination of the wetted length and wetted area.

No turbulence stimulators have been used since the model scale and speed were considered to be large enough to yield reliable results. No towing speeds below 1.0 m/s were used.

4. Measurement scheme

For the 30^o deadrise series, 4 L_p/B_{px} ratios have been developed including the parent model. For each of these L_p/B_{px} ratios each possible combination of the loading coefficients $A_p/\nabla^{2/3}$ (4, 5.5, 7, and 8.5) and the longitudinal position of the centre of gravity (0, 2, 4, and 8% of L_p aft of the Centroid of A_p) were tested in the speed range of Fn_∇ 0.75 to 3.0. The total number of test runs of the 30^o deadrise series was approximately 570.

5. Results of the 30^o deadrise tests

The results of the experiments are presented in Appendix 1. For every L_p/B_{px}, $A_p/\nabla^{2/3}$, and LCG combination as a function of model speed are listed:

- the total resistance of the model R_{tm}
- the wetted length over the keel L_k
- the wetted length over the chines L_c
- the trim angle, positive for an upward displaced bow, relative to the position at $v_m = 0$
- the rise of the centre of gravity (positive for upward displacement) relative to its position at $v_m = 0$.

Some combinations of small values of $A_p/\nabla^{2/3}$ and LCG 8% aft of Centroid A_p have been omitted due to the fact that the aft deck was submerged at rest. These situations were considered to be impractical.

6. Polynomial model of experimental data

Based on the experimental results, polynomial expressions have been formulated to approximate the total resistance, the trim angle and the rise of centre of gravity of the planing hull. The expressions are dependent of the L_p/B_{px} ratio, the loading coefficient $A_p/\nabla^{2/3}$, and the longitudinal centre of gravity LCG and fitted to separate datasets for every deadrise-Fn_∇ combination. Describing the (non-dimensional) resistance, trim and (non-dimensional) sinkage for a number of discrete values of Fn_∇ proved to give a better fit than the description of these parameters by means of one polynomial for the entire speed range.

The total resistance of the planing hull can be predicted by interpolating the R_t/Δ fitted to separate datasets, each containing the total model resistance scaled to a different volume of displacement. Separating the total model resistance into a residual resistance coefficient and a wetted length and wetted surface would have reduced the number of fitted coefficients, but also reduces the accuracy of the resistance prediction. Sets of coefficients have been determined for a volume of displacement ranging from 2.5 m^3 to 5000 m^3. For the expansion of the resistance data, use has been made of the ITTC '57 friction line.

The polynomials have the following form:

$$\left.\begin{matrix} R_t/\Delta \\ \theta \\ RCG/\nabla^{1/3} \end{matrix}\right\} = \begin{aligned} & a_0 + a_1\ L_p/B_{px} + a_2\ L_p/B_{px}^2 + a_3\ L_p/B_{px}^3 + a_4\ A_p/\nabla^{2/3} + \\ & a_5\ A_p/\nabla^{2/3^2} + a_6\ A_p/\nabla^{2/3^3} + a_7\ LCG + a_8\ LCG^2 + \\ & a_9\ LCG^3 + a_{10}\ LCG\ A_p/\nabla^{2/3} + a_{11}\ L_p/B_{px}\ A_p/\nabla^{2/3} + \\ & a_{12}\ LCG\ L_p/B_{px}. \end{aligned} \tag{1}$$

Appendix 2 contains 120 sets of coefficients $a_0 \ldots a_{12}$, i.e., for every deadrise, volumetric Froude number combination, two sets for R_t/Δ for a volumes of displacement of 5 m^3 and 50 m^3 [1)], a set for trim angle, and a set for $RCG/\nabla^{1/3}$.

[1)] To minimize the amount of listed coefficients, the R_t/Δ coefficients are given for two volumes of displacement. The complete set of coefficients for R_t/Δ ranging from 2.5 m^3 to 5000 m^3 are obtainable at the Delft University of Technology, Ship Hydromechanics Laboratory.

7. Verification of the polynomial model

The goodness of fit of the polynomial expressions is demonstrated in the Figures 10 to 18 for three respective models of the systematic series. The deadrise, L_p/B_{px}, $A_p/\nabla^{2/3}$, and LCG parameters of these models, based on a medium, light and heavy weight of displacement, are listed in Table 4.

Table 4. Models used to validate polynomial results.

model	β	L_p/B_{px}	$A_p/\nabla^{2/3}$	LCG
PHF1	25	5.5	5.5	-4
PHF2	25	5.5	8.5	-12
PHF3	25	2.0	4.0	0

The largest discrepancies occur for the heavy model with low L_p/B_{px} value. The total resistance is underpredicted in the speed region below Fn_∇ 1.75 and overpredicted for higher speeds. Also for this model, the trim calculation underpredicts the measured values for speeds higher than Fn_∇ 1.25. The RCG values agree satisfactory for these three models.

To validate the polynomials for the use in predicting the resistance trim and sinkage of arbitrary planing ships, three models tested at the Delft University of Technology, Ship Hydromechanics Laboratory, were used for a comparison with the polynomial results. In Figures 5 to 7 the body plans of a coastal patrol vessel, a planing motor yacht (R410) and a coastal rescue boat are shown. The main dimensions of these craft are listed in Tables 5 to 7.

In Figures 19 to 27 both measured and calculated results are presented for these three vessels. Also in these cases the prediction is reasonably accurate.

It appeared, however, that the interpolation of the 12.5 and 25^o deadrise for the patrol boat, as well as for the motor yacht resulted in a better fit to experiments when a linear interpolation with respect to deadrise angle β was used instead of a quadratic interpolation over all available data. Since many planing vessels designed for operation in coastal areas have deadrise angles close to 20^o, the influence of deadrise on resistance trim and sinkage in the range of 12.5^o to 25^o needs to be investigated more extensively. Therefore, it was decided to test an additional 19^o deadrise series in the Delft towing tank facilities in the near future.

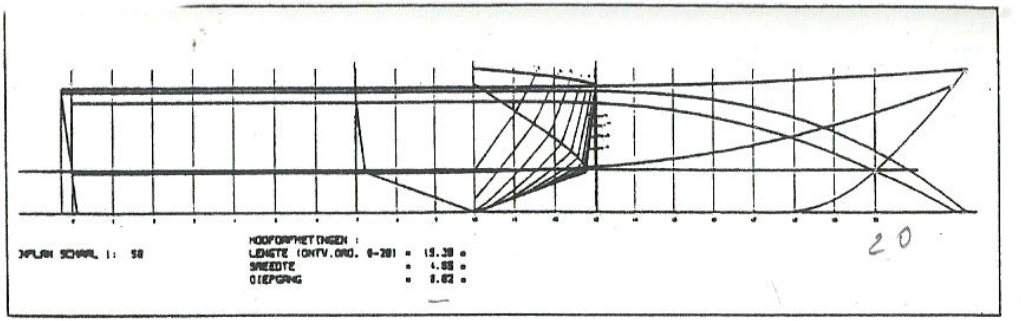

Figure 5. Body plan of coastal patrol vessel.

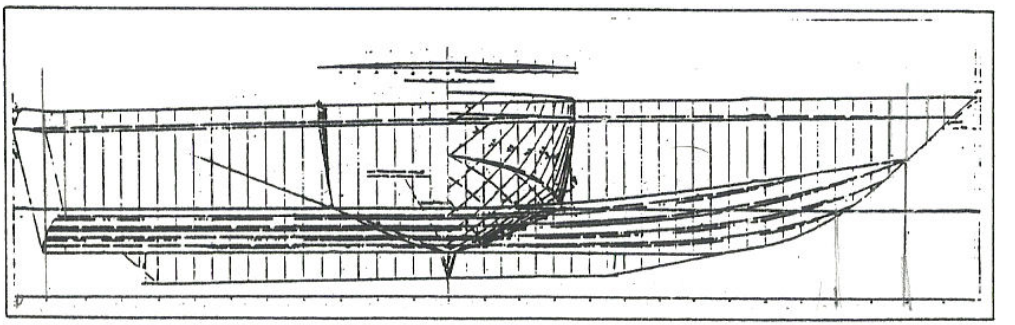

Figure 6. Body plan of motor yacht R410.

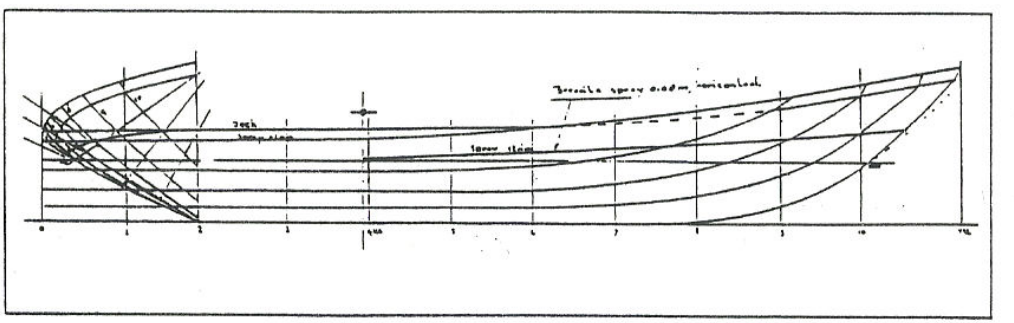

Figure 7. Body plan of coastal rescue boat.

Table 5. Main dimensions patrol vessel. R 409

L_p	16.8	m
B_{px}	4.22	m
A_p	60.5	m^2
∇	23.7	m^3
C_{A_p} rel to ord 0	39.3	$\%L_p$
β	20	deg.
L_p/B_{px}	4.0	-
$A_p/\nabla^{2/3}$	7.36	-
LCG rel to C_{A_p}	-3.9	$\%L_p$

Table 6. Main dimensions motor yacht R410.

L_p	19.2	m
B_{px}	5.05	m
A_p	84.3	m^2
∇	44.9	m^3
C_{A_p} rel to ord 0	45.8	$\%L_p$
β	21	deg.
L_p/B_{px}	3.8	-
$A_p/\nabla^{2/3}$	6.67	-
LCG rel to C_{A_p}	-5.31	$\%L_p$

Table 7. Main dimensions coastal rescue boat. R 411

L_p	11.21	m
B_{px}	3.30	m
A_p	35.3	m^2
∇	13.3	m^3
C_{A_p} rel to ord 0	36.9	$\%L_p$
β	26	deg.
L_p/B_{px}	3.3	-
$A_p/\nabla^{2/3}$	6.3	-
LCG rel to C_{A_p}	-4.8	$\%L_p$

8. Twisted bottom models

Many planing hull form designs do not have the prismatic aft body of the parent models of the previously described series, but show a variation in deadrise angle over the length and rising centreline in the aft part of the hull, which allows the propeller shaft to have a lower inclination angle. To investigate the possible influence of these effects on resistance, trim and sinkage, two models with a strong resemblance to the 25^o deadrise parent model have been tested in the speed range Fn_∇ 0.75 ... 3 [4].

Both models have a twisted bottom, i.e., a deadrise variation of 25^o at ordinate 10 to 5^o deadrise at ordinate 0. The two models had a different centreline, however. For model 232-A the average inclination angle of the centreline is -4.9^o, whereas this angle for model 232-B equals -2.6^o. In order to maintain sufficient buoyancy in the aft body, the width of the chines had to be increased. Although this parameter clearly influences the characteristics of a planing hull and hereby the validity of a comparison of characteristics between the twisted bottom models and the prismatic hull forms, this was accepted to obtain realistic models. The sections forward of ordinate 10 are equal to those of the parent model of the 25^o deadrise series. The body plans of the two models are shown in Figures 8 and 9. Propeller clearances and shaft inclination were equal to those used for the prismatic hull forms. The main particulars of the models are listed in Table 8.

Table 8. Main particulars of twisted bottom models.

	Model		
	232-A	232-B	
L_p/B_{px}	4.09	4.09	-
L_p	1.5	1.5	m
A_p	0.4589	0.4540	m^2
B_{pa}	0.306	0.303	m
B_{px}	0.367	0.367	m
B_{pt}	0.32	0.31	m
L_p/B_{pa}	4.9	4.9	-
B_{px}/B_{pa}	1.2	1.2	-
B_{pt}/B_{px}	0.872	0.844	-
C_{A_p} rel to ord 0	48.8	48.8	$\%L_p$

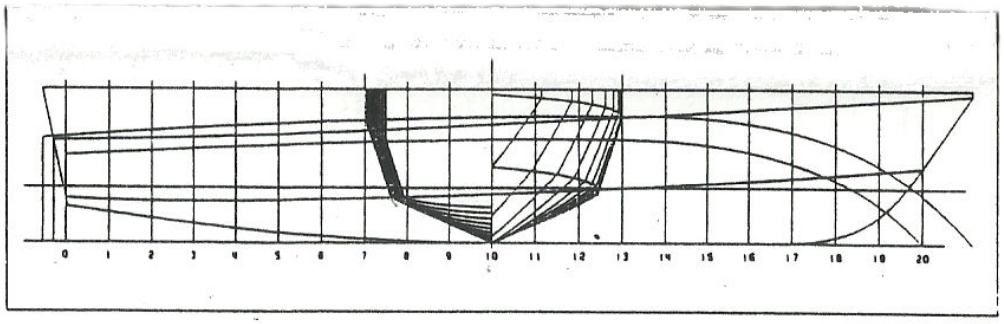

Figure 8. Body plan of twisted bottom model 232-A.

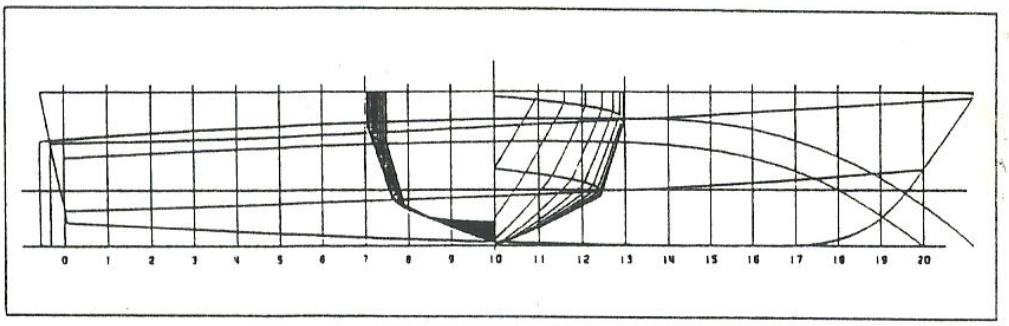

Figure 9. Body plan of twisted bottom model 232-B.

The experimental set-up was equal to the set-up used in the 25 and 30^o deadrise series and described in Section 3.

The measurement scheme was equal to the scheme used for the previously described series, i.e., $A_p/\nabla^{2/3}$ values of 4.0, 5.5, 7.0, 8.5 and LCG values of 0, 4, 8, and 12% L_p aft of the Centroid of A_p.

Some combinations of heavy weight of displacement and position of the centre of gravity were not tested due to excessive trim which caused flooding of the model at rest.

The results of the tests are listed in Appendix 3.

8.1. *Polynomial model of the twisted bottom results*

The effect of twist and rising centreline can be described by the difference in resistance, trim and sinkage of the twisted bottom models and the parent model of the 25^o deadrise series. To ease the work of interpolating the experimental results, these terms are represented by polynomials, in which a linear dependency on the centreline inclination angle γ and the twist angle ϵ, as well as coupling between these angles and the loading coefficient and LCG is assumed. The polynomials have the following

form:

$$\left.\begin{matrix}\Delta R_t/\Delta \\ \Delta\theta \\ \Delta RCG/\nabla^{1/3}\end{matrix}\right\} = \begin{matrix} a_0\,\gamma + a_1\,\epsilon + a_2\,\gamma\,A_p/\nabla^{2/3} + a_3\,\gamma\,LCG + \\ a_4\,\epsilon\,A_p/\nabla^{2/3} + a_5\,\epsilon\,LCG + a_6\,\gamma\,A_p/\nabla^{2/3^2} + \\ a_7\,\gamma\,LCG^2. \end{matrix} \qquad (2)$$

Also in this case, the regression analysis has been performed for separate data sets for each Fn_∇. The experimental $\Delta R_t/\Delta$ values have been scaled to the same weights of displacement as used in Section 6. The polynomial coefficients are listed in Appendix 4 [2].

8.2. *Verification of the twisted bottom polynomial model*

The results of the polynomial approximations are validated by a comparison of calculated and measured values of $\Delta R_t/\Delta$, $\Delta\theta$, and $\Delta RCG/\nabla^{1/3}$. The selected twisted bottom models for this comparion are listed in Table 9.

Table 9. Twisted bottom models used to validate polynomials.

model	$A_p/\nabla^{2/3}$	LCG
232A-1	5.5	0
232A-2	5.5	-8
232B-1	7.0	-4

In Figures 28 to 36 the results of the experiments of the twisted bottom and the 25^o deadrise parent model as well as the experimental difference and its polynomial values are presented. In these figures, $PHF\ exp$ denotes the experimental value of the 25^o deadrise model, $TB\ exp$ denotes the experimental value of a twisted bottom model, $TB\text{–}PHF\ exp$ denotes the difference between these two values, and $TB\text{–}PHF\ polyn$ denotes the polynomial approximation of $TB\text{–}PHF\ exp$. The agreement is in all cases satisfactory for the resistance as well as for the trim and rise of centre of gravity.

[2] To minimize the amount of listed coefficients, the R_t/Δ coefficients are given for two volumes of displacement. The complete set of coefficients for $\Delta R_t/\Delta$ ranging from 2.5 m^3 to 5000 m^3 are obtainable at the Delft University of Technology, Ship Hydromechanics Laboratory.

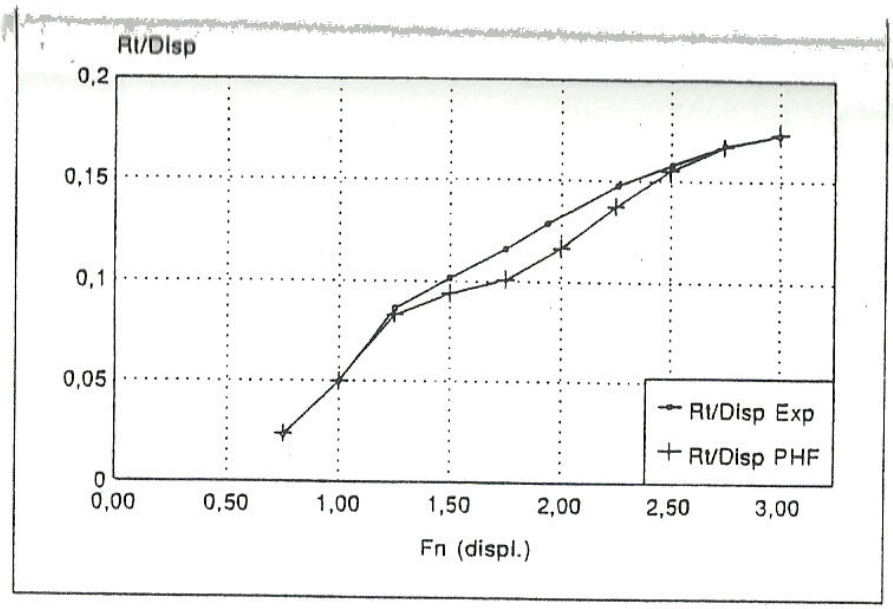

Figure 10. PHF 1 Experimental and calculated R_t/Δ.

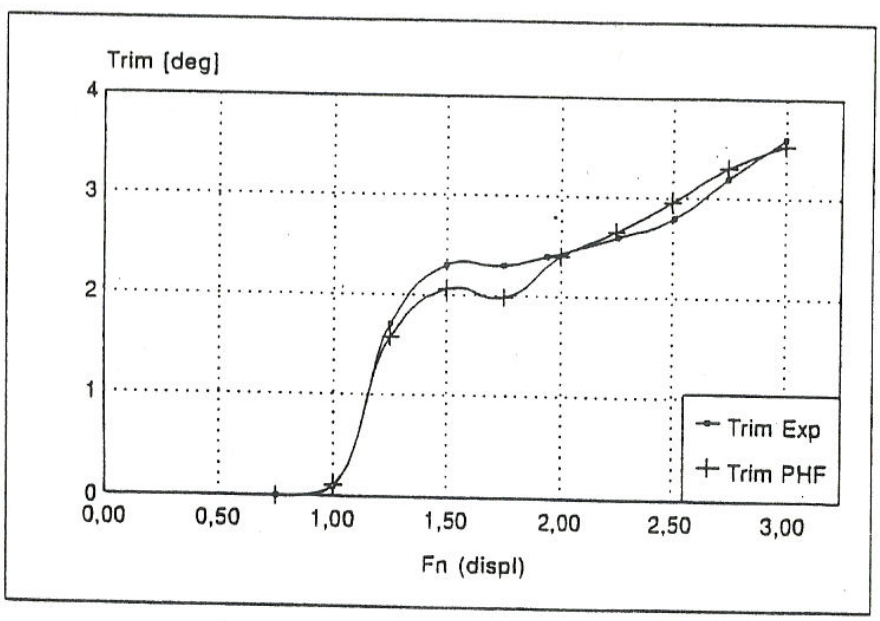

Figure 11. PHF 1 Experimental and calculated trim.

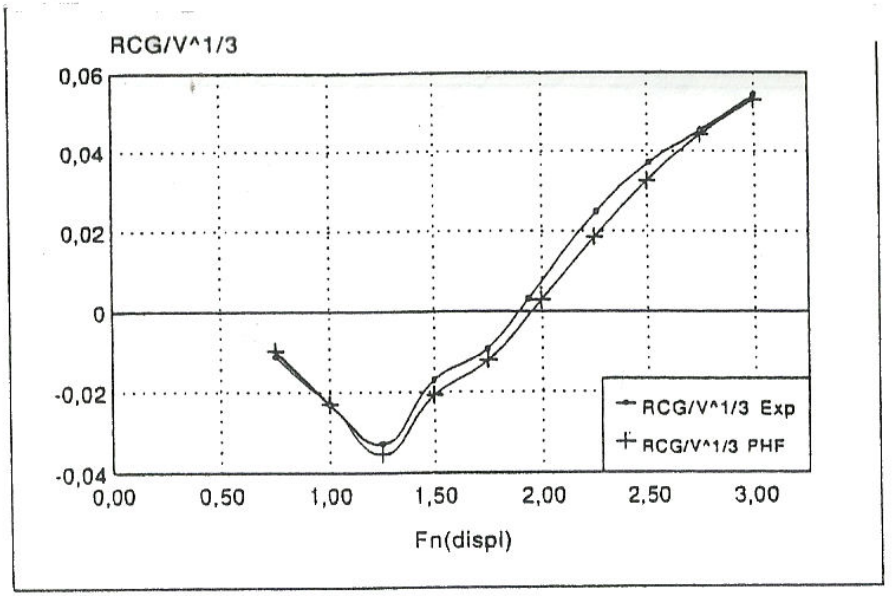

Figure 12. PHF 1 Experimental and calculated $RCG/\nabla^{1/3}$.

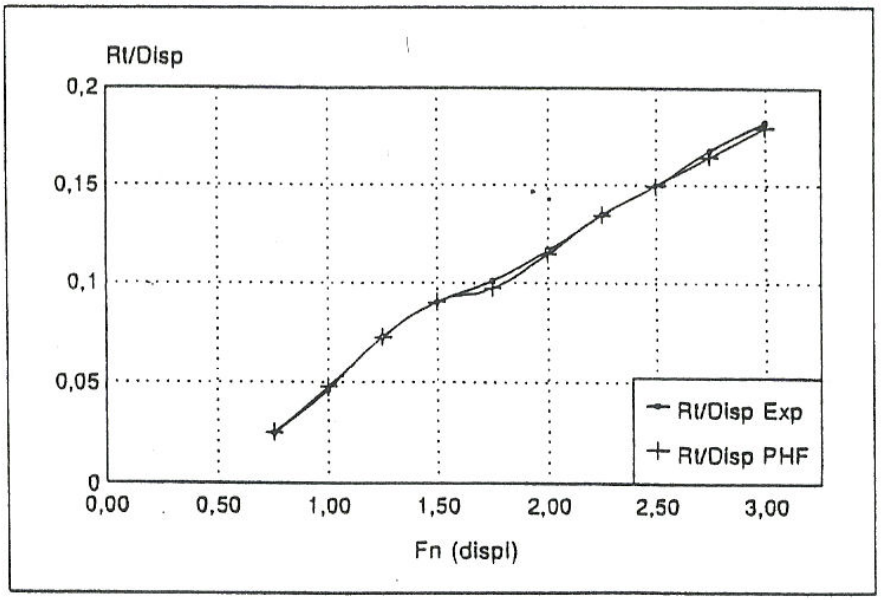

Figure 13. PHF 2 Experimental and calculated R_t/Δ.

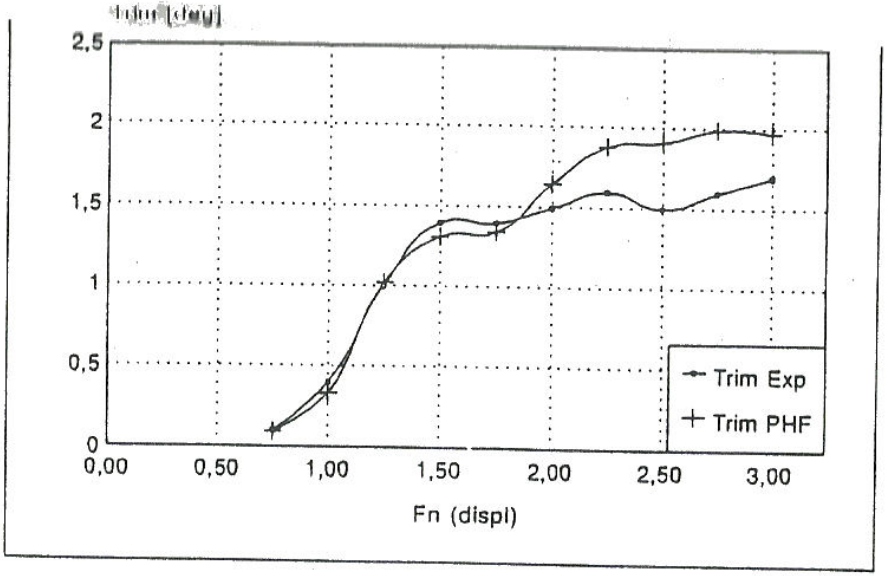

Figure 14. PHF 2 Experimental and calculated trim.

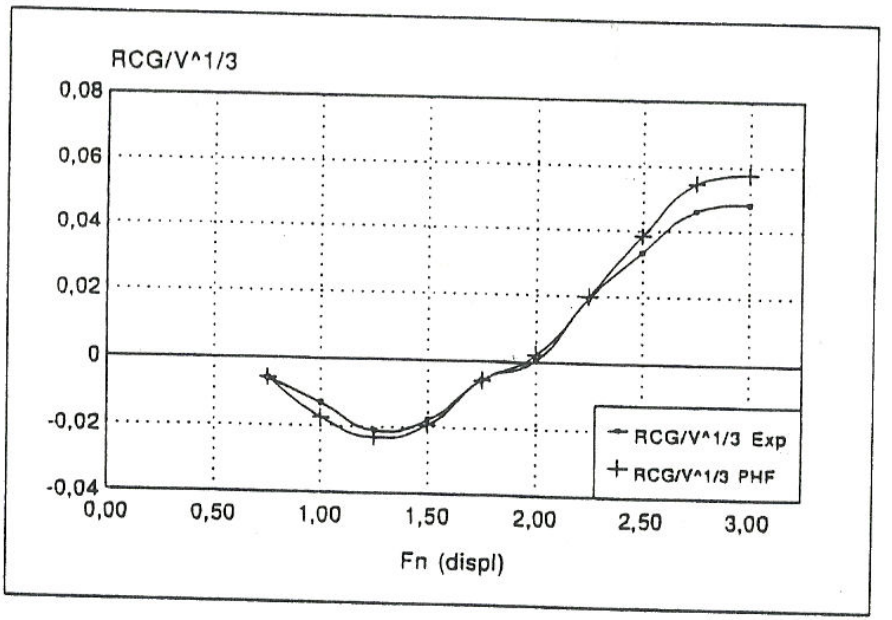

Figure 15. PHF 2 Experimental and calculated $RCG/\nabla^{1/3}$.

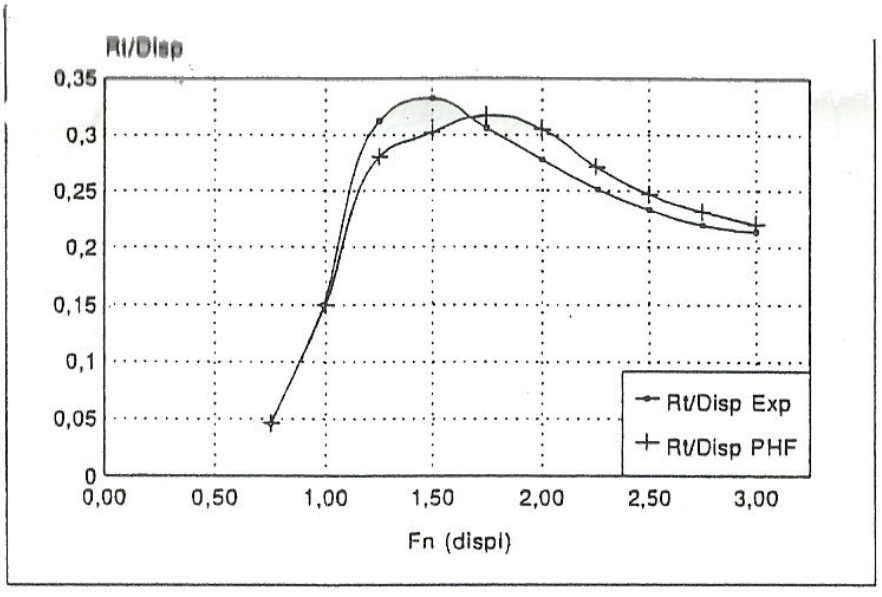

Figure 16. PHF 3 Experimental and calculated R_t/Δ.

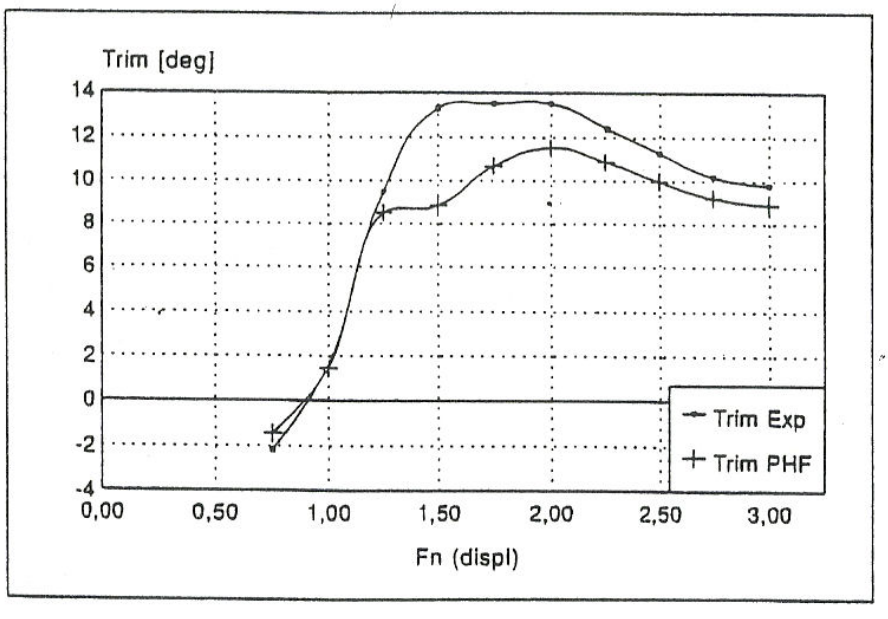

Figure 17. PHF 3 Experimental and calculated trim.

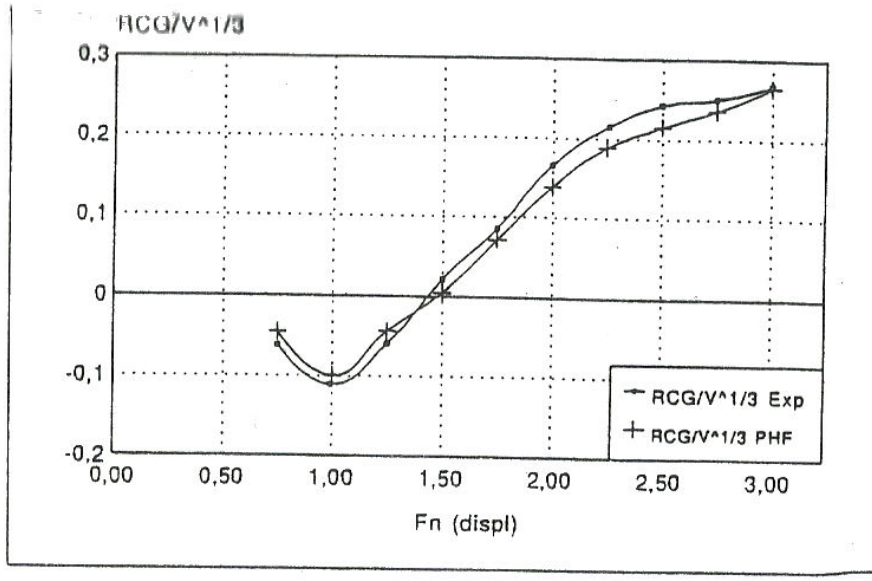

Figure 18. PHF 3 Experimental and calculated $RCG/\nabla^{1/3}$.

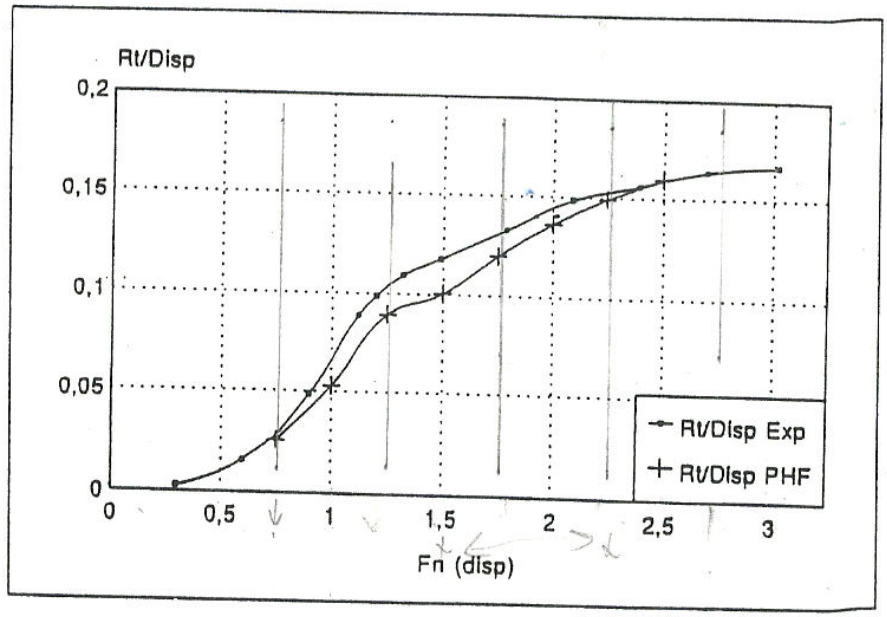

Figure 19. Coastal Patrol Vessel Experimental and calculated R_t/Δ.

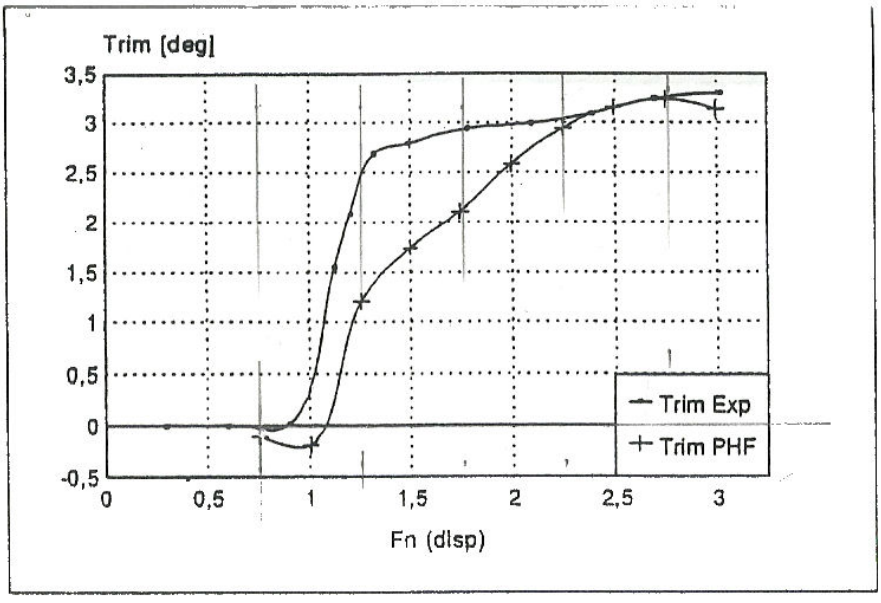

Figure 20. Coastal Patrol Vessel Experimental and calculated trim.

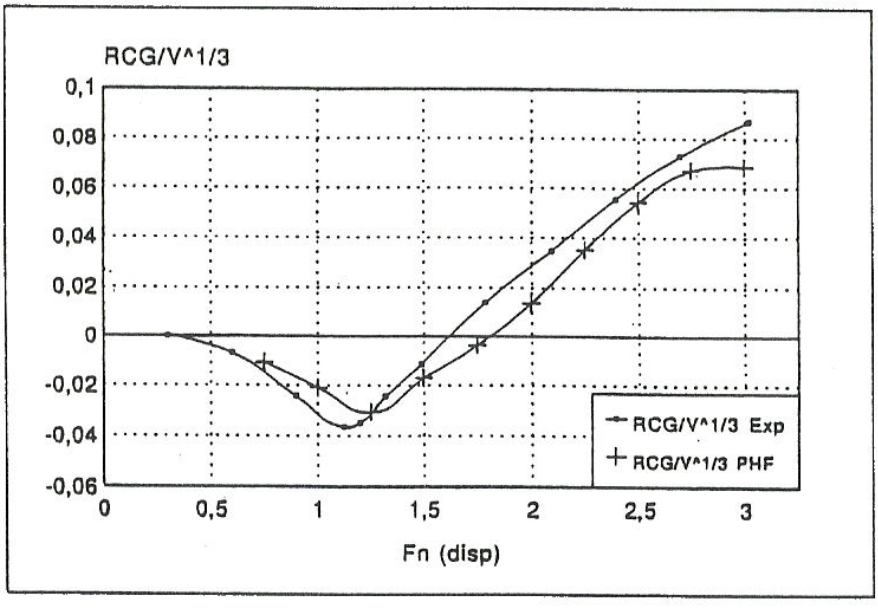

Figure 21. Coastal Patrol Vessel Experimental and calculated $RCG/\nabla^{1/3}$.

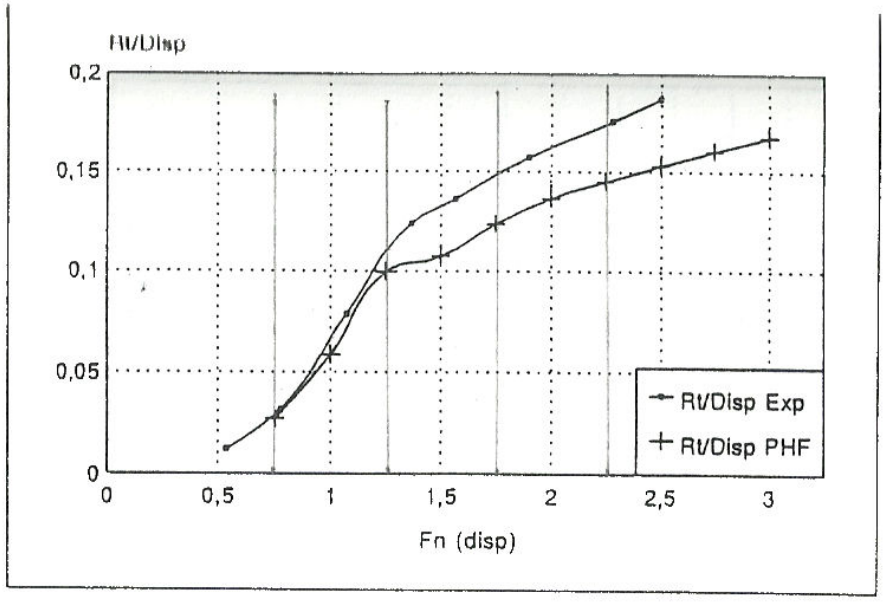

Figure 22. Motor Yacht R410 Experimental and calculated R_t/Δ.

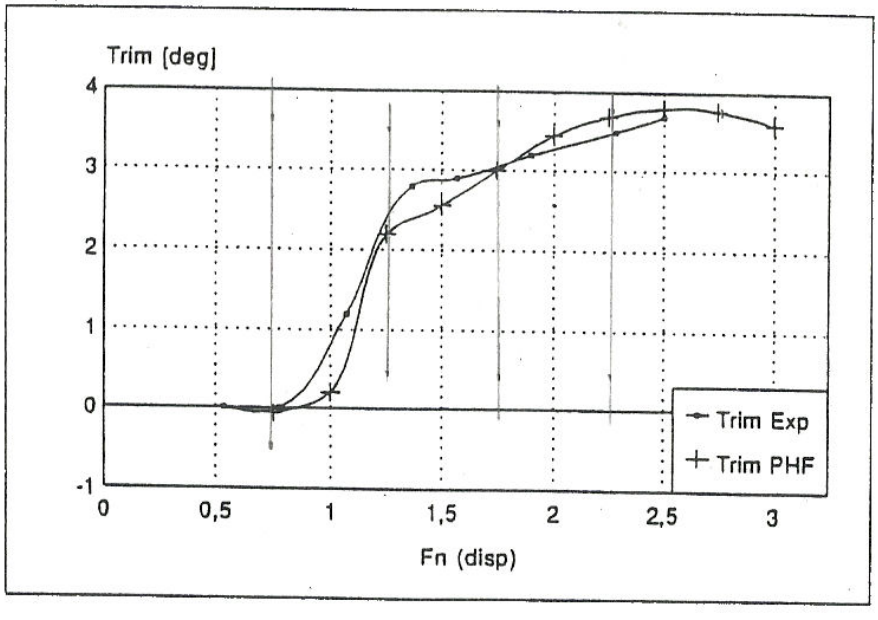

Figure 23. Motor Yacht R410 Experimental and calculated trim.

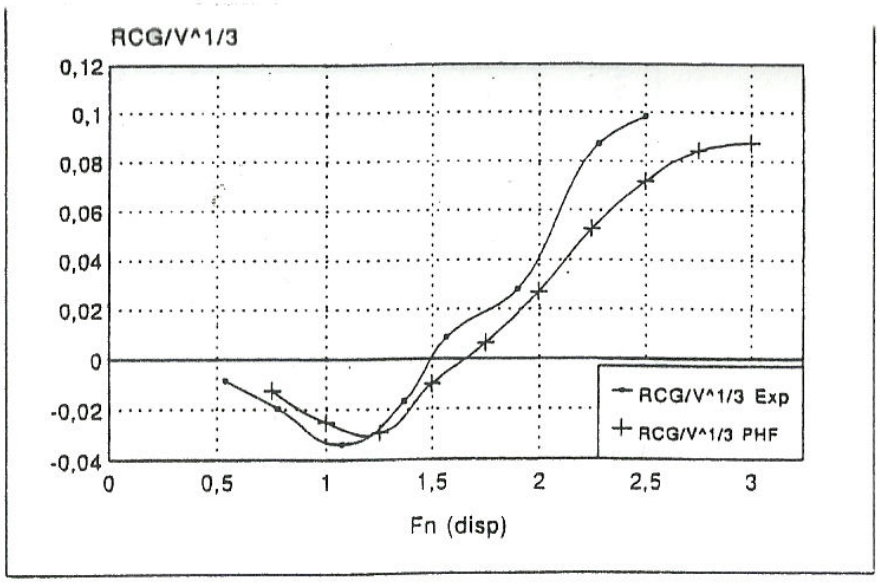

Figure 24. Motor Yacht R410 Experimental and calculated $RCG/\nabla^{1/3}$.

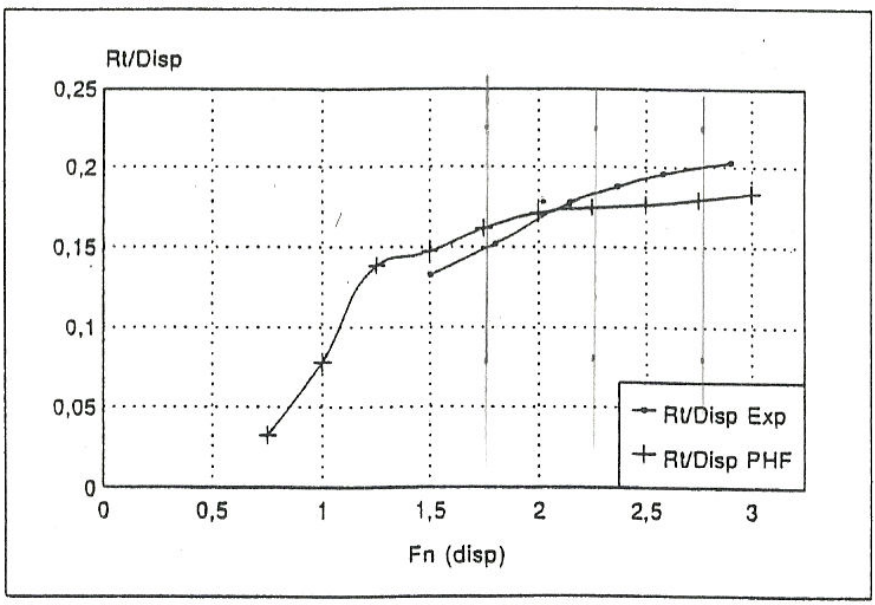

Figure 25. Coastal Rescue Boat Experimental and calculated R_t/Δ.

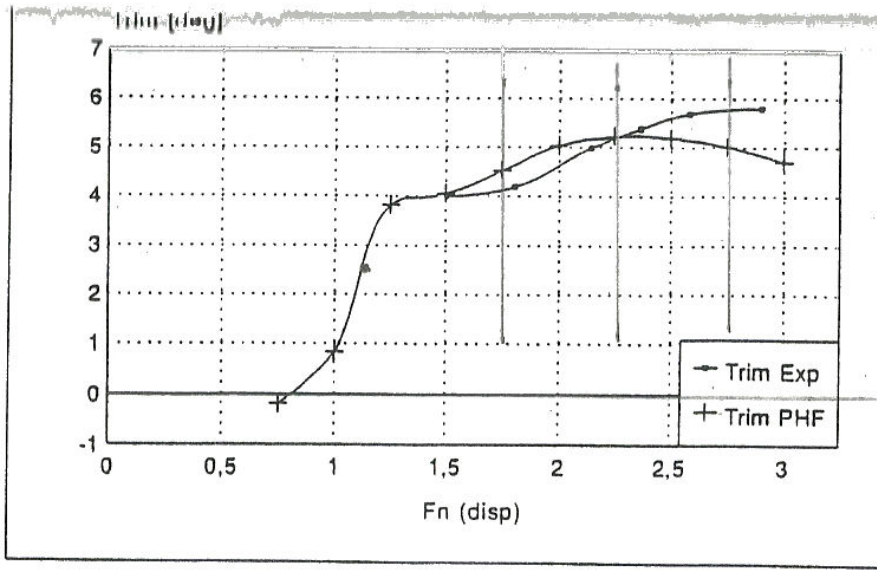

Figure 26. Coastal Rescue Boat Experimental and calculated trim.

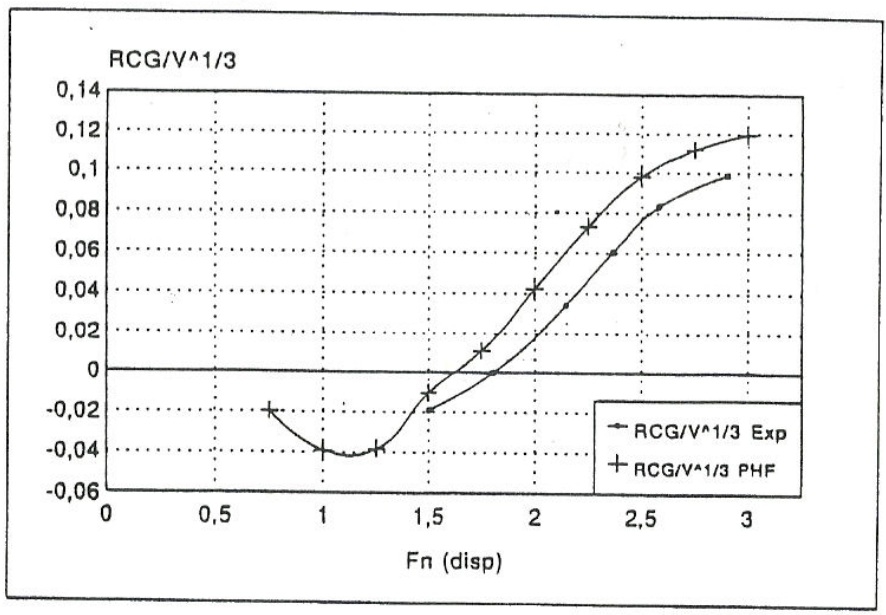

Figure 27. Coastal Rescue Boat Experimental and calculated $RCG/\nabla^{1/3}$.

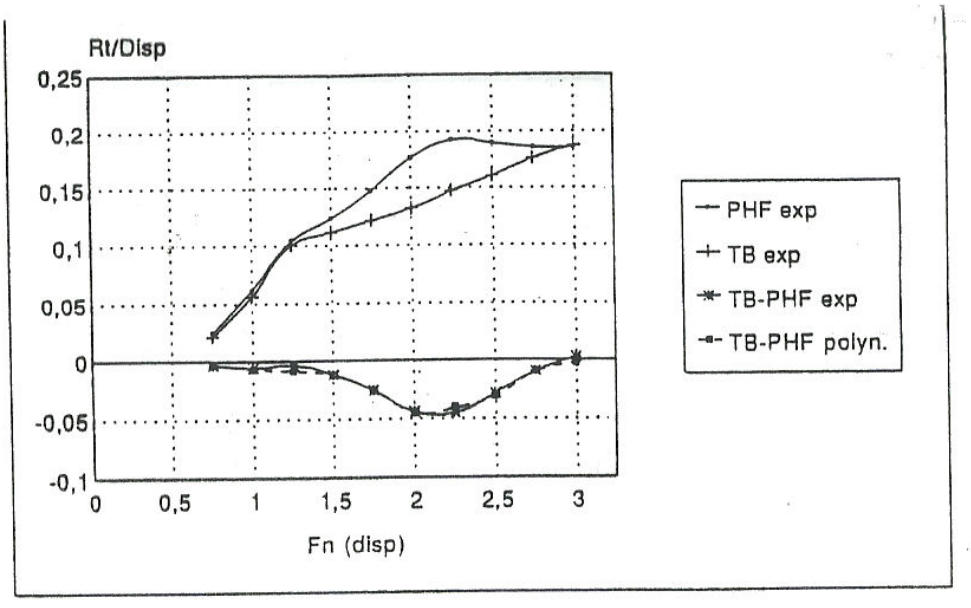

Figure 28. Model 232A-1 Experimental and calculated $\Delta R_t/\Delta$.

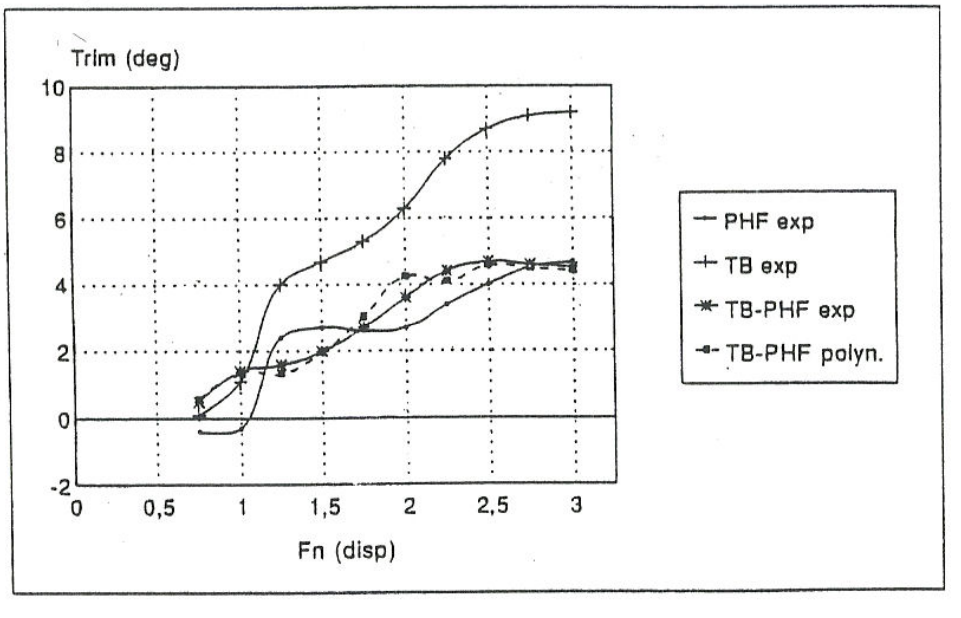

Figure 29. Model 232A-1 Experimental and calculated $\Delta\theta$.

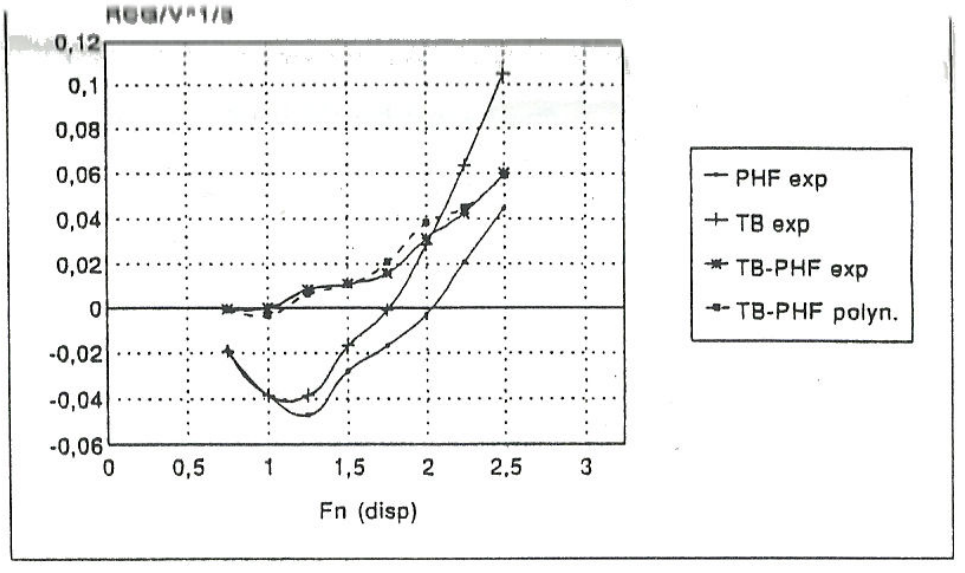

Figure 30. Model 232A-1 Experimental and calculated $\Delta RCG/\nabla^{1/3}$.

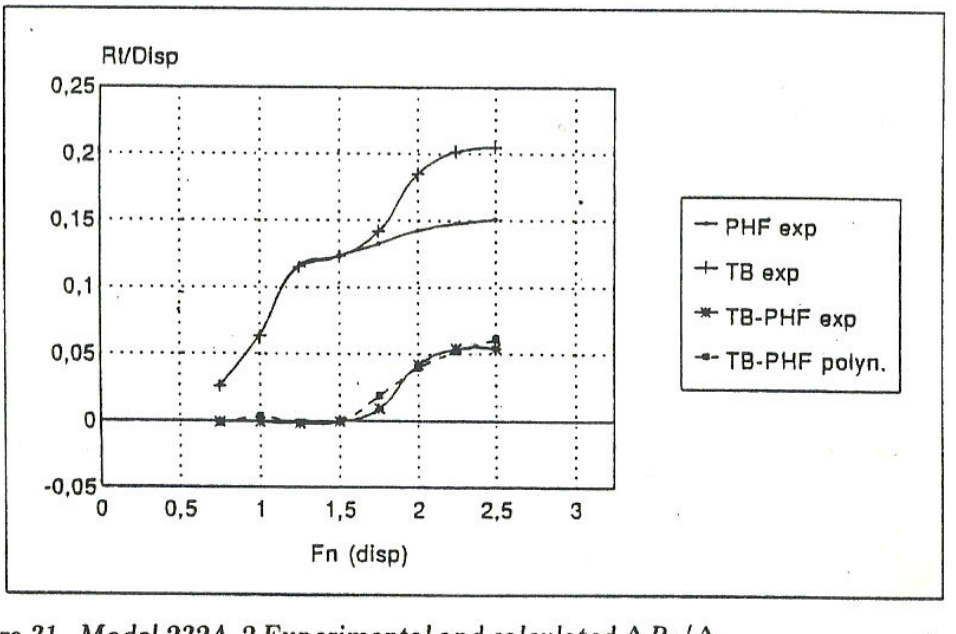

Figure 31. Model 232A-2 Experimental and calculated $\Delta R_t/\Delta$.

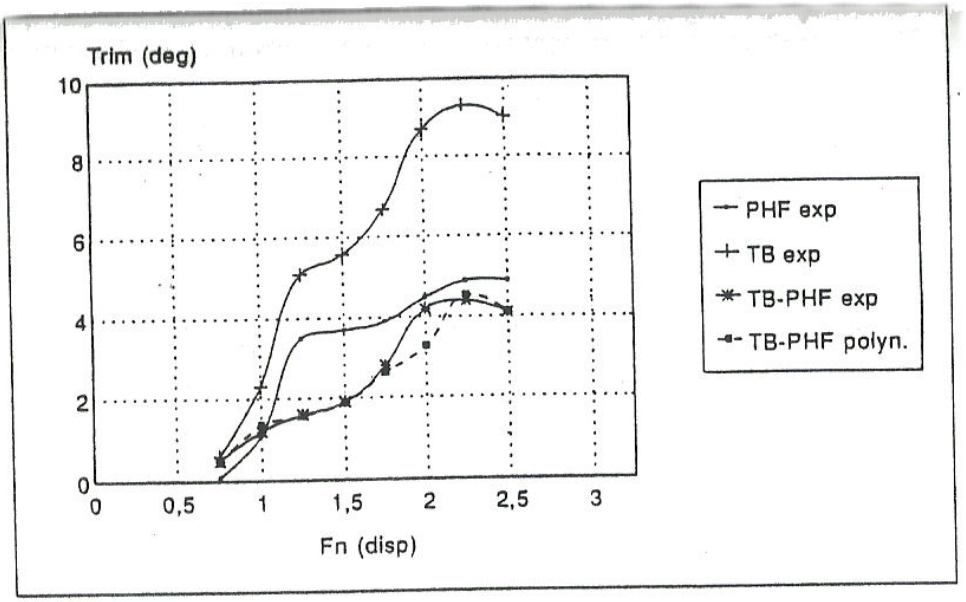

Figure 32. Model 232A-2 Experimental and calculated $\Delta\theta$.

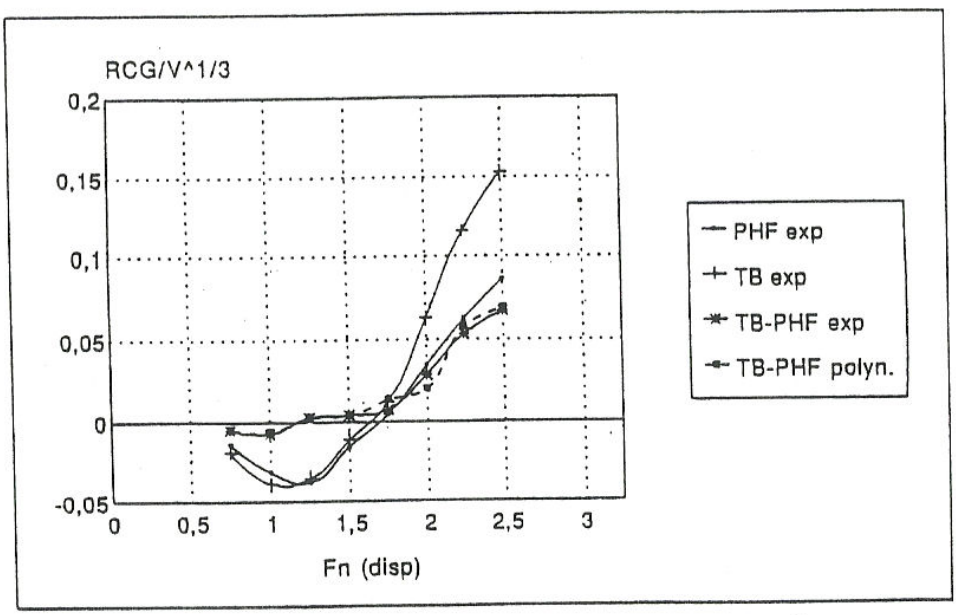

Figure 33. Model 232A-2 Experimental and calculated $\Delta RCG/\nabla^{1/3}$.

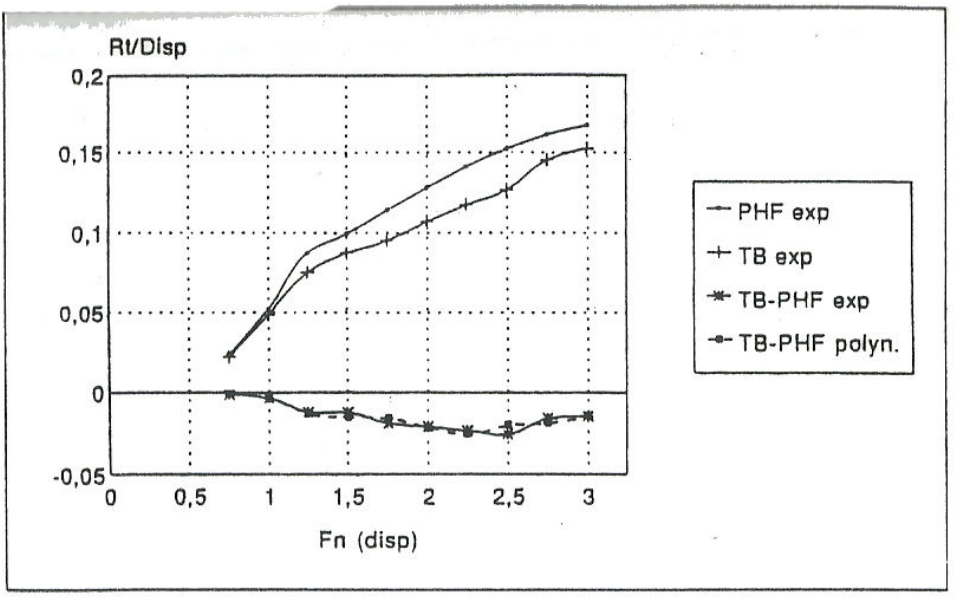

Figure 34. Model 232B-1 Experimental and calculated $\Delta R_t/\Delta$.

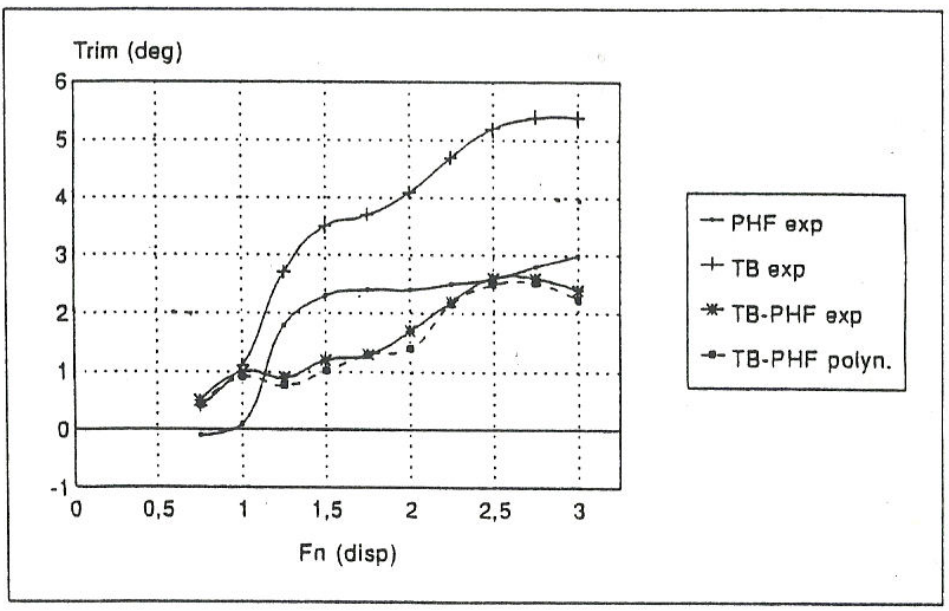

Figure 35. Model 232B-1 Experimental and calculated $\Delta\theta$.

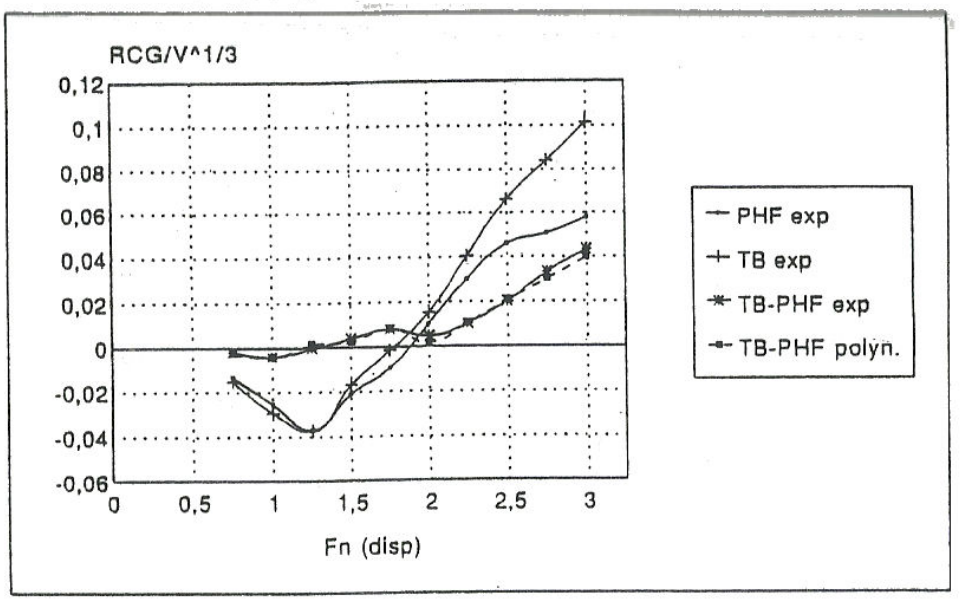

Figure 36. Model 232B-1 Experimental and calculated $\Delta RCG/\nabla^{1/3}$.

9. Conclusions

The experimental data presented in this paper provides resistance information necessary in the design trade off between seakeeping characteristics (high deadrise) and low resistance (small deadrise angles).

The trim and rise of centre of gravity data give the still water position of the vessel at speed, which are shown to have a significant effect on seakeeping calculations [3].

The combined series data represented in a polynomial model provide an easy way to interpolate over a wide range of planing hull forms. It appeared, however, that additional experimental data is needed in the deadrise range from 12.5 to 25^o.

The experimental data and polynomial representation of the twisted bottom models give insight into the influence of a varying deadrise and inclined buttock lines in the aft body of the planing craft. The results obtained with the polynomial expressions for the difference in resistance, trim and rise of centre of gravity due to change of deadrise and centreline inclination show a good fit with the measured data. The use of this correction for arbitrary designs, however, should be considered with care because they are based only on a limited amount of experimental data.

[1] Clemens, E.P. and Blount, D.L., Resistance tests of a systematic series of planing hull forms, *Trans. SNAME*, 1963.

[2] Keuning, J.A. and Gerritsma, J., Resistance tests of a systematic series of planing hull forms with 25^o deadrise angle, *Int. Shipbuild. Progr.*, Vol. 29, No. 337 (1982).

[3] Keuning, J.A., Non-linear heave and pitch motions of fast ships in irregular head seas, Intersoc. High Performance Marine Vehicle Conf. and Exhibit, HPMV, Arlington, 1992.

[4] Keuning, J.A., 'Resistance tests of two planing boats with twisted bottom', Report No. 731, Ship Hydromechanics Laboratory, Delft Univ. of Technology.

[5] Versluis, A., 'Computer added design of shipform by afine transformation', Report No. 438-P, Ship Hydromechanics Laboratory, Delft Univ. of Technology.

Appendix 1: Experimental results 50° deadrise series

model 241

L/B [-]	Depl [N]	LCG [%Lp]	Ap/V [-]
3.41	488.500	0.000	4.00

run	Vm [m/s]	Rtm [N]	Lk [m]	Lc [m]	S [m2]	Trim [deg]	RCG [mm]
794	1.425	18.210	1.25	1.25	0.456	−0.75	−15.0
795	1.900	57.540	1.25	1.25	0.456	3.25	−27.0
796	2.375	105.930	1.25	1.25	0.456	6.90	−20.0
797	2.850	115.140	1.25	1.25	0.456	6.00	−15.0

model 231

L/B [-]	Depl [N]	LCG [%Lp]	Ap/V [-]
3.41	303.100	0.000	5.50

run	Vm [m/s]	Rtm [N]	Lk [m]	Lc [m]	S [m2]	Trim [deg]	RCG [mm]
743	1.333	10.349	1.25	1.25	0.456	−0.65	−10.0
744	1.790	29.053	1.25	1.25	0.456	1.25	−20.0
745	2.193	51.729	1.25	1.25	0.456	5.20	−16.0
746	2.632	54.902	1.25	1.25	0.456	4.32	−6.5

model 240

L/B [-]	Depl [N]	LCG [%Lp]	Ap/V [-]
3.41	488.500	−2.000	4.00

run	Vm [m/s]	Rtm [N]	Lk [m]	Lc [m]	S [m2]	Trim [deg]	RCG [mm]
789	1.425	18.950	1.25	1.25	0.456	−0.35	−14.0
790	1.900	56.200	1.25	1.25	0.456	3.70	−24.0
791	2.375	108.680	1.25	1.25	0.456	7.40	−17.0
792	2.850	115.720	1.25	1.25	0.456	7.20	−12.0
793	3.344	132.050	1.25	1.25	0.456	7.60	−6.5

model 230

L/B [-]	Depl [N]	LCG [%Lp]	Ap/V [-]
3.41	303.100	−2.000	5.50

run	Vm [m/s]	Rtm [N]	Lk [m]	Lc [m]	S [m2]	Trim [deg]	RCG [mm]
747	1.316	10.660	1.25	1.25	0.456	−0.55	−8.5
748	1.755	28.530	1.25	1.25	0.456	1.70	−18.0
749	2.211	53.850	1.25	1.25	0.456	5.60	−13.0
750	2.649	59.370	1.25	1.25	0.456	5.30	−5.5
751	3.070	68.740	0.88	1.16	0.402	6.50	1.0
753	3.527	66.910	0.81	1.16	0.388	8.45	14.5
752	3.946	65.750	0.75	1.16	0.373	8.85	31.0
754	4.404	62.880	0.75	1.16	0.373	8.90	42.5
755	4.842	61.660	0.63	1.16	0.345	8.40	48.0
756	5.264	61.130	0.59	1.16	0.335	8.00	53.5
757	5.702	63.500	0.55	1.16	0.325	7.65	57.0

model 242

L/B [-]	Depl [N]	LCG [%Lp]	Ap/V [-]
3.41	488.500	−4.000	4.00

run	Vm [m/s]	Rtm [N]	Lk [m]	Lc [m]	S [m2]	Trim [deg]	RCG [mm]
784	1.425	19.430	1.25	1.25	0.456	−0.15	−13.0
785	1.900	57.070	1.25	1.25	0.456	4.20	−22.0
786	2.375	110.400	1.25	1.25	0.456	7.90	−15.5
787	2.850	121.930	1.25	1.25	0.456	8.40	−8.0
788	3.325	144.770	1.25	1.25	0.456	13.20	17.0

model 232

L/B [-]	Depl [N]	LCG [%Lp]	Ap/V [-]
3.41	303.100	−4.000	5.50

run	Vm [m/s]	Rtm [N]	Lk [m]	Lc [m]	S [m2]	Trim [deg]	RCG [mm]
758	1.316	10.620	1.25	1.25	0.456	−0.35	−8.5
759	1.772	29.890	1.25	1.25	0.456	2.35	−16.5
760	2.211	56.590	1.19	1.25	0.461	5.95	−11.5
761	2.632	60.480	0.94	1.19	0.421	6.10	−3.5
762	3.070	65.470	0.84	1.16	0.394	7.40	5.5
763	3.527	65.590	0.75	1.16	0.373	9.10	20.5
764	3.983	63.530	0.69	1.16	0.359	9.10	36.5
765	4.386	61.780	0.63	1.13	0.338	8.60	44.5
766	4.825	59.850	0.56	1.09	0.313	8.10	51.5
767	5.264	59.650	0.56	1.09	0.313	7.45	56.5
768	5.702	60.000	0.56	1.09	0.313	6.75	60.0

model 243

L/B [-]	Depl [N]	LCG [%Lp]	Ap/V [-]
3.41	488.500	−6.000	4.00

run	Vm [m/s]	Rtm [N]	Lk [m]	Lc [m]	S [m2]	Trim [deg]	RCG [mm]
780	1.425	21.200	1.25	1.25	0.456	0.65	−12.0
781	1.900	61.660	1.25	1.25	0.456	5.55	−17.0
782	2.375	118.010	0.94	1.19	0.421	9.00	−8.0
783	2.869	139.900	0.88	1.19	0.409	12.10	5.5

model 233

L/B [-]	Depl [N]	LCG [%Lp]	Ap/V [-]
3.41	303.100	−6.000	5.50

run	Vm [m/s]	Rtm [N]	Lk [m]	Lc [m]	S [m2]	Trim [deg]	RCG [mm]
769	1.316	11.640	1.25	1.25	0.456	0.20	−7.5
770	1.755	31.660	1.25	1.25	0.456	3.25	−14.0
771	2.193	61.830	0.91	1.22	0.421	7.00	−10.0
772	2.632	65.030	0.75	1.16	0.373	7.85	1.0
773	3.070	69.950	0.69	1.13	0.352	9.80	14.5
774	3.509	70.390	0.59	0.94	0.289	9.80	29.5
775	3.948	68.800	0.53	0.93	0.273	9.20	44.5
776	4.389	65.140	0.53	0.91	0.269	8.30	54.0
777	4.825	62.010	0.50	0.91	0.262	7.30	60.5
778	5.264	61.520	0.47	0.91	0.255	6.45	64.0
779	5.702	60.260	0.44	0.88	0.243	5.60	67.5

model 211

L/B [-]	Depl [N]	LCG [%Lp]	Ap/V [-]
3.41	210.900	0.000	7.00

run	Vm [m/s]	Rtm [N]	Lk [m]	Lc [m]	S [m2]	Trim [deg]	RCG [mm]
705	1.222	6.260	1.25	1.25	0.456	−0.60	−5.5
706	1.652	17.700	1.25	1.25	0.456	0.10	−14.0
707	2.064	30.870	1.25	1.25	0.456	3.65	−13.5
708	2.477	35.640	1.19	1.25	0.461	3.55	−7.0
709	2.890	42.810	1.13	1.25	0.462	3.40	−5.5
710	3.287	50.400	1.06	1.25	0.456	4.15	0.0
711	3.716	51.730	0.97	1.22	0.433	5.15	9.0
712	4.129	50.390	0.88	1.19	0.409	5.80	18.5
713	4.556	50.020	0.79	1.17	0.384	6.05	23.5
714	4.971	50.140	0.69	1.16	0.359	6.10	29.0
715	5.368	52.000	0.69	1.16	0.359	6.00	33.0
716	5.781	53.700	0.69	1.16	0.359	5.90	38.0

model 211

L/B [-]	Depl [N]	LCG [%Lp]	Ap/V [-]
3.41	157.9	0.0	8.5

run	Vm [m/s]	Rtm [N]	Lk [m]	Lc [m]	S [m2]	Trim [deg]	RCG [mm]
630	1.180	4.572	1.25	1.25	0.456	−0.40	−5.5
631	1.590	12.310	1.25	1.25	0.456	−0.10	−10.2
632	1.999	21.399	1.06	1.25	0.456	2.60	−11.0
633	2.408	25.263	0.97	1.25	0.440	2.75	−6.0
634	2.754	29.413	0.94	1.25	0.434	2.70	−4.5
635	3.148	34.500	0.89	1.22	0.416	2.85	−0.5
636	3.541	38.800	0.83	1.22	0.405	3.30	4.0
637	3.962	41.531	0.78	1.19	0.388	3.50	10.0
638	4.344	42.758	0.72	1.19	0.372	3.80	12.0
639	4.721	43.655	0.69	1.17	0.361	4.10	17.0
640	5.115	44.945	0.63	1.16	0.345	4.25	20.0
641	5.508	46.800	0.57	1.16	0.330	4.30	24.0
642	5.902	48.000	0.50	1.16	0.313	4.40	29.0

model 220

L/B [-]	Depl [N]	LCG [%Lp]	Ap/V [-]
3.41	210.900	−2.000	7.00

run	Vm [m/s]	Rtm [N]	Lk [m]	Lc [m]	S [m2]	Trim [deg]	RCG [mm]
718	1.222	6.670	1.25	1.25	0.456	−0.35	−5.5
719	1.652	17.400	1.25	1.25	0.456	0.55	−13.5
720	2.064	31.730	1.25	1.25	0.456	4.05	−12.0
721	2.477	35.440	1.00	1.25	0.446	4.10	−5.0
722	2.890	40.510	0.88	1.25	0.422	4.30	−1.0
723	3.303	44.020	0.81	1.19	0.393	4.95	6.5
724	3.716	43.480	0.75	1.19	0.379	5.70	15.5
725	4.129	43.420	0.69	1.19	0.365	6.00	22.5
726	4.556	43.480	0.63	1.19	0.351	6.00	28.0
727	4.971	43.890	0.59	1.16	0.335	5.90	32.0
728	5.368	45.800	0.56	1.16	0.327	5.70	36.0
729	5.781	47.600	0.53	1.16	0.320	5.60	40.5

model 210

L/B [-]	Depl [N]	LCG [%Lp]	Ap/V [-]
3.41	157.9	−2.0	8.5

run	Vm [m/s]	Rtm [N]	Lk [m]	Lc [m]	S [m2]	Trim [deg]	RCG [mm]
644	1.180	5.066	1.25	1.25	0.456	−0.25	−5.0
645	1.590	12.055	1.25	1.25	0.456	0.20	−10.0
646	1.997	20.699	1.06	1.25	0.456	2.90	−11.0
647	2.378	23.650	0.94	1.25	0.434	3.10	−4.5
648	2.723	26.716	0.86	1.22	0.415	3.00	−1.8
649	3.148	30.695	0.81	1.19	0.393	3.15	2.0
650	3.541	33.613	0.75	1.19	0.379	3.50	7.0
651	3.935	35.000	0.70	1.17	0.360	3.80	13.0
652	4.359	36.095	0.59	1.16	0.335	4.05	18.0
653	4.769	37.406	0.56	1.16	0.327	4.25	21.0
654	5.115	39.461	0.53	1.16	0.320	4.25	23.0
655	5.508	41.000	0.51	1.16	0.315	4.25	26.5

model 222

L/B [-]	Depl [N]	LCG [%Lp]	Ap/V [-]
3.41	210.900	−4.000	7.00

run	Vm [m/s]	Rtm [N]	Lk [m]	Lc [m]	S [m2]	Trim [deg]	RCG [mm]
730	1.222	6.960	1.25	1.25	0.456	−0.25	−5.5
731	1.652	17.390	1.25	1.25	0.456	1.05	−12.5
733	2.064	31.690	1.06	1.22	0.450	4.40	−11.0
734	2.477	34.330	1.00	1.22	0.439	4.40	−3.5
735	2.890	37.800	0.88	1.19	0.409	4.80	2.0
736	3.303	39.430	0.69	1.19	0.365	5.65	10.0
737	3.716	39.270	0.63	1.19	0.351	6.15	20.5
738	4.129	39.210	0.63	1.19	0.351	6.15	27.0
739	4.556	39.790	0.59	1.16	0.335	6.00	32.0
740	4.971	39.410	0.56	1.16	0.327	5.80	37.0
741	5.368	40.200	0.51	1.16	0.315	5.50	40.5
742	5.781	43.000	0.50	1.16	0.313	5.25	44.0

model 212

L/B [-]	Depl [N]	LCG [%Lp]	Ap/V [-]
3.41	157.9	−4.0	8.5

run	Vm [m/s]	Rtm [N]	Lk [m]	Lc [m]	S [m2]	Trim [deg]	RCG [mm]
666	1.180	5.122	1.25	1.25	0.456	−0.15	−4.0
667	1.590	11.895	1.25	1.25	0.456	0.50	−9.0
668	1.997	20.069	1.00	1.19	0.433	3.05	−10.0
669	2.378	22.606	0.81	1.19	0.393	3.40	−3.5
670	2.723	24.940	0.75	1.19	0.379	3.32	−0.5
671	3.148	27.892	0.69	1.25	0.378	3.60	5.0
672	3.573	29.529	0.66	1.25	0.371	4.00	10.5
673	3.935	30.900	0.63	1.17	0.347	4.20	16.5
674	4.297	31.293	0.59	1.16	0.335	4.25	20.0
675	4.721	32.400	0.56	1.16	0.327	4.30	23.0
676	5.115	33.696	0.50	1.16	0.313	4.25	26.5
677	5.461	35.955	0.47	1.16	0.305	4.15	29.0
678	5.902	38.600	0.45	1.16	0.300	4.00	32.0

model 223

L/B [-]	Depl [N]	LCG [%Lp]	Ap/V [-]
3.41	210.900	−8.000	7.00

run	Vm [m/s]	Rtm [N]	Lk [m]	Lc [m]	S [m2]	Trim [deg]	RCG [mm]
693	1.239	7.500	0.88	1.25	0.422	0.30	−5.0
694	1.652	17.440	0.88	1.25	0.422	1.85	−11.0
695	2.064	32.860	0.88	1.19	0.409	5.10	−9.0
696	2.477	33.660	0.78	1.16	0.380	5.25	0.0
697	2.890	34.950	0.72	1.16	0.366	5.90	7.0
698	3.303	35.650	0.63	1.13	0.338	6.60	17.0
699	3.716	36.400	0.56	1.06	0.307	6.55	26.5
700	4.145	36.750	0.53	1.06	0.300	6.10	34.0
701	4.542	36.700	0.50	1.03	0.286	5.70	39.0
702	4.971	37.240	0.47	1.03	0.279	5.20	42.0
703	5.368	38.400	0.44	1.00	0.266	4.75	45.0
704	5.781	40.000	0.44	1.00	0.266	4.35	49.0

model 213

L/B [-]	Depl [N]	LCG [%Lp]	Ap/V [-]
3.41	157.900	−8.000	8.50

run	Vm [m/s]	Rtm [N]	Lk [m]	Lc [m]	S [m2]	Trim [deg]	RCG [mm]
680	1.180	5.518	0.69	1.25	0.378	0.15	−4.0
681	1.590	12.024	0.69	1.25	0.378	1.20	−8.0
682	1.997	20.722	0.81	1.16	0.388	3.70	−8.7
683	2.345	21.538	0.69	1.16	0.359	3.75	−1.0
684	2.738	22.605	0.66	1.16	0.352	3.90	3.0
685	3.148	23.857	0.63	1.16	0.345	4.30	9.5
686	3.557	25.036	0.58	1.16	0.332	4.50	17.0
687	3.950	25.546	0.52	1.16	0.316	4.45	25.5
688	4.312	26.355	0.47	1.11	0.295	4.25	26.0
689	4.721	27.200	0.44	1.10	0.285	4.10	28.5
690	5.115	28.959	0.41	1.09	0.277	3.80	31.5
691	5.508	31.310	0.39	1.09	0.272	3.50	32.5

[redacted]

model 341

L/B [–]	Depl [N]	LCG [%Lp]	Ap/V [–]
4.09	369.900	0.000	4.00

run	Vm [m/s]	Rtm [N]	Lk [m]	Lc [m]	S [m2]	Trim [deg]	RCG [mm]
138	1.360	11.229	1.50	1.50	0.536	−0.45	−9.0
139	1.814	27.874	1.50	1.50	0.536	0.75	−19.0
140	2.267	52.604	1.50	1.50	0.536	4.30	−16.0
141	2.775	57.931	1.50	1.50	0.536	4.05	−11.0
142	3.174	65.541	1.50	1.50	0.536	3.65	−8.5

model 331

L/B [–]	Depl [N]	LCG [%Lp]	Ap/V [–]
4.09	229.500	0.000	5.50

run	Vm [m/s]	Rtm [N]	Lk [m]	Lc [m]	S [m2]	Trim [deg]	RCG [mm]
126	1.256	6.116	1.28	1.50	0.534	−0.30	−5.5
127	1.692	14.769	1.13	1.50	0.511	−0.05	−11.0
128	2.094	27.300	1.05	1.50	0.496	2.30	−14.0
129	2.546	31.662	1.13	1.46	0.502	2.75	−8.5
130	2.948	37.361	1.13	1.46	0.502	2.84	−5.0
131	3.350	43.515	1.13	0.46	0.502	2.85	−1.4
132	3.769	47.936	1.05	1.46	0.467	3.55	4.0
133	4.186	49.810	1.01	1.46	0.476	4.10	10.0
134	4.606	49.828	0.98	1.43	0.464	4.60	16.5
135	5.075	49.963	0.86	1.43	0.436	5.00	21.0
136	5.444	51.000	0.79	1.43	0.419	5.20	25.5

model 340

L/B [–]	Depl [N]	LCG [%Lp]	Ap/V [–]
4.09	369.900	−2.000	4.00

run	Vm [m/s]	Rtm [N]	Lk [m]	Lc [m]	S [m2]	Trim [deg]	RCG [mm]
171	1.360	11.175	1.50	1.50	0.536	−0.33	−8.0
172	1.814	27.457	1.50	1.50	0.536	1.10	−18.0
173	2.265	54.013	1.50	1.50	0.536	4.40	−16.2
174	2.739	59.712	1.50	1.50	0.536	4.35	−9.5
175	3.156	66.247	1.35	1.43	0.533	4.65	−4.0
176	3.646	75.757	1.20	1.43	0.510	6.05	5.5
178	4.081	75.000	1.09	1.43	0.466	7.65	22.0
177	4.534	72.000	0.94	1.35	0.437	8.00	36.0
179	4.986	71.000	0.88	1.31	0.415	7.80	43.0

model 330

L/B [–]	Depl [N]	LCG [%Lp]	Ap/V [–]
4.09	229.500	−2.000	5.50

run	Vm [m/s]	Rtm [N]	Lk [m]	Lc [m]	S [m2]	Trim [deg]	RCG [mm]
114	1.256	6.373	1.20	1.50	0.525	−0.15	−5.2
115	1.675	14.730	1.16	1.50	0.517	0.25	−10.5
116	2.094	26.300	1.09	1.50	0.503	2.60	−13.0
117	2.529	30.525	1.13	1.43	0.496	2.98	−7.0
118	2.948	35.249	1.13	1.43	0.496	3.10	−3.5
119	3.350	39.483	1.09	1.43	0.486	3.50	2.0
120	3.769	42.411	1.05	1.43	0.480	3.95	8.0
121	4.186	42.927	0.96	1.43	0.464	4.50	14.5
122	4.606	43.225	0.86	1.43	0.436	4.80	19.0
123	5.075	44.624	0.79	1.43	0.419	5.00	24.0
124	5.444	46.200	0.75	1.39	0.401	5.10	29.0

model 342

L/B [–]	Depl [N]	LCG [%Lp]	Ap/V [–]
4.09	369.900	−4.000	4.00

run	Vm [m/s]	Rtm [N]	Lk [m]	Lc [m]	S [m2]	Trim [deg]	RCG [mm]
160	1.360	11.282	1.50	1.50	0.536	−0.15	−7.5
161	1.814	27.254	1.50	1.50	0.536	1.35	−16.5
162	2.267	55.000	1.43	1.50	0.535	4.80	−13.5
163	2.775	61.816	1.28	1.50	0.534	4.95	−6.5
164	3.192	66.974	1.13	1.43	0.496	5.50	0.0
165	3.664	71.485	1.09	1.35	0.470	7.00	12.0
166	4.081	73.000	0.98	1.35	0.447	8.05	26.5
167	4.607	69.549	0.90	1.31	0.420	8.00	36.0
168	5.006	70.247	0.79	1.20	0.370	7.75	46.0
169	5.568	71.693	0.79	1.20	0.370	7.40	54.0

model 332

L/B [–]	Depl [N]	LCG [%Lp]	Ap/V [–]
4.09	229.500	−4.000	5.50

run	Vm [m/s]	Rtm - [N]	Lk [m]	Lc [m]	S [m2]	Trim [deg]	RCG [mm]
102	1.256	6.646	1.31	1.50	0.539	0.00	−4.8
103	1.692	15.124	1.28	1.50	0.534	0.55	−9.8
104	2.094	26.567	1.20	1.50	0.525	2.88	−12.5
105	2.529	29.507	1.16	1.46	0.508	3.16	−6.5
106	2.948	33.353	1.13	1.46	0.502	3.40	−1.5
107	3.350	36.583	1.01	1.43	0.471	3.70	4.0
108	3.769	38.208	0.98	1.43	0.464	4.25	11.0
109	4.236	39.049	0.86	1.43	0.436	4.75	18.0
110	4.623	40.162	0.79	1.39	0.410	5.00	22.5
111	5.075	41.870	0.71	1.35	0.382	5.00	27.0
112	5.444	43.700	0.71	1.35	0.382	5.00	30.5
113	5.863	44.250	0.71	1.33	0.378	5.05	32.5

model 343

L/B [–]	Depl [N]	LCG [%Lp]	Ap/V [–]
4.09	369.900	−6.000	4.00

run	Vm [m/s]	Rtm [N]	Lk [m]	Lc [m]	S [m2]	Trim [deg]	RCG [mm]
144	1.360	12.445	1.50	1.50	0.536	0.32	−7.5
145	1.866	33.331	1.35	1.50	0.530	2.60	−15.5
146	2.265	61.430	1.20	1.50	0.525	5.70	−13.0
147	2.721	64.671	1.09	1.43	0.488	6.20	−5.0
148	3.192	70.978	1.01	1.38	0.460	7.55	6.0
149	3.700	77.471	0.90	1.28	0.413	8.60	22.0
150	4.045	77.856	0.75	1.24	0.369	8.65	34.5
151	4.571	77.305	0.75	1.24	0.369	8.10	48.5
153	4.988	78.000	0.71	1.20	0.351	7.55	56.0
154	5.441	75.000	0.71	1.20	0.351	6.90	53.0

model 333

L/B [–]	Depl [N]	LCG [%Lp]	Ap/V [–]
4.09	229.500	−6.000	5.50

run	Vm [m/s]	Rtm [N]	Lk [m]	Lc [m]	S [m2]	Trim [deg]	RCG [mm]
88	1.256	6.866	1.13	1.50	0.511	0.15	−4.5
89	1.675	14.810	1.13	1.50	0.511	1.00	−9.0
90	2.094	27.632	1.09	1.43	0.488	3.40	−11.2
91	2.513	29.900	1.05	1.43	0.480	3.75	−4.5
92	2.948	31.891	0.98	1.43	0.464	4.00	1.5
93	3.367	34.066	0.86	1.43	0.436	4.55	8.5
94	3.786	36.053	0.83	1.39	0.420	5.10	16.3
95	4.204	37.819	0.75	1.35	0.392	5.20	23.0
96	4.640	39.316	0.71	1.35	0.382	5.15	28.0
97	5.059	40.452	0.68	1.35	0.374	5.05	32.5
101	5.444	42.000	0.68	1.35	0.369	4.90	36.5
98	5.863	44.400	0.64	1.31	0.356	4.80	41.5

[redacted]

run	Vm [m/s]	Rtm [N]	Lk [m]	Lc [m]	S [m2]	Trim [deg]	RCG [mm]
44	1.163	3.997	1.13	1.50	0.511	−0.18	−4.0
45	1.577	9.937	1.13	1.50	0.511	−0.18	−7.0
46	1.987	16.177	1.13	1.50	0.511	1.55	−10.5
47	2.365	19.236	1.13	1.46	0.502	2.10	−7.5
48	2.775	23.309	1.05	1.46	0.457	2.20	−4.5
49	3.170	27.675	1.05	1.46	0.457	2.25	−2.0
50	3.580	32.429	1.01	1.46	0.476	2.25	2.0
51	3.974	36.939	0.94	1.46	0.461	2.48	4.9
52	4.384	40.499	0.94	1.44	0.457	2.70	6.0
53	4.794	42.553	0.90	1.44	0.446	3.05	8.0
184	5.125	43.000	0.83	1.43	0.429	3.35	10.5
186	5.519	44.300	0.75	1.43	0.409	3.70	16.0

[redacted]

run	Vm [m/s]	Rtm [N]	Lk [m]	Lc [m]	S [m2]	Trim [deg]	RCG [mm]
3	1.127	2.799	0.98	1.46	0.471	−0.15	−2.9
4	1.517	6.359	0.98	1.46	0.471	−0.28	−5.4
5	1.878	10.243	0.98	1.46	0.471	0.75	−8.8
6	2.254	12.708	0.98	1.46	0.471	1.55	−0.7
9	2.629	15.612	0.98	1.46	0.471	1.90	−5.5
8	3.020	19.113	0.94	1.46	0.461	1.75	−3.0
1	3.380	22.429	0.98	1.46	0.471	1.79	−1.0
2	3.771	26.869	0.98	1.46	0.471	1.70	1.8
7	4.132	29.843	0.98	1.46	0.471	1.75	2.3
10	4.507	35.252	0.94	1.46	0.461	1.85	1.5
200	4.883	38.250	0.75	1.43	0.409	2.10	2.5
183	5.258	40.750	0.68	1.39	0.382	2.50	6.0
182	5.634	42.500	0.62	1.39	0.362	2.85	9.0

model 320

L/B [−]	Depl [N]	LCG [%Lp]	Ap/V [−]
4.09	159.600	−2.000	7.00

run	Vm [m/s]	Rtm [N]	Lk [m]	Lc [m]	S [m2]	Trim [deg]	RCG [mm]
54	1.163	4.217	1.05	1.50	0.498	−0.15	−3.8
55	1.577	9.390	1.05	1.50	0.498	0.00	−7.0
56	1.971	15.649	1.05	1.50	0.498	1.65	−10.5
57	2.365	18.183	1.05	1.46	0.457	2.12	−7.2
58	2.775	21.457	1.05	1.46	0.457	2.20	−4.2
59	3.154	25.110	1.01	1.46	0.476	2.30	−5.0
60	3.564	28.957	0.94	1.46	0.461	2.40	3.5
61	3.956	32.153	0.86	1.44	0.438	2.52	7.0
62	4.337	34.500	0.79	1.44	0.421	2.65	8.5
63	4.731	36.300	0.79	1.44	0.421	3.20	10.5
187	5.125	38.200	0.71	1.35	0.382	3.50	13.0
188	5.519	39.400	0.64	1.35	0.364	3.75	18.0

model 310

L/B [−]	Depl [N]	LCG [%Lp]	Ap/V [−]
4.09	119.500	−2.000	8.50

run	Vm [m/s]	Rtm [N]	Lk [m]	Lc [m]	S [m2]	Trim [deg]	RCG [mm]
11	1.127	2.923	1.05	1.46	0.457	−0.08	−3.0
12	1.502	6.270	1.05	1.46	0.457	−0.01	−5.0
13	1.878	10.008	1.05	1.46	0.457	0.88	−8.0
14	2.269	12.790	1.05	1.46	0.457	1.75	−6.0
15	2.644	15.989	1.05	1.46	0.457	1.73	−4.3
16	3.035	17.857	1.01	1.46	0.476	1.88	−1.5
17	3.410	20.847	0.96	1.46	0.471	1.90	1.4
18	3.771	23.972	0.94	1.46	0.461	1.92	4.0
19	4.132	27.300	0.90	1.46	0.452	1.95	5.0
20	4.492	30.602	0.86	1.46	0.442	2.05	4.5
190	4.883	33.200	0.64	1.31	0.356	2.25	5.5
191	5.258	34.600	0.60	1.31	0.349	2.60	9.0
192	5.634	36.676	0.60	1.35	0.354	2.95	11.0

model 322

L/B [−]	Depl [N]	LCG [%Lp]	Ap/V [−]
4.09	159.600	−4.000	7.00

run	Vm [m/s]	Rtm [N]	Lk [m]	Lc [m]	S [m2]	Trim [deg]	RCG [mm]
64	1.163	4.381	0.98	1.50	0.480	0.00	−3.4
65	1.563	9.125	0.98	1.50	0.480	0.18	−6.1
66	1.987	15.494	0.98	1.50	0.480	1.85	−9.5
67	2.365	17.628	0.98	1.46	0.471	2.30	−6.5
68	2.760	20.481	0.94	1.46	0.461	2.35	−3.0
69	3.170	23.557	0.90	1.46	0.452	2.50	1.6
70	3.564	26.283	0.83	1.46	0.435	2.60	5.0
71	3.942	28.515	0.79	1.46	0.425	2.75	9.0
72	4.352	30.822	0.75	1.43	0.409	3.10	11.0
73	4.776	31.994	0.71	1.43	0.399	3.45	14.0
197	5.125	33.200	0.56	1.37	0.347	3.65	17.0
196	5.519	35.700	0.56	1.35	0.343	3.70	20.0

model 312

L/B [−]	Depl [N]	LCG [%Lp]	Ap/V [−]
4.09	119.500	−4.000	8.50

run	Vm [m/s]	Rtm [N]	Lk [m]	Lc [m]	S [m2]	Trim [deg]	RCG [mm]
21	1.127	3.043	1.05	1.46	0.457	0.00	−2.5
22	1.502	6.124	1.05	1.46	0.457	0.00	−4.5
23	1.878	9.837	1.05	1.46	0.457	0.98	−8.0
24	2.254	12.250	1.05	1.46	0.457	1.74	−6.0
25	2.629	14.378	1.05	1.46	0.457	1.80	−3.0
26	3.005	16.821	1.05	1.46	0.457	1.93	−1.0
27	3.380	19.266	0.90	1.46	0.452	2.00	2.2
29	3.756	21.955	0.77	1.46	0.420	2.00	5.8
28	4.132	24.800	0.79	1.46	0.425	2.00	6.0
30	4.522	27.386	0.75	1.46	0.415	2.25	7.0
31	4.883	29.800	0.75	1.46	0.415	2.50	8.5
193	5.258	31.400	0.54	1.35	0.336	2.80	10.5
195	5.634	32.200	0.53	1.31	0.327	2.90	13.0

model 323

L/B [−]	Depl [N]	LCG [%Lp]	Ap/V [−]
4.09	159.600	−6.000	7.00

run	Vm [m/s]	Rtm [N]	Lk [m]	Lc [m]	S [m2]	Trim [deg]	RCG [mm]
74	1.163	4.550	0.98	1.46	0.471	0.17	−2.8
75	1.577	9.210	0.90	1.46	0.452	0.60	−5.5
76	1.987	15.867	0.75	1.46	0.416	2.25	−9.5
77	2.365	17.642	0.75	1.46	0.416	2.62	−5.5
78	2.760	19.498	0.75	1.43	0.409	2.75	−1.5
79	3.170	21.328	0.79	1.43	0.419	2.85	4.0
80	3.564	22.933	0.79	1.43	0.419	3.05	9.0
81	3.942	24.404	0.79	1.39	0.410	3.30	13.0
82	4.368	26.373	0.68	1.39	0.382	3.50	16.5
83	4.810	30.220	0.64	1.39	0.372	3.55	19.0
84	5.125	32.200	0.60	1.35	0.354	3.55	21.0
86	5.519	34.000	0.56	1.35	0.338	3.55	24.0
87	5.914	35.700	0.53	1.28	0.323	3.60	28.0

model 313

L/B [−]	Depl [N]	LCG [%Lp]	Ap/V [−]
4.09	119.500	−6.000	8.50

run	Vm [m/s]	Rtm [N]	Lk [m]	Lc [m]	S [m2]	Trim [deg]	RCG [mm]
32	1.127	3.213	0.90	1.43	0.446	0.14	−2.5
33	1.502	6.300	0.83	1.43	0.429	0.31	−5.0
34	1.878	10.284	0.83	1.43	0.429	1.40	−7.5
35	2.254	12.099	0.83	1.43	0.429	1.98	−5.0
36	2.644	13.714	0.79	1.43	0.419	2.05	−2.5
37	3.020	15.382	0.75	1.43	0.409	2.10	1.0
38	3.380	17.145	0.68	1.43	0.391	2.20	5.4
39	3.756	18.784	0.60	1.43	0.370	2.20	8.2
40	4.102	20.639	0.56	1.43	0.359	2.38	10.0
41	4.522	22.823	0.53	1.43	0.340	2.60	11.3
42	4.883	25.200	0.53	1.31	0.327	2.75	12.5
199	5.258	27.320	0.49	1.35	0.347	2.70	15.0
198	5.634	30.300	0.49	1.31	0.317	2.75	18.0

[illegible]

[illegible]

run	Vm [m/s]	Rtm [N]	Lk [m]	Lc [m]	S [m2]	Trim [deg]	RCG [mm]
380	1.263	5.972	1.50	1.50	0.400	−0.20	−5.0
381	1.684	12.600	1.50	1.50	0.400	0.70	−11.0
382	2.089	24.520	1.50	1.50	0.400	2.43	−13.0
383	2.527	27.856	1.50	1.50	0.400	2.86	−10.0
384	2.948	31.629	1.50	1.50	0.400	2.63	−6.0
385	3.369	36.923	1.50	1.50	0.400	2.15	−4.8
386	3.790	43.796	1.50	1.50	0.400	1.70	−6.0

run	Vm [m/s]	Rtm [N]	Lk [m]	Lc [m]	S [m2]	Trim [deg]	RCG [mm]
314	1.151	3.228	1.50	1.50	0.389	−0.12	−3.
315	1.558	7.155	1.50	1.50	0.389	−0.20	−6.
316	1.946	12.144	1.50	1.50	0.394	1.20	−10.
317	2.349	15.085	1.50	1.50	0.400	1.95	−9
318	2.736	17.479	1.50	1.50	0.400	1.95	-

model 440

L/B [−]	Depl [N]	LCG [%Lp]	Ap/V [−]
5.5	237.400	−2.000	4.00

run	Vm [m/s]	Rtm [N]	Lk [m]	Lc [m]	S [m2]	Trim [deg]	RCG [mm]
387	1.263	6.075	1.50	1.50	0.400	−0.10	−6.0
388	1.684	13.410	1.50	1.50	0.400	0.45	−10.0
389	2.106	24.453	1.50	1.50	0.400	2.65	−12.5
390	2.527	28.366	1.43	1.50	0.400	3.20	−9.0
391	2.948	32.604	1.43	1.46	0.398	3.20	−4.0
392	3.369	37.158	1.43	1.46	0.398	3.00	0.0
393	3.790	43.527	1.43	1.46	0.398	2.65	2.0
394	4.211	49.860	1.50	1.50	0.400	2.60	5.0
395	4.616	58.412	1.50	1.50	0.400	2.40	0.0

model 442

L/B [−]	Depl [N]	LCG [%Lp]	Ap/V [−]
5.5	237.400	−4.000	4.00

run	Vm [m/s]	Rtm [N]	Lk [m]	Lc [m]	S [m2]	Trim [deg]	RCG [mm]
396	1.247	6.220	1.50	1.50	0.400	0.00	−4.0
397	1.668	13.357	1.50	1.50	0.400	0.60	−10.0
398	2.106	25.733	1.50	1.50	0.400	2.90	−11.5
399	2.510	29.209	1.39	1.44	0.396	3.40	−8.0
400	2.914	32.536	1.35	1.43	0.393	3.35	−3.5
401	3.369	36.414	1.31	1.43	0.390	3.45	1.0
402	3.807	40.832	1.24	1.43	0.383	3.90	6.0
403	4.228	42.301	1.13	1.39	0.362	4.70	11.0
404	4.649	43.440	1.01	1.33	0.337	5.75	18.0
405	5.053	42.047	0.94	1.29	0.319	5.85	23.0
406	5.475	42.191	0.90	1.28	0.310	5.70	34.0

model 443

L/B [−]	Depl [N]	LCG [%Lp]	Ap/V [−]
5.5	237.400	−6.000	4.00

run	Vm [m/s]	Rtm [N]	Lk [m]	Lc [m]	S [m2]	Trim [deg]	RCG [mm]
366	1.247	6.209	1.50	1.50	0.400	0.20	−4.0
369	1.684	14.453	1.43	1.46	0.398	1.20	−9.0
370	2.106	25.320	1.28	1.43	0.388	3.15	−11.0
371	2.510	26.628	1.24	1.37	0.375	3.45	−6.0
372	2.948	29.118	1.16	1.39	0.370	3.60	−2.0
373	3.369	30.740	1.13	1.37	0.359	3.80	4.0
374	3.807	30.934	1.11	1.33	0.350	4.30	9.0
375	4.228	29.999	0.99	1.31	0.332	4.70	15.0
376	4.649	27.328	0.88	1.22	0.297	5.25	20.0
377	5.037	28.423	0.83	1.20	0.284	5.25	26.0
378	5.475	31.300	0.79	1.16	0.274	5.10	31.5
379	5.896	35.500	0.77	1.14	0.265	4.80	36.5

model 432

L/B [−]	Depl [N]	LCG [%Lp]	Ap/V [−]
5.5	147.300	−4.000	5.50

run	Vm [m/s]	Rtm [N]	Lk [m]	Lc [m]	S [m2]	Trim [deg]	RCG [mm]
338	1.167	3.474	1.50	1.50	0.400	0.00	−3.8
339	1.556	7.558	1.50	1.50	0.400	0.30	−6.5
340	1.945	12.938	1.35	1.43	0.393	1.75	−8.2
341	2.349	15.045	1.24	1.43	0.383	2.31	−4.1
342	2.736	16.803	1.16	1.41	0.370	2.25	−2.0
343	3.142	19.228	1.13	1.39	0.362	2.36	1.0
344	3.516	21.416	1.09	1.39	0.357	2.45	5.0
345	3.920	23.514	1.05	1.39	0.353	2.69	8.5
346	4.278	25.000	0.96	1.37	0.336	2.75	9.5
347	4.667	26.364	0.96	1.37	0.334	3.13	10.5
348	5.056	27.420	0.94	1.37	0.331	3.25	13.2
350	5.445	29.000	0.86	1.35	0.315	3.35	15.0
351	5.834	31.700	0.83	1.35	0.308	3.80	16.5

model 433

L/B [−]	Depl [N]	LCG [%Lp]	Ap/V [−]
5.5	147.300	−6.000	5.50

run	Vm [m/s]	Rtm [N]	Lk [m]	Lc [m]	S [m2]	Trim [deg]	RCG [mm]
352	1.167	3.550	1.50	1.50	0.400	0.00	−2.5
353	1.556	7.799	1.35	1.46	0.398	0.20	−6.0
354	1.945	13.354	1.20	1.43	0.378	1.90	−9.5
355	2.349	15.197	1.13	1.39	0.362	2.50	−5.0
356	2.736	16.815	1.05	1.39	0.353	2.53	−2.0
357	3.158	18.656	1.01	1.37	0.344	2.60	1.0
359	3.516	20.033	0.94	1.37	0.331	2.60	5.0
360	3.869	21.567	0.92	1.37	0.326	2.80	8.0
361	4.294	22.719	0.86	1.35	0.315	3.25	11.0
362	4.683	23.959	0.83	1.33	0.304	3.40	14.0
363	5.040	25.407	0.79	1.31	0.295	3.40	16.0
366	5.445	27.000	0.75	1.31	0.289	3.35	19.5
367	5.834	29.000	0.69	1.29	0.276	3.20	25.0

L/B [-]	Depl [N]	LCG [%Lp]	Ap/V [-]
5.5	102.600	0.000	7.00

run	Vm [m/s]	Rtm [N]	Lk [m]	Lc [m]	S [m2]	Trim [deg]	RCG [mm]
287	1.064	2.156	1.50	1.50	0.363	−0.10	−2.5
288	1.465	4.789	1.50	1.50	0.380	−0.15	−4.0
289	1.831	7.589	1.50	1.50	0.380	0.00	−6.5
290	2.197	9.744	1.35	1.50	0.384	1.30	−5.5
291	2.563	11.654	1.20	1.49	0.378	1.35	−4.5
292	2.929	14.643	1.16	1.49	0.376	1.42	−2.5
293	3.281	16.777	1.13	1.48	0.369	1.42	0.0
294	3.679	19.643	1.09	1.49	0.364	1.40	1.0
295	4.043	23.126	1.05	1.43	0.350	1.35	1.5
296	4.396	26.606	1.01	1.43	0.352	1.35	0.0
297	4.775	30.092	0.96	1.48	0.347	1.50	−1.0
298	5.128	33.200	0.94	1.48	0.341	1.60	−0.5
299	5.493	36.000	0.90	1.43	0.334	1.75	1.0

[illegible]			
5.5	76.600	0.000	8.50

run	Vm [m/s]	Rtm [N]	Lk [m]	Lc [m]	S [m2]	Trim [deg]	RCG [mm]
201	1.046	1.607	1.35	1.50	0.357	−0.10	−1.8
202	1.395	3.371	1.28	1.50	0.343	−0.08	−3.0
203	1.758	5.035	1.20	1.50	0.340	0.25	−4.3
204	2.107	6.815	1.20	1.50	0.340	0.95	−4.8
205	2.456	7.999	1.05	1.50	0.331	0.95	−3.5
206	2.804	9.723	0.96	1.43	0.319	0.95	−3.0
207	3.139	12.000	0.96	1.43	0.319	1.00	−2.5
208	3.486	14.006	0.96	1.43	0.333	1.05	0.0
209	3.836	16.819	0.96	1.43	0.339	1.00	2.5
210	4.213	20.582	0.96	1.43	0.347	0.90	3.0
211	4.534	23.000	0.96	1.43	0.347	0.90	−1.0
212	4.883	26.300	0.96	1.43	0.347	0.85	−2.0
213	5.231	31.200	0.96	1.43	0.347	0.90	−2.0
214	5.580	35.200	0.96	1.43	0.347	0.90	−2.2

model 420

L/B [-]	Depl [N]	LCG [%Lp]	Ap/V [-]
5.5	102.600	−2.000	7.00

run	Vm [m/s]	Rtm [N]	Lk [m]	Lc [m]	S [m2]	Trim [deg]	RCG [mm]
300	1.099	2.272	1.50	1.50	0.360	−0.05	−3.0
301	1.460	4.725	1.50	1.50	0.377	−0.02	−4.3
302	1.831	7.554	1.43	1.50	0.360	0.72	−6.5
303	2.197	9.546	1.43	1.50	0.366	1.40	−5.0
304	2.563	11.104	1.35	1.46	0.362	1.46	−4.0
306	2.929	13.040	1.28	1.46	0.363	1.52	−2.5
307	3.296	15.557	1.16	1.46	0.376	1.52	0.0
308	3.662	18.066	1.05	1.43	0.359	1.50	3.5
309	4.043	20.633	0.96	1.43	0.347	1.45	4.0
310	4.423	23.491	0.90	1.43	0.334	1.50	3.0
311	4.780	26.207	0.86	1.43	0.326	1.65	2.5
312	5.128	29.400	0.83	1.43	0.320	1.70	2.5
312	5.493	30.626	0.80	1.43	0.317	1.80	4.0
313	5.673	34.251	0.79	1.43	0.313	1.95	7.0

model 410

L/B [-]	Depl [N]	LCG [%Lp]	Ap/V [-]
5.5	76.600	−2.000	8.50

run	Vm [m/s]	Rtm [N]	Lk [m]	Lc [m]	S [m2]	Trim [deg]	RCG [mm]
215	1.046	1.635	1.35	1.50	0.357	−0.05	−1.4
216	1.395	3.300	1.24	1.46	0.348	−0.05	−2.7
217	1.744	5.442	1.20	1.46	0.350	0.20	−4.5
219	2.093	6.700	1.05	1.44	0.338	1.00	−4.8
220	2.427	7.683	0.96	1.43	0.330	1.00	−3.0
221	2.804	9.416	0.94	1.43	0.327	1.05	−2.6
222	3.139	11.282	0.94	1.43	0.330	1.10	−1.5
223	3.502	13.348	0.94	1.43	0.333	1.10	−1.5
224	3.850	15.664	0.94	1.43	0.341	1.00	2.5
225	4.199	18.407	0.94	1.43	0.341	0.95	2.0
226	4.548	21.519	0.90	1.43	0.334	0.80	0.0
227	4.897	24.665	0.83	1.43	0.320	0.80	−1.0
0	0.000	0.000	0.00	0.00	0.000	0.00	0.0
228	5.580	31.400	0.79	1.43	0.313	0.85	0.0

model 422

L/B [-]	Depl [N]	LCG [%Lp]	Ap/V [-]
5.5	102.600	−4.000	7.00

run	Vm [m/s]	Rtm [N]	Lk [m]	Lc [m]	S [m2]	Trim [deg]	RCG [mm]
274	1.064	2.340	1.35	1.50	0.366	0.00	−2.0
275	1.465	4.797	1.43	1.50	0.366	0.10	−3.5
276	1.831	7.503	1.35	1.50	0.364	0.80	−6.0
273	2.197	9.400	1.35	1.50	0.362	1.25	−5.0
277	2.563	10.400	1.28	1.43	0.363	1.50	−3.5
278	2.929	12.559	1.05	1.43	0.559	1.60	−1.5
279	3.296	14.650	1.01	1.43	0.352	1.65	1.5
280	3.662	16.800	1.01	1.43	0.352	1.60	4.5
281	4.043	19.914	0.96	1.43	0.347	1.60	5.0
282	4.423	21.594	0.96	1.43	0.344	1.60	4.0
283	4.780	23.800	0.94	1.43	0.341	1.70	4.0
286	5.128	26.317	0.90	1.43	0.334	1.65	5.0
284	5.493	29.800	0.86	1.43	0.326	2.00	6.5
285	5.859	31.000	0.79	1.41	0.310	2.10	10.5

model 412

L/B [-]	Depl [N]	LCG [%Lp]	Ap/V [-]
5.5	76.600	−4.000	8.50

run	Vm [m/s]	Rtm [N]	Lk [m]	Lc [m]	S [m2]	Trim [deg]	RCG [mm]
230	1.046	1.711	1.35	1.50	0.354	−0.05	−1.5
231	1.381	3.371	1.31	1.50	0.366	0.05	−2.5
232	1.744	4.690	1.28	1.50	0.371	0.05	−4.2
233	2.093	6.548	1.20	1.43	0.359	1.05	−5.0
234	2.441	7.486	1.13	1.43	0.355	1.05	−2.5
235	2.804	9.059	1.13	1.43	0.358	1.05	−2.5
236	3.153	10.750	1.05	1.43	0.359	1.10	0.0
237	3.516	12.629	0.98	1.43	0.347	1.10	2.2
238	3.864	14.592	0.96	1.43	0.347	1.05	4.5
239	4.213	17.114	0.96	1.43	0.347	0.95	3.5
240	4.562	19.852	0.96	1.43	0.347	0.90	1.5
241	4.883	22.800	0.96	1.43	0.347	0.90	0.5
243	5.231	25.200	0.90	1.43	0.334	1.00	1.5
242	5.580	28.000	0.90	1.43	0.334	1.05	2.5
244	5.929	30.600	0.90	1.43	0.334	1.10	3.5

model 423

L/B [-]	Depl [N]	LCG [%Lp]	Ap/V [-]
5.5	102.600	−6.000	7.00

run	Vm [m/s]	Rtm [N]	Lk [m]	Lc [m]	S [m2]	Trim [deg]	RCG [mm]
259	1.064	2.414	1.35	1.50	0.374	0.10	−2.5
260	1.460	4.774	1.28	1.50	0.377	0.28	−5.0
261	1.831	7.804	1.16	1.43	0.353	1.20	−7.0
262	2.197	9.481	1.05	1.43	0.353	1.70	−5.0
263	2.563	10.536	0.98	1.43	0.347	1.75	−3.0
264	2.915	11.961	0.90	1.43	0.334	1.60	0.0
265	3.310	13.564	0.83	1.43	0.320	1.60	2.5
266	3.676	15.177	0.79	1.41	0.310	1.60	6.0
267	4.028	16.905	0.75	1.39	0.301	1.75	7.0
268	4.394	18.500	0.75	1.35	0.295	1.90	7.0
269	4.760	20.330	0.75	1.35	0.295	2.00	7.0
270	5.126	22.000	0.68	1.35	0.281	2.05	9.5
272	5.493	24.000	0.64	1.35	0.273	2.15	11.0
271	5.859	25.800	0.64	1.35	0.273	2.20	13.0

model 413

L/B [-]	Depl [N]	LCG [%Lp]	Ap/V [-]
5.5	76.600	−6.000	8.50

run	Vm [m/s]	Rtm [N]	Lk [m]	Lc [m]	S [m2]	Trim [deg]	RCG [mm]
245	1.046	1.847	1.35	1.50	0.354	0.05	−1.5
246	1.395	3.563	1.35	1.50	0.360	0.20	−2.5
247	1.744	5.254	1.20	1.43	0.362	0.70	−5.0
249	2.107	6.587	1.13	1.43	0.352	1.20	−4.5
250	2.441	7.517	0.96	1.43	0.336	1.25	−2.0
248	2.790	8.719	0.96	1.43	0.336	1.25	−1.0
251	3.139	9.991	0.43	1.43	0.320	1.30	1.0
252	3.488	11.515	0.71	1.43	0.300	1.21	3.5
253	3.836	13.118	0.71	1.41	0.300	1.10	5.5
254	4.213	15.049	0.71	1.41	0.296	1.05	5.5
256	4.534	17.000	0.68	1.43	0.291	1.05	4.5
255	4.883	19.000	0.68	1.41	0.291	1.05	5.0
257	5.231	21.300	0.68	1.41	0.291	1.10	6.0
258	5.580	23.500	0.68	1.41	0.291	1.20	7.5

run	Vm [m/s]	Rtm [N]	Lk [m]	Lc [m]	S [m2]	Trim [deg]	RCG [mm]
596	1.173	3.484	1.50	1.50	0.324	−0.05	−4.0
597	1.570	7.556	1.50	1.50	0.324	0.00	−7.0
598	1.966	13.169	1.50	1.50	0.324	1.40	−10.0
599	2.363	16.603	1.50	1.50	0.324	2.30	−8.0
600	2.759	19.994	1.50	1.50	0.324	2.40	−5.0
601	3.045	20.753	1.50	1.50	0.324	2.35	−4.0
602	3.568	25.110	1.50	1.50	0.324	2.15	0.0
603	3.960	29.310	1.50	1.50	0.324	1.80	0.0

run	Vm [m/s]	Rtm [N]	Lk [m]	Lc [m]	S [m2]	Trim [deg]	RCG [mm]
530	1.084	2.005	1.50	1.50	0.323	0.00	0.0
531	1.464	4.346	1.50	1.50	0.323	−0.10	−4.0
532	1.816	6.882	1.50	1.50	0.323	0.70	−6.0
533	2.162	9.066	1.50	1.50	0.323	1.40	−8.0
534	2.548	10.786	1.50	1.50	0.323	1.55	−4.0
535	2.958	12.844	1.50	1.50	0.323	1.65	−2.5
536	3.280	14.848	1.50	1.50	0.323	1.60	−1.8
537	3.681	16.239	1.50	1.50	0.323	1.50	0.3
538	4.041	21.887	1.50	1.50	0.323	1.30	1.0

model 540

L/B [−]	Depl [N]	LCG [%Lp]	Ap/V [−]
7	165.200	−2.000	4.00

run	Vm [m/s]	Rtm [N]	Lk [m]	Lc [m]	S [m2]	Trim [deg]	RCG [mm]
604	1.173	3.384	1.50	1.50	0.324	0.00	−3.0
605	1.570	7.560	1.50	1.50	0.324	0.10	−6.0
606	1.966	13.536	1.50	1.50	0.324	1.50	−10.0
607	2.363	16.892	1.50	1.50	0.324	2.30	−7.0
608	2.775	19.277	1.50	1.50	0.324	2.50	−5.0
609	3.171	22.473	1.50	1.50	0.324	2.50	−1.0
610	3.568	25.758	1.50	1.50	0.324	2.40	1.0
611	3.980	29.460	1.50	1.50	0.324	2.30	3.0
612	4.361	33.773	1.50	1.50	0.324	2.55	3.0

model 530

L/B [−]	Depl [N]	LCG [%Lp]	Ap/V [−]
7	102.400	−2.000	5.50

run	Vm [m/s]	Rtm [N]	Lk [m]	Lc [m]	S [m2]	Trim [deg]	RCG [mm]
541	1.084	2.015	1.50	1.50	0.323	−0.05	−2.0
540	1.450	4.267	1.50	1.50	0.323	0.00	−4.0
542	1.830	7.200	1.50	1.50	0.323	0.80	−7.0
543	2.196	9.523	1.50	1.50	0.323	1.70	−6.0
544	2.548	10.774	1.50	1.50	0.323	1.75	−4.0
545	2.928	12.491	1.35	1.46	0.316	1.80	−2.0
546	3.294	14.248	1.35	1.46	0.316	1.75	0.0
547	3.675	16.473	1.31	1.46	0.315	1.80	2.0
548	4.056	18.654	1.28	1.46	0.314	1.90	4.0
554	4.437	20.998	1.24	1.46	0.310	2.10	3.0
550	4.786	22.270	1.13	1.43	0.296	2.40	8.0
0	0.000	0.000	0.00	0.00	0.000	0.00	0.0
551	5.491	24.700	0.98	1.43	0.278	3.00	9.0

model 542

L/B [−]	Depl [N]	LCG [%Lp]	Ap/V [−]
7	165.200	−4.000	4.00

run	Vm [m/s]	Rtm [N]	Lk [m]	Lc [m]	S [m2]	Trim [deg]	RCG [mm]
613	1.158	3.612	1.50	1.50	0.324	0.00	−3.0
614	1.602	8.079	1.50	1.50	0.324	0.30	−7.0
615	1.966	14.013	1.50	1.50	0.324	1.80	−10.0
616	2.379	17.781	1.50	1.50	0.324	2.70	−7.0
617	2.775	19.564	1.50	1.50	0.324	2.65	−4.0
618	3.171	22.080	1.50	1.50	0.324	2.70	−1.0
619	3.568	24.790	1.50	1.50	0.324	2.70	2.0
620	3.996	27.236	1.35	1.43	0.307	2.95	6.0
622	4.377	29.408	1.13	1.39	0.290	3.70	9.0
623	4.757	30.500	1.07	1.39	0.283	4.35	12.0
625	5.154	31.000	0.91	1.36	0.257	5.00	16.0
624	5.550	31.400	0.90	1.33	0.253	5.30	22.0
626	5.946	33.000	0.88	1.30	0.247	5.10	27.0

model 532

L/B [−]	Depl [N]	LCG [%Lp]	Ap/V [−]
7	102.400	−4.000	5.50

run	Vm [m/s]	Rtm [N]	Lk [m]	Lc [m]	S [m2]	Trim [deg]	RCG [mm]
555	1.099	2.417	1.50	1.50	0.323	0.00	−2.5
556	1.450	4.492	1.50	1.50	0.323	0.05	−4.0
557	1.816	7.285	1.50	1.50	0.323	1.05	−7.5
558	2.182	9.156	1.50	1.50	0.323	1.70	−6.0
559	2.548	10.436	1.28	1.46	0.316	1.80	−3.8
560	2.928	12.090	1.28	1.43	0.310	1.85	−2.0
562	3.280	13.739	1.20	1.43	0.303	1.90	1.0
563	3.646	15.431	1.16	1.43	0.299	2.00	4.0
564	4.027	17.056	1.13	1.43	0.296	2.10	6.0
565	4.407	18.912	1.09	1.43	0.291	2.30	5.8
566	4.759	20.151	1.05	1.43	0.286	2.60	5.7
567	5.227	21.201	0.94	1.39	0.267	2.90	8.0
568	5.491	22.100	0.86	1.39	0.255	3.00	10.0
569	5.901	24.641	0.83	1.39	0.251	3.00	12.0

model 543

L/B [−]	Depl [N]	LCG [%Lp]	Ap/V [−]
7	165.200	−6.000	4.00

run	Vm [m/s]	Rtm [N]	Lk [m]	Lc [m]	S [m2]	Trim [deg]	RCG [mm]
584	1.158	3.679	1.50	1.50	0.323	0.20	−4.0
585	1.586	8.611	1.50	1.50	0.323	0.70	−8.0
586	1.982	15.021	1.35	1.46	0.316	2.15	−10.0
587	2.363	19.299	1.28	1.43	0.310	3.05	−8.0
588	2.759	20.483	1.24	1.43	0.300	3.05	−4.0
589	3.156	22.526	1.16	1.43	0.299	3.30	0.0
590	3.568	24.929	1.13	1.43	0.296	3.60	4.0
591	3.984	27.363	1.01	1.43	0.281	4.20	9.0
592	4.377	29.278	0.94	1.35	0.261	4.65	13.0
593	4.741	31.001	0.90	1.28	0.247	5.50	17.0
594	5.154	30.945	0.84	1.24	0.233	5.45	21.5

model 533

L/B [−]	Depl [N]	LCG [%Lp]	Ap/V [−]
7	102.400	−6.000	5.50

run	Vm [m/s]	Rtm [N]	Lk [m]	Lc [m]	S [m2]	Trim [deg]	RCG [mm]
570	1.099	2.318	1.35	1.46	0.316	0.05	−2.0
571	1.464	4.859	1.35	1.46	0.316	0.04	−4.0
572	1.830	8.052	1.28	1.43	0.310	1.35	−6.0
573	2.182	9.541	1.16	1.43	0.299	1.85	−5.0
574	2.562	10.530	1.09	1.41	0.288	2.00	−2.0
575	2.928	12.027	1.09	1.41	0.288	2.05	−1.0
576	3.280	13.522	1.01	1.41	0.278	2.20	1.0
577	3.646	15.030	0.96	1.39	0.272	2.30	4.0
578	4.041	16.348	0.94	1.39	0.267	2.50	8.0
579	4.407	17.945	0.86	1.39	0.255	2.80	7.0
580	4.773	18.756	0.83	1.39	0.251	3.10	9.0
581	5.169	20.153	0.79	1.35	0.240	3.15	12.0
582	5.491	21.800	0.75	1.35	0.234	3.20	14.5
583	5.857	23.400	0.71	1.31	0.223	3.10	16.5

model 531

L/B [-]	Depl [N]	LCG [%Lp]	Ap/V [-]
7	71.300	0.000	7.00

run	Vm [m/s]	Rtm [N]	Lk [m]	Lc [m]	S [m2]	Trim [deg]	RCG [mm]
469	1.034	1.357	1.29	1.46	0.306	−0.05	−1.5
469	1.376	2.757	1.28	1.46	0.306	−0.02	−3.0
470	1.723	4.230	1.28	1.46	0.306	0.30	−4.2
471	2.068	5.745	1.26	1.46	0.311	0.99	−5.0
472	2.399	6.717	1.29	1.43	0.310	1.10	−3.8
473	2.757	8.133	1.28	1.43	0.310	1.20	−2.0
474	3.102	9.600	1.24	1.43	0.309	1.20	−1.5
475	3.446	11.025	1.24	1.43	0.308	1.20	0.5
476	3.816	13.049	1.24	1.43	0.308	1.15	2.0
477	4.136	15.537	1.24	1.43	0.308	1.20	2.0
478	4.484	17.614	1.24	1.46	0.308	1.30	0.0
479	4.852	19.619	1.20	1.43	0.308	1.40	0.0
480	5.169	21.600	1.20	1.43	0.309	1.50	0.0
482	5.514	23.600	1.19	1.40	0.292	1.70	2.5
484	5.859	25.600	1.05	1.40	0.282	1.85	5.0

model 511

L/B [-]	Depl [N]	LCG [%Lp]	Ap/V [-]
7	53.400	0.000	8.50

run	Vm [m/s]	Rtm [N]	Lk [m]	Lc [m]	S [m2]	Trim [deg]	RCG [mm]
407	0.965	1.117	1.38	1.50	0.299	−0.05	−1.0
409	1.340	2.106	1.31	1.50	0.303	0.00	−2.0
410	1.642	3.101	1.31	1.50	0.297	0.14	−3.0
411	1.970	4.026	1.29	1.50	0.304	0.50	−4.0
413	2.312	4.926	1.20	1.49	0.296	0.63	−2.2
414	2.627	5.924	1.13	1.49	0.289	0.85	−3.0
412	2.958	7.109	1.20	1.50	0.301	0.90	−2.0
415	3.284	8.369	1.13	1.43	0.290	0.95	0.0
416	3.629	10.036	1.09	1.43	0.291	0.93	2.0
417	3.954	11.804	1.05	1.43	0.286	0.90	2.2
418	4.283	13.725	1.01	1.43	0.281	0.85	0.0
419	4.611	15.932	1.01	1.43	0.281	0.90	−2.0
420	4.926	18.000	1.01	1.43	0.281	0.90	−2.0
422	5.294	20.523	1.01	1.43	0.281	0.90	−1.0

model 520

L/B [-]	Depl [N]	LCG [%Lp]	Ap/V [-]
7	71.300	−2.000	7.00

run	Vm [m/s]	Rtm [N]	Lk [m]	Lc [m]	S [m2]	Trim [deg]	RCG [mm]
485	1.034	1.448	1.38	1.46	0.306	−0.03	−2.0
486	1.378	2.800	1.38	1.46	0.306	0.03	−2.5
487	1.723	4.300	1.38	1.46	0.306	0.40	−4.0
488	2.068	5.861	1.31	1.44	0.305	0.92	−5.0
489	2.412	6.714	1.26	1.44	0.306	1.15	−2.2
490	2.771	8.070	1.29	1.43	0.309	1.20	−2.0
491	3.102	9.400	1.23	1.43	0.306	1.22	−1.2
492	3.460	11.053	1.20	1.43	0.303	1.30	1.8
493	3.791	12.482	1.16	1.43	0.299	1.30	4.0
494	4.204	14.567	1.13	1.43	0.296	1.30	4.0
495	4.508	16.331	1.09	1.43	0.291	1.35	1.0
496	4.825	18.437	1.05	1.41	0.284	1.45	2.0
497	5.169	19.900	1.05	1.39	0.281	1.50	2.0
499	5.542	21.600	0.98	1.39	0.272	1.70	4.0
498	5.859	23.200	0.90	1.39	0.261	1.80	5.5

model 510

L/B [-]	Depl [N]	LCG [%Lp]	Ap/V [-]
7	53.400	−2.000	8.50

run	Vm [m/s]	Rtm [N]	Lk [m]	Lc [m]	S [m2]	Trim [deg]	RCG [mm]
423	0.965	1.120	1.38	1.46	0.291	0.00	−1.5
425	1.327	2.195	1.38	1.46	0.297	0.00	−2.0
426	1.642	3.085	1.38	1.46	0.299	0.20	−2.0
427	1.970	4.105	1.31	1.43	0.298	0.58	−4.0
430	2.378	5.111	1.26	1.43	0.310	0.80	−3.0
431	2.627	5.825	1.20	1.43	0.303	0.80	−3.0
429	2.962	7.405	1.13	1.43	0.296	0.90	−1.5
432	3.297	8.856	1.05	1.43	0.286	0.95	0.0
433	3.626	9.727	1.01	1.43	0.281	0.95	2.0
434	3.967	11.522	0.98	1.43	0.278	0.90	2.5
435	4.283	13.330	0.90	1.43	0.266	0.90	1.0
436	4.611	15.242	0.86	1.43	0.260	0.90	−0.5
437	4.926	16.660	0.84	1.42	0.256	1.00	0.0
439	5.256	19.000	0.84	1.41	0.256	1.00	0.0
438	5.583	21.000	0.84	1.41	0.256	1.05	1.0

model 522

L/B [-]	Depl [N]	LCG [%Lp]	Ap/V [-]
7	71.300	−4.000	7.00

run	Vm [m/s]	Rtm [N]	Lk [m]	Lc [m]	S [m2]	Trim [deg]	RCG [mm]
500	1.034	1.517	1.28	1.46	0.303	0.00	−2.5
501	1.378	2.800	1.28	1.46	0.303	0.10	−4.0
502	1.709	4.304	1.26	1.46	0.303	0.60	−5.0
503	2.054	5.549	1.26	1.43	0.306	1.00	−6.0
504	2.412	6.519	1.20	1.43	0.300	1.20	−3.0
505	2.757	7.853	1.16	1.43	0.301	1.25	−2.0
506	3.102	9.000	1.16	1.43	0.299	1.30	0.0
507	3.446	10.328	1.09	1.41	0.286	1.35	2.0
508	3.791	11.866	1.09	1.41	0.286	1.35	4.0
509	4.149	13.507	1.05	1.41	0.284	1.35	4.0
510	4.508	15.401	1.04	1.39	0.280	1.35	2.0
511	4.825	16.991	1.04	1.39	0.280	1.55	3.0
514	5.183	18.806	1.04	1.39	0.280	1.65	4.0
513	5.610	20.112	1.00	1.39	0.280	1.80	6.0

model 512

L/B [-]	Depl [N]	LCG [%Lp]	Ap/V [-]
7	53.400	−4.000	8.50

run	Vm [m/s]	Rtm [N]	Lk [m]	Lc [m]	S [m2]	Trim [deg]	RCG [mm]
441	0.965	1.131	1.28	1.43	0.282	0.00	−1.0
440	1.314	2.169	1.26	1.43	0.282	0.10	−2.0
442	1.642	3.067	1.20	1.43	0.280	0.32	−3.5
443	1.970	3.991	1.20	1.43	0.283	0.60	−4.0
444	2.298	4.829	1.13	1.43	0.282	0.65	−2.5
445	2.640	5.882	1.13	1.43	0.282	0.85	−2.5
446	2.969	6.811	1.01	1.43	0.281	1.00	−1.0
447	3.284	7.791	1.01	1.43	0.281	1.00	0.0
448	3.613	9.353	0.98	1.43	0.278	1.00	1.8
449	3.941	11.023	0.94	1.43	0.272	0.98	3.0
450	4.296	12.842	0.90	1.43	0.266	0.95	2.0
451	4.624	14.564	0.90	1.41	0.263	0.95	1.0
452	4.926	16.000	0.83	1.41	0.254	1.00	1.0
453	5.255	17.850	0.83	1.39	0.251	1.05	2.0

model 523

L/B [-]	Depl [N]	LCG [%Lp]	Ap/V [-]
7	71.300	−6.000	7.00

run	Vm [m/s]	Rtm [N]	Lk [m]	Lc [m]	S [m2]	Trim [deg]	RCG [mm]
515	1.034	1.512	1.26	1.43	0.299	0.06	−1.0
516	1.378	3.056	1.26	1.43	0.299	0.20	−2.0
517	1.709	4.717	1.24	1.43	0.295	0.80	−5.0
518	2.068	5.751	1.16	1.41	0.286	1.20	−5.0
519	2.412	6.566	1.05	1.41	0.281	1.30	−2.2
520	2.743	7.523	1.05	1.39	0.284	1.30	−2.0
522	3.102	9.000	0.98	1.39	0.272	1.45	0.5
523	3.432	10.366	0.90	1.39	0.261	1.50	2.0
521	3.763	11.366	0.90	1.37	0.256	1.50	5.7
524	4.122	12.660	0.83	1.39	0.251	1.50	6.0
525	4.464	14.166	0.83	1.37	0.249	1.60	4.0
526	4.839	15.634	0.79	1.35	0.240	1.80	6.0
527	5.169	17.000	0.75	1.35	0.234	1.90	6.5
528	5.528	18.843	0.79	1.35	0.240	1.95	8.0
526	5.859	20.600	0.75	1.33	0.232	2.00	10.5

model 513

L/B [-]	Depl [N]	LCG [%Lp]	Ap/V [-]
7	53.400	−6.000	8.50

run	Vm [m/s]	Rtm [N]	Lk [m]	Lc [m]	S [m2]	Trim [deg]	RCG [mm]
454	0.965	1.191	1.16	1.43	0.271	0.05	−1.0
455	1.314	2.290	1.16	1.43	0.279	0.20	−2.0
456	1.642	3.231	1.13	1.37	0.277	0.45	−3.0
457	1.970	4.052	0.98	1.37	0.262	0.72	−4.0
458	2.298	4.952	0.98	1.37	0.270	0.95	−2.0
459	2.627	5.826	0.94	1.37	0.264	0.95	−2.0
460	2.956	6.820	0.87	1.37	0.254	1.00	−1.0
461	3.284	7.748	0.83	1.37	0.249	1.05	2.0
462	3.626	8.921	0.83	1.37	0.249	1.02	4.0
463	3.954	10.121	0.83	1.37	0.249	1.00	5.0
464	4.269	11.477	0.83	1.37	0.249	1.00	5.0
465	4.624	13.271	0.79	1.37	0.243	1.00	3.0
466	4.926	14.686	0.75	1.37	0.237	1.10	3.0
467	5.294	16.509	0.71	1.37	0.230	1.20	4.0

Appendix 2: Coefficients of polynomial model

β	Fn_∇		a_0	a_1	a_2	a_3	a_4	a_5	a_6
			a_7	a_8	a_9	a_{10}	a_{11}	a_{12}	
12.5	.75	R_t/Δ, ∇=5	.1120E+00	-.1289E-01	.1197E-02	-.3479E-04	-.2297E-01	.2924E-02	-.1347E-03
			-.7272E-03	9765E-04	.4226E-05	.1256E-04	.2713E-03	.1774E-03	
		R_t/Δ, ∇=50	.1115E+00	-.1290E-01	.1199E-02	- 3510E-04	- 2300E-01	.2917E-02	- 1344E-03
			-.7217E-03	9901E-04	.4318E-05	.1130E-04	.2728E-03	.1786E-03	
		θ	.1129E+01	.1696E+01	- 3130E+00	.2169E-01	-.2760E+01	.4720E+00	- 2433E-01
			- 3112E+00	.1163E-01	.5206E-03	.2458E-01	-.3180E-02	.3304E-01	
		$RCG/\nabla^{1/3}$	-.4074E+00	.9876E-01	-.2147E-01	.1515E-02	.9922E-01	-.1388E-01	.7181E-03
			- 6410E-02	.2775E-03	.1503E-04	.1030E-02	-.4586E-03	.1524E-04	
	1.00	R_t/Δ, ∇=5	.3996E+00	- 9231E-01	.1192E-01	-.6086E-03	- 4127E-01	.2720E-02	- 5832E-04
			.1094E-02	.3815E-03	.9987E-05	.2345E-03	.1766E-02	.5378E-04	
		R_t/Δ, ∇=50	.4002E+00	- 9267E-01	.1201E-01	- 6158E-03	-.4170E-01	.2753E-02	- 5955E-04
			.1136E-02	.3879E-03	.1025E-04	.2308E-03	.1773E-02	.5885E-04	
		θ	.1515E+02	-.9005E+00	.1166E+00	- 4535E-02	-.6366E+01	.8357E+00	-.3731E-01
			-.7934E+00	.1718E-01	.4324E-03	.5055E-01	.9474E-01	.9864E-01	
		$RCG/\nabla^{1/3}$	-.3261E+00	.9289E-01	-.2020E-01	.1426E-02	.2227E-01	.1884E-03	-.3914E-04
			-.1948E-01	.2537E-03	.1417E-04	.2314E-02	.3813E-03	.7261E-03	
	1.25	R_t/Δ, ∇=5	.8393E+00	-.1246E+00	.1461E-01	- 6615E-03	-.1753E+00	.2255E-01	-.1016E-02
			.4165E-02	6591E-03	.1478E-04	.8072E-03	.1433E-02	-.7895E-03	
		R_t/Δ, ∇=50	.8375E+00	- 1248E+00	.1466E-01	-.6656E-03	- 1748E+00	2243E-01	- 1009E-02
			.4036E-02	.6488E-03	1417E-04	.8146E-03	.1445E-02	-.7806E-03	
		θ	.9889E+01	- 7061E+01	.9620E+00	-.5360E-01	.5572E+01	- 1291E+01	.7367E-01
			- 3946E+00	3410E-01	.1764E-02	.1420E-01	.2198E+00	.7282E-01	
		$RCG/\nabla^{1/3}$	-.1057E+01	.6355E-01	-.2372E-01	.1890E-02	4602E+00	- 7229E-01	3700E-02
			-.1873E-01	.4248E-03	.2053E-04	.2296E-02	.3490E-02	.1174E-02	
	1.50	R_t/Δ, ∇=5	.7786E+00	-.1016E+00	.9022E-02	- 2943E-03	-.1539E+00	.1795E-01	-.7779E-03
			.3499E-02	.1219E-02	.3137E-04	.1069E-02	.3079E-02	.1622E-04	
		R_t/Δ, ∇=50	.7830E+00	-.1028E+00	.9261E-02	- 3111E-03	- 1560E+00	.1823E-01	-.7923E-03
			.3454E-02	.1226E-02	.3162E-04	.1069E-02	.3087E-02	3045E-04	
		θ	.4786E+02	- 9164E+01	.1350E+01	-.7826E-01	-.9693E+01	.1005E+01	- 3806E-01
			-.3616E+00	.1714E-01	.6256E-03	.3080E-01	.2011E+00	.3556E-01	
		$RCG/\nabla^{1/3}$	- 5638E+00	- 2403E-01	-.1195E-01	.1194E-02	.3355E+00	- 5715E-01	3043E-02
			-.2849E-01	- 8738E-03	-.4271E-04	.2585E-02	.5695E-02	.8498E-03	
	1.75	R_t/Δ, ∇=5	.5817E+00	2683E-01	-.1742E-01	.1476E-02	-.1538E+00	.1827E-01	-.7977E-03
			9107E-03	1048E-02	2881E-04	.1050E-02	.2770E-02	.1664E-03	
		R_t/Δ, ∇=50	.5824E+00	.2586E-01	- 1725E-01	.1465E-02	- 1542E+00	.1826E-01	- 7975E-03
			8446E-03	1059E-02	.2918E-04	1052E-02	.2781E-02	.1844E-03	
		θ	.3161E+02	- 6006E+01	.6319E+00	- 2905E-01	- 2892E+01	- 7939E-01	1623E-01
			- 4067E-01	.1568E-01	.6076E-03	- 1308E-02	.1856E+00	.1581E-01	
		$RCG/\nabla^{1/3}$	7918E-01	3672E-01	- 2361E-01	.2115E-02	.5393E-01	- 1695E-01	.1139E-02
			-.1168E-01	-.1828E-03	- 2390E-04	5145E-03	.3081E-02	.1509E-02	

12.5	2.00	R_t/Δ, ∇=5	.4372E+00	.6303E-01	-.2146E-01	.1633E-02	-.1229E+00	.1416E-01	-.6035E-03
			.1789E-02	.9401E-03	.2507E-04	.7046E-03	.2017E-02	3221E-03	
		R_t/Δ, ∇=50	.4373E+00	.6227E-01	-.2136E-01	.1627E-02	-.1232E+00	.1413E-01	-.6023E-03
			.1756E-02	.9546E-03	.2561E-04	.6993E-03	.2028E-02	.3424E-03	
		θ	.1322E+02	-.2002E+01	-.1667E+00	.2536E-01	.3508E+01	-.1046E+01	.6417E-01
			.1978E+00	.3248E-02	-.2820E-03	-.2124E-01	.1421E+00	-.5899E-02	
		$RCG/\nabla^{1/3}$	.3061E+00	.5434E-01	-.2693E-01	.2561E-02	-.3087E-01	-.5601E-02	.6545E-03
			-.1355E-01	-.8926E-03	-.6666E-04	.5779E-03	.2339E-02	1237E-02	
	2.25	R_t/Δ, ∇=5	.4683E+00	.4320E-01	-.1361E-01	.1000E-02	-.1418E+00	.1779E-01	-.7790E-03
			.9081E-03	.9836E-03	.3078E-04	.8248E-03	.1317E-02	.3086E-03	
		R_t/Δ, ∇=50	.4695E+00	.4205E-01	-.1342E-01	.9850E-03	-.1423E+00	.1773E-01	-.7758E-03
			.9280E-03	.1002E-02	.3148E-04	.8095E-03	.1326E-02	.3277E-03	
		θ	.2005E+02	-.8878E+00	-.2429E+00	.2151E-01	-.1223E+01	-.2412E+00	.2287E-01
			.4608E+00	.3414E-01	.1530E-02	-.1894E-01	.8043E-01	-.3643E-01	
		$RCG/\nabla^{1/3}$	.9376E-01	-.7904E-02	-.1772E-01	.1632E-02	.1013E+00	-.2329E-01	.1340E-02
			-.1703E-01	-.1087E-02	-.5905E-04	.1185E-02	.4634E-02	.2907E-03	
	2.50	R_t/Δ, ∇=5	.3276E+00	.2996E-01	-.7670E-02	.5118E-03	-.7863E-01	.8623E-02	-.3192E-03
			.1414E-02	.7821E-03	.2343E-04	.6311E-03	.5793E-03	1716E-03	
		R_t/Δ, ∇=50	.3278E+00	.2871E-01	-.7447E-02	4925E-03	-.7886E-01	.8539E-02	-.3161E-03
			.1371E-02	.7906E-03	.2369E-04	.6169E-03	.5856E-03	.1842E-03	
		θ	.5497E+01	-.1505E+00	-.2074E+00	.1446E-01	.4538E+01	-.1070E+01	6381E-01
			.5650E+00	.1284E-01	.2049E-03	-.2930E-01	.1067E-01	-.5021E-01	
		$RCG/\nabla^{1/3}$	.5347E+00	.2676E-01	-.2602E-01	.2249E-02	-.1207E+00	.1309E-01	-.5889E-03
			.2506E-02	.1169E-02	.5121E-04	.4842E-03	.4146E-02	.1570E-04	
	2.75	R_t/Δ, ∇=5	.2864E+00	.2157E-01	-.4537E-02	.2855E-03	-.6463E-01	.7329E-02	-.2793E-03
			.2635E-02	.8383E-03	.2825E-04	.5046E-03	.3729E-03	.1657E-03	
		R_t/Δ, ∇=50	.2891E+00	.1934E-01	-.4014E-02	.2408E-03	-.6574E-01	.7390E-02	-.2841E-03
			.2672E-02	.8536E-03	.2874E-04	.4875E-03	.3528E-03	.1661E-03	
		θ	.5251E+01	-.2136E+00	-.4981E-01	-.2390E-03	.3763E+01	-.8703E+00	5193E-01
			.7439E+00	3604E-01	.1549E-02	-.2963E-01	-.3124E-01	-.6563E-01	
		$RCG/\nabla^{1/3}$	.4987E+00	-.2149E-01	-.8807E-02	.8621E-03	-.6185E-01	.3117E-02	-.3261E-04
			.7517E-02	.8079E-03	.3312E-04	-.3072E-03	.2070E-02	-.2094E-03	
	3.00	R_t/Δ, ∇=5	.2041E+00	.2262E-01	-.4611E-02	.3277E-03	-.3360E-01	.3327E-02	-.9487E-04
			.2499E-02	.6954E-03	.2360E-04	.4707E-03	.1737E-03	.8781E-04	
		R_t/Δ, ∇=50	.2085E+00	.1942E-01	-.3751E-02	.2557E-03	-.3523E-01	.3475E-02	-.1039E-03
			.2569E-02	.7122E-03	.2412E-04	.4573E-03	.9270E-04	.6799E-04	
		θ	.2750E+01	-.6138E+00	.1493E+00	-.1441E-01	.4592E+01	-.9479E+00	.5502E-01
			.8403E+00	.3900E-01	.1814E-02	-.3527E-01	-.7550E-01	-.7209E-01	
		$RCG/\nabla^{1/3}$	.5527E+00	-.8569E-01	.6848E-02	-.2166E-03	-.4469E-01	5517E-03	.9890E-04
			.7751E-02	.3866E-03	.2107E-04	-.6350E-03	.1068E-02	-.7190E-03	

25	.75	R_t/Δ, ∇=5	.1266E+00	-.2424E-01	.3491E-02	-.1893E-03	-.2136E-01	.2706E-02	-.1263E-03
			-.1462E-02	-.4897E-05	-.4912E-06	.3145E-05	.2632E-03	.2009E-03	
		R_t/Δ, ∇=50	.1260E+00	-.2365E-01	.3359E-02	-.1802E-03	-.2152E-01	.2711E-02	-.1265E-03
			-.1457E-02	-.5151E-05	-.5195E-06	.2379E-05	.2653E-03	.2007E-03	
		θ	-.2791E+01	.6060E+00	-.1479E-01	-.8580E-03	.4449E-01	.1737E-01	-.3669E-03
			-.3048E+00	-.2215E-02	-.6126E-04	.1374E-01	-.2986E-01	.2900E-01	
		$RCG/\nabla^{1/3}$	-.5631E-01	.1358E-01	.1978E-03	-.9157E-04	-.1305E-01	.3252E-02	-.1867E-03
			-.2090E-02	.6262E-04	.5807E-05	.3741E-04	-.5312E-03	.3005E-03	
	1.00	R_t/Δ, ∇=5	.3665E+00	-.1043E+00	.1400E-01	-.7408E-03	-.1966E-01	-.6496E-03	.1031E-03
			-.1763E-02	.3776E-04	-.5533E-05	.2222E-03	.2048E-02	.2132E-03	
		R_t/Δ, ∇=50	.3659E+00	-.1036E+00	.1385E-01	-.7299E-03	-.2000E-01	-.6113E-03	.1012E-03
			-.1767E-02	.3688E-04	-.5624E-05	.2198E-03	.2048E-02	.2160E-03	
		θ	.1064E+02	-.2476E+01	.2907E+00	-.1443E-01	-.1992E+01	.9811E-01	-.2754E-03
			-.6578E+00	.2138E-03	.3172E-05	.2929E-01	.1417E+00	.7013E-01	
		$RCG/\nabla^{1/3}$	-.2468E+00	.5017E-01	-.5742E-02	.2944E-03	.2368E-01	-.1508E-02	.4642E-04
			-.7365E-02	-.8799E-04	.3699E-06	.2715E-03	-.8045E-03	.7947E-03	
	1.25	R_t/Δ, ∇=5	.7346E+00	-.1753E+00	.2059E-01	-.1003E-02	-.6923E-01	.3296E-02	-.3195E-04
			-.2975E-02	.1928E-03	-.4883E-05	.7575E-03	.4465E-02	.1095E-04	
		R_t/Δ, ∇=50	.7331E+00	-.1744E+00	.2037E-01	-.9872E-03	-.6949E-01	.3290E-02	-.3134E-04
			-.2984E-02	.1955E-03	-.4780E-05	.7530E-03	.4459E-02	.1806E-04	
		θ	.2407E+02	-.6571E+01	.7093E+00	-.3195E-01	-.1193E+01	-.1873E+00	1544E-01
			-.3438E+00	.7800E-02	.4234E-03	.1579E-01	2244E+00	.3405E-01	
		$RCG/\nabla^{1/3}$	-.2845E-01	-.4699E-01	.7296E-02	-.3960E-03	.2604E-01	-.5517E-02	.3090E-03
			-.8058E-02	-.1553E-03	-.4078E-05	.2832E-03	.2089E-02	.8162E-03	
	1.50	R_t/Δ, ∇=5	.8278E+00	-.1938E+00	.2319E-01	-.1139E-02	-.8753E-01	.4455E-02	-.1599E-05
			-.6563E-02	.2575E-03	-.1677E-04	.1527E-02	.5371E-02	.2796E-03	
		R_t/Δ, ∇=50	.8263E+00	-.1927E+00	2293E-01	-.1119E-02	-.8797E-01	.4460E-02	-.1314E-05
			-.6591E-02	.2606E-03	-.1666E-04	.1521E-02	5364E-02	.2897E-03	
		θ	.2832E+02	-.8269E+01	.1002E+01	-.4986E-01	-.3671E+00	-.3866E+00	2851E-01
			-.7646E+00	-.2883E-02	-.2796E-03	.5567E-01	.2880E+00	.6108E-01	
		$RCG/\nabla^{1/3}$	.5694E-01	-.1061E+00	.1742E-01	-.9896E-03	.4806E-01	-.8546E-02	.4183E-03
			-.1034E-01	-.1755E-03	-.7328E-05	.3267E-03	.2052E-02	.1164E-02	
	1.75	R_t/Δ, ∇=5	.9566E+00	-.1196E+00	.7891E-02	-.1443E-03	-.1932E+00	.2134E-01	-.8377E-03
			-.3208E-02	.7299E-03	-.3397E-06	.1896E-02	.4743E-02	-.6219E-04	
		R_t/Δ, ∇=50	.9550E+00	-.1183E+00	.7563E-02	-.1185E-03	-.1938E+00	.2133E-01	-.8361E-03
			-.3264E-02	7311E-03	-.3583E-06	.1890E-02	.4738E-02	-.4953E-04	
		θ	.3901E+02	-.6757E+01	.5287E+00	-.1651E-01	-.6611E+01	4903E+00	-.1453E-01
			-.6147E+00	-.5014E-02	-.4529E-03	.4609E-01	.3434E+00	.4319E-01	
		$RCG/\nabla^{1/3}$	.3378E+00	-.1661E+00	.2435E-01	-.1350E-02	.8538E-04	-.4868E-02	.3050E-03
			-.1249E-01	-.1158E-03	-.5414E-05	.3944E-03	4640E-02	.1473E-02	

#	F.n.		a_0	a_1	a_2	a_3	a_4	a_5	a_6	a_7
			a_8	a_9	a_{10}	a_{11}	a_{12}	a_{13}	a_{14}	a_{15}
25	2.00	R_t/Δ, ∇=5	.9093E+00	-.6004E-01	-.2084E-03	.3004E-03	.2244E+00	.7901E-01	-.1173E-02	
			.1494E-02	.1223E-02	.2299E-04	.1875E-02	.2861E-02	-.3119E-03		
		R_t/Δ, ∇=50	.9074E+00	-.5865E-01	-.5893E-03	.3005E-03	-.2249E+00	.2787E-01	-.1171E-02	
			.1423E-02	.1228E-02	.2317E-04	.1866E-02	.2848E-02	-.2987E-03		
		θ	.4651E+02	-.5594E+01	.4061E+00	-.1428E-01	-.1074E+02	.1163E+01	-.4941E-01	
			-.3024E+00	-.1047E-01	-.6648E-03	.2291E-01	.2767E+00	.4257E-02		
		$RCG/\nabla^{1/3}$	.6440E+00	-.2007E+00	.2825E-01	-.1576E-02	-.8261E-01	.6147E-02	-.2399E-03	
			-.1344E-01	-.3522E-03	-.1875E-04	.3414E-03	.5541E-02	.1394E-02		
	2.25	R_t/Δ, ∇=5	.7267E+00	-.3065E-01	-.4856E-03	.1254E-03	-.1832E+00	.2340E-01	-.9550E-03	
			.1759E-02	.1136E-02	.1964E-04	.1832E-02	.1057E-02	-.3018E-03		
		R_t/Δ, ∇=50	.7238E+00	-.2946E-01	-.8423E-03	.1554E-03	-.1830E+00	.2322E-01	-.9432E-03	
			.1652E-02	.1129E-02	.1914E-04	.1825E-02	.1035E-02	-.2923E-03		
		θ	.3930E+02	-.3838E+01	.1671E+00	-.1504E-02	-.9002E+01	.9844E+00	-.4198E-01	
			-.5436E-01	-.5073E-02	-.2881E-03	.1382E-01	.1938E+00	-.3012E-01		
		$RCG/\nabla^{1/3}$	.7810E+00	-.2062E+00	.2691E-01	-.1457E-02	-.1138E+00	.9881E-02	-.4012E-03	
			-.1288E-01	-.2335E-03	-.1484E-04	.4903E-03	.5972E-02	.1138E-02		
	2.50	R_t/Δ, ∇=5	.5911E+00	-.1332E-02	-.2723E-02	.1880E-03	-.1582E+00	.2103E-01	-.8556E-03	
			.2990E-02	.1367E-02	.3447E-04	.1735E-02	-.2485E-04	-.8911E-04		
		R_t/Δ, ∇=50	.5896E+00	.5678E-03	-.3241E-02	.2295E-03	-.1594E+00	.2106E-01	-.8555E-03	
			.2934E-02	.1372E-02	.3467E-04	.1722E-02	-.6421E-04	-.8239E-04		
		θ	.3457E+02	-.2448E+01	.3596E-01	.3139E-02	-.8405E+01	.9749E+00	-.4280E-01	
			.4796E-01	-.1524E-01	-.5625E-03	.6950E-02	.1132E+00	-.5600E-01		
		$RCG/\nabla^{1/3}$	.9096E+00	-.1932E+00	.2314E-01	-.1211E-02	-.1710E+00	.1877E-01	-.8557E-03	
			-.1322E-01	-.1999E-03	-.1303E-04	.6159E-03	.6142E-02	.9184E-03		
	2.75	R_t/Δ, ∇=5	.5063E+00	.3047E-01	-.7043E-02	.4750E-03	-.1525E+00	.2178E-01	-.9195E-03	
			.5580E-02	.1404E-02	.4042E-04	.1406E-02	-.1424E-02	-.1939E-03		
		R_t/Δ, ∇=50	.5042E+00	.3293E-01	-.7703E-02	.5276E-03	-.1538E+00	.2182E-01	-.9199E-03	
			.5526E-02	.1411E-02	.4076E-04	.1391E-02	-.1479E-02	-.1887E-03		
		θ	.2718E+02	-.1949E+01	.7036E-01	-.2685E-02	-.5753E+01	.6084E+00	-.2452E-01	
			.1545E+00	-.1495E-01	-.5452E-03	.5244E-02	.6356E-01	-.6772E-01		
		$RCG/\nabla^{1/3}$	.1010E+01	-.1952E+00	.2321E-01	-.1272E-02	-.2037E+00	.2262E-01	-.1013E-02	
			-.1367E-01	-.3822E-03	-.2246E-04	.6646E-03	.6673E-02	.6786E-03		
	3.00	R_t/Δ, ∇=5	.4725E+00	2993E-01	-.7451E-02	5195E-03	-.1502E+00	.2257E-01	-.9848E-03	
			.4185E-02	.1587E-02	.5345E-04	.1713E-02	-.7806E-03	-.1318E-03		
		R_t/Δ, ∇=50	.4693E+00	.3357E-01	-.8372E-02	.5913E-03	-.1520E+00	.2269E-01	-.9906E-03	
			.4146E-02	.1587E-02	.5357E-04	.1687E-02	-.8693E-03	-.1363E-03		
		θ	.2337E+02	.1400E+00	-.1892E+00	.1559E-01	-.5536E+01	.6424E+00	-.2701E-01	
			.6203E+00	.8787E-02	.4819E-03	-.3054E-01	-.6558E-01	-.7799E-01		
		$RCG/\nabla^{1/3}$	.1152E+01	-.1663E+00	.1819E-01	-.9180E-03	-.2701E+00	.3175E-01	-.1428E-02	
			-.7406E-02	.1002E-03	-.2626E-05	.2663E-03	.5604E-02	.6099E-03		

			-.1066E-02	-.6606E-04	-.4616E-05	-.7651E-05	.4227E-03	.9094E-04	
		R_t/Δ, ∇=50	.2441E+00	-.1069E+00	.1843E-01	-.1084E-02	-.5458E-02	-.9167E-05	.1467E-04
			-.1061E-02	-.6654E-04	-.4901E-05	-.9439E-05	.4219E-03	.9157E-04	
		θ	-.3308E+01	.2550E+01	-.4395E+00	.2636E-01	-.1037E+01	.1771E+00	-.8958E-02
			-.2613E+00	-.3974E-02	-.4585E-03	.1186E-01	-.7422E-02	.2557E-01	
		$RCG/\nabla^{1/3}$	-.3177E+00	.1208E+00	-.2063E-01	.1227E-02	.2717E-01	-.3003E-02	.1355E-03
			-.6540E-03	.3208E-03	.2741E-04	.5574E-05	-.7106E-03	.2287E-03	
	1.00	R_t/Δ, ∇=5	.9682E+00	-.4393E+00	.7588E-01	-.4470E-02	-.2704E-01	.1049E-02	-.5175E-05
			-.9952E-03	.1588E-03	.2220E-05	.2921E-03	.1925E-02	-.4311E-04	
		R_t/Δ, ∇=50	.9787E+00	-.4453E+00	.7700E-01	-.4538E-02	-.2747E-01	.1085E-02	-.6608E-05
			-.9873E-03	.1573E-03	.1994E-05	.2893E-03	.1921E-02	-.4144E-04	
		θ	.5441E+02	-.2288E+02	.3988E+01	-.2386E+00	-.5056E+01	.5340E+00	-.2318E-01
			-.4847E+00	.9449E-02	.5464E-03	.2527E-01	.1910E+00	.4970E-01	
		$RCG/\nabla^{1/3}$	-.4817E+00	.1940E+00	-.3240E-01	.1881E-02	.1884E-01	-.9944E-03	.2894E-04
			-.5076E-02	-.1482E-03	-.1146E-04	.2403E-03	-.8347E-03	.4546E-03	
	1.25	R_t/Δ, ∇=5	.1893E+01	-.8457E+00	.1457E+00	-.8577E-02	-.6406E-01	.3342E-02	-.7825E-04
			-.5532E-02	-.2505E-03	-.3509E-04	.5791E-03	.3928E-02	.1844E-03	
		R_t/Δ, ∇=50	.1908E+01	-.8539E+00	.1472E+00	-.8671E-02	-.6465E-01	.3390E-02	-.8027E-04
			-.5525E-02	-.2523E-03	-.3551E-04	.5756E-03	.3924E-02	.1879E-03	
		θ	.8265E+02	-.3612E+02	.6187E+01	-.3627E+00	-.4466E+01	.3828E+00	-.1584E-01
			-.3732E+00	.8297E-02	.4187E-03	.2140E-01	.1987E+00	.3160E-01	
		$RCG/\nabla^{1/3}$	.1322E+00	-.9430E-01	.1822E-01	-.1159E-02	-.2056E-01	.2794E-02	-.1375E-03
			-.7445E-02	-.3535E-03	-.2478E-04	.3577E-03	.1312E-02	.6003E-03	
	1.50	R_t/Δ, ∇=5	.1858E+01	-.8280E+00	.1431E+00	-.8422E-02	-.5704E-01	.2596E-02	-.2847E-04
			-.5175E-02	-.4050E-03	-.4045E-04	.7328E-03	.3278E-02	-.1106E-03	
		R_t/Δ, ∇=50	.1879E+01	-.8404E+00	.1454E+00	-.8563E-02	-.5732E-01	.2571E-02	-.2619E-04
			-.5174E-02	-.4052E-03	-.4082E-04	.7261E-03	.3271E-02	-.1054E-03	
		θ	.6978E+02	-.3135E+02	.5460E+01	-.3225E+00	-.2889E+01	.1742E+00	-.4266E-02
			-.6324E+00	.1348E-02	.1646E-03	.3824E-01	.1397E+00	.5171E-01	
		$RCG/\nabla^{1/3}$	.2261E-01	-.1064E+00	.2000E-01	-.1204E-02	.6209E-01	-.9628E-02	.5027E-03
			-.5670E-02	.4477E-03	.3335E-04	.4417E-03	-.1045E-03	.6196E-03	
	1.75	R_t/Δ, ∇=5	.1702E+01	-.7709E+00	.1305E+00	-.7581E-02	-.6966E-02	-.5282E-02	.3696E-03
			-.1824E-02	-.1237E-02	-.1262E-03	.6829E-03	.3235E-02	-.6792E-03	
		R_t/Δ, ∇=50	.1733E+01	-.7893E+00	.1339E+00	-.7791E-02	-.7524E-02	-.5292E-02	.3716E-03
			-.1813E-02	-.1224E-02	-.1256E-03	.6794E-03	.3231E-02	-.6722E-03	
		θ	.7224E+02	-.3562E+02	.6161E+01	-.3609E+00	.3320E+00	-.3862E+00	.2447E-01
			-.9607E+00	-.2280E-01	-.2228E-02	.5705E-01	.2030E+00	.7807E-01	
		$RCG/\nabla^{1/3}$	.4322E+00	-.2972E+00	.5325E-01	-.3187E-02	.4307E-01	-.8474E-02	.4483E-03
			-.1120E-01	.1239E-04	.5205E-05	.4255E-03	.1557E-02	.1150E-02	

[illegible]	[illegible]	[illegible]	[illegible]	[illegible]	[illegible]	[illegible]	[illegible]	[illegible]	[illegible]	[illegible]
3.00		R_t/Δ, ∇=45	[illegible]	[illegible]	[illegible]	[illegible]	[illegible]	[illegible]	[illegible]	[illegible]
			.6126E-03	-.3166E-03	-.6663E-04	.7336E-03	.3907E-03	-.1388E-03		
		R_t/Δ, ∇=50	.1694E+01	-.7039E+00	.1177E+00	-.6804E-02	-.4649E-01	.9008E-03	.7014E-04	
			.5933E-02	-.3613E-03	-.7191E-04	.7270E-03	.2913E-02	-.1273E-02		
		θ	.8804E+02	-.3982E+02	.6620E+01	-.3810E+00	-.2136E+01	-.1155E+00	.1139E-01	
			-.1008E+01	-.3554E-01	-.2607E-02	.5899E-01	.3045E+00	.6854E-01		
		$RCG/\nabla^{1/3}$	.8667E+00	-.4740E+00	.8228E-01	-.4842E-02	.1408E-01	-.5696E-02	.3229E-03	
			-.1656E-01	.1728E-03	.2300E-04	.7306E-03	.2799E-02	.1625E-02		
2.25		R_t/Δ, ∇=5	.1463E+01	-.5376E+00	.9138E-01	-.5364E-02	-.8717E-01	.9157E-02	-.3582E-03	
			.1024E-01	.2689E-03	-.3268E-04	.7508E-03	.1368E-02	-.1379E-02		
		R_t/Δ, ∇=50	.1606E+01	-.5676E+00	.9695E-01	-.5702E-02	-.8862E-01	.9234E-02	-.3604E-03	
			.1017E-01	.2831E-03	-.3217E-04	.7504E-03	.1373E-02	-.1365E-02		
		θ	.9557E+02	-.3926E+02	.6365E+01	-.3630E+00	-.4819E+01	.2255E+00	-.4879E-02	
			-.5270E+00	.1016E-01	.1224E-02	.3807E-01	.3517E+00	.3216E-01		
		$RCG/\nabla^{1/3}$	.1353E+01	-.6515E+00	.1099E+00	-.6388E-02	-.2494E-01	-.2037E-02	.1454E-03	
			-.1627E-01	.1617E-03	.2885E-04	.5353E-03	.4753E-02	.1634E-02		
2.50		R_t/Δ, ∇=5	.9319E+00	-.2954E+00	.5024E-01	-.2921E-02	-.6361E-01	.8261E-02	-.3369E-03	
			.1184E-01	.8303E-03	.5622E-06	.9069E-03	-.7135E-03	-.1244E-02		
		R_t/Δ, ∇=50	.9948E+00	-.3296E+00	.5657E-01	-.3304E-02	-.6611E-01	.8461E-02	-.3445E-03	
			.1181E-01	.8371E-03	.5183E-06	.8959E-03	-.7075E-03	-.1236E-02		
		θ	.9824E+02	-.3926E+02	.6440E+01	-.3724E+00	-.5970E+01	.3969E+00	-.1310E-01	
			-.4028E+00	-.5026E-01	-.3700E-02	.2618E-01	.3341E+00	-.4590E-02		
		$RCG/\nabla^{1/3}$	.1842E+01	-.8079E+00	.1355E+00	-.7899E-02	-.9085E-01	.5616E-02	-.1970E-03	
			-.1795E-01	-.1024E-02	-.7721E-04	.4877E-03	.6345E-02	.1413E-02		
2.75		R_t/Δ, ∇=5	.6313E+00	-.1312E+00	.2362E-01	-.1399E-02	-.7721E-01	.1184E-01	-.5199E-03	
			.1186E-01	.9825E-03	.2873E-05	.8766E-03	-.1911E-02	-.7917E-03		
		R_t/Δ, ∇=50	.7086E+00	-.1717E+00	.3109E-01	-.1850E-02	-.8123E-01	.1225E-01	-.5382E-03	
			.1182E-01	.9787E-03	.2031E-05	.8611E-03	-.1907E-02	-.7870E-03		
		θ	.9066E+02	-.3365E+02	.5499E+01	-.3163E+00	-.7182E+01	.5379E+00	-.2509E-01	
			-.4376E-01	.5334E-02	.1064E-02	.1525E-01	.2526E+00	-.2757E-01		
		$RCG/\nabla^{1/3}$	.2129E+01	-.9369E+00	.1570E+00	-.9168E-02	-.9685E-01	.4548E-02	-.1089E-03	
			-.1769E-01	-.9548E-03	-.7379E-04	.6547E-03	.7716E-02	.1153E-02		
3.00		R_t/Δ, ∇=5	.3244E+00	.3275E-01	-.5660E-02	.2629E-03	-.8965E-01	.1499E-01	-.6978E-03	
			.3986E-02	.7377E-04	-.6592E-04	.1683E-02	-.1222E-02	-.8664E-03		
		R_t/Δ, ∇=50	.4106E+00	-.1235E-01	.2636E-02	-.2355E-03	-.9399E-01	.1542E-01	-.7167E-03	
			.4036E-02	.5876E-04	-.6810E-04	.1653E-02	-.1243E-02	-.8652E-03		
		θ	.7509E+02	-.2554E+02	.4114E+01	-.2306E+00	-.8603E+01	.6169E+00	-.2355E-01	
			.1718E+00	-.1843E-01	-.1362E-02	-.9041E-02	.1296E+00	-.3701E-01		
		$RCG/\nabla^{1/3}$	.2406E+01	-.9778E+00	.1612E+00	-.9288E-02	-.1598E+00	.1235E-01	-.4494E-03	
			-.1356E-01	-.3565E-03	-.2769E-04	.4475E-03	.8148E-02	.1005E-02		

[redacted]

Disp [N]	LCG [%Lp]	Ap/V [ ]
164.71	0	7.0

run [–]	vm [m/s]	Rtm [N]	Lk [m]	Lc [m]	S [m^2]	Trim [deg]	RCG [mm]
225	0.795	0.990	0.66	1.49	0.448	0.0	−1.0
226	1.199	3.750	1.32	1.51	0.460	0.1	−4.0
227	1.585	8.490	1.20	1.51	0.490	0.6	−8.3
228	1.979	14.240	1.13	1.48	0.487	2.8	−12.4
229	2.378	18.710	0.96	1.45	0.476	3.6	−4.9
230	2.765	19.080	0.96	1.42	0.483	4.0	−1.1
231	3.163	21.120	0.90	1.40	0.444	4.7	4.6
232	3.572	23.560	0.87	1.36	0.421	5.5	11.1
233	3.971	26.460	0.75	1.26	0.389	6.7	20.9
234	4.378	30.270	0.72	1.14	0.348	7.3	29.5
235	4.797	33.620	0.65	1.05	0.320	7.5	35.2

Disp [N]	LCG [%Lp]	Ap/V [ ]
236.42	0	5.5

run [–]	vm [m/s]	Rtm [N]	Lk [m]	Lc [m]	S [m^2]	Trim [deg]	RCG [mm]
236	0.847	1.430	1.05	1.52	0.495	0.0	−2.0
237	1.273	5.600	1.26	1.54	0.526	0.1	−5.6
238	1.686	14.200	1.56	1.56	0.555	1.1	−11.2
239	2.124	25.160	1.32	1.48	0.529	4.0	−11.2
240	2.531	28.130	1.10	1.47	0.493	4.7	−4.9
241	2.942	30.990	1.09	1.43	0.482	5.3	−0.3
242	3.361	33.930	1.00	1.40	0.460	6.3	8.3
243	3.790	37.890	0.91	1.33	0.425	7.8	18.4
244	4.239	41.370	0.79	1.22	0.382	8.7	30.4
245	4.686	45.390	0.74	1.12	0.346	9.1	40.1
247	5.103	48.470	0.70	1.06	0.323	9.2	46.1

model 232−A

Disp [N]	LCG [%Lp]	Ap/V [−]
164.71	−4	7.0

run [–]	vm [m/s]	Rtm [N]	Lk [m]	Lc [m]	S [m^2]	Trim [deg]	RCG [mm]
213	0.796	1.150	0.65	1.48	0.412	0.1	−1.6
214	1.201	3.830	0.79	1.49	0.432	0.3	−4.4
215	1.596	8.600	0.75	1.47	0.447	1.2	−9.0
216	1.993	13.610	0.97	1.43	0.454	2.9	−10.8
217	2.390	16.110	0.91	1.41	0.449	3.7	−4.5
218	2.786	18.110	0.89	1.38	0.434	4.2	−0.9
219	3.158	21.100	0.87	1.33	0.414	5.3	4.7
220	3.572	24.560	0.87	1.18	0.386	6.7	14.4
221	3.972	29.060	0.69	1.09	0.355	7.4	25.7
222	4.371	31.400	0.64	1.02	0.320	7.7	32.3
223	4.798	34.330	0.59	0.97	0.280	7.7	37.8

model 232−A

Disp [N]	LCG [%Lp]	Ap/V [−]
236.42	−4	5.5

run [–]	vm [m/s]	Rtm [N]	Lk [m]	Lc [m]	S [m^2]	Trim [deg]	RCG [mm]
249	0.847	1.660	0.91	1.51	0.463	0.1	−2.0
250	1.262	5.940	1.56	1.54	0.555	0.3	−6.0
252	1.687	14.520	1.32	1.56	0.542	1.7	−11.4
253	2.123	25.290	1.13	1.44	0.482	4.4	−11.1
254	2.539	27.900	1.02	1.29	0.452	5.1	−4.5
255	2.956	30.220	0.96	1.37	0.434	5.6	1.2
256	3.377	35.630	0.87	1.28	0.403	6.9	10.1
257	3.785	42.200	0.79	1.15	0.367	8.4	27.2
258	4.228	46.640	0.75	1.04	0.332	8.8	36.6
259	4.666	49.060	0.66	0.96	0.307	8.8	44.6
260	5.059	50.470	0.64	0.93	0.294	8.6	50.1

model 232−A

Disp [N]	LCG [%Lp]	Ap/V [−]
164.71	−8	7.0

run [–]	vm [m/s]	Rtm [N]	Lk [m]	Lc [m]	S [m^2]	Trim [deg]	RCG [mm]
201	0.794	1.310	0.74	1.46	0.420	0.1	−1.5
202	1.198	4.190	0.78	1.44	0.424	0.5	−4.6
203	1.593	9.320	0.67	1.42	0.426	1.6	−9.4
204	1.990	15.190	0.95	1.37	0.425	3.3	−10.5
205	2.386	17.310	0.86	1.32	0.415	3.7	−4.3
206	2.783	20.260	0.79	1.25	0.393	4.6	0.5
207	3.182	24.540	0.75	1.12	0.362	5.9	8.7
208	3.569	28.760	0.67	1.01	0.325	7.0	21.2
209	3.971	32.330	0.62	0.90	0.279	7.2	31.4

model 232−A

Disp [N]	LCG [%Lp]	Ap/V [−]
236.42	−8	5.5

run [–]	vm [m/s]	Rtm [N]	Lk [m]	Lc [m]	S [m^2]	Trim [deg]	RCG [mm]
262	0.844	2.040	0.87	1.48	0.496	0.2	−1.8
263	1.269	6.570	0.91	1.47	0.457	0.6	−5.5
264	1.684	15.760	1.13	1.43	0.491	2.3	−11.2
265	2.116	26.270	0.99	1.35	0.446	5.1	−10.1
266	2.536	30.560	0.90	1.30	0.424	5.6	−3.2
267	2.955	35.430	0.87	1.24	0.396	6.7	3.6
268	3.374	45.910	0.79	1.06	0.356	8.7	18.3
269	3.801	50.160	0.70	0.96	0.315	9.3	33.6
270	4.235	51.310	0.61	0.91	0.283	9.0	44.4

model 232−A

Disp [N]	LCG [%Lp]	Ap/V [−]
164.71	−12	7.0

run [–]	vm [m/s]	Rtm [N]	Lk [m]	Lc [m]	S [m^2]	Trim [deg]	RCG [mm]
188	0.794	1.930	0.68	1.43	0.400	0.2	−1.5
189	1.199	4.530	0.68	1.41	0.397	0.7	−4.6
190	1.583	11.250	0.71	1.37	0.396	2.1	−10.0
192	1.978	18.310	0.83	1.25	0.395	4.3	−9.2
193	2.384	20.900	0.79	1.15	0.378	4.9	−1.9
194	2.781	24.810	0.71	1.04	0.351	6.1	5.3
195	3.190	31.660	0.67	1.03	0.313	7.8	19.7

model 232−A

Disp [N]	LCG [%Lp]	Ap/V [−]
236.42	−12	5.5

run [–]	vm [m/s]	Rtm [N]	Lk [m]	Lc [m]	S [m^2]	Trim [deg]	RCG [mm]
274	0.847	2.420	0.83	1.46	0.497	0.3	−2.1
275	1.262	7.090	0.83	1.44	0.440	0.9	−6.0
276	1.687	19.030	0.95	1.38	0.497	3.1	−11.9
277	2.102	34.720	0.90	1.25	0.410	6.1	−10.0
278	2.526	38.490	0.83	1.13	0.368	6.7	−0.7
280	2.936	49.920	0.75	1.03	0.330	8.8	10.4
279	3.364	56.900	0.66	0.89	0.295	10.0	26.8

run [–]	vm [m/s]	Rtm [N]	Lk [m]	Lc [m]	S [m^2]	Trim [deg]	RCG [mm]
38	0.795	1.140	0.79	1.50	0.445	0.0	−1.5
39	1.189	3.900	1.56	1.51	0.551	0.1	−4.3
40	1.584	6.610	1.56	1.49	0.550	0.7	−7.9
41	1.980	13.920	1.32	1.51	0.532	2.3	−10.1
42	2.377	16.600	1.13	1.48	0.501	3.2	−4.9
43	2.783	19.010	1.06	1.46	0.478	3.5	−1.6
44	3.180	21.670	0.96	1.44	0.456	3.9	2.5
45	3.580	23.490	0.90	1.42	0.439	4.3	8.3
46	3.980	26.050	0.83	1.38	0.421	4.9	13.7
47	4.383	28.720	0.79	1.34	0.404	5.4	18.3
48	4.789	29.860	0.75	1.29	0.388	5.6	22.5

run [–]	vm [m/s]	Rtm [N]	Lk [m]	Lc [m]	S [m^2]	Trim [deg]	RCG [mm]
49	0.794	1.380	1.13	1.54	0.512	0.0	−1.6
50	1.187	4.740	1.56	1.56	0.562	0.1	−4.9
51	1.583	14.600	1.56	1.56	0.552	1.0	−11.1
61	1.847	19.370	1.45	1.53	0.552	2.1	−13.7
52	2.066	24.630	1.40	1.52	0.547	3.5	−12.2
53	2.526	28.330	1.23	1.46	0.523	4.2	−5.5
54	2.943	31.630	1.15	1.45	0.500	4.7	−0.5
55	3.373	34.820	1.05	1.43	0.475	5.3	6.0
56	3.794	36.150	0.96	1.41	0.451	6.1	13.7
57	4.234	38.680	0.89	1.36	0.426	6.9	22.6
59	4.652	40.570	0.83	1.31	0.406	7.2	29.7
60	5.094	42.300	0.79	1.25	0.386	7.3	34.7

model 232–8

Disp [N]	LCG [%Lp]	Ap/V [–]
164.71	−4	7.0

run [–]	vm [m/s]	Rtm [N]	Lk [m]	Lc [m]	S [m^2]	Trim [deg]	RCG [mm]
26	0.795	1.310	0.75	1.48	0.429	0.1	−1.4
27	1.189	4.160	1.26	1.50	0.526	0.4	−3.9
28	1.584	8.820	1.16	1.48	0.507	1.1	−7.6
29	1.981	13.570	1.05	1.46	0.481	2.7	−9.6
30	2.386	15.980	0.94	1.41	0.457	3.5	−4.3
31	2.783	17.730	0.90	1.40	0.439	3.7	−0.4
32	3.180	20.110	0.90	1.38	0.426	4.1	3.9
33	3.578	22.370	0.83	1.35	0.418	4.7	10.4
34	3.980	24.410	0.78	1.28	0.403	5.2	17.0
35	4.366	27.780	0.75	1.22	0.377	5.4	21.6
36	4.792	29.330	0.83	1.11	0.336	5.4	26.0

model 232–8

Disp [N]	LCG [%Lp]	Ap/V [–]
236.42	−4	5.5

run [–]	vm [m/s]	Rtm [N]	Lk [m]	Lc [m]	S [m^2]	Trim [deg]	RCG [mm]
63	0.846	1.970	1.05	1.50	0.490	0.2	−1.9
64	1.264	6.470	1.49	1.51	0.548	0.4	−5.4
65	1.676	14.750	1.56	1.56	0.552	1.9	−10.5
67	2.001	23.640	1.23	1.47	0.516	3.6	−12.5
66	2.121	25.080	1.16	1.44	0.505	4.0	−10.6
69	2.525	27.560	1.05	1.43	0.476	4.4	−4.7
70	2.934	30.270	0.98	1.40	0.462	5.0	1.9
71	3.364	33.160	0.90	1.35	0.428	5.8	8.9
72	3.807	35.930	0.87	1.31	0.406	6.5	18.5
73	4.247	40.240	0.79	1.23	0.384	7.0	27.8
74	4.663	39.930	0.75	1.15	0.364	6.9	34.0
75	5.001	41.510	0.72	1.12	0.347	6.7	38.1

model 232–8

Disp [N]	LCG [%Lp]	Ap/V [–]
164.71	−8	7.0

run [–]	vm [m/s]	Rtm [N]	Lk [m]	Lc [m]	S [m^2]	Trim [deg]	RCG [mm]
14	0.791	1.540	0.68	1.48	0.408	0.2	−1.0
15	1.189	4.490	0.79	1.50	0.436	0.5	−3.7
17	1.584	9.500	1.09	1.48	0.500	1.5	−7.9
25	1.828	13.520	1.05	1.42	0.468	3.0	−10.1
16	1.991	14.630	0.94	1.43	0.451	3.4	−9.3
19	2.386	16.870	0.87	1.36	0.426	4.0	−3.3
20	2.792	18.690	0.83	1.33	0.409	4.1	0.9
21	3.190	21.210	0.79	1.30	0.396	4.8	6.6
22	3.560	23.230	0.75	1.17	0.370	5.3	14.0
23	3.970	25.190	0.68	1.10	0.335	5.8	22.0
24	4.375	27.690	0.65	1.05	0.320	5.5	27.1

model 232–8

Disp [N]	LCG [%Lp]	Ap/V [–]
236.42	−8	5.5

run [–]	vm [m/s]	Rtm [N]	Lk [m]	Lc [m]	S [m^2]	Trim [deg]	RCG [mm]
77	0.845	2.310	0.83	1.48	0.445	0.2	−1.6
78	1.269	7.220	1.26	1.49	0.521	0.6	−5.0
80	1.674	15.370	1.13	1.48	0.497	2.0	−10.1
81	2.000	26.140	1.05	1.42	0.473	4.0	−11.6
82	2.141	27.650	1.02	1.40	0.463	4.5	−9.7
83	2.537	29.490	0.94	1.37	0.441	5.0	−2.8
84	2.966	32.610	0.90	1.30	0.416	5.5	3.6
85	3.366	36.300	0.83	1.21	0.387	6.4	12.6
86	3.805	40.110	0.75	1.10	0.354	7.3	24.7
87	4.234	41.720	0.72	1.05	0.331	6.9	34.4
88	4.660	41.630	0.68	1.02	0.314	6.6	39.6
89	5.046	41.340	0.60	1.00	0.301	6.0	43.6

model 232–8

Disp [N]	LCG [%Lp]	Ap/V [–]
164.71	−12	7.0

run [–]	vm [m/s]	Rtm [N]	Lk [m]	Lc [m]	S [m^2]	Trim [deg]	RCG [mm]
3	0.795	1.790	0.68	1.45	0.400	0.1	−1.0
9	1.189	4.910	0.75	1.42	0.415	1.1	−4.0
4	1.585	11.060	0.98	1.41	0.452	1.7	−6.3
13	1.827	16.170	0.90	1.37	0.437	3.2	−10.5
2	2.021	17.570	0.87	1.35	0.423	3.6	−8.1
5	2.386	19.230	0.79	1.26	0.394	3.8	−1.9
10	2.791	21.650	0.75	1.17	0.360	4.7	3.8
6	3.183	24.620	0.68	1.05	0.325	5.5	11.6
11	3.597	26.630	0.60	0.97	0.295	5.8	22.8
7	3.995	28.550	0.60	0.94	0.283	5.8	30.3
12	4.411	29.190	0.60	0.90	0.264	5.5	34.1
8	4.812	29.000	0.53	0.89	0.306	4.7	36.7

model 232–8

Disp [N]	LCG [%Lp]	Ap/V [–]
236.42	−12	5.5

run [–]	vm [m/s]	Rtm [N]	Lk [m]	Lc [m]	S [m^2]	Trim [deg]	RCG [mm]
91	0.846	2.610	0.87	1.45	0.443	0.3	−1.8
92	1.262	7.460	0.98	1.40	0.454	0.6	−5.2
102	1.677	18.500	0.98	1.29	0.452	2.6	−10.8
97	1.886	28.630	0.98	1.36	0.442	4.3	−12.6
93	2.123	32.630	0.91	1.28	0.426	5.1	−9.3
94	2.529	34.970	0.87	1.21	0.390	5.7	−0.4
95	2.948	39.620	0.79	1.10	0.354	6.6	7.8
96	3.366	47.340	0.72	0.99	0.322	8.0	22.3
98	3.767	47.270	0.65	0.92	0.298	7.8	35.7
99	4.236	43.740	0.64	0.87	0.278	7.1	42.6
100	4.655	43.950	0.60	0.86	0.269	6.6	49.6
101	5.095	43.150	0.60	0.81	0.264	5.9	53.2

[illegible]

run [–]	vm [m/s]	Rtm [N]	Lk [m]	Lc [m]	S [m^2]	Trim [deg]	RCG [mm]
38	0.795	1.140	0.79	1.50	0.445	0.0	−1.5
39	1.189	3.900	1.56	1.51	0.551	0.1	−4.3
40	1.584	6.810	1.56	1.49	0.550	0.7	−7.9
41	1.980	13.920	1.32	1.51	0.532	2.3	−10.1
42	2.377	16.600	1.13	1.48	0.501	3.2	−4.9
43	2.783	19.010	1.06	1.46	0.478	3.5	−1.6
44	3.160	21.670	0.95	1.44	0.458	3.9	2.5
45	3.560	23.490	0.90	1.42	0.439	4.3	8.3
46	3.960	26.050	0.83	1.38	0.421	4.9	13.7
47	4.383	26.720	0.79	1.34	0.404	5.4	16.3
48	4.789	29.660	0.75	1.29	0.388	5.8	22.5

[illegible]

run [–]	vm [m/s]	Rtm [N]	Lk [m]	Lc [m]	S [m^2]	Trim [deg]	RCG [mm]
49	0.794	1.360	1.13	1.54	0.512	0.0	−1.6
50	1.187	4.740	1.56	1.56	0.552	0.1	−4.9
51	1.583	14.600	1.56	1.56	0.552	1.0	−11.1
61	1.847	19.370	1.45	1.53	0.552	2.1	−13.7
52	2.068	24.630	1.40	1.52	0.547	3.5	−12.2
53	2.526	28.330	1.23	1.46	0.523	4.2	−5.5
54	2.943	31.690	1.16	1.45	0.500	4.7	−0.5
55	3.373	34.820	1.06	1.43	0.475	5.3	5.0
56	3.794	36.150	0.96	1.41	0.451	6.1	13.7
57	4.234	38.660	0.86	1.36	0.426	6.9	22.6
59	4.652	40.570	0.83	1.31	0.406	7.2	28.7
60	5.094	42.300	0.79	1.25	0.386	7.3	34.7

model 232–B

Disp [N]	LCG [%Lp]	Ap/V [–]
164.71	−4	7.0

run [–]	vm [m/s]	Rtm [N]	Lk [m]	Lc [m]	S [m^2]	Trim [deg]	RCG [mm]
26	0.795	1.310	0.75	1.48	0.429	0.1	−1.4
27	1.189	4.160	1.26	1.50	0.526	0.4	−3.9
28	1.584	8.820	1.16	1.48	0.507	1.1	−7.6
29	1.981	13.570	1.05	1.46	0.481	2.7	−9.6
30	2.386	15.960	0.94	1.41	0.457	3.5	−4.3
31	2.785	17.730	0.90	1.40	0.439	3.7	−0.4
32	3.180	20.110	0.90	1.38	0.426	4.1	3.9
33	3.578	22.370	0.83	1.35	0.418	4.7	10.4
34	3.980	24.410	0.76	1.26	0.403	5.2	17.0
35	4.366	27.760	0.75	1.22	0.377	5.4	21.6
36	4.792	29.330	0.63	1.11	0.336	5.4	26.0

model 232–B

Disp [N]	LCG [%Lp]	Ap/V [–]
236.42	−4	5.5

run [–]	vm [m/s]	Rtm [N]	Lk [m]	Lc [m]	S [m^2]	Trim [deg]	RCG [mm]
63	0.846	1.970	1.05	1.50	0.490	0.2	−1.9
64	1.264	6.470	1.49	1.51	0.548	0.4	−5.4
65	1.676	14.750	1.56	1.56	0.552	1.6	−10.5
67	2.001	23.640	1.23	1.47	0.516	3.6	−12.5
66	2.121	25.060	1.16	1.44	0.505	4.0	−10.6
69	2.525	27.560	1.05	1.43	0.476	4.4	−4.7
70	2.954	30.270	0.96	1.40	0.462	5.0	1.9
71	3.364	33.160	0.90	1.35	0.428	5.8	8.9
72	3.807	35.930	0.87	1.31	0.406	6.5	19.5
73	4.247	40.240	0.79	1.23	0.384	7.0	27.8
74	4.663	39.930	0.75	1.15	0.364	6.9	34.0
75	5.001	41.510	0.72	1.12	0.347	6.7	38.1

model 232–B

Disp [N]	LCG [%Lp]	Ap/V [–]
164.71	−8	7.0

run [–]	vm [m/s]	Rtm [N]	Lk [m]	Lc [m]	S [m^2]	Trim [deg]	RCG [mm]
14	0.791	1.540	0.68	1.48	0.406	0.2	−1.0
15	1.189	4.490	0.79	1.50	0.436	0.5	−3.7
17	1.584	9.500	1.09	1.45	0.500	1.5	−7.9
25	1.826	13.520	1.05	1.42	0.466	3.0	−10.1
18	1.991	14.630	0.94	1.43	0.451	3.4	−9.3
19	2.386	16.670	0.87	1.38	0.426	4.0	−3.3
20	2.792	18.630	0.83	1.33	0.409	4.1	0.9
21	3.190	21.210	0.79	1.30	0.396	4.6	6.6
22	3.560	23.230	0.75	1.17	0.370	5.3	14.0
23	3.970	25.190	0.68	1.10	0.335	5.5	22.0
24	4.375	27.690	0.65	1.05	0.320	5.5	27.1

model 232–B

Disp [N]	LCG [%Lp]	Ap/V [–]
236.42	−8	5.5

run [–]	vm [m/s]	Rtm [N]	Lk [m]	Lc [m]	S [m^2]	Trim [deg]	RCG [mm]
77	0.845	2.310	0.63	1.48	0.445	0.2	−1.6
78	1.269	7.220	1.26	1.49	0.521	0.6	−5.0
80	1.674	15.370	1.13	1.48	0.497	2.0	−10.1
81	2.000	26.140	1.05	1.42	0.473	4.0	−11.6
82	2.141	27.650	1.02	1.40	0.463	4.5	−9.7
83	2.537	29.490	0.94	1.37	0.441	5.0	−2.8
84	2.966	32.610	0.90	1.30	0.416	5.5	3.6
85	3.366	36.300	0.83	1.21	0.387	6.4	12.6
86	3.805	40.110	0.75	1.10	0.354	7.3	24.7
87	4.234	41.720	0.72	1.05	0.331	6.9	34.4
88	4.650	41.830	0.68	1.02	0.314	6.6	39.6
89	5.046	41.340	0.60	1.00	0.301	6.0	43.6

model 232–B

Disp [N]	LCG [%Lp]	Ap/V [–]
164.71	−12	7.0

run [–]	vm [m/s]	Rtm [N]	Lk [m]	Lc [m]	S [m^2]	Trim [deg]	RCG [mm]
3	0.795	1.790	0.68	1.45	0.400	0.1	−1.0
9	1.189	4.910	0.75	1.42	0.415	1.1	−4.0
4	1.585	11.060	0.98	1.41	0.452	1.7	−6.3
13	1.827	16.170	0.90	1.37	0.437	3.2	−10.5
2	2.021	17.570	0.87	1.35	0.423	3.6	−8.1
5	2.386	19.230	0.79	1.26	0.394	3.8	−1.9
10	2.791	21.650	0.75	1.17	0.360	4.7	3.8
6	3.183	24.620	0.68	1.05	0.325	5.5	11.6
11	3.597	26.630	0.60	0.97	0.295	5.8	22.8
7	3.995	28.550	0.60	0.94	0.283	5.8	30.3
12	4.411	29.190	0.60	0.90	0.264	5.5	34.1
8	4.812	29.000	0.53	0.89	0.306	4.7	36.7

model 232–B

Disp [N]	LCG [%Lp]	Ap/V [–]
236.42	−12	5.5

run [–]	vm [m/s]	Rtm [N]	Lk [m]	Lc [m]	S [m^2]	Trim [deg]	RCG [mm]
91	0.846	2.610	0.87	1.45	0.443	0.3	−1.6
92	1.262	7.460	0.98	1.40	0.454	0.6	−5.2
102	1.677	18.500	0.98	1.29	0.452	2.6	−10.8
97	1.886	28.630	0.98	1.36	0.442	4.3	−12.6
93	2.123	32.630	0.91	1.28	0.426	5.1	−9.3
94	2.529	34.970	0.87	1.21	0.390	5.7	−0.4
95	2.946	39.620	0.79	1.10	0.354	6.6	7.8
96	3.366	47.340	0.72	0.99	0.322	8.0	22.3
98	3.767	47.270	0.65	0.92	0.298	7.8	35.7
99	4.236	43.740	0.64	0.87	0.278	7.1	42.6
100	4.655	43.950	0.60	0.86	0.269	6.6	49.6
101	5.095	43.150	0.60	0.81	0.264	5.9	53.2

[redacted]

Disp [N]	LCG [%Lp]	Ap/V [-]
381.22	0	4.0

run [-]	vm [m/s]	Rtm [N]	Lk [m]	Lc [m]	S [m^2]	Trim [deg]	RCG [mm]
128	0.915	2.690	1.56	1.56	0.555	0.1	-3.3
129	1.370	11.660	1.56	1.56	0.555	0.1	-9.2
130	1.815	28.220	1.56	1.56	0.555	1.9	-16.6
136	2.036	42.120	1.56	1.56	0.555	4.2	17.9
131	2.261	52.090	1.56	1.56	0.555	5.8	-14.3
132	2.726	58.210	1.45	1.52	0.555	6.3	-6.9
133	3.185	64.600	1.26	1.47	0.525	7.0	2.0
134	3.644	68.650	1.13	1.44	0.492	8.5	14.2
135	4.110	70.590	1.00	1.34	0.449	10.0	30.6
136	4.591	71.940	0.85	1.26	0.402	10.0	45.2
137	5.161	71.260	0.85	1.19	0.388	10.0	54.0

model 232-8

Disp [N]	LCG [%Lp]	Ap/V [-]
381.22	-4	4.0

run [-]	vm [m/s]	Rtm [N]	Lk [m]	Lc [m]	S [m^2]	Trim [deg]	RCG [mm]
118	0.917	3.210	1.56	1.56	0.555	0.3	-2.8
119	1.378	12.630	1.56	1.56	0.555	0.7	-7.7
120	1.818	31.160	1.56	1.56	0.555	2.6	-14.0
126	2.021	47.290	1.56	1.56	0.555	5.3	-15.4
121	2.265	55.530	1.26	1.47	0.524	6.6	-12.0
122	2.731	59.620	1.13	1.49	0.491	7.0	-3.3
123	3.190	65.390	1.05	1.37	0.461	8.2	6.8
124	3.648	72.560	0.96	1.29	0.432	9.5	21.3
125	4.111	78.440	0.91	1.24	0.205	10.0	39.5

model 232-8

Disp [N]	LCG [%Lp]	Ap/V [-]
381.22	-8	4.0

run [-]	vm [m/s]	Rtm [N]	Lk [m]	Lc [m]	S [m^2]	Trim [deg]	RCG [mm]
110	0.916	3.660	1.13	1.51	0.508	0.4	-2.6
111	1.372	12.720	1.56	1.56	0.555	1.0	-7.1
112	1.817	34.920	1.32	1.47	0.526	3.6	-13.6
113	2.273	62.940	1.13	1.39	0.484	7.4	-10.3
114	2.731	66.970	1.05	1.32	0.444	6.1	0.4
115	3.187	75.990	0.94	1.23	0.405	9.3	12.7
116	3.649	91.670	0.88	1.06	0.367	10.0	34.0

model 232-8

Disp [N]	LCG [%Lp]	Ap/V [-]
381.22	-12	4.0

run [-]	vm [m/s]	Rtm [N]	Lk [m]	Lc [m]	S [m^2]	Trim [deg]	RCG [mm]
104	0.917	4.750	1.05	1.48	0.485	0.5	-2.4
105	1.363	13.020	1.20	1.47	0.514	1.3	-7.2
106	1.829	40.620	1.13	1.41	0.467	4.8	-14.2
107	2.284	76.800	0.98	1.26	0.424	8.3	-9.8
108	2.732	88.770	0.91	1.16	0.393	9.5	2.8
109	3.201	79.320	0.91	1.13	0.366	10.0	-0.3

Appendix A: Coefficients of twisted bottom polynomial model

Fn		a_0	a_1	a_2	a_3	a_4	a_5
		a_6	a_7				
.75	$\Delta R_t/\Delta$, ∇=5	.4983E-03	-.1485E-03	- 1233E-03	.2533E-05	.1277E-04	-.1850E-04
		.1597E-04	.4245E-05				
	$\Delta R_t/\Delta$, ∇=50	.4209E-03	-.1563E-03	- .9512E-04	.1984E-05	.1354E-04	-.1906E-04
		.1309E-04	.4288E-05				
	$\Delta\theta$	-.4610E-01	.4631E-01	.1214E-01	-.1037E-01	-.3454E-02	- 6250E-03
		-.8404E-03	-.6243E-03				
	$\Delta RCG/\nabla^{1/3}$	.3776E-02	- .9268E-04	-.1424E-02	-.1246E-03	.9463E-05	.1850E-06
		.1331E-03	-.3086E-05				
1.00	$\Delta R_t/\Delta$, ∇=5	-.7109E-02	.4784E-03	.2702E-02	- .7780E-05	-.1321E-03	-.5580E-04
		-.2408E-03	-.6455E-05				
	$\Delta R_t/\Delta$, ∇=50	- .7171E-02	.4771E-03	.2730E-02	-.8632E-05	-.1333E-03	-.5657E-04
		-.2446E-03	-.6400E-05				
	$\Delta\theta$	-.7175E+00	.9020E-01	.2028E+00	.1298E-03	- .7746E-02	.5703E-03
		-.1607E-01	-.1538E-03				
	$\Delta RCG/\nabla^{1/3}$	- .3234E-02	.5587E-03	.1200E-02	.3996E-04	-.7873E-04	.4558E-06
		- .7148E-04	.1229E-04				
1.25	$\Delta R_t/\Delta$, ∇=5	-.1611E-01	.6872E-03	.5469E-02	- .3476E-03	- .2235E-03	-.3902E-04
		- .4749E-03	- .4774E-04				
	$\Delta R_t/\Delta$, ∇=50	-.1611E-01	.6947E-03	.5484E-02	- .3426E-03	- .2256E-03	-.3927E-04
		- .4779E-03	- .4737E-04				
	$\Delta\theta$	-.1492E+01	.1383E+00	.4799E+00	-.5107E-02	-.1694E-01	- .8203E-04
		-.4096E-01	-.1271E-02				
	$\Delta RCG/\nabla^{1/3}$	- .2576E-02	.2884E-03	-.6448E-04	- .1077E-03	.1450E-05	- .1085E-04
		.9325E-04	.3125E-05				
1.50	$\Delta R_t/\Delta$, ∇=5	- .1156E-01	.1010E-02	.4347E-02	- .7582E-04	- .2816E-03	- .2185E-04
		- .3944E-03	- .4035E-04				
	$\Delta R_t/\Delta$, ∇=50	- .1153E-01	.1002E-02	.4325E-02	- .7148E-04	- .2804E-03	-.2218E-04
		- .3924E-03	- .3996E-04				
	$\Delta\theta$	-.1747E+01	.1264E+00	.5078E+00	-.8632E-02	-.1203E-01	.2301E-02
		- .3979E-01	-.1961E-02				
	$\Delta RCG/\nabla^{1/3}$	-.1265E-01	.1279E-02	.4050E-02	- .3522E-03	-.1449E-03	.9500E-05
		-.3254E-03	- .2848E-04				
1.75	$\Delta R_t/\Delta$, ∇=5	- .1781E-01	- .2777E-02	.3988E-02	.1913E-02	.3926E-03	.1714E-03
		- .4276E-04	.6918E-05				
	$\Delta R_t/\Delta$, ∇=50	- .1781E-01	- .2802E-02	.3962E-02	.1923E-02	.3985E-03	.1724E-03
		-.3853E-04	.7212E-05				
	$\Delta\theta$	- .2105E+01	.8404E-01	.5106E+00	- .1442E-01	- .6604E-03	.9035E-02
		- .3282E-01	-.5075E-02				
	$\Delta RCG/\nabla^{1/3}$	-.1976E-01	- .3741E-03	.4480E-02	.1019E-03	.2446E-03	.1656E-03
		- .1706E-03	- .4848E-04				

2.00	$\Delta R_t/\Delta$, ∇=5	-.1696E-01	-.1133E-02	.3922E-02	.2811E-02	-.8412E-04	.9946E-05
		-.3640E-03	.7771E-04				
	$\Delta R_t/\Delta$, ∇=50	-.1891E-01	-.1142E-02	.5881E-02	.2814E-02	-.8078E-04	.1088E-04
		-.3603E-03	.7762E-04				
	$\Delta\theta$	-.2695E+01	.1853E+00	.6910E+00	-.6575E-01	-.1953E-01	.8210E-02
		-.5452E-01	-.9311E-02				
	$\Delta RCG/\nabla^{1/3}$	-.5989E-01	.2930E-02	.1785E-01	-.1535E-02	-.3801E-03	6120E-04
		-.1412E-02	-.1650E-03				
2.25	$\Delta R_t/\Delta$, ∇=5	-.3588E-01	.1388E-03	.1107E-01	.3152E-02	-.3984E-03	-.1834E-04
		-.8323E-03	.1092E-03				
	$\Delta R_t/\Delta$, ∇=50	-.3725E-01	.3248E-03	.1161E-01	.3158E-02	-.4257E-03	-.1554E-04
		-.8667E-03	.1081E-03				
	$\Delta\theta$	-.1525E+01	-.1723E-01	.1660E+00	.2115E-01	.5883E-02	.1806E-02
		-.5244E-02	.3020E-03				
	$\Delta RCG/\nabla^{1/3}$	-.6100E-01	.9271E-03	.1565E-01	-.2120E-03	-.1254E-03	.8236E-04
		-.1101E-02	-.1095E-03				
2.50	$\Delta R_t/\Delta$, ∇=5	-.5260E-02	-.3146E-02	-.2567E-02	.3263E-02	.1492E-04	-.1185E-03
		.4336E-03	.1739E-03				
	$\Delta R_t/\Delta$, ∇=50	-.5245E-02	-.3185E-02	-.2639E-02	.3267E-02	.2341E-04	-.1145E-03
		.4400E-03	.1723E-03				
	$\Delta\theta$	-.2302E+00	.3193E-01	-.1812E+00	-.1211E-01	-.1979E-02	.2759E-03
		.1277E-01	-.2276E-03				
	$\Delta RCG/\nabla^{1/3}$	-.1935E-01	.1547E-02	.2596E-02	-.3649E-03	-.3085E-03	.1805E-04
		-.2492E-03	-.8810E-04				
2.75	$\Delta R_t/\Delta$, ∇=5	-.3454E-01	-.6475E-02	.1387E-02	.1848E-02	.3586E-03	-.3693E-03
		.3447E-03	.2075E-03				
	$\Delta R_t/\Delta$, ∇=50	-.3502E-01	-.6477E-02	.1490E-02	.1836E-02	.3595E-03	-.3669E-03
		.3317E-03	.2062E-03				
	$\Delta\theta$	.4111E-01	.7245E-01	-.1804E+00	.7383E-02	-.6458E-02	.7109E-02
		.6386E-02	-.2195E-02				
	$\Delta RCG/\nabla^{1/3}$	-.1573E-01	.1805E-02	.8777E-03	-.2462E-03	-.3616E-03	.6562E-04
		-.1874E-03	-.8928E-04				
3.00	$\Delta R_t/\Delta$, ∇=5	.1001E-01	-.5544E-02	-.1342E-01	.1636E-02	.1327E-03	-.5689E-03
		.1475E-02	.3445E-03				
	$\Delta R_t/\Delta$, ∇=50	.8563E-02	-.5354E-02	-.1287E-01	.1634E-02	.1020E-03	-.5691E-03
		.1413E-02	.3475E-03				
	$\Delta\theta$	-.1607E+01	.1098E+00	.3775E+00	.1483E-01	-.1283E-01	.1036E-01
		-.3977E-01	-.2998E-02				
	$\Delta RCG/\nabla^{1/3}$	-.7659E-02	.1821E-02	-.9599E-03	-.2954E-03	-.3330E-03	.7094E-04
		-.1434E-03	-.7165E-04				

RESISTANCE TESTS OF TWO PLANING BOATS WITH TWISTED BOTTOM

Ir. J.A. Keuning

December 1986

Report no 731

Delft University of Technology
Ship Hydromechanics Laboratory
Mekelweg 2
2628 CD Delft
The Netherlands
Phone 015 - 78 68 82

Contents

Summary

In this report experiments with two models derived from the parent model of the Keuning-Gerritsma series with a twisted planing bottom in the after body are described.
The results of the test are presented and compared with those of the Clement-Blount and the Keuning-Gerritsma series with prismatic after bodies.
From the comparison it is concluded that not so much the decrease in deadrise angle but the slope of the buttock lines in the after body is important.
The twisted bottom yields favourable results under certain circumstances.

I Introduction

For the calculation of the resistance of a planing boat a number of well known methods based on experimental results derived from modeltests with systhematic series are available, for instance Clement and Blount Ref. [1] and Keuning and Gerritsma Ref. [2]. However the models used for these series all had prismatic after bodies, i.e. the deadrise of the planing hull bottom remained constant from the midships section aft to the transom.

In the actual design practice however designers often prefer a change in deadrise angle towards the transom in order to improve the position of the propellers in such a way that they do not protrude to much under the keel of the vessel. This change in deadrise results in a "twisted" bottom of the planing hull. As a result of this also the immersed area of the transom may be reduced, which is believed to be advantageous for the resistance at relatively low speeds.

To investigate the influence of the twisted bottom on the resistance of the vessel in the whole speed range two models have been tested, each with a twisted bottom in the aft ship but with different aft buttock inclination and immersed transom area. These models have been tested using the same parameter variations as used in the original Clement and Blount series. The results of these tests are presented in this report and due to the similarity with the parent models of Clement and Keuning the influence of a twisted bottom may be reduced from these data.

II The models

Two models have been used during the experiments. The models have been developed from the lines of the parent model of the Keuning-Gerritsma series with a 25° degrees deadrise angle. The fore bodies of the newly developed models were identical to this parent model, i.e. from (midship) section to the stem. In the aft body the deadrise angle has been gradually decreased from 25° degrees at ordinate 10 midship to 5° degrees at ordinate 0 (the transom).

In order to maintain sufficient buoyancy in the aft body the chine area, i.e. the width over the chines, had to be increased significantly.

This is however a important factor influencing the behaviour of the craft with respect to resistance and trim. So by doing this the validity of a comparison with the prismatic after bodied models is limited.

In order to produce realistic models however it was never-the-less decided to do so.

The difference between the two models used i.e. 233 A and 233 B, is the immersed transom area and the inclination of the buttock lines in the after body.

Model 233 A has less immersed transom area and the centre-line is more tilted upwards. As a result of this the chine and the buttock lines of model 233 A are more of less curved while of model 233-B the chine and the half-width buttock are straight lines, sloping downwards and horizontal respectively.

The filosophy behind the lines of model 233-A was to determine how far the centre line may be raised in order to gain room for the propellors and minimising immersed transom area before severe penalties in resistance and trim have to be paid.

Both models are composed of developable surfaces which has its effect on the sectionshape in particular in the aft body due to the rotation of the bottom plating. The sections become convex there.

The lines of both models are presented in the figure 1 for model 233-A and 233-B respectively. The main particulars are presented in Table 1.

For reference the lines of the parent models of the Clement-Blount series and the Keuning-Gerritsma series are presented in figure 2.
The shaft centre line is shown for each model in the body plans. The same values as used in the previous series for shaft rake and propellor clearance have been used for these models.
All models had spray strips attached over the full length of the chine. The bottom of the spray lines followed the line of the bottom of the model from ordinate 0 (transom) to ordinate 10 (midship) and was horizontal from ordinate 12 to ordinate 20 (the stem) with a transition in the region from ordinate 10 to ordinate 12. The width of the spray strips was approximately 4 mm and they had non radiused edges.
The models have been constructed of glass fibre reinforced polyester.

Tabel 1

	model 232-A	model 232-B
deadrise ord 10	25°	25°
ord 20	5°	5°
L_p	1.500 m	1.500 m
B_{pA}	0.306 m	0.303 m
B_{px}	0.367 m	0.367 m
B_{pT}	0.320 m	0.310 m
A_p	0.4589 m^2	0.4540 m^2
L_p/B_{pA}	4.90	4.90
Lp/B_{px}	4.09	4.09
B_{px}/B_{pA}	1.20	1.20
B_{pT}/B_{px}	0.872	0.844
C_{AP} from ord 0 in % L_p	48.8	48.8

III Experimental set up

The tests have been carried out in the no 1 towing tank of the Ships Hydromechanics Laboratory of the Delft University of Technology. Dimensions of the tank are: length 150 m width 4.50 m and depth 2.5 m.

The models have been connected to the towing carriage in such a way that they were free to pitch and heave but the models were restrained in all other modes of motion. The pivoting point of this suspension frame was located in the intersection of the assumed shaft line with the transverse plane through the centre of gravity of the model.

A strain gauge type dynamometer has been placed on the hinge to measure the resistance force. The vertical displacement of the centre of gravity and the trim have been measured using wire over potentiometer type displacement meters.

During each run a photo has been taken through the transparent bottom of the hull of the model at the given speed to determine the wetted surface of the hull after wards.

No turbulence stimulators have been used on the models since model scale and towing speeds were considered to be large enough to yield reliable results. No towing speed below 1.0 m/sec has been used.

IV Measurement scheme

The test program consisted of variations in displacement and position of the centre of gravity, i.e. all combinations of the following parameters:

$L/B = 4.09$

$A_p/\nabla^{2/3} = 4.0,\ 5.5,\ 7.0,\ 8.5$

LCG = 0, 4, 8, 12 % L aft of centroid A_p

The test were conducted in the speedrange

of $Fn_\nabla = \frac{V}{\sqrt{g\nabla^{1/3}}}$

$0.75 < Fn_\nabla < 3.00$

corresponding with model speeds between

$1.0\ m/s < Vm < 5.0\ m/sec$

Some combinations of heavy displacement and position of the centre of gravity were not feasable due to excessive trim of the model, causing flooding of the model at rest.
The range of parameters investigated corresponds to the range used in the Keuning-Gerritsma series with 25 degrees deadrise and the Clement and Blount series with 12.5 degrees deadrise, although the later used a higher speed range.

V The Results

The results of the experiment are presented partly as tabulated data for each run in the Appendix to this report and partly in a number of figures.
The tabulated data present all relevant model data, such as speed, resistance, sinkage, trim and wetted area.
The later refer to the area of the bottom of the model in contact with solid water only and have been derived from the photographs.
The relatively small parts of the sides of the models in contact with the solid water at the lowest speeds only have been omitted.The figures contain data expanded from these model data for actual ships with a displacement of 45 kN and 450 kN respectively, being the same procedure as used by Clement and Blount originally.
For the expansion of the resistance data use has been made of the Schoenherr friction coefficients with zero roughness allowance.
The Schoenherr coefficients has been used rather than the usual ITTC 57 friction line because of the conformity with the Clement and Blount data.
The resistance/weight of displacement ratio for the 45 kN boat are presented in the figures 3 to 9 and for the 450 kN boat in the figures 10 to 16.
The figures are arranged in order of increasing loading factor $A_p/\nabla^{2/3}$ for first model 232 A and thereafter model 232 B.

VI Discussion of the results

From the figures it may be concluded that there is a marked influence on resistance from both the loading factor and the position of the centre of gravity with respect to the centroid of A_p.

Due to the larger "rocker" in the aft body of model 232 A when compared with model 232 B the resistance of model A is consistently higher. This difference diminishes with increasing loading factor (i.e. lighter ships), with a more forward position of the centre of gravity and with increasing speed. The trim angles of both models are generally high, sometimes higher than 10 degrees.

The difference between model 232-A and 232-B is evident from these results. It should be noted that the twist in the planing bottom of the two hulls is identical, i.e. 25^o degrees at section 10 (midship) and 5^o at section 20 (transom). From this it may be concluded that the inclination of the buttock lines is much more important, this being the actual difference between the two models. The resulting considerably larger submerged transom area of the model 232-B causes hardly an increase in resistance in the lower speed range.

This is also clearly demonstrated in the figures 17 to 21 in which the results of the models 232-A and B are compared with the according data of the parent model of the Clement-Blount and the Keuning-Gerritsma series.

These figures are compiled for three loading factors, i.e. $A_p/\nabla^{2/3}$ = 4.0, 5.5 and 7.0, and two longitudinal positions of the centre of gravity, i.e. LCG = 4% and 8%.

From these figures it may be concluded that the resistance in the lower speed range ($1 < Fn_\nabla < 2.0$) of the model 232-B with the straight half width buttock and the twisted bottom is generally lower than the others, with exception of the 12^5 deadrise angle model of Clement and Blount.

This is in particular so in the 4% LCG situation. The difference increases with decreasing weight of the models.

The trim angle of the models 232-A and B is consitently higher than those of the models with the prismatic after body.
It may be so that the "rocker" in the buttock lines of the models with the twisted bottoms is responsable for this as can be concluded from the difference between model 232-A and B. Decreasing the deadrise angle in the aft body whilst keeping the centre line straight (horizontal) and sloping the buttocks slightly down from the horizontal might even yield better results. The resistance increase due to the higher immersed transom area in the lowest speed range ($Fn_{\nabla} < 1.0$) may be rather small as shown by the comparison of model 232-A and B in this speed region.

References

[1] E.P. Clement and D.L. Blount
Resistance tests of a Systematic Series of Planing Hull Forms
SNAME 1963

[2] J.A. Keuning and J. Gerritsma
Resistance tests of a series planing hull forms with 25 degrees deadrise angle
I.S.P. (29) 1982 no. 337

List of Symbols

A_p	projected planing area
B_{pA}	average width over chine
B_{px}	maximum width over chine
B_{pT}	width over chine at transom
C_{AP}	centroid of Ap
Fn_∇	volumetric Froude number $Fn_\nabla = \frac{V}{\sqrt{g\nabla^{1/3}}}$
L_p	length over chine
L_K	wetted length chine
L_C	wetted length keel
R_{TM}	resistance total of the model
V_m	model speed
z	vertical displacement centre of gravity
α	deadrise angle
∇	volume of displacement
Δ	weight of displacement
θ	trim angle

List of Figures

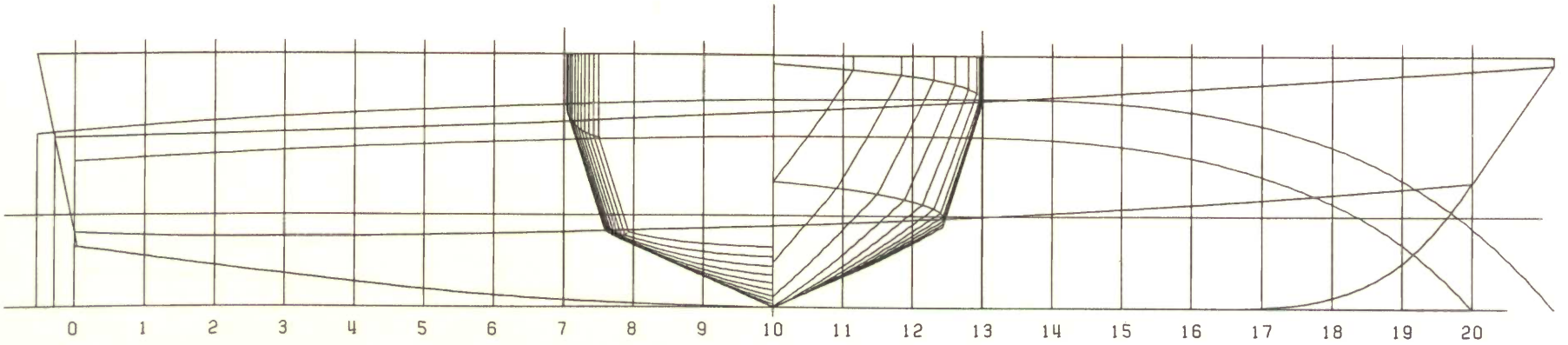

HOOFDAFMETINGEN:

LENGTE (ONTW.ORD.0-20)	=	15.00	M
BREEDTE	=	4.480	M
DIEPGANG	=	0.980	M

Figure 1a. Model 232-A.

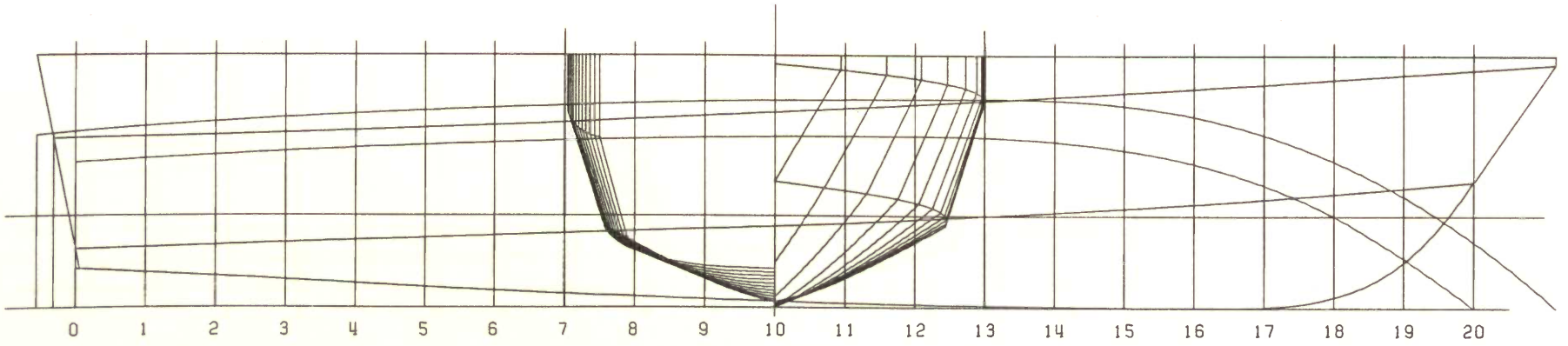

HOOFDAFMETINGEN:

LENGTE (ONTW.ORD.0-20)	=	15.00	M
BREEDTE	=	4.480	M
DIEPGANG	=	0.980	M

Figure 1b. Model 232-B.

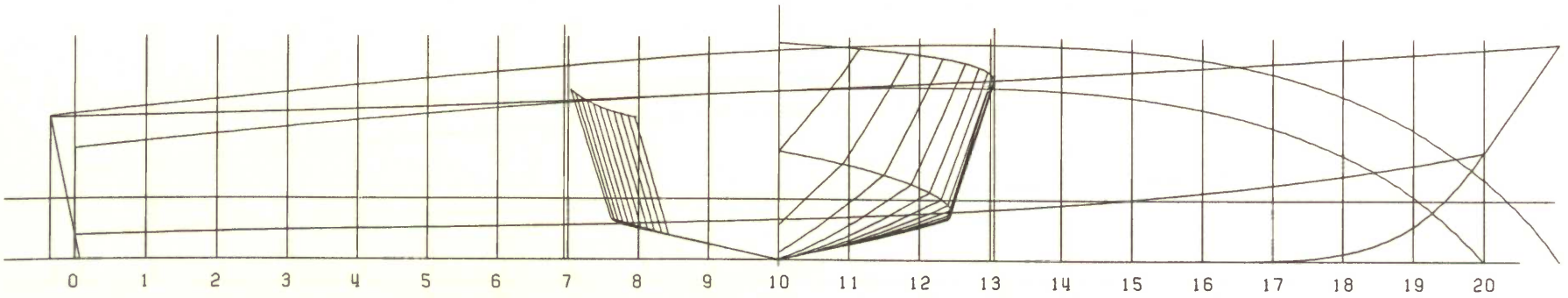

HOOFDAFMETINGEN:

LENGTE (ONTW.ORD.0-20)	=	15.00	M
BREEDTE	=	4.580	M
DIEPGANG	=	0.640	M

Figure 2a. Parent model 12^5 degrees deadrise.
(Clement-Blount).

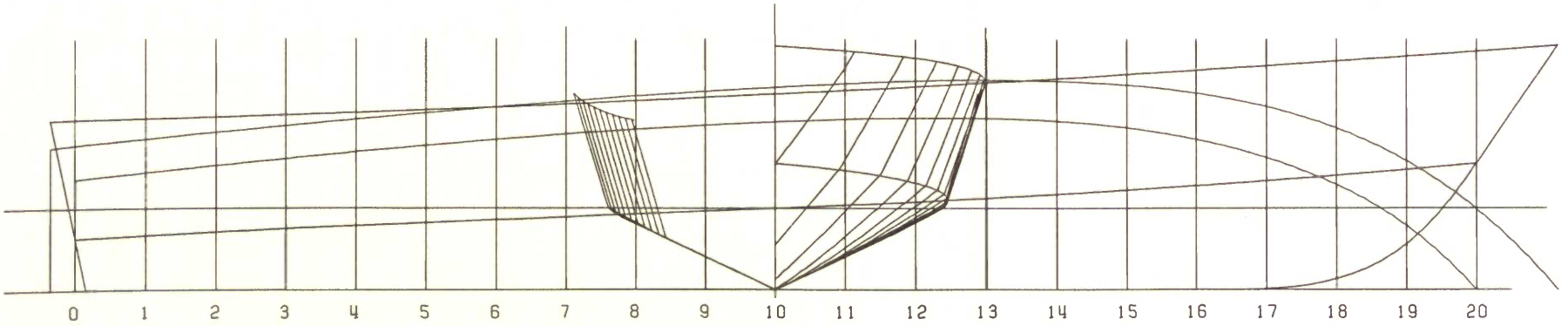

HOOFDAFMETINGEN:

LENGTE (ONTW.ORD.0-20)	=	15.00	M
BREEDTE	=	4.480	M
DIEPGANG	=	0.870	M

Figure 2b. Parent model 25 degrees deadrise.
(Keuning - Gerritsma)

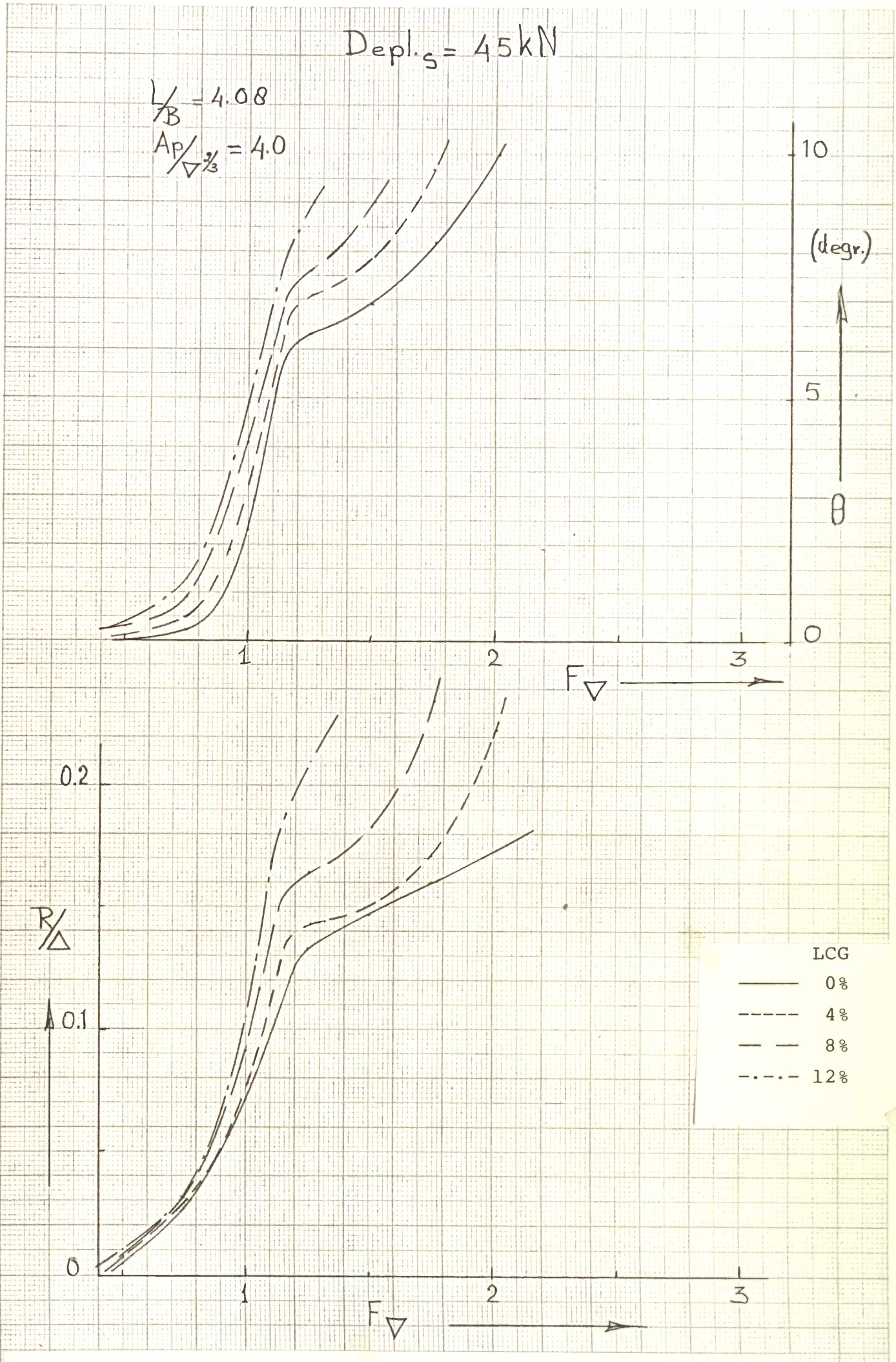

Figure 3. Model 232-A, Δ = 45kN.

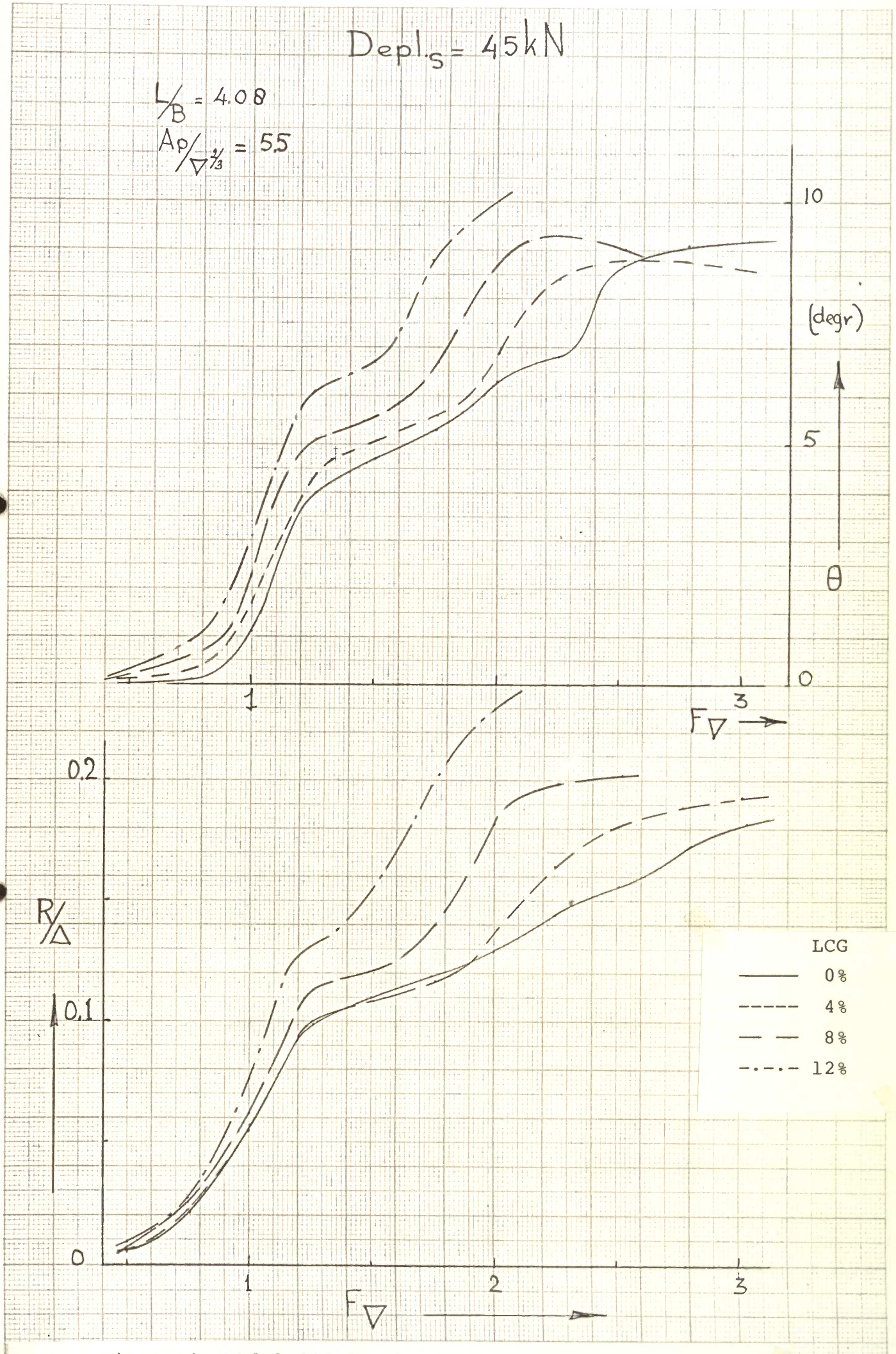

Figure 4. Model 232-A, Δ = 45kN.

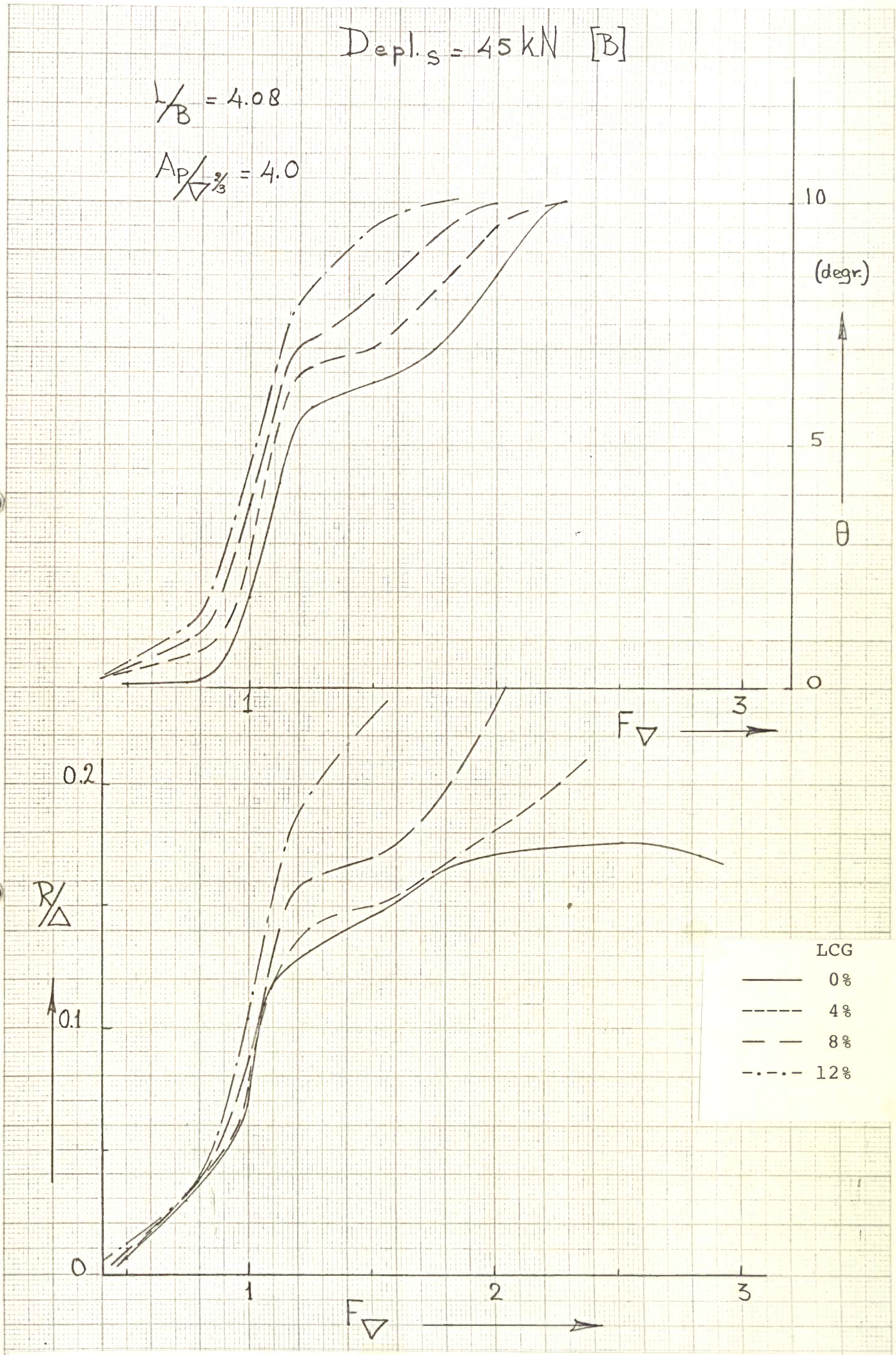

Figure 6. Model 232-B, Δ = 45kN.

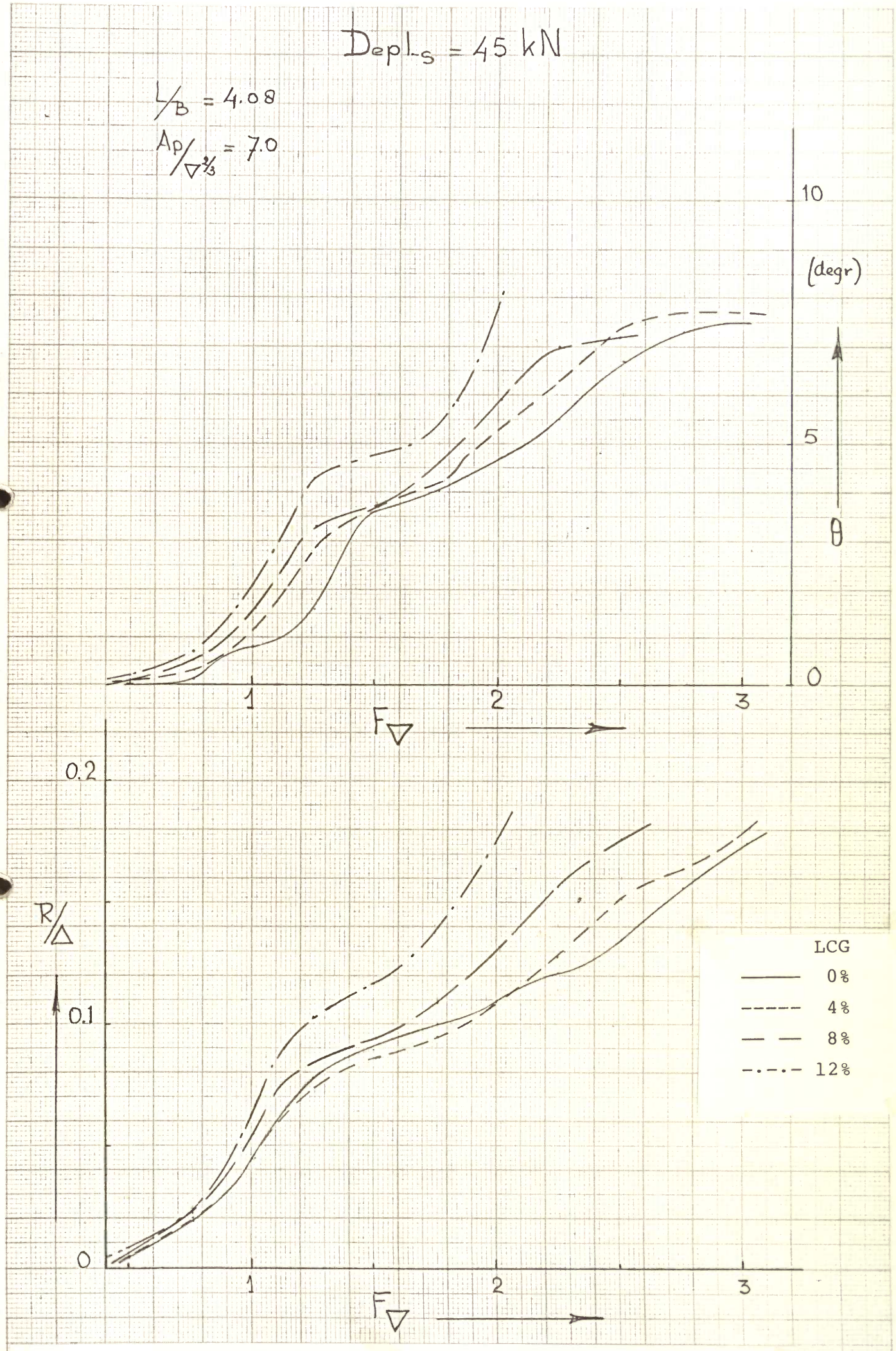

Figure 5. Model 232-A, Δ = 45kN.

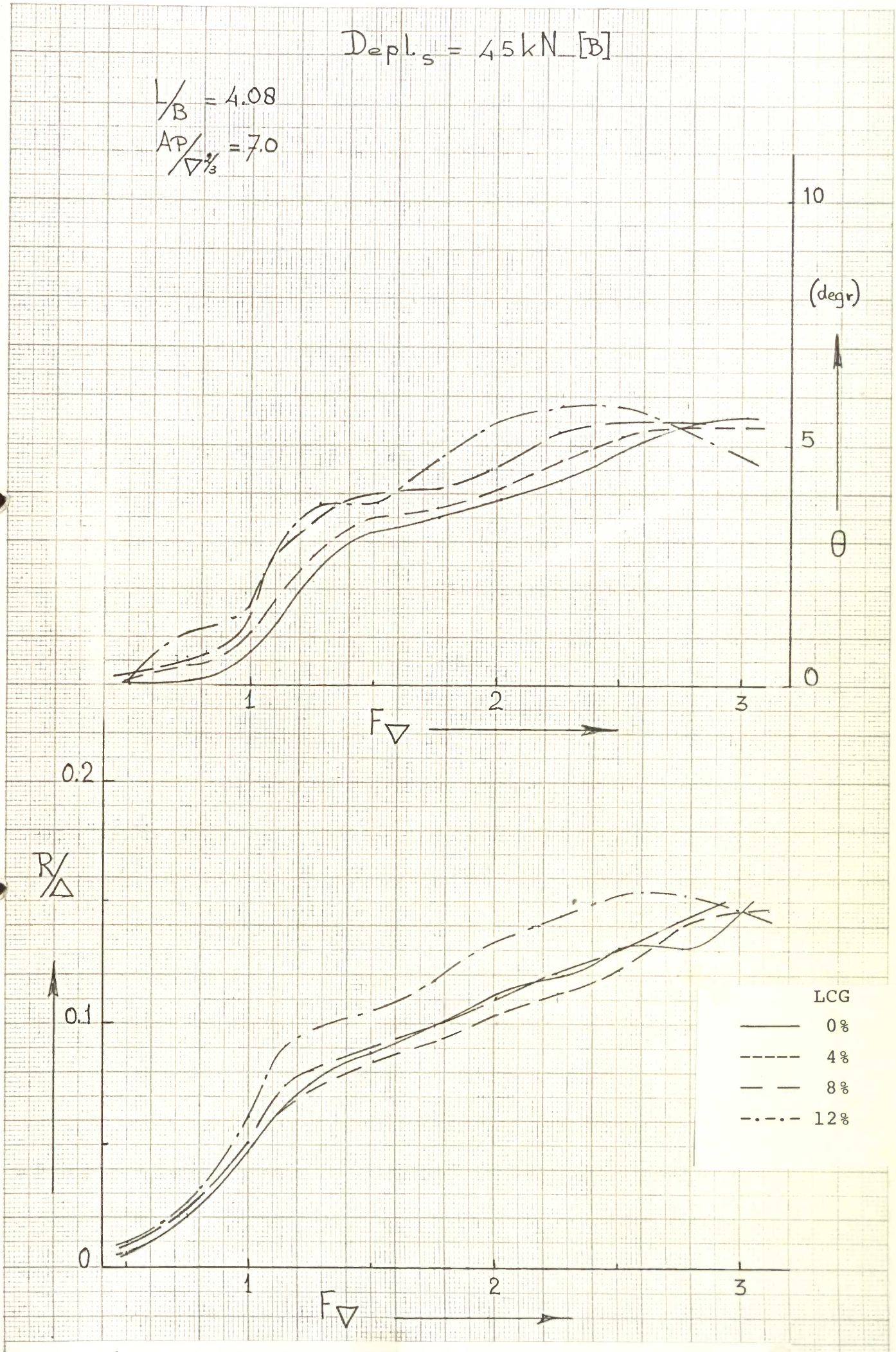

Figure 8. Model 232-B, Δ = 45kN.

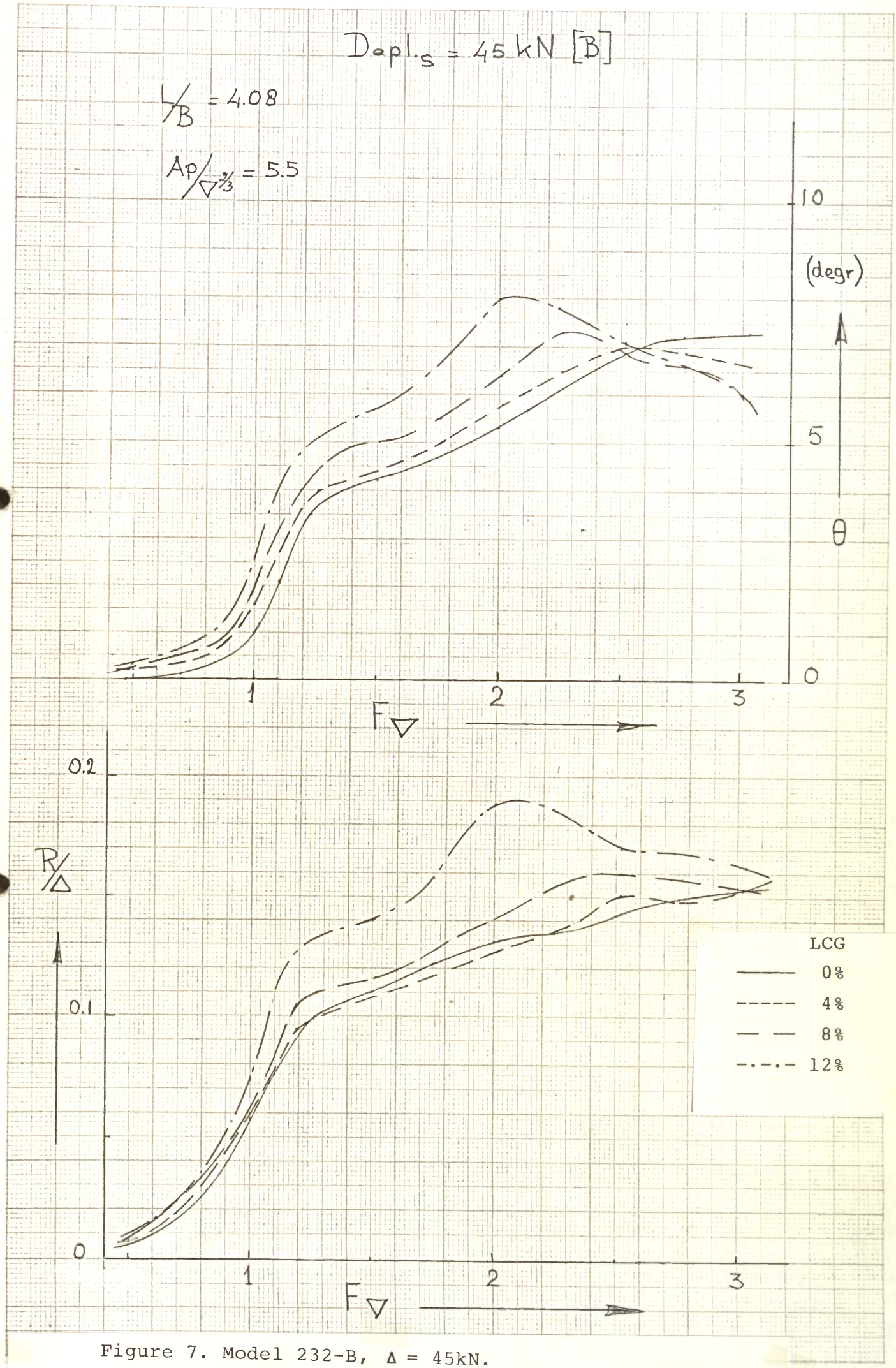

Figure 7. Model 232-B, Δ = 45kN.

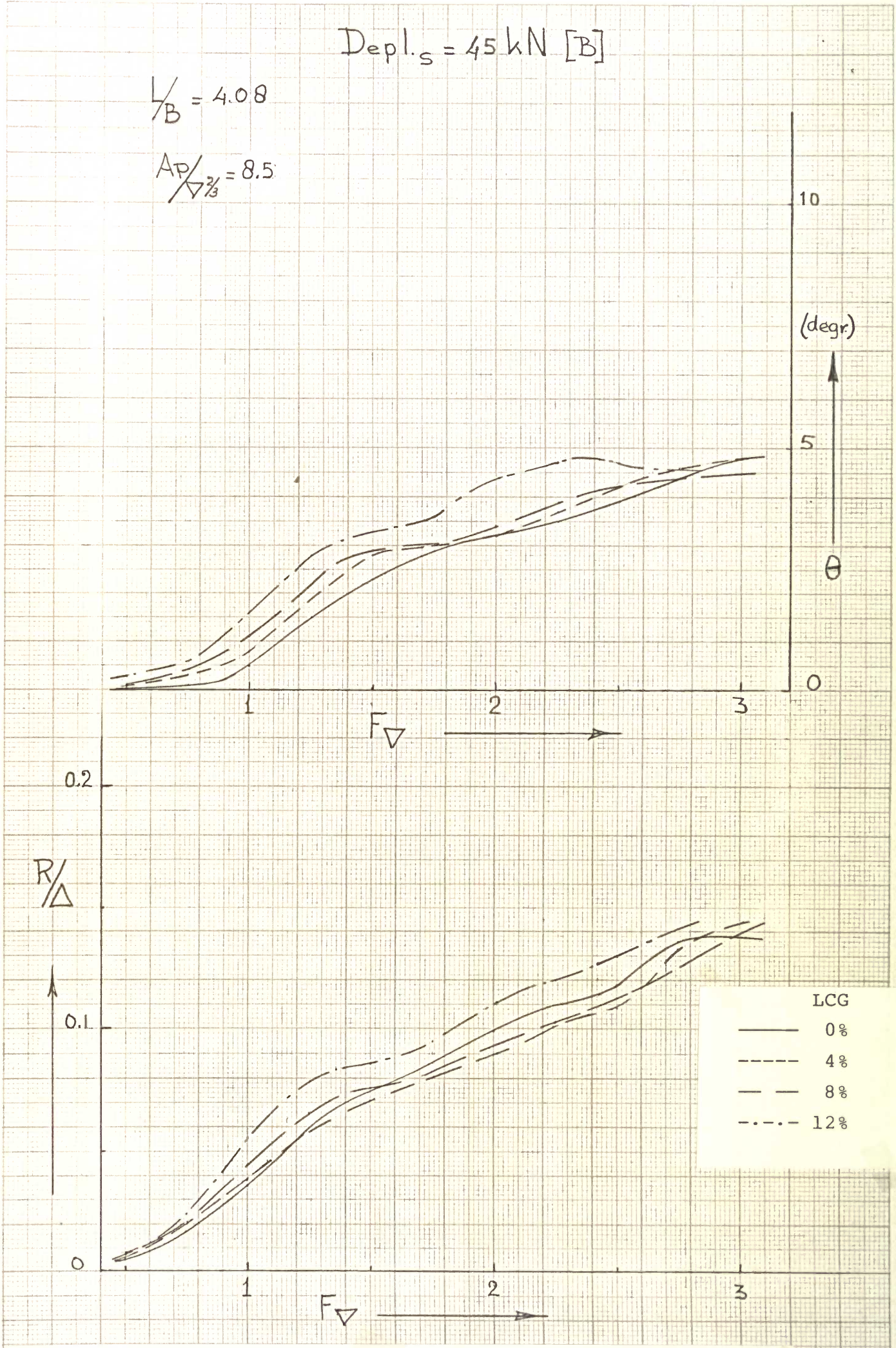

Figure 9. Model 232-B, Δ = 45kN.

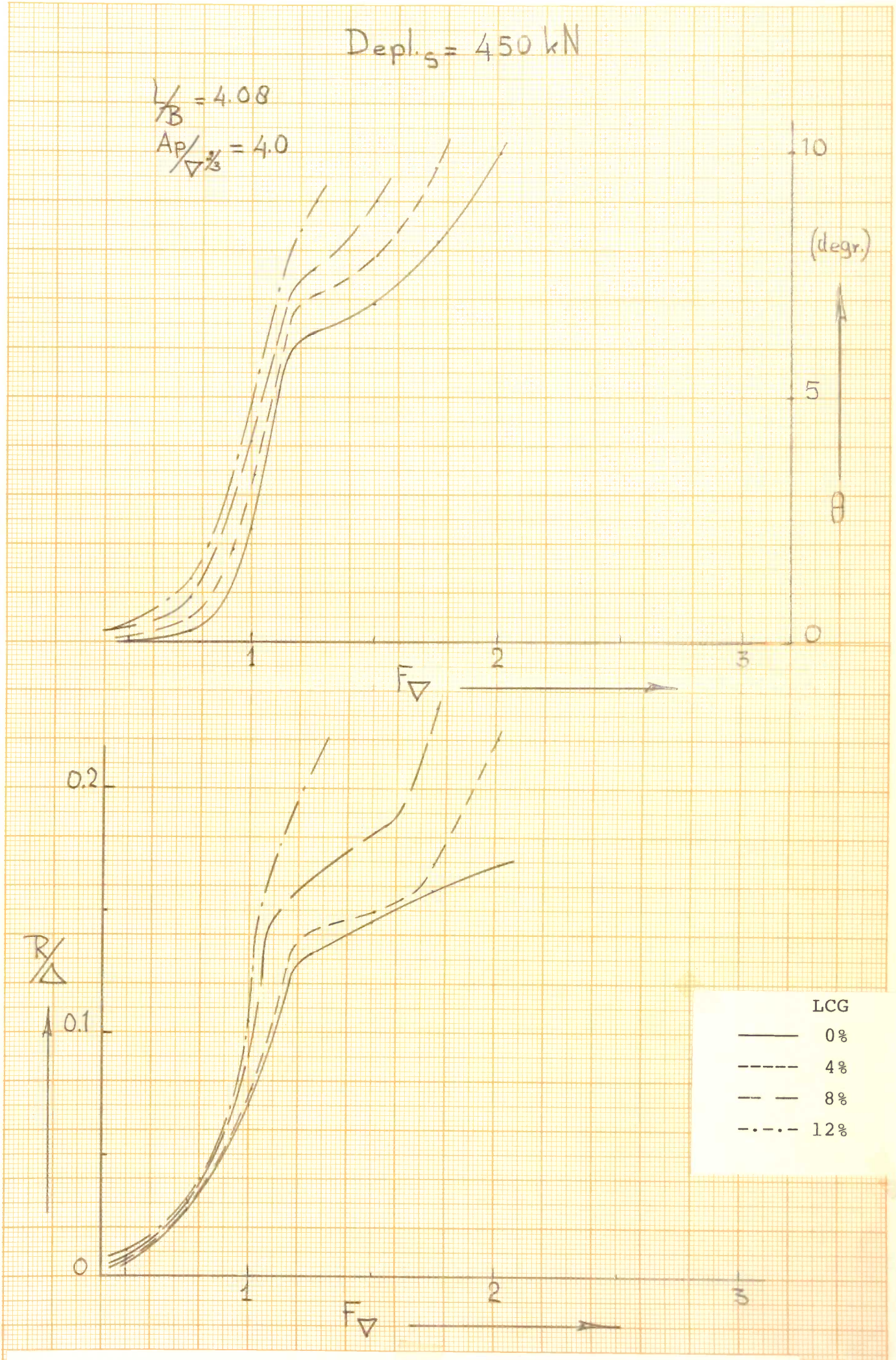

Figure 10. Model 232-A, Δ = 450kN.

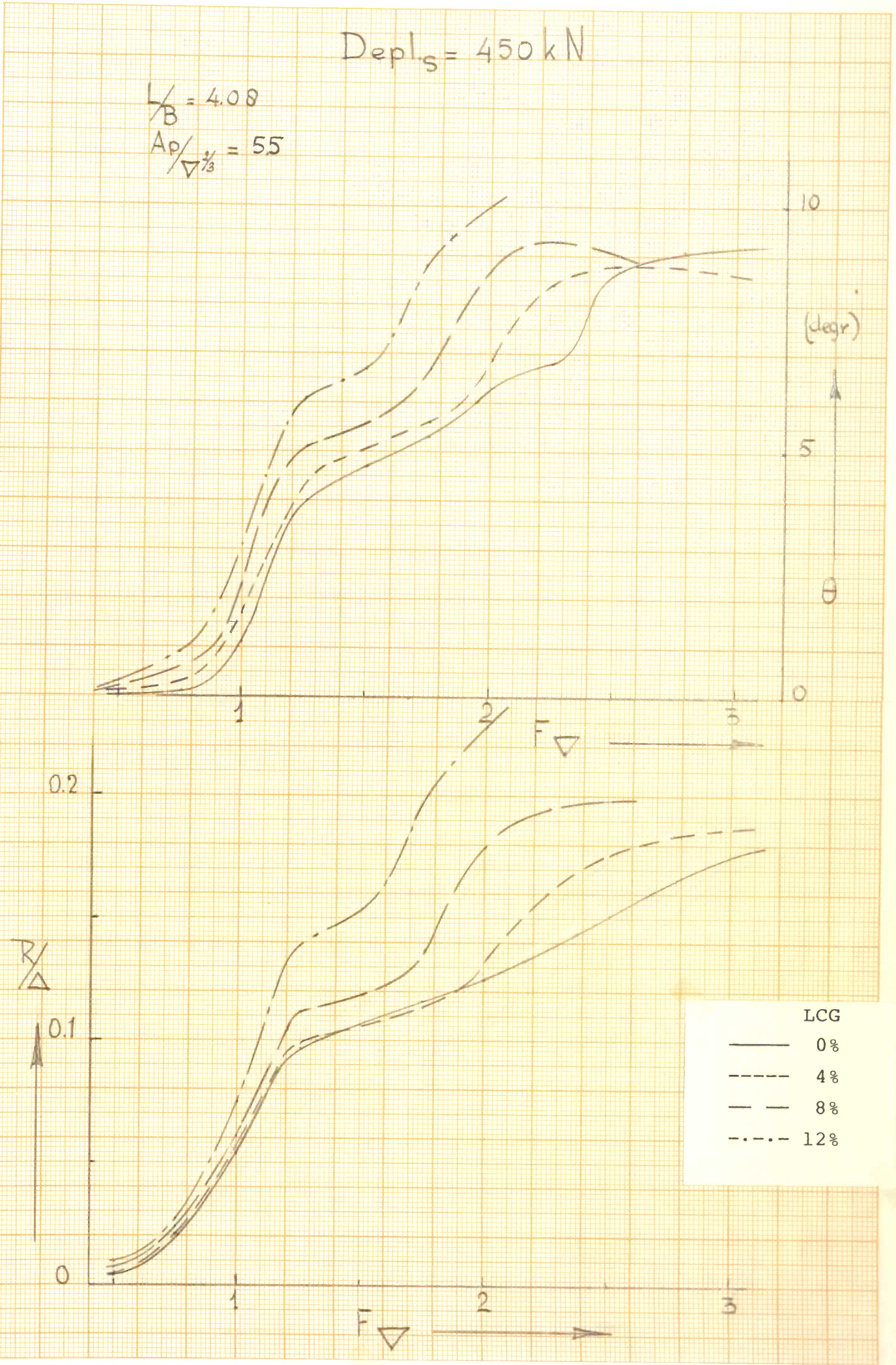

Figure 11. Model 232-A, Δ = 450kN.

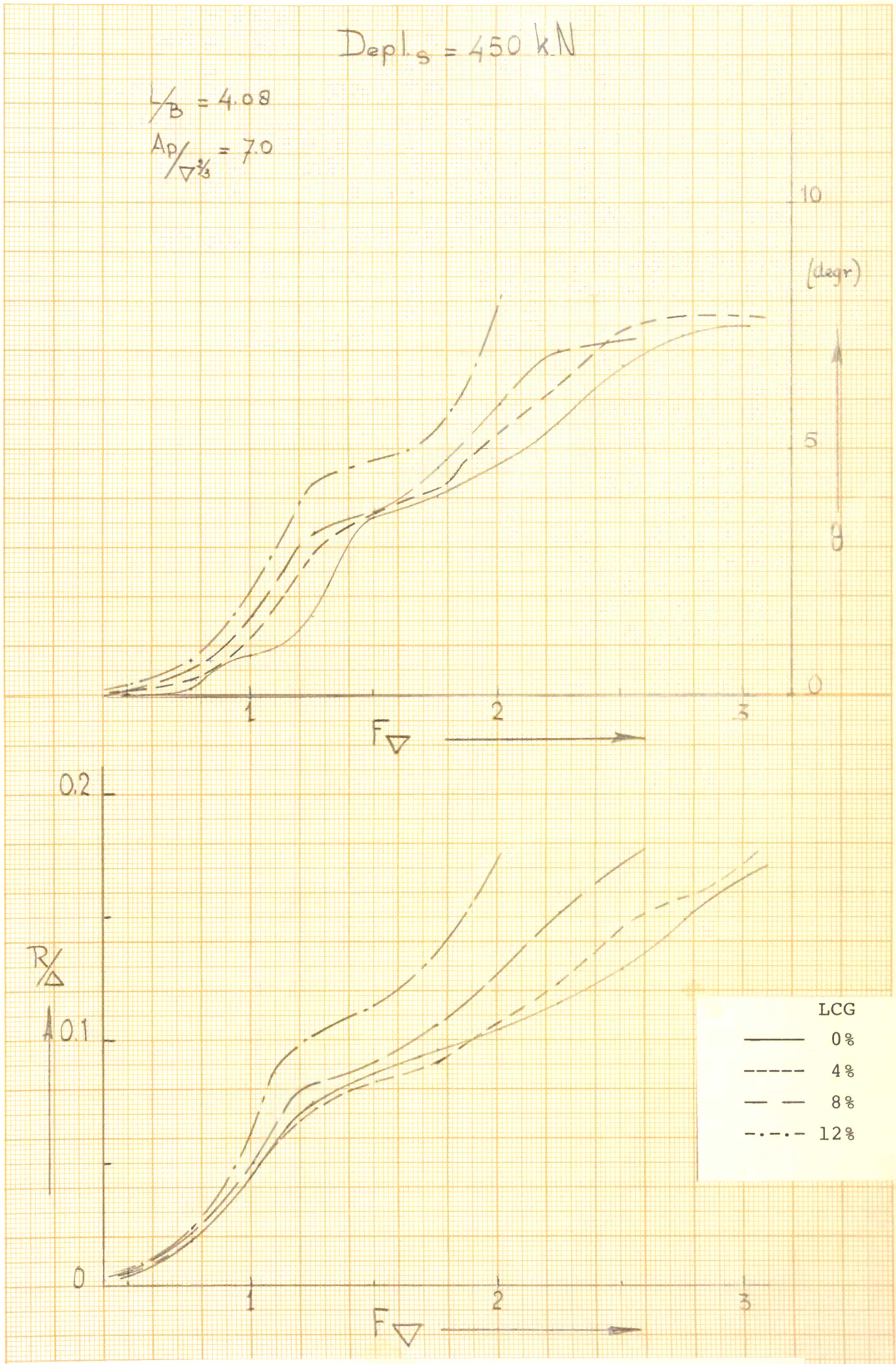

Figure 12. Model 232-A, Δ = 450kN.

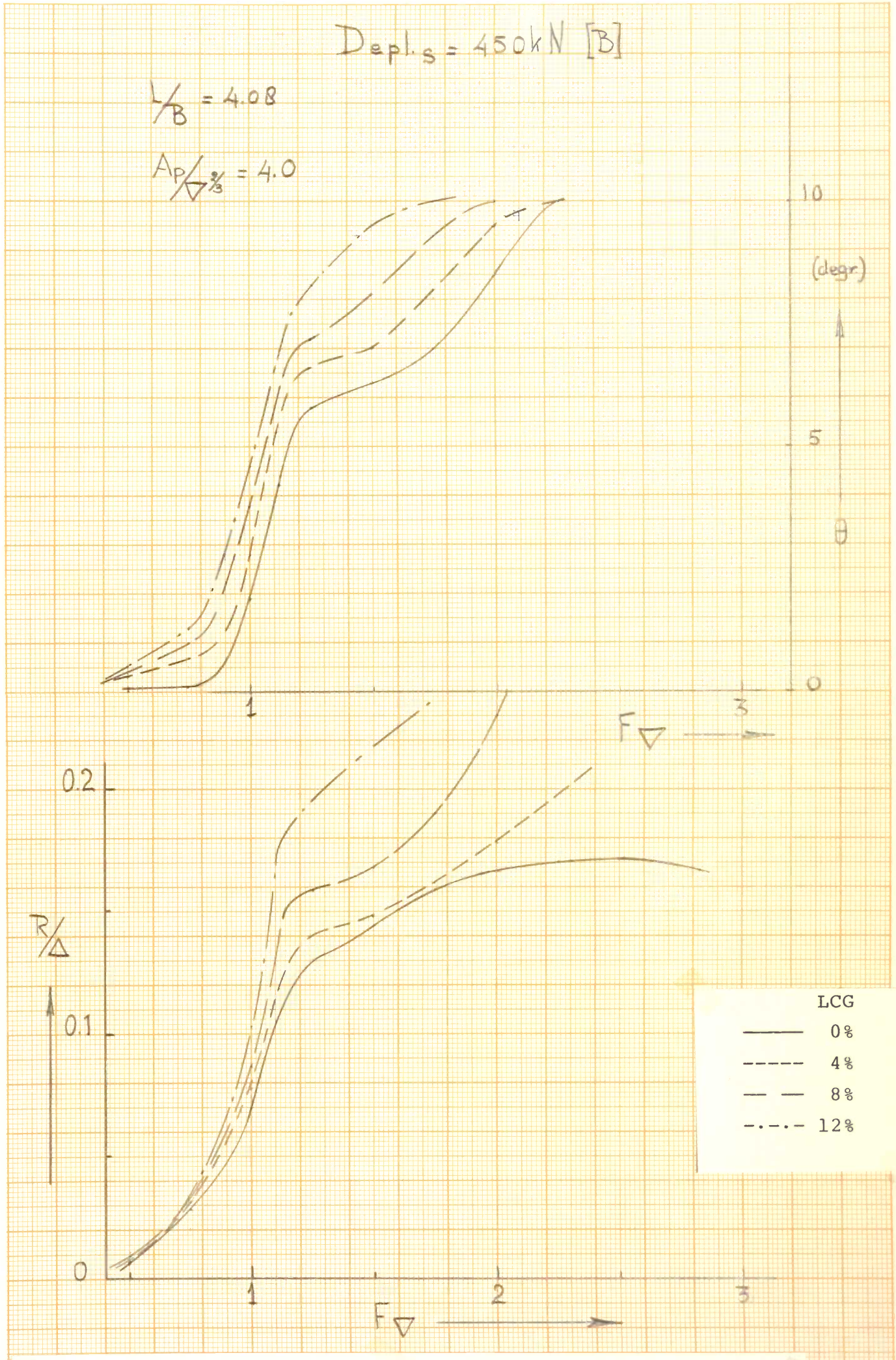

Figure 13. Model 232-B, Δ = 450kN.

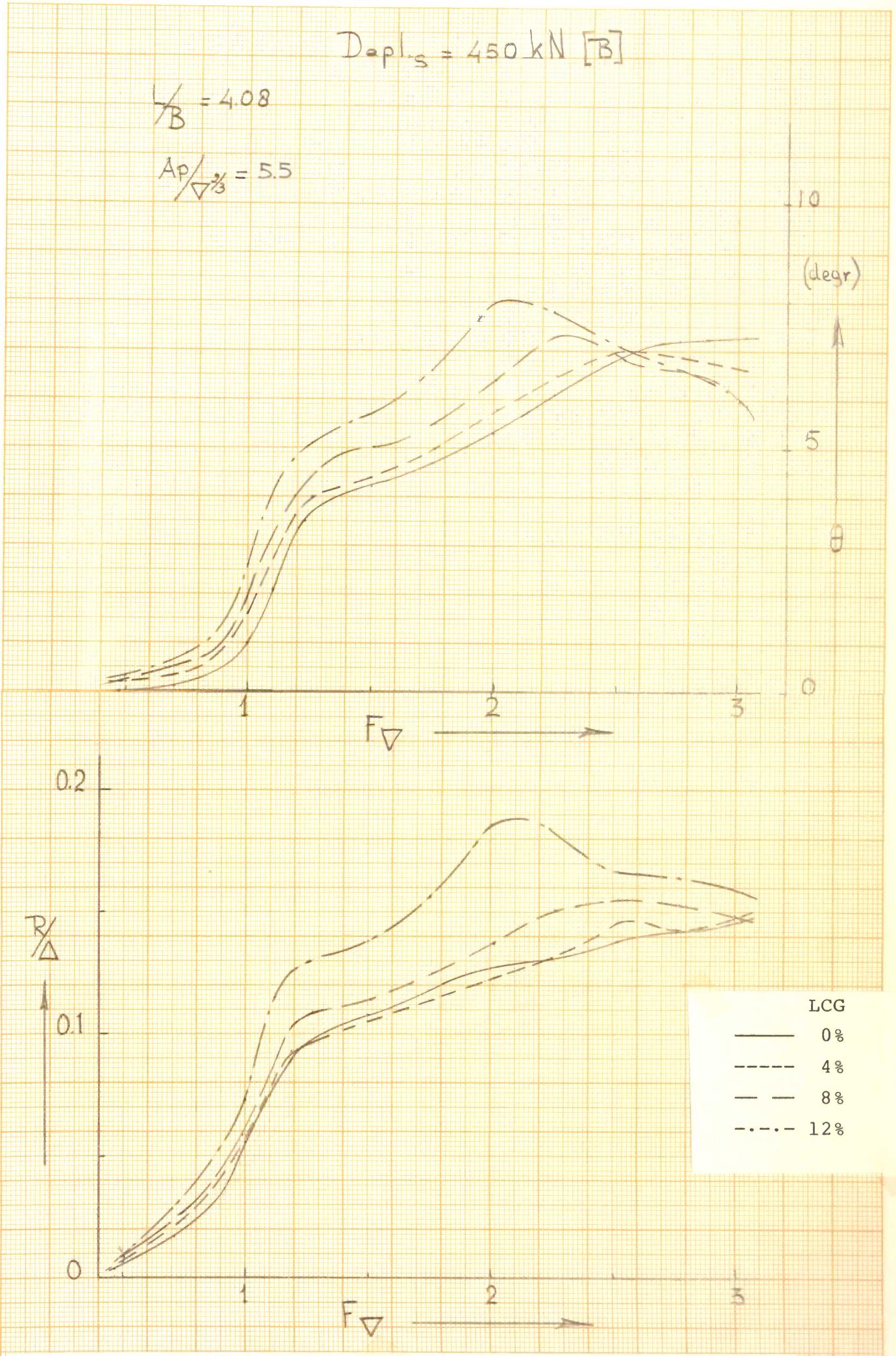

Figure 14. Model 232-B, Δ = 450kN.

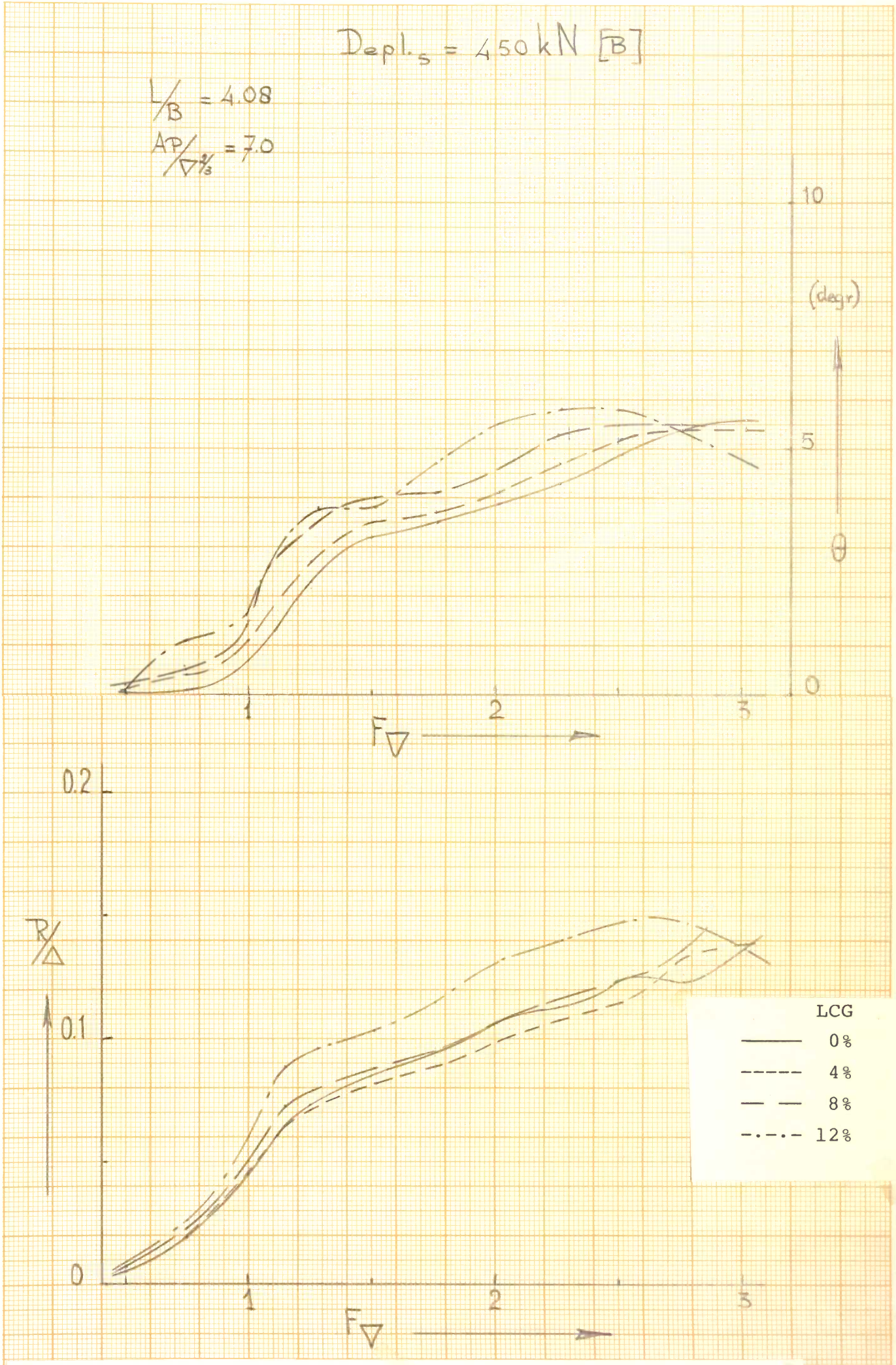

Figure 15. Model 232-B, Δ = 450kN.

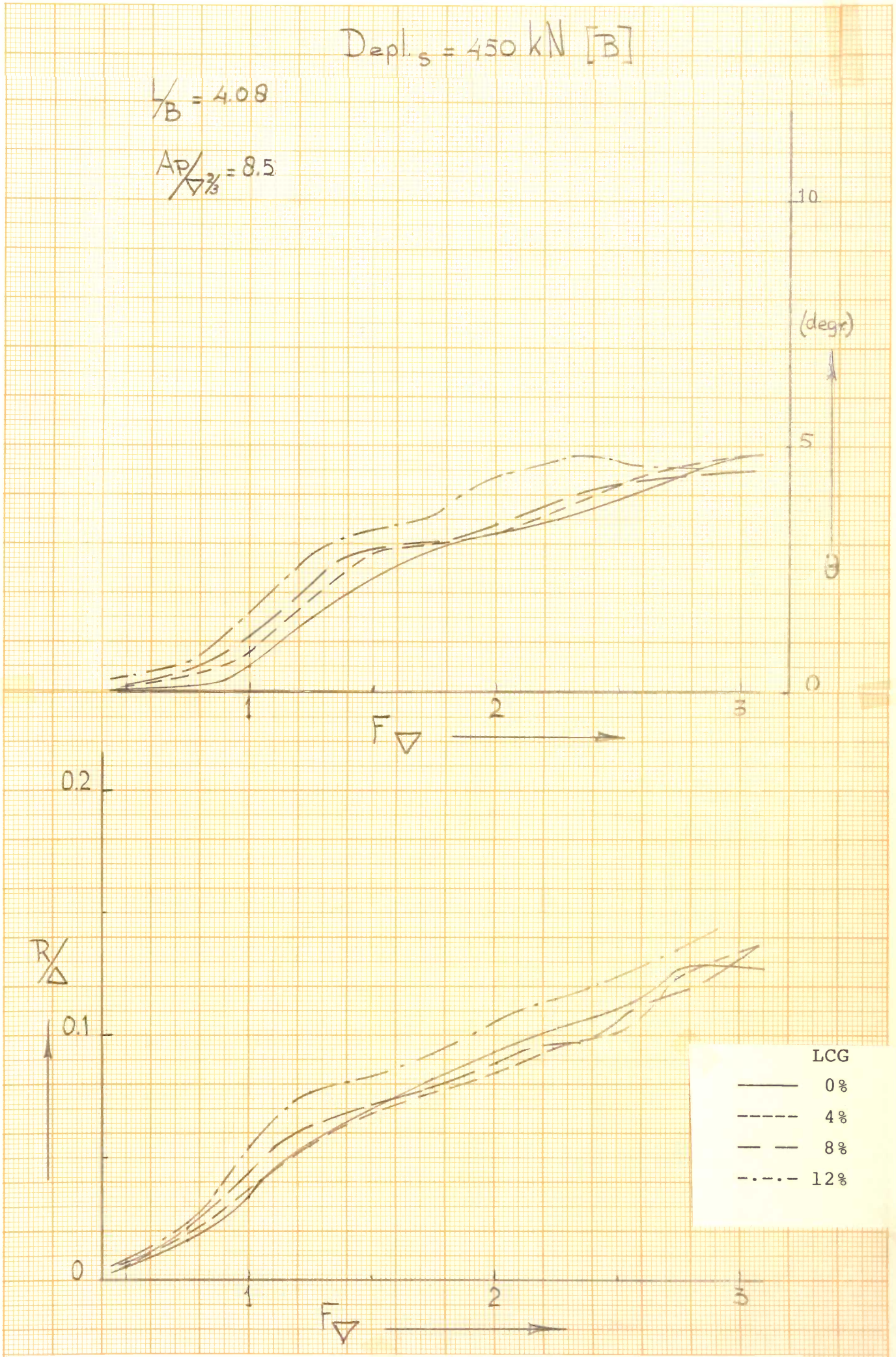

Figure 16. Model 232-B, Δ = 450kN.

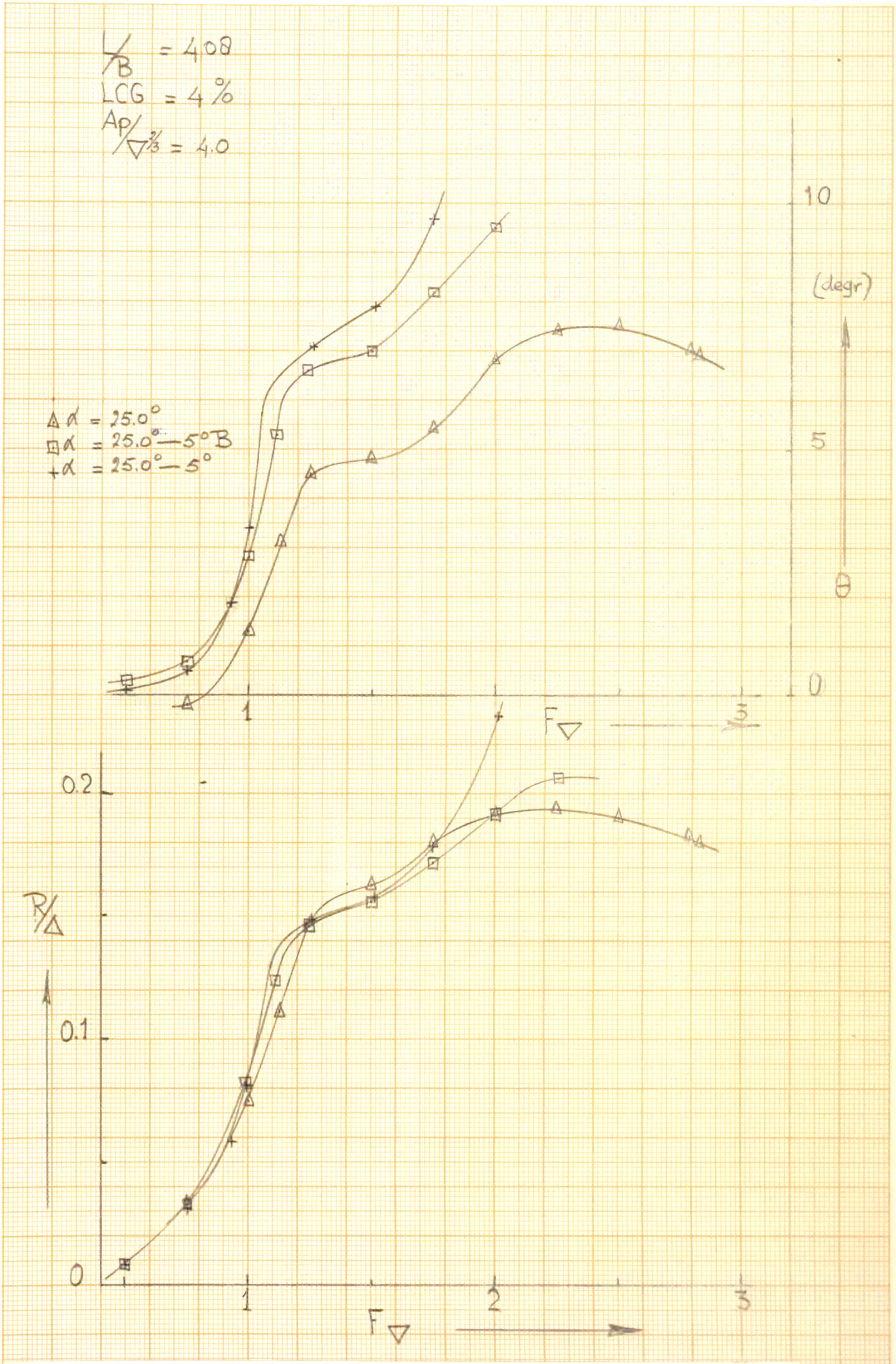

Figure 17. Comparison 4 parent models.

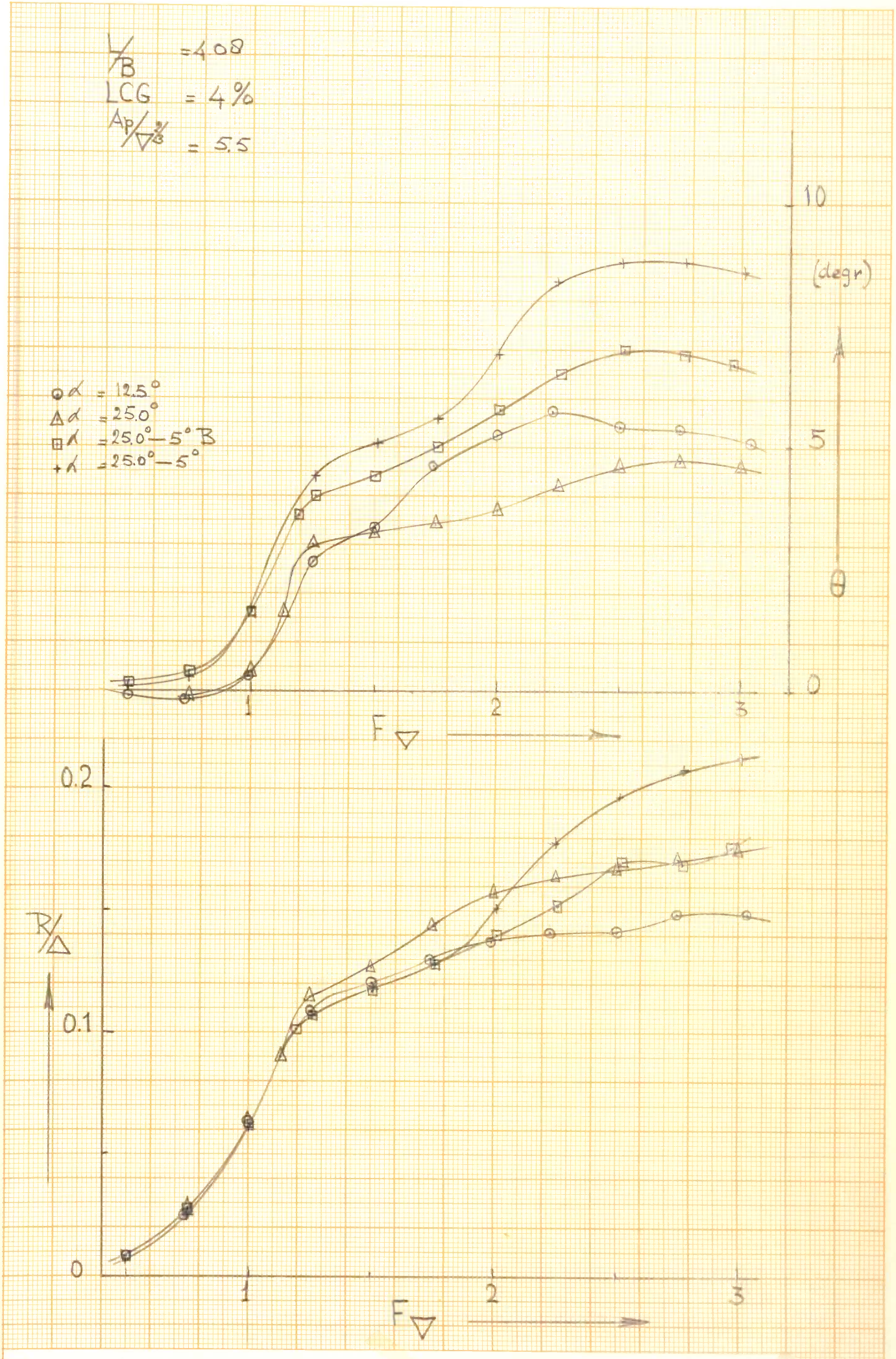

Figure 18. Comparison 4 parent models.

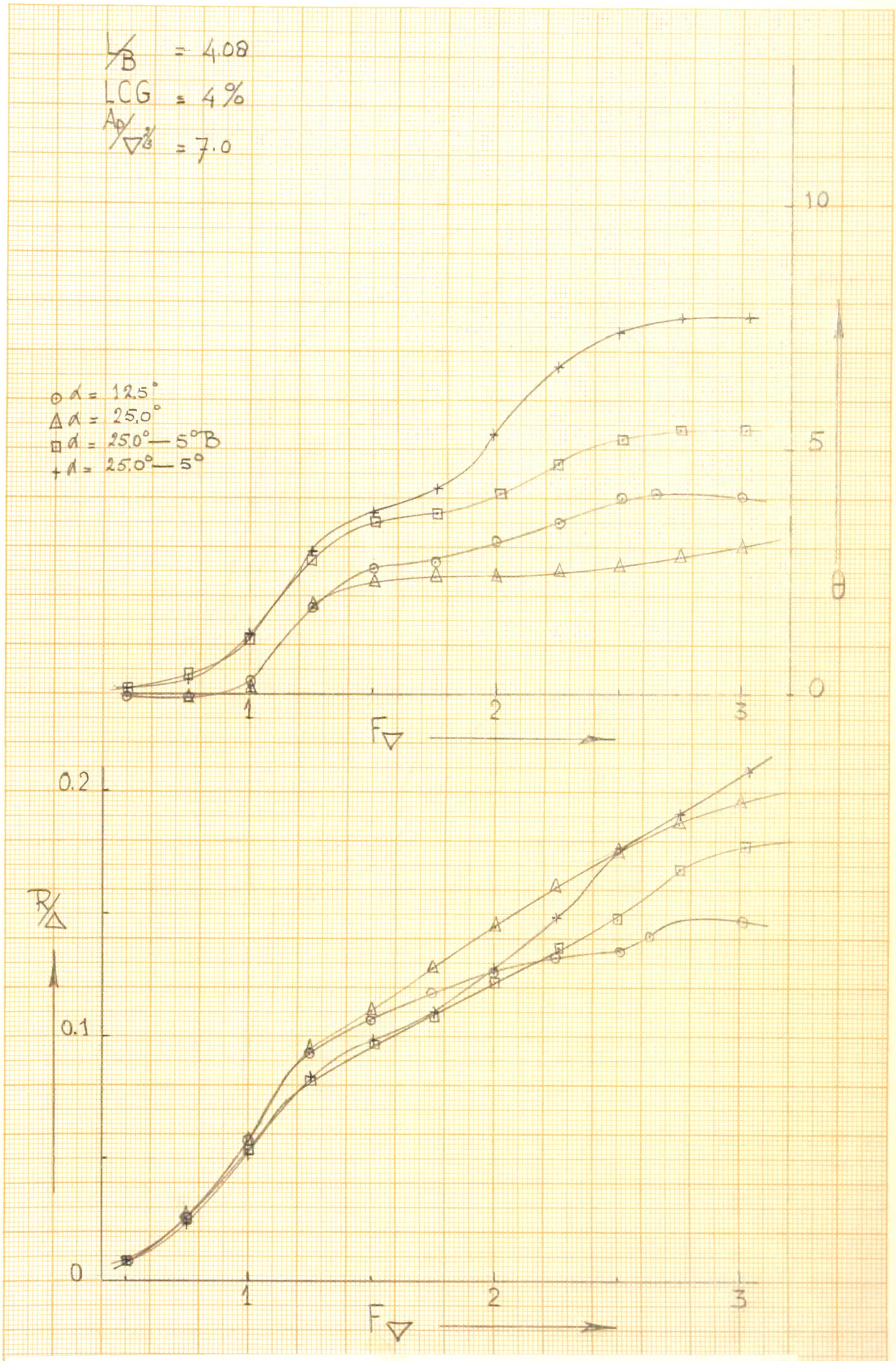

Figure 19. Comparison 4 parent models.

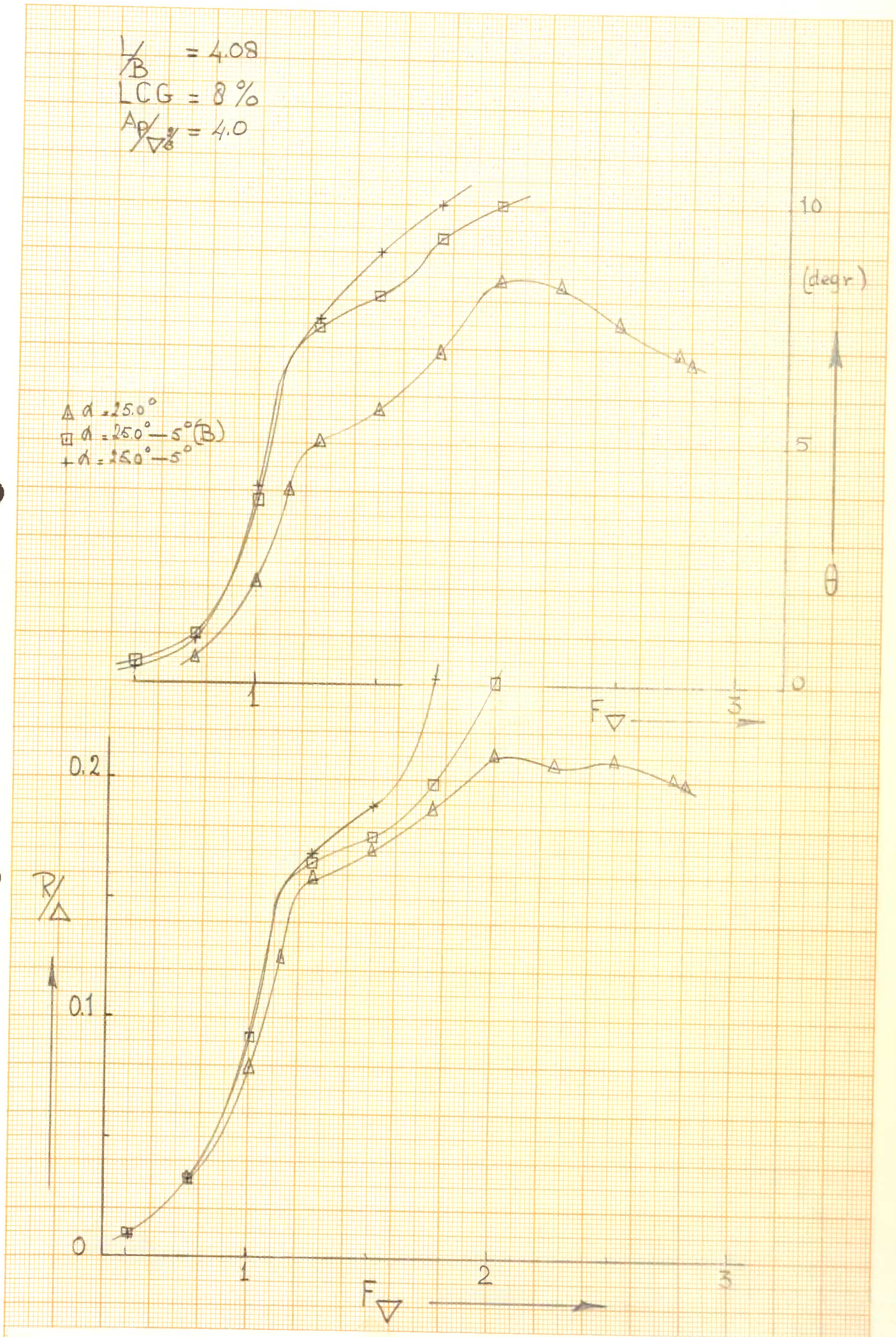

Figure 20. Comparison 4 parent models.

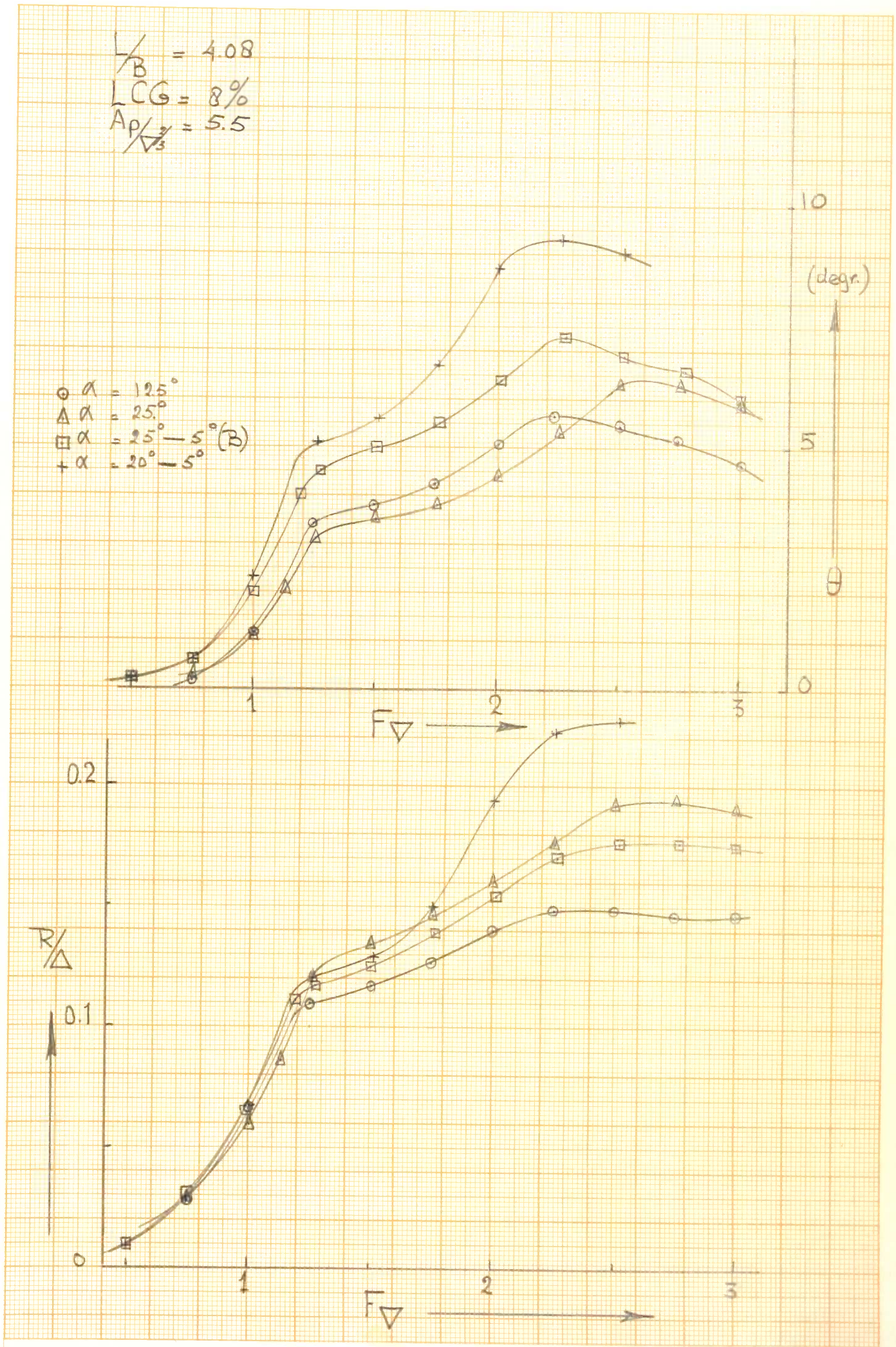

Figure 21. Comparison 4 parent models.

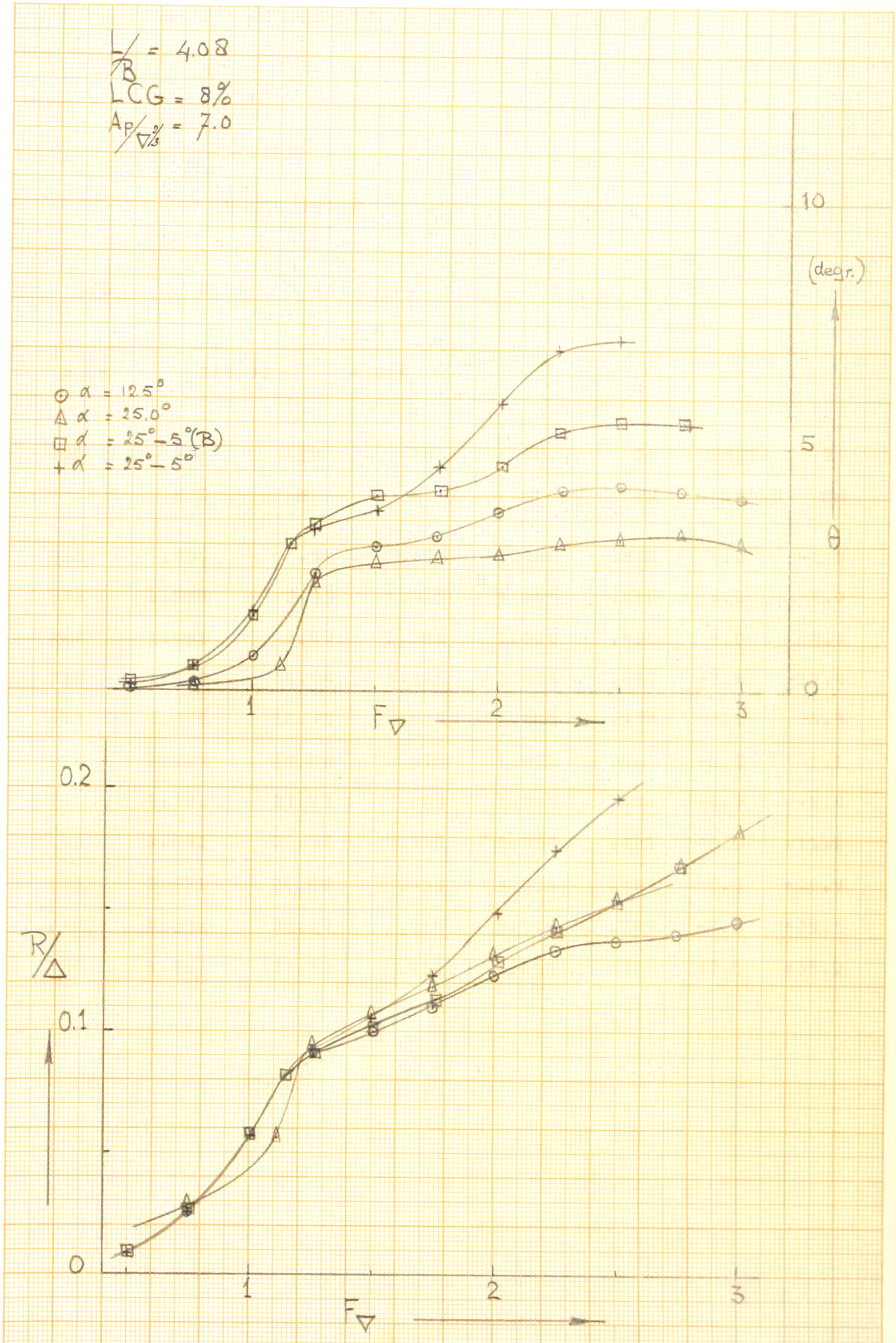

Figure 22. Comparison 4 parent models.

MODEL 233 A

L/B	DEPL	LCG
	N	M
4.08	164.71	+.000

RUN	VM	RTM	LK	LC	S	THETA	Z
	M/S	N	M	M	M2	GRADEN	MM
225	.795	.99	.675	1.485	.448	+.0	-1.0
226	1.199	3.75	1.315	1.505	.480	+.1	-4.0
227	1.585	8.49	1.200	1.510	.490	+.8	-8.3
228	1.979	14.24	1.125	1.475	.487	+2.6	-12.4
229	2.378	16.71	.980	1.445	.478	+3.6	-4.9
230	2.785	19.08	.975	1.420	.463	+4.0	-1.1
231	3.183	21.12	.900	1.395	.444	+4.7	+4.6
232	3.572	23.56	.865	1.360	.421	+5.5	+11.1
233	3.971	26.48	.750	1.255	.389	+6.7	+20.9
234	4.378	30.27	.715	1.140	.349	+7.3	+29.5
235	4.787	33.82	.650	1.050	.320	+7.5	+35.2

MODEL 233 A

L/B	DEPL	LCG
	N	M
4.08	164.71	-.060

RUN	VM	RTM	LK	LC	S	THETA	Z
	M/S	N	M	M	M2	GRADEN	MM
213	.796	1.15	.650	1.475	.412	+.1	-1.6
214	1.201	3.83	.785	1.490	.432	+.3	-4.4
215	1.596	8.60	.750	1.465	.447	+1.2	-9.0
216	1.993	13.61	.970	1.430	.454	+2.9	-10.8
217	2.390	16.11	.905	1.405	.449	+3.7	-4.5
218	2.786	18.11	.890	1.355	.434	+4.2	-.9
219	3.158	21.10	.865	1.330	.414	+5.3	+4.7
220	3.572	24.56	.870	1.180	.386	+6.7	+14.4
221	3.972	29.08	.690	1.085	.355	+7.4	+25.7
222	4.371	31.40	.638	1.015	.320	+7.7	+32.3
223	4.798	34.33	.590	.965	.280	+7.7	+37.8

MODEL 233 A

L/B	DEPL	LCG
	N	M
4.08	164.71	-.120

RUN	VM	RTM	LK	LC	S	THETA	Z
	M/S	N	M	M	M2	GRADEN	MM
201	.794	1.31	.740	1.460	.420	+.1	-1.5
202	1.198	4.19	.780	1.440	.424	+.5	-4.6
203	1.593	9.32	.670	1.420	.426	+1.6	-9.4
204	1.990	15.19	.950	1.365	.425	+3.3	-10.5
205	2.386	17.31	.860	1.315	.415	+3.7	-4.3
206	2.783	20.28	.785	1.245	.393	+4.6	+.5
207	3.182	24.54	.750	1.120	.362	+5.9	+8.7
208	3.569	28.76	.670	1.305	.325	+7.0	+21.2
209	3.971	32.33	.620	.900	.279	+7.2	+31.4

MODEL 233 A

L/B	DEPL	LCG
	N	M
4.08	164.71	-.180

RUN	VM	RTM	LK	LC	S	THETA	Z
	M/S	N	M	M	M2	GRADEN	MM
188	.794	1.53	.675	1.425	.400	+.2	-1.5
189	1.199	4.53	.675	1.410	.397	+.7	-4.6
190	1.583	11.25	.713	1.365	.396	+2.1	-10.0
192	1.978	18.31	.825	1.250	.395	+4.3	-9.2
193	2.384	20.90	.785	1.145	.378	+4.9	-1.9
194	2.781	24.81	.710	1.040	.351	+6.1	+5.3
195	3.190	31.68	.670	1.025	.313	+7.8	+13.7

MODEL 233 A

L/B	DEPL	LCG
	N	M
4.08	236.42	+.000

RUN	VM	RTM	LK	LC	S	THETA	Z
	M/S	N	M	M	M2	GRADEN	MM
236	.847	1.43	1.050	1.520	.495	+.0	-2.0
237	1.273	5.60	1.260	1.540	.528	+.1	-5.6
238	1.688	14.20	1.560	1.560	.555	+1.1	-11.2
239	2.124	25.16	1.315	1.475	.529	+4.0	-11.2
240	2.531	28.13	1.100	1.465	.493	+4.7	-4.9
241	2.942	30.99	1.088	1.430	.482	+5.3	-.3
242	3.361	33.93	1.000	1.395	.460	+6.3	+8.3
243	3.790	37.89	.905	1.325	.425	+7.8	+18.4
244	4.233	41.37	.790	1.220	.382	+8.7	+30.4
248	4.688	45.39	.740	1.115	.346	+9.1	+40.1
247	5.103	48.47	.700	1.055	.323	+9.2	+46.1

MODEL 233 A
==========

L/B	DEPL	LCG
	N	M
4.08	236.42	-.060

RUN	VM	RTM	LK	LC	S	THETA	Z
	M/S	N	M	M	M2	GRADEN	MM
249	.847	1.66	.905	1.505	.463	+.1	-2.0
250	1.262	5.94	1.560	1.535	.555	+.3	-6.0
252	1.687	14.52	1.315	1.560	.542	+1.7	-11.4
253	2.123	25.29	1.125	1.440	.482	+4.4	-11.1
254	2.539	27.90	1.015	1.290	.452	+5.1	-4.5
255	2.958	30.22	.975	1.370	.434	+5.6	+1.2
256	3.377	35.63	.865	1.280	.403	+6.9	+10.1
257	3.785	42.20	.785	1.150	.367	+8.4	+27.2
258	4.228	46.64	.750	1.035	.332	+8.8	+36.6
259	4.666	49.06	.675	.960	.307	+8.8	+44.6
260	5.059	50.47	.640	.930	.294	+8.6	+50.1

MODEL 233 A

L/B	DEPL	LCG
	N	M
4.08	236.42	-.120

RUN	VM	RTM	LK	LC	S	THETA	Z
	M/S	N	M	M	M2	GRADEN	MM
262	.844	2.04	.865	1.480	.495	+.2	-1.8
263	1.269	6.57	.910	1.470	.457	+.6	-5.5
264	1.684	15.78	1.130	1.430	.491	+2.3	-11.2
265	2.118	28.27	.985	1.345	.446	+5.1	-10.1
266	2.536	30.59	.900	1.295	.424	+5.6	-3.2
267	2.955	35.43	.870	1.235	.396	+6.7	+3.6
268	3.374	45.91	.785	1.055	.356	+8.7	+18.3
269	3.801	50.16	.700	.960	.315	+9.3	+33.6
270	4.235	51.31	.610	.905	.283	+9.0	+44.4

MODEL 233 A

L/B	DEPL	LCG
	N	M
4.08	236.42	-.180

RUN	VM	RTM	LK	LC	S	THETA	Z
	M/S	N	M	M	M2	GRADEN	MM
274	.847	2.42	.825	1.455	.437	+.3	-2.1
275	1.262	7.09	.825	1.435	.440	+.9	-6.0
276	1.687	19.03	.950	1.375	.437	+3.1	-11.9
277	2.102	34.72	.900	1.250	.410	+6.1	-10.0
278	2.528	38.49	.825	1.130	.368	+6.7	-.7
280	2.936	48.92	.750	1.025	.330	+8.8	+10.4
279	3.364	56.90	.675	.890	.295	+10.0	+28.8

MODEL 233 A

L/B	DEPL	LCG
	N	M
4.08	381.22	+.000

RUN	VM	RTM	LK	LC	S	THETA	Z
	M/S	N	M	M	M2	GRADEN	MM
307	.917	2.36	1.560	1.560	.555	+.0	-3.1
308	1.372	11.11	1.560	1.560	.555	+.2	-8.8
309	1.828	28.30	1.560	1.560	.555	+2.3	-17.0
310	2.284	52.66	1.560	1.560	.555	+6.3	-13.1
311	2.741	58.39	1.320	1.530	.530	+6.9	-5.5
312	3.199	64.20	1.200	1.435	.498	+8.2	+4.5
313	3.671	69.48	1.050	1.360	.462	+10.0	+19.8

MODEL 233 A

L/B	DEPL	LCG
	N	M
4.08	381.22	-.060

RUN	VM	RTM	LK	LC	S	THETA	Z
	M/S	N	M	M	M2	GRADEN	MM
298	.916	3.04	1.560	1.560	.555	+.1	-3.4
299	1.370	11.76	1.560	1.560	.555	+.5	-8.8
300	1.693	22.65	1.560	1.560	.555	+1.9	-13.9
301	1.837	31.05	1.560	1.560	.555	+3.4	-15.8
302	2.292	56.29	1.200	1.435	.517	+7.1	-12.0
303	2.750	59.83	1.125	1.400	.475	+7.9	-2.8
304	3.198	67.88	1.015	1.330	.435	+9.7	+8.1
305	3.666	88.30	.870	1.150	.392	+10.0	+28.1

MODEL 233 A
=========

L/B	DEPL	LCG
	N	M
4.08	381.22	-.120

RUN	VM	RTM	LK	LC	S	THETA	Z
	M/S	N	M	M	M2	GRADEN	MM
291	.917	3.54	1.125	1.515	.508	+.3	-2.0
292	1.373	12.40	1.560	1.495	.550	+.9	-7.6
293	1.828	35.71	1.320	1.455	.513	+4.1	-14.6
294	2.285	64.28	1.050	1.360	.468	+7.6	-10.4
295	2.752	71.98	.975	1.270	.423	+9.0	+.1
296	3.200	92.15	.865	1.090	.378	+10.0	+15.3

MODEL 233 A
==========

L/B	DEPL	LCG
	N	M
4.08	381.22	-.180

RUN	VM	RTM	LK	LC	S	THETA	Z
	M/S	N	M	M	M2	GRADEN	MM
286	.917	4.26	1.015	1.460	.475	+.4	-2.8
287	1.372	12.54	1.200	1.440	.478	+1.3	-7.8
288	1.827	41.26	1.090	1.395	.460	+4.9	-14.9
289	2.293	81.55	.980	1.235	.424	+9.0	-10.2

MODEL 233 B

L/B	DEPL	LCG
	N	M
4.08	123.02	+.000

RUN	VM	RTM	LK	LC	S	THETA	Z
	M/S	N	M	M	M2	GRADEN	MM
140	.753	.87	.600	1.475	.396	+.0	-1.9
141	1.136	2.73	1.315	1.510	.535	+.1	-4.3
142	1.510	5.48	1.560	1.500	.550	+.5	-7.0
143	1.885	8.76	1.260	1.470	.523	+1.5	-9.4
145	2.639	13.04	.890	1.430	.444	+2.9	-1.4
146	3.020	15.11	.865	1.420	.437	+3.2	+2.4
147	3.405	17.09	.825	1.405	.426	+3.5	+7.0
148	3.773	18.59	.825	1.370	.412	+3.9	+8.9
149	4.156	21.44	.750	1.330	.393	+4.4	+13.5
150	4.553	22.37	.675	1.270	.373	+4.8	+16.0

MODEL 233 B

L/B	DEPL	LCG
	N	M
4.08	123.02	-.060

RUN	VM	RTM	LK	LC	S	THETA	Z
	M/S	N	M	M	M2	GRADEN	MM
151	.754	.99	.550	1.470	.385	+.1	-1.3
152	1.127	2.90	.600	1.480	.396	+.3	-3.0
154	1.511	5.74	1.125	1.500	.504	+.8	-5.7
155	1.883	8.52	1.050	1.490	.488	+1.9	-8.2
156	2.268	10.55	.900	1.415	.444	+2.8	-4.5
157	2.654	12.22	.785	1.395	.418	+3.0	-1.8
158	3.032	13.96	.785	1.380	.413	+3.2	+1.4
159	3.388	15.82	.750	1.365	.403	+3.7	+6.1
160	3.768	17.34	.720	1.305	.385	+4.2	+11.7
161	4.159	20.78	.670	1.245	.363	+4.6	+16.0
162	4.548	22.70	.620	1.165	.337	+4.8	+18.6

MODEL 233 B

L/B	DEPL	LCG
	N	M
4.08	123.02	-.120

RUN	VM	RTM	LK	LC	S	THETA	Z
	M/S	N	M	M	M2	GRADEN	MM
164	.752	1.11	.525	1.445	.374	+.1	-.9
165	1.134	3.12	.550	1.440	.378	+.4	-3.1
166	1.509	6.43	.715	1.440	.411	+1.1	-5.9
167	1.883	9.34	.780	1.365	.413	+2.2	-8.0
168	2.258	11.00	.825	1.350	.411	+2.9	-3.9
169	2.644	12.41	.780	1.340	.402	+3.0	-.6
170	3.033	14.28	.730	1.285	.386	+3.4	+4.8
171	3.391	15.89	.700	1.225	.367	+3.9	+11.6
172	3.777	17.58	.630	1.125	.342	+4.2	+15.6
173	4.169	19.57	.590	1.050	.315	+4.4	+19.9
174	4.549	21.51	.555	1.035	.286	+4.5	+22.9

MODEL 233 B
==========

L/B	DEPL	LCG
	N	M
4.08	123.02	-.180

RUN	VM	RTM	LK	LC	S	THETA	Z
	M/S	N	M	M	M2	GRADEN	MM
176	.754	1.26	.525	1.430	.362	+.3	-1.3
177	1.128	3.39	.500	1.380	.359	+.6	-3.7
178	1.512	7.68	.550	1.360	.362	+1.6	-6.9
179	1.887	10.97	.825	1.275	.400	+2.8	-7.0
180	2.272	12.20	.750	1.225	.376	+3.3	-2.5
181	2.638	13.67	.713	1.195	.350	+3.6	+1.8
183	3.035	15.98	.638	1.050	.324	+4.4	+8.0
184	3.390	17.48	.590	.995	.303	+4.7	+15.2
182	3.647	18.56	.600	.965	.289	+4.8	+20.4
185	3.774	19.08	.600	.885	.283	+4.7	+22.9
186	4.158	20.87	.555	.875	.263	+4.6	+26.6

MODEL 233 B

L/B	DEPL	LCG
	N	M
4.08	164.71	+.000

RUN	VM	RTM	LK	LC	S	THETA	Z
	M/S	N	M	M	M2	GRADEN	MM
38	.795	1.14	.785	1.500	.445	+.0	-1.5
39	1.189	3.90	1.560	1.505	.551	+.1	-4.3
40	1.584	8.81	1.560	1.490	.550	+.7	-7.9
41	1.980	13.92	1.315	1.505	.532	+2.3	-10.2
42	2.377	16.60	1.125	1.480	.501	+3.2	-4.9
43	2.783	19.01	1.050	1.460	.478	+3.5	-1.6
44	3.180	21.67	.945	1.435	.458	+3.9	+2.5
45	3.580	23.43	.900	1.420	.439	+4.3	+8.3
46	3.980	26.05	.825	1.380	.421	+4.9	+13.7
47	4.383	26.72	.785	1.340	.404	+5.4	+18.3
48	4.789	29.86	.750	1.290	.388	+5.6	+22.5

MODEL 233 B

L/B	DEPL	LCG
	N	M
4.08	164.71	-.060

RUN	VM	RTM	LK	LC	S	THETA	Z
	M/S	N	M	M	M2	GRADEN	MM
26	.795	1.31	.750	1.480	.429	+.1	-1.4
27	1.189	4.16	1.260	1.500	.526	+.4	-3.9
28	1.584	8.82	1.160	1.475	.507	+1.1	-7.6
29	1.981	13.57	1.050	1.455	.481	+2.7	-9.6
30	2.386	15.98	.940	1.410	.457	+3.5	-4.3
31	2.783	17.73	.900	1.395	.439	+3.7	-.4
32	3.180	20.11	.900	1.380	.426	+4.1	+3.9
33	3.578	22.37	.825	1.345	.418	+4.7	+10.4
34	3.980	24.41	.760	1.275	.403	+5.2	+17.0
35	4.366	27.78	.750	1.220	.377	+5.4	+21.6
36	4.792	29.33	.630	1.110	.338	+5.4	+26.0

MODEL 233 B

L/B	DEPL	LCG
	N	M
4.08	164.71	-.120

RUN	VM	RTM	LK	LC	S	THETA	Z
	M/S	N	M	M	M2	GRADEN	MM
14	.791	1.54	.675	1.455	.406	+.2	-1.0
15	1.189	4.49	.785	1.495	.436	+.5	-3.7
17	1.584	9.50	1.090	1.450	.500	+1.5	-7.9
25	1.828	13.52	1.050	1.420	.468	+3.0	-10.1
18	1.991	14.83	.940	1.425	.451	+3.4	-9.3
19	2.386	16.87	.865	1.380	.426	+4.0	-3.3
20	2.792	18.63	.825	1.330	.409	+4.1	+.9
21	3.190	21.21	.785	1.295	.396	+4.6	+6.6
22	3.560	23.23	.750	1.170	.370	+5.3	+14.0
23	3.970	25.19	.675	1.100	.335	+5.5	+22.0
24	4.375	27.69	.650	1.050	.320	+5.5	+27.1

MODEL 233 B

L/B	DEPL	LCG
	N	M
4.08	164.71	-.180

RUN	VM	RTM	LK	LC	S	THETA	Z
	M/S	N	M	M	M2	GRADEN	MM
3	.795	1.79	.675	1.445	.400	+.1	-1.0
9	1.189	4.91	.750	1.415	.415	+1.1	-4.0
4	1.585	11.06	.975	1.407	.452	+1.7	-8.3
13	1.827	16.17	.900	1.365	.437	+3.2	-10.5
2	2.021	17.57	.870	1.345	.423	+3.8	-8.1
5	2.388	19.23	.785	1.275	.394	+3.8	-1.9
10	2.791	21.65	.750	1.165	.360	+4.7	+3.8
6	3.183	24.62	.675	1.050	.325	+5.5	+11.6
11	3.597	26.63	.600	.970	.295	+5.8	+22.8
7	3.995	28.55	.600	.938	.283	+5.8	+30.3
12	4.411	29.19	.600	.895	.284	+5.5	+34.1
8	4.812	29.00	.525	.890	.306	+4.7	+36.7

MODEL 233 B

L/B	DEPL	LCG
	N	M
4.08	236.42	+.000

RUN	VM	RTM	LK	LC	S	THETA	Z
	M/S	N	M	M	M2	GRADEN	MM
49	.794	1.38	1.125	1.535	.512	+.0	-1.6
50	1.187	4.74	1.560	1.550	.552	+.1	-4.9
51	1.683	14.60	1.560	1.550	.552	+1.0	-11.1
61	1.847	19.37	1.450	1.525	.552	+2.1	-13.7
52	2.068	24.63	1.400	1.520	.547	+3.5	-12.2
53	2.526	28.33	1.230	1.455	.523	+4.2	-5.5
54	2.943	31.63	1.150	1.450	.500	+4.7	-.5
55	3.373	34.52	1.050	1.425	.475	+5.3	+6.0
56	3.794	36.15	.975	1.410	.451	+6.1	+13.7
57	4.234	38.68	.890	1.355	.428	+6.9	+22.6
59	4.652	40.57	.825	1.305	.406	+7.2	+28.7
60	5.094	42.30	.785	1.245	.386	+7.3	+34.7

MODEL 233 B
==========

L/B	DEPL	LCG
	N	M
4.08	236.42	-.060

RUN	VM	RTM	LK	LC	S	THETA	Z
	M/S	N	M	M	M2	GRADEN	MM
63	.846	1.97	1.050	1.500	.490	+.2	-1.9
64	1.264	6.47	1.490	1.510	.548	+.4	-5.4
65	1.676	14.75	1.560	1.560	.552	+1.6	-10.5
67	2.001	23.84	1.230	1.470	.516	+3.6	-12.5
68	2.121	25.09	1.160	1.440	.505	+4.0	-10.6
69	2.525	27.58	1.050	1.430	.476	+4.4	-4.7
70	2.954	30.27	.975	1.400	.452	+5.0	+1.9
71	3.384	33.16	.900	1.350	.428	+5.8	+8.9
72	3.807	35.93	.865	1.305	.406	+6.5	+18.5
73	4.247	40.24	.785	1.225	.384	+7.0	+27.8
74	4.663	39.93	.750	1.150	.364	+6.9	+34.0
75	5.001	41.51	.715	1.120	.347	+6.7	+38.1

MODEL 233 B

L/B	DEPL	LCG
	N	M
4.08	236.42	-.120

RUN	VM	RTM	LK	LC	S	THETA	Z
	M/S	N	M	M	M2	GRADEN	MM
77	.845	2.31	.825	1.480	.445	+.2	-1.6
78	1.269	7.22	1.260	1.485	.521	+.6	-5.0
80	1.674	15.37	1.125	1.460	.497	+2.0	-10.1
81	2.000	26.14	1.050	1.415	.473	+4.0	-11.6
82	2.141	27.65	1.015	1.400	.463	+4.5	-9.7
83	2.537	29.49	.940	1.370	.441	+5.0	-2.8
84	2.966	32.81	.900	1.300	.416	+5.5	+3.6
85	3.386	36.30	.825	1.210	.387	+6.4	+12.6
86	3.805	40.11	.750	1.095	.354	+7.3	+24.7
87	4.234	41.72	.715	1.050	.331	+6.9	+34.4
88	4.660	41.83	.675	1.020	.314	+6.6	+39.6
89	5.046	41.34	.600	.995	.301	+6.0	+43.8

MODEL 233 B

L/B	DEPL	LCG
	N	M
4.08	236.42	-.180

RUN	VM	RTM	LK	LC	S	THETA	Z
	M/S	N	M	M	M2	GRADEN	MM
91	.846	2.61	.865	1.450	.443	+.3	-1.8
92	1.262	7.46	.975	1.395	.454	+.8	-5.2
102	1.677	18.50	.955	1.290	.452	+2.6	-10.8
97	1.886	28.63	.975	1.355	.442	+4.3	-12.6
93	2.123	32.63	.905	1.275	.426	+5.1	-9.3
94	2.529	34.97	.865	1.205	.390	+5.7	-.4
95	2.948	39.62	.785	1.100	.354	+6.6	+7.8
96	3.366	47.34	.715	.985	.322	+8.0	+22.3
98	3.767	47.27	.650	.920	.298	+7.8	+35.7
99	4.236	43.74	.640	.870	.278	+7.1	+42.6
100	4.655	43.95	.600	.855	.269	+6.6	+49.6
101	5.095	43.15	.600	.805	.264	+5.9	+53.2

MODEL 233 B

L/B	DEPL	LCG
	N	M
4.08	381.22	+.000

RUN	VM	RTM	LK	LC	S	THETA	Z
	M/S	N	M	M	M2	GRADEN	MM
128	.915	2.69	1.560	1.555	.555	+.1	-3.3
129	1.370	11.66	1.560	1.560	.555	+.1	-9.2
130	1.815	28.22	1.560	1.555	.555	+1.9	-16.8
136	2.038	42.12	1.560	1.555	.555	+4.2	-17.9
131	2.281	52.09	1.560	1.555	.555	+5.8	-14.3
132	2.728	58.21	1.450	1.515	.555	+6.3	-6.9
133	3.185	64.80	1.280	1.470	.525	+7.0	+2.0
134	3.644	68.85	1.130	1.440	.492	+8.5	+14.2
135	4.110	70.59	1.000	1.340	.449	+10.0	+30.8
138	4.591	71.94	.850	1.260	.402	+10.0	+43.2
137	5.161	71.26	.850	1.190	.388	+10.0	+54.0

MODEL 233 B
==========

L/B	DEPL	LCG
	N	M
4.08	381.22	-.060

RUN	VM	RTM	LK	LC	S	THETA	Z
	M/S	N	M	M	M2	GRADEN	MM
118	.917	3.21	1.560	1.555	.555	+.3	-2.8
119	1.373	12.63	1.560	1.555	.555	+.7	-7.7
120	1.818	31.18	1.560	1.555	.555	+2.8	-14.0
126	2.021	47.29	1.560	1.555	.555	+5.3	-15.4
121	2.265	55.53	1.260	1.470	.524	+6.6	-12.0
122	2.731	59.62	1.125	1.430	.491	+7.0	-3.3
123	3.190	65.39	1.050	1.370	.461	+8.2	+6.8
124	3.648	72.58	.975	1.290	.432	+9.5	+21.3
125	4.111	78.44	.910	1.235	.205	+10.0	+39.5

MODEL 233 B
==========

L/B	DEPL	LCG
	N	M
4.08	381.22	-.120

RUN	VM	RTM	LK	LC	S	THETA	Z
	M/S	N	M	M	M2	GRADEN	MM
110	.916	3.86	1.125	1.505	.506	+.4	-2.6
111	1.372	12.72	1.560	1.555	.555	+1.0	-7.1
112	1.817	34.92	1.315	1.470	.528	+3.8	-13.6
113	2.273	62.94	1.125	1.390	.484	+7.4	-10.3
114	2.731	66.97	1.050	1.315	.444	+8.1	+.4
115	3.187	75.99	.940	1.225	.405	+9.3	+12.7
116	3.649	91.87	.825	1.050	.367	+10.0	+34.0

MODEL 233 B

L/B	DEPL	LCG
	N	M
4.08	381.22	-.180

RUN	VM	RTM	LK	LC	S	THETA	Z
	M/S	N	M	M	M2	GRADEN	MM
104	.917	4.75	1.050	1.475	.485	+.5	-2.4
105	1.363	13.02	1.200	1.470	.514	+1.3	-7.2
106	1.829	40.62	1.125	1.410	.487	+4.6	-14.2
107	2.284	76.60	.975	1.260	.424	+8.3	-9.8
108	2.732	88.77	.905	1.155	.393	+9.5	+2.8
109	3.201	79.32	.905	1.125	.386	+10.0	-.3

Stellingen:

1.
De pieken in de verticale versnellingen, welke een snelvarend schip in golven ervaart, zijn maatgevend voor de inzetbaarheid van het schip, ongeacht de grootte van het momentane significante versnellingsniveau.

2.
Het ware beter bij het opstellen van een mathematisch model voor de beschrijving van een physisch gebeuren het toepassen van een niet-lineair model niet te beschouwen als een ongewenste complicatie maar het gebruik van een lineair model als een onvermijdelijke simplificatie.

3.
Het onderzoek naar operationele criteria welke de werkbaarheid van (snelle) schepen in zeegang begrenzen verdient aanzienlijk meer aandacht dan het nu krijgt.

4.
Bij het beschouwen van ontwerpen van snelle schepen kan geconcludeerd worden, dat de eisen welke aan geluidsniveau's gesteld worden zwaarder wegen dan die welke aan de toelaatbare bewegingen gesteld moeten worden.

5.
Het ware beter een andere benaming te gebruiken voor de "significante" amplituden om de schijn te vermijden dat alleen die "van belang" zouden zijn.

6.
Veel rapporten waarin verslag wordt gedaan van een wetenschappelijk onderzoek vertonen een dermate logische opbouw dat het vrijwel zeker is dat het betreffende onderzoek nooit in die volgorde is uitgevoerd.

7.
Het feit dat op de Nederlandse binnenwateren de pleziervaart moet wijken voor beroepsvaart getuigt van een arbeidsethos welk niet meer van deze tijd is.

8.
Het veelvuldig werken met lineaire modellen kan aanleiding geven tot onwetenschappelijke rechtlijnigheid.

9.
Dogma's worden eenvoudiger afgezworen dan een dogmatische levenshouding.

10.
Niet door een overmaat aan vlijt is het wiel ontdekt.

Nonlinear Behaviour of Fast Monohulls in Head Waves

Jan Alexander Keuning

CIP-DATA KONINKLIJKE BIBLIOTHEEK, DEN HAAG

Keuning, Jan Alexander

Nonlinear behaviour of fast monohulls in head waves / Jan Alexander Keuning. - Delft : Delft University of Technology, Faculty of Mechanical Engineering and Marine Technology. - Fig.
Thesis Technische Universiteit Delft. - With ref.
ISBN 90-370-0109-2
Subject headings: monohulls ; nonlinear behaviour.

Opmerkingen:

Deze CIP-gegevens alleen afdrukken in de proefschrifteditie.

Technische Universiteit Delft, Fac. Werktuigbouwkunde en Maritieme Techniek,
Bibliotheek WbMT
Mekelweg 2,
2628 CD Delft

Deze CIP-gegevens ongewijzigd afdrukken op de copyrightpagina van het boek, incl. het kopje "CIP-GEGEVENS KONINKLIJKE BIBLIOTHEEK, DEN HAAG".
Voor informatie: tel.: 070-3140414.

NONLINEAR BEHAVIOUR OF

FAST MONOHULLS IN HEAD WAVES

PROEFSCHRIFT

ter verkrijging van de graad van doctor
aan de Technische Universiteit Delft
op gezag van de Rector Magnificus
Prof.ir. K.F.Wakker,
in het openbaar te verdedigen
ten overstaan van een commissie
door het College van Dekanen aangewezen
op woensdag 14 september 1994 te 16:00 uur

door

Jan Alexander KEUNING
scheepsbouwkundig ingenieur

geboren te Enschede

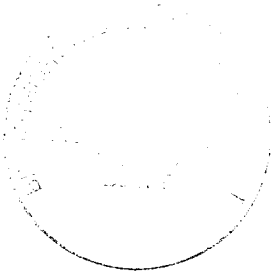

Dit proefschrift is goedgekeurd door de promotor:
Prof.ir. J.Gerritsma.

Table of Contents

Chapter 1

Introduction

The search for high speeds for marine vehicles, although very vivid during the last decades, has not been restricted to this period of time. During the complete history of marine vehicles, man has always been striving for higher speeds, be it for warfare, or trade or plain pleasure. But speeds attainable by wind propelled vehicles reached more or less their maximum at the end of 1800's due to lack of adequate construction materials available and lack of interest due to the forthcoming of mechanically propelled vessels. Attention shifted to these kind of vessels which showed a higher reliability because of their seemable independency of the prevailing wind conditions with regard to relative wind direction and strength and also the decoupling of deliverable thrust and transverse static stability of the craft.

In effect this search for higher speeds attained by marine vehicles started as early as in the late 1800's when C. Ramus proposed the development of a 2500 ton deadweight "planing" ship. At that time however the society was not ready for such a development and the idea was generally rejected as being "unrealistic", amongst others by William Froude. In 1894 Sir Charles Parsons produced the first marine propulsion plant based on a steam turbine engine in the well known ship "Turbinia". This ship displaced 45 tons of water and had a long and slender hullform. She was capable of speeds upto 35 knots, which she finally reached in 1896 when suitable propellors had been fitted.

After her acceptance as a feasible and even promising concept for marine warfare the development of so-called Motor Torpedo Boats and Torpedo Boat Destroyers started. This development was greatly enhanced by the introduction of the internal combustion type piston engines, which were capable of delivering the power to weight ratio necessary for attaining these high speeds. Also, at that time the typical design features for planing craft as we know them nowadays started to develop: the hard chines and the cut off transom stern and sometimes even some transverse steps in the planing bottom, i.e. the so-called "stepped hull", meant to reduce unnecessary wetted surface. The speeds went up and in 1910 Thornycroft designed a 7.5 meter single stepped planing hull capable of 35 knots which finally led to the design and production of a 16.5 meter Coastal Motorboat of 14 tons displacement carrying two torpedo's and a crew of five at speeds upto 46 knots.

This boat was designed for use in the rough environment of the North Sea,

where she proved to be very succesful during the First World War.
Development continued between World War 1 and World War 2. The hard chined planing hull evolved to become more and more accepted in relation to the round bilge hull so well developed until then. Leading countries in the development of fast monohulls at that time were Great Britain, Germany and the United States, each with their own preference with respect to hull shape, i.e. the UK and the USA favouring hard chines and Germany favouring round bilges. Hull construction material varied between steel, wood and aluminium. Speeds varied from 30 to well over 40 knots. During World War 2 refinement of design reached a stage in wich most of the designs were of the hard chine type. Well known examples of these craft were the MTB's, the Motor Torpede Boats, which served during World War 2 but also later in the sixties. A benchmark speed reached in that period of time was well over 50 knots attained by the British "Brave" class equipped with Rolls Royce Proteus gasturbines.
The development until then was more or less dominated by the military applications. Although there was a lot of research going on in the field of planing hull hydrodynamics the prime attention was focussed on still water performance and aimed at the highest speeds possible and very little emphasis was being placed on the seakeeping properties of these fast craft. Studies in the field of impact loads on planing surfaces were mostly initiated by the designers of waterplanes, who were confronted with similar problems in this respect during take-off and landing of these planes from the water surface. The problems encountered with high speed vessels travelling in a seaway, and those appeared to be quite a few, were dealt with the attitude that the designer had to optimise for speed in still water and that resistance increase, and, in particular, the motions and accelerations in waves were something "one had to live with".
The interest in high speed marine vehicles for military applications has continued to grow, in the last two decades, however, there is also an increasing interest in the application of these craft in other areas of marine transportation, i.e. as patrol boats, passenger ferries, lifeboats, service vessels and pleasure craft. In these applications much more emphasis has to be placed on the behaviour of the ships in a seaway, in particular with respect to passenger- and crew comfort as well as their safety. The afore-mentioned attitude towards the seakeeping behaviour of the high speed craft was no longer acceptable. However, both the physical understanding of the phenomena involved as the tools to calculate or optimise the behaviour of fast monohulls in waves were not generally available. Therefore, the use of high speed craft in these applications remained restricted to the more or less sheltered areas like rivers, lakes, estuaries and coastal seas in which the sea climate could generally be described as "mild".

In the late sixties much more interest developed in improving the seakeeping characteristics of high speed planing craft. Noticeable work in this field was carried out by Van den Bosch (6) in 1969 and Fridsma (13, 14) in 1971. Particularly Fridsma was one of the first to carry out extensive systematic research on the seakeeping behaviour of fast (planing) monohulls. This work has later been extended by D. Savitsky (53) to yield results which were more suited

for practical application by the designers.

The combination of high forward speeds and "acceptable" motions and more in particular acceptable levels of the vertical accelerations in a seaway onboard a fast moving monohull proved to be difficult.

In the continuing search for this combination all kinds of so called "advanced" concepts have been designed, evaluated, built and used, each of them however with its specific benefits and shortcommings. Among these "advanced" concepts the Hydrofoil-boat, the Air Cushion Vehicle, the Surface Effect Ship, the Catamaran, the Small Waterplane Area Twin Hull Ship and, more recently, the Wing In Ground should be mentioned. A conceptional layout of these various craft is presented in Figure 1.1. Their design philosophy is partly aimed at attaining high speed by reducing resistance (buoyancy or wetted area) and partly at minimising motions in waves at speed by reducing wave exciting forces (by reducing waterplane area, buoyancy etc).

All these concepts have reached a certain stage of perfection over the last decades. Compared to the relatively "simple" monohull, however, be it a round bilge or a hard chine design, all these "advanced" concepts are considerably more complicated and therefore tend to be considerably more expensive, both in construction and operation.

Therefore : the role of the fast monohull as a high speed and performance marine vehicle is certainly not over yet.
However, the applicability of this fast monohull in waves needed improvement over the performance realised until the late sixties. A large factor in the determination of succesful task fulfilment is the realised operability of these craft in waves. So improving the operability of the fast monohull means improving the seakeeping behaviour of the concept, in particular, in irregular (head) seas.

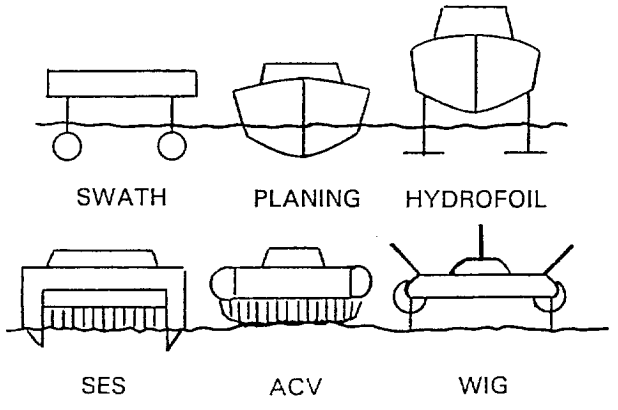

Figure 1.1: Conceptual drawings of advanced marine vehicles

At first this was done by making use of the general information derived from seakeeping tests with similar designs which have been systematically varied with respect to the main parameters of importance for seakeeping. This approach is particularly attractive when much insight in the phenomena involved still has to be gained. A very noticeable publication with results from extensive systematic model tests on seakeeping was presented by Fridsma (13, 14) in his pioneering approach to assess the seakeeping behaviour of planing boats. By systematically changing the deadrise of the planing bottom, the length to beam ratio of the chine area, the running trim of the craft at speed, the loading factor and the longitudinal position of the Centre of Gravity during tests in regular head waves, he obtained considerable information on the influence of these parameters on the seakeeping behaviour of planing boats. The results obtained during these tests were systematically analysed and presented in the form of "design charts" for use by designers. These design charts presented valuable information on the parameters involved and showed the designer how the seakeeping behaviour of a fast craft could be influenced in the design stage. The information was more of a qualitative then of a quantitative nature.
No specific information on actual designs under consideration could be derived and the data presented permitted no excursions too far away from the parent model used because the parameter range of the systematic series, they were originally derived from, was rather limited. This was partly due to the schematic nature of the hull geometries used. Widening the applicability of these results would mean extending the systematic model test series. This has been done amongst others by Savitsky (53), Hadler (20), Van den Bosch (5). Savitsky derived empirical formulations for the calculation of vertical motions and accelerations based on the results of Fridsma and using data available in an early design stage only.

In conjunction with these tests another kind of model experiments of a more fundamental nature was carried out by amongst others Von Karman, aimed at gaining insight in the physical phenomena involved. Quite often experiments with planing wedges, as a physical analogon of the ship hull, were used. The aim of these experiments was to gain insight in the nature of the planing phenomena and the development of dynamic lift on the ships hull at high speeds and to determine the relevance of the use of the ship motions mathematical models primarily developed for "ordinary" displacement ships in highspeed situations.

In the field of naval hydrodynamics the theory to calculate the motions of ships in waves was under development and in particular since the 50's the possibility to calculate shipmotions was investigated by many authors.
Naval hydrodynamics in shipmotion calculation routine development were largely based on the 2-D linear strip theory approach. This theory was based on the work of Krylov reported as early as 1898. In 1954 Ursell (66) formulated an analytical method for the calculation of the added mass and damping of a heaving cilinder in the free surface. By means of the use of conformal transfor-

mation techniques both Grim and Tasai (61) showed the way to use these results to calculate the added mass and damping of an arbitrary 2-D cross section. In 1957 Korvin Kroukovsky and Jacobs (36) derived the expression to calculate the hydrodynamic coefficients and wave forces for a ship with forward speed, which were further analysed and verified by Gerritsma and Beukelman (16) in 1960. It is a linear theory which means that the ship moving in the waves is considered to be a linear system. This implies that the ship is considered to perform motions with infinite small amplitudes around its still water reference position at zero speed. The motions amplitudes of the ship response are linearily related to the height of the incoming disturbant wave. The hydrodynamic reaction forces experienced by the ship due to its motions in the surrounding water and the forces excited on the ship by the incoming waves are being calculated by integration over the length of the ship of 2-D cross-sectional values for added mass and damping. The magnitude of these inphase and quadrature forces with respect to the motions are considered to be constant over a certain span of the shiplength. They are derived either by some kind of conformal mapping from a known solution of an oscillating cilinder of infinite length in the free surface (Lewis) or by a 2-D diffraction technique (Frank). Interaction effects between the cross-sections is considered to be small for ship hull-form and therefore neglected. The influence of the forward speed of the ship on the motions is taken into account by a correction on the hydrodynamic forces incorporating among others the length-wise distribution of the 2-D sectional added mass and damping over the shiplength. No influence of the velocity distribution of the water along the hull moving at speed is taken into account.
Three-dimensional methods have also been developed. These are based on the solution of the velocity potential by defining the proper boundary conditions on the body in three dimensions and the free surface. This method is described among others by Faltinsen (11), Hogben (18) and Standing and Newman (46). Originally the solution of the velocity potential was restricted to the problem of an oscillating 3-D body at the free surface without forward speed. Inglis and Price (23) and Kobayashi (34) have extended the method to be able to handle ships with low forward speeds. Recently Sclavounos and Nakos (45) have extended the method to include the solution of the boundary value problem of the ship in steady forward motion.

All these methods are basically linear and the resulting motions in an irregular sea are calculated using the linear superposition principle as originally formulated for naval applications by Denis and Pierson (10). This enabled the designer to optimise his design with respect to operability for a specific area when the statistics of the environmental conditions were known.
In particular the linear strip theory method has evolved in the past decades into a powerful tool for the prediction of the motions of ships with forward speed. The use of the theory is widespread, its applicability is high, it is easy to handle with relatively short runtimes even on Personal Computers and the computational results compare generally very well with model experiment results.

As outlined before, the impact of the seakeeping behaviour on the design of fast monohulls is probably greater than for "normal" speed commercial vessels, so the availability of a reliable prediction tool of the relevant motions is of significant importance for the evolution of the concept. However, some of the underlying assumptions and constraints may not justify the use of the developed linear strip theory for fast ships.

To investigate the applicability of the 2-D linear strip theory for these fast ships Blok and Beukelman (2) performed in 1984 extensive shipmotion calculations with 9 models of the High Speed Displacement Hull Form Series of which the responses to regular head waves had been measured at the facilities of MARIN in Wageningen in a project under joint sponsorship by the Royal Netherlands Navy, the David Taylor Research Centre (USA) and the Royal Australian Navy. All 9 models used in this series were derived from one round bilge parent model from which the bodyplan is depicted in Figure 1.2.

In this study Blok and Beukelman found rather good correlation between measured and calculated results for heave and pitch motions in head seas for really high speeds upto Fn = 1.14, being the highest speed used in the MARIN experiments. A typical example of their results is presented in the Figure 1.3 for the heave and pitch transfer-function at the highest Froude number.
Unfortunately, no information is available about measured vertical accelerations. Only the response operators derived from the tests in regular waves have been compared.

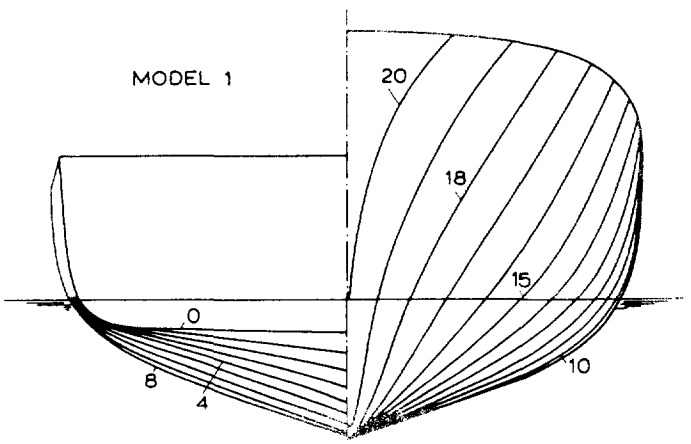

Figure 1.2: Bodyplan of the parent hull of the HSDHF Series

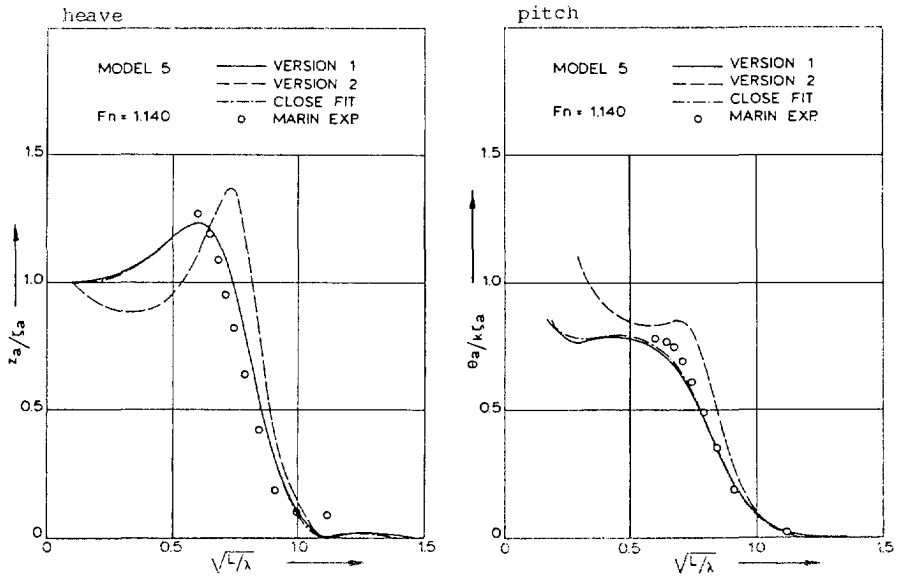

Figure 1.3: Heave and pitch transfer function of HSDHF series parent hull at Fn = 1.14. From (2)

This good result for these round bilge monohulls at high forward speeds lead Beukelman (1) to use this 2-D linear strip theory calculation method also for the motion calculations of hard chine planing hull forms in head seas. He measured and calculated the heave- and pitch transfer functions as well as the vertical accelerations at the midship section and at the bow of a hard chine planing hull at two different forward speeds. The hull geometry of the model used is shown in Figure 1.4 and both the measured and calculated transfer functions are shown in Figure 1.5 for heave and pitch respectively.

From his results there appears to be no significant difference in correlation between measured and predicted results for the transfer function in the case of a round bilge or hard chine design.
To investigate the linearity of the system of a planing hull in waves additional measurements and calculations were performed in two irregular wave conditions as well. General conclusions drawn from this work were that the heave motion is reasonably well predicted by the linear strip theory both in regular and irregular waves but that the correlation for pitch is less satisfactory.
The results for the vertical accelerations at the bow showed some large discrepancies.
For the assessment of the motions of a fast monohull or planing craft in waves the linear strip theory approach could, however, well remain attractive due to its relatively short processing time needed for the computations. The motions in various sea spectra may be obtained easily by using the linear superpositioning

principle once the transfer functions are known. This may well explain its widespread use, for instance, in design studies were operability optimisation is used, because in those studies the motions have to be calculated for a variety of designs in a large array of seastates.

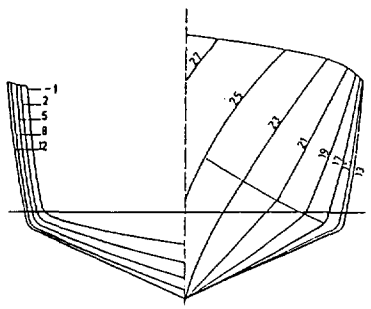

Figure 1.4: Bodyplan planing hull. From (1)

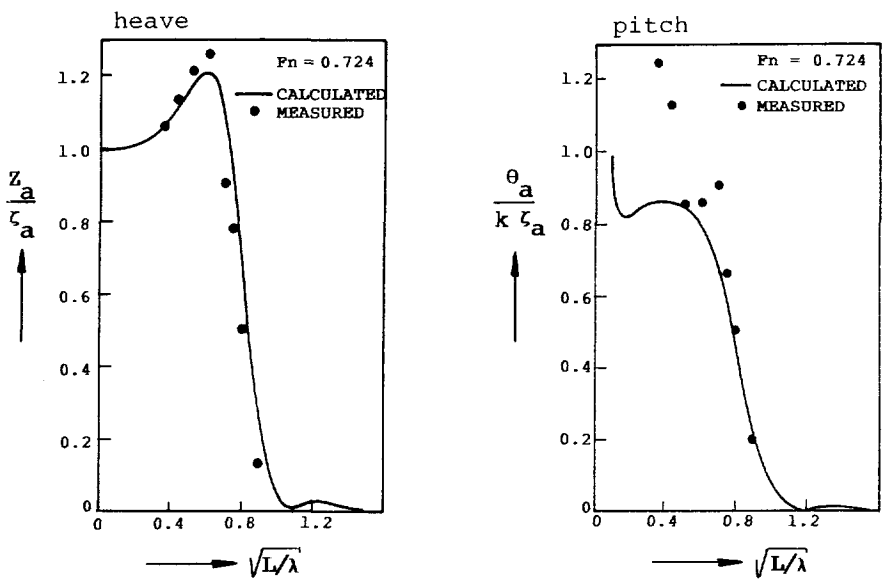

Figure 1.5 : Heave and pitch transferfunctions of the planing hull. From (1)

Typical constraints of the application of a linear theory when assessing the motions of fast ships are:

- the assumed linearity, which implies that the hydrodynamic forces are linearily dependent on the amplitude of the incomming wave and that the amplitudes of the resulting motions are small. Theoretically the calculations are carried out for a zero amplitude of motions.

- the forward speed influence is only partly taken into account, which generally restricts the use to moderate forward speeds

- hull forms with no significant changes in hull geometry in the region just above (and below) the still-waterline around which the craft is considered to perform its motions.

Both from experience with actual fast craft at sea and model experiments it is known that the motions of a fast monohull in head waves and in particular the vertical accelerations may be strongly nonlinear with respect to the amplitude of the disturbant waves.
When performing tests with high speed models in regular waves it has been found that the response in heave and pitch show a nonlinear dependence on the wave amplitude. This nonlinear response behaviour is dependent on a number of hullform parameters but in particular on the deadrise angle of the planing bottom.
Also the vertical accelerations measured in regular waves, at different positions along the length of the ship, may show a considerable non harmonic character with large peaks exceeding the amplitude of the harmonic response by a factor of two or more. There is a pronounced difference between the vertical accelerations measured at midship or at the bow in this respect, the later tending to behave generally more nonharmonic. Again this nonlinear behaviour increases with increasing wave amplitude and forward speed and is dependent on hullform parameters also.

Although the influence on the motions of these peaks in the accelerations is rather limited, their occurrence is of great importance for the determination of the operability of the ship. From full scale experience it is known that the occurrence of peaks in the vertical accelerations, associated with "slams", are the limiting phenomena with regard to possible damage to the crew and/or the ship and generally lead to a "voluntary" speed reduction of the ship in waves.

Many actual applications of fast ships consist of relatively small ships, i.e. passenger ferries, service craft, patrol boats, lifeboats, pleasure craft etc. Related to the environmental conditions this usually means that the waves are relatively large with respect to the size of the ship. In addition the high forward speed of the ships under consideration implies that waves which excite the ship in or near its natural period for heave and pitch are generally longer with respect to the shiplength than customary for ships sailing with "normal" speeds. This implies that in particular in those conditions which must be considered to be of special interest or even critical with respect to the operability of the ship, for

instance high forward speed and relatively large waveheights, large (relative) motions may occur. Significant bow submergence and occurrence of moments in which the ship is partly or even completely airborne are not impossible for fast ships.
This implies that the small motion amplitude assumption underlying the linear theory may no longer be justifiable. The influence on the hydrodynamic forces of the changing geometry of the ship in contact with the water whilst performing large amplitude relative motions may have to be taken into the calculations to account for these effects. In particular bow sub- and emergence may have a considerable nonlinear effect on the magnitude of the exciting forces in particular so because of the significant flare or V-shape of many fast monohulls designs in that section.

It is also known that fast monohulls at high speeds experience a considerable change in vertical position of the ship in the water due to the forward speed only. This change in "reference" position of the ship in calm water is generally referred to as "sinkage" (steady state heave) and "trim" (steady state pitch). Both are caused by a change in the pressure distribution over the length of the ship due to hydrodynamic effects which may differ largely when compared with the assumed hydrostatic pressure distribution at zero forward speed. For ships at "normal" forward speeds this may generally be neglected, but for the ships under consideration in the present study with high forward speeds, this sinkage and trim may become considerable. This results not only in a change of the submerged geometry of the ship, i.e. a change of waterplane area, cross-sectional curves etc, but also in a change of the submerged volume because part of the ship's weight is been carried by the hydrodynamic lift.
In the usual linear theory this is not easily accounted for. Sinkage and trim may be taken into account by changing the still water reference position and by doing so account for the change in sumberged hull geometry, but this will most likely yield a considerable difference between the weight of the ship and the weight of displaced water by the hull. This will result in an imbalance in the equations discribing the motions of the ship in vertical plane, i.e. heave and pitch. In addition a major force contribution in this plane is neglected, which force may also show considerable changes in time due to the motions and the related changes in submerged hull geometry.

The hypothesis put forward in this thesis is that nonlinear effects have to be taken into the computational model for the calculation of the heave and pitch motions and vertical accelerations of fast mono-hulls in head seas in order to be able to predict the peak values of the vertical accelerations properly. Because of the fact that the occurrence of these peaks is the true limiting phenomenon on which the criteria for the (safe) operation of fast ships in waves is based, an adequate prediction of these is necessarry. The use of linear computational models may lead to erroneous results and even reverse design trends.

The outline of this thesis is as follows:

In **Chapter 2** a series of model experiments with planing hulls in calm water and in waves will be discussed and analysed.
The nonlinear behaviour of this system of "a fast monohull in waves" will be demonstrated and the importance of these nonlinearities on the phenomena of interest shown. If the experimental setup permits, the nonlinear behaviour will be attributed to some design parameters and/or occurring phenomena. Largely on basis of these experimental results a selection will be made of sources of non-linear behaviour in the system which have to be taken into account in the computational model.

In **Chapter 3** the computational model will be described that will be used for the calculations. Based on the findings of Chapter 2 special emphasis will be put on the following aspects:

- the determination of the calm water steady state equilibrium position, i.e. sinkage and trim of the ship at high forward speed. An extensive series of experiments with a systematic series of planing hulls will be described aimed at measuring resistance sinkage and trim as function of some first order design parameters. These results will be used to derive polynomial equations based on these design parameters only from which the sinkage and trim of an arbitrary design may be derived. Using this sinkage and trim as an input in the equations describing the steady state planing in calm water the lengthwise hydrodynamic pressure distribution may be found which is used to determine the lift force on the hull at speed.

- the distribution over the length of the ship of the hydrodynamic reaction forces, i.e. added mass and damping, at high forward speed. These have been measured in a forced oscillation experiment using a segmented model. The applicability of 2-D added mass calculations with no forward speed effect will be shown if the proper vertical lift distribution over the length due to the high forward speed of the hull is taken into account.

- the domination in the wave exciting forces, in the case of a fast moving monohull in head waves, by the Froude Kriloff component. This will be shown by analysing the results of an experiment in which the wave forces have been measured on a captive model at high forward speeds using the same segmented model as mentioned above.

- the influence of large relative motions. This will be introduced by making the added mass calculation dependent on the submerged cross-sectional shape of the ship whilst performing large motions in waves. Similarly the wave exciting forces are calculated by using the Froude Kriloff com-

ponent over the momentaneous submerged volume of the ship under the same condition.

- irregular waves. A special calculation routine has been implemented in the computational model to make simulations possible in irreggular waves.

In **Chapter 4** the results of the calculations using the developed computercode FASTSHIP based on the computational model derived in Chapter 3 will be compared with the results of measurements with a systematic series of planing models in waves to check the applicability and the accuracy of the derived computational model. In addition a sensitivity analysis will be made of the computational results with regard to some of the assumptions made and the importance of the nonlinear effects introduced into the calculations. Hereto also a comparison between the results of a linear versus the presented nonlinear model will be made.

In **Chapter 5** the effect of the use of a linear or a nonlinear computational model for the prediction of the motions and accelerations of a fast monohull in a seaway will be discussed. It will be shown that the nature of the operability criteria to be used for fast monohulls necessitates the use of nonlinear models.

Chapter 2

Nonlinearities in the behaviour of fast monohulls

2.1 Introduction

In this Chapter the necessity to use a nonlinear computational model to predict the motions and operability of a fast monohull in waves will be discussed.

In the context of shipmotions studies nonlinear behaviour is considered to be the nonlinear dependency of the amplitude of motions, velocities and accelerations on the amplitude of the incomming disturbant wave. If non-linearities in the behaviour prove to be of any significance then their source of origination should be localised and possibly introduced into the computational model.

To illustrate the nonlinear behaviour of the fast monohull in head waves use will be made of the results of model experiments carried out by Fridsma a.o. (13, 14) and Van den Bosch (6). They carried out experiments with systematically varied models as early as 1970 to clarify the dependency of the motions and accelerations of planing craft on some design parameters such as forward speed, deadrise angle of the planing bottom, longitudinal position of the Centre of Gravity and the associated trim angle.

An important phenomenon in the behaviour of fast ships not accounted for in linear computational models, although not strictly a nonlinear effect in the sense as defined above, is the change in reference position of the ship at speed, due to the afore-mentioned sinkage (stationary heave) and trim (stationary pitch). To demonstrate the magnitude of this sinkage and trim and to show their dependency on some design parameters, results of tests carried out by Clement and Blount (9) with a systematic series of planing models will be used. This change in reference position originates from the presence of substantial hydrodynamic lift. It will be shown that this lift is an important aspect in the behaviour of the ship in waves.

In addition to these tests and within the framework of the present study, experiments have been carried out with planing hull models showing different bow deadrise angles and bow flare. The results of these tests will be used to show the nonlinear effects introduced by the geometry of the ship and the above water (bow) geometry whilst performing large relative motions in irregular head waves.

2.2 The effect of forward speed on sinkage and trim

Due to the forward speed of a ship in calm water the pressure distribution around the hull changes with respect to the hydrostatic pressure distribution around the hull at zero speed of advance. In the case of "normal" ships with moderate forward speeds, i.e. Froude numbers to Fn = 0.35 or Fn = 0.40, this generally leads to a downward displacement of the Centre of Gravity at lower speeds changing into a small rise when the speed increases together with a bow up attitude, both of which are small in magnitude. The change in total submerged volume of the hull is generally negligible, which means that the assumption that the total weight of the ship is carried by the buoyancy force is justifiable.
In the case of high forward speeds, however, the sinkage and trim may become quite significant, in particular with hard chined planing hulls. In fact, this is one of the design objectives of this fast ship concept: due to the rise of the Centre of Gravity and the trim a significant reduction of the wetted surface of the hull may be achieved and so the frictional resistance is reduced. In addition, the actual submerged volume of the hull is reduced, which in its turn leads to a reduction of the wave making resistance. Both reductions of these components in the total resistance of a ship make the high design speeds feasible at the cost of still economic amounts of installed power.

In linear ship motion calculation models, be it 2-D or 3-D, these stationary heave and pitch motions are neglected: in the computational procedure the ship is kept on its calm water zero forward speed reference position irrespective of its actual forward speed. The existence of any dynamic liftforce (and moment) in the equations of motions is neglected, and therefore also any interaction between the motions and this dynamic lift.
The justification of this approach for ships with forward speeds upto Fn = 0.40 has been amply demonstrated by many authors, who compared measured and calculated motions of ships in waves.

However, to illustrate the possible magnitude of the sinkage and trim in the case of a planing monohull as well as their dependency on the hull geometry and some design parameters, the results of a study presented by Clement and Blount (9) will be used.

In order to supply designers with information about the resistance, sinkage and trim of planing hulls, Clement and Blount carried out extensive experiments with a systematic series of planing hullforms. As a parent model for this series they chose an optimised contemporary design of a planing hull with a deadrise angle of 12.5 degrees and a prismatic afterbody. The bodyplan of this model is depicted in Figure 2.1.
In their systematic series they varied the aspect ratio (length to beam over the chine), the loading (weight related to chine area) of the lifting surface and the longitudinal position of the Centre of Gravity.

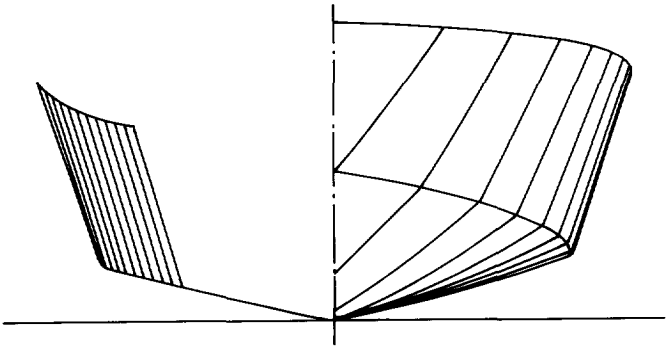

Figure 2.1: Bodyplan of the Clement Series 62 parent model

The hulls were derived from the selected parent hullform by means of a linear transformation technique guaranteeing a close similarity between all hulls. The difference in chine projections of the various models is depicted in Figure 2.2.

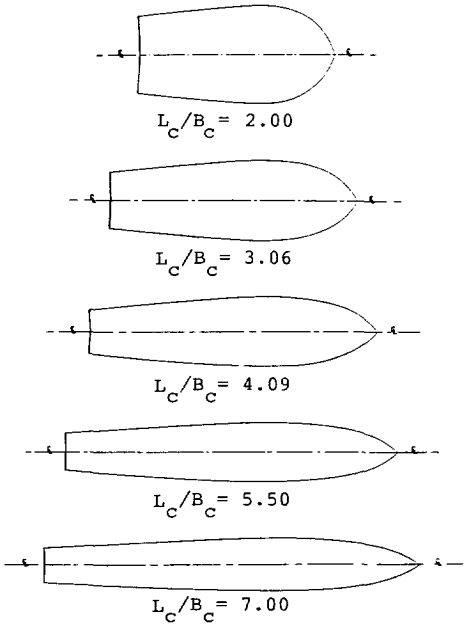

Figure 2.2: Chine projections of the 12.5 degrees deadrise systematic models. From (9)

The results for sinkage and trim of their parent model over the speed range of interest is shown in Figure 2.3.

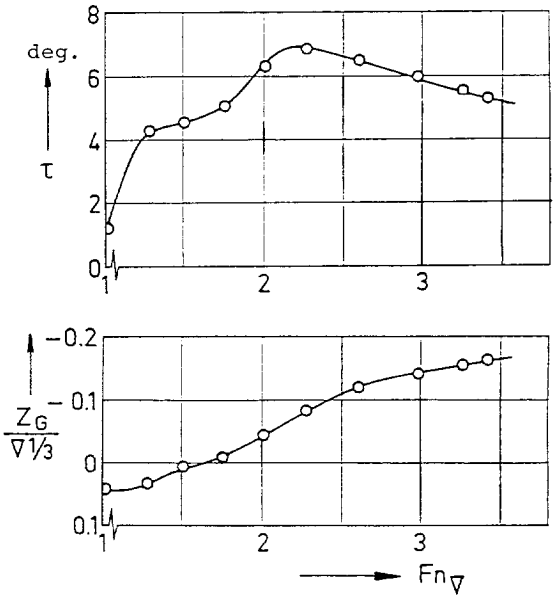

Figure 2.3: Sinkage and trim of the Clement parent model as function of forward speed

From these results it is apparent how large the contribution of the dynamic lift in the weight carrying process with increasing forward speed may become. The sinkage may easily become more than half the draft and the trim angle may vary between 2 and 6 degrees for well designed ships. This contributes to a considerable change in submerged volume of the hull. At a Fn_∇ = 3.0 it was approximated for the parent model that only 40 percent of the weight of the ship was still being carried by the buoyancy "lift" and the remaining 60 percent by the dynamic lift. This was done by calculating the displaced volume of the hull under the waterline at speed and assuming hydrostatic pressure over the submerged part of the hull.
From their results it may also be concluded that the sinkage and trim are strongly dependent on the geometry of the particular hull under consideration This may also be seen from Figure 2.4, showing, as an example, the measured trim as function of the length to beam ratio of the models. Similar results were obtained for the dependency of sinkage and trim on the other design parameters investigated in these experiments, i.e. the loading factor ($Ap/\nabla^{2/3}$) and the longitudinal position of the Centre of Gravity (LCG).

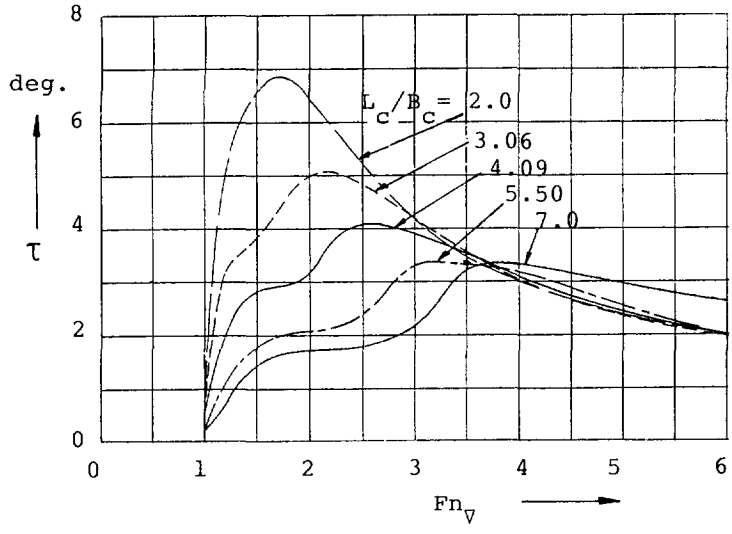

Figure 2.4: Trim as function of (L_c/B_c) and speed. From (9)

Therefore a rough approximation of the sinkage and trim, assuming these to be only dependent on the speed and not on the geometry of the actual hull under consideration, appears to be not justifiable.

Dependent on the particular hull under consideration and the forward speed the change in still water reference position of a fast monohull may be considerable. The absolute magnitude of the sinkage and trim varies considerably with increasing forward speed and is also strongly dependent on the geometry and layout of the particular ship under consideration.

However the pure existence of sinkage and trim in the case of fast monohulls and their magnitude is not sufficient to necessitate their introduction into a computational model. Their influence on the motions and vertical accelerations has to be demonstrated.

2.3 The effect of sinkage and trim

No tests were available in the literature on the possible influence of an isolated change of either sinkage or trim on the motions. The set-up of such a test would also be hard to envisage because a change in just one of the two with all other design parameters constant is physically not possible. However, some results are available on the combined effect with an emphasis on the influence of trim.
To show the effect of the trim angle (steady state pitch) on the motions of a fast monohull in waves, use is made of the comprehensive study on the rough water performance of planing boats as reported by Fridsma (13). He tested a planing hull with a constant deadrise angle of 20 degrees over the entire length of the hull. The bodyplan of this model is depicted in Figure 2.5.

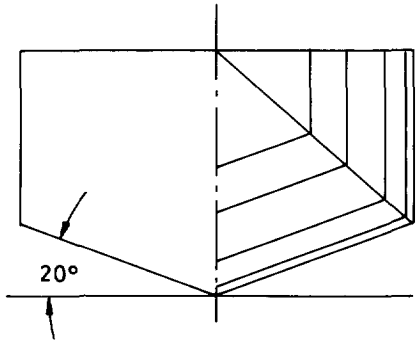

Figure 2.5: Bodyplan 20 degrees deadrise model of Fridsma (13)

The model was tested in regular head waves. During the tests the wavelength/-shiplength ratio (λ/L_c) varied between 1 and 6. The tests were performed at two different forward speeds.
To investigate the influence of the trim angle on the vertical motions the model was towed at each speed with two different trim angles, i.e. 4 and 6 degrees respectively. The difference in the trim angle whilst maintaining a constant forward speed and weight of the model, was established by changing the longitudinal position of the Centre of Gravity from 59 percent of L_c to 65.5 percent of L_c measured from the stern respectively. Although not explicitly mentioned by Fridsma a small associated change in the sinkage appeared inevitable.

From the results of these tests it became obvious that a change in the trim angle of 2 degrees had a significant effect on the heave- and pitch motions in particular in the longer wavelengths. At resonance the heave motion was increased by some 35 percent and the pitch motion even with 65 percent. A typical result of these measurements is shown in Figure 2.6.

The effect of the trim angle on the motions was considerably smaller at the lowest forward speed investigated. This is attributed to the fact that at this speed the hydrodynamic lift is less significant and (vertical) forces are still dominated by hydrostatic buoyancy. This closely matches the situation found with ships sailing at "normal" speeds, for which condition linear calculation models have proved to be quite usable.

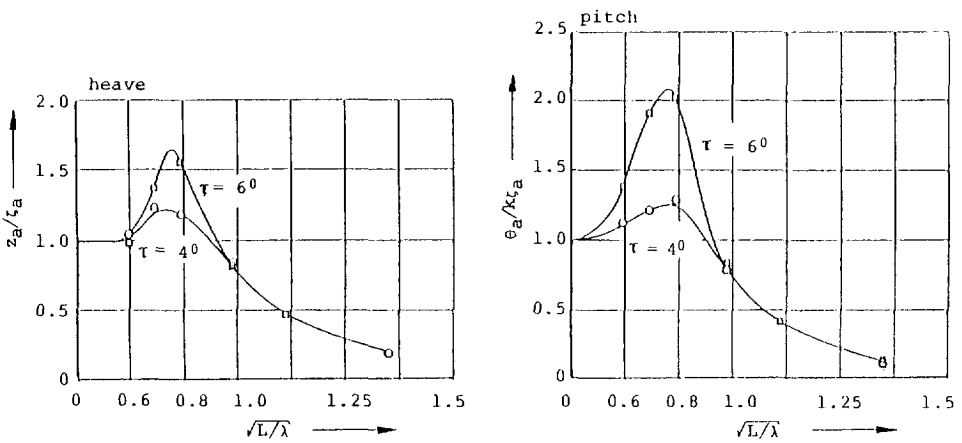

Figure 2.6: Influence of trim on heave and pitch motion. From (13)

When the forward speed increases, however, to "semi-planing" or "full-planing" condition and the magnitude of the dynamic lift increases, the effect of the trim angle on the motions becomes of considerable importance. It should be noted that the effect of the trim may not be isolated from the effect of the dynamic lift because these are closely related.
The effect of the trim angle on the vertical accelerations was found to be even more pronounced and this over the entire wavelength range investigated. The increase in trim angle from 4 degrees to 6 degrees produced 50 percent to 100 percent higher values for the vertical accelerations both at the Centre of Gravity as well as at the bow. Some typical results of the vertical accelerations at the bow and the Centre of Gravity versus the trim angle are presented in Figure 2.7.

Linear computational models only deal with the (hydro)dynamic forces arising from the presence of disturbant waves and the resulting response of the ship. Stationary forces such as the steady state dynamic lift are neglected. Therefore, it is of interest to investigate whether feeding only the changed reference position of the ship into the otherwise linear calculations is sufficient to account for the effects associated with high forward speeds. By doing so only the changed geometry of the submerged part of the hull and its changed position in

the water is considered to be of importance and therefore properly accounted for.
Using both procedures, the calculated vertical response of the hard chined planing boat at high forward speed was compared with the measured results. This is shown in Figure 2.8. The sinkage and trim of this craft at the particular speed used in the calculations were derived from model experiments.
From the comparison of these results it may be concluded that modifying the linear calculations by introducing the described procedure does not yield sufficiently different results when compared with the regular method and still does not predict the large vertical accelerations. Apparently, some coupling between the dynamic lift, the changed attitude of the ship, the high forward speed and the large motion amplitudes does exist, which is not accounted for by just introducing the final result of the presence of the dynamic lift, i.e. the sinkage and trim, in the computations only.

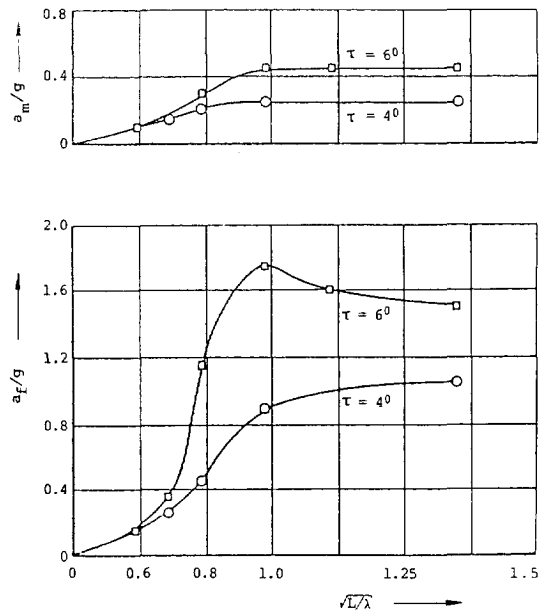

Figure 2.7: Influence of trim on the vertical accelerations. From (13)

In the present study the effect of the vertical accelerations on the performance of fast monohulls in waves is considered to be of prime importance for the prediction of the operability of these ships in waves. The exclusion of sinkage and trim and, more in particular, of the dynamic lift in a computational model to be used for the predictions of the behaviour of fast ships in waves seems therefore not justifiable.

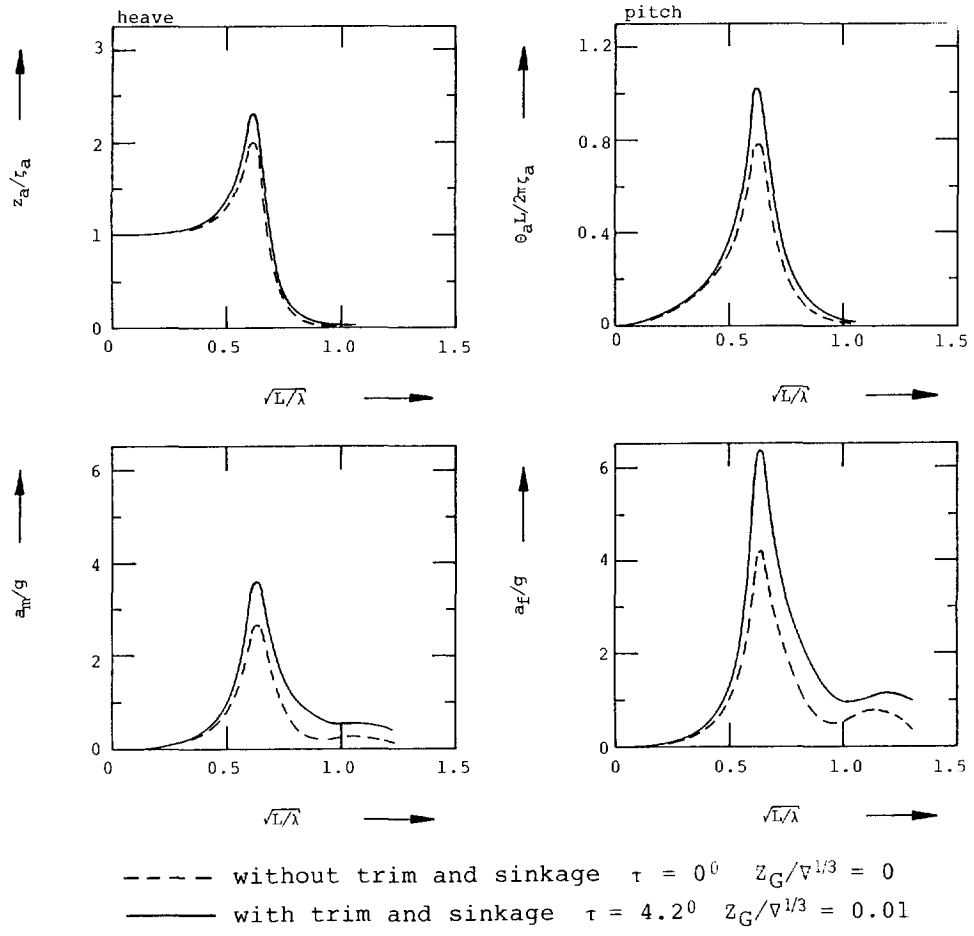

Figure 2.8: Calculations using a linear theory with and without adapted reference position

2.4 The effect of the deadrise angle

Fridsma (13) also analysed the influence of the deadrise angle on the seakeeping behaviour of planing hulls. In his study on the rough water performance of planing hulls he actually used a small systematic series of three models with different deadrise, i.e. with 10, 20 and 30 degrees respectively.
The main particulars of these three models are presented in Table 2.1. The bodyplans of the models are presented in Figure 2.9.

TABLE 2.1

#	L / B	β	τ	v / $\sqrt{L}$	K
A	5	20	4	4	25.1
B	5	20	4	6	25.5
E	5	20	6	4	26.2
H	5	10	4	2	25.6

in which: L/B = length beam ratio
β = deadrise angle
τ = trim angle
K = radius of gyration % L_c
V/$\sqrt{L}$ = velocity parameter

As may be seen fom these bodyplans the bow shapes of the models were unconventional because a constant deadrise angle was maintained over the entire length of the models. This is rather unrealistic from a practical point of view. However it was felt necessary in order to be able to isolate the effect of the deadrise on the motions and the bow accelerations in particular as much as possible.
All models were tested over a variety of wavelength to shiplength ratios (λ/L_c) ranging from 1 to 6. A limited number of tests were repeated in at least three different waveheights to be able to obtain a check on the linearity of the vertical motions and accelerations with respect to the amplitude of the oncoming wave.

During the tests the models were free to heave and pitch and by using an additional servo-controlled sub-towing carriage the models were also allowed to surge.
Measurements were taken of the heave, the pitch, the surge, the average speed of the towing carriage and the vertical accelerations at the bow and at CG.

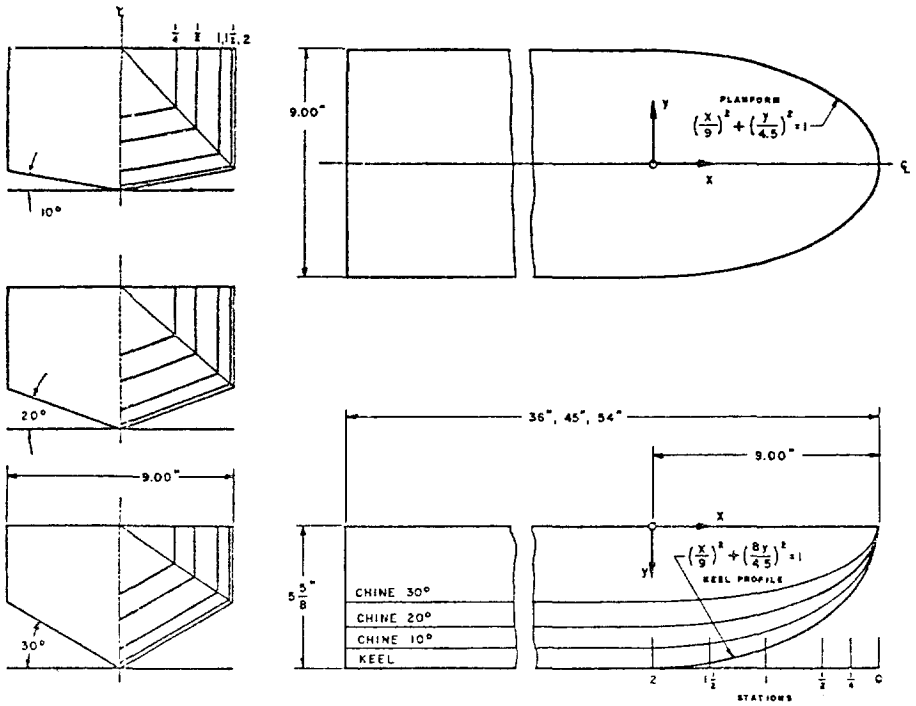

Figure 2.9: Bodyplans of the Fridsma models. From (13)

The tests were carried out at three different forward speeds corresponding to Fn = 0.66, Fn = 1.22 and Fn = 2.0. The speed at Fn = 0.66 is a so-called "prehump" condition in which the vertical forces are dominated by hydrostatic buoyancy. There is only a small contribution of the dynamic lift. At the speed of Fn = 1.22 both the hydrodynamic lift and the buoyancy are significant. The boat is beginning to plane and this condition may be referred to as "posthump". At Fn = 2.00 the boat is "fully planing" and the buoyancy contribution is only small.

To show the linearity of the response the results of the measurements of the heave and pitch motion of the 20 degrees deadrise model at Fn = 1.22 for three different waveheights are depicted in Figure 2.10.

As may be concluded from these results the heave and pitch response are both nonlinear in particular in the wavelength range near resonance.

This nonlinear behaviour proved to be small at the lowest Froude number but increased considerably with increasing forward speed. As may be seen from Figure 2.11 the low deadrise hull shows already considerable non linear behaviour at the lowest speed used in the tests.

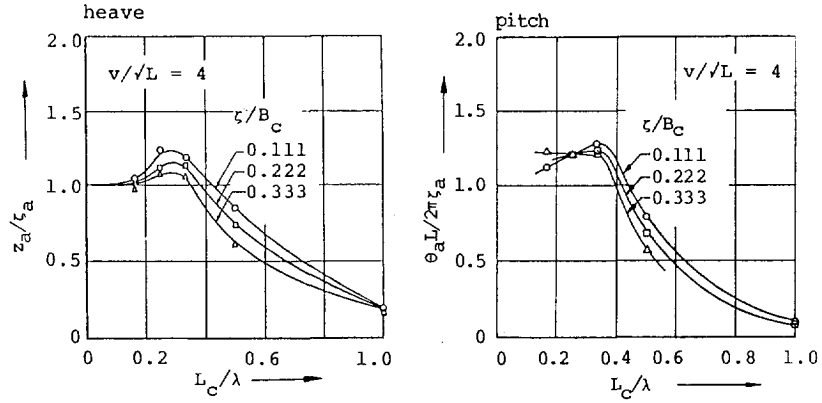

Figure 2.10: Linearity of the heave and pitch response at Fn = 1.22 and β = 20 degrees. From (13)

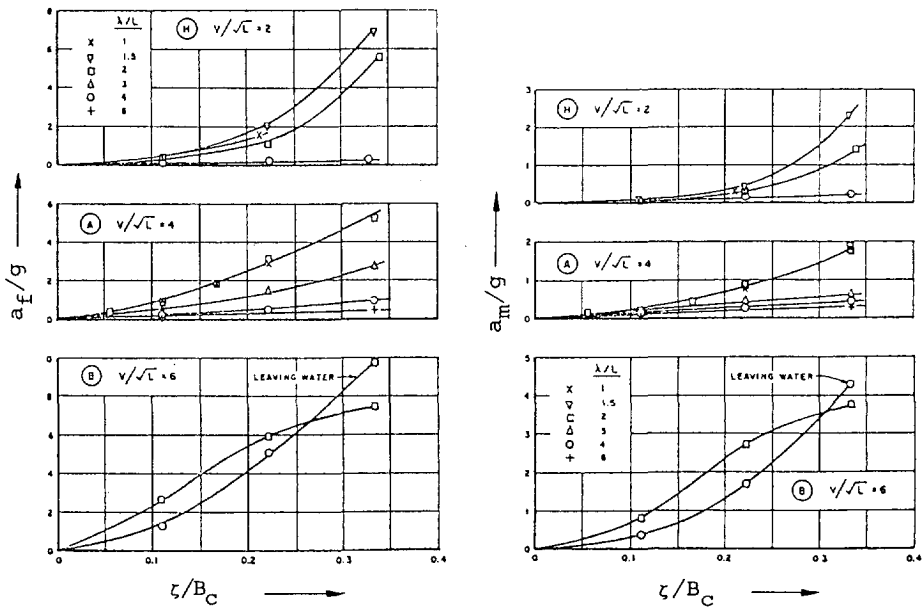

Figure 2.11: Vertical accelerations at CG and the bow for Fn = 0.66, 1.22 and 2.0 versus wave height. From (13)

The results of measurements of the vertical accelerations at the CG and at the bow for the three different speeds and for the 10, 20 and 30 degrees deadrise models are shown in Figure 2.12. Results for different wave amplitudes are only available for the 10 and 20 degrees deadrise models.

The nonlinearity of the vertical accelerations with respect to the amplitude of the oncoming wave is obvious. Unfortunately, no information is available to a comparison between different deadrise angles at the same speed enable.
It should be noted that in particular the strong nonlinearity found with the 10 degrees deadrise model at the lowest forward speed tested is of interest because in this condition speed effects such as sinkage and trim and hydrodynamic lift are considered to be still of only minor importance. Apparently the low deadrise hull already delivers significant dynamic lift even at those speeds. The dependency of the vertical accelerations on the deadrise angle of the models is also apparent in particular because the results of the high deadrise model are from the tests at the highest speed and those of the low deadrise model at the lowest speed investigated.
Since the geometry of the hull as a whole is considered to be of importance for a fast ship performing large relative motions in waves the peculiar bow shape of the Fridsma models might have been of influence on the behaviour.
To investigate this and the nonlinear response of a planing hull in more detail, Van den Bosch (6) carried out experiments in both regular and irregular waves with the parent model of the Clement and Blount series with 12.5 degrees deadrise and an additional, almost similar model, having 25 degrees of deadrise. All design characteristics, such as the chine projected area, the lengthwise distribution of deadrise and the centreline profile, were kept the same as much as possible. The bow shape of these designs, however, was much more realistic than those used by Fridsma. The bodyplans of these models are depicted in Figure 2.12.

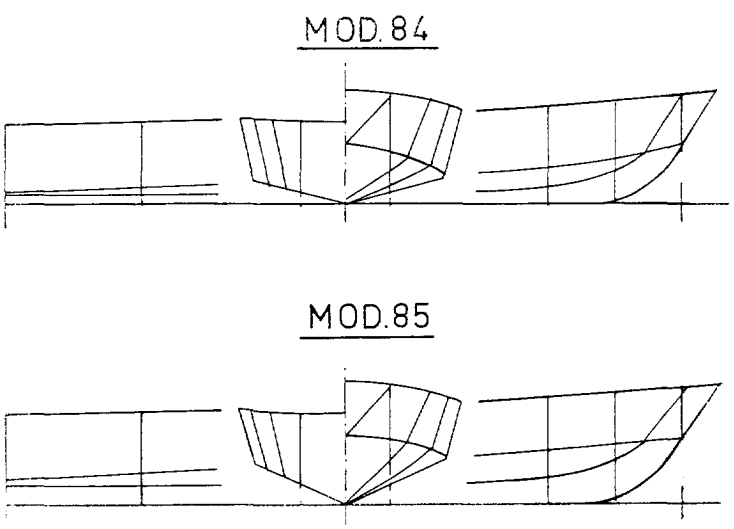

Figure 2.12: Deadrise models used by Van den Bosch. From (6)

From these tests Van den Bosch concluded that the deadrise has a considerable influence on the motions and vertical accelerations. The absolute values of the vertical accelerations at the bow were smaller than found by Fridsma, possibly due to the difference in deadrise angles and bow geometry. He attributed the differences in vertical accelerations between the two models also to the change in trim between the two models: the increase in deadrise decreases the capabilities of the hull to generate dynamic lift. This results in a difference in trim which is clearly shown in Figure 2.13: the high deadrise hull "sits" deeper in the water with less trim. This reduction in trim will decrease the motions and accelerations as shown previously. Another explanation might be that the hull which generates the least dynamic lift produces also the smallest vertical accelerations, which highlights the importance of the dynamic lift.

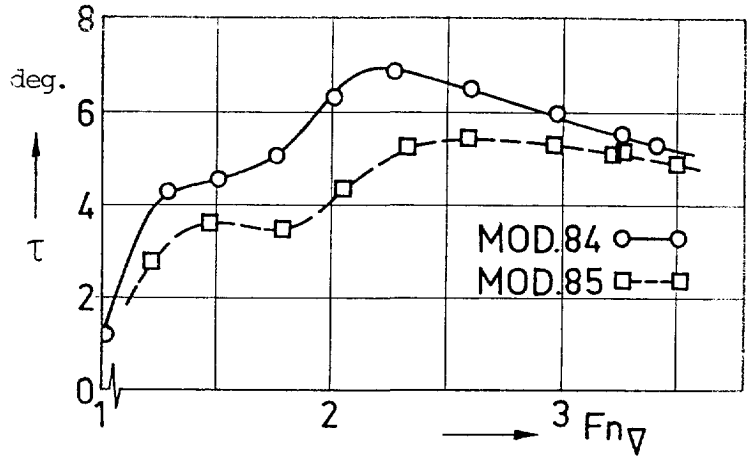

Figure 2.13: Trim versus deadrise. From (6)

To demonstrate the nonlinear response of the ship, tetst were performed in regular waves with two different waveheights. During these tests recordings were made of the heave, pitch and vertical accelerations signals of both models. A typical example of such a record is presented in Figure 2.14 for a wavelength of two times the model length and at a forward speed of the model during the test corresponding to $Fn_{\nabla} = 2.9$

From these sample recordings the nonlinear reaction of the models in heave and pitch with respect to the (sinusoidal) incoming wave is evident. There is a strong dependency on deadrise and also the wave steepness: i.e. the low dead-

rise hull and the steeper wave yield the most pronounced nonlinear response. This nonlinear behaviour and its dependency on the deadrise is even more apparent when the vertical accelerations at the bow of the two models are examined. A typical example of such a recording under identical conditions for both models is presented in Figure 2.15.

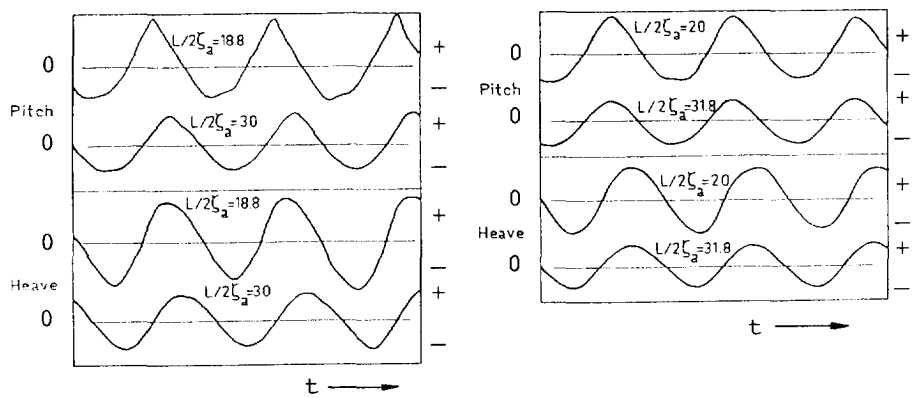

model 84
Fn_∇ = 2.9
λ / L_C = 2

model 85
Fn_∇ = 2.9
λ / L_C = 2

Figure 2.14: Sample recording of the measured heave and pitch motion in regular waves. From (6)

Again the nonlinear character of the responses is obvious for both models. The steep rise in the acceleration occurs when the bow is (re)entering the water. The low deadrise hull shows significant higher peaks in the accelerations. The effect of these high peaks in the accelerations on the motion signals (the two times integrated signals) as presented in figure 2.15 remains limited.
Using linear computational models, the predicted difference between these two models is only small and the large difference in the measured level of vertical accelerations is not predicted. The difference between the shape of the submerged part of the hulls of the models in their still water zero speed reference position is obviously too small.

The large differences in response between all these models may also be explained by the considerable change in actual momentaneous submerged volume of the model whilst performing large relative motions in waves. This sudden change in submerged volume and hull shape may generate large peaks in the wave excited (vertical) forces and also changes in "added mass" and "damping" of the hull.

If this time-dependent change in submerged geometry is important then these forces should be strongly related to the deadrise angle of the planing bottom but even more to the bowshape and bowflare of the ship under consideration, because the relative motions in head seas are largest at the bow.

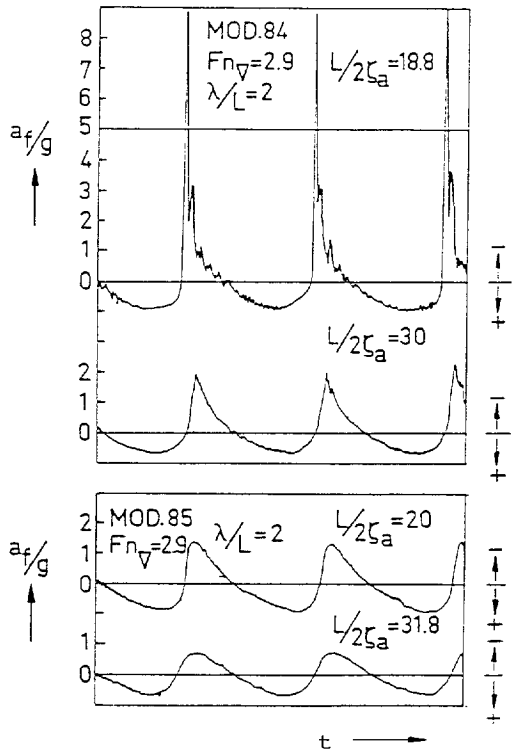

Figure 2.15 *Sample recording of the measured vertical accelerations at the bow in regular waves. From (6)*

2.5 Large relative motions

The natural periods for heave and pitch of a ship are important parameters when assessing its seakeeping behaviour.

In actual applications of fast monohulls, the ship length in most cases is relatively small, i.e. the shiplength for typical high speed applications ranges from 15 to 40 m. From both experience and theory it is known that the longer waves with respect to the shiplength are capable of generating relatively larger exciting forces.
This may lead to large motions the more so when these forces are exerted on the system in or near its resonance frequency. In the case of a fast ship moving against the waves, resonance occurs at relatively longer (and therefore larger) waves due to its high forward speed. Resonance effects will therefore result in larger motions, when compared to "normal" ships.
Both from experience with actual ships and from model experiments it is known that large relative motions do occur indeed: the foreship may become completely emerged and in some conditions the ship may even become completely "airborne". This may imply that the geometry of the ship in contact with the water changes considerably in time. This is especially true for high speed planing hulls which usually have strongly V-shaped sections below the chine and also in the foreship above the chine. So even smaller relative motions may already lead to significant changes in the hull shape of the ship in contact with the water.
The generally underlying assumption of small motion amplitudes and the associated unchanged hull geometry used in the linear computational models might therefore no longer be justifiable for those conditions.

To investigate this an experiment with the 25 degrees parent model previously used by Van den Bosch was carried out by Keuning (27) in irregular head waves and the results of these tests were compared with the results of similar tests obtained by Blok (3) using two additional models having different bowshapes.
The aftbodies of these three models from transom to midship were identical, having a 25 degrees deadrise prismatic shape. The deadrise of the hull below the chine at the foreship (at ordinate 18) however was changed from 35 to 45 and 55 degrees respectively. The inclination of the topsides above the chine was kept the same as with the Van den Bosch model. This resulted in a different deckline. The shape of the still-waterline was kept as much the same as possible for all three models. The bodyplans of the three models are compared in Figure 2.16. The main specifics of the models are presented in Table 2.2.

From a comparison of these measurements it may be concluded that the heave motion was not strongly influenced by the difference in deadrise shape of the forebody, although the model with 45 degrees deadrise at ord 18 (the parent) showed the largest response. The pitch motions however proved to be more dependent on forebody shape and was largest again for the parent model.

Table 2.2. Main specifics of the foreship shape variation models.

	Model II	Parent I	Model III
Deadrise	25	25	25
Deadrise ord. 18	35	45	55
Length	15.0	15.0	15.0
Beam	3.67	3.67	3.67
Disp.	23.40	23.40	23.40
K in % of Lc	25	25	25

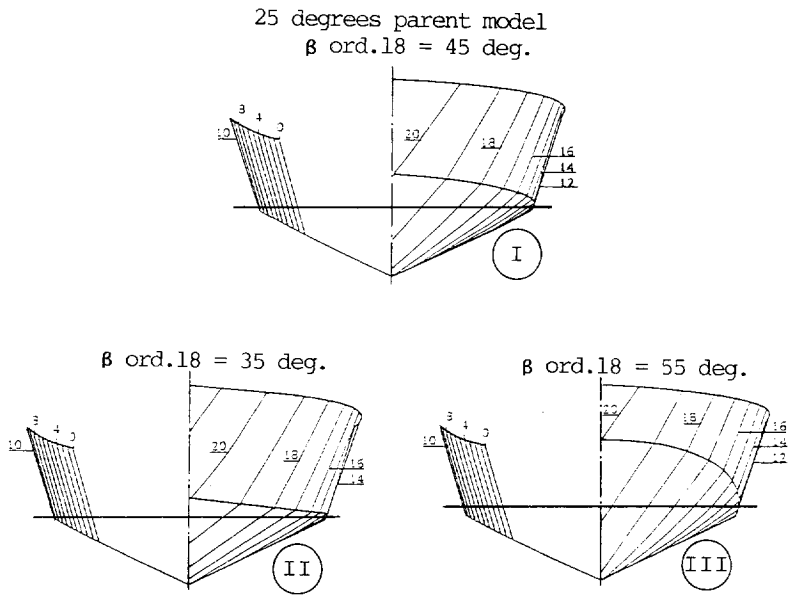

Figure 2.16: Bodyplans of the bowshape variations models From (3)

The dependency of heave and pitch on bowshape deadrise is shown in Figure 2.17. There was some nonlinear behaviour in heave and pitch which increased with increasing forward speed and the pitch motion was more affected than the heave motion.

The same tendency but much more pronounced is shown in Figure 2.18 in which the maximum measured vertical accelerations at the bow are depicted on the basis of the different forebody shape. Although the results for the low deadrise ship at the highest speed and in the highest wave spectrum are somewhat in contradiction with the expectations, the dependency of the maximum vertical accelerations on the forebody shape is quite obvious.
When analysing these results it should be emphasised that the submerged parts of the hull of these systematic models showed no considerable differences, but the above water part did.
An exact measurement of the relative motions at the bow during the measurements proved to be unfeasible due to the high forward speed. This high speed caused ventilation of the wire type waveheight meters used for the determination of these relative motions.

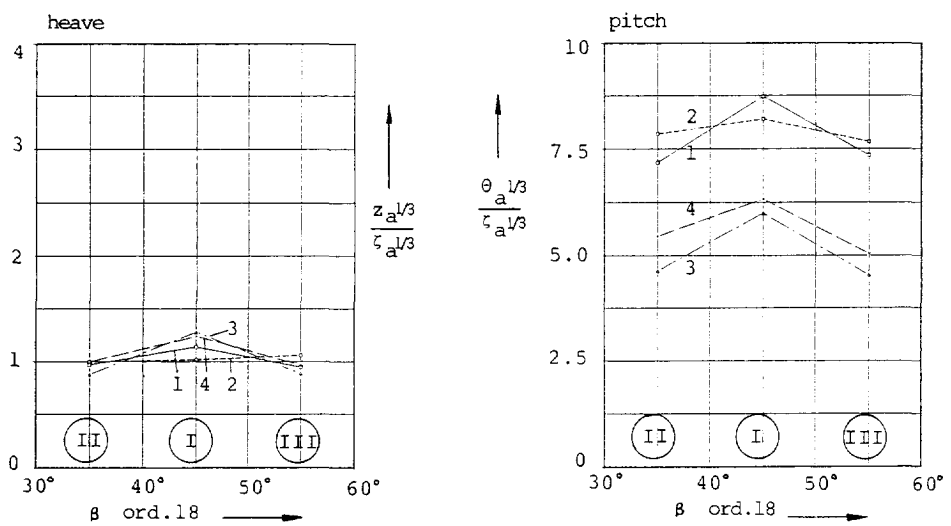

#	$H_{1/3}$	V_s
1	0.59	16.7
2	0.59	27.8
3	1.72	16.7
4	1.72	27.8

Figure 2.17: Heave and pitch of the bowshape variation models From (3)

In addition, the generated spray caused difficulties in defining the exact height of the solid water surface in contact with the hull. So visual observations and video recordings were used to qualify the differences in behaviour of the three models. From these observations it was obvious that the models had a large tendency for bow emergence, but this and the reentrance into the water was more severe with the lower bow deadrise model. Using a linear approximation of the system when calculating the motions in waves, these differences have to be neglected.
In addition, the V-shaped sections of a planing boat in particular in the foreship may yield strong nonlinearities in both the wave exciting forces and the hydrodynamic reaction forces when its being pushed in and out of the water when the ship is performing large relative motions. This obviously affects the motions and accelerations as may be seen from these experimental results.

From the above results it may be concluded that the effects associated with the large relative motions and the change in submerged geometry of the hull have to be taken into account in particular when a more reliable prediction of the vertical accelerations is needed.

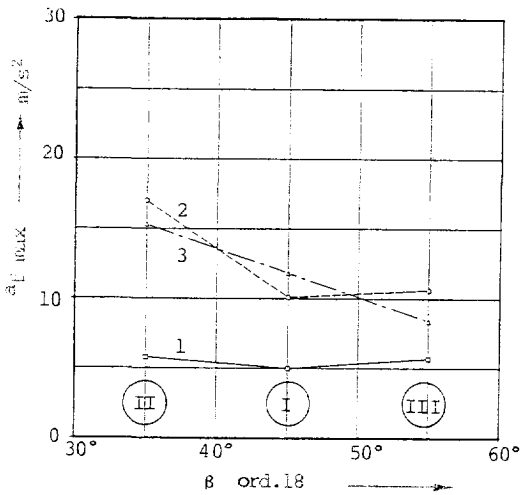

#	H1/3	V_s
1	0.59	16.7
2	0.59	27.8
3	1.72	16.7
4	1.72	27.8

Figure 2.18: Maximum vertical accelerations at the bow versus forebody shape. From (3)

2.6 Irregular waves

The nonlinear character of the responses as shown so far makes it necessarry to simulate the motions and vertical accellerations of the fast monohull in irregular head waves in the time domain. Since peak vertical accelerations are considered to be the limiting phenomena in the safe operation of the ship its is essential to predict the frequency of occurence of these peak values as well as their magnitude.
If the system is considered to be a linear system and the heights of the incoming waves as being Rayleigh distributed then the amplitudes of the motions and accelerations should also be Rayleigh distributed. If the system however is nonlinear with respect to the amplitude of the disturbant waves then this relation between the distribution of the input and output is no longer valid.

An example of this is shown in Figure 2.19, in which the distribution of the maxima of the vertical accelerations at the bow is presented for the two previously mentioned models as tested by Van den Bosch with 12.5 and 25 degrees deadrise respectively. The difference between the two distributions is obvious: the distribution of the measured maxima in the vertical accelerations in the case of the low deadrise model shows considerably higher peaks than the high deadrise model. The heights of the incoming waves during the tests were more or less Rayleigh distributed and the deviation of the measured distribution of the vertical accelerations at the bow with respect of the Rayleigh distribution may be considered as a measure of the nonlinearity of the system. The high deadrise model behaves more linear in this respect than the low deadrise model.

So simulations in realistic wave spectra are necessarry to properly predict both the frequency of occurence and the absolute value of the peak vertical accelerations which determine the limits of safe operability. The use of extrapolation procedures based on assumed Rayleigh distributions of the responses, as normal practise in shipmotion analyses, are no longer valid due to the nonlinearity of the system "fast monohull in head waves". This nonlinear behaviour appears to be dependend on hull form parameters and speed.

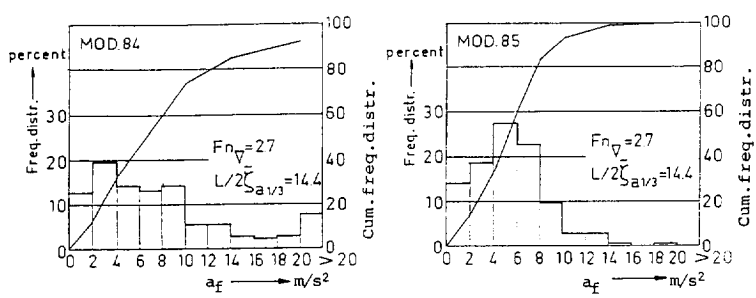

Figure 2.19: Distribution of the maxima of bow vertical accelerations as function of deadrise. From (6)

2.7 Conclusions

In general it may be concluded that an proper implementation of the effects of the forward speed, the hydrodynamic lift, the change in reference position, the irregularity of the waves and the dependency of the wave exciting forces and hydrodynamic reaction forces on the large relative motion amplitudes and the time depend hull shape all seem to play an important role in the determination of the responses of a planing boat to the waves. In particular the vertical accelerations seem strongly dependend on these parameters and show a considerable nonlinear relationship with the amplitude of the incoming wave. Since these vertical accelerations and in particular the peak values are the limiting phenomena for the safe and comfortable operation of fast ship it appears to be important to incorporate all these effects into the computational model.

Chapter 3

Computational model

3.1 Introduction

In this chapter the computational model that will be used to assess the operability of the fast monohull in waves will be described.

From the analysis of the experimental data and the results of calculations using linear models it became evident that the discrepancies could not be improved by introducing refinements into the otherwise linear calculations. So probably more emphasis must be placed on the introduction of the nonlinear effects as mentioned in the earlier chapters and which are considered to be of importance.
Within the scope of the present study it will not always be feasible to present formulations for these effects which are entirely based on exact analytical expressions but rather empirical or generaly formulations suitable for introducing the effects into the computational model will be used. This is justifiable since the intention of this study is to establish whether or not the introduction of these nonlinear effects yields an improvement in the predictions of the motions and vertical accelerations in comparison with results obtained with linear models and this rather in a qualitative than in a quantative way.

The basis of the present computational model is formed by the work of Zarnick (73) who formulated a nonlinear model for the heave and pitch-motion of planing boats in regular head waves. This model has been extended to incorporate a formulation for the sinkage and trim of the ship at high speed and the associated hydrodynamic lift distribution along the length of the ship as well as the non linear added mass and wave exciting forces in both regular and irregular waves.

The limits of operability of a fast monohull in waves are usually met first in the head wave condition. If an allround workability is required the head sea condition will therefore be the limiting condition. Although this is generally true it remains a simplification of the problem. There may certainly be other conditions, for instance rolling in beam seas or broaching in heavy following seas, which also

may impose limits on the safe workabilty of the ship. Within the framework of the present study, however, only the motions in head seas will be considered, i.e. heave and pitch and the associated vertical accelerations.

First a general description of the equations of motion of a fast ship in head seas and of the forces involved will be given. With the formulations used in the ordinary strip theory as a starting point the equations for a fast moving hull will be derived, with special emphasis on the lift- and wave forces.
Secondly the derivation of an empirical polynomial equation for the stationary sinkage and trim of the ship at forward speed will be presented. The sinkage and trim will be used to assess the distribution between the hydrodynamic and hydrostatic lift.
Thereafter the added mass formulations will be further investigated using a series of oscillation experiments with a segmented model towed at high forward speed. The influence of this high forward speed on the added mass and its distribution along the length of the ship will be discussed.
Then the wave exciting forces will be discussed using the same model. These forces are assumed to be dominated by the component associated with the pressure in the undisturbed wave over the actual submerged volume of the ship.
Finally, the equations for the generation of the irregular waves into the computational model will be developed by which the instanteneous wave elevation along the length of the ship sailing in irregular waves is obtained.

3.2 The equations of motion

The coordinate system used in the computational model is presented in Figure 3.1. It consists of an earth fixed system with X-, Y- and Z- axes with the X-axis lying in the undisturbed water surface pointing in the direction of travel of the ship and a body fixed coordinate system with ξ-, χ- and ζ-axes, of which the ξ-axis is the longitudinal axis of the ship pointing forward.
A schematic presentation is shown in Figure 3.1.

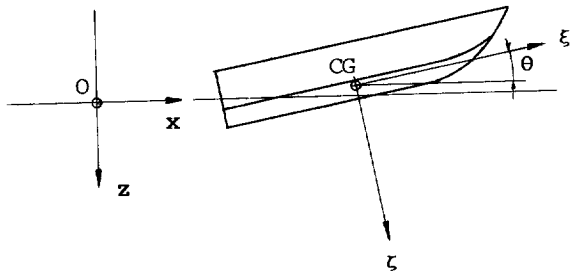

Figure 3.1: Coordinate system

In the present model only the motions in the vertical plane will be considered. Therefore the surge, heave and pitch equation may be written as:

$$\textit{surge:} \qquad M\ddot{x}_{CG} = T_x - N \sin\theta - D\cos\theta$$

$$\textit{heave:} \qquad M\ddot{z}_{CG} = T_z - N\cos\theta + D\sin\theta + W$$

$$\textit{pitch:} \qquad I\ddot{\theta} = Nx_c - Dx_d + Tx_p$$

in which:

M	=	mass of the ship including added mass
T	=	thrust of the propellor
N	=	normal force on the planing hull
D	=	frictional drag force along the hull
W	=	weight of the ship
I	=	mass moment of inertia in pitch
θ	=	pitch angle
x_{CG}	=	X-coordinate Centre of Gravity
z_{CG}	=	Z-coordinate Centre of Gravity
x_p	=	moment arm of thrust force
x_c	=	moment arm of normal force
x_d	=	moment arm of frictional drag force

The definition of these forces is presented in Figure 3.2.

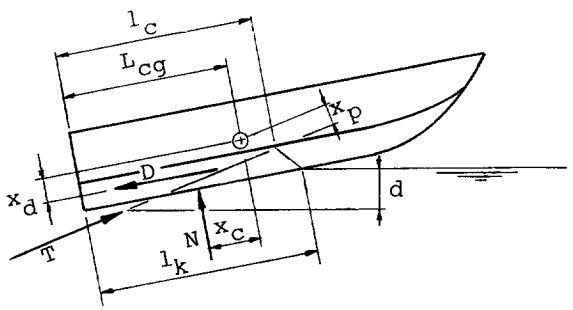

Figure 3.2: Definition of forces

Further simplification of the model is now introduced by assuming that the change in forward velocity of the ship is small in comparison with its forward speed, i.e.:

$$\dot{X}_{CG} = constant$$

This generally corresponds with the way at which model experiments are being carried out and therefore seems a very justifiable simplification in this stage. It should be noted, however, that sudden voluntary reductions in delivered thrust imposed by the crew will lead to an abrupt speed reduction of the ship due to its high power to weight ratio. By doing so severe impacts by foreseeable high waves may be evaded. This may strongly attribute to the safe operation of fast monohulls in waves, even in conditions where a constant forward speed might otherwise have led to the exceedence of the limiting criteria with respect to peak accelerations.
In addition it is supposed that the working line of the frictional resistance force D and the thrust force T are acting through the Centre of Gravity of the ship and that the vertical components of these forces are small with respect to the other hydrodynamic forces involved and may therefore be neglected.
This reduces the equations to:

surge: $\ddot{x}_{CG} = 0$

heave: $M\ddot{z}_{CG} = -N \cos\theta + W$

pitch: $I\ddot{\theta} = N x_c$

In which the hydrodynamic forces on the hull still need to be determined.

To calculate the integral forces and moments on the ship as a whole with forward speed a strip theory approach has been adopted: the forces are calculated using a lengthwise integration of sectional values found for segments of the hull, which are considered to be part of a cylinder with infinite length and constant cross-sectional shape. Interaction effects between the segments are neglected. Forward speed effects are accounted for by lengthwise derivatives of the sectional values.

As a typical example of the strip theory the approach of Korvin Kroukovsky will be summarised here. In his approach the ship is defined in an earth fixed coordinate system and a body fixed coordinate system as shown in Figure 3.3. The cross-section of the ship under consideration is positioned at x_b.
For small pitch angles θ this may be written as:

$$x_b = x_o - V t \qquad \text{and so} \qquad \dot{x}_b = -V$$

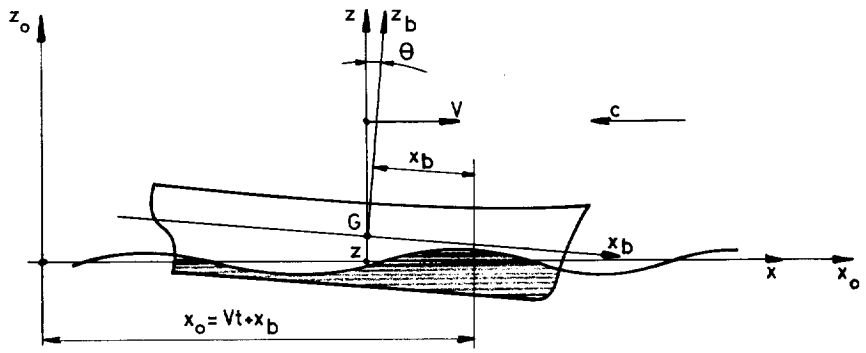

Figure 3.3: Definition according to Korvin Kroukovsky

The cross-section at the position x_b has a vertical relative velocity with respect to the wave corresponding to:

displacement: $S_z = z - x_b\theta - \zeta^*$

velocity: $V_z = \dot{z} - x_b\dot{\theta} + V\theta - \zeta^*$

and acceleration: $\dot{V}_z = \ddot{z} - x_b\ddot{\theta} + 2V\dot{\theta} - \ddot{\zeta}^*$

in which ζ^* is the "effective" waveheight.

The hydrodynamic force on the cross-section in this approximation is defined by:

$$F' = - d/dt (m_a' V_z) - N' V_z - 2 \rho y_w S_z$$

in which: m_a' = 2-D cross-sectional added mass
N' = 2-D cross-sectional damping
y_w = half waterline beam of section

The first term in F' is the result of the so-called "slender body theory", the second one is damping associated with the generated surface waves and the third one is the hydrostatic reaction due to the vertical displacement of the section.
In the linear strip theory approximation, the first term derivative is written as:

$$\frac{dm_a'}{dt} = \frac{dm_a'}{dx_b}\frac{dx_b}{dt} = -V\frac{dm_a'}{dx_b}$$

and thus:

$$F' = -m_a'\dot{V}_z - (N' - V\frac{dm_a'}{dx_b})V_z - 2\rho g y_w S_z$$

The equations of motion for the heaving and pitching ship with its forward velocity V sailing in head waves becomes:

$$\textit{Heave:} \quad \rho\nabla\ddot{z} = \int_L (F_1' + F_2' + F_3')dx_b$$

$$\textit{Pitch:} \quad I_{yy}\ddot{\theta} = -\int_L (F_1' + F_2' + F_3')x_b\, dx_b$$

in which:

$$F_1' = - 2\rho g y_w(z - x_b\theta - \zeta^*)$$

$$F_2' = - N'(\dot{z} - x_b\dot{\theta} + V\theta - \dot{\zeta}^*)$$

$$F_3' = - \frac{d}{dt} m_a'(\dot{z} - x_b\dot{\theta} + V\theta - \dot{\zeta}^*)$$

$$= - m_a'(\ddot{z} - x_b\ddot{\theta} + 2V\dot{\theta} - \dot{\zeta}^*) + V\frac{dm_a'}{dx_b}(\dot{z} - x_b\dot{\theta} + V\theta - \dot{\zeta}^*)$$

and:

$$\zeta^* = \zeta e^{-kT^*} = \zeta_a e^{-kT^*} \cos(kx_b + \omega_e t)$$

$$\dot{\zeta}^* = - \zeta_a \omega e^{-kT^*} \sin(kx_b + \omega_e t)$$

$$\ddot{\zeta}^* = - \zeta_a \omega^2 e^{-kT^*} \cos(kx_b + \omega_e t)$$

in which ζ^* is the local "effective" wave height approximated by:

$$\zeta^* = \zeta e^{-kT^*} \text{ and } T^* = - \frac{1}{k} \ln(1 - \frac{k}{y_w}) \int_{-T} y_b e^{kz_b} dz_b$$

Integration of F' along the length of the ship leads to the following equations:

$$a_{zz}\ddot{z} + b_{zz}\dot{z} + c_{zz}z - d_{z\theta}\ddot{\theta} - e_{z\theta}\dot{\theta} - g_{z\theta}\theta = F_{za} \cos(\omega_e t + \epsilon)$$

$$A_{\theta\theta}\ddot{\theta} + B_{\theta\theta}\dot{\theta} + C_{\theta\theta}\theta - D_{\theta z}\ddot{z} - E_{\theta z}\dot{z} - G_{\theta z}z = M_{\theta a} \cos(\omega_e t + \epsilon)$$

in which, after some elaboration, for the coefficients is found in the heave equation:

$$a_{zz} = \rho\nabla + \int_L m_a' dx_b \qquad d_{z\theta} = \int_L m_a' x_b dx_b$$

$$b_{zz} = \int_L (N' - V\frac{dm_a'}{dx_b}) dx_b \qquad e_{z\theta} = \int_L (N'x_b - 2m_a'V - Vx_b \frac{dm_a'}{dx_b}) dx_b$$

$$c_{zz} = 2\rho g \int_L y_w dx_b \qquad g_{z\theta} = 2\rho g \int_L y_w x_b dx_b - Vb_{zz}$$

and in the pitch equation:

$$A_{\theta\theta} = I_{yy} + \int_L m_a' x_b^2 \, dx_b \qquad D_{\theta z} = \int_L m' x_b dx_b$$

$$B_{\theta\theta} = \int_L (N'x_b^2 - 2Vm_a'x_b - Vx_b^2 \frac{dm_a'}{dx_b}) dx_b$$

$$E_{\theta z} = \int_L (Nx_b' - Vx_b \frac{dm_a'}{dx_b}) dx_b$$

$$C_{\theta\theta} = 2\rho g \int_L y_w x_b^2 \, dx_b - Ve_{\theta z} \qquad G_{\theta z} = 2\rho g \int_L y_w x_b \, dx_b$$

For the inphase and quadrature component of the wave exciting forces and moment:

$$\frac{F_{za}}{\zeta_a} \begin{matrix}\cos\\ \sin\end{matrix} \epsilon_{F\zeta} = \int_L y_w e^{-kT^*} \begin{matrix}\cos\\ \sin\end{matrix} kx_b \, dx_b +$$

$$\mp \omega \int_L (N' - V \frac{dm_a'}{dx_b}) e^{-kT^*} \begin{matrix}\sin\\ \cos\end{matrix} kx_b \, dx_b$$

$$- \omega^2 \int_L m_a' e^{-kT^*} \begin{matrix}\cos\\ \sin\end{matrix} kx_b \, dx_b$$

$$\frac{M_{\theta a}}{\zeta_a} \begin{matrix}\cos\\ \sin\end{matrix} \epsilon_{M\zeta} = - 2\rho g \int_L y_w x_b e^{-kT^*} \begin{matrix}\cos\\ \sin\end{matrix} kx_b \, dx_b$$

$$\pm \omega \int_L (N' - V \frac{dm_a'}{dx_b}) x_b e^{-kT^*} \begin{matrix}\sin\\ \cos\end{matrix} kx_b \, dx_b$$

$$+ \omega^2 \int_L m_a' x_b e^{-kT^*} \begin{matrix}\cos\\ \sin\end{matrix} kx_b \, dx_b$$

These equations are known as the Ordinary Strip-theory Method and contain only sectional values for added mass and damping and a.o. the derivative of the added mass along the length of the model multiplied with the forward speed to account for forward speed effects.

The results of this method for the calculation of motions of ships in waves with forward speed are generally good, although some mass coefficients lack symmetry. This has led to the development of the modified strip theory by Tuck, Salvesen and Faltinsen (52). This will be discussed in Chapter 3.5.
Zarnick extended this method for the situation of planing boats in regular head waves.

Although the mathematical justification for using a strip theory approach is not very rigorous, both Zarnick (73) and Martin (43) obtained results for the motions of fast monohulls in regular head waves which compared very well with the results obtained from experiments. The basis of the formulations used by Zarnick and Martin are similar.

Implicit with a strip theory approach is the need to define the two-dimensional hydrodynamic forces acting on a arbitrary cross-section. These forces on a strip of a fast monohull are somewhat different from the previous model and are represented in Figure 3.4.

The actual flow phenomena around a fast moving hull in head waves are rather complicated: one part of the process could best be characterised by unsteady planing, while at the moment of bow entrance into the coming wavecrest, impact loads are predominant, followed by a condition in which buoyancy forces are most important.

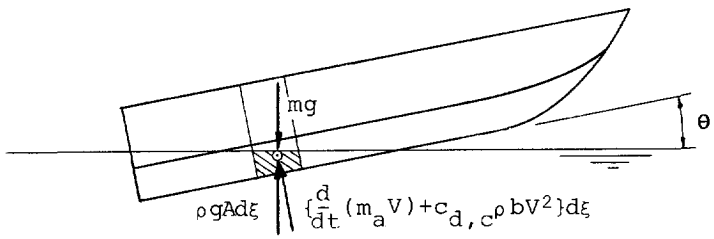

Figure 3.4: Forces on a strip of a fast hull

Zarnick (73) separates the 2-D flow around the strip in two separate flow conditions, assumed to represent the cross flow over the section of a ship at high forward speed depending whether the flow is separated at the chine or not. These conditions are schematically presented in Figure 3.5.

Figure 3.5: Flow conditions around the hull

The hull of a fast monohull can be devided in four different regions each representing a different flow condition. These regions are defined in Figure 3.6.

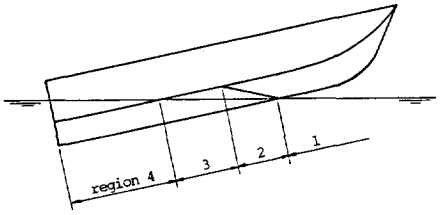

Figure 3.6: Definition of various flow-regions along the length of a planing hull

Region 1 represents that part of the hull which is not in contact with the water. In Region 2 the keel is submerged but the chines are not. This is a dry chine Region.
The chines are submerged in Region 3 but the flow separates at the chines. The hull above the chine remains "dry". In Region 4 the topsides are submerged also. The section is "wet" till well over the chine.
The height of the water on each cross-section is calculated using the known sinkage and trim as well as the undisturbed wave elevation along the length of the ship. This will be dealt with in more detail later.

In the present computational model the hydrodynamic forces are calculated treating the unsteady flow around the hull as quasi steady. Surface wave generation and unsteady circulary flow phenomena are neglected.

Since the paper of Von Karman (70) on the sea plane hull impacts during landing, the theory used for the calculation of hydrodynamic loads on the hull during planing has been based on the concept of "added mass". In concept this theory corresponds with the slender body theory used to calculate the side force on low aspect ratio wings and surface ships under leeway.

Using this theory the normal force on a transverse section of a hull is given by the rate of change of momentum of the oncoming fluid expressed in terms of the "added mass" of the particular cross-section under consideration :

$$f = \frac{D}{Dt} (m_a V)$$

in which:

f	=	the dynamic force developed at right angles to the planing hull section
m_a	=	the added mass of the local cross-section
V	=	the water velocity component normal to the local planing surface

The rate of change of momentum of the fluid at a particular section may be further elaborated to:

$$\frac{D}{Dt}\,(\,m_a V\,) = m_a\dot{V} + V\dot{m}_a - \frac{d}{d\xi}\,(\,m_a V\,)\,\frac{d\xi}{dt}$$

The difference with the formulation used by Korvin Kroukovsky is found in the time dependency of the added mass. The last term of this expression takes into account the variation of the added mass along the length of the hull.
This contribution can be visualised by considering the 2-D flow plane as a substantive surface moving along the hull with a velocity $U = -d\xi/dt$ tangent to the baseline. As the surface moves along the body the section geometry in the moving surface may be considered to change with as a result a change in added mass. This is the lift generating term in the steady state planing condition in which the first two terms in the equation equal to zero.
If the disturbance of waves and resulting motions is temporarily neglected and we therefore constrain ourselves to the condition of steady state planing of a prismatic hull, then:

$$V = U_o \sin\theta$$

$$m_a = \frac{\pi}{2}\,\rho\, y^2\, Cm$$

in which:

U_o	=	horizontal velocity of the planing surface
θ	=	trim angle
ρ	=	mass density of water
y	=	half width of wetted section
Cm	=	added mass coefficient

Von Karman based his theory on the flow around a wedge penetrating the undisturbed free surface with a constant velocity. This is still considered as a first step approach to impact load and Lewis (41), Taylor (63) and Wagner (71) calculated the added mass of such an impacting wedge. They came up with the following approximation:

$$m_a' = C_m'\,\frac{\pi}{2}\,\rho\, y^2$$

in which:

$$C_m' = (\,1 - \frac{\beta}{2\pi}\,)^2$$

$$0 \le \beta \le \frac{\pi}{2}$$

This approximation will be used in the dry chine regions of the planing hull.
Wagner suggested that the lateral dimensional width of the section at the waterline (y) in the equation should be the "splashed-up" half width y_1.

See Figure 3.7.

$$1 + \psi = \frac{\pi}{2} \quad so\ that:\ y_1 = \frac{\pi}{2}\frac{Z}{\tan\beta}$$

The factor $\pi/2$ is generally referred to as "pile-up" correction with:
The "pile-up" correction used, therefore, was unaffected by the deadrise angle β. This procedure has been used extensively until Payne (48) pointed out that by using this appproximation too high impact loads were found when compared with experiments and he suggested to neglect the pile-up correction and to use y_0 instead.
In his recent publication, however, Payne (49) finds that the results originally found by Pierson, in which he formulated a deadrise dependent pile-up correction agreed very well with the results found by Zhao and Faltinsen (12). They used a boundary element method as a numerical analysis of the impacting wedge with constant velocity. Pierson's formulation is:

$$(1 + \psi) = \frac{\pi}{2} - \beta (1 - \frac{2}{\pi})$$

The correlation between his results and the numerical results of Zhao and Faltinsen is shown in Figure 3.7.

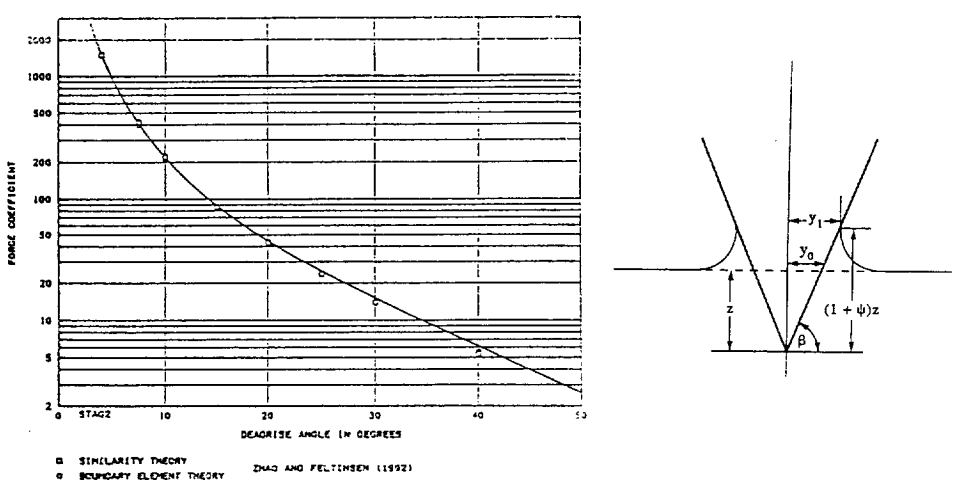

Figure 3.7: The impacting wedge

The added mass is considered to be proportional to on the wetted beam of the section, which corresponds to the 2-D high frequency approximation of the added mass equalling the volume of a demi-circle with the half beam of the section as a radius.

In the wet chine Region the half beam of the cross-section does not change (or only marginally) because the section has more or less vertical topsides due to wave elevation and motions. The added mass therefore becomes constant.

In Region 2 and 4 however the submerged breadth of the section is changing constantly in time. Therefore the change of added mass with respect to time becomes:

$$\frac{dm_a}{dt} = \rho\pi\, c_m\, y\, \frac{dy}{dt}$$

in which for Region 2:

$$y = \frac{\pi}{2}\left\{ \frac{h_w}{\cos\theta - v\sin\theta} \right\} \cdot \frac{1}{\tan\beta}$$

and for Region 4:

$$y = Y + \left\{ \frac{h_w}{\cos\theta - v\sin\theta} - Y\tan\beta \right\} \cdot \frac{1}{\tan\beta}$$

and:

$$h_w = z_{cg} - \xi\sin\theta + \zeta\cos\theta - \zeta_w$$

h_w	=	instantaneous local submergence of the cross-section
y	=	instantaneous breadth of section
Y	=	maximum breadth of section
ζ_w	=	wave elevation at section

So for steady state planing the lift becomes:

$$\frac{dL}{dx} = U_o\sin\tau\, \frac{dm_a'}{dt} = U_o\sin\tau\, \frac{dm_a'}{dx}\, \frac{dx}{dt}$$

$$= U_o^2\, \sin\tau\, \cos\tau\, \frac{dm_a'}{dx} = \frac{1}{2}\, U_o^2\, \sin 2\tau\, \frac{dm_a'}{dx}$$

in which: $dm_a'/dx = \pi\,\rho\, Cm\, y\, dy/dx$

We restrict our considerations first to the planing hulls with a prismatic constant beam aftbodies as used by a.o. Shufold for their fundamental studies on planing hulls. These hulls have a finite value of dy/dx in the dry chine region and so a positive normal force is being developed. In the wet chine region, however, where the chines are immersed:

$$dy/dx = 0 \quad \text{and so:} \quad dm_a/dx = 0 \quad \text{and thus:} \quad dL/dx = 0$$

This was in contradiction with the experimental results available on the hydrodynamic load distribution along such a planing hull. So, an additional lift term was introduced into the formulations based on the "cross flow drag" principle:

$$\frac{df}{dx} = \frac{1}{2}\rho \, (U_o \sin\theta)^2 \, b \, C_{D,c}$$

in which: $C_{D,c}$ = cross flow drag coefficient
b = 2 y = local beam (chine tot chine)

Many researchers have used these formulations with good result, although Payne (48) points out that the introduction of this cross flow drag may be omitted when another formulation of the added mass in the wet chine region is introduced, i.e.:

$$m_a = \frac{\pi}{2} \rho \, y^2 \, Cm \qquad \text{for the dry chine region in which } y < Y$$

and:

$$m_a = \frac{\pi}{2} \rho \, y^2 \, Cm(1 + f (\frac{zc}{Y})) \text{ for the wet chine region in which } y = Y$$

in which: zc = keel submergence of the section.

By doing so Payne suggests that the added mass of a section must increase with increasing chine immersion according to:

$$f(\frac{zc}{Y}) = \frac{4}{3} (\frac{zc}{Y})$$

The differences between the results for the hydrodynamic load distribution of the two approaches are not very significant but will be further dealt with in the chapter on steady state planing.
The cross flow drag coefficient according to Shufold (57) may be approximated for V shaped sections by:

$$C_{D,c} = 1.15 \cos(\beta)$$

in which: β = deadrise angle of the section

Finally a buoyancy force still works on the segment of the planing hull. This force is assumed to work in a vertical direction and to be equal to the equivalent static buoyancy of the section multiplied with a correction factor a_{bf} :

$$f_B = a_{bf} \rho \, 9.81 \, A$$

in which: A = cross-sectional area of the section

The full amount of the static buoyancy is not realised because at the high speeds under consideration the flow separates from the chines and the stern, reducing the pressures at these locations to the atmospheric pressure. Therefore the total pressure distribution deviates considerably from the hydrostatic pressure distribution when applying Archimedes Law. The value of a_{bf} will be assessed in more detail in the paragraph on steady state planing.

The total hydrodynamic force on the ship is obtained by the summation of the three force components for each segment and by integration along the length of the ship of these sectional forces. This yields for the total force in the Z-direction:

$$F_z(t) = -N\cos\theta = \int_L f\cos\theta\, d\xi + \int_L f_B\, d\xi$$

$$= -\Big[\int_L \{ m_a(\xi,t)\dot{V}(\xi,t) + \dot{m}_a(\xi,t)V(\xi,t) - U(\xi,t)\frac{\partial}{\partial\xi}[m_a(\xi,t)V(\xi,t)]$$

$$+ C_{D,c}(\xi,t)\rho b(\xi,t)V^2(\xi,t)\}\cos\theta\, d\xi + a_{bf}\, A d\xi\Big]$$

in which the integration is taken of the instantaneous wetted length L of the ship, i.e. the wetted length under influence of the motions and wave elevation. Similarly the force in the X-direction is given by:

$$F_x(t) = \int_L f\sin\theta\, d\xi$$

$$= -\int_L \{ m_a(\xi,t)\dot{V}(\xi,t) + \dot{m}_a(\xi,t)V(\xi,t)$$

$$- U(\xi,t)\frac{\partial}{\partial\xi}(m_a(\xi,t)V(\xi,t)) +$$

$$+ C_{D,c}(\xi,t)\rho\, b(\xi,t)V^2(\xi,t)\}\sin\theta\, d\xi$$

The hydrodynamic moment around the Centre of Gravity of the ship is obtained in a similar manner by integration over the instantaneous wetted length of the ship of the normal force on each cross-section times its lever with respect to the Centre of Gravity of the ship:

$$F_\theta(t) = -\int_L f(\xi,t)\xi d\xi - \int_L f_B\cos\theta\xi\, d\xi$$

$$= \int_L \{ m_a(\xi,t)\, \dot{V}(\xi,t) + \dot{m}_a(\xi,t)\, V(\xi,t)$$

$$- U(\xi,t)\, \frac{\partial}{\partial \xi} (m_a(\xi,t)\, V(\xi,t)) + C_{D,c}(\xi,t)\rho\, b(\xi,t)\, V^2(\xi,t)$$

$$+ a_{bf}\, \rho g A \cos\theta \}\, \xi\, d\xi$$

The wave exciting forces on the ship are obtained by neglecting the diffraction forces and assuming that the wave excitation is caused by both the geometrical properties of the wave, altering the wetted length and the draft of the ship and by the vertical component of the orbital velocities in the waves. Because the ships under consideration are generally shallow with respect to the height of the waves, the orbital velocity is taken at the undisturbed water surface in the plane Z = 0. The influence of the horizontal orbital velocities is neglected, because these are considered relatively small in comparison with the forward speed of the ship.

So the velocity U along and V normal to the baseline of the ship may be expressed by the following formulation:

$$U(\xi,t) = \dot{x}_{CG}(t) \cos\theta(t) - \{ \dot{z}_{CG}(t) - w_z(\xi,t) \} * \sin\theta(t)$$

$$V(\xi,t) = \dot{x}_{CG}(t) \sin\theta(t) - \{ \dot{z}_{CG}(t) - w_z(\xi,t) \} \cos\theta(t) - \dot{\theta}(t)\xi$$

in which: w_z is the vertical component of the wave orbital velocity.

The depth of submergence h of the cross-section at any point $P(\xi,\zeta)$ and time may be determined by:

$$h(\xi,\zeta,t) = Z_{CG}(t) - \xi \sin\theta(t) + \zeta \cos\theta(t) - r(\xi,t)$$

in which $r(\xi,t)$ = instantaneous wave elevation at point $P(\xi,\zeta)$.
At point $P(\xi,\zeta)$:

$$x(t) = x_{CG}(t) + \xi \cos\theta(t) + \zeta \sin\theta(t)$$

in which:

$$x_{CG}(t) = \int_{t=t_o}^{t=t} \dot{x}_{CG}(t)\, dt$$

and the depth of submergence of the strip is approximated by:

$$d \approx \frac{h(\xi,\zeta,t)}{\cos\theta(t) - v \sin\theta(t)}$$

in which v = local wave slope.

The formulation of the wave elevation and vertical orbital velocity will be given in more detail in the section on irregular waves.

The vertical relative acceleration of the water V may be obtained by differentiation with respect to time, yielding:

$$\dot{V} = \ddot{x}_{CG} \sin\theta + (\ddot{z}_{CG} - \dot{w}_z) \cos\theta - \ddot{\theta}\, \xi +$$

$$+ \dot{\theta} (\dot{x}_{CG} \cos\theta) - (z_{CG} - w_z\theta) \sin\theta$$

in which:

$$\frac{dw_z}{dt} = \dot{w}_z - U \frac{\partial w_z}{d\xi} \qquad \text{and}$$

$$\int_L UV \frac{\partial m_a}{d\xi} = - \frac{UVm_a}{stern} - \int_L m_a \frac{\partial UV}{\partial \xi}\, d\xi$$

The final formulations for the vertical force and the pitch moment become:

$$F_z(t) = \{ - M_z \cos\theta\, \ddot{z}_{CG} - M_a \sin\theta\, \ddot{x}_{CG} + Q_a\ddot{\theta}$$

$$+ M_a\dot{\theta}(\dot{z}_{CG} \sin\theta - \dot{x}_{CG} \cos\theta) + \int_L m_a \frac{dw_z}{dt} \cos\theta\, d\xi$$

$$- \int_L m_a w_z\dot{\theta} \sin\theta\, d\xi - \int_L m_a V \frac{\partial w_z}{\partial \xi} \sin\theta\, d\xi + \int_L m_a U \frac{\partial w_z}{\partial \xi} \cos\theta\, d\xi$$

$$- \frac{UVm_a}{stern} - \int_L V\dot{m}_a d\xi - \rho \int_L C_{D,c}\, bV^2\, d\xi \} \cos\theta + \int_L a_{bf}\rho g A d\xi$$

in which:

$$M_a = \int_L m_a d\xi$$

and:

$$Q_a = \int_L m_a \xi\, d\xi$$

A similar expression is found for:

$$F_\theta(t) = I_a\ddot{\theta} + Q_a \cos\theta\, \ddot{z}_{CG} - Q_a\dot{\theta}(\dot{z}_{CG}\sin\theta - \dot{x}_{CG}\cos\theta)$$

$$- \int_L m_a \cos\theta \frac{dw_z}{dt} \xi\, d\xi + \int_L m_a\dot{\theta} \sin\theta\, w_z \xi\, d\xi$$

$$+ \int_L V\dot{m}_a\xi\, d\xi + \int_L \rho C_{D,C}\, bV^2\xi\, d\xi + m_a UV\xi|_{stern}$$

$$- \int_L m_a U \frac{\partial w_z}{\partial \xi} \cos\theta\, \xi\, d\xi + \int_L a_{bf}\, \rho g A \cos\theta\, \xi\, d\xi$$

$$+ \int_L m_a VU\, d\xi + \int_L m_a V \frac{\partial w_z}{\partial \xi} \sin\theta\, \xi\, d\xi$$

in which:

$$Q_a = \int_L m_a\xi\, d\xi$$

$$I_a = \int_L m_a\xi^2\, d\xi$$

$$M_a = \int_L m_a\, d\xi$$

In the next sections a more detailed examination of the remaining unknowns, such as the stationary heave and pitch in steady state planing, the load distribution over the length of the ship, the added mass distribution and the wave exciting forces will be presented.

3.3 Determination of the steady state still water reference position of the craft at speed

As demonstrated in Chapter 2 fast monohulls may experience a considerable stationary heave (sinkage) and pitch (trim) due to their high forward speed. It has been demonstrated that in particular the trim angle has a strong influence on the pitch motion and the vertical accelerations.

For the introduction of the sinkage and trim of the craft into the calculations, use can be made of experimental results obtained from a towing tank experiment with a model of the actual design. This is an accurate way of obtaining these data, however it requires a model experiment. To enable the calculation of the wave induced motions in an early design stage, a method for determining the sinkage and trim of an arbitrary planing hull should be available.
It should be mentioned, however, that not only the overall result of the changing pressure distribution over the wetted bottom of the hull is of interest, i.e. the sinkage and trim, but also the distribution itself. This will be discussed in more detail in section 3.5.
Different procedures to obtain the sinkage and trim data as function of forward speed for an arbitrary design are possible:

First satisfactory results for moderate speeds upto around Fn = 0.4 may be obtained for non transom type hulls by solving the velocity potential in three dimensions using a boundary integral equation for the velocity potential which simultaneously satisfies both the hull surface and the free surface conditions. The boundary integral methods can be roughly divided in two categories: one using the Green's type boundary element and the other is the so-called Rankine source method.
In particular, the latter has been developed extensively for realistically shaped marine vessels and is based on the method originally brought forward by Dawson in 1977. The results show a dependency on the panel discretisation of the hull used. In 1988 Raven (51) used the method also for transom type navy vessels .The calculation of the velocity distribution over the hull appears reasonably accurate, although validation of this aspect is still difficult. The pressure integration over the surface of the hull to yield wave resistance and sinkage and trim is subject to local singularities which may negatively affect the results.

With planing craft the hydrodynamics involved are more complicated and are rather different from low speed displacement type vessels. Partly this is caused by separation effects both at the submerged transom as well as on part of the chines. Due to this separation at the transom large waves may develop in the wake of the hull which introduce nonlinear effects.
Linearized theories have been used to examine the cases of planing ships but only with very simple geometries, not resembling the shape of the actual craft.
Hino a.o. (21) present in 1991 results of such a computation, but only results

for wave elevation along the length of the ship and velocity distributions are shown. They found reasonable agreement, but modelling the pressure peak in the sprayroot area appeared to be an unsurmountable problem which had an important negative effect on the overall results. Spray is a highly nonlinear phenomenon and its mathematical formulation is extremely difficult. In linear theory the final position of the craft at speed is part of the presumed solution.
An iterative procedure must be followed to find the final equilibrium position of the craft at its appropriate forward speed, using the results of the previously obtained pressure distribution over the hull to define a new position for the next calculation. In this process new meshes have to be defined for each step, due to the changing geometry of the hull in contact with the water. This is a rather complicated and time consuming procedure with a too low level of accuracy yet in the speed range of interest in the case of the planing hulls to make the effort worthwhile for the present motion calculation procedure.

Another method to calculate the hydrodynamic lift distribution along the hull could be based on the work of Sottorf (59), Sedov (58), and Van den Bosch (5) a.o. who used towing tank experiments with planing wedges of varying shapes under different conditions to measure the pressure distribution over the wetted area of these "planing hulls" at speed.
The efforts of these researchers resulted in a large amount of test data on the hydrodynamic characteristics of constant deadrise planing hullforms moving with constant trim, fixed mean wetted length and constant forward speed. These data have been used to formulate empirical expressions for the pressure distribution over the hull of an arbitrary design.

These basic planing equations have been used a.o. by Savitsky (53) in 1964 to formulate expressions for prediction of the running trim and sinkage of prismatic planing hulls. The computational method involves the determination of the running trim and the resistance which will provide for an equilibrium condition of the hull at a given running speed, loading, and longitudinal position of the Centre of Gravity. He defines the forces according to Figure 3.8:

The equations used for relating vertical and horizontal forces are:

Vertical : $T \sin(\tau+\epsilon) + N \cos(\tau) - D_f \sin(\tau) - \Delta = 0$

Horizontal : $T \cos(\tau+\epsilon) - N \sin(\tau) - D_f \cos(\tau) = 0$

Trim : $Nc + D_f a - Tf = 0$

in which:

T	=	propeller trust
Δ	=	weight of the boat
D_f	=	frictional resistance

N	=	resultant of pressure on the bottom
c	=	distance between N and CG
τ	=	trimangle in steady state planing condition
a	=	vertical lever thrust

For a given boat design the weight, the position and inclination of the propeller shaft, the longitudinal position of the Centre of Gravity and the deadrise are known quantities. Using an iterative procedure labda and tau are being solved using the following empirical formulae for the hydrodynamic and hydrostatic forces on the submerged hull:

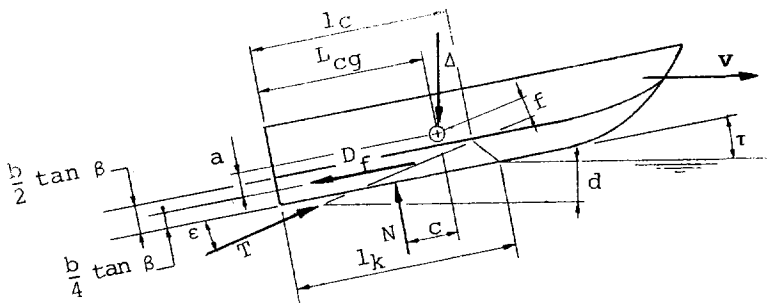

Figure 3.8: Definition sketch according to Savitsky

- lift coefficient for a flat plate:

$$C_{l_o} = \frac{\Delta}{\frac{1}{2}\rho V^2 b^2} = \tau^{1.1}(0.012\sqrt{\lambda_s + \frac{0.0055\lambda_s^{5/2}}{C_v^2}})$$

in which: $\lambda_s = \frac{Lk + Lc}{2y}$ $\qquad C_v = \frac{V}{\sqrt{g * b}}$

$\tau^{1.1}\ 0.012\sqrt{\lambda_s}$ *the hydrodynamic lift*

and

$\tau^{1.1}\ \frac{0.0055\lambda_s^{5/2}}{C_v^2}$ *the hydrostatic lift*

- lift coefficient correction for deadrise:

$$Cl_\beta = Cl_o - 0.0065\beta\, Cl_o^{0.6}$$

- distance of the centre of pressure to CG:

$$c = LCG - xC_\nabla \qquad \textit{in which:} \qquad xC_\nabla = \{ (0.75 - \frac{1}{5.21 \frac{C_v^2}{\lambda_s^2} + 2.39}) \} * \lambda_s b$$

The results of this approximation of the sinkage and trim is reasonably accurate when compared with measured data as may be seen from Figure 3.9. But in particular for higher length to beam ratio hulls and LCG positions further aft than 4% of Lpp with respect to the centroid of the planing area large discrepancies may occur.

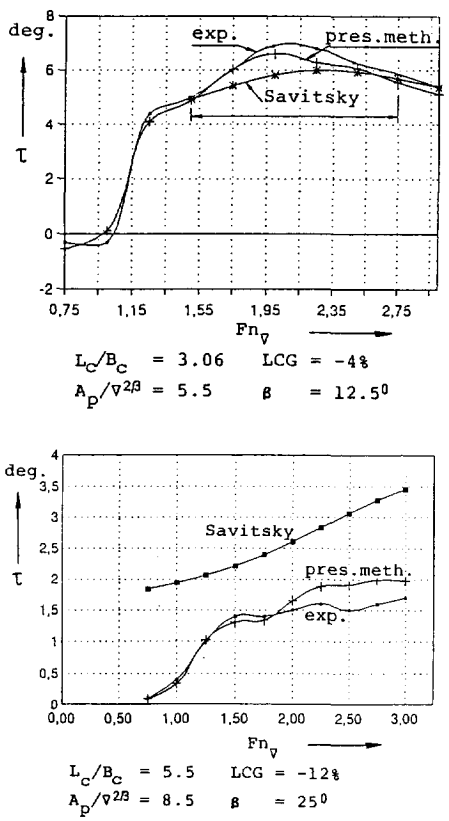

Figure 3.9: Measured and calculated sinkage and trim according to Savitsky

In the present study a third and somewhat different approach has been used:

Here use is being made of an approximation of the sinkage and trim of the planing hull obtained from polynomial expressions derived from experimental data obtained from a large number of towing tank experiments with a number of systematic series of planing hullforms. By doing so the still water reference position of an arbitrary hull, characterised by hull form parameters, which should be within the range of these systematic series, may be obtained.
To formulate these polynomial expressions use has been made of the work presented in 1963 by Clement and Blount (9) on the resistance, sinkage and trim of a series of planing hull forms generally known as the TMB Series 62 or the "Clement Series".
This series has been extended with two additional systematic series to cover a larger range of deadrise angles.

3.3.1 The Delft Systematic Deadrise Series of planing hull forms

The results of Clement in 1963, based on an extensive series of model experiments, showed the influence of a number of hullform parameters, such as length to beam ratio, the longitudinal position of the Centre of Gravity with respect to the centroid of the planing area and the displacement-planing area ratio of the craft on the resistance, sinkage and running trim. He performed the experiments with five systematically derived variations of one parent model. All models had a deadrise of 12.5 degrees at the midship section which was kept constant from there over the remaining aftbody of the hull. These experimental data have been extensively used by designers of planing boats to predict and optimise the performance in the design stage.
In 1982 Keuning and Gerritsma (31) extended this Clement series by a systematic series with a similar setup but now with models with 25 degrees deadrise and in 1992 another extension to this series was published by Keuning, Gerritsma and Van Terwisga (32) for hulls with 30 degrees deadrise. These extensions were felt necessary because in the search for improved seakeeping capability of planing craft, increasing the deadrise proved to be an important aspect. The original series as tested by Clement in 1963 was more aimed at the lowest still water resistance and therefore restricted to low deadrise angles, which were considered to be favourable in that respect.
For the 25 and 30 degrees deadrise series new parent models had to be developed. For the development of these parents use has been made of the lines of the 12.5 degrees parent model as originally used by Clement and Blount. This was considered to be essential for the consistency between the three different series. Much effort has been put into the design of these parent models to keep them as similar to Clement's parent as possible. This resulted in:

- the length over the chine is the same for all models;

- the maximum breadth on the chine and the vertical projection of the chine (B_p/B_{pa}) has been kept the same for all models;

- the vertical projection of the deck line has been kept the same for all models;

- the keelline has been kept the same for all models, except from ordinate 16 forwards, in which region due to the increased deadrise the stem profile had to be adjusted to maintain the proper length over the chine;

- the hulls consist entirely of developable surfaces, similar to Clement's parent model;

- the transom slope has been maintained.

Only the deadrise angle was changed from 12.5 to 25.0 and 30.0 degrees respectively. The bodyplans of the three parents are depicted in Figure 3.10. From these bodyplans it may be seen that the three parent models show a close resemblance. The main particulars of the three parent models are presented in Table 3.1.

TABLE 3.1

β degrees	30	25	12.5
L_c m	1.5	1.5	2.436
B_c m	0.3	0.3	0.487
L_c/B_c	4.087	4.087	4.09
C_{AP} rel to Ord. 0	48.8	48.8	48.8

The additional models of each series were length to beam ratio variations derived from the parent models by means of an afine transformation technique as described a.o. by Versluis (69). This technique uses (linear) functions to transform the beam and the depth of the sections and if necessary also the ordinate spacing to generate a new linesplan of predetermined dimensions and hydrostatic characteristics. Using this technique a great similarity between the models is guaranteed.
Some slight additional modifications, however, have been made to the aft bodies of the models with the lower length to beam ratios, i.e. 3.06 and 2.00.
This was done in exactly the same way as done by Clement in his original series. The main particulars of the 25 degrees deadrise series are presented in Table 3.2 and of the 30 degrees deadrise series in Table 3.3. All the models had spray strips attached over the entire length of the chine. The bottom of the spray strips followed the athwart ships inclination of the bottom of the model

from ordinate 0 (the transom) to ordinate 10 (midship) and was horizontal from ordinate 12 to ordinate 20 (the stem) with a transition zone between ordinate 10 and ordinate 12. The width of the spraystrips was approximately 4 mm and they had non-radiused edges. The models were constructed of transparant material which allowed through hull photography for the determination of the wetted surface during each run.

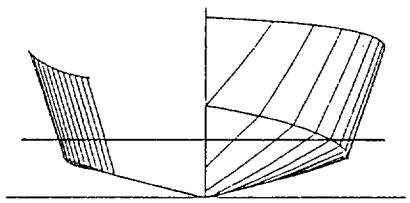

$\beta = 12.5^0$

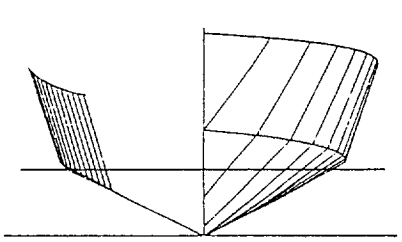

$\beta = 25^0$

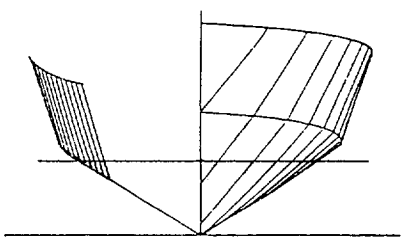

$\beta = 30^0$

Figure 3.10: Bodyplans of the parents of the 12.5, 25.0 and 30.0 deadrise series. From (32)

All the tests with the models were carried out in the #1 towing tank of the Delft Shiphydromechanics Laboratory of the Delft University of Technolgy.
The dimensions of this tank are 142 meters length, 4.22 meters width and maximum waterdepth 2.5 meters. The maximum attainable speed of the towing carriage is 7.0 meters/second.

TABLE 3.2

A_p	m^2	0.4296	0.4277	0.4500	0.3347	0.2628
$L_p = L_c$	m	1.000	1.250	1.500	1.500	1.500
B_c	m	0.500	0.408	0.367	0.273	0.214
L_c/B_c		2.00	3.06	4.08	5.49	7.01
C_{AP} rel to ord. 0 in %		47.1	47.8	48.8	48.8	48.8

TABLE 3.3

A_p	m^2	0.384	0.449	0.334	0.262
L_c	m	1.25	1.5	1.5	1.5
B_c	m	0.367	0.367	0.273	0.214
L_c/B_c		3.41	4.09	5.5	7.0
C_{AP} rel to ord. 0	%	47.9	48.8	48.6	48.6

The models were connected to the towing carriage in such a way that they were free to heave and pitch but restrained in all other modes of motion. The pivot of the connection between the towing carriage and the model was situated at the intersection of the cross-section through the Centre of Gravity of the model and the assumed shaftline of the main propulsors.
The linesplans of the models with 25 and 30 degrees deadrise are presented in Figures 3.11 and 3.12.

The position and inclination of these shaftlines are similar to those used by Clement in his series.
A straingauge type dynamometer was placed on the hinge for the measurement of the resistance force.
It was always parallel to the undisturbed water surface. The vertical displacement fore and aft were measured with two "wire-over-potentiometer" type displacement meters to yield the sinkage and trim of the craft.
Through-hull photography was used at each run to determine the position of the sprayroot, the wetted length over the keel and the chine and the instantaneous wetted surface. No turbulence stimulators were used during the experiments because the modelscale and the speeds used were considered to be large enough to yield reliable results. No modelspeeds below 1.0 m/s was used during the experiments.

All models tests were performed with every combination arising from the variation of the parameters as presented in Table 3.4.
The range of speeds used during the experiments with the 25 and 30 degrees

deadrise models was smaller than the range used by Clement with his models due to physical limitations imposed by the equipment in the Delft Towing Tank.

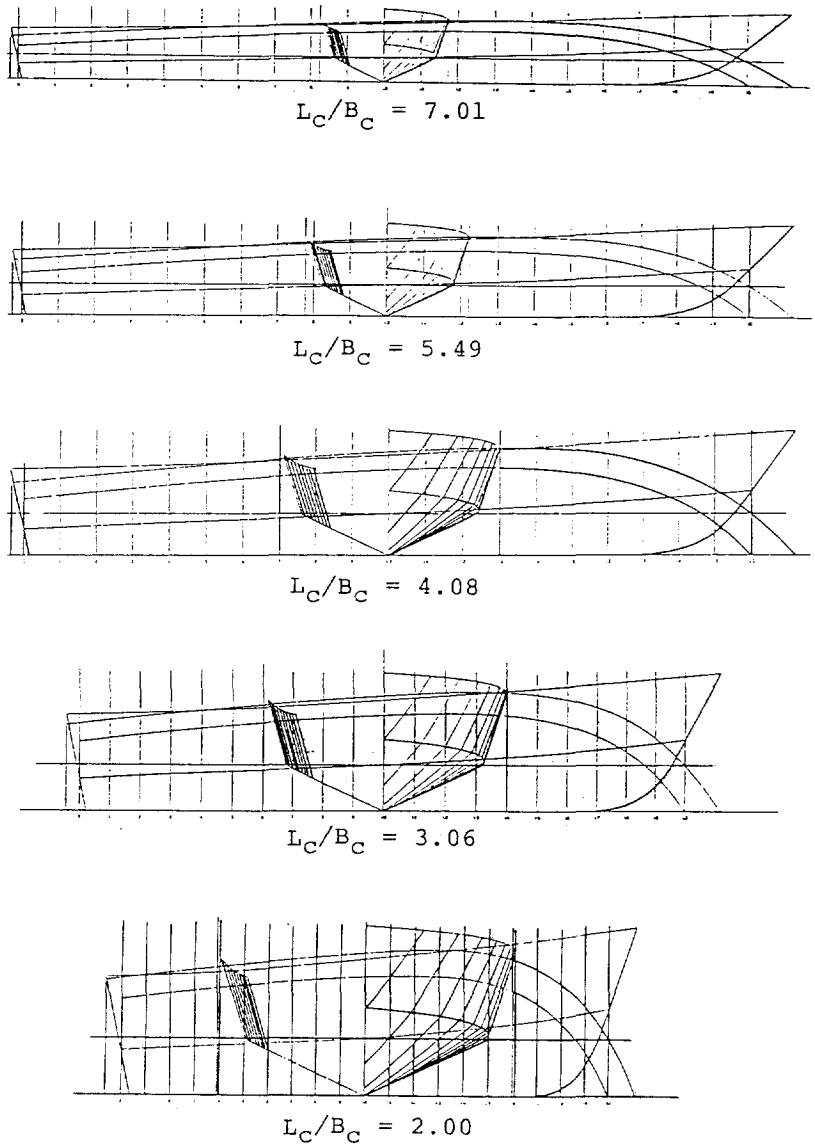

Figure 3.11: Linesplans of the 25 degrees deadrise models

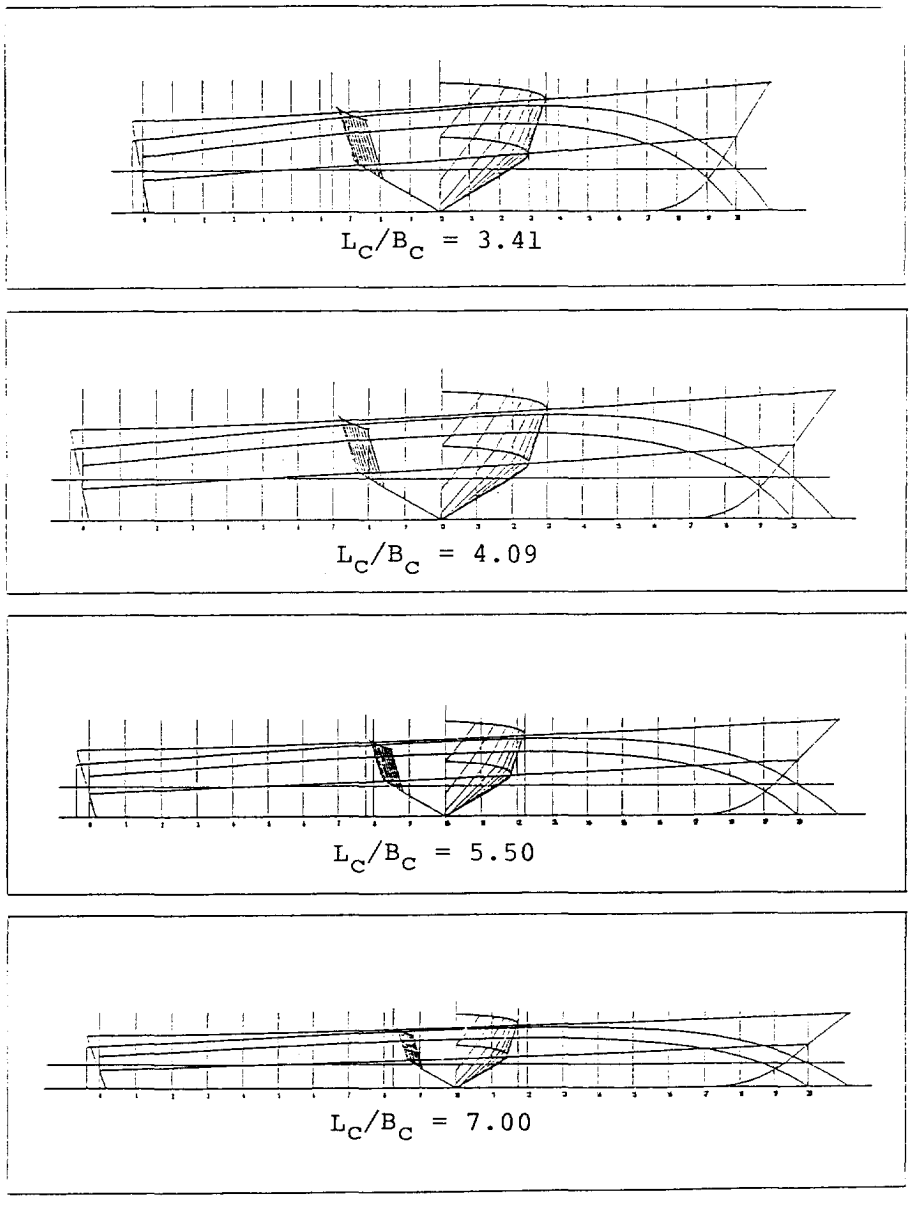

Figure 3.12 Linesplans of the 30 degrees deadrise models

Table 3.4: Parameter range of the Delft Systematic Deadrise Series

L_c/B_c	2.00	3.06	4.09	5.50	7.00
$A_p/\nabla^{2/3}$	4.0	5.5	7.0	8.5	
L_{CG}	0 %	4 %	8 %	12 %	L_p after centroid A_p
Fn_∇	0.75	1.00	1.25	1.50	1.75
	2.00	2.25	2.50	2.75	3.00

3.3.2 The polynomial expressions

The three systematic series i.e. Clement and Blount, Keuning and Gerritsma, and Keuning, Gerritsma and Van Terwisga have been combined and will be referred to from here as the Delft Systematic Deadrise Series (DSDS).
All the measured results from the DSDS have been combined to yield polynomial expressions for the approximation of the resistance, the trim and the sinkage of an arbitrary hard chined hull at high forward speeds. These polynomial expressions are based solely on the parameters varied during the experiments, i.e.:

- length to beam ratio (L_c/B_c)
- loading coefficient ($A_p/\nabla^{2/3}$)
- longitudinal position of the Centre of Gravity (LCG)
- the dearise angle (β).

After extensive analysis of a variety of expressions using a root mean square method for the determination of the coefficients, the following expressions proved to yield the most satisfactory results:

$$\left.\begin{matrix} R_t/\Delta \\ \theta \\ R_{CG}/\nabla^1/3 \end{matrix}\right\} = a_0 + a_1 \frac{L_c}{B_c} + a_2 \left(\frac{L_c}{B_c}\right)^2 + a_3 \left(\frac{L_c}{B_c}\right)^3 + a_4 \frac{A_p}{\nabla^{2/3}} +$$

$$a_5 \left(\frac{A_p}{\nabla^{2/3}}\right)^2 + a_6 \left(\frac{A_p}{\nabla^{2/3}}\right)^3 + a_7 LCG^2 + a_8 LCG^2 + a_9 LCG^3 +$$

$$a_{10} LCG \frac{A_p}{\nabla^{2/3}} + a_{11} \frac{L_c}{B_c} \frac{A_p}{\nabla^{2/3}} + a_{12} LCG \frac{L_c}{B_c}$$

The coefficients for these polynomial expressions have been determined as function of the forward speed, i.e. Fn_∇. The accuracy of the approximations is significantly increased by this approach as is the number of coefficients. In addition the polynomial expressions for the resistance assess the total resistance instead of the residuary resistance only. This makes it necessary to have different sets of coefficients for different weights of displacements.

One set of coefficients for one displacement is given in Appendix I.

The correctness of fit of the approximations using the polynomial expressions to the measured data is shown in Figure 3.13 and Figure 3.14 for two models of the series of which the main particulars are shown in the following Table:

TABLE 3.5

model	β degr.	L_c/B_c	$A_p/\nabla^{2/3}$	L_{CG} %
#1	25	5.5	5.5	-4
#2	25	2.0	4.0	0

As may be seen from comparison of results presented in these figures the largest discrepancies between the approximated and measured values occur for the heaviest model with the lowest L/B ratios. In general, the error of fit of the polynomials to the measured data was within 5 percent and in most conditions considerably less. The correlation coefficients obtained during the fitting process were always in excess of 0.98. In addition, considerable attention has been paid to guarantee that in particular the trend in variation of the quantity under consideration with the hullform parameters and the forward speed was always properly predicted by the polynomial approximations when using the derived coefficients. This enables small excursions outside the parameter range of the series used, whithout the risk of big errors occurring.

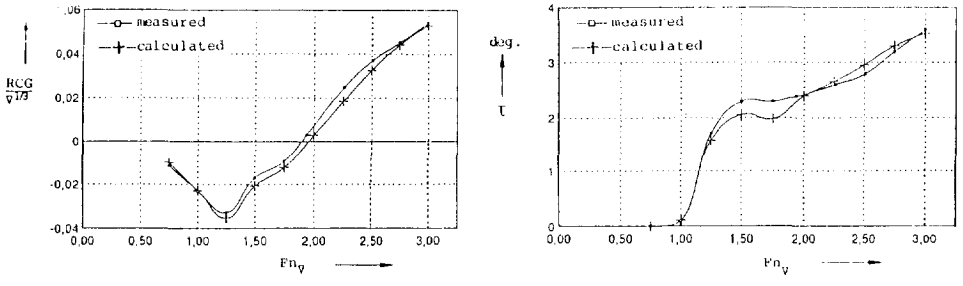

Figure 3.13: Comparison between measured and approximated trim and sinkage, model #1

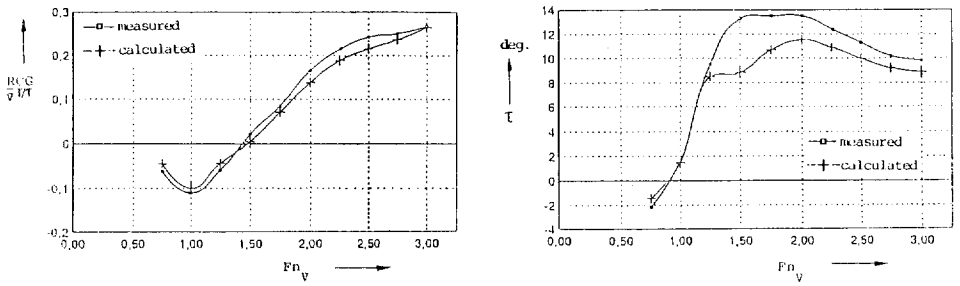

Figure 3.14: Comparison between measured and approximated trim and sinkage, model #2

To validate the polynomials for the use with arbitrary designs, the large data set available at the Delft Shiphydromechanics Laboratory has been used. This contains model test data on some 25 quite different designs all tested in the Laboratory, using a consistent measurement technique throughout the systematic series.

Three models were selected of which the main parameters were considered to be representative for present day designs. The craft used for the validation were:

- a coastal patrol boat for the North Sea
- a fast planing motor yacht
- a North Sea coastal rescue boat

The lines plans of these ships are depicted in Figure 3.15.
The comparison between the measured and the approximated results for sinkage and trim are presented in Figure 3.16. As may be seen from this figure the correlation is satisfactory.
A linear interpolation routine is being used to obtain results for values of the dead rise angles in between 12.5, 25 or 30 degrees. An extension of the systematic series with models having 20 degrees deadrise is foreseen to improve the predictions in this rather important area.

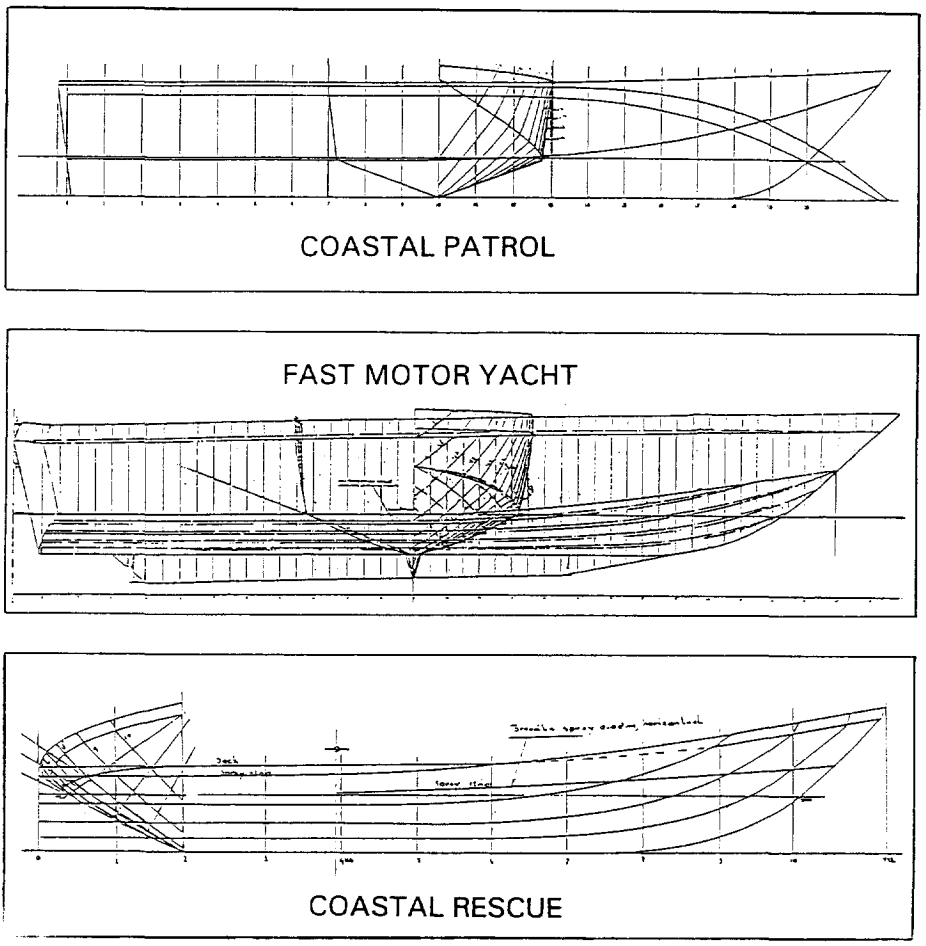

Figure 3.15: Linesplans of the ships used for validation

3.3.3 Correction for the wharped bottom

When observing actual designs it is evident that many ships do not have a prismatic constant deadrise aft body like the models of the DSDS, but show a changing deadrise over the aftbody between midship and transom yielding a convex centreline profile and/or buttock shape. This enables the installation of a larger propellor and reduces the inclination of the shafts, which increases the overall propulsive efficiency. In addition, a large number of planing craft, in particular those used for patrol- or surveillance tasks, are being operated at relatively low speeds for a relatively large amount of time.

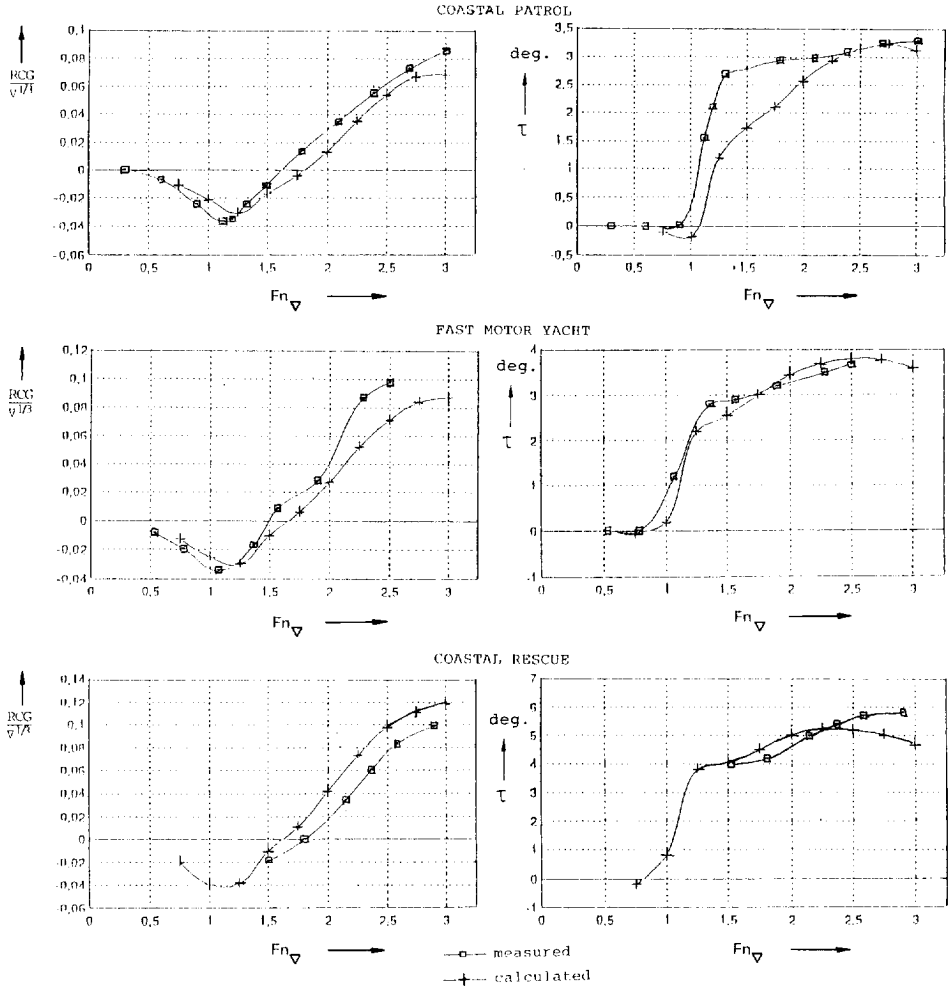

Figure 3.16: Comparison between measured and approximated sinkage and trim for the test fleet

Reduction of the submerged area of the transom has a favourable effect on the resistance at sub-hump speeds. This variation in deadrise, however, will effect the sinkage and running trim of these craft and therefore this influence should be incorporated in the prediction.

To be able to account for this effect in the polynomial approximations, an additional small sub-series of two models similar to the 25 degrees deadrise

parent model but with a non prismatic aftbody were tested. The intention was to develop an expression to "correct" the running trim and sinkage of a hull with a non prismatic aftbody as obtained from the polynomial expressions based on the prismatic hulls series only. The underlying assumption being that the correction would effect all the other models in the same way.

The aftbody deadrise of the two models in this sub-series changed from 25 degrees at ordinate 10 (midship) to 5 degrees at ordinate 0 (transom). The difference between the two models was the "average" inclination of the centre-buttock aft, which was -4.9 degrees for model 232-A and -2.6 degrees for model 232-B, see Figure 3.17. In order to be able to maintain the same distribution of the submerged volume the width over the chine was increased compared to the 25 degrees parent model. The deviation from the parent hull shape arising herefrom, however, was considered to be of minor importance. The sections from ordinate 10 to ordinate 20 were exactly similar to those of the 25 degrees parent model. The main particulars of the models are presented in Table 3.6.

The measurement scheme for these two models was equal to the measurement scheme used for the other models, so the same variations of $A_p/\nabla^{2/3}$ and LCG have been tested. The effect of the wharped bottom and rise of the centreline could be expressed as differentials in resistance, sinkage and trim in comparison with the parent model.
These differentials have been expressed as polynomial expressions in which a linear dependency is assumed on the average centreline inclination angle (γ) and the twist angle (ϵ_t), being the difference in deadrise at ordinate 10 and 0, as well as the coupling between these angles and the loading coefficient and LCG. The resulting polynomials are of the following form:

$$\Delta \begin{Bmatrix} \Delta Rt \\ \Delta\theta \\ \Delta\left(\frac{R_{CG}}{\nabla^{1/3}}\right) \end{Bmatrix} = a_0\,\gamma + a_1\,\epsilon_t + \frac{A_p}{\nabla^{2/3}} + a_3\,\gamma\,LCG +$$

$$+ a_4\,\epsilon_t\,\frac{A_p}{\nabla^{2/3}} + a_5\,\epsilon_t\,LCG + a_6\,\gamma\,\frac{A_p}{\nabla^{2/3^2}} + a_7\,\gamma\,LCG^2$$

Similar to the previously obtained polynomials the coefficients were derived by using a root mean square method on the datasets for a specific number of volumetric Froude numbers at fixed intervals.
In Figure 3.18 a comparison is made between the measured and the approximated sinkage and trim for one typical example.
As may be concluded from the data presented in Figure 3.17 the correctness of fit of the polynomials to the data is satisfactory, in particular for the sinkage and trim of the hulls. The derived approximation yields insight in the change in sinkage and trim of the hull due to the combined effect of twist and centreline rise and appears sufficiently accurate to be implemented in the procedure to

calculate the reference position of a planing hull at speed in the motion calculations. The use of the correction for arbitrary designs however should be considered with some care, because the correctional polynomial expressions are based on a rather limited amount of experimental data.

TABLE 3.6

		Model	Model
		232-A	232-B
A_P	m	0.4589	0.4540
L_c	m	1.50	1.50
B_c	m	0.3670	0.3670
L_c/B_c		4.09	4.09
C_{AP} rel to ord 0	% L_c	48.8	48.8

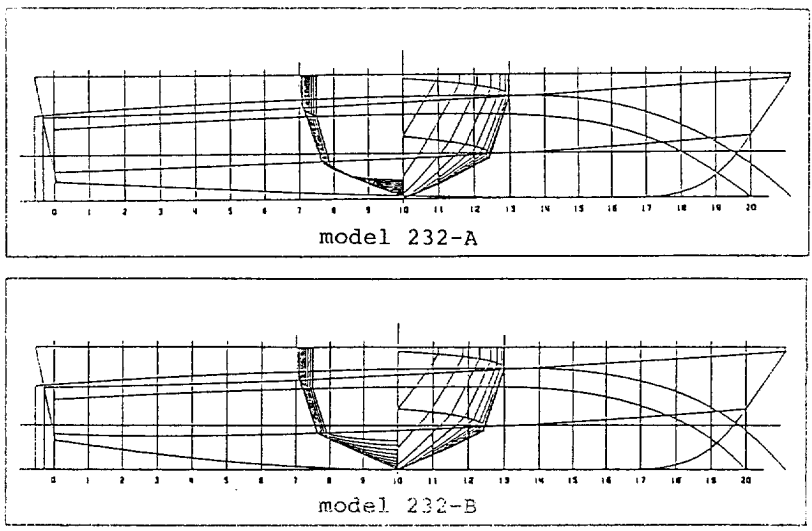

Figure 3.17: Linesplans of the twisted bottom models 232-A and 232-B

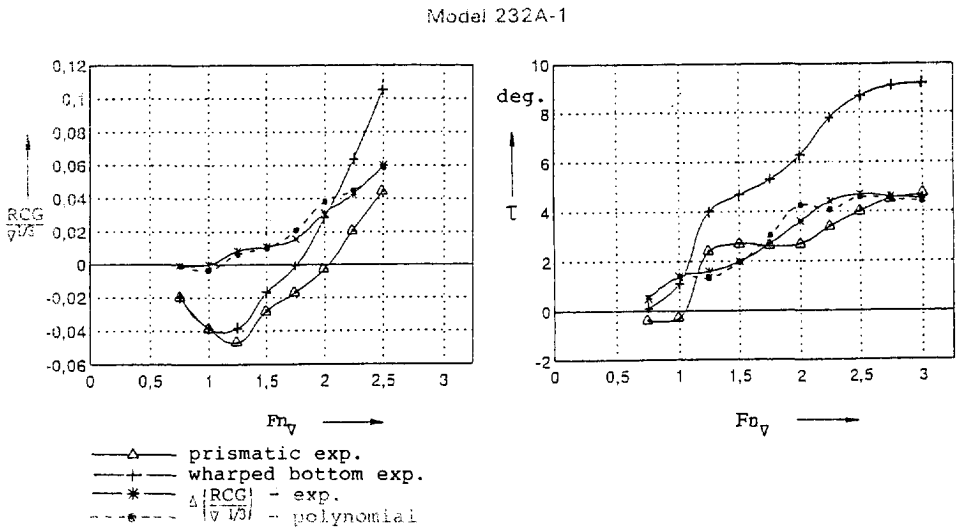

Figure 3.18: Comparison measured and approximated sinkage and trim of twisted bottom models

It should be noted also that the validity of the assumption that the derived correction may be used for other designs having a wharped planing bottom could not be checked sufficiently due to the limited availability of such designs in the data base of the Laboratory mentioned previously. Nevertheless the predicted trend of the correction corresponds with the explications and so it will be used from here on.

3.4 The determination of the buoyancy correction factor

The equilibrium condition of the craft in its steady state planing condition at speed is used to assess the relative magnitude of the hydrodynamic and the hydrostatic part of the lift force.

As may be seen from the equations the hydrodynamic force is supposed to consist of three components: i.e. a hydrodynamic lift associated with the change of fluid momentum, the cross flow drag and a buoyancy part. The latter term is expressed in the equations by:

$$f_B = a_{bf}\, \rho\, g\, A$$

It is considered to be equal to the hydrostatic buoyancy taken over the actually submerged part of the hull multiplied with a correction coefficient a_{bf}. This a_{bf} is smaller than unity and is added to account for the effect that the pressure distribution over the submerged hull deviates from the assumed hydrostatic pressure distribution: the flow is separated at the transom and part of the chines reducing the pressure in these regions to the atmospheric pressure. Zarnick in his model used a fixed value for this correction of 0.5 and added an additional correction on the pitch moment of again 0.5 to arrive at reasonable values for sinkage and trim in his steady state solution. These values were derived from the work of Shufold (57) for the very high speed region.
In a validation study of the Zarnick model carried out by Verkerk (68) it was found that the calculated reference position for a particular planing craft at lower Froude numbers using these fixed values for a_{bf} (and Cm) did not yield satisfactory results when compared with the results of measurements carried out in the towing tank with the same model. Furthermore it became apparent that by introducing the actual reference position obtained from a model test into the calculations the agreement between the measured and calculated response operators for heave and pitch was improved even though this accounted only for the change in geometry of the wetted hull and the associated forces herewith and not for a change in pressure distribution over the hull, since still the same values for a_{bf} and Cm were being used in the instationary calculations.
A short study by Kring (38) in 1988 revealed the importance of, for instance, this a_{bf} value on the vertical bow accelerations as may be seen from Figure 3.19, in which the results of calculations using two different values of a_{bf} are presen- ted, i.e. one for very high speeds (a_{bf} = 0.5) and one for low speeds (a_{bf} = 1.0). The correlation between the measured and the calculated data is not correct using the Zarnick values and the sensitivity of the solution with respect to the value of a_{bf} is evident.

So a proper assessment of the value of a_{bf} (and Cm) obviously is essential. In the present computational model the following approach will be used:

The equations of motion will be used to describe the equilibrium of the craft at speed in calm water. The solution of this is known using the approximated values for the sinkage and trim derived as a result from the previously developed polynomial expressions. The remaining unknowns in the equations, i.e. a_{bf} and Cm, yielding the proper hydrodynamic pressure distribution along the length of the ship, may now be solved.
If only steady state planing is considered the following simplification may be introduced into the equations:

$$\ddot{\theta} = \ddot{Z}cg = \ddot{X}cg = 0$$

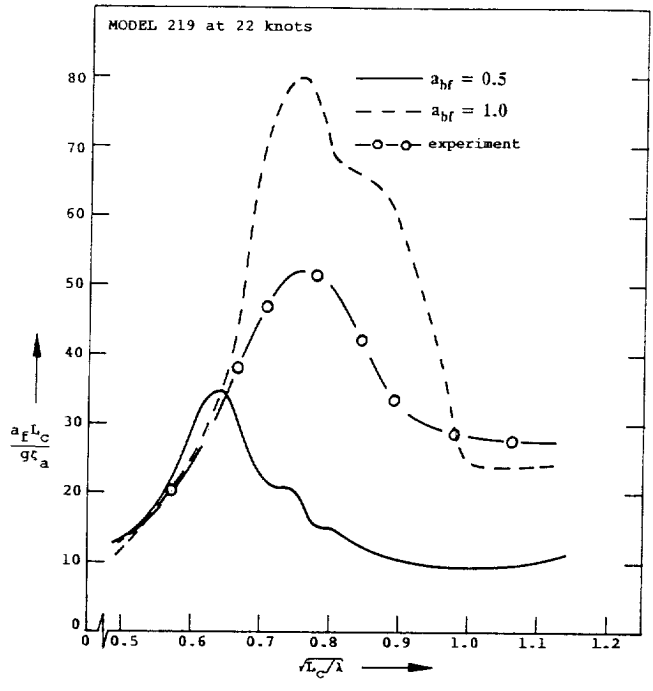

Figure 3.19: Vertical bow accelerations as function of a_{bf}.

and:

$$U = \dot{X}cg \cos\theta$$

$$V = \dot{X}cg \sin\theta$$

The resulting equations describing the steady state planing equilibrium become:

$$W + F_z = 0$$

$$F_\theta + W * Xcg = 0$$

and:

$$F_z = \int_L ((UV \frac{dm_a}{d\xi} - C_{D,c}\, \rho b V^2)\cos\theta - a_{bf}\, \rho g A)d\xi$$

$$F_\theta = \int_L ((UV \frac{dm_a}{d\xi} - C_{D,c}\, \rho b V^2) - a_{bf}\, \rho g A \cos\theta)\xi d\xi$$

in which θ, A and b are known given the approximated sinkage and trim of the ship. The unkowns are the added mass distribution, which will be discussed in the next section, the buoyancy correction coefficient a_{bf} and the cross flow drag coefficient $C_{D,c}$. Since only two equations are available one of these unknowns has to be fixed on a predetermined value. The absolute magnitude of the lift due to the cross flow drag is rather small compared with the other components, so the solution of C_m and a_{bf} was found using a known value for $C_{D,c}$. According to Shufold (57) the cross flow drag coefficient $C_{D,c}$ of a section with deadrise angle beta may be approximated by:

$$C_{D,c} = 1.33 * cos(\beta)$$

and this value has been used throughout this study.

This procedure has been used on a variety of planing boat designs of which model test data on sinkage and trim were available to yield values for Cm and a_{bf}. The main particulars of the models used are presented in the Tables 3.7 and 3.8 together with the obtained values of a_{bf} and Cm. The results are derived from the validation work carried out by Quadvlieg (67).
The obtained results using this approach show a good correlation with the results obtained by Shufold (57) for planing wedges tested at corresponding speeds and trim angles.

With the derived values for the coefficients it is also possible to approximate the load distribution over the length of the model caused by the hydrodynamic and hydrostatic lift including the cross flow effect.
This distribution for one particular case is shown in Figure 3.20. In this Figure the different contributions are shown separately.
It is evident that the hydrodynamic lift prevails in the fore part of the wetted length of the planing ship and the hydrostatic part dominates the lift force in the aft part of the ship. The lift force due to the cross flow drag component is of minor importance for the conditions under consideration, i.e. not very high for-

ward speeds and moderate trim angles.
From the formulation of the dynamic lift force it is obvious that the change of sectional added mass over the length plays an important role. Since the added mass of the sections is being related to the beam of the section at the momentaneous waterline and the beam of planing craft hulls generally decreases in the aftbody to minimise wetted area, a negative lift could occur in the aftbody using these formulations. As stated earlier Payne (48) uses a different formulation for the added mass of these sections with the wetted chine to overcome this problem. In the present formulation the negative slope of the added mass is neglected if it occurs and the hydrodynamic lift force arising from the fluid momentum set to zero for these sections.

TABLE 3.7

Model #		276	277	251	85
Deadrise	degr.	12.5	25	30	25
Length	m	1.5	1.5	1.5	1.5
Max. Breadth at chine	m	0.367	0.367	0.367	0.450
Displacement	m^3	0.0234	0.0234	0.0234	0.0273
Projected area	m^2	0.45	0.45	0.45	0.55
Position of CG in length		-4 %	-4 %	-4 %	-4.3 %
L/B		4.09	4.09	4.09	3.33
$A_\nabla/\nabla^{2/3}$		5.5	5.5	5.5	6.11
Depth of CG in neutral position	m	0.0741	0.0945	0.1041	0.1041
Trim angle in neutral position	degr.	-0.18	-0.25	-0.34	-0.11
T average	m	0.742	0.942	1.05	1.05

TABLE 3.8

$C_{D,c}$ = 1.33	Model 251	Cm	0.8526
		a_{bf}	0.6395
	Model 277	Cm	0.8473
		a_{bf}	0.7206
	Model 276	CM	1.2658
		a_{bf}	0.6239

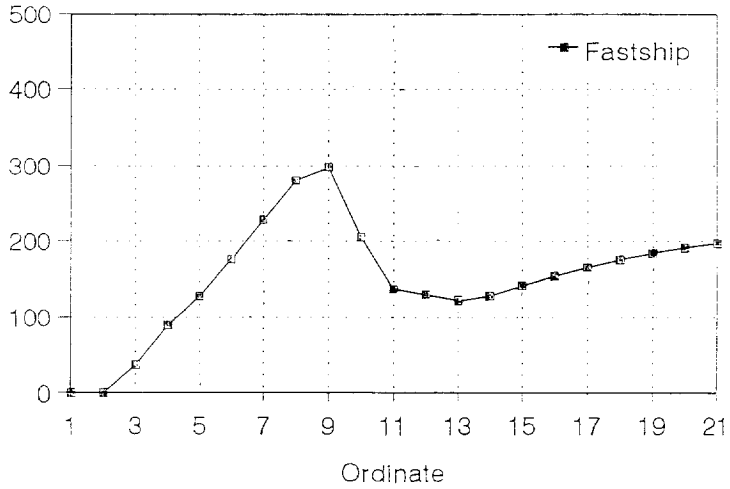

Figure 3.20: *Load distribution over the length of a planing ship. From (67)*

3.5 Distribution of the added mass and damping along the length of a ship at high forward speed

3.5.1 Introduction

The importance of an adequate formulation of the added mass distribution over the length of a ship moving at high forward speed has already been touched upon in section 2 and 5 when dealing with the determination of the hydrodynamic lift force on the planing bottom. According to this "change of fluid momentum" theory the magnitude of this hydrodynamic lift force is proportional to the change in added mass along the wetted length of the ship.

The method most commonly used for the calculation of the distribution of the added mass and damping along the length of a ship moving at forward speed is based on the so-called "ordinary strip theory". The total hydrodynamic reaction as well as the wave exciting forces are calculated by integration over the design waterline length of the ship of the 2-D cross-sectional values. These 2-D added mass and damping values are derived either by some kind of "conformal mapping" of the actual cross-sectional shape to the unit semi circle of which the analytical solution is known or by a 2-D diffraction technique. The influence of the forward speed is taken into account by a correction procedure applied to the zero speed calculations incorporating amongst others the distribution of the added mass and damping along the length of the ship.

The applicability of these linear strip theory based calculation routines for the motions of monohulls moving at high forward speeds in head waves has been shown by Blok and Beukelman (2). They measured the heave and pitch motions of 9 different models of the High Speed Displacement Hull Form Series and compared these with the results of calculations performed with an "ordinary strip theory" computer code. They found good correlation between measured and calculated pitch and heave response in regular head waves for speeds upto Froude numbers of 1.14. It should be noted, however, that this linear strip theory calculation method is pushed far beyond its generally accepted limits of applicability, in particular with respect to the forward speed.

Since Blok and Beukelman only compared motions, the question may arise whether the good correlation on the "motion-level" which they found also implied that the added mass and damping were properly predicted at these high forward speeds or that this good correlation was due to a cumulation of errors cancelling each others effect.

Therefore it was decided to carry out an extensive series of forced oscillation tests with high forward speed at the Delft Hydromechanics Laboratory of the Delft University of Technology. These experiments have been carried out with

the parent model of the High Speed Displacement Hull Form Series similar to the one used by Blok and Beukelman in their study. This High Speed Displacement Hull Form Series was a long term fundamental research project aimed at optimising resistance and seakeeping characteristics of fast frigate type monohulls carried out at MARIN, Wageningen, and has been jointly sponsored by the Royal Netherlands Navy, The Royal Australian Navy, the David Taylor Research Centre (USA) and MARIN.

The main objective of the oscillation experiment was to determine the hydromechanic coefficients of this model moving at high forward speed and in particular the distribution of the added mass and the damping over the length of the model and to compare these with the results of calculations using the linear strip theory type approximations.

3.5.2 The model and measurement set-up

The experiments have been carried out in the #1 towing tank of the Delft Shiphydromechanic Laboratory of the Delft University of Technology. The dimensions of this tank are: length 142 meters, width 4.22 meters and the waterdepth during the experiments was 2.5 meters.

The parent model of the High Speed Displacement Hull Form Series was selected as a model for these experiments for the following reasons, i.e:

- all data on measured resistance, trim and sinkage at speeds upto Fn = 1.14 were available and kindly put to our disposal by the participants in the HSDHF Series, as well as all data on the heave and pitch motions of the model in regular head waves.

- from the computational results derived by Blok and Beukelman it may be concluded that for this model the calculation of the motions in waves yielded good results using the linear strip theory approach even at the highest Froude number of Fn = 1.14.

The main particulars of the model are presented in Table 3.9.

Since in the determination of the dynamic lift the distribution of the added mass over the length of the model plays such an important role and because two different versions of the strip theory exist each taking a different approach to the speed influence on the distribution of the added mass and damping over the length of the model, it was felt to be of importance to measure the distribution of these quantities over the length of the model.
So the tests have been performed with two versions of the same model, i.e.: one unsegmented model and one segmented model. The unsegemented model was a rigid monocoque model constructed from glass fibre reinforced polyester

as customary for tests in the Laboratory.

TABLE 3.9

length test waterline	2.00	m
beam test waterline	0.25	m
draft	0.0624	m
displacement	0.01248	m^3
length-beam ratio	8.0	
beam-draft ratio	4.0	
block coefficient	0.396	
cross section coefficient	0.633	
LCB in % of Lwl	-5.11 %	
LCF in % of Lwl	-8.68 %	

The segmented model was the same but now devided into seven "sections" of equal length, yielding seven sections with a length of 0.285 meters. Each of the segments was provided with a watertight bulkhead at the front and at the rear, making it a watertight box. Each segment was connected to a strain gauge type dynamometer measuring only the vertical forces on that particular segment. The resulting total of seven dynamometers were rigidly mounted on a stiff steel girder extending over the total length of the model and being the "backbone" of the model whilst keeping each particular segment on its predetermined position to constitute the "complete" model. The separation between the segments was approximately of 0.0005 meter. On top of the first girder a second steel girder was placed to provide for the connection to the pushing rods of the vertical oscillator.

The oscillator of the Laboratory used for the experiments consists of two mechanical oscillators of the "scotch-yoke" type, which perform pure sinusoidal vertical motions with frequencies ranging from ω = 1 rad/s to ω = 20 rad/s with an amplitude ranging from 0.0 to 0.10 meter. The distance between the two oscillating pushing rods is 1.0 meter. The phase of the motion of the two pushing rods of the oscillators with respect to each other may be varied to impose either a pure heave or a pure pitch motion on the connected model. The oscillator was connnected mechanically to an electronic measurement system, consisting primarily of a series of resolver sets, by which its is possible to measure the in-phase and quadrature component of the reaction forces between the segments and the oscillator. The in-phase and quadrature component were determined using the vertical displacement of the model as a reference. In addition, a harmonic analysis has been performed directly on the force signals of each of the dynamometers, yielding the same outcome.
Great emphasis was placed on the rigidity and stiffness of the construction as a whole, assuring resonance frequencies of the complete set-up and the individual

segments well away from the frequency range used during the experiments as well as a fixed position of the segments relative to each other.
Prior to the actual oscillation measurements a series of additional measurements was carried out to establish whether the goals of these efforts had been achieved. These proved to be successful.

An impression of the segmented model may be obtained from the following photograph.

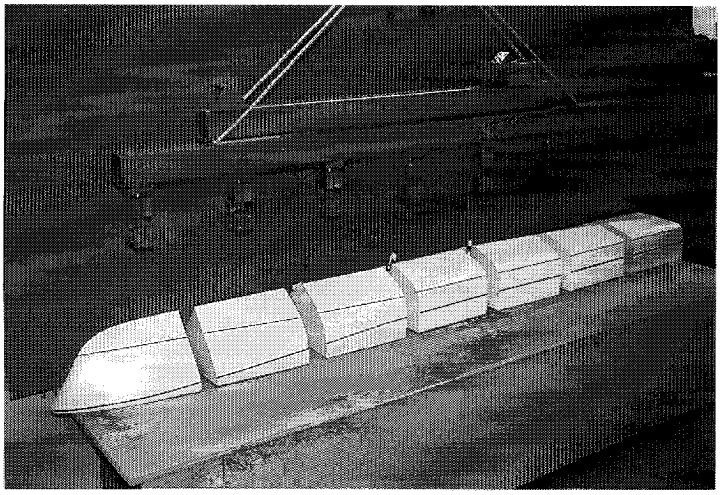

Figure 3.21: Photograph of the segmented model

The unsegmented model has only been used to check the accuracy of the results obtained with the segmented model. Integration of the sectional values obtained with the segmented model should yield the same results as those obtained from the unsegmented model as a whole. Comparison of both results enabled quantitative assessment of the possible influence of the small gaps between the segments on the pressure distribution around the model. From these comparisons for both the oscillation tests and the wave force measurements was concluded that there was no measurable influence from the gaps on the overall results. Also, by visual observation during the experiments no "leakage" effects arising from these gaps could be observed.

The force signals of each segment measured during the tests were decomposed in the afore mentioned in-phase and quadrature component with respect to the motion. From these the well-known expressions for the added mass and the damping in heave for each section have been derived using the commonly used method. The sectional values have been obtained by normalisation using the segment length.

The equations used for the elaboration of the measured in-phase and quadrature force components in the hydrodynamic mass and damping are:

$$a'_{zz} = \frac{1}{z_a\,\omega^2}\,(\,F_{inphase}\;c'_{zz}\;z_a\,) - \rho\,\nabla$$

$$b'_{zz} = \frac{1}{z_a\,\omega}\,(\,F_{quadrature})$$

In which:

a'_{zz}	=	sectional added mass
b'_{zz}	=	sectional damping
c'_{zz}	=	hydrostatic restoring force of the section
z_a	=	oscillation amplitude
ω	=	frequency of oscillation
$\rho * \nabla$	=	mass of the section

The dependency of the sectional c'_{zz} on the amplitude of oscillation is evident but may be approximated as being constant if the oscillation amplitude does not exceed 0.01 m.
The mass of each of the seven segments of the model have been measured by carrying out an oscillation experiment with the model suspended in air.
The sectional hydrostatic restoring coefficient C_{zz} of the model as a whole and of each individual section has been measured. This has also been done with the model in the two different reference positions but both with zero advance speed to coincide with the standard calculation and measurement procedure. The results of these measurements are presented in Figure 3.22.

Finally for all reference positions and corresponding speeds of advance the wave profile along the length of the model has been measured. Care has been taken to define the local height of the solid waterline at speed without the disturbing influence of the spray. The goal of these measurements was to investigate whether the introduction of the actual waterline of the craft under speed would have a significant effect on the calculation of sectional added mass and damping. This will be discussed in more detail in the section dealing with the analysis of the results. The measured wave profiles are presented in Figure 3.23.

3.5.3 The measurement scheme

The experiment consisted of a series of vertical oscillation tests covering the whole frequency range of interest for a high speed craft in head waves, i.e. ω = 4 to ω = 15 rad/s and were performed at two different speeds, corresponding to Fn = 0.57 and Fn = 1.14. During the tests two different oscillation amplitudes were used, i.e z_a = 0.01 and z_a = 0.02 meter.

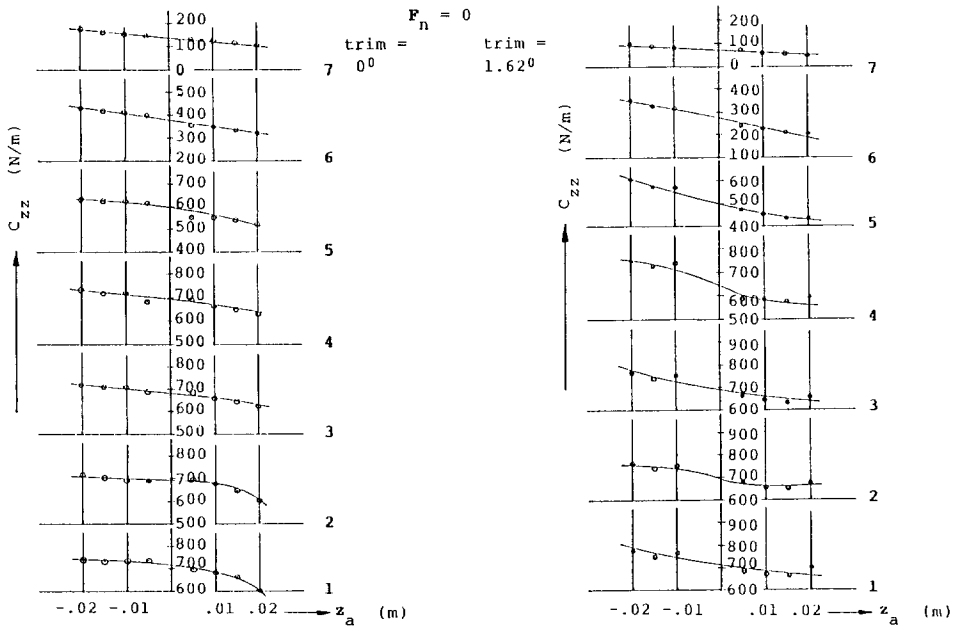

Figure 3.22: Sectional C_{zz} at Fn = 0 and two different reference positions

As will be discussed in the part containing the analysis of the results, these tests were performed at different reference positions of the craft. The reference position is the position of the model at zero amplitude of oscillation. The different reference positions used were:

- the reference position at zero speed without sinkage and trim
- the reference position at speed with the correct sinkage and trim

The first reference position is derived from the linesplan and corresponds to the model on its design waterline. This is the usual reference position at which oscillation tests are carried out.

The second reference position is the position which the free running craft at speed would assume. The precise values of the sinkage and trim of the model at the two particular speeds under consideration were derived from the experimental data as presented by MARIN.

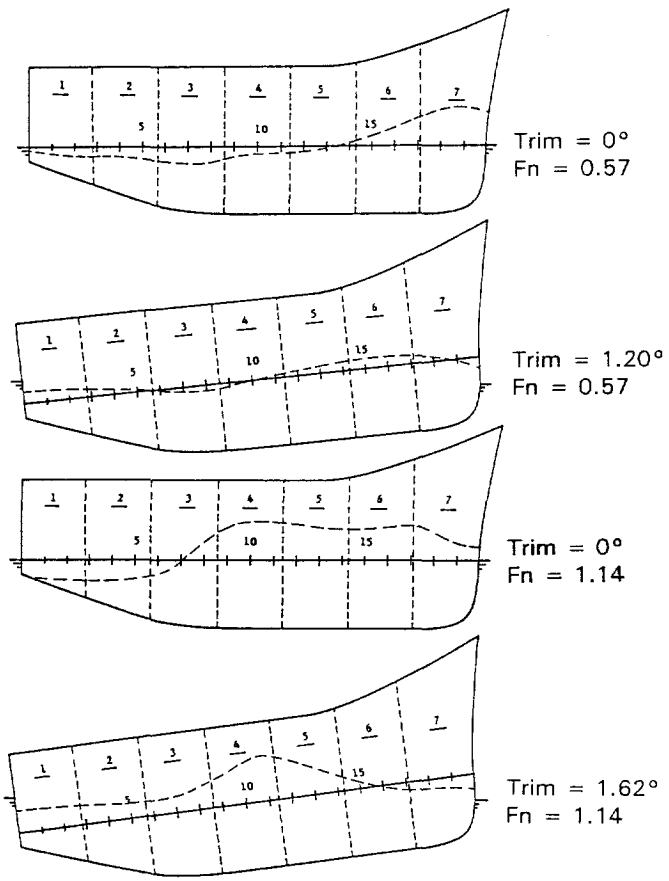

Figure 3.23: *Measured wave profile along the length of the model at three different speeds in still water*

An additional series of tests has been carried out to measure the hydrodynamic lift distribution along the length of the model at speed.

3.5.4 Results

The measurements were evaluated in the usual way to yield the added mass and damping values of each segment. These results are presented in the Figures 3.24 to 3.27.

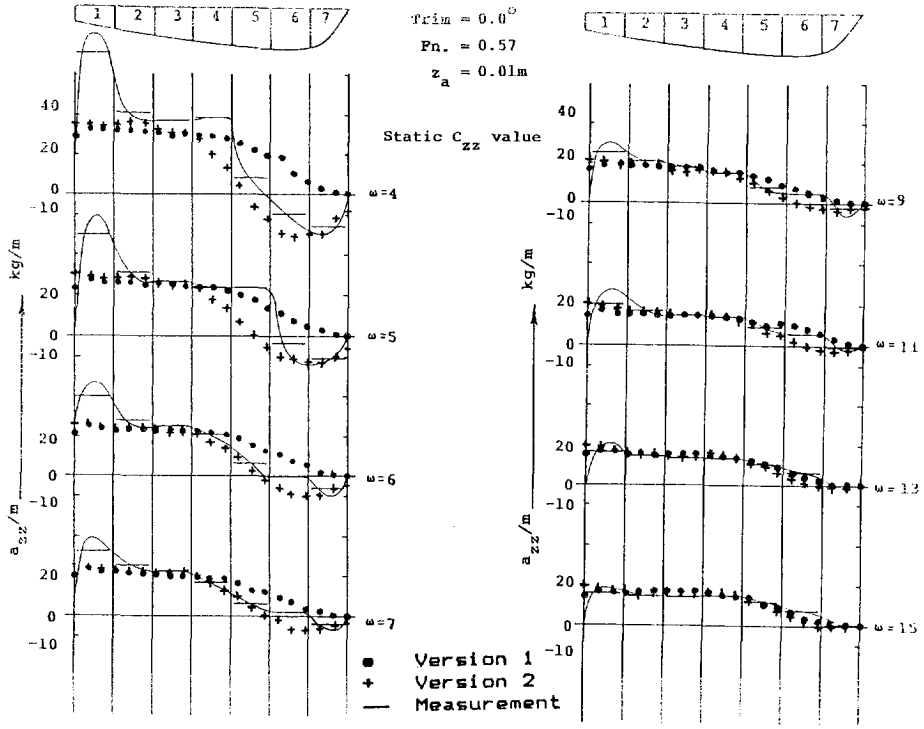

Figure 3.24: Added mass distribution at Fn = 0.57. No trim!

When analysing these figures it should be noted that the actual added mass and damping are being averaged along the length of the segments. These values are indicated in the figures by the straight lines over the length of the segments.
The curves of the solid lines which have been drawn through these lines is a "best estimate" of how the distribution may look like over the length of the model taking into account that the integrated (averaged) value should correspond to the area underneath the straight line.
The results of the in-phase component of the hydrodynamic reaction force in these figures has been evaluated by using the static value of the C_{zz} coefficient, i.e. the value found at zero forward speed both in the still water reference position without trim and sinkage as in the reference position corresponding to the position of the craft at speed with regard to sinkage and trim, but again measured with zero forward speed.

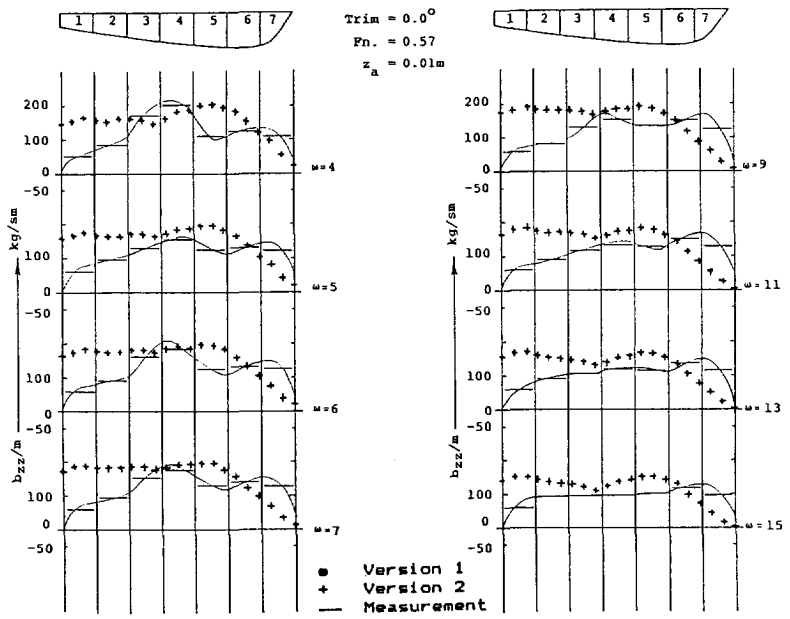

Figure 3.25: Damping distribution at Fn = 0.57. No trim!

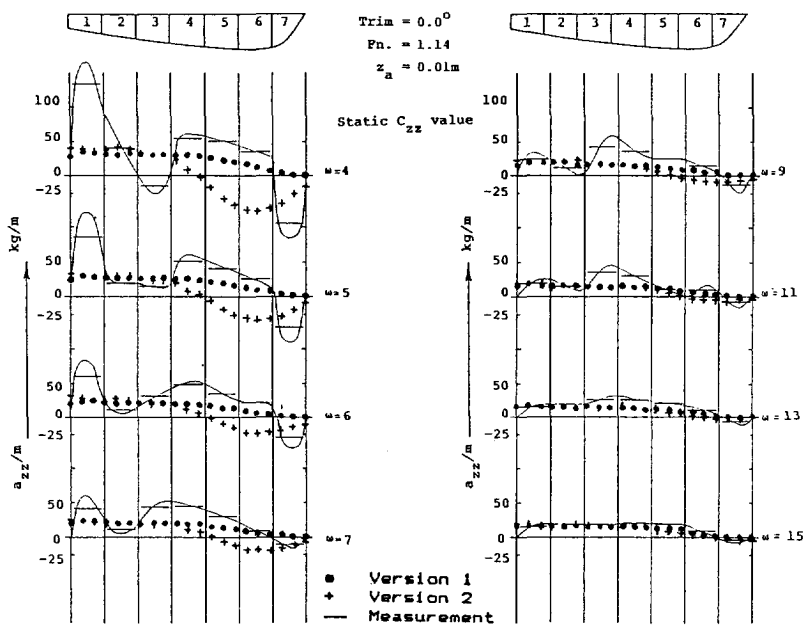

Figure 3.26: Added mass distribution at Fn = 1.14. No trim!

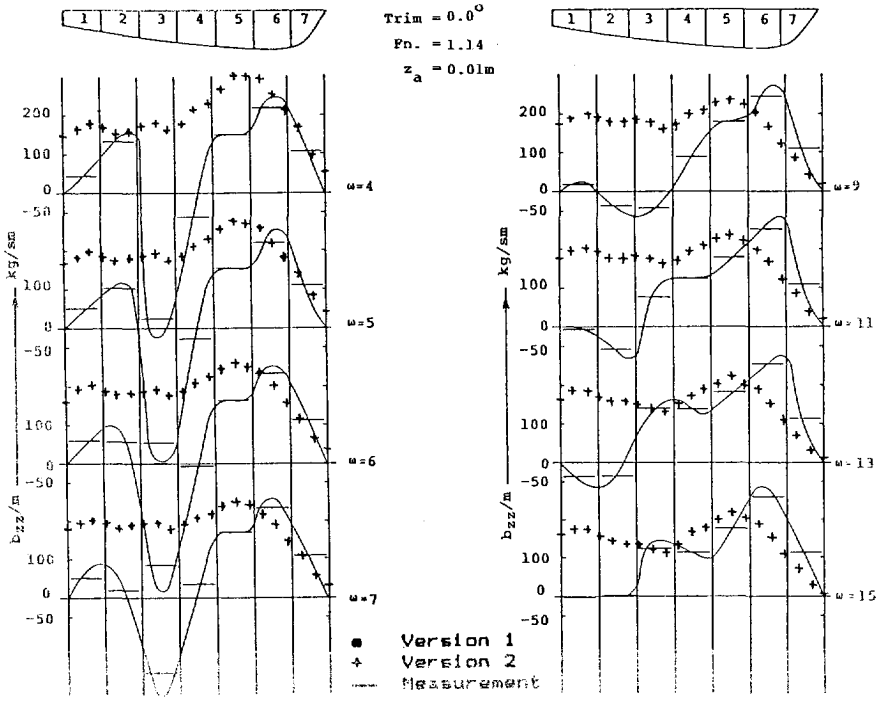

Figure 3.27: Damping distribution at Fn = 1.14 No trim!

3.5.5 Numerical computations

The measuered added mass and damping properties of the entire model and the distribution along the length of the model, using the sectional data of the segmented model, have been compared with the results of numerical computations, using a linear strip theory method. Using this method the two-dimensional approximation of the linear velocity potential is calculated and herewith the hydrodynamic or added mass and the damping for a total of 20 (or more) sections. This is done by conformal transformation of the actual section to the unit circle of which the analytical solution as derived by Ursell (66) for an oscillating cylinder at the free surface is known. The transformation formula is given by:

$$W = a \{ \zeta + \sum_{n=o}^{N} a_{2n+1} \zeta^{-(2n+1)} \}$$

For n = 2 the so-called "Lewis" transformation is obtained which in general yields results with satisfactory accuracy. The "Lewis" transformation determines the ship cross-section by its beam to draft ratio and the sectional area coefficient. The procedure for this transformation of the shiplike cross-section

has been described by Tasai (61). The same procedure has been used by Blok and Beukelman when they calculated the motions of this model. A more detailed description of the actual shipsection may be obtained by the "close fit" transformation method for which case the value of N = 5 in the presented transformation formula. The results of this transformation technique for the model under consideration yielded no significant improvement of the outcome of the added mass and damping calculations when compared with the "Lewis" transformation.For the sections in the after body of the model also a two-dimensional diffraction technique known as the "Frank-close-fit" method has been used because of the high beam to draft ratio of these sections. In the figures presented hereby the "Lewis" transformation technique has been used with the exception of the last 4 (out of a total of 21 sections) in the after body of the model for which the "Frank-close-fit" technique has been used.
In the linear strip theory two approaches exist which result in a different formulation by which the influence of the forward speed on the distribution of added mass and damping is been taken into account:

- *Version 1,* best known as the Ordinary Strip Theory Method.

This is a somewhat intuitive approach based on the work of Korvin Kroukovsky. The coefficients of the resulting equations of motion are presented in section 3.2. It uses a set of coefficients which lacks some of the symmetry relations in the mass coupling coefficients. In this version the speed influence is taken into account only for distribution over the length of the ship of the damping by introducing the derivative of the added mass over the shiplength. This is done by the term: V * dm'/dx in the calculation of the damping. The distribution of the added mass along the length of the ship is not influenced by the forward speed of the ship.

- *Version 2,*

This is a more fundamental approach in which the hydrodynamic force on the strip is calculated using:

$$F_h' = \rho * \int_S \left(\frac{d}{dt} - V \frac{d}{dx} \right) (V_z \varphi) \cos(n, z) \, ds$$

in which: $V_z\varphi$ = velocity potential as function of the position on the ship
S = ships wetted surface
n = normal vector on the ship surface

By writing:

$$\rho \int_S \varphi \cos(n, z) \, ds = \rho \int_S \varphi \frac{d\varphi}{dn} \, ds = -m'(x) + \frac{i}{\omega_e} N'(x)$$

this may be elaborated into:

$$F'h = - \left(\frac{d}{dt} - V \frac{d}{dx} \right) \left(\left(\dot{z} - x_b \dot{\theta} + V \theta \right) * \left(m' - \frac{iN'}{\omega_e} \right) \right)$$

yielding :

$$F'h = - a'\ddot{z} - b'\dot{z} + d' \ddot{\theta} + e' \dot{\theta}$$

in which:

$$a' = m' + V/\omega_e^2 \, dN'/dx_b$$

$$b' = N' - V \, dm'/dx_b$$

$$d' = m' x_b + 2 V/\omega_e^2 N' + x_b V/\omega_e^2 \, dN'/dx_b - V^2/\omega_e^2 \, dN'/dx_b$$

$$e' = N' x_b - 2m' V - V x_b \, dm'/dx_b - V^2/\omega_e^2 \, dN'/dx_b$$

For the present study the difference in the added mass distribution along the length of the ship with respect to version 1 is the introduction of the derivative of the sectional damping over the length.

A more detailed description of the theory behind both versions has been presented by Gerritsma, Beukelman and Glansdorp at the ONR Symposium 1974 (17).

Blok and Beukelman found in their study that generally spoken the agreement between the calculated results using Version 1 compared better with the measurements than those using Version 2, although Version 2 is theoretically more suited for the high speed application.

In the present study the linear strip theory calculations have been carried out with the computer code "SEAWAY" described in Reference (25) capable of producing results according to both approaches. The computations have been carried out with the model in both its still water reference position and the reference positions with the proper sinkage and trim corresponding to the particular speed under consideration. Also the wave profile along the length of the hull as measured during the tests has been brought into the calculations when that was considered to be appropriate. This will be discussed in more detail in the following section. The restoring force coefficients used in these calculations are based exclusively on the waterline area of the sections and no forward speed effects are taken into account here.

3.5.6 Discussion of the results

3.5.6.1 Untrimmed reference position

For verification of the calculation method used by Blok and Beukelman the results presented in the figures 3.24 to 3.27 need to be considered. These show the results of the added mass and damping in the no trim reference position at both forward speeds. For the elaboration of the added mass from the measured force signals the "static" (no speed) hydrostatic restoring force coefficient C_{zz} has been used. From these figures the following observations may be made:

- *At Fn = 0.57* the correlation between the measured and the calculated results of the added mass is reasonable, especially, when the results of the calculations using Version 2 are considered. These calculations adequately predict the "negative added mass" at the forebody. At the lower frequencies large deviations do occur at the aft sections, however. At the higher frequencies the correlation between the measured and calculated values is good. For the damping the correlation is worse at all frequencies except for the highest, in which case the correlation appears to be reasonable.

- *At Fn = 1.14* the agreement between the calculated and the measured added mass is poor for both Versions, except for the highest frequencies for which the correlation is good. The correlation between the measured and calculated damping, however, remains poor over the whole frequency range.

The measurements at Fn = 1.14 show a pronounced negative peak in the damping at section #3, which increases considerably with decreasing frequency of oscillation. From a physical point of view this phenomenon is not understood and its occurrence certainly not anticipated. Also the damping of the sections in the after body is considerably smaller than would be expected considering the relatively large beam to draft ratio of these sections. The calculated values for the damping of these sections are considerably larger. It was questioned whether these phenomena originated from possible shortcomings in the measurement technique or setup used.

One possible shortcoming could be the use of not sufficiently small amplitudes of oscillation considering the size of the model. The results of the tests with 0.01 and 0.02 meter amplitude of oscillation showed excellent consistency however.

Another source of inaccuracy could be the fact that the tests at the highest Froude number Fn = 1.14 were performed at a speed of the towing carriage of 5.04 meter/second which is quite close to the critical speed at the waterdepth in the towing tank during the experiments of 2.5 meters. Therefore the complete series of tests performed at the highest Froude number of Fn = 1.14 have

been repeated in the facilities of MARIN at Wageningen but now in a towing tank with a waterdepth of 5.0 meter. The results of both tests, i.e. with a waterdepth of 2.5 and 5.0 meter, coincided within a few percent for all frequencies investigated both for the damping and the added mass. So it may be concluded that the waterdepth during the tests has not influenced the results.

Blok and Beukelman found that the results of their calculations of the ship motions correlated well with the experimental results. Hence also a good correlation between the measured and the calculated hydrodynamic coefficients was anticipated. This good correlation on the motion "level" can be partly attributed to the fact that the high forward speed implies high frequencies of encounter with the oncoming waves and from the results of the oscillation experiments shown it may be concluded that the correlation between measured and calculated hydrodynamic coefficients increases with increasing frequency of oscillation. No information is available yet about the degree of correlation between calculated and measured motions at lower encounter frequencies (and high speeds!). For practical purposes, however, these lower frequencies are of minor importance, because the response of the ship to these frequencies is not significant when the operability of a fast ship in head waves has to be determined.
They also concluded that the results of the computations using Version 1 compared better with the measurements than those obtained using Version 2.

From the results shown from the present study on the correlation between the measured and calculated hydrodynamic coefficients this is not completely obvious. On the contrary : from the results shown here it could be concluded that Version 2 should yield better results although the discrepancies between the calculations using both versions decreases with increasing frequency of oscillation. It should be noted also that the actual motion calculation incorporates more than just the added mass and damping and also the correlation of, for instance, the wave exciting forces under those conditions is of interest.

3.5.6.2 Trimmed reference position

When considering ships moving at high forward speed it is known that these may experience a considerable change in their position in the water due to the change in the pressure distribution around the hull. This change in position is usually referred to as sinkage and trim. So when analysing the behaviour of ships at high speed in waves it appears to be more appropriate to include the sinkage and trim instead of using the zero speed position.
During the oscillation tests when using the no trim reference position some peculiar phenomena did occur, in particular, at the stern and the bow with the model at the highest speed. A very large bow wave occurred at the bow and the immersion of the aft section became minimal, which effect was even endorsed by the oscillatory motion itself.

Therefore the oscillation tests at both speeds have been carried out also with the model in its proper reference position.
The following observations may be made from the results of these experiments:

- *At Fn = 0.57* the added mass seems to be adequately predicted by the results of the calculations using Version 2 and the correlation between measured and calculated damping is good. The measured added mass appears only slightly influenced by the introduction of the proper sinkage and trim. The measured damping although not shown here, however, is strongly influenced and increases considerably in particular at the aft sections of the model.

- *At Fn = 1.14* the discrepancy between the calculated and measured added mass is still considerable, in particular at the lower frequencies and the aft sections. However, the high negative peak in the measured damping disappears when the proper sinkage and trim is introduced into the measurement procedure. The results of Version 2 correlate better because they predict the negative added mass of the fore sections in contradiction to Version 1. This discrepancy diminishes with increasing frequency of oscillation.

In general the improvement in the correlation between the measured and calculated results due to the introduction of sinkage and trim may be mainly attributed to the change in the measured results, which changes are considerably more pronounced than the change in the results of the calculations. This may however strongly depend on the specific hull geometry under consideration.
These results and the comparison with calculations using the strip theory, which were performed with the model in its proper reference position also, are presented in the Figures 3.28 and 3.29. From these it may be concluded that the correlation is significantly increased.

3.5.6.3 Introduction of the actual restoring force

As may be seen from the equations by which the measured in-phase forces on the model are elaborated, the hydrostatic restoring force is an important component in the determination of the added mass of the ship or the section. In the oscillation technique it is common practice to use the values of these forces by determination of the hydrostatic restoring force coefficient C_{zz} obtained either by hydrostatic calculations or static measurements on the model. This is carried out without taking into consideration the change in reference position of the model due to sinkage and trim and at zero speed of advance. For moderate speeds upto Fn = 0.35 this has always proved to be a justifiable simplification. Even for the relatively high Froude number of Fn = 0.57 under consideration in the present study, this procedure still works reasonably well judged from the correlation between the measured and calculated values of the added mass.

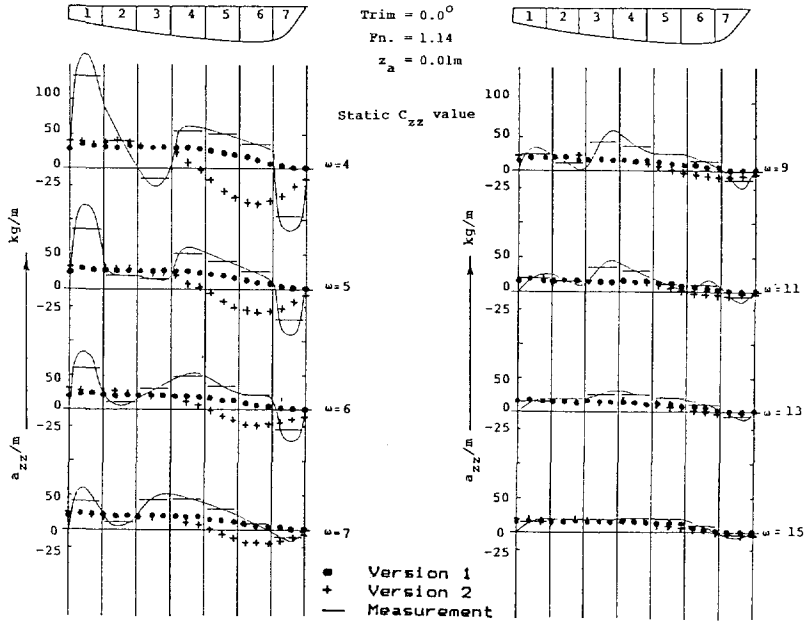

Figure 3.28: Added mass distribution Fn = 0.57. With trim.

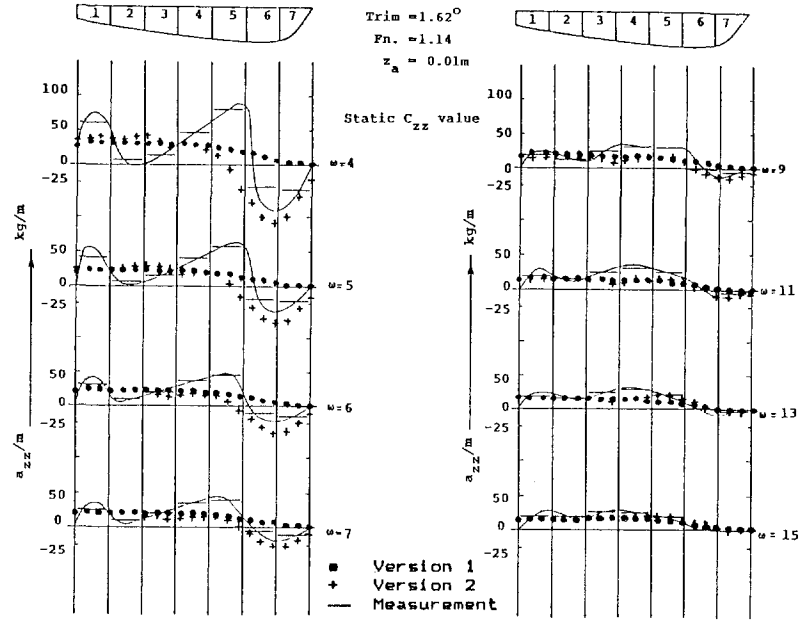

Figure 3.29: Damping distribution Fn = 0.57. With trim.

From a theoretical point of view however it may be questioned whether this is a proper approach. At high forward speeds the "hydrostatic" restoring force will change almost certainly due to the change in pressure distribution along the length of the hull moving at high forward speed.

This may be even more evident in the case of the determination of the sectional C_{zz} value of a segmented model, because pressure peaks may be present at particular parts of the model. It has been a discussion in the field of the strip theory, whether the forward speed influence used in the calculations takes into account anything that originates from the fact that the forward speed is not equal to zero or that the added mass and damping are solely the components of the hydrodynamic reaction force due to the oscillatory motion of the ship alone. In that case additional forces have to be introduced which originate from the steady state forward speed condition of the ship and the hydrostatic coefficient C_{zz} has to be determined with the ship at speed.

Thes latter procedure is the approach used in the calculation model presented in this present study: the pressure distribution along the length of the model originating from its high forward speed is taken into account as a separate component of the hydrodynamic reaction force in the equations and the added mass and damping are considered to originate solely from the oscillatory motion.

To test this hypothesis additional tests have been carried out with the segmented model at the highest Froude number of Fn = 1.14, in which condition the results of this approach should be the most evident. At this Froude number the forces due to the vertical displacement of the model from its reference position have been separated from the forces due to the vertical motion of the model. This has been done by measuring the vertical force on each segment of the model at a speed corresponding to Fn = 1.14 caused by the vertical displacement of the model from its reference position in steps of 0.0025 meter in a quasi steady way.

$$Fz\ (static) = F\ (x,z)\ at\ \omega = 0 \qquad V = 5.04\ m/s$$

By displacing the model vertically both upwards and downwards from its reference position with steps of 2.5 millimeter the "static" forces Fz on each segment due to the displacment z at forward speed were known over the trajectory of the vertical displacement covered by the model during the oscillation tests carried out with an amplitude of oscillation of 10 millimeter. These measurements have been carried out both with the model in its still water reference position and in the reference position with the proper sinkage and trim at Fn = 1.14.

The results of these measurements are presented in Figure 3.30 and Figure 3.31.

From these figures the change in the vertical force on each segment due to the vertical displacement of the segment is obvious and differs considerably from the values obtained at zero forward speed. Also, the introduction of sinkage and trim has a marked influence on the results. In particular, in the trimmed position the force distribution over the aft segments is remarkable and the nature of this fluctuation may be due to the fact that the chosen values for sinkage and trim do not correspond exactly to the condition chosen. However, this will not influence the investigation into the validity of the hypothesis since the oscillation experiment covers exactly the same range of vertical displacements.
In order to obtain the added mass using these data on Fz the following procedure has been followed:

- the vertical reaction force on each segment due to the vertical displacement z of the section, (Fz "static"), has been approximated by a least square fit procedure to obtain this Fz "static" as a continous function of the displacement z using the measured data as an input.

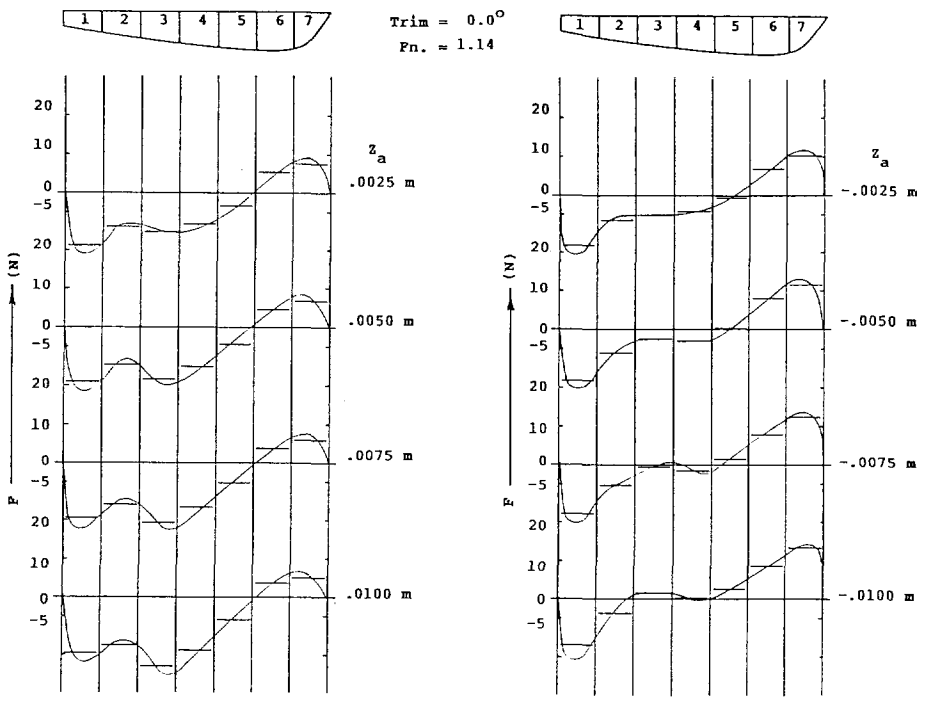

Figure 3.30: Force distribution along the length of the model at Fn = 1.14 due to vertical displacement Z_a. No trim

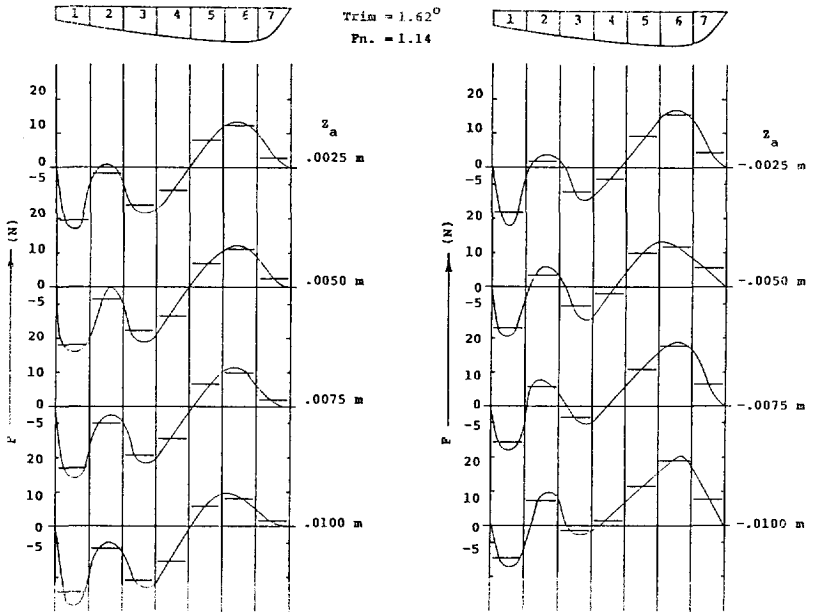

Figure 3.31: Force distribution along the length of the model at Fn = 1.14 due to vertical displacement Z_a. With trim.

- the force signals of the dynamometers on each segment as obtained during the measurements have been digitized at a rate of 500 samples per second during a predetermined number of cycles. This yielded:

$$Fz\ (dynamic) = Fz(x,\ z,\ \frac{dz}{dt},\ \frac{d^2z}{dt^2},\ t)\ \omega \neq 0 \qquad V = 5.04\ m/s$$

- From these signals the "static" Fz due to the displacement z has been subtracted using a simple time domain calculation routine, yielding:

$$Fz\ (corr),t) \quad = \quad Fz\ (dynamic) - Fz\ (static)$$

- the resulting force signals Fz (corr) have been split in the usual in-phase and quadrature component with respect to the vertical displacement.

The results obtained by using this procedure are presented in the Figures 3.32. The results of the calculations presented in these figures are those obtained with the use of Version 1, which means no speed influence in the added mass. From a comparison with the results obtained using the static C_{zz} the change in "measured" added mass distribution is evident:

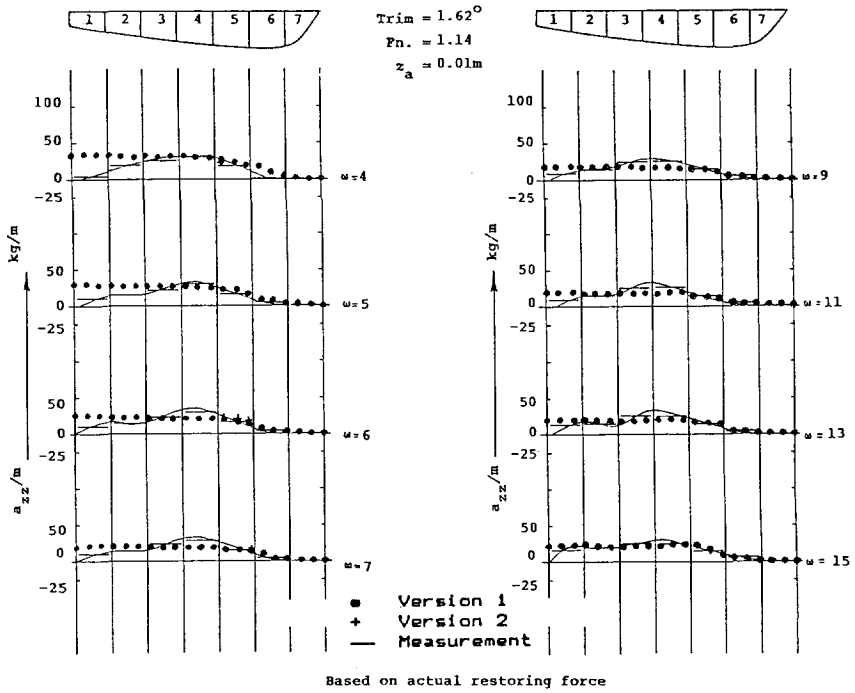

Figure 3.32: Added mass distribution at Fn = 1.14 using the actual restoring force. With trimmed reference position.

In the trimmed reference position the distribution of the added mass over the length of the model is rather smooth. The differences with the added mass measurements using the static C_{zz} are obvious, in particular the disappearance of the negative added mass phenomenon. For the higher part of the oscillation frequencies under consideration the distribution of the added mass along the length of the model, both quantitatively as qualitatively, becomes almost independent of the oscillation frequency.
The correlation with the calculated values is largely improved, although at the lowest frequencies the calculated added mass remains significantly higher than the measured added mass.

From these results it may be concluded that the sectional added mass is not strongly influenced by the oscillation frequency in the range of interest for a fast moving monohull. Its distribution along the length of the ship is hardly influenced by the forward speed of the craft if the stationary hydrodynamic forces associated with the high forward speed are considered separately.

3.5.6.4 Damping distribution

Obviously, the measured damping is not affected by this new approach, because only the in-phase forces are corrected by the forces related to the vertical displacement z.
However, in the formulation of the forward speed influence in the strip theory method the distribution along the length of the added mass influences the distribution of the damping, because herein the derivative of the added mass with respect to the length of the ship is taken into account. The influence of this derivative on the damping distribution is rather important because it is multiplied with the forward speed of the ship to yield the correction on the damping distribution found at zero speed and in the present situation with the high speed ship the forward speed is rather high.

Since the calculated and measured distribution of the added mass show some discrepancies and therefore the derivative with respect to the length will differ, it is of interest to investigate how the distribution of the calculated damping is influenced. When either the measured or calculated added mass distribution is used.
This calculation has been performed for three different frequencies of oscillation and the results are shown in Figure 3.33.

From these figures it may be seen that the correlation between the measured and calculated damping distribution improves considerably when the measured added mass distribution is put into the calculations. In particular the character of the distribution over the length is in good agreement. It should be noted that these results are sensitive to the chosen added mass distribution curve which is drawn through only seven measured data points and therefore is not undisputable.

The correction due to the forward speed influence of the 2-D sectional damping distribution calculated with zero forward speed through the use of the lengthwise derivative of the added mass, as described in Version 1 of the strip theory method, appears to be validated by these results.

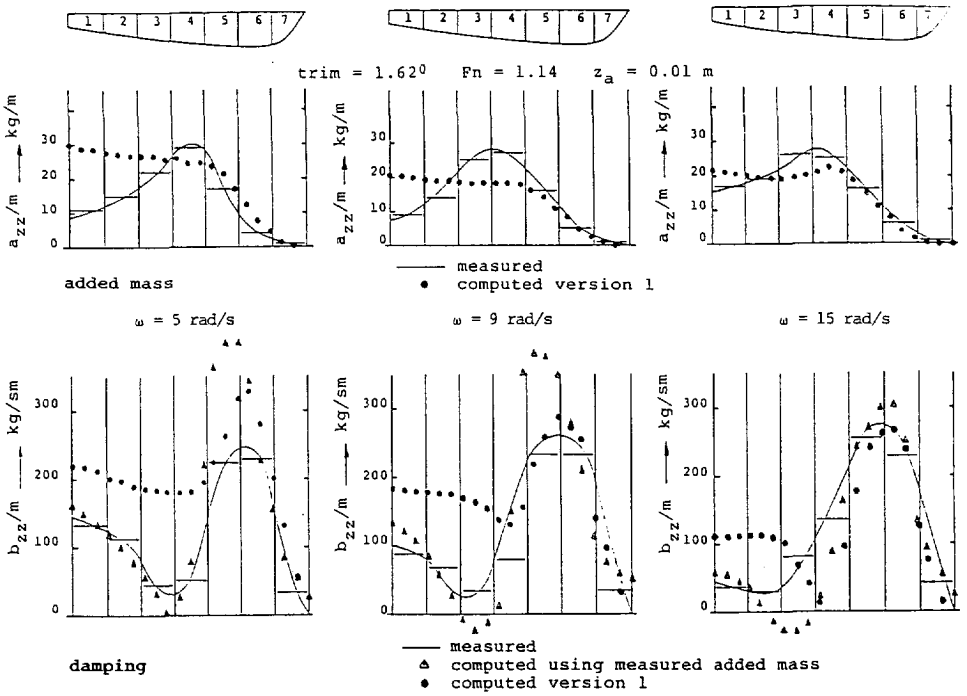

Figure 3.33: Effect of added mass distribution on the damping distribution at Fn = 1.14

3.6 Wave force measurements

3.6.1 Introduction

The intention of this part of the present study is to demonstrate that the wave exciting forces on a fast monohull may be approximated by using the Froude Kriloff component only, i.e. the integrated pressure over the ship hull arising from the undisturbed oncoming wave. If this approximation is justified then the nonlinearities in the wave exciting forces due to the large relative motions of the ship in head waves and the large changes in submerged volume of the hull may be taken into the computational model.

3.6.2 Measurement Set-up

To check the hypothesis that the wave forces of interest for fast ships are Froude Kriloff dominated, an experiment was set-up. In this experiment the same segmented model as used for the previously described oscillation measurements was used to determine the wave exciting forces and their distribution along the length of the model at high forward speed.
During these experiments the model was restrained in all modes of motion whilst being fixed in position by means of the vertical oscillator. In all other respects the measurement set-up was identical to the one in the previously described oscillation experiment.
The tests have been carried out with the model towed at the same two forward speeds as used in the oscillation experiment, i.e. Fn = 0.57 and Fn = 1.14 respectively. At each speed a range of wave lengths was used varying from λ = 1.40 meter to λ = 6.5 meter, yielding a variation in the wavelength to shiplength ratio from 0.6 to 3.0 approximately.

For each wavelength two different wave heights have been applied to obtain a check on the linearity of the exciting forces with respect to waveheight.

3.6.3 Results

The results of these measurements have been elaborated to yield the vertical wave force per meter wave height per unit length of the model, i.e. :

$$Fz\ (section) / (\zeta * section\ length)$$

The results obtained with the model in the trimmed reference position are presented in Figure 3.34 for both speeds investigated. These are presented in the figure by the solid and straight lines indicating an average of the force per meter over each segment.

3.6.4 Numerical Results

In the figures 3.34 and 3.35 also the results of numerical computations using the two dimensional linear strip theory have been plotted. These calculations have been made using the code SEAWAY as described in Reference (25). In the calculations a total of 21 sections has been used.

In the strip theory the vertical wave exciting force on the ship as a whole is found by integration over the length of the sectional waveforces.
In the Ordinary Strip Theory Method this wave exciting force for heave on a re-

trained cross-section of a ship in waves is given by:

$$K'_{w3} = +FK'_3 + \frac{D}{Dt}\left[M'_{33} * \dot{\zeta}_{w3}{}^* \right] + N'_{33}\,\dot{\zeta}_{w3}{}^*$$

$$= +FK'_3 + M'_{33}\,\ddot{\zeta}_{w3}{}^* + \left[N'_{33} - V\frac{dM'_{33}}{dx_b} \right]\dot{\zeta}_{w3}{}^*$$

in which FK_3 stands for the Froude Krilov force on the section in the vertical direction, i.e.:

$$FK'_3 = -\int_{-T}^{\zeta}\int_{-y_b}^{+y_b} \frac{\partial p}{\partial z_b}\,dy_b\,dz_b = +\rho\int_{-T}^{\zeta}\int_{-y_b}^{+y_b} \left(g + \ddot{\zeta}'_{w3} \right) dy_b\,dz_b$$

in deep water this is approximated by:

$$FK'_3 = \rho * \left[\frac{-2y_w}{k} * \frac{\sin(-ky_w \sin\mu)}{-ky_w \sin\mu} + A_{sh} \right] (-k\zeta_a\, g) \cos(\omega_e t - kx_b \cos\mu)$$

$$A_{sh} = 2\int_{-T}^{0} \frac{\sin(-ky_b \sin\mu)}{-ky_b \sin\mu}\,\frac{\sinh k(h + z_b)}{\cosh kh}\,y_b\,dz_b$$

When expanding the Froude Krilov force in deep water with $\lambda >> 2\pi * y_w$ and $\lambda >> 2\pi$ T in series, it is found:

$$FK'_3 = \rho\left[\left(\frac{-2y_w}{k} \right) + \left(A + S_y k + I_y * \frac{1}{2}k^2 + \ldots \right) \right] *$$

$$(-k\zeta_a\, g) \cos(\omega e_t - kx_b \cos\mu)$$

yielding:

$$FK'_3 = 2\rho g y_w \zeta + \rho A\,\ddot{\zeta}^*_{w3}$$

with:

$$\zeta_{w3}{}^* = (-k\,\zeta_{a3}{}^*\, g) * \cos(\omega_e t - kx_b \cos\mu)$$

$$\ddot{\zeta}_{w3}{}^* = \left(+k\,\zeta_{a3}{}^* \frac{g}{\omega} \right) * \sin(\omega_e t - kx_b \cos\mu)$$

For the total sectional vertical wave exciting vertical force it then follows:

$$X_{w3} = +\int_L FK'_3\,dx_b + \int_L M'_{33}\,\ddot{\zeta}_{w3}{}^*\,dx_b +$$

$$\frac{+V}{\omega\ \omega_e}\int_L \frac{dN'_{33}}{dx_b}\,\zeta_{w3}^*\ dx_b\ +$$

$$+\int_L \left[\ \frac{\omega}{\omega_e}\,N'_{33} - V\,\frac{dM'_{33}}{dx_b}\ \right]\zeta_{w3}^*\ dx_b$$

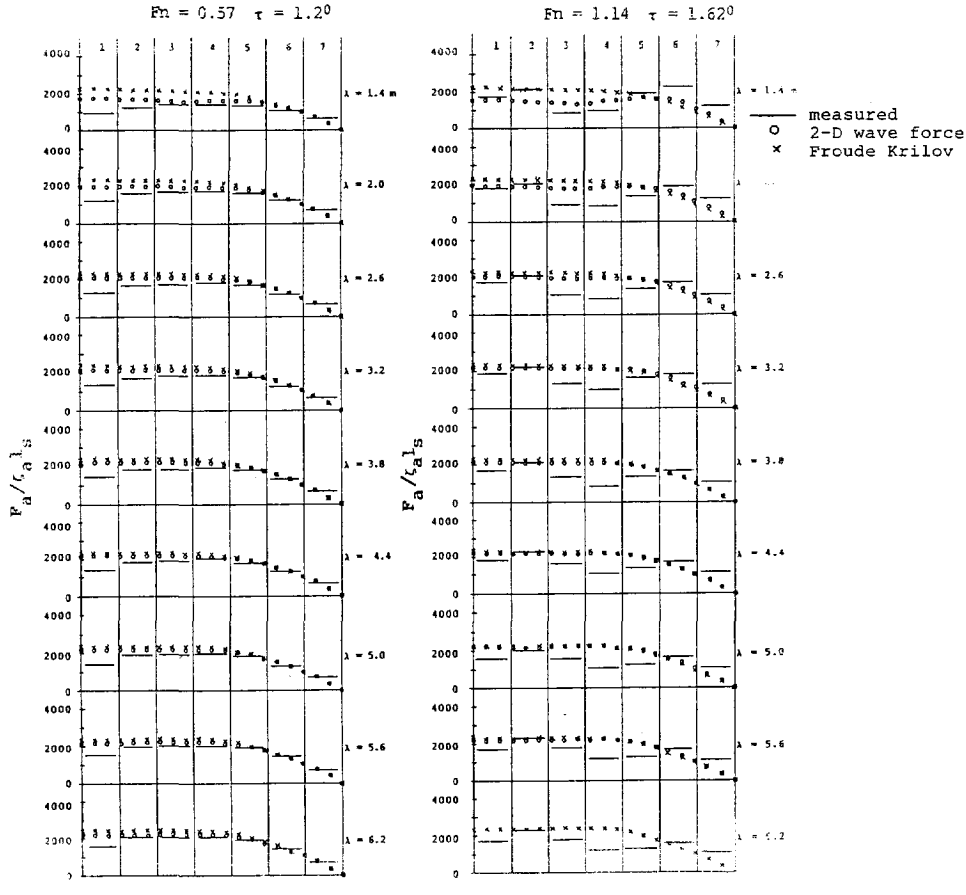

Figure 3.34: Wave force distribution at Fn = 0.57 and Fn = 1.14. With trim!

The "Modified Strip Theory Method" includes the underlined terms. When ignoring these terms the "Ordinary Strip Theory Method" is presented.
The results of both calculations are presented in the figures, i.e.:

- the results of the calculation using the complete formulation with the sectional added mass and damping terms accounting for the contribution of diffraction and radiation forces; and
- the results of the Froude Krilov component only.

3.6.5 Discussion of the results

From the comparison of the measured and calculated results it became obvious that the measurements carried out with the model in the trimmed reference position show a better correlation.
In particular the results at Fn = 0.57 show a rather good agreement except for the aftermost section which seems consistently overpredicted by the calculations.

Two possible explanations for these phenomena are:

- even the smallest wave amplitude used during the experiments, i.e. circa 0.01 meter, made the transom section clear the water surface at the passage of the wavethrough;

- pressure leakage effects due to the forward speed of the craft and the specific geometry of the aft body.

To investigate whether the high forward speed had any effect on this, a series of additional experiments was carried out at very low forward speed, i.e. Fn = 0.10. The results of these measurements are presented in Figure 3.35. Obviously, a similar trend may be seen as in the high speed cases. Therefore it may be concluded that this effect is probably not due to the high forward speed.If the effect of decreasing sectional wave force at the stern is caused by the wave clearing the section at the stern, this effect should be more pronounced in the "non-trimmed" reference position than in the "trimmed" reference position, since the trim is stern down and therefore increasing the submergence of the transom section. Comparison of the measurement results obtained in those two situations strengthens this assumption.

The measurements with the model at the highest speed of Fn = 1.14 show less satisfactory agreement with the calculations. From analysis of the recorded force signals of the dynamometers in this situation it was found that considerable disturbance of the force signals did occur during these tests, in particular at the sections #3 and #4. This may be partly attributed to the fact that the sections themselves were not rigid enough to remain completely free of resonance effects during these measurements. Nevertheless even under these extreme conditions the agreement between measured and calculated results sufficiently justify the use of the proposed calculation method.

From the results of the calculations using the strip theory approximation of the vertical wave forces, it is obvious that for all but the shortest wave length the wave induced exciting forces are dominated to a very large extent by the Froude Krilov component. In the case of fast ships in head waves the larger wave lengths are of real interest because due to the high forward speed these are the waves which encounter frequencies near resonance of the ship in heave and pitch.

Considering the high forward speed of the ships under consideration in the present study the use of a Froude Krilov approximation of the vertical wave exciting forces in head waves is justifiable.

By using the Froude Krilov approximation of the wave forces, however, it becomes possible to take into account an important nonlinear effect in the calculation of the motions of fast ships in head waves. This is the effect that the "not small" relative motions between the craft and the incoming waves have on the wave exciting motions. These large relative motions cause a significant change in the submerged geometry of the craft and the high speed of this change may lead to considerable peaks in the wave exciting forces.

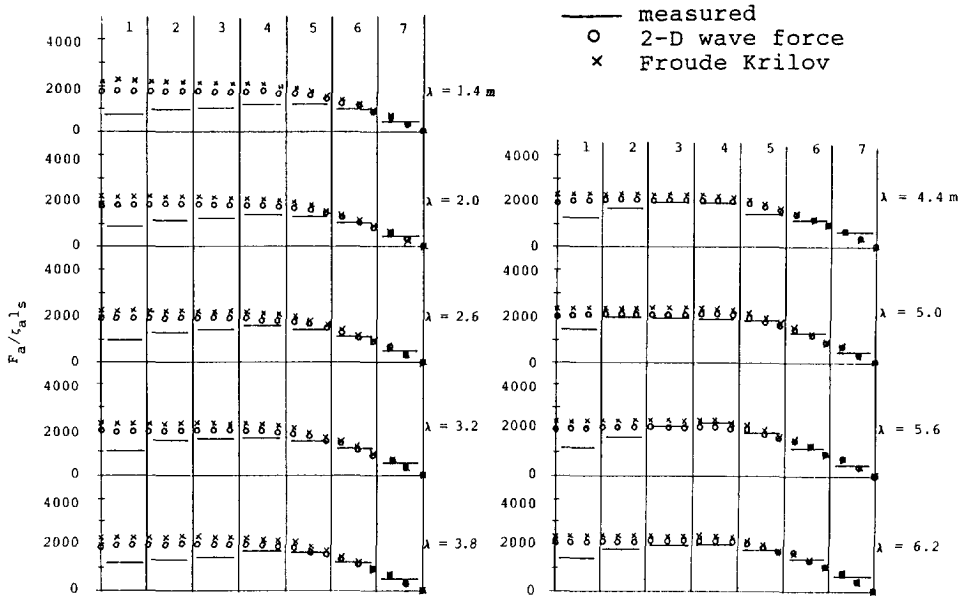

Figure 3.35: Wave force distribution at Fn = 0.10

By integration of the undisturbed wave pressure over the actual submerged volume of the craft whilst performing non small motions in waves in a time domain simulation, the momentaneous Froude Krilov wave exciting force may be calculated which introduces a significant nonlinear effect into the wave exciting forces on a fast ship. This will lead to high peaks in the vertical accelerations.

As will be shown in Chapter 4 this improved the correlation between measured and calculated motions and accelerations considerably.

3.7 Irregular waves

3.7.1 Introduction

In the prediction of the motions and accelerations of fast monohulls in head waves the nonlinear behaviour of the system plays an important role. Therefore it is not sufficient to restrain the calculations to the case of regular waves only, because this may result in an faulty prediction, especially, of the vertical accelerations. Also, a comparison between different designs based on results in regular waves only may be insufficient. In addition, the spectral analysis technique used for linear systems and based on the linear superposition principle, as introduced into the ship motion calculations by Dennis and Pierson (10), is not applicable in the case of a fast monohull in head waves, due to its strong nonlinear respons. Introducing irregular waves into the computational model necessitated the implementation of a "wave generator", capable of producing the irregular wave profile along the moving model as function of time and place.

3.7.2 The irregular wave generation model

The implementation of the irregular waves into the computational model produces a time history of the wave elevation along the length of the ship and the corresponding orbital velocities.
The wave spectrum in which the motions of the ship have to be calculated is discretised in a given number of frequency intervals represented by its centre frequency and a wave amplitude which results in the same energy for that wave as for the interval of the spectrum it represents.
The random phase representation of the wave elevation is given by the following expression:

$$\zeta_w(x,t) = \sum_{i=1}^{N} \zeta_w(i) * \sin(\omega_i t) + k_i x + \phi_i)$$

in which :

$$\omega(i) = 2\pi/T(i)$$
$$k(i) = 2\pi/\lambda(i)$$

The spectral shape may be defined either by specific information of one particular spectrum or by an energy distribution over the frequency range as formulated by Pierson Moskowitz and requiring as an input only a significant wave height and a zero crossing period, i.e.:

$$S(\omega) = \frac{0.0081\, g^2}{\omega^5} \exp\left(- \frac{0.74\, g^4}{\omega^4 V^{w^4}} \right)$$

in which:

$S(\omega)$ = spectral density (m^2/Hz)
V_w = wind velocity in m/s

The horizontal orbital velocity induced by wave component (i) may be written as:

$$U_w = -\omega_i \zeta_i \frac{\cosh k_i (h + z)}{\sinh k_i h} * \sin \phi$$

and the vertical orbital velocity as:

$$V_w = -\omega_i \zeta_i \frac{\sinh k_i (h + z)}{\sinh k_i h} \cos \phi$$

in which:

$$\psi = \omega_i t + k_i x$$

Using the well-known dispersion relation for waves travelling on deep water a time history is generated for the wave elevation and the velocities along the length of the ship at each time.
In the calculation model for the heave and pitch motion the wave elevation and the orbital velocities along the length of the model must be known because these are used in the determination of the Froude Kriloff forces, the instantaneous geometry dependent added mass and the cross flow drag, as discussed in the previous sections. By using the mentioned technique these quantities are known both as a function of t and as a function of X. In the simulation model the ship is actually moving against these waves, yielding the desired values at each time step used in the simulation.

3.7.3 Repetition intervals

The repetition time in which the irregular wave pattern is repeating itself using the above procedure of wave generation may be obtained from the following approach:

Take component $i = 1$ and component $i = 2$ of which $\omega(i) = 2 \pi f(i)$.
The time t in which these components repeat themselves is for both components respectively:

$$\omega_1 * t = n\ 2\ \pi \qquad \text{and} \qquad \omega_2 * t = m\ 2\ \pi$$

in which n and m are positive integers. This yields as repetition time for their combination:

$$t = n/f(1) = m/f(2) \quad \text{and so:} \quad n = m\ f(1)/f(2) \quad \text{and:} \quad n/m = f(1)/f(2)$$

Because n and m are positive integers the largest common denominator (lcd) of f(1) and f(2) determines the smallest t. So if

$$fg = \text{lcd van } f(1) \text{ and } f(2) \text{ then}$$

$$n = f(1)/fg \quad \text{and} \quad m = f(2)/fg$$

yielding:

$$t = n/f(1) = m/f(2) = 1/fg$$

So by proper selection of the value of fg for the generation of the irregular wave train the repetition time of this wave realisation can be chosen outside the duration of the simulation.

Using a similar approach but now on the distance X over which the wave pattern will repeat itself it can be found that this distance is:

$$X = 2\pi/kg \qquad \text{in which:} \qquad kg = (2\pi fg)^2/9.81$$

$$k = 2\pi/\lambda = \text{wave number} \qquad fg = \text{lcd of } f(1) \text{ and } f(2)$$

3.8 Solution of the equations

The solution of the set-up derived equations of motion is complicated by the strong nonlinear character of the differential equations. They form a set of three coupled second order nonlinear differential equations, which will be solved in the time domain using standard numerical techniques. Hereto the set of equations is transformed into a set of six coupled first order nonlinear differen-tial equations by introducing the following vector X:

$$\begin{aligned} x_1 &= x \\ x_2 &= z_{CG} \\ x_3 &= \theta \\ x_4 &= x_{CG} \\ x_5 &= z_{CG} \\ x_6 &= \theta \end{aligned}$$

The equations of motion may then be written as:

$$A * \dot{X} = F$$

in which:

$$A = \textit{mass matrix}$$

$$F = \textit{force vector}$$

$$\dot{X} = (\ddot{x}_{CG}, \ddot{z}_{CG}, \ddot{\theta})$$

This yields, since $\ddot{x}_{CG} = 0$

$$(M + M_a \cos^2\theta) \ddot{z}_{CG} - (Q_a \cos\theta) \ddot{\theta} = T_z + F_z' + D \sin\theta + W$$

$$(Q_a \cos\theta) \ddot{z}_{CG} + (I + I_a) \ddot{\theta} = F_\theta' - D * x_d + T * x_p$$

in which:

$$M_a(t) = \int_L m_a (\xi,t) \, d\xi$$

$$I_a (t) = \int_L m_a (\xi,t) \, \xi^2 \, d\xi$$

$$F_z' = F_z - (\textit{ appropriate accelerations terms })$$

$$F_\theta' = F_\theta - (\textit{ appropriate accelerations terms })$$

The solution of this set may befound by:

$$\dot{X} = A^{-1} * F$$

The procedure used to solve these equations is the Runge-Kutta-Merson method. Knowing the state vector at t_o the equations are simultaneously solved for the small time increment Δt to yield the solution on $t_o + \Delta t$.

Chapter 4

Validation

4.1 Introduction

The computational model as presented in Chapter 3 has been programmed in FORTRAN 77 to yield the code FASTSHIP. It is a time domain simulation program and at the Laboratory the program runs on a CONVEX computer. Typical runtime on that machine for one particular speed in one particular spectrum is about 10 minutes for a simulation of 800 sec. duration. A verification of the results for the heave and pitch motions of a fast monohull in head waves obtained with this code will be made with the aid of a series of model experiments carried out with the three parent models of the Delft Systematic Deadrise Series having 12.5, 25.0 and the 30.0 degrees deadrise respectively. In addition some of the experimental results of Fridsma and Van den Bosch will be used, to check the capability of the computational model to predict nonlinear behaviour.
Calculations with this code will also be used to assess the contributions of some of the nonlinear effects introduced into the present computational model. An analysis will be made with regard to their respective contribution to the prediction of the heave and pitch motions of the fast monohull in head waves, with particular emphasis on the vertical accelerations at CG and the bow. Special attention will be paid to the differences in the predicted motions and accelerations using either a linear computational model based on the Ordinary Strip Theory or the presently described nonlinear computational model.
In addition, the influence of the solution method will be analysed with respect to the number of harmonic components used in the realisation of the irregular wave train and the magnitude of the time step used in the simulation in particular with respect to the predicted magnitude of the vertical peak accelerations.

4.2 The validation

4.2.1 Regular waves

To validate the results of the computational model in regular waves, use will be made of some of the tests carried out by Fridsma (13), which were performed in the high speed range and from tests carried out by Van den Bosch (6) and Verkerk (68) in the middle speed range, i.e. $1.5 < Fn_\nabla < 3.0$.
In 1972 Van den Bosch developed two models with 12.5 and 25.0 degrees deadrise respectively to investigate the influence of the deadrise on the motions of planing ships in head waves. The 12.5 degrees deadrise model was identical to the parent model originally used by Clement for his systematic series. The 25 degrees model was obtained by transformation of the 12.5 degrees model. The bodyplans of these two models are already depicted in Figure 3.11 of Chapter 3. Van den Bosch, however, used only a very limited number of wave lengths during his tests in regular waves. To extend the work of Van den Bosch in this respect additional motion measurements were carried out by Verkerk using the same models. In addition, he performed a full set of forced oscillation tests in the vertical plane to determine the added mass and the damping of these two models. These tests were carried out in 1982 in the Towing Tank of the Delft Shiphydromechanics Laboratory.
The models used during these experiments were completely unappended except for a pair of spray strips of 4 mm width running over the entire length of the chines. The longitudinal radius of gyration of the models was fixed at 25 percent of the length over the chines. The models were connected to the towing carriage in such a way that they were free to heave and pitch but restrained in all other modes of motion. The pivot of the connecting device placed between the model and the towing carriage was located at the intersection of the assumed shaftline and a transverse plane through the Centre of Gravity of the model. This corresponded with the position used during the trim, sinkage and resistance measurements carried out with these models previously.
During the motion experiments the heave and pitch motion of the models were measured using "wire over potentiometer" displacement meters. Two accelerometers were used to measure the vertical accelerations at two different positions in the model: i.e. one at the midship section (ordinate 10) and one at a position 10 percent of the length abaft the bow (ordinate 18). Also two wave height probes were used: one connected to the towing carriage at a specific distance in front of the Centre of Gravity of the model, which was used for the determination of the phase between the response and the oncoming wave, and another one in a fixed position in the towing tank at some distance from the wave generator, which was used for the determination of the waveheight. This method of using two probes overcomes the problems associated with possible ventilation of the wires of the wave probes when used at high speed. The wave generator consisted of a hydraulically actuated flap.
In Figure 4.1 the calculated heave and pitch response of the model with 25 de-

grees deadrise at $Fn_\nabla = 2.7$ to the regular head waves is compared with the measured results. The wave height in the simulations is the same as during the experiments.

As may be concluded from this figure the correlation between the measured and the predicted motions is quite good. Similar results were obtained for the 12.5 degrees deadrise model, although for that particular model it proved to be of considerable importance to obtain an accurate approximation of the reference position of the craft in the steady state planing condition.

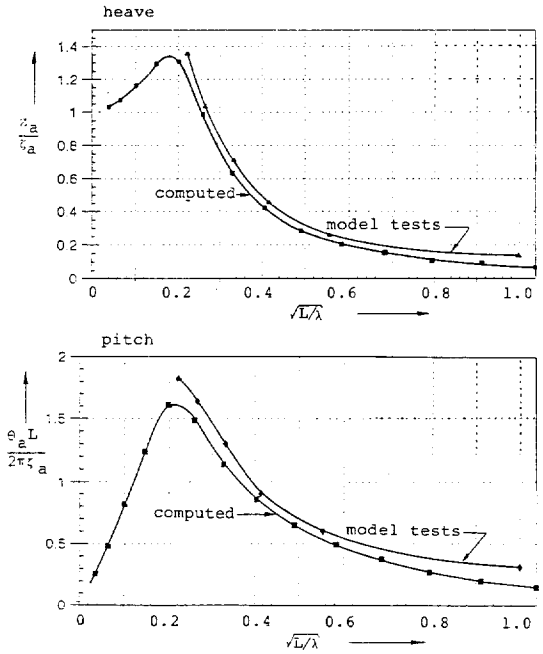

Figure 4.1: Heave and pitch response of 25 degrees deadrise model $Fn_\nabla = 2.7$

The results obtained with the linear theory also show a rather satisfactory agreement in particular for the 25.0 degrees deadrise model. Of more interest in this respect is a comparison between the measured and calculated vertical accelerations using both theories. The results hereof are shown in Figure 4.2 for both the 12.5 and the 25.0 degrees deadrise model.
From the results of these figures it may be concluded that the vertical accelerations are properly predicted by the present theory, although an unsatisfactory discrepancy still does occur in the case of the 12.5 degrees deadrise model. For this model under these conditions the accelerations are underpredicted, in particular, in the frequency range near resonance.

The general character of the calculated transfer functions, however, shows reasonable similarity to the measured ones. The improvement when compared with the predictions using a linear model, however, is evident.

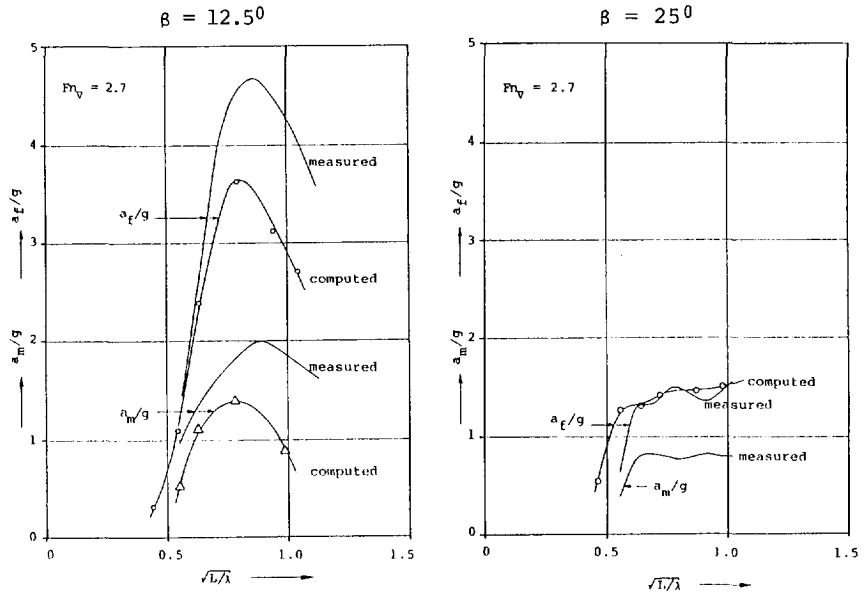

Figure 4.2: Vertical accelerations at CG and the bow for the 12.5 and 25.0 degr. deadrise models in regular head waves. Fn_{∇}= 2.7

The capability of the present model to predict the nonlinear behaviour of the fast monohull in head waves by the present computational model is also clearly demonstrated by the results presented in Figure 4.3. Here a time recording of the vertical acceleration at the bow in one particular regular head wave is presented for both models.
The signal obtained from the measurements by Van den Bosch is compared with the calculated one by simulation with the present computational model. As may be concluded from this figure there is a striking similarity between the two recordings. The actual height of the peak with the 12.5 degrees model may of course be influenced by both testing technique aspects like sample rate, type of accelerometer etc. as well as by the magnitude of the time step used in the simulations.
To check the capability of the computational model to properly predict the nonlinear dependency of the motions and accelerations with respect to the waveheight, the experimental results of Fridsma's study on the rough water performance of planing hulls were used. For one particular wavelength the 20 degrees deadrise model was tested at three different waveheights.

The results for the pitch motion and the vertical accelerations at the bow are compared with the results of the simulations with similar conditions using FAST-SHIP in Figure 4.4.

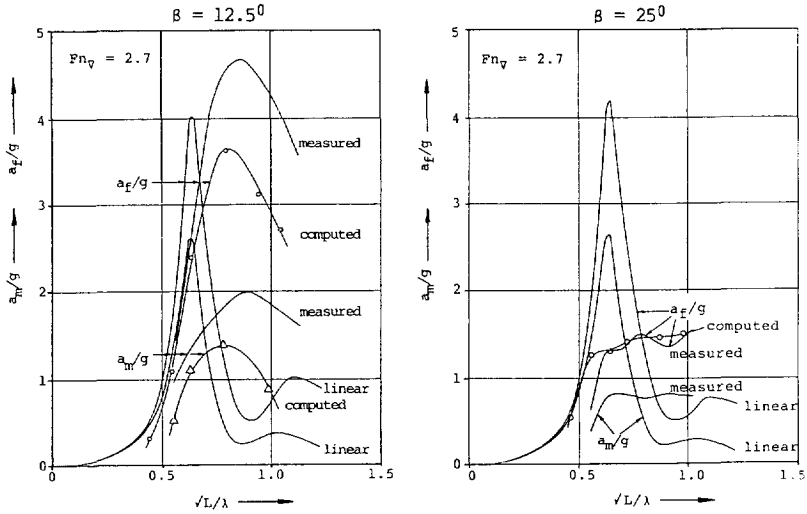

Figure 4.3: Simulated and measured time recording of vertical acceleration at the bow in regular head waves

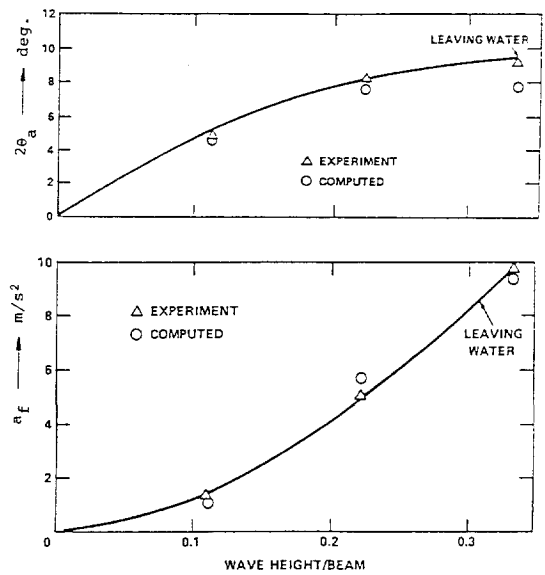

Figure 4.4: Comparison measured and calculated dependency of pitch and vertical accelerations at the bow on waveheight. β = 20 degrees, Fn = 1.8, λ/L = 4

The results indicate that the nonlinear dependency on waveheight is being adequately predicted. Once again the simulations on the 10 degrees deadrise model showed larger discrepancies, which may be attributed to the strong dependency of the results on an accurate prediction of the steady state planing condition, which is not exactly known from Fridsma's report and which may be poorly approximated by the polynomials for sinkage and trim for these somewhat unrealistically shaped models.

4.2.2 Irregular waves

To validate the results of the calculations in irregular waves using the presently described computational model, a series of model experiments was carried out in the Shiphydromechanics Laboratory of the Delft University of Technology.
The models used in these experiments were the three parent models of the Delft Systematic Deadrise Series having a deadrise angle of 12.5, 25.0 and 30.0 degrees respectively. The main particulars and body plans of these models are depicted in Table 3.1 and Figure 3.10 of Chapter 3.
These models were also completely unappended except for the spray strips over the entire length of the chines. The longitudinal radius of gyration of the models was 25 percent of the length over the chine.
The steering signal of the wave generator used for the generation of the irregular waves was made using the random phase method and recorded on magtape. It had a duration of about 30 minutes. This signal was then subsequently used for all tests with the three models. Each test consisted of a series of at least 20 different runs with the model. Each one of these runs used another time interval of the recorded steering signal of the wave-generator. Each measurement was started applying a specific timelag after the wave generator was switched on. By using this procedure a high level of confidence was achieved with respect to the assumption that each run was carried out in a different part of the irregular wavetrain realisation, while on the other hand the conditions met by each of the three models were as much similar to each other as feasible. Three different wave realisations were used derived from wave spectra representing a Brettschneider distribution of the energy over the frequency range. The characteristic data of these spectra were full scale (with assumed modelscale of 1:10):

TABLE 4.1

	significant waveheight	peak period
Spectrum #1	$H_{1/3}$ = 0.55 meter	Tp = 5.9 sec
Spectrum #2	$H_{1/3}$ = 1.10 meter	Tp = 6.7 sec
Spectrum #3	$H_{1/3}$ = 1.60 meter	Tp = 9.0 sec

The formulation for the energy distribution according to Brettschneider is defined by:

$$S_{\zeta\zeta}(\omega) = \frac{A}{\omega^r} \exp\left(-\frac{B}{\omega^s}\right)$$

in which:

ω = wave frequency

$A = 487\ \overline{H}_{1/3}^2 / T_p^4$

$B = 1948 / T_p^2$

$r = 5$

$s = 4$

$H_{1/3}$ = significant wave height

T_p = peak period of spectrum

$T_p = 1.3\ \overline{T}_1$

The tests were carried out at two different forward speeds, i.e. at an assumed cruising speed ($Fn_\nabla = 1.62$) and at full speed ($Fn_\nabla = 2.70$). For a 15 meter ship these speeds correspond to 16 and 28 knots respectively. Each model was tested at these two Froude numbers in each of these three spectra.

All the signals from the transducers were digitised using a 50 Hz sampling frequency, being the highest sampling frequency available at that time stored on disc, to be processed afterwards into spectra etc with the aid of ASYST. The highest achievable sampling frequency was considered necessarry to be able to deal with the expected high peaks of short duration in the signals of the vertical accelerations.

The results of the measurements at $Fn_\nabla = 2.7$ carried out in the wave realisation obtained from the spectra #2 and #3 are presented here only, because these conditions represent the environmental conditions closest to the limits with respect to ship operability. The results of the other tests show similar trends. The calculations with FASTSHIP were carried out for the same conditions. The duration of the simulations was 300 seconds on model scale, i.e. 945 sec full scale for the 15 m ship.

The measured and computed significant amplitudes of the heave and pitch motions in wave spectrum #2 are compared in Figure 4.5 and in wave spectrum #3 in Figure 4.6. The significant vertical accelerations amplitudes at the bow and the CoG in the same conditions are presented in Figure 4.7 and Figure 4.8.
The measured and calculated significant and maximum amplitudes of the vertical

peak accelerations at the bow are compared for the wave spectrum #3 only in Figure 4.9. All results are plotted on the basis of the midship deadrise angle of the models and are non dimensionalised by dividing them by the significant wave amplitude.

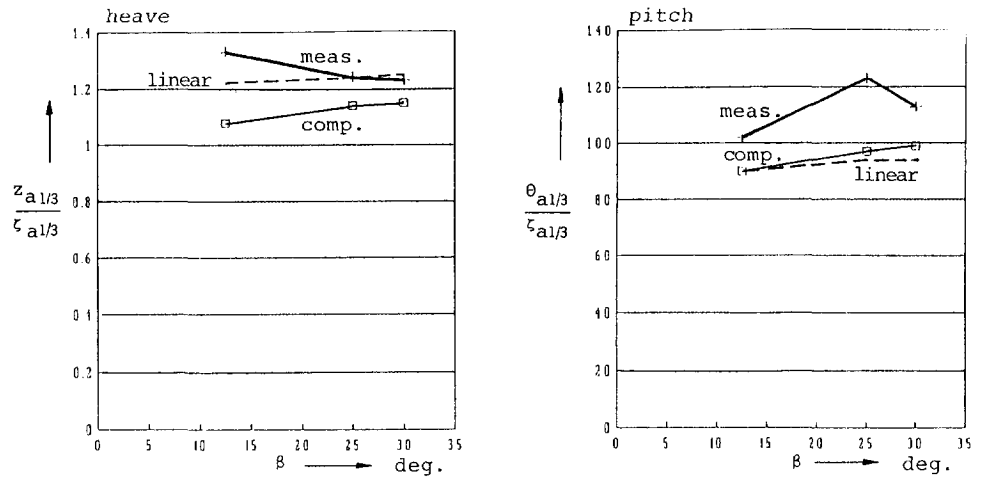

Figure 4.5: Heave and pitch respons of the DSDS models in spectrum #2

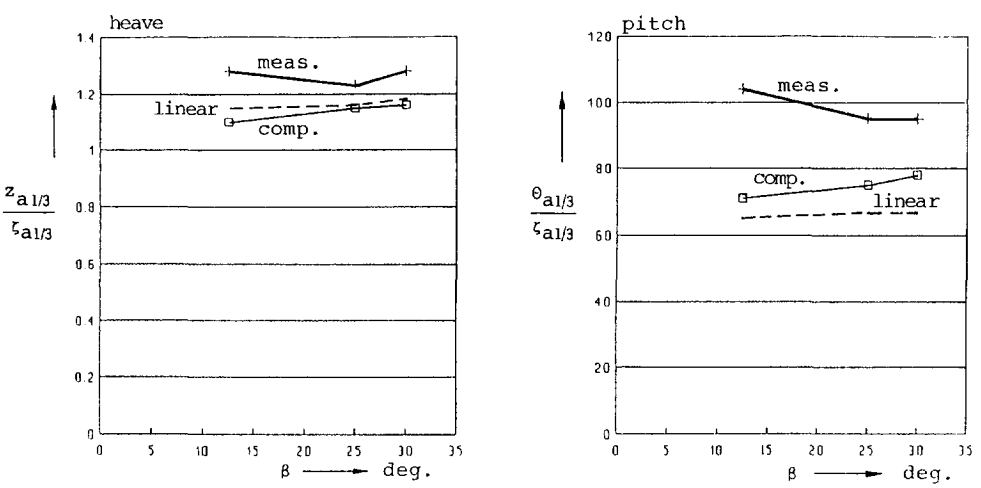

Figure 4.6: Heave and pitch respons of the DSDS models in spectrum #3

From a comparison of these results it may be seen that the correlation between the measured and the computed responses is reasonable. The trend over the deadrise is not predicted correctly. This is caused by the fact that the heave and pitch motion of the 12.5 degrees deadrise model are generally more underpredicted in both spectra. This may be due to the fact that the low deadrise model is highly sensitive to improper prediction of the sinkage and trim and herewith of the added mass coefficient Cm and the buoyancy correction coefficient a_{bf}. The influence hereof will be discussed in more detail in the next paragraph.

It is interesting to note that the differences in significant motion amplitudes between the three models with such a considerable change in deadrise angle is limited to roughly 10 percent. Both motions tend to increase with increasing deadrise this predicted trend is not confirmed by the measurements.
The results of the calculated significant vertical acceleration amplitudes as presented in Figure 4.7 and 4.8 also show an underprediction with respect to the measured results. Although the trend is generally better predicted than for the motions. The largest discrepancies occur for the 12.5 degrees deadrise model in particular for the vertical accelerations at the CG. The accelerations at the bow show a much better correlation.
In Figure 4.5 the measured and predicted distributions of the vertical accelerations at the bow are presented for the 12.5 and 25.0 degrees deadrise ships. The results for the 30 degrees model have been left out because they differ only slightly from the 25 degrees model.
The waveheights in the wave realisations during the physical experiments and the simulation were both found to be closely resembling a Rayleigh distribution.

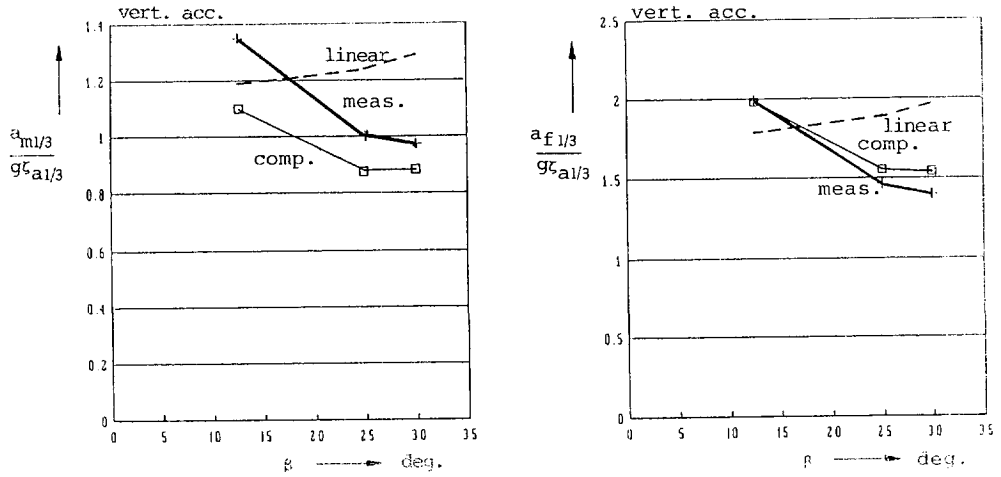

Figure 4.7: Significant vertical accelerations at the CG and the bow of the DSDS models in spectrum #2

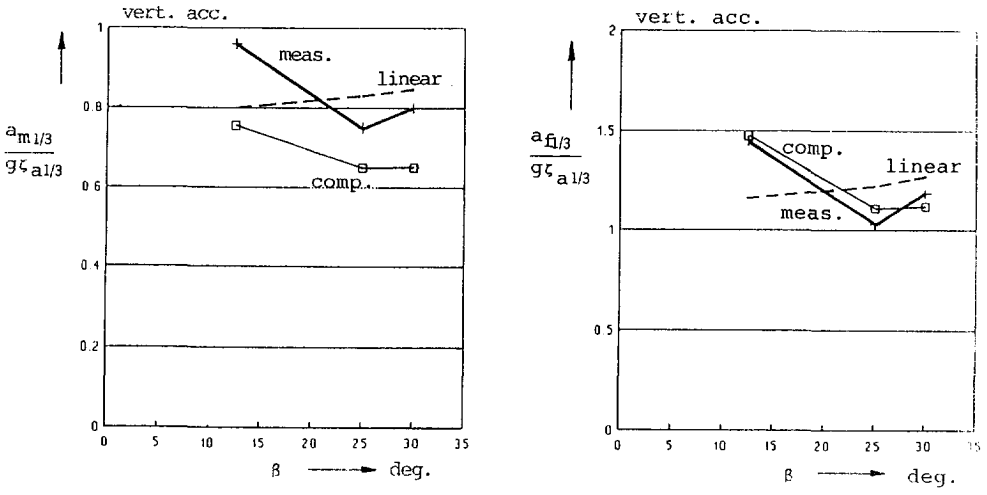

Figure 4.8: Significant vertical accelerations at the CG and the bow of the DSDS models in spectrum #3

Should the response of the system "fast monohull in waves" to the disturbant waves be linear then this would imply that the vertical accelerations should also be Rayleigh distributed. In that case, the Rayleigh distribution may be used for the prediction of the maximum values given a predetermined chance of occurrence. If the 1/1000 chance of exceedence would be used as an estimation of the maximum value to be expected, the use of which value is more or less general practice when predicting extremes in shipmotions studies, then the difference between the absolute value of the significant height and this maximum (1/1000) value would be almost factor 2. These are well known values obtained from the Rayleigh distribution, which is defined as:

$$p(x) = \frac{x}{m_{ox}} \exp\left(- \frac{x^2}{2m_{ox}} \right)$$

with: $x_{a1/3} \cong 2\sqrt{m_{ox}}$

and: $x_{a1/1000} \cong 4\sqrt{m_{ox}}$

To show the difference between the magnitude of predicted maximum using the Rayleigh distribution assumption, resulting from the general use of a linear computational model and the actual measured ones, the Rayleigh distribution for both conditions is plotted in the figure as well.

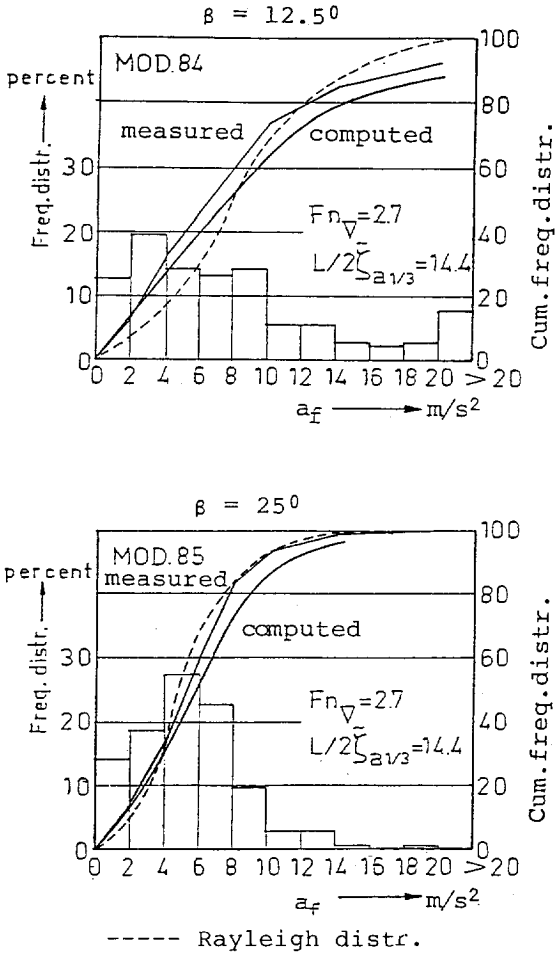

Figure 4.9: Measured and predicted distributions of the vertical accelerations at the bow of the 12.5 and 25.0 degrees deadrise models of the DSDS

From the results of these measurements it is obvious that the assumption of a Rayleigh distribution is certainly not valid for the lower deadrise hulls. Although some discrepancies between the measured and predicted distributions using the present nonlinear model still do occur these results indicate that in particular the trend as function of the deadrise angle is properly predicted. There is a considerable improvement of the prediction of the extremes using the present nonlinear model when compared with the results of a similar prediction based on the use of the Rayleigh distribution.

In the present study no attempt has been made to find a more accurate fromulation of the distribution of the vertical accelerations at either the C_oG or the bow derived from simulations based on the use of the nonlinear computational model, although this would have enabled the determination of the extreme values of the vertical accelerations with greater accuracy. Within the scope of the present study it was considered sufficient to base all simulations on a run in exactly the same irregular wavetrain realisation for all models, in which the ship encounters roughly 1000 waves and to determine the maximum value of the vertical accelerations by taking the average of the two highest peaks encountered. This will clearly show the difference between the designs and will suffice to illustrate the need of the use of a nonlinear computational model for the behaviour of fast ships in head seas when predicting the operability. The use of these maximum values in the figures is more illustrative to show the differences in the behaviour between the various designs.

The procedure as described above for the determination of the maximum values of the vertical accelerations from the computed recording of the simulations has also been applied to the recordings obtained during the physical experiments with the three models in the towing tank. Although mathematically not a rigorously solid procedure for the determination of the maxima in such a highly nonlinear behaviour it is nevertheless consistent.

From Figure 4.10 it may be concluded that the (peak) vertical accelerations at the bow for all models using the described procedure compare reasonably well with those predicted by the present computational model. In particular, the predicted dependency of the maximum vertical accelerations on the deadrise angle at ord. 10 closely resembles the trend found from the measurements. In the case of the maximum accelerations at the bow this is of particular interest because here the strong nonlinear character of the system is at its "best". The relation between the significant and the maximum values in both the measurements and the simulations appears to be strongly dependent on the deadrise of the planing hull. With decreasing deadrise this factor may increase to a value of almost 5 for the 12.5 degrees deadrise model. This is a strong deviation from the results found when using the Rayleigh distribution, customary for linear models for which the relation between the significant ($a_{1/3}$) and $a_{1.1000}$ is roughly a factor of two. It is important to note that this difference between significant and maximum values and its dependency on deadrise will also lead to the necessity to use a nonlinear model when assessing the operability of fast ships in waves based on limiting criteria using the occurrence of peaks in the vertical accelerations.

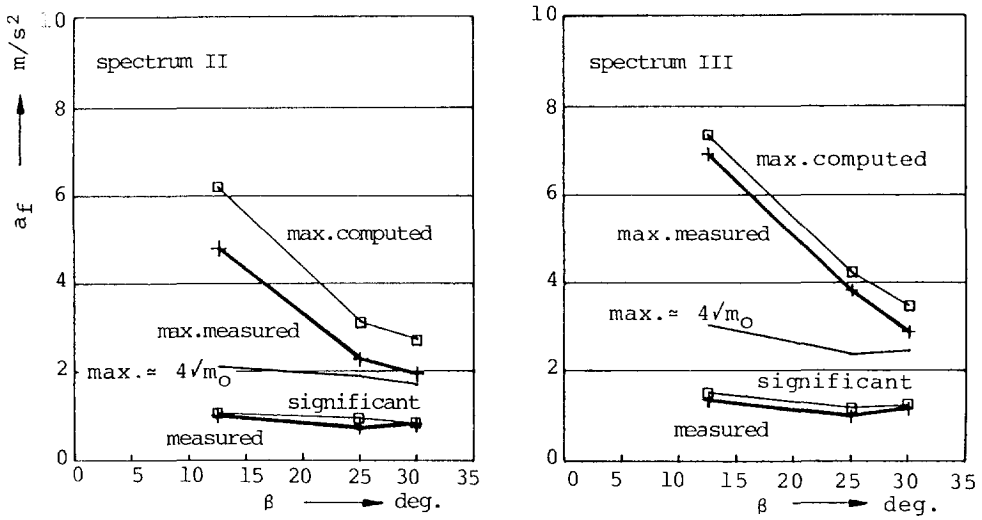

Figure 4.10: Significant and maximum vertical accelerations at the bow of the DSDS models in spectrum #2 and #3

4.3 The influence of the lift

As may be seen from the expressions in the computational model as described in Chapter 3, the hydrodynamic lift is an important nonlinear component in the equations. Therefore it is considered to be of interest to check its effect on the determination of the motions and accelerations using the described nonlinear computational model and to compare these with the results obtained by linear computations in which the effects of dynamic lift are not taken into account.
Zarnick in his model used constant values for Cm and a_{bf} in the expressions of the dynamic and static lift component, which he derived from the work of a.o. Shufold (57). In addition, he corrected the longitudinal distribution of the hydrostatic lift by another constant factor to obtain more realistic results for the trim angle. The trim and sinkage of the craft under consideration were approximated using the expressions describing the steady state planing condition containing these constant values for both parameters.
In the present computational model this process is reversed: i.e. the trim and sinkage of the craft under consideration is approximated using the polynomial expression derived from the systematic DSDS series. By doing so the solution of the equations of motion describing the steady state planing is known. Substituting these values for sinkage and trim in the equations of motions enables the solution of the values of Cm and a_{bf} using the same equations.
The models used to check the validity of the determination of the a_{bf} and Cm values and their sensitivity to the calculation procedure used, are the three parent models of the Delft Systematic Deadrise Series as previously described.
First the calculated results for the sinkage and trim will be compared with the measured results. Since all three models were part of the Delft Systematic Deadrise Series the correlation between these results is rather satisfactory.
Secondly the difference in the determined values for a_{bf} and Cm will be shown when both procedures, i.e. the method used by Zarnick and the present method, are applied to the same models.In both methods the value for $C_{D,c}$ has been kept constant. The results of the Cm values will be checked against some experimental results obtained by Verkerk (68).

The contribution of the lift due to the cross flow drag on the total lift of the hull at speed in the steady state condition is rather small when compared with the other two components, so fixing this value has only a marginal effect on the calculated values for both Cm and a_{bf}.
The main particulars of the three parent models are presented in Table 3.1 in Chapter 3, and only summarized below.

The results of the calculated and measured trim and sinkage of the three models over the entire speed range are presented in Figure 4.11. The sensitivity of the calculated values of sinkage and trim to a change in input parameters is also shown in Figure 4.11 by the dotted line corresponding to a 10 percent change in $Ap/\nabla^{2/3}$.

This appeared to be the most influencial parameter in the polynomial expression. As may be seen from the results the influence on the calculated values is rather large, in particular for the trim.

TABLE 4.2

model #	deadrise	L/B	$Ap/\nabla^{2/3}$	LCG
276	12.5	4.09	5.5	4.0%
277	25.0	4.09	5.5	4.0%
251	30.0	4.09	5.5	4.0%

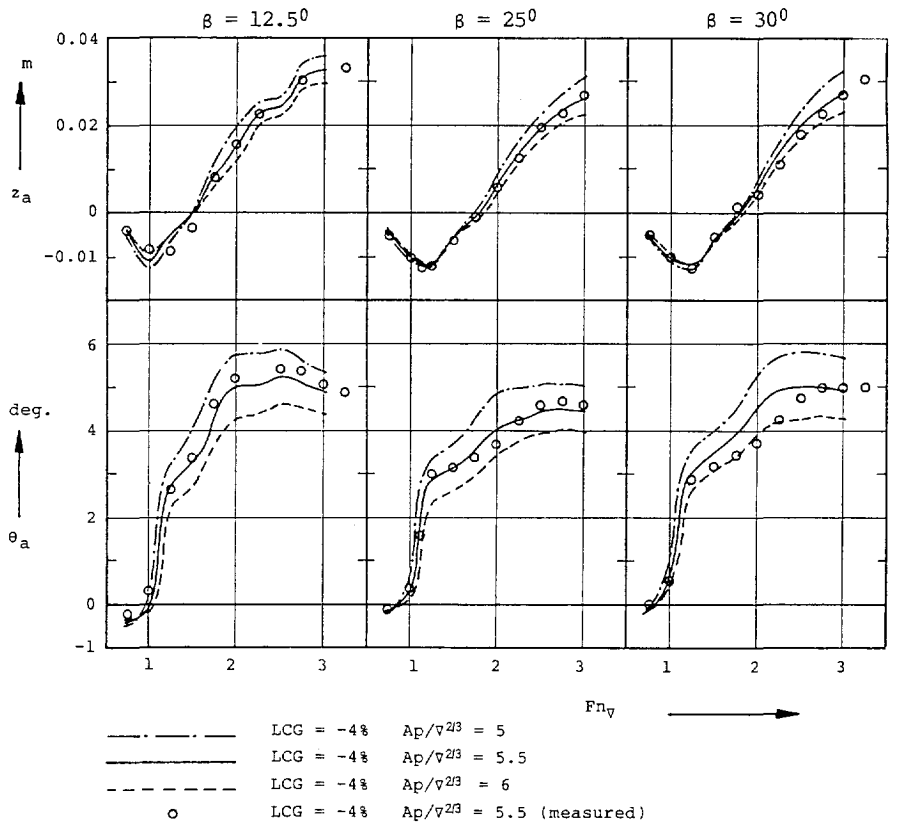

Figure 4.11: Comparison of measured and calculated trim and sinkage for the three parent models of the Delft Sytematic Deadrise Series

The results obtained for the values of Cm and a_{bf} in the complete range of forward speeds of the ships are presented in Table 4.3 for the 25 degrees deadrise model. The value Zarnick used for $C_{D,c}$, i.e. $C_{D,c}$ = 1.13, has been used.

TABLE 4.3

Fn_∇	z	τ	a_{bf}	Cm
1.00	-0.0094	0.13	0.83	-8.00
1.62	-0.0024	3.09	0.74	1.01
2.00	0.0082	3.82	0.77	0.96
2.70	0.0247	4.22	0.79	0.83
3.00	0.0277	4.15	0.79	0.74

From this table it may be seen that the values found for a_{bf} and Cm give realistic results when the described procedure is used above speeds corresponding to Fn_∇ = 1.6.
The results for the three parent models at a speed of Fn_∇ = 3.0 using both the Zarnick method and the present method are compared in Table 4.4:

TABLE 4.4

	Zarnick			Present		
model #	$C_{D,c}$	Cm	a_{bf}	$C_{D,c}$	Cm	a_{bf}
251	1.15	1.20	0.50	1.33	0.85	0.64
277	1.15	1.20	0.50	1.33	0.84	0.72
276	1.15	1.20	0.50	1.33	1.26	0.62

The total force distribution along the length of the models according to the two methods are compared in Figure 4.12.
The limited validity of the method used by Zarnick is clearly demonstrated, he restricted his method to very high speeds. The coefficients he used were derived from the work of Shufold for the case of high forward speeds and low deadrise hulls. As may be seen the results of both methods more or less coincide for that condition, i.e. the 12.5 degrees deadrise hull at the highest Froude number. When the deadrise of the hull is increased, however, considerable differences between the two derived results occur. For calculations performed on high deadrise hulls, which may be favoured for rough sea conditions, the present method should yield more reliable results. The influence of the dynamic part of

the lift is overestimated by Zarnick by using the same values in all conditions when compared to the present method. From the results using this method it can be found that the hydrostatic part in the total lift force plays on increasingly dominant role with increasing deadrise. This coincides with the physical interpretation of the effects of the high deadrise hull, i.e. the hydrodynamic lift decreases due to the higher inclination of the hull with respect to the flow and so the hydrostatic part of the weight carrying force must, therefore, remain larger.
By carefull interpretation of the results presented by Shufold (57) it can be postulated that he found values for a_{bf} of the same order of magnitude, i.e around 0.75 - 0.60, in his tests under more comparible conditions, i.e. lower trim angles, higher deadrise and slower speeds.

The applicability of the original Zarnick model has therefore been extended by the introduction of the present method, because the values of a_{bf} and Cm take into account the actual hull geometry, the forward speed and the lift generating capabilities of the ship in more detail and are differentiating more between the various design parameters. By doing so the hydrodynamic lift is brought into the computational model with a higher level of accuracy than in the Zarnick model.

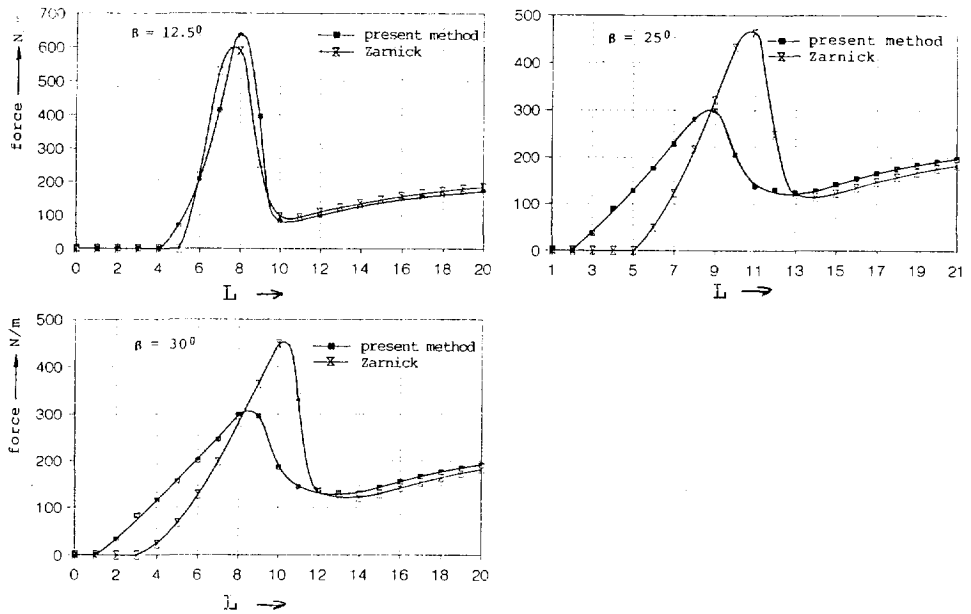

Figure 4.12: The force distribution along the length of the parent hulls of the Delft Systematic Deadrise Series at Fn_∇ = 3.0

However, implicit with the present method of determination of the added mass coefficient Cm and the buoyancy correction coefficient a_{bf} is the importance of an accurate prediction of the sinkage and trim of the ship at speed. In the present study, however, these are approximated by the polynomial expressions based on a systematic series with an inevitable limited range of parameters and variations.
Another shortcomming might be the determination of the submerged volume of the hull in its steady state position at speed with trim and sinkage which remains questionable because the exact flow regime and so the pressure distribution over the hull is not exactly known, but only solved generally.
If the values for stationary trim and sinkage are systematically varied, different values of a_{bf} and Cm may be found for the same hull under otherwise identical conditions. This may have an effect on the calculated motions and vertical accelerations of the ship in waves. To check this effect a sensitivity analysis was carried out for the 25 degrees deadrise parent model.
A variation of the value of Cm and a_{bf} will also illustrate the importance of the incorporation of the lift-component in the computational model for the results.

Hereto the coefficients a_{bf} and Cm have been calculated with a deliberate change in the trim angle of 0.5 degree either side (corresponding to a change of model scale approximately plus and minus 15 percent) and with a change of the sinkage of 2 centimeters (corresponding to a change of approximately plus and minus 20 percent) either side with respect to the proper reference position of the ship at speed. These changes are rather large and the accuracy of the polynomial approximation of the sinkage and trim should normally be well inside this range. The effect of these changes on the values of a_{bf} and Cm are shown in Table 4.5.

TABLE 4.5

sinkage	trim	a_{bf}	Cm	condition #
0.024	4.2	0.72	0.84	1 - (proper ref pos)
0.024	3.7	0.80	0.83	2 - (low trim)
0.024	4.7	0.65	0.85	3 - (high trim)
0.044	4.2	0.72	1.72	4 - (sits high in the water)
0.004	4.2	0.60	0.53	5 - (sits low in the water)

As may be seen from these results an error in the steady state trim predominantly affects the buoyancy correction factor: a high trim angle causes more of the aftbody to be immersed which calls for a lower value of a_{bf} since the total lift remains roughly unchanged and vice versa. An error in the sinkage of the ship

predominatly affects the added mass coefficient: a high rise of the Centre of Gravity calls for a high lift, both dynamic and static while at the same time only little displaced volume is being left which is mainly concentrated in the aft body. This causes a higher buoyancy correction factor to counteract the trimming moment caused by the dynamic lift and vice versa.

To investigate the influence of a change in the coefficients a_{bf} and Cm on the motions and accelerations of the ship in head waves, calculations were performed using the following combinations :

position #1	Cm = 0.84	a_{bf} = 0.72
position #6	Cm = 0.76	a_{bf} = 0.80
position #7	Cm = 0.93	a_{bf} = 0.65

The position #1 is still the proper reference position of the actual ship at its high forward speed corresponding to Fn_∇ = 2.7. The additional positions #6 and #7 were introduced into the motion calculations because these yielded more realistic reference positions of the craft at speed than the conditions #2 to #5 since a high Cm is combined with a decreased value for a_{bf} and vice versa.
The results of these motion calculations are shown in Figure 4.13, showing the heave and pitch transfer function of the model in the three reference positions. The calculations have all been performed with a allmost similar wave steepness of 1/35 except for the two longest waves for which the waveheight was fixed at L/25 for practical reasons.
From these results it is obvious that the effect on the motions is almost proportional to the change in Cm in the range of relatively shorter wavelengths ($\lambda <$ 1.5 times L). For the longer waves the difference is marginal.
The results of the vertical accelerations at CG and the bow in the same conditions are shown in Figure 4.14. The difference between the three different combinations of the lift distribution is also evident.
The condition of high dynamic lift causes considerable higher vertical accelerations both at the Centre of Gravity and at the bow and almost over the entire wavelength range.
Since the occurrence and the magnitude of the peak values of the vertical accelerations are best analysed in irregular waves a further analysis of the effect of the dynamic lift has been carried out by performing a number of motion simulations with the code FASTSHIP in irregular waves. Of these simulations only the results for one forward speed corresponding to Fn_∇ = 2.7 and one particular spectrum will be presented here. The results of this simulation were found to be typical for all other runs which showed similar tendencies.
In order to enable a reliable comparison between the different models possible in a reasonably short simulation runtime and in only a limited length of the wave realisations, great care has been taken to make the irregular wave realisations, used in the simulations for each model, as identical as possible.

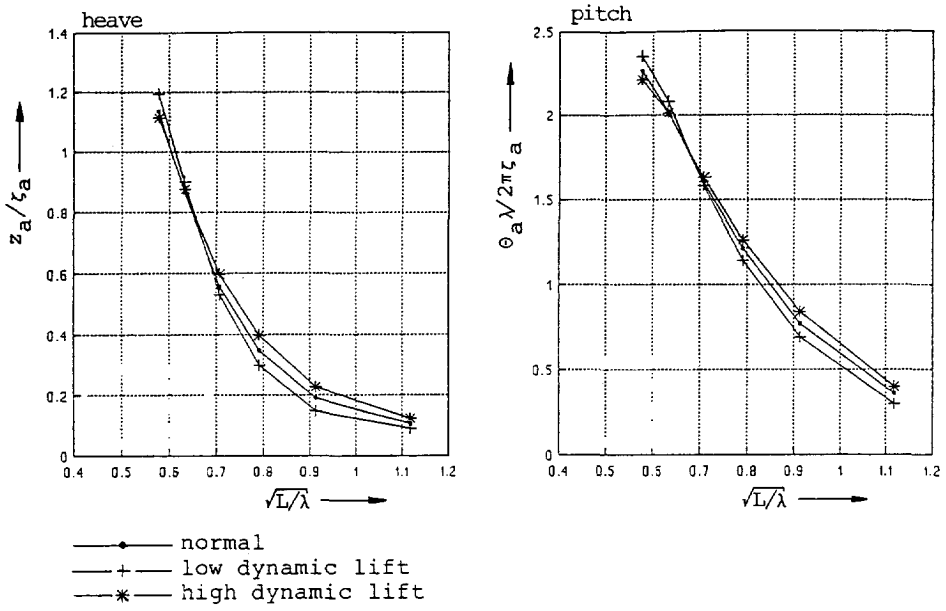

Figure 4.13: Heave and pitch response operators for different lift contributions

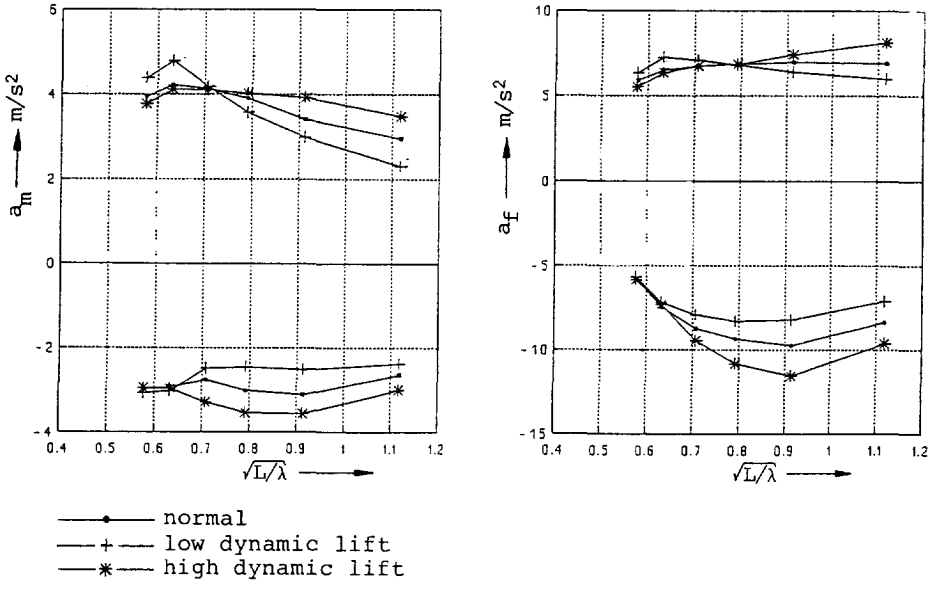

Figure 4.14: Vertical accelerations at CG and the bow for different lift contributions in regular head waves

Hereto the random phase generation of the harmonic components has been overruled in these comparative testsruns to yield the same irregular wave elevation realisation as function of the time in each run.
This had the additional advantage of facilitation of the determination of the maximum values in the registrations of the motions and more in particular of the vertical accelerations. Due to the highly nonlinear character of the reponse it is obvious that from a statistical point of view these maximum values determined in this way are not the maxima associated with a predetermined chance of exceedence based on an obtained distribution of maxima of the signal from the time history. Therefore they lack general applicability. However as a comparative tool to distinct different tendencies between the different models the described method is quite useful.
For the conditions as indicated before, the results are presented in Table 4.6:

TABLE 4.6

cond. #	$z_{1/3}/\zeta_{1/3}$	$\theta_{1/3}/\zeta_{1/3}$	$acg_{1/3}$	acg_{max}		$af_{1/3}$	af_{max}	
				up	down		up	down
1	1.15	1.31	5.8	-9.6	9.8	9.9	-36.9	11.7
2	1.19	1.36	6.3	-8.5	9.8	10.4	-36.3	11.9
3	1.13	1.28	5.6	-10.5	9.4	9.8	-36.5	11.5
4	1.14	1.32	7.0	19.4	9.6	12.7	-53.7	14.6
5	1.20	1.27	5.4	-7.5	9.8	7.9	-22.5	11.9
6	1.21	1.37	6.3	-8.0	9.8	10.3	-32.0	12.0
7	1.13	1.29	5.8	-11.9	9.4	10.3	-40.1	11.4

From these results it may be concluded that the effect of the changes in the respective relative magnitude of the hydrostatic and hydrodynamic lift on the significant heave and pitch amplitudes is rather limited, in particular, when the large changes between the conditions with respect to the values of a_{bf} and Cm are considered. The changes in predicted levels of vertical accelerations at the bow and the CG show considerable more dependency on the magnitude of the dynamic lift under consideration. The predicted peak values show a very strong dependency on the imposed magnitude of the dynamic lift. The highest peak values are predicted in those conditions which have the highest values for Cm.
In addition, a high value for Cm seems to increase the accelerations at the bow and a high value of a_{bf} the accelerations at the Centre of Gravity. This may be explained by the nature of the lift component these respective parameters are influencing most, i.e. Cm the lift in the spray zone were the change in added

mass momentum is largest and a_{bf} the lift in the aft body, where displaced volume is largest.

To obtain a more realistic picture of what might be the influence of a difference in the distribution between hydrodynamic and hydrostatic lift and of how big the influence of the dynamic lift on the peak accelerations is, two additional variations with respect to the actual model have been calculated in the same spectrum. The change between the conditions was a change in the longitudinal position of the Centre of Gravity of the ship from its normal position at 4 percent abaft the centroid of the planing area to 2 percent and 6 percent respectively.
The results of this change in LCG on the values of sinkage and trim and so on a_{bf} and c_m are summarized in Tabel 4.7. The results of the motion calculations are presented in Table 4.8.

These results coincide very well with the results of Fridsma (13): i.e. reducing the trim angle reduces the pitching motion significantly and to a much lesser extent the heave motion. The peak accelerations at the bow, however, are reduced considerably with the reduction of the steady state trim. An increment in running trim leads to the opposite effect. The results of the present computational model show a similar trend.

TABLE 4.7

sinkage	trim	a_{bf}	Cm	condition #
0.024	4.2	0.72	0.84	1 - (proper ref pos)
0.0268	4.5	0.78	0.84	8 - (lcg at 6%)
0.0209	3.9	0.68	0.88	9 - (lcg at 2%)

TABLE 4.8

cond. #	$z_{1/3}/\zeta_{1/3}$	$\theta_{1/3}/\zeta_{1/3}$	$acg_{1/3}$	acg_{max}		$af_{1/3}$	af_{max}	
				up	down		up	down
1	1.15	1.31	5.8	-9.6	9.8	9.9	-36.9	11.7
8	1.17	1.45	6.6	-13.5	9.8	12.0	-44.6	11.9
9	1.13	1.16	5.0	-7.5	9.6	7.6	-28.9	11.4

4.4 The influence of nonlinear added mass

In the present computational model the added mass of each section is approximated by using a formulation which takes into account the change in actual submerged geometry of the ship whilst performing large relative motions with respect to the actual momentaneous wave surface. The frequency dependency of the added mass is herewith neglected, i.e. the formulation used is the same for all frequencies. The use of such a procedure is justified by the results presented in Chapter 3 which shows the added mass of a fast monohull to be almost frequency independent in particular in the frequency range of interest when considering the case of a fast ship in head waves.

To investigate the influence of these assumptions on the motions and vertical accelerations a number of calculations have been carried out with the Van den Bosch models using both methods, i.e. :

- a frequency dependent added mass which is independent of the change in geometry and is based on the submerged geometry of the craft at its still water zero forward speed reference position; and

- a frequency independent added mass which is dependent on the momentaneous submerged geometry of the ship

The frequency dependent added mass was calculated using a Lewis transformation of the sections as customarely used in the Ordinary Strip Theory. The time dependent added mass was calculated using the formulations as described in Chapter 3. All calculations have been carried out for $Fn_\nabla = 2.7$ which corresponds to the speed used during the model experiments, and corresponding waveheights were used.
The results of these calculations are presented in Figure 4.15 for the heave and pitch motion of the 12.5 degrees deadrise model and in Figure 4.16 for the 25 degrees deadrise model.

As may be seen from these figures the effect on the motions of the method used to approximate the added mass is quite significant. In particular the pitch motion is strongly affected. Similar results were found for the vertical accelerations. It should be noted that the measured results as found by Van den Bosch closely resembled the results obtained using the nonlinear added mass approximations of the present method and therefore the results obtained by a method using linear added mass only should be considered as definitely inferior to the the results obtained with the nonlinear added mass approximation, even though this implies in the present model that the frequency dependency of the added mass is being neglected.

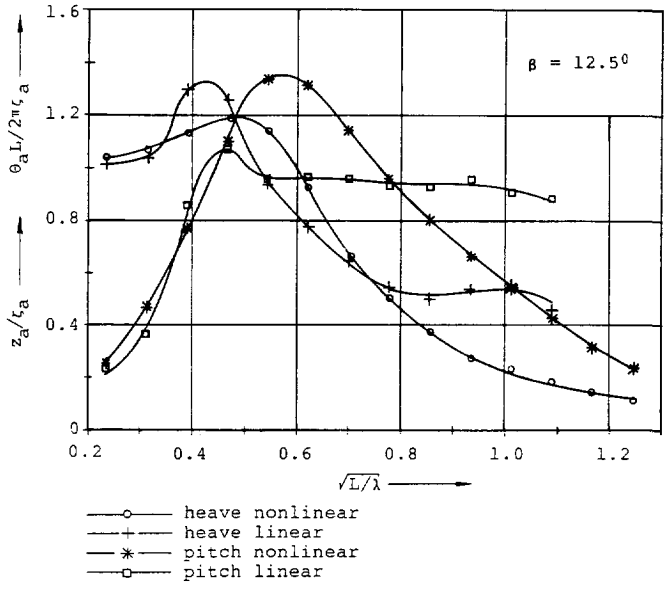

Figure 4.15: Heave and pitch motion of the 12.5 degrees deadrise model with and without nonlinear added mass

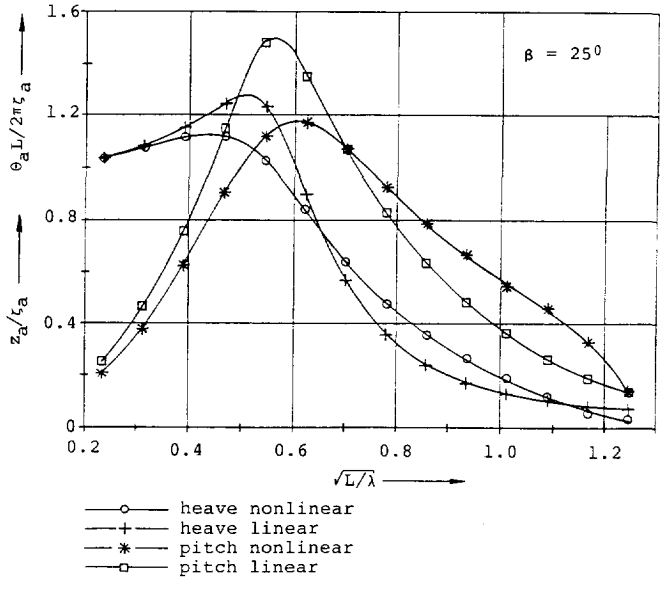

Figure 4.16: Heave and pitch motion of the 25 degrees deadrise model with and without nonlinear added mass

4.5 The effect of nonlinear waveforces

A similar exercise as with the added mass was carried out for analysing the effect of the nonlinear wave forces on the prediction of motions and accelerations.
Implementation in the computational model appeared to be only feasible for the area above the chine of the model, i.e. the shape of the model above the chine could be made either prismatic with vertical sidewalls or non prismatic with the topsides above the chine inclined to match the actual shape of the sections. A schematic representation hereof is presented in Figure 4.17. The prismatic shape corresponds with the assumption used by Zarnick in his original model.

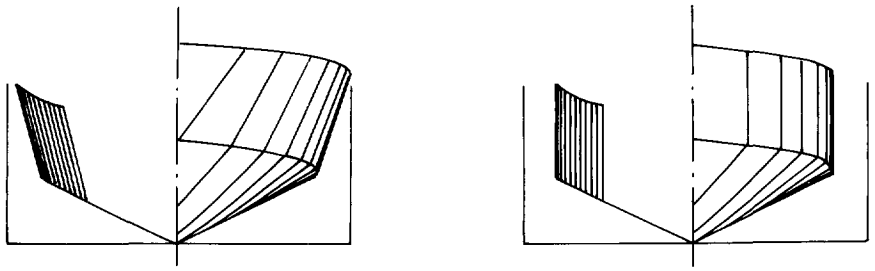

Figure 4.17: Geometries used for the evaluation of wave force effects

So the nonlinear effect is restricted to the above chine region only. This implied that only a very limited analysis of the effect of the nonlinear wave forces on the motions could be made. The difference between the two geometries as depicted in Figure 4.16 is rather limited in the aft body and in the foreship the actual difference is constricted to an area that will be submerged only when the ship is performing large relative motions. Therefore at short waves the difference between the two methods will be negligible and largest differences should occur on and near resonance. This may be seen from the results obtained for the vertical accelerations at the bow in regular head waves as computed for the 12.5 and 25.0 degrees deadrise models of Van den Bosch as shown in Figure 4.18.
Both the heave and pitch motion are reduced by the introduction of the non prismatic hull shape and in conjunction also the vertical accelerations. This means that for the motions the correlation between the measured and the calculated response operators is improved by the introduction of the nonlinear wave force effect and that the correlation for the vertical accelerations at the bow, which were underpredicted, in particular, for the 12.5 degrees model. It should be noted, however, that an inevitable small change in the values of a_{bf} and Cm also occurred due to the small change of submerged geometry of the craft

during the steady state planing condition. This also affected the predicted behaviour of the ships. From simulations in irregular waves, however, it became obvious that the absolute value of the encountered peaks of the vertical accelerations was somewhat increased by introduction of the nonlinear wave forces.

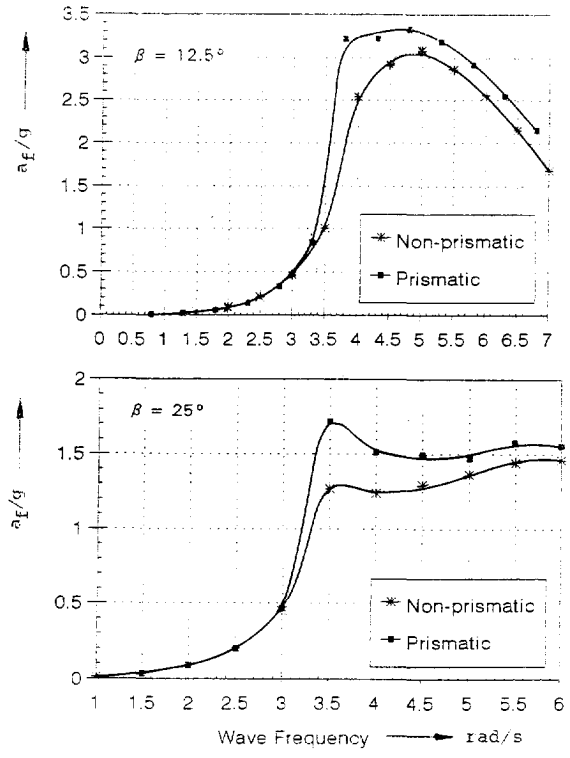

Figure 4.18: Bow accelerations of the 12.5 and 25.0 degrees deadrise models with and without prismatic hull shape above the chine. $Fn_\nabla = 2.7$

From a visualisation program used in order to "animate" the generated output of FASTSHIP on a PC screen it was obvious, however, that the highest peaks in the vertical accelerations at the bow did occur on those moments in which the under chine part of the hull was reimmersed into the water rather than on those moments in which the bow of the ship was plunged completely into the face of the incoming waves. Therefore, the proper introduction of the lift forces into the computational model should be considered of greater importance for the prediction of peak accelerations than the introduction of the nonlinear wave forces.

4.6 The influence of the timestep in the simulations

The solution of the equations of motion in the computer code FASTSHIP is being performed in the time domain. Since special attention in the output is paid to peak phenomena, i.e. peak acclerations, an influence of the magnitude of the timestep used in the simulation is to be expected. A very small magnitude could yield higher values for these phenomena and vice versa. However, also the computer run-time of a simulation is significantly increased by decreasing the magnitude of the timestep. So a proper trade off between accuracy and time needed has to be made.
In the code an optimisation routine is being used which divides the time step stipulated in the input file by a factor 2 if a specified error criterium in the solutions is being surpassed. The solution is then recalculated using this smaller timestep and the timestep is kept at this level for two successive timesteps before being switched back to the previous (original) value (or not).
Most calculations carried out for the validation of the computational model, of which the results are presented above, were carried out with a timestep of 0.02 seconds or 50 Hz (modelscale).
To check the influence of the timestep magnitude on the computational results a number of calculations on the DSDS parents in irregular waves have been repeated using a time step of 0.01 seconds or 100 Hz. The results of a comparison between the two simulations carried out for one particular combination of speed and wave spectrum are presented in Table 4.9.

The results in this Table may be considered typical for the other results and for other conditions which were simulated. The particular combination of the forward speed and wave spectrum used in this simulation, however, was chosen because it guaranteed a substantial magnitude of the peak accelerations. The differences found for the less severe, and therefore more realistic conditions, were considerably less pronounced.
As may be seen from these results, the significant amplitudes of the vertical accelerations are hardly affected by a change in timestep. The peak values, however, may be affected by almost 20 percent in the case of the lower deadrise hulls, for which the peaks are by far the most pronounced and the behaviour of the fast monohull in this respect is by far the most nonlinear.
It is worth noting however that, although the absolute magnitude of the peaks is affected by the magnitude of the timestep used in the simulation, the general trend over the three deadrise models is not affected. Therefore conclusions based on calculations which are being carried out using a smaller timestep will not be affected.
An optimum timestep could not be found. Each reduction led to an increment in the peaks although a reduction to 0.0075 seconds led only to an increase in the peak values of approximately 5 percent.
Considering the validation purposes for which the calculations were made it should be mentioned that also the registration of the peaks during the model experiments is an era of uncertainty. For these highly peaked phenomena of

short duration the determination of the absolute maximum from these measured recordings is also difficult. By using the same frequency for the sampling rate of these signals as for the time step in simulations, a comparison between the two was considered consistent.
A typical time recording of a peak acceleration found with both simulation steps is shown in Figure 4.19.

TABLE 4.9

	$\beta = 12.5°$	
	50 Hz	100 Hz
af_{max}	60.2	74.4
$af_{1/3}$	11.2	11.7
am_{max}	22.2	31
$am_{1/3}$	6.0	5.9
	$\beta = 25°$	
	50 Hz	100 Hz
af_{max}	41.9	48.5
$af_{1/3}$	9.0	9.0
am_{max}	12.6	13.5
$am_{1/3}$	5.2	5.2
	$\beta = 30°$	
	50 Hz	100 Hz
af_{max}	44.7	44.6
$af_{1/3}$	8.9	8.9
am_{max}	13.0	13.0
$am_{1/3}$	5.3	5.3

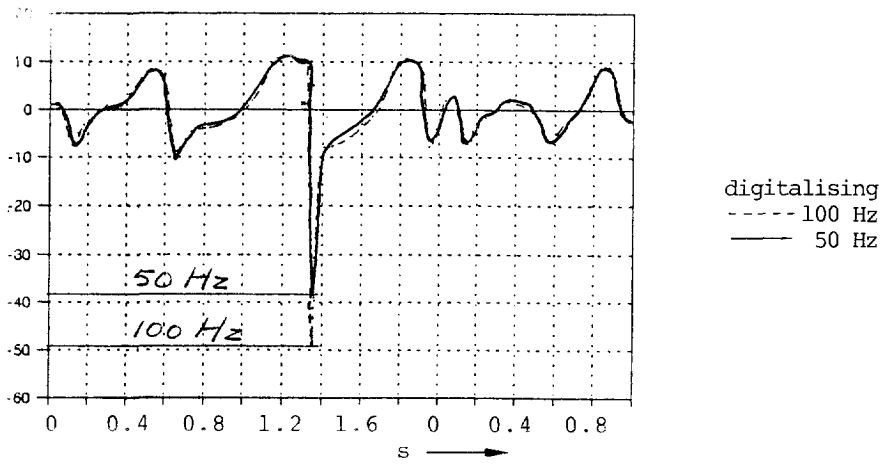

Figure 4.19: Simulated recording of vertical acceleration at the bow with time step 0.02 and 0.01 second.

It should be noted that the duration of the peak appears not to be influenced significantly by the shorter time steps, although a detailed analysis in this respect has not been carried out yet.

4.7 The influence of the number of components in the irregular wave realisation

Another aspect that might be of influence on the magnitude of the peak values found during the simulations, is the number of harmonic components which is being used in the generation of the irregular wave train realisation.
As formulated in Chapter 3 the irregular wave train realisation is based on a random phase model using a predetermined number of harmonic components to represent a wave energy distribution over the frequency range according to the Brettschneider formulation with predetermined significant wave height and peak period. For the purpose of a proper comparison between the different models the random phase generation for the respective spectra was "overruled" to yield the same realisation for each simulation run.
In particular because much emphasis is being put on the prediction of the highly nonlinear peaks in the vertical acceleration the actual shape of the irregular wave train realisation in time will be of importance. Steeper waves in this irregular wave elevation realisation may occur when more components are being used for its generation.
Therefore, the sensitivity of the results with respect to the number of components used was made.
To check the sensitivity of the calculated results on the number of components used in the wave realisation a number of calculations was carried out with the three parent models of the DSDS in the same spectrum but using 15, 30 and 60 components to describe the spectrum respectively.
The influence hereof on the significant wave height is presented in table 4.10.

TABLE 4.10

		15 comp	30 comp	60 comp
$h_{1/3}$	[m]	1.08	1.09	1.09
T_{peak}	[s]	6.76	6.67	6.77

As may be concluded from these data the significant waveheight derived by statistical analysis of the wave elevation realisation is not affected by the number of components, nor is the general shape of the distribution of crests and throughs.
The influence of the wave elevation realisations on the computed maximum vertical accelerations is presented in table 4.11. Again as maximum value for the accelerations the average of the two highest values obtained from the simulated recording of the vertical accelerations was used.
These results indicate that there is an influence of the number of components used in the realisation on the peak accelerations. The dependency of the magnitude of the peak accelerations on the deadrise, however, is not affected.

TABLE 4.11

	$\beta = 12.5^{\circ}$	
	15 comp	60 comp
af_{max}	60.1	60.2
am_{max}	22.6	22.2

	$\beta = 25^{\circ}$	
	15 comp	60 comp
af_{max}	34.7	41.9
am_{max}	11.1	12.6

	$\beta = 30^{\circ}$	
	15 comp	60 comp
af_{max}	29.7	44.7
am_{max}	9.2	13.0

4.8 Time histories

As a demonstration of the capabilities of the computational model a few time histories of the response of the ship in both regular and irregular waves are presented. The nonlinear response of the ship in regular waves is evident and obviously properly handed by the simulation. When these results are compared with the recordings taken onboard the models by Van den Bosch, as presented in Figures 2.14 and 2.15 the similarity between the signals is also quite satisfactory. It should be noted that the recordings are not to scale.

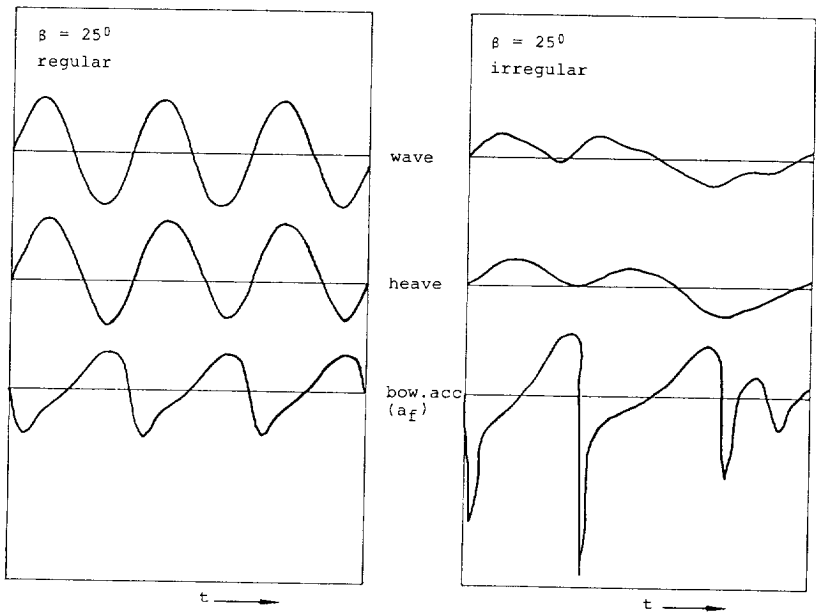

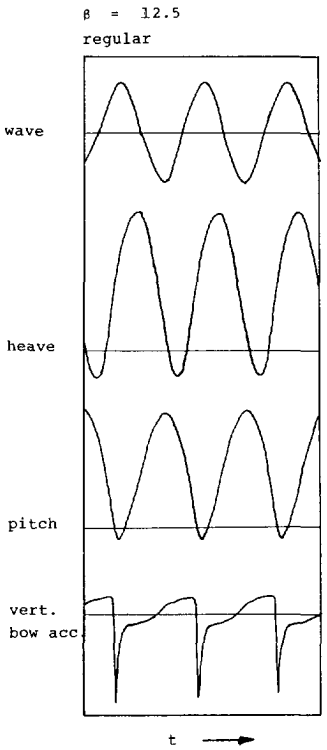

4.9 Conclusions

From the comparison between the results obtained with FASTSHIP and the results obtained from measurements it may be concluded that the present computational model yields valuable results, in particular, for the nonlinear behaviour of the fast monohulls such as the vertical accelerations. The trends in this behaviour between different designs are generally well predicted, although discrepancies in the absolute magnitude of the responses still occur. The improvement over using a linear theory, however, is evident. The prediction of the operability of these craft which is based on criteria containing nonlinear behaviour should therefore be improved in comparison with predictions based on linear computations.

Chapter 5

The effect of nonlinear behaviour on operability

5.1 Introduction

As mentioned previously the availability of a reliable computational model capable of predicting the nonlinear behaviour of a fast monohull in waves is an essentional tool for assessing the operability of these ships in waves.
Based on the conclusions of the previous Chapter it may be stated that the present computational model should be able to predict the differences in operability between different designs more adequatly than a linear model, especially, when the limiting criteria, which are being employed to establish the limits of this operability, are based on nonlinear behaviour. In the case of fast ships in waves it is known that these limiting criteria are largely based on the occurrence of peaks in the vertical accelerations. In this Chapter the importance of taking into account these nonlinear phenomena when assessing the operability of these craft will be shown. Although the necessary effort for such an exercise increases considerably when using a nonlinear simulation technique instead of the usual linear computational models, it will be illustrated that this is essential. Otherwise considerable differences in absolute values of the predicted outcome and also reverse design trends may occur.
To be able to assess the safe (and comfortable) operation of fast ships in waves, it is necessary to formulate limiting criteria with respect to the acceptable level of motions and accelerations in waves. A short description of some criteria used in the operability analyses of fast ships will be given and their relevance discussed.
The influence of the use of either a linear or a nonlinear computational model will be shown using the results of such a study which was carried out for a coastal patrol boat for the North Sea area in 1988.

5.2 The limiting criteria

In the mid 80's the Netherlands Shipping Authority felt the need of formulating limiting criteria for the safe operation of their coastal patrol ships used by the Customs, the Law Enforcement and Pilot Departments, which were operated in he Dutch North Sea area and estuaries. In that period these ships became signifcantly faster than their predecessors because of new operational requirements leading to fewer ships with the associated need for more rapid deployment.
The operational criteria used for fast small patrol boats at that time were primarily dealing with noise levels (dB's) in the accommodation and the wheelhouse and with Motion Sickness Incidence (seasickness) based on an ISO interpretation of the work in this area carried out by a.o. Hanlon and MacCaulghy (42).
No other criteria for motions or accelerations which were generally applicable at that time existed. The only criteria in use were some criteria obtained from specific mission requirements for one particular kind of boat or, for instance, based on the use of a specific instrument like a sonar etc. In order to obtain some insight in these criteria, a study was set up by the Delft Shiphydromechanics Laboratory in cooperation with the Netherlands Authorities which was aimed at obtaining the levels of acceptable vertical motions (heave and pitch) and vertical accelerations by professional crews. Hereto a number of experiments were undertaken on board patrol boats on the North Sea.
During these full scale experiments the selected ships were under command of their regular crews. The ships ranged in size from 18 to 35 meters length overall and speeds varied between 20 and 30 knots. Although all ships had a specific task for which they were actually designed, i.e. as patrol boat, as pilot launch e.a., which generally imposed limits on the motions and accelerations considered acceptable for performing that specific task, these were not considered in this study. Instead, general information was sought on the limits for a safe (or comfortable) operation of these ships through the waves.
All ships were instrumented by the Shiphydromechanics Laboratory for the trails. The heave motion, the pitch motion, the heading of the ship with respect to the waves, the speed of the ship and the vertical accelerations at midship and at the bow, approximately 10 percent of the length over the chines abaft the Forward Perpendicular, were measured during all runs. In a number of experiments a disposable wavebuoy developed by the Laboratory was used to measure the spectrum of the waves. During the other tests these data were obtained from WAVERIDER buoys deployed by Public Works Department of the Ministry of Transportation and Public Works and kindly put at our disposal.
During the tests the crews of the ships were asked to maintain the maximum forward speed which they considered still acceptable for the given wave condition. During these test runs all relevant data were recorded. Voluntary speed reductions, when occurring, were filed on the measurement logs. The crews were asked to maintain a constant speed during the runs and not to use the customary sudden speed reduction to prevent a foreseeable slam of the ship into an oncoming wave.

During all tests a measurement team of the Laboratory was onboard to get their own impression of circumstances, the behaviour of the ship and the crews reaction.

An important conclusion drawn from this study was that generally spoken all crews imposed a voluntary speed reduction at roughly the same conditions. The real measure for imposing this voluntary speed reduction appeared not to be taken from the prevailing magnitude of the significant heave and pitch motion at the time nor from the significant magnitude of the vertical accelerations, but rather from the occurrence of one big "slam", i.e. a peak in the vertical accelerations. Another interesting conclusion from the experiments on the operability in waves was that all ships had their wheelhouse rather far forward. Although from a ship motion point of view this position of the wheelhouse appears not to be a very sensible design option, apparently most designers (of these ships) opted for this solution. It enabled them to create the maximum distance between the main engines and propellers and the wheelhouse, in which the noise level had to be kept below certain limits. These required maximum noise levels therefore prevailed over the limiting motion levels in the wheelhouse, because these criteria did not exist at the time.

The conclusion on the importance of the peaks in the vertical accelerations was supported by the experience from others working with fast ships and also frequently mentioned in the literature. However, in the few reports on operability analyses of fast ships in waves the peaks in the vertical accelerations are hardly being used as limiting criteria.

This may well be attributed to the lack of reliable nonlinear computational models capable to predict these peak values. Shipmotion calculations at that time were (and still are) predominantly based on linear computational models. Operability studies a.o. are based on the results obtained with these models and with good results as long as nonlinear behaviour is relatively unimportant. Limiting criteria concerning the operability are, therefore, generally restricted to threshold values on significant amplitudes of motions and accelerations. If the nonlinear phenomena, such as the peak accelerations, become the limiting factor, as apparently is the case for these fast ships, the use of these linear models may no longer be justifiable. On the other hand as long as linear models are being used exclusively as tools in the operability studies the formulation of criteria based on nonlinear phenomena is of little or no use.
Therefore as a result of this study new limiting criteria were formulated which were based on the significant values of the vertical accelerations at midship and at the bow, even though it was known that these were not the actual limiting phenomena. A "translation" from peak values to significant values had to be made.
These criteria were:

$$af_{1/3} < 0.50 * g\ m/s^2$$
$$am_{1/3} < 0.36 * g\ m/s^2$$

The basic underlying assumption used to formulate these criteria was the supposed linear response of the ship to the waves. The waveheights in an ocean wave spectrum are assumed to be Rayleigh distributed. This assumption is verified in many occasions and is commonly accepted for shipmotion analyses purposes. For a linear system this implies that the responses of the system to these waves are also Rayleigh distributed. The formulation for the Rayleigh distribution reads:

$$p(x) = \left(\frac{x}{m_o x} * \exp \left(- \frac{x^2}{2 * m_o x} \right) \right.$$

in which:

$$m_o = \int_0^\infty S(\omega) d\omega \; m$$

For the significant waveheight, being the average of the highest one third part of the waves it may be found:

$$X_{a_{1/3}} \cong 2 * \sqrt{m_o}$$

As the maximum value of the response of the ship in shipmotions studies generally the value with a 1/1000 chance of exceedence is used:

$$X_{a1/1000} \cong 4 * \sqrt{m_o} = 2 * X_{a1/3}$$

So the peak values found in the full scale experiments on board the fast ships as mentioned above, which were found to be the threshold values for the voluntary speed reduction by the crews, were divided by a factor two to yield the limiting criteria expressed as significant threshold values. From the results on the motion analysis on the DSDS parent models as described in the previous Chapter, it is known that this assumption is not valid for the lower deadrise hulls. The use of this assumption in the formulation of the criteria may therefore strongly favour these low deadrise hulls. It should be emphasized that the derived criteria, be it the peak values or the significant values, are both based on the described study which had only a very limited scope. It was set up and carried out only to provide some guidelines in the area of acceptable acceleration levels aboard fast ships within a rather short period of time. Its outcome should not be regarded as to be near an allround and robust solution to the criteria formulation problem because, it still certainly lacks general applicability. Nevertheless it provides some useful grip on the problem and made the operability analyses carried out to optimise designs feasible. A more extensive study to attack this problem, incorporating long term full scale measurements along the same lines onboard a larger variety of ships, was formulated and set up but is still being retarded due to lack of adequate funding. In addition, a long term research project was started to investigate the motion sickness incidence aboard ships in order to be able to define acceptable levels of accelerations in irregular waves

and combined motions. This may yield a completely different set of criteria which are of special interest for passenger ferries etc.

5.3 Operability calculations

In 1985 the Netherlands Ministry of Justice commissioned an optimisation study to be carried out on a new design of a patrol vessel with respect to its operability. The ship was going to be deployed in the Dutch coastal areas of the North Sea. The general description of the design was known, i.e.

Length on the waterline	=	21	meter
Beam on the waterline	=	4.4	meter
Draft	=	1.3	meter
Displacement	=	44.0	$meter^3$
Design speed	=	25	knots

The design had to be a hard chined planing hull with one chine on either side. An impression of the bodyplan of the preliminary design may be obtained from Figure 5.1.

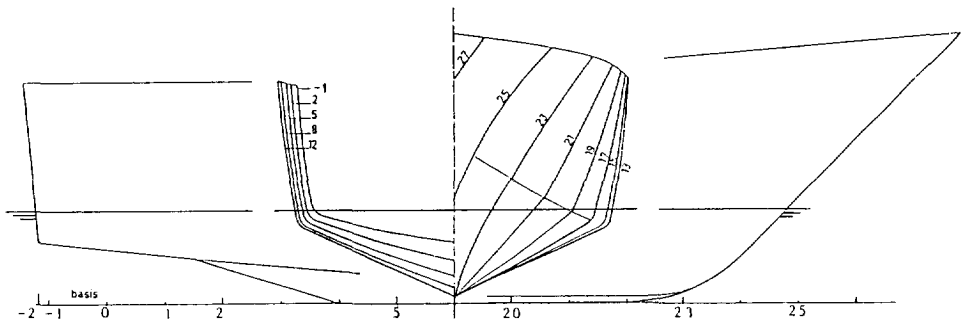

Figure 5.1: Linesplan of the coastal patrol boat

An optimisation of the calm water resistance was not to be taken into account. The prime design parameters to be investigated were: the length, the beam and the draft of the ship.

The study was carried out by applying the aforementioned criteria on the acceptable levels of vertical accelerations only. The results of this study, orginally carried out using a linear computational model and the described limiting criteria based on significant values, will be used to show the effect on the outcome of the use of a nonlinear computational model and the use of the peak-accelerations in the criteria.

The ship having the main dimensions as presented in the Table was chosen as the parent model of a small systematic series of design variations. The length of the parent design was changed to 15 and 25 meters respectively, keeping beam and draft constant. The draft was changed to 0.90 and 1.5 meters respectively on the 21 meter long design only, keeping the beam constant and finally the beam was changed to 4.82 and 5.36 meters respectively again only on the 21 meter parent design whilst keeping the draft constant. The total number of design variations within the series was seven. A schematic representation of the design variation is presented in Figure 5.2. For all these design variations the operability in the given sea area was determined.

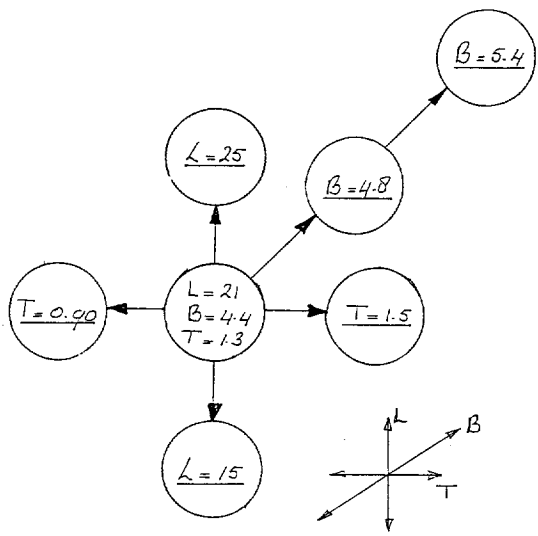

Figure 5.2 Design variations

The operability calculations were carried out using the well known technique based on the available scatter diagrams of the area under consideration. In these scatter diagrams the relation between the significant waveheight, the peak period of the spectrum and the percentage of occurrence of that particular combination is presented. This data is available on a monthly or an all-year basis and is derived from long term observations in that specific area.

In order to be able to calculate the operability of any particular ship the relevant response of that ship to all those different wave spectra has to be calculated. In the present study on the coastal patrol vessel, the relevant responses of the ship were the vertical accelerations at the bow and midship. For each particular combination of significant wave height and peak period, as presented in the scatter diagram, it was checked whether the threshold values, given by the criteria, were surpassed or not. The percentage of time in which the ship under consideration can be operated may then be approximated.

To calculate the responses of all the design variations for this particular study use was made of the motion calculation code TRIAL of the Shiphydromechanics Laboratory. This code computes the vertical motions of ships in head and following waves using a linear computational model based on the Ordinary Strip Theory, both Version1 and Version 2. For the present calculations Version 1 was used, a decision based on the experience obtained from the study carried out by Blok and Beukelman (2) with the parent of the HSDHF Series.
In order to check the accuracy of the calculation method used for predicting the motions, a series of experiments in both reguar and irregular waves was carried out with the parent model.

From a comparison of the measured and calculated results it was concluded that the heave motion was predicted rather well but that the pitch motion showed a considerable underprediction, particularly near resonance. Unfortunately the vertical accelerations were only measured at a position near the midship section (ord 12) and although in regular waves the difference between measured and predicted results remained within 10 percent, in irregular waves the vertical accelerations were significantly underpredicted by a margin of more than 25 percent.

A typical example of such an operability calculation using the known scatter diagram is presented in Figure 5.3 for the parent hull at 25 knots.

No attempt was made to bring a "mission profile" of the ship into the calculations, because for comparison between the different designs this was not felt necessary. In general the limiting conditions of fast ships in waves, when only criteria are being used based on the vertical acceleration levels, are most frequently encountered in head waves. Therefore the assumption is being used that the ships sail in head waves during 100 percent of the time. Without going into further details concerning the outcome of this optimisation study, one particular design variation will be selected to show the importance of the use of nonlinear computational models in these kinds of operability calculations.

Not all results of this study will be shown here but only the particular variation that will be considered for the comparison: the beam variation. With the parent hull as a starting point two other designs were generated having a smaller and a larger beam respectively, whilst keeping the length and the draft constant. The main particulars of these models are presented in Table 5.1.
By changing the beam with constant length, the length to beam ratio of the ships changes considerably. From experience with the Ordinary Strip Theory it is known that these changes can be dealt with for ordinary ships. In the case of planing vessels, however, the steady state planing condition will also be affected, resulting in a difference in sinkage and trim, which is not accounted for in the linear theory.

By changing the beam with constant draft, the beam to draft ratio is also changed considerably. In the case of a planing hull with hard chines this implies

specifically a change in deadrise angle of the planing bottom at midship. Since the hulls of the design variations were obtained from the parent hull by using an afine transformation technique, this change in deadrise angle at ordinate 10 results also in a change of the deadrise over the entire length of the ship. For the design variations under consideration the difference in the deadrise angle at ordinate 10 ranged from 28 degrees on model #3 with B/T = 3.48 to 22 degrees for model #5 with B/T = 4.22. Such a considerable change in the deadrise should influence the motions and in particular the vertical accelerations.

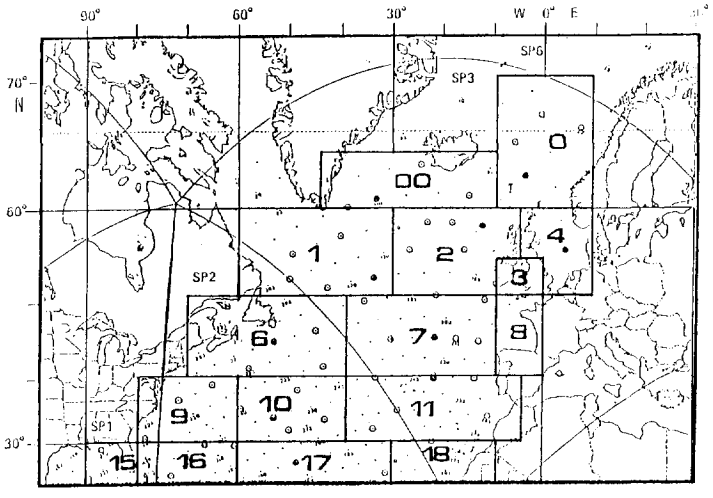

No.	T_p sec.	% frequency of $\bar{H}_{1/3}$	% operability	$\bar{H}_{1/3}$ (metres) 0.5	1.5	2.5	3.5	4.5	5.5	6.5	7.5	8.5	9.5
1	3.2	2.4	2.4	2.4	-	-	-	-	-	-	-	-	-
2	4.8	3.5	3.5	1.8	1.7	-	-	-	-	-	-	-	-
3	6.3	11.0	10.8	3.4	7.4	0.2	-	-	-	-	-	-	-
4	7.5	14.3	10.8	4.2	6.6	3.6	-	-	-	-	-	-	-
5	8.8	13.3	6.8	3.2	3.6	5.6	0.9	-	-	-	-	-	-
6	9.7	17.6	7.1	3.7	3.4	5.3	4.6	0.5	-	-	-	-	-
7	10.9	10.1	4.3	2.1	2.2	1.6	1.8	2.0	0.4	-	-	-	-
8	12.4	9.8	4.3	2.1	2.2	1.1	0.9	1.2	1.6	0.6	0.1	-	-
9	13.8	5.2	3.3	1.3	1.3	0.7	0.5	0.3	0.1	0.3	0.3	0.1	-
10	15.0	8.7	6.7	3.4	2.1	1.2	0.8	0.3	0.2	0.2	0.2	0.2	0.1
11	16.4	3.7	2.8	0.8	0.8	0.7	0.5	0.3	0.2	0.1	0.1	0.05	0.1
Total		99.6	62.8										

Figure 5.3: Typical example scatter diagram for determining operability of the parent model. Speed is 25 knots

TABLE 5.1

model #	3	4	5
length m	21.0	21.0	21.0
beam m	4.42	4.85	5.36
draft m	1.27	1.27	1.27
∇ m^3	44.0	48.0	53.0
L/B	4.66	4.25	3.84
B/T	3.48	3.82	4.22

The results obtained for these three ships using the linear computational model only a small difference in response between ship #3 and #4. The yields response of ship #5 was significantly lower. The effect on the operability is shown in Figure 5.4.

As may be seen from this figure the operability increases with increasing beam when the ship motion calculations are performed with linear computational model. Even though not all design parameters were completely kept constant, such as displacement and L/B ratio, the influence of a change in deadrise angle would intuitively affect the operability of these ships just the other way around: i.e. increasing the beam decreases the deadrise angle of the planing hull and this leads to a decreased operability of the ship in waves.

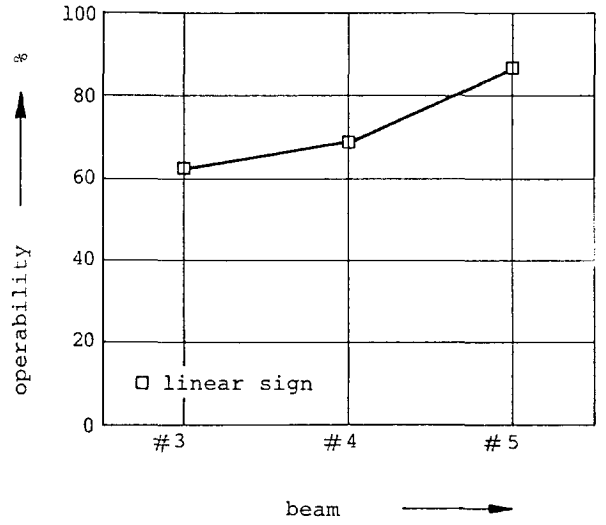

Figure 5.4: Operability of the beam variations of the parent model

To investigate whether the use of the present nonlinear computational model would yield the same results as obtained with the linear model, simulations were carried out with FASTSHIP using the same design variations.
For each particular combination of the significant wave height and the peak period of the wave spectrum as presented in the scatter diagram, a simulation of the behaviour of these ships in that particular wavespectrum was made. All simulation runs extended over a period of roughly 300 seconds sailing time on model scale for the spectrum with the small peak period to roughly 600 seconds for the spectrum with the large peak period. The number of wave encounters was considered to be high enough for comparison purposes. As may be realised this amounted already to a large number of lengthy simulations to be carried out. The results for the three models with respect to the staionary planing condition as approximated in FASTSHIP by using the derived polynomials, are presented in Table 5.2

The speed under consideration is rather low, which explains the relatively small rise of the Centre of Gravity of these designs. The variation of the sinkage and trim over the three designs shows a trend as to be expected: the wider ship produces more lift and trim angle in comparison with the narrow hull.

TABLE 5.2

model #	3	4	5
trim (degr)	2.9	2.5	2.2
Rcg m	0.03	0.01	0.00
Fn_∇	1.93	1.96	2.00
Cm	1.204	1.258	1.281
a_{bf}	0.69	0.74	0.77

First the operability of the ships has been predicted using the regular limiting criteria based on the significant values of the vertical accelerations. Hereto the simulated recordings of the vertical accelerations at the bow and midship were analysed to yield the significant values, which were used in conjuction with data of the scatter diagram to determine the operability of the ships.

The results of the obtained operability are presented in Figure 5.5 on a basis of the beam of the ship and compared with the results obtained with the linear motion prediction.
As may be seen from this figure the trend of the dependency of the operability of the ship with respect to the variation in the beam is reversed when compared with the results obtained previously with the linear computational model. Increasing the beam leads to a reduction of the operability. The decrease in

deadrise angle obviously leads to a decrement of the operability.
The absolute magnitude of the trend with respect to the change in deadrise, however, is influenced by the choice of the design variations:

The model with the largest beam and the lower deadrise has considerable more displacement with respect to the parent model. Similarly, the narrow and high deadrise hull has considerably less displacement. The absolute magnitude of the vertical accelerations is influenced by this change in displacement which leads to lower values for the heavier model and higher values for the lighter model when compared with the situation in which the ships had exactly the same displacement. The influence of the change in deadrise angle is therefore somewhat masked by this effect. Nevertheless the reversed trend is obvious.
Secondly full use was made of the nonlinear computational model to assess the operability.
The use of a nonlinear computational model gives the opportunity to use the actual limiting criteria with respect to the operability of the fast ships in waves such as found during the described full scale experiments onboard the real craft. These proved to be the occurrence of peaks in the vertical accelerations rather than the level of the prevailing significant values. As explained the use of the criteria based on the significant values originated from the use of linear computational models. The peak accelerations which provoked the voluntary speed reductions by the crew were, as explained before, twice the values used for the significant values.

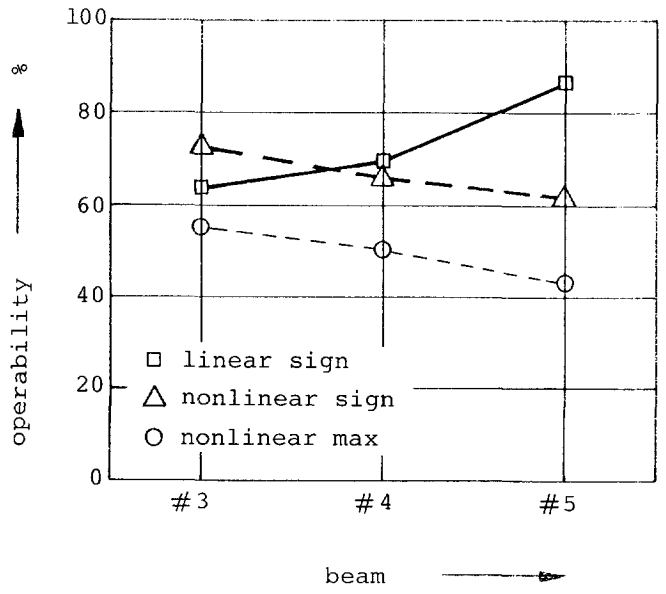

Figure 5.5: Operability comparison as function of the beam using both linear and nonlinear computational models.

If the occurrence of such a peak in the simulations is used as a limiting criterium rather than the significant values of the vertical accelerations, a new assessment of the operability can be made. The criteria then become:

$$af_{max} < 1.0 * g\ m/sec^2$$

and

$$am_{max} < 0.7 * g\ m/sec^2$$

The results of the computed operability of the beam variations using these criteria were also plotted in Figure 5.4. As may be seen from these results the predicted operability is significantly lower than the operability based on the significant values of the vertical accelerations. Although no specific attention should be paid to the absolute values of the calculated operability using the described procedure, it may be concluded that the operability calculations based on the peak values in the vertical accelerations are roughly 15 to 20 percent lower. The trend found from the calculations based on the significant values is similar to the one found from the calculations based on the peak values, although with decreasing deadrise the absolute difference between the two increases.

From the results of this study on the use of nonlinear computational models it may be concluded that their use has a significant effect on the operability prediction of fast monohulls. This is particularly true for the design variations under consideration are sensitive to the nonlinear behaviour of the ship, such as in the demonstrated case of deadrise changes. The full use of peak accelerations as limiting criteria with a nonlinear computational model also strongly affects the results of an operability analysis.

Conclusions

From the results obtained by the present studies the following conclusions with respect to the prediction of the behaviour of fast monohulls in head seas may be drawn:

- the heave and pitch motions of a fast monohull in head waves are nonlinear with respect to the amplitudes of the incoming waves. In particular the vertical accelerations show strong nonlinearities, which increase with increasing forward speed and decreasing deadrise angle.

- the motions and accelerations of a fast monohull in waves are strongly influenced by the the steady state trim and sinkage of the ship at its forward speed. These should be taken into the computations, even when using linear computational models.

- the introduction of nonlinear effects, such as the hydrodynamic lift and the effects associated with the large relative motions which these craft may experience, into a computational model used to predict the motions and accelerations in waves, is important for obtaining a more accurate prediction of the motions and in particular of the peak vertical accelerations.

- the vertical added mass and its distribution along the length of a fast moving monohull in head wave conditions is found to be hardly dependent on the forward speed and the associated surface disturbances if the hydrodynamic load distribution along the length of the ship due to its high forward speed is taken into account.

- the introduction of timedependent added mass into a computational model is of great importance for an accurate prediction of the fluctuating hydrodynamic lift on the fast monohull while moving in head waves. It has a strong influence on the predicted heave and pitch motions and in particular on the peaks in the vertical accelerations.

- the peaks in the vertical accelerations are the limiting factors for a safe operation of fast ships in waves. The exclusive use of criteria, which limit the safe operability of fast ships in waves based solely on significant values for vertical acclerations only, may lead to a considerable overestimation of the operability. It should be strongly recommended that further investigations are carried out in this area. In particular the present limitation to head seas conditions only should be taken into consideration.

The availability of a simulation program for the computation of time histories of the heave- and pitchmotions as well as the vertical accelerations in any given seastate provides the opertunity to use a set of more advanced criteria, which better represent the actual practice aboard of these ships.

- the accurate prediction of the absolute peakvalues in the vertical accellerations remains hazardous. In the computed outcome using the presented procedure there is a dependency on the magnitude of the time step used in the computations, as well as on the number of components used in the irregular wave train realisation. A possible solution may be found in taking the energy content of the peaks rather than the absolute height of them. For comparison purposes as used in the present study these difficulties may be partly overcome and are therefore of less significance.

- the use of linear computational models for the prediction of the operability of fast monohulls in waves may lead to erroneous results and design trends.
By using a computational model which includes the important nonlinear effects it becomes possible to predict the operability with a higher accurracy. In particular the influence on the operability of the ship in waves of some design parameters, such as speed, deadrise, trim and bowshape may be better predicted by using such a computational model.

Appendix

β	Fn_∇		a_0	a_1	a_2	a_3	a_4	a_5	a_5
			a_7	a_8	a_9	a_{10}	a_{11}	a_{12}	
12.5	.75	R_t/Δ, ∇=5	.1120E+00	-.1289E-01	.1197E-02	-.3479E-04	-.2297E-01	.2924E-02	-.1347E-03
			-.7272E-03	.9765E-04	.4226E-05	.1256E-04	.2713E-03	.1774E-03	
		R_t/Δ, ∇=50	.1115E+00	-.1290E-01	.1199E-02	-.3510E-04	-.2300E-01	.2917E-02	-.1344E-03
			-.7217E-03	.9901E-04	.4318E-05	.1130E-04	.2728E-03	.1786E-03	
		θ	.1129E+01	.1696E+01	-.3130E+00	.2169E-01	-.2760E+01	.4720E+00	-.2433E-01
			-.3112E+00	.1163E-01	.5206E-03	.2458E-01	-.3180E-02	.3304E-01	
		$RCG/\nabla^{1/3}$	-.4074E+00	.9876E-01	-.2147E-01	.1515E-02	.9922E-01	-.1388E-01	.7181E-03
			-.6410E-02	.2775E-03	.1503E-04	.1030E-02	-.4586E-03	.1524E-04	
	1.00	R_t/Δ, ∇=5	.3996E+00	-.9231E-01	.1192E-01	-.6086E-03	-.4127E-01	.2720E-02	-.5832E-04
			.1094E-02	.3815E-03	.9987E-05	.2345E-03	.1766E-02	.5378E-04	
		R_t/Δ, ∇=50	.4002E+00	-.9267E-01	.1201E-01	-.6158E-03	-.4170E-01	.2753E-02	-.5955E-04
			.1136E-02	.3879E-03	.1025E-04	.2308E-03	.1773E-02	.5885E-04	
		θ	.1515E+02	-.9005E+00	.1166E+00	-.4535E-02	-.6366E+01	.8357E+00	-.3731E-01
			-.7934E+00	.1718E-01	.4324E-03	.5055E-01	.9474E-01	.9864E-01	
		$RCG/\nabla^{1/3}$	-.3251E+00	.9289E-01	-.2020E-01	.1426E-02	.2227E-01	.1884E-03	-.3914E-04
			-.1948E-01	.2537E-03	.1417E-04	.2314E-02	.3813E-03	.7281E-03	
	1.25	R_t/Δ, ∇=5	.8393E+00	-.1246E+00	.1461E-01	-.6615E-03	-.1753E+00	.2255E-01	-.1016E-02
			.4165E-02	.6591E-03	.1478E-04	.8072E-03	.1433E-02	-.7895E-03	
		R_t/Δ, ∇=50	.8375E+00	-.1248E+00	.1466E-01	-.6656E-03	-.1748E+00	.2243E-01	-.1009E-02
			.4036E-02	.6488E-03	.1417E-04	.8146E-03	.1445E-02	-.7806E-03	
		θ	.9889E+01	-.7061E+01	.9620E+00	-.5360E-01	.5572E+01	-.1291E+01	.7367E-01
			-.3946E+00	.3410E-01	.1764E-02	.1420E-01	.2198E+00	.7282E-01	
		$RCG/\nabla^{1/3}$	-.1057E+01	.6355E-01	-.2372E-01	.1890E-02	.4602E+00	-.7229E-01	.3700E-02
			-.1873E-01	.4248E-03	.2053E-04	.2296E-02	.3490E-02	.1174E-02	
	1.50	R_t/Δ, ∇=5	.7786E+00	-.1016E+00	.9022E-02	-.2943E-03	-.1539E+00	.1795E-01	-.7779E-03
			.3499E-02	.1219E-02	.3137E-04	.1069E-02	.3079E-02	.1622E-04	
		R_t/Δ, ∇=50	.7830E+00	-.1028E+00	.9261E-02	-.3111E-03	-.1560E+00	.1823E-01	-.7923E-03
			.3454E-02	.1226E-02	.3162E-04	.1069E-02	.3087E-02	.3045E-04	
		θ	.4786E+02	-.9164E+01	.1350E+01	-.7826E-01	-.9693E+01	.1005E+01	-.3806E-01
			-.3616E+00	.1714E-01	.6256E-03	.3080E-01	.2011E+00	.3556E-01	
		$RCG/\nabla^{1/3}$	-.5638E+00	-.2403E-01	-.1195E-01	.1194E-02	.3355E+00	-.5715E-01	.3043E-02
			-.2849E-01	-.8738E-03	-.4271E-04	.2585E-02	.5695E-02	.8498E-03	
	1.75	R_t/Δ, ∇=5	.5817E+00	.2683E-01	-.1742E-01	.1476E-02	-.1538E+00	.1827E-01	-.7977E-03
			.9107E-03	.1048E-02	.2881E-04	.1050E-02	.2770E-02	.1664E-03	
		R_t/Δ, ∇=50	.5824E+00	.2586E-01	-.1725E-01	.1465E-02	-.1542E+00	.1826E-01	-.7975E-03
			.8446E-03	.1059E-02	.2918E-04	.1052E-02	.2781E-02	.1844E-03	
		θ	.3161E+02	-.6006E+01	.6319E+00	-.2905E-01	-.2892E+01	-.7939E-01	.1623E-01
			-.4067E-01	.1568E-01	.6076E-03	-.1308E-02	.1856E+00	.1581E-01	
		$RCG/\nabla^{1/3}$	.7918E-01	.3672E-01	-.2361E-01	.2115E-02	.5393E-01	-.1695E-01	.1139E-02
			-.1168E-01	-.1828E-03	-.2390E-04	.5145E-03	.3081E-02	.1509E-02	

β	Fn_∇		a_0	a_1	a_2	a_3	a_4	a_5	a_6
			a_7	a_8	a_9	a_{10}	a_{11}	a_{12}	
12.5	2.00	R_t/Δ, ∇=5	.4372E+00	.6303E-01	-.2146E-01	.1633E-02	-.1229E+00	.1416E-01	-.6035E-03
			.1789E-02	.9401E-03	.2507E-04	.7046E-03	.2017E-02	.3221E-03	
		R_t/Δ, ∇=50	.4373E+00	.6227E-01	-.2136E-01	.1627E-02	-.1232E+00	.1413E-01	-.6023E-03
			.1758E-02	.9548E-03	.2561E-04	.6993E-03	.2028E-02	.3424E-03	
		θ	.1322E+02	-.2002E+01	-.1887E+00	.2538E-01	.3508E+01	-.1046E+01	.5417E-01
			.1978E+00	.3248E-02	-.2820E-03	-.2124E-01	.1421E+00	-.5899E-02	
		$RCG/\nabla^{1/3}$	.3061E+00	.5434E-01	-.2893E-01	.2561E-02	-.3087E-01	-.5601E-02	.6545E-03
			-.1355E-01	-.8926E-03	-.6666E-04	.5779E-03	.2339E-02	.1237E-02	
	2.25	R_t/Δ, ∇=5	.4683E+00	.4320E-01	-.1361E-01	.1000E-02	-.1418E+00	.1779E-01	-.7790E-03
			.9081E-03	.9836E-03	.3078E-04	.8248E-03	.1317E-02	.3086E-03	
		R_t/Δ, ∇=50	.4695E+00	.4205E-01	-.1342E-01	.9850E-03	-.1423E+00	.1773E-01	-.7758E-03
			.9280E-03	-.1002E-02	.3148E-04	.8095E-03	.1326E-02	.3277E-03	
		θ	.2005E+02	-.8878E+00	-.2429E+00	.2151E-01	-.1223E+01	-.2412E+00	.2287E-01
			.4608E+00	.3414E-01	.1530E-02	-.1894E-01	.8043E-01	-.3643E-01	
		$RCG/\nabla^{1/3}$	.9376E-01	-.7904E-02	-.1772E-01	.1632E-02	.1013E+00	-.2329E-01	.1340E-02
			-.1703E-01	-.1087E-02	-.5905E-04	.1185E-02	.4634E-02	.2907E-03	
	2.50	R_t/Δ, ∇=5	.3276E+00	.2996E-01	-.7670E-02	.5118E-03	-.7863E-01	.8623E-02	-.3192E-03
			.1414E-02	.7821E-03	.2343E-04	.6311E-03	.5793E-03	.1716E-03	
		R_t/Δ, ∇=50	.3278E+00	.2871E-01	-.7447E-02	.4925E-03	-.7886E-01	.8539E-02	-.3161E-03
			.1371E-02	.7906E-03	.2369E-04	.6169E-03	.5856E-03	.1842E-03	
		θ	.5497E+01	-.1505E+00	-.2074E+00	.1448E-01	.4538E+01	-.1070E+01	.6381E-01
			.5650E+00	.1284E-01	.2049E-03	-.2930E-01	.1067E-01	-.5021E-01	
		$RCG/\nabla^{1/3}$	.5347E+00	.2676E-01	-.2502E-01	.2249E-02	-.1207E+00	.1309E-01	-.5889E-03
			.2506E-02	.1169E-02	.5121E-04	.4842E-03	.4146E-02	.1570E-04	
	2.75	R_t/Δ, ∇=5	.2864E+00	.2157E-01	-.4537E-02	.2855E-03	-.6463E-01	.7329E-02	-.2793E-03
			.2635E-02	.8383E-03	.2825E-04	.5046E-03	.3729E-03	.1657E-03	
		R_t/Δ, ∇=50	.2891E+00	.1934E-01	-.4014E-02	.2408E-03	-.6574E-01	.7390E-02	-.2841E-03
			.2672E-02	.8536E-03	.2874E-04	.4875E-03	.3528E-03	.1661E-03	
		θ	.5251E+01	-.2136E+00	-.4981E-01	-.2390E-03	.3763E+01	-.8703E+00	.5193E-01
			.7439E+00	.3604E-01	.1549E-02	-.2963E-01	-.3124E-01	-.6563E-01	
		$RCG/\nabla^{1/3}$	.4987E+00	-.2149E-01	-.8807E-02	.8621E-03	-.6185E-01	.3117E-02	-.3261E-04
			.7517E-02	.8079E-03	.3312E-04	-.3072E-03	.2070E-02	-.2094E-03	
	3.00	R_t/Δ, ∇=5	.2041E+00	.2262E-01	-.4611E-02	.3277E-03	-.3360E-01	.3327E-02	-.9487E-04
			.2499E-02	.6954E-03	.2360E-04	.4707E-03	.1737E-03	.8781E-04	
		R_t/Δ, ∇=50	.2085E+00	.1942E-01	-.3751E-02	.2557E-03	-.3523E-01	.3475E-02	-.1039E-03
			.2569E-02	.7122E-03	.2412E-04	.4573E-03	.9270E-04	.6799E-04	
		θ	.2750E+01	-.6138E+00	.1493E+00	-.1441E-01	.4592E+01	-.9479E+00	.5502E-01
			.8403E+00	.3900E-01	.1814E-02	-.3527E-01	-.7550E-01	-.7209E-01	
		$RCG/\nabla^{1/3}$	.5527E+00	-.8569E-01	.6848E-02	-.2166E-03	-.4469E-01	.5517E-03	.9890E-04
			.7751E-02	.3866E-03	.2107E-04	-.6350E-03	.1068E-02	-.7190E-03	

β	Fn_∇		a_0	a_1	a_2	a_3	a_4	a_5	a_6
			a_7	a_8	a_9	a_{10}	a_{11}	a_{12}	
25	.75	R_t/Δ, ∇=5	.1268E+00	-.2424E-01	.3491E-02	-.1893E-03	-.2136E-01	.2706E-02	-.1283E-03
			-.1462E-02	-.4897E-05	-.4912E-06	.3145E-05	.2632E-03	.2009E-03	
		R_t/Δ, ∇=50	.1260E+00	-.2365E-01	.3359E-02	-.1802E-03	-.2152E-01	.2711E-02	-.1285E-03
			-.1457E-02	-.5151E-05	-.5195E-06	.2379E-05	.2653E-03	.2007E-03	
		θ	-.2791E+01	.6060E+00	-.1479E-01	-.8580E-03	.4449E-01	.1737E-01	-.3669E-03
			-.3048E+00	-.2215E-02	-.6126E-04	.1374E-01	-.2986E-01	.2900E-01	
		$RCG/\nabla^{1/3}$	-.5631E-01	.1358E-01	.1978E-03	-.9157E-04	-.1305E-01	.3252E-02	-.1867E-03
			-.2090E-02	.6262E-04	.5807E-05	.3741E-04	-.5312E-03	.3005E-03	
	1.00	R_t/Δ, ∇=5	.3665E+00	-.1043E+00	.1400E-01	-.7408E-03	-.1955E-01	-.6496E-03	.1031E-03
			-.1763E-02	.3776E-04	-.5533E-05	.2222E-03	.2048E-02	.2132E-03	
		R_t/Δ, ∇=50	.3659E+00	-.1036E+00	.1385E-01	-.7299E-03	-.2000E-01	-.6113E-03	.1012E-03
			-.1767E-02	.3688E-04	-.5624E-05	.2198E-03	.2048E-02	.2160E-03	
		θ	.1064E+02	-.2476E+01	.2907E+00	-.1443E-01	-.1992E+01	.9811E-01	-.2754E-03
			-.6578E+00	.2138E-03	.3172E-05	.2929E-01	.1417E+00	.7013E-01	
		$RCG/\nabla^{1/3}$	-.2468E+00	.5017E-01	-.5742E-02	.2944E-03	.2368E-01	-.1508E-02	.4642E-04
			-.7365E-02	-.8799E-04	.3699E-06	.2715E-03	-.8045E-03	.7947E-03	
	1.25	R_t/Δ, ∇=5	.7346E+00	-.1753E+00	.2059E-01	-.1003E-02	-.6923E-01	.3296E-02	-.3195E-04
			-.2975E-02	.1928E-03	-.4883E-05	.7575E-03	.4465E-02	.1095E-04	
		R_t/Δ, ∇=50	.7331E+00	-.1744E+00	.2037E-01	-.9872E-03	-.6949E-01	.3290E-02	-.3134E-04
			-.2984E-02	.1955E-03	-.4780E-05	.7530E-03	.4459E-02	.1806E-04	
		θ	.2407E+02	-.6571E+01	.7093E+00	-.3195E-01	-.1193E+01	-.1873E+00	.1544E-01
			-.3438E+00	.7800E-02	.4234E-03	.1579E-01	.2244E+00	.3405E-01	
		$RCG/\nabla^{1/3}$	-.2845E-01	-.4699E-01	.7296E-02	-.3960E-03	.2604E-01	-.5517E-02	.3090E-03
			-.8058E-02	-.1553E-03	-.4078E-05	.2832E-03	.2089E-02	.8162E-03	
	1.50	R_t/Δ, ∇=5	.8278E+00	-.1938E+00	.2319E-01	-.1139E-02	-.8753E-01	.4455E-02	-.1599E-05
			-.6563E-02	.2575E-03	-.1677E-04	.1527E-02	.5371E-02	.2796E-03	
		R_t/Δ, ∇=50	.8263E+00	-.1927E+00	.2293E-01	-.1119E-02	-.8797E-01	.4460E-02	-.1314E-05
			-.6591E-02	.2606E-03	-.1666E-04	.1521E-02	.5364E-02	.2897E-03	
		θ	.2532E+02	-.8269E+01	.1002E+01	-.4986E-01	-.3671E+00	-.3866E+00	.2851E-01
			-.7646E+00	-.2883E-02	-.2796E-03	.5567E-01	.2880E+00	.6108E-01	
		$RCG/\nabla^{1/3}$	.5694E-01	-.1061E+00	.1742E-01	-.9896E-03	.4806E-01	-.8546E-02	.4183E-03
			-.1034E-01	-.1755E-03	-.7328E-05	.3267E-03	.2052E-02	.1164E-02	
	1.75	R_t/Δ, ∇=5	.9566E+00	-.1196E+00	.7891E-02	-.1443E-03	-.1932E+00	.2134E-01	-.8377E-03
			-.3208E-02	.7299E-03	-.3397E-06	.1896E-02	.4743E-02	-.6219E-04	
		R_t/Δ, ∇=50	.9550E+00	-.1183E+00	.7563E-02	-.1185E-03	-.1938E+00	.2133E-01	-.8361E-03
			-.3264E-02	.7311E-03	-.3583E-06	.1890E-02	.4738E-02	-.4953E-04	
		θ	.3901E+02	-.6757E+01	.5287E+00	-.1651E-01	-.6611E+01	.4903E+00	-.1453E-01
			-.6147E+00	-.5014E-02	-.4529E-03	.4609E-01	.3434E+00	.4319E-01	
		$RCG/\nabla^{1/3}$	.3378E+00	-.1661E+00	.2435E-01	-.1350E-02	.8538E-04	-.4868E-02	.3050E-03
			-.1249E-01	-.1158E-03	-.5414E-05	.3944E-03	.4640E-02	.1473E-02	

β	Fn_∇		a_0	a_1	a_2	a_3	a_4	a_5	a_6
			a_7	a_8	a_9	a_{10}	a_{11}	a_{12}	
25	2.00	R_t/Δ, ∇=5	.9093E+00	-.6004E-01	-.2084E-03	.2698E-03	-.2244E+00	.2790E-01	-.1173E-02
			.1494E-02	.1223E-02	.2299E-04	.1875E-02	.2861E-02	-.3119E-03	
		R_t/Δ, ∇=50	.9074E+00	-.5865E-01	-.5893E-03	.3005E-03	-.2249E+00	.2787E-01	-.1171E-02
			.1423E-02	.1228E-02	.2317E-04	.1868E-02	.2848E-02	-.2987E-03	
		θ	.4651E+02	-.5594E+01	.4061E+00	-.1428E-01	-.1074E+02	.1163E+01	-.4941E-01
			-.3024E+00	-.1047E-01	-.6648E-03	.2291E-01	.2767E+00	.4257E-02	
		$RCG/\nabla^{1/3}$	.6440E+00	-.2007E+00	.2825E-01	-.1576E-02	-.8261E-01	.6147E-02	-.2399E-03
			-.1344E-01	-.3522E-03	-.1875E-04	.3414E-03	.5541E-02	.1394E-02	
	2.25	R_t/Δ, ∇=5	.7267E+00	-.3065E-01	-.4856E-03	.1254E-03	-.1832E+00	.2340E-01	-.9550E-03
			.1759E-02	.1136E-02	.1964E-04	.1832E-02	.1057E-02	-.3018E-03	
		R_t/Δ, ∇=50	.7238E+00	-.2946E-01	-.8423E-03	.1554E-03	-.1830E+00	.2322E-01	-.9432E-03
			.1652E-02	.1129E-02	.1914E-04	.1825E-02	.1035E-02	-.2923E-03	
		θ	.3930E+02	-.3838E+01	.1671E+00	-.1504E-02	-.9002E+01	.9844E+00	-.4198E-01
			-.5436E-01	-.5073E-02	-.2881E-03	.1382E-01	.1938E+00	-.3012E-01	
		$RCG/\nabla^{1/3}$	.7810E+00	-.2062E+00	.2691E-01	-.1457E-02	-.1138E+00	.9881E-02	-.4012E-03
			-.1288E-01	-.2335E-03	-.1484E-04	.4903E-03	.5972E-02	.1138E-02	
	2.50	R_t/Δ, ∇=5	.5911E+00	-.1332E-02	-.2723E-02	.1880E-03	-.1582E+00	.2103E-01	-.8556E-03
			.2990E-02	.1367E-02	.3447E-04	.1735E-02	-.2485E-04	-.8911E-04	
		R_t/Δ, ∇=50	.5896E+00	.5678E-03	-.3241E-02	.2295E-03	-.1594E+00	.2106E-01	-.8555E-03
			.2934E-02	.1372E-02	.3467E-04	.1722E-02	-.6421E-04	-.8239E-04	
		θ	.3457E+02	-.2448E+01	.3596E-01	.3139E-02	-.8405E+01	.9749E+00	-.4280E-01
			.4796E-01	-.1524E-01	-.5625E-03	.6950E-02	.1132E+00	-.5600E-01	
		$RCG/\nabla^{1/3}$	.9096E+00	-.1932E+00	.2314E-01	-.1211E-02	-.1710E+00	.1877E-01	-.8557E-03
			-.1322E-01	-.1999E-03	-.1303E-04	.6159E-03	.6142E-02	.9184E-03	
	2.75	R_t/Δ, ∇=5	.5063E+00	.3047E-01	-.7043E-02	.4750E-03	-.1525E+00	.2178E-01	-.9195E-03
			.5580E-02	.1404E-02	.4042E-04	.1406E-02	-.1424E-02	-.1939E-03	
		R_t/Δ, ∇=50	.5042E+00	.3293E-01	-.7703E-02	.5276E-03	-.1538E+00	.2182E-01	-.9199E-03
			.5526E-02	.1411E-02	.4076E-04	.1391E-02	-.1479E-02	-.1887E-03	
		θ	.2718E+02	-.1949E+01	.7036E-01	-.2685E-02	-.5753E+01	.6084E+00	-.2452E-01
			.1545E+00	-.1495E-01	-.5452E-03	.5244E-02	.6356E-01	-.6772E-01	
		$RCG/\nabla^{1/3}$	.1010E+01	-.1952E+00	.2321E-01	-.1272E-02	-.2037E+00	.2262E-01	-.1013E-02
			-.1367E-01	-.3822E-03	-.2246E-04	.6646E-03	.6673E-02	.6786E-03	
	3.00	R_t/Δ, ∇=5	.4725E+00	.2993E-01	-.7451E-02	.5195E-03	-.1502E+00	.2257E-01	-.9848E-03
			.4185E-02	.1587E-02	.5345E-04	.1713E-02	-.7806E-03	-.1318E-03	
		R_t/Δ, ∇=50	.4693E+00	.3357E-01	-.8372E-02	.5913E-03	-.1520E+00	.2269E-01	-.9906E-03
			.4146E-02	.1587E-02	.5357E-04	.1687E-02	-.8693E-03	-.1363E-03	
		θ	.2337E+02	.1400E+00	-.1892E+00	.1559E-01	-.5536E+01	.6424E+00	-.2701E-01
			.6203E+00	.8787E-02	.4819E-03	-.3054E-01	-.6558E-01	-.7799E-01	
		$RCG/\nabla^{1/3}$	.1152E+01	-.1663E+00	.1819E-01	-.9180E-03	-.2701E+00	.3175E-01	-.1428E-02
			-.7406E-02	.1002E-03	-.2626E-05	.2663E-03	.5604E-02	.6099E-03	

β	Fn_∇		a_0	a_1	a_2	a_3	a_4	a_5	a_6
			a_7	a_8	a_9	a_{10}	a_{11}	a_{12}	
30	.75	R_t/Δ, ∇=5	.2375E+00	-.1031E+00	.1772E-01	-.1041E-02	-.5205E-02	-.2773E-04	.1531E-04
			-.1068E-02	-.6608E-04	-.4816E-05	-.7651E-05	.4227E-03	.9094E-04	
		R_t/Δ, ∇=50	.2441E+00	-.1069E+00	.1843E-01	-.1084E-02	-.5458E-02	-.9167E-05	.1467E-04
			-.1061E-02	-.6654E-04	-.4901E-05	-.9439E-05	.4219E-03	.9157E-04	
		θ	-.3308E+01	.2550E+01	-.4395E+00	.2636E-01	-.1037E+01	.1771E+00	-.8958E-02
			-.2613E+00	-.3974E-02	-.4585E-03	.1186E-01	-.7422E-02	.2557E-01	
		$RCG/\nabla^{1/3}$	-.3177E+00	.1208E+00	-.2063E-01	.1227E-02	.2717E-01	-.3003E-02	.1353E-03
			-.6540E-03	.3208E-03	.2741E-04	.5574E-05	-.7108E-03	.2287E-03	
	1.00	R_t/Δ, ∇=5	.9682E+00	-.4393E+00	.7588E-01	-.4470E-02	-.2704E-01	.1049E-02	-.5175E-05
			-.9952E-03	.1588E-03	.2220E-05	.2921E-03	.1925E-02	-.4311E-04	
		R_t/Δ, ∇=50	.9787E+00	-.4453E+00	.7700E-01	-.4538E-02	-.2747E-01	.1085E-02	-.6608E-05
			-.9873E-03	.1573E-03	.1994E-05	.2893E-03	.1921E-02	-.4144E-04	
		θ	.5441E+02	-.2288E+02	.3988E+01	-.2386E+00	-.5056E+01	.5340E+00	-.2318E-01
			-.4847E+00	.9449E-02	.5464E-03	.2527E-01	.1910E+00	.4970E-01	
		$RCG/\nabla^{1/3}$	-.4817E+00	.1940E+00	-.3240E-01	.1881E-02	.1884E-01	-.3944E-03	.2894E-04
			-.5076E-02	-.1482E-03	-.1146E-04	.2403E-03	-.8347E-03	.4546E-03	
	1.25	R_t/Δ, ∇=5	.1893E+01	-.8457E+00	.1457E+00	-.8577E-02	-.6406E-01	.3342E-02	-.7825E-04
			-.5532E-02	-.2505E-03	-.3509E-04	.5791E-03	.3928E-02	.1844E-03	
		R_t/Δ, ∇=50	.1908E+01	-.8539E+00	.1472E+00	-.8671E-02	-.6465E-01	.3390E-02	-.8027E-04
			-.5525E-02	-.2523E-03	-.3551E-04	.5756E-03	.3924E-02	.1879E-03	
		θ	.8265E+02	-.3612E+02	.6187E+01	-.3627E+00	-.4466E+01	.3828E+00	-.1584E-01
			-.3732E+00	.8297E-02	.4187E-03	.2140E-01	.1987E+00	.3160E-01	
		$RCG/\nabla^{1/3}$	.1322E+00	-.9430E-01	.1822E-01	-.1159E-02	-.2056E-01	.2794E-02	-.1375E-03
			-.7445E-02	-.3535E-03	-.2478E-04	.3577E-03	.1312E-02	.6003E-03	
	1.50	R_t/Δ, ∇=5	.1858E+01	-.8280E+00	.1431E+00	-.8422E-02	-.5704E-01	.2596E-02	-.2847E-04
			-.5175E-02	-.4050E-03	-.4045E-04	.7328E-03	.3278E-02	-.1106E-03	
		R_t/Δ, ∇=50	.1879E+01	-.8404E+00	.1454E+00	-.8563E-02	-.5732E-01	.2571E-02	-.2619E-04
			-.5174E-02	-.4052E-03	-.4082E-04	.7281E-03	.3271E-02	-.1054E-03	
		θ	.6978E+02	-.3135E+02	.5460E+01	-.3225E+00	-.2889E+01	.1742E+00	-.4266E-02
			-.6324E+00	.1348E-02	.1646E-03	.3824E-01	.1397E+00	.5171E-01	
		$RCG/\nabla^{1/3}$	.2261E-01	-.1064E+00	.2000E-01	-.1204E-02	.6209E-01	-.9628E-02	.5027E-03
			-.5670E-02	.4477E-03	.3335E-04	.4417E-03	-.1045E-03	.6196E-03	
	1.75	R_t/Δ, ∇=5	.1702E+01	-.7709E+00	.1305E+00	-.7581E-02	-.6966E-02	-.5282E-02	.3696E-03
			-.1824E-02	-.1237E-02	-.1262E-03	.6829E-03	.3235E-02	-.6792E-03	
		R_t/Δ, ∇=50	.1733E+01	-.7893E+00	.1339E+00	-.7791E-02	-.7524E-02	-.5292E-02	.3716E-03
			-.1813E-02	-.1224E-02	-.1256E-03	.6794E-03	.3231E-02	-.6722E-03	
		θ	.7224E+02	-.3582E+02	.6161E+01	-.3609E+00	.3320E+00	-.3882E+00	.2447E-01
			-.9607E+00	-.2280E-01	-.2228E-02	.5705E-01	.2030E+00	.7807E-01	
		$RCG/\nabla^{1/3}$	.4322E+00	-.2972E+00	.5325E-01	-.3187E-02	.4307E-01	-.8474E-02	.4483E-03
			-.1120E-01	.1239E-04	.5205E-05	.4255E-03	.1557E-02	.1150E-02	

β	Fn_∇		a_0	a_1	a_2	a_3	a_4	a_5	a_6
			a_7	a_8	a_9	a_{10}	a_{11}	a_{12}	
30	2.00	R_t/Δ, ∇=5	.1656E+01	-.6805E+00	.1134E+00	-.6550E-02	-.4770E-01	.1274E-02	.4691E-04
			.6126E-02	-.3168E-03	-.6683E-04	.7238E-03	.2907E-02	-.1289E-02	
		R_t/Δ, ∇=50	.1694E+01	-.7038E+00	.1177E+00	-.6804E-02	-.4649E-01	.9008E-03	.7014E-04
			.5933E-02	-.3613E-03	-.7191E-04	.7270E-03	.2913E-02	-.1273E-02	
		θ	.8804E+02	-.3982E+02	.6620E+01	-.3810E+00	-.2136E+01	-.1155E+00	.1139E-01
			-.1008E+01	-.3554E-01	-.2607E-02	.5899E-01	.3045E+00	.6854E-01	
		$RCG/\nabla^{1/3}$	.8667E+00	-.4740E+00	.8228E-01	-.4842E-02	.1408E-01	-.5696E-02	.3229E-03
			-.1656E-01	.1728E-03	.2300E-04	.7306E-03	.2799E-02	.1625E-02	
	2.25	R_t/Δ, ∇=5	.1453E+01	-.5376E+00	.9138E-01	-.5364E-02	-.8717E-01	.9157E-02	-.3582E-03
			.1024E-01	.2689E-03	-.3268E-04	.7508E-03	.1368E-02	-.1379E-02	
		R_t/Δ, ∇=50	.1506E+01	-.5676E+00	.9695E-01	-.5702E-02	-.8862E-01	.9234E-02	-.3604E-03
			.1017E-01	.2831E-03	-.3217E-04	.7504E-03	.1373E-02	-.1365E-02	
		θ	.9557E+02	-.3926E+02	.6365E+01	-.3630E+00	-.4819E+01	.2255E+00	-.4879E-02
			-.5270E+00	.1015E-01	.1224E-02	.3807E-01	.3517E+00	.3215E-01	
		$RCG/\nabla^{1/3}$	.1353E+01	-.6515E+00	.1099E+00	-.6388E-02	-.2494E-01	-.2037E-02	.1454E-03
			-.1627E-01	.1617E-03	.2885E-04	.5353E-03	.4753E-02	.1634E-02	
	2.50	R_t/Δ, ∇=5	.9319E+00	-.2954E+00	.5024E-01	-.2921E-02	-.8361E-01	.8261E-02	-.3369E-03
			.1184E-01	.8303E-03	.5622E-06	.9069E-03	-.7135E-03	-.1244E-02	
		R_t/Δ, ∇=50	.9948E+00	-.3296E+00	.5657E-01	-.3304E-02	-.6611E-01	.8461E-02	-.3445E-03
			.1181E-01	.8371E-03	.5183E-06	.8959E-03	-.7075E-03	-.1236E-02	
		θ	.9824E+02	-.3926E+02	.6440E+01	-.3724E+00	-.5970E+01	.3969E+00	-.1310E-01
			-.4028E+00	-.5026E-01	-.3700E-02	.2618E-01	.3341E+00	-.4590E-02	
		$RCG/\nabla^{1/3}$	.1842E+01	-.8079E+00	.1355E+00	-.7899E-02	-.9085E-01	.5616E-02	-.1970E-03
			-.1795E-01	-.1024E-02	-.7721E-04	.4877E-03	.6345E-02	.1413E-02	
	2.75	R_t/Δ, ∇=5	.6313E+00	-.1312E+00	.2362E-01	-.1399E-02	-.7721E-01	.1184E-01	-.5199E-03
			.1186E-01	.9825E-03	.2873E-05	.8766E-03	-.1911E-02	-.7917E-03	
		R_t/Δ, ∇=50	.7086E+00	-.1717E+00	.3109E-01	-.1850E-02	-.8123E-01	.1225E-01	-.5382E-03
			.1182E-01	.9787E-03	.2031E-05	.8611E-03	-.1907E-02	-.7870E-03	
		θ	.9068E+02	-.3365E+02	.5499E+01	-.3163E+00	-.7182E+01	.6379E+00	-.2509E-01
			-.4376E-01	.5334E-02	.1064E-02	.1525E-01	.2526E+00	-.2757E-01	
		$RCG/\nabla^{1/3}$	.2129E+01	-.9369E+00	.1570E+00	-.9168E-02	-.9685E-01	.4548E-02	-.1089E-03
			-.1769E-01	-.9548E-03	-.7379E-04	.6547E-03	.7718E-02	.1153E-02	
	3.00	R_t/Δ, ∇=5	.3244E+00	.3275E-01	-.5660E-02	.2629E-03	-.8965E-01	.1499E-01	-.6978E-03
			.3986E-02	.7377E-04	-.6592E-04	.1683E-02	-.1222E-02	-.8664E-03	
		R_t/Δ, ∇=50	.4106E+00	-.1235E-01	.2636E-02	-.2355E-03	-.9399E-01	.1542E-01	-.7167E-03
			.4036E-02	.5876E-04	-.6810E-04	.1653E-02	-.1243E-02	-.8652E-03	
		θ	.7509E+02	-.2554E+02	.4114E+01	-.2306E+00	-.6603E+01	.6169E+00	-.2355E-01
			.1718E+00	-.1843E-01	-.1362E-02	-.9041E-02	.1298E+00	-.3701E-01	
		$RCG/\nabla^{1/3}$	.2406E+01	-.9778E+00	.1612E+00	-.9288E-02	-.1598E+00	.1235E-01	-.4494E-03
			-.1356E-01	-.3565E-03	-.2769E-04	.4475E-03	.8148E-02	.1005E-02	

Fn_∇		a_0	a_1	a_2	a_3	a_4	a_5
		a_6	a_7				
.75	$\Delta R_t/\Delta$, ∇=5	.4983E-03	-.1485E-03	-.1233E-03	.2533E-05	.1277E-04	-.1850E-04
		.1597E-04	.4245E-05				
	$\Delta R_t/\Delta$, ∇=50	.4209E-03	-.1563E-03	-.9512E-04	.1984E-05	.1354E-04	-.1906E-04
		.1309E-04	.4288E-05				
	$\Delta\theta$	-.4610E-01	.4631E-01	.1214E-01	-.1037E-01	-.3454E-02	-.6250E-03
		-.8404E-03	-.6243E-03				
	$\Delta RCG/\nabla^{1/3}$	.3776E-02	-.9268E-04	-.1424E-02	-.1246E-03	.9463E-05	.1850E-06
		.1331E-03	-.3086E-05				
1.00	$\Delta R_t/\Delta$, ∇=5	-.7109E-02	.4784E-03	.2702E-02	-.7780E-05	-.1321E-03	-.5580E-04
		-.2408E-03	-.6455E-05				
	$\Delta R_t/\Delta$, ∇=50	-.7171E-02	.4771E-03	.2730E-02	-.8632E-05	-.1333E-03	-.5657E-04
		-.2446E-03	-.6400E-05				
	$\Delta\theta$	-.7175E+00	.9020E-01	.2028E+00	.1298E-03	-.7746E-02	.5703E-03
		-.1607E-01	-.1538E-03				
	$\Delta RCG/\nabla^{1/3}$	-.3234E-02	.5587E-03	.1200E-02	.3996E-04	-.7873E-04	.4558E-06
		-.7148E-04	.1229E-04				
1.25	$\Delta R_t/\Delta$, ∇=5	-.1611E-01	.6872E-03	.5469E-02	-.3476E-03	-.2235E-03	-.3902E-04
		-.4749E-03	-.4774E-04				
	$\Delta R_t/\Delta$, ∇=50	-.1611E-01	.6947E-03	.5484E-02	-.3426E-03	-.2256E-03	-.3927E-04
		-.4779E-03	-.4737E-04				
	$\Delta\theta$	-.1492E+01	.1383E+00	.4799E+00	-.5107E-02	-.1694E-01	-.8203E-04
		-.4096E-01	-.1271E-02				
	$\Delta RCG/\nabla^{1/3}$	-.2576E-02	.2884E-03	-.6448E-04	-.1077E-03	.1450E-05	-.1085E-04
		.9325E-04	.3125E-05				
1.50	$\Delta R_t/\Delta$, ∇=5	-.1156E-01	.1010E-02	.4347E-02	-.7582E-04	-.2816E-03	-.2185E-04
		-.3944E-03	-.4035E-04				
	$\Delta R_t/\Delta$, ∇=50	-.1153E-01	.1002E-02	.4325E-02	-.7148E-04	-.2804E-03	-.2218E-04
		-.3924E-03	-.3996E-04				
	$\Delta\theta$	-.1747E+01	.1264E+00	.5078E+00	-.8632E-02	-.1203E-01	.2301E-02
		-.3979E-01	-.1961E-02				
	$\Delta RCG/\nabla^{1/3}$	-.1265E-01	.1279E-02	.4050E-02	-.3522E-03	-.1449E-03	.9500E-05
		-.3254E-03	-.2848E-04				
1.75	$\Delta R_t/\Delta$, ∇=5	-.1781E-01	-.2777E-02	.3988E-02	.1913E-02	.3926E-03	.1714E-03
		-.4276E-04	.6918E-05				
	$\Delta R_t/\Delta$, ∇=50	-.1781E-01	-.2802E-02	.3962E-02	.1923E-02	.3985E-03	.1724E-03
		-.3853E-04	.7212E-05				
	$\Delta\theta$	-.2105E+01	.8404E-01	.5106E+00	-.1442E-01	-.6604E-03	.9035E-02
		-.3282E-01	-.5075E-02				
	$\Delta RCG/\nabla^{1/3}$	-.1976E-01	-.3741E-03	.4480E-02	.1019E-03	.2446E-03	.1656E-03
		-.1706E-03	-.4848E-04				

Fn_∇		a_0	a_1	a_2	a_3	a_4	a_5
		a_6	a_7				
2.00	$\Delta R_t/\Delta,\ \nabla$=5	-.1896E-01	-.1133E-02	.5922E-02	.2811E-02	-.8412E-04	.9948E-05
		-.3640E-03	.7771E-04				
	$\Delta R_t/\Delta,\ \nabla$=50	-.1891E-01	-.1142E-02	.5881E-02	.2814E-02	-.8078E-04	.1088E-04
		-.3603E-03	.7762E-04				
	$\Delta\theta$	-.2695E+01	.1853E+00	.6910E+00	-.6575E-01	-.1953E-01	.8210E-02
		-.5452E-01	-.9311E-02				
	$\Delta RCG/\nabla^{1/3}$	-.5989E-01	.2930E-02	.1785E-01	-.1535E-02	-.3801E-03	.6120E-04
		-.1412E-02	-.1650E-03				
2.25	$\Delta R_t/\Delta,\ \nabla$=5	-.3588E-01	.1388E-03	.1107E-01	.3152E-02	-.3984E-03	-.1834E-04
		-.8323E-03	.1092E-03				
	$\Delta R_t/\Delta,\ \nabla$=50	-.3725E-01	.3245E-03	.1161E-01	.3158E-02	-.4257E-03	-.1554E-04
		-.8867E-03	.1081E-03				
	$\Delta\theta$	-.1525E+01	-.1723E-01	.1660E+00	.2115E-01	.5883E-02	.1806E-02
		-.5244E-02	.3020E-03				
	$\Delta RCG/\nabla^{1/3}$	-.6100E-01	.9271E-03	.1565E-01	-.2120E-03	-.1254E-03	.8236E-04
		-.1101E-02	-.1095E-03				
2.50	$\Delta R_t/\Delta,\ \nabla$=5	-.5260E-02	-.3146E-02	-.2567E-02	.3263E-02	.1492E-04	-.1185E-03
		.4338E-03	.1739E-03				
	$\Delta R_t/\Delta,\ \nabla$=50	-.5245E-02	-.3185E-02	-.2639E-02	.3267E-02	.2341E-04	-.1145E-03
		.4400E-03	.1723E-03				
	$\Delta\theta$	-.2302E+00	.3193E-01	-.1812E+00	-.1211E-01	-.1979E-02	.2759E-03
		.1277E-01	-.2276E-03				
	$\Delta RCG/\nabla^{1/3}$	-.1935E-01	.1547E-02	.2596E-02	-.3649E-03	-.3085E-03	.1805E-04
		-.2492E-03	-.8810E-04				
2.75	$\Delta R_t/\Delta,\ \nabla$=5	-.3454E-01	-.6475E-02	.1387E-02	.1848E-02	.3588E-03	-.3693E-03
		.3447E-03	.2075E-03				
	$\Delta R_t/\Delta,\ \nabla$=50	-.3502E-01	-.6477E-02	.1490E-02	.1836E-02	.3595E-03	-.3669E-03
		.3317E-03	.2062E-03				
	$\Delta\theta$	.4111E-01	.7245E-01	-.1804E+00	.7383E-02	-.6458E-02	.7109E-02
		.6386E-02	-.2195E-02				
	$\Delta RCG/\nabla^{1/3}$	-.1573E-01	.1805E-02	.8777E-03	-.2462E-03	-.3616E-03	.6562E-04
		-.1874E-03	-.8928E-04				
3.00	$\Delta R_t/\Delta,\ \nabla$=5	.1001E-01	-.5544E-02	-.1342E-01	.1636E-02	.1327E-03	-.5689E-03
		.1475E-02	.3445E-03				
	$\Delta R_t/\Delta,\ \nabla$=50	.8563E-02	-.5354E-02	-.1287E-01	.1634E-02	.1020E-03	-.5691E-03
		.1413E-02	.3475E-03				
	$\Delta\theta$	-.1607E+01	.1098E+00	.3775E+00	.1483E-01	-.1283E-01	.1036E-01
		-.3977E-01	-.2998E-02				
	$\Delta RCG/\nabla^{1/3}$	-.7659E-02	.1821E-02	-.9599E-03	-.2954E-03	-.3330E-03	.7094E-04
		-.1434E-03	-.7165E-04				

List of References

[1] BEUKELMAN, W.: *"Prediction of Operability of Fast Semiplaning Vessels in a Seaway"*, TU-Delft, Shiphydromechanics Laboratory, Report 700

[2] BLOK, J.J. and BEUKELMAN, W.: *"The High Speed Displacement Hull Forms - Seakeeping Characteristics"*, SNAME Transactions, Vol 921-984, p 125 - 150

[3] BLOK, J.J. and ROELOFS, H.W.: *"De Invloed van Voorschips-vlaktilling op het Zeegangsgedrag"*, MARIN, Report No 49207-1-HT, april 1989

[4] BOSCH, J.J. van den: *"Comparitive tests of four fast motor boat models"*, Nederlands Scheepsstudiecentrum TNO, Report No 196 S, December 1974

[5] BOSCH, J.J. van den: *"Over de vaareigenschappen van planerende motorboten"*, TU-Delft, Laboratorium voor Scheepsbouwkunde, Report 238, juni 1969

[6] BOSCH, J.J. van den: *"Tests with Two Planing Boats in Waves"*, TU-Delft, Shiphydromechanics Laboratory, Report no 266, February 1970

[7] CHUANG, S.L.: *"Slamming Tests of Three Dimensional Bodies in Calm Water and Waves"*, NSRDC, Report 4095, September 1973

[8] CHIU, F. and FUJINO, M.: *"Nonlinear prediction of Vertical Motions and Waveloads of High Speed Craft in Head Seas"*, Int. Shipbuilding Progress, No 406, 1989, p 193 - 232

[9] CLEMENT, E.P. and BLOUNT, D.L.: *"Resistance Tests of a Systematic Series Planing Hull Forms"*, Transactions SNAME, 1963

[10] DENIS, M.St. and PIERSON,W.J.: *"On the Motions of Ships in Confused Seas"* , Transactions SNAME, 1953

[11] FALTINSEN, O. and MICHELSEN, F.C.: *"Motions of Large Structures in Waves at Zero Froude number"*, Int. Symposium on the Dynamics of Marine Vehicles and Structures in Waves, Mech. Eng. Publ., London, 1975, p 273 - 292

[12] FALTINSEN, O. and ZHAO, R.: *"Numerical predictions of ship motions at high forward speed"*, Phil. Trans. R. Soc, London, 1994, p 241-252

[13] FRIDSMA, G.: *"A Systematic Study of the Rough-water Performance-of Planing Boats"*, Stevens Institute of Technology, Davidson Laboratory, Report 1275, November 1969

[14] FRIDSMA, G.: *"A systematic Study of the Rough-water Performanceof Planing Boats Part 2 Irregular Waves"*, Stevens Institute of Technology, Davidson Laboratory, March 1971

[15] GERRITSMA, J. and BEUKELMAN, W.: *"Analysis of a Modified Strip-Theory for the Calculation of Ship Motions and Wave Bending Moments"*, Netherlands Ship Research Centre, Report 96 S, June 1967

[16] GERRITSMA, J. and BEUKELMAN, W.: *"The Distribution of the Hydrodynamic Forces on a Heaving and Pitching Shipmodel in Still Water"*, Int. Shipbuilding Progress, 1964

[17] GERRITSMA, J. BEUKELMAN, W. and GLANSDORP, C.C.: *"The Effects of Beam on the Hydromechanic Characteristics of Ship Hulls"*, Transactions 10 th ONR Symposium, Boston, June 1974

[18] HOGBEN, N. and STANDING, R.G.: *"Wave loads on Large bodies"*, Int. Symposium on the Dynamics of Marine Vehicles and Structures in Waves, Mech. Eng. Publ., London, 1975

[19] HOGBEN, N. and LUMB, F.E.: *"Ocean Wave Statistics"*, National Physical Laboratory, HMSO, 1967

[20] HADLER, J.B. e.a.: *"Planing Hull Feasibility Model - its Role in Improving Patrol Craft Design"*, RINA Symposium on Small Fast Warships and Security Vessels, London, England, March 1978

[21] HINO, T., HIRATA, N. and HORI, T.: *"Calculation of Free Surface Flows Generated by Planing Craft"*,Proceedings FAST 91, Trondheim, June 1991

[22] INGLIS, R.B. and PRICE, W.G.: *"The Hydrodynamic Coefficients of an Oscillating Ellipsoid Moving in the Free Surface"*, Journal of Hydronautics, 14 (4), 1980

[23] INGLIS, R.B. and PRICE, W.G.: *"A Three Dimensional Ship Motion Theory - Comparison between Theoretical Predictions and Experimental Data of the Hydrodynamic Coefficients with Forward Speed"*, RINA Transactions, 1981

[24] INGLIS, R.B. and PRICE, W.G.: *"Calculation of the Velocity Potential of a Translating Pulsating Source"*, RINA Transactions, 1980

[25] JOURNEE, J.M.J.: *"Seaway Delft"*, User Manual of Release 4.0, TU-Delft, Shiphydromechanics Laboratory, Report 910, 1992

[26] KANT, R.: *"Tijdsdomein Simulatie programma voor de Bewegingen van Planerende Schepen in Golven"*, TU-Delft, Shiphydromechanics Laboratory, Student Thesis, 1989

[27] KEUNING, J.A.: *"Optimalisatie van een Planerend Patrouille Vaartuig naar Gedrag in Zeegang"*, TU-Delft, Shiphydromechanics Laboratory, Report 741-O, April 1987

[28] KEUNING, J.A.: *"Zeegangsgedrag van geavanceerde schepen"*, Zeegangsdag, KIVI, maart 1984

[29] KEUNING, J.A.: *"Nonlinear Heave and Pitch Motions of Fats Ships in Irregular Head Waves"*, ASNE High Speed Marine Vehicles Conference, Washington, June 1992

[30] KEUNING, J.A.: *"Distribution of Added Mass and Damping along the Length of a Ship model at High Forward Speed"*, Int. Shipbuilding Progress, No 410, 1990 p 123-150

[31] KEUNING, J.A. and GERRITSMA, J.: *"Resistance Tests of a Series Planing Hull Forms with 25 Degrees Deadrise Angle"*, Int Shipbuilding Progress, Vol. 29, No 337, 1982

[32] KEUNING, J.A., GERRITSMA, J. and TERWISGA, P.F. van: *"Resistance Tests of a Series Planing Hull Forms with 30 degrees Deadrise and a Calculation Method Based on this and Similar Series"*, Int. Shipbuilding Progress, December 1993

[33] KEUNING, J.A.: *"Nonlinear Motions of Fast Ships and the Effect on the Operability"*, MARIN Jubilee Conference, Wageningen, May 1992

[34] KOBAYASHI, H.: *"On the Hydrodynamic Forces on an Arbitrary Floating Body with Constant Forward Speed"*, J.S.N.A., Vol. 20, 1982

[35] KORVIN-KROUKOFSKY, B.V.: *"Lift of Planing Surfaces"*, Stevens Institute of Technology, Experimental Towing Tank, Paper Journal of Aeronautical Sciences, September 1950

[36] KORVIN-KROUKOFSKY, B.V. and JACOBS, W.R.: *"Pitching and Heaving Motions of a Ship in Regular Waves"*, SNAME Transactions, Vol. 65, 1957

[37] KOELBEL, J.G.: *"Seakeeping Considerations in Design and Operation of Hard Chine Planing Hulls"*, The Naval Architect, RINA, March 1979

[38] KRING, D.: *"Investigation of the Zarnick Nonlinear Model of Planing Craft Motions"*, TU-Delft, Shiphydromechanics Laboratory, Report 786, February 1988

[39] KRING, D. and SCLAVOUNOS, P.D.: *"A New Method for Analysing the Seakeeping of Multi Hull Ships"*, Proceedings FAST 91, Trondheim, June 1991

[40] LATHIHARJU, E. e.a.: *"Resistance and Seakeeping Charateristics of Fast Transom Stern Hulls with Systematically Varied Form"*, SNAME Transactions, Vol. 99, 1991, p 85 - 118

[41] LEWIS, F.M.: *"The Inertia of Water Surrounding a Vibrating Ship"*, SNAME Transactions, 37, 1929, p 1-20

[42] McCAULGHY, e.a.: *"Motion Sickness Incidence: Exploratory Studies of Habituation, Pitch and Roll and the Refinements of a Mathematical Model"*, Human Factors Research Inc., Technical Report 1733-2, Goleta, California 1976.

[43] MARTIN, M.: *"Theoretical Prediction of Motions of High Speed Planing Boats in Waves"*, Journal of Shipresearch, Vol. 22, No 3, September 1978

[44] MOLYNEUX, D. and RODDAN, G: *"Model Experiments on a Simplified Planing Hull in Regular and Irregular Waves"*

[45] NAKOS, D.E., NESTEGARD, A. and SCLAVOUNOS, P.D.: *"Seakeeping Analysis of Surface Effects Ships"*, Proceedings FAST 91, Trondheim, June 1991

[46] NEWMAN, J.N.: *"Shipmotions in Regular Waves"*, Numerical Methods Applied to Shipbuilding, Oslo, October 1963

[47] NEWMAN, J.N.: *"The Exciting Forces on a Moving Body in Waves"*, David Taylor Model Basin, Washington, Report 5110, February 1965

[48] PAYNE, P.R.: *"A Unification in the Added Mass Theory of Planing"*, Ocean Engeneering, Vol. 19, p 39-55

[49] PAYNE, P.R.: *"Recent Developments in Added Mass Planing Theory"*, Ocean Engineering, Vol. 21, No 3, 1994, p 257-309

[50] PIERSON, J.D., DINGEE, D.A. and NIEDINGER, J.W.: *"A Hydrodynamics Study of the Chines Dry Planing Body"*, Stevens Institute of Technology, Davidson Laboratory, Report SIT DL 54-492

[51] RAVEN, H.C.: *"Variations on a Theme by Dawson"*, Transactions of the 17th ONR Symposium, The Hague, The Netherlands, 1989

[52] SALVESEN, N., TUCK, E.O. and FALTINSEN, O.: *"Ship Motions and Sealoads"*, SNAME Transactions, Vol. b78, 1970

[53] SAVITSKY, D.: *"Hydrodynamic Design of Planing Hulls"*, Marine Technology, Vol. 1, No 1, October 1964

[54] SAVITSKY, D. and GORE, J.L.: *"A re-evaluation of the Planing Hull Forms"*, AIAA Report 79-2028, 1979

[55] SAVITSKY, D.: *"Seakeeping Considerations in Design and Operation of Hard Chine Planing Hulls"*, The Naval Architect, March 1979, p 55-59

[56] SAVITSKY, D. e.a.: *"Hydrodynamic Development of a High Speed Planing Hull"*, 9th Symposium on Naval Hydrodynamics, Paris 1972

[57] SHUFOLD, C.L.: *"A Theoretical and Experimental Study of Planing Surfaces Including Effects of Cross Section and Plan Form"*, NACA-Technical Memorandum, Report 1355, 1958

[58] SEDOV, L.: *"Scale Effects and Optimum Relations for Sea Surface Planing"*, NACA Technical Memorandum, No 1097, 1947

[59] SOTTORF, W.: *"Experiments with Planing Surfaces"*, NACA Technical Memorandum, TM 661, March 1932

[60] STAVOVY, A.B. and CHUANG, S.L.: *"Analytical Determination of Slamming Pressures for High Speed Vehicles in Waves"*, Journal of Ship Research, Vol. 20, No 4, December 1976, p 180-198

[61] TASAI, F.: *"On the Damping Force and Added Mass of Ships Heavingand Pitching"*, Report of Research Institute of Applied Mechanics, Kyushu University, Japan 1960

[62] TASAI, F.: *"Improvements in the Theory of Shipmotions in Longitudinal Waves"*, Transactions ITTC, Rome 1969, pp 677

[63] TAYLOR, J.L.: *"Hydrodynamical Inertia Coefficients"*, Phylosophical Magazine, 9, 1930, p 161-183

[64] TIMMAN, J. and NEWMAN, J.N: *"The Coupled Damping Coefficients of a Symmetric Ship"*, David Taylor Model Basin, Washington, June 1961

[65] TROESCH, A.W. and HICKS, J.D.: *"The Efficient Use of Simulation in Planing Hull Motion Analysis"*, ASME High Performance Marine Vehicles Conference, Washington, June 1992

[66] URSELL, F.: *"On the Vertical Added Mass and Damping of Floating Bodies at Zero Speed ahead"*, Proceedings Symposium of Ships in Seaway, NSMB, Wageningen 1957

[67] QUADVLIEG, F.H.H.A.: *"Nonlinear Motions of Planing Ships"*, TU-Delft, Shiphydromechanics Laboratory, Student Thesis, June 1992

[68] VERKERK, F.: *"Planerende Schepen in Golven"*, TU-Delft, Shiphydromechanics Laboratory, Student Thesis, Report 598-M, Oktober 1983

[69] VERSLUIS, A.: *"Computer Aided Design of Shipforms by Afine Transformation"*, TU-Delft, Shiphydromechanics Laboratory, Report 438-P

[70] VON KARMAN, W.: *"The Impact of Seaplane Floats During Landing"*, NACA Technical Memorandum, TN 321, 1929

[71] WAGNER, H. von: *"Uber Stoss und Gleitvorgange an der Oberfläche von Flüssigkeiten"*, Zeitschrifft für Angewandete Mathematik und Mechanik, Band 12, Heft 4, 1932

[72] WANG, L.W.: *"A study on Motions of High Speed Planing Boats with Controlable Flaps"*, Int. Shipbuilding Progress, No 365, January 1985, p 6-23

[73] ZARNICK, E.E.: *"A Nonlinear Mathematical Model of Motions of Planing Boats in Regular Head Waves"*, DTNSRDC, Report 78-032, March 1978

Nomenclature

a_{bf}	buoancy correction coefficient
a_f	vertical acceleration at the bow
a_m	vertical acceleration at midship
A	cross sectional area
a_{zz}	heave added mass coefficient
$a_{\theta\theta}$	pitch added mass coefficient
B_c	beam over the chine
b_{zz}	heave damping coefficient
Cap	Centroid of Ap in % of L_c
CG	Center of Gravity
Cm	added mass coefficient
$C_{D,C}$	Cross flow drag coefficient
C_{Lo}	flat plate lift coefficient
$C_{L\beta}$	lift coefficient as function of deadrise
C_{zz}	heave restoring force coefficient
$C_{\theta\theta}$	pitch restoring moment coefficient
Fn	Froude number $Fn = V / \sqrt{gL}$
Fn_∇	Volumetric Froude number $Fn_\nabla = V / \sqrt{g\nabla^{1/3}}$
f	hydrodynamic lift force
f_B	buoyancy force
g	acceleration due to gravity
h_w	depth of submergence of section
$H_{1/3}$	significant wave height
I_a	mass moment of inertia
K	radius of gyration

k	$k = 2\pi/\lambda$ = wave number
L	instanteneous wetted length
L_c	length over chine
l_c	wetted length chine
l_k	wetted length keel
LCG	Longitudinal position of CG
LCB	Longitudinal position of the Centre of Buoyancy
m	mass
m_a	added mass
m_a'	sectional added mass
N'	sectional damping
N	normal force
R_T	total resistance
R_{CG}	Rise of the Centre of Gravity
S	wetted surface
t	time
T^*	effective draft
T_p	peak period
T_x	thrust force
U_w	horizontal water velocity
V_w	vertical water velocity
Y_w	local waterline half beam
V_s	ship forward speed
W	weight of the ship
Z	heave motion
Z_a	heave amplitude
$Z_{a1/3}$	significant heave amplitude
β	deadrise angle
γ	centre line inclination angle
ϵ_t	twist angle
ϵ	phase angle

∇	volume of displacement
Δ	weight of displacement
ζ	body fixed coordinate
ξ	body fixed coordinate
μ	wave heading
λ	wave length
λ_s	averaged wetted length
ρ	density of water
τ	trime angle
ω	wave frequency
ωe	frequency of encounter
θ	pitch motion
θ_a	pitch amplitude
$\theta_{a1/3}$	significant pitch amplitude
ζ_a	wave amplitude
$\zeta_{a1/3}$	significant wave amplitude
ζ^*	effective wave height

List of Tables

Chapter 2

Chapter 3

Chapter 4

Chapter 5

List of Figures

Chapter 1

Chapter 2

Chapter 3

Chapter 4

Chapter 5

Abstract

In this study the behaviour of fast monohulls in head waves will be investigated. The occurrence of high peaks in the vertical accelerations experienced by these ships while sailing in head waves is the limiting factor for the safe operation. The methods most commonly used for the calculation of the motions and acceleations of these ships in waves are not capable of predicting these peak values with great accuracy. Therefore an adapter computational method is sought for the prediction of the operability of these fast ships in the design stage. This new computational method will have to incorporate a number of the phenomena which are considered to be of importance for the nonlinear behaviour of these ships in waves and which are not accounted for in the linear theories.

The methods commonly used uptill now for the prediction of the motions of (fast) ships in waves are based on linear theories. Among other things this implies that the ship is considered to perform small amplitude motions around its calm water zero forward speed equilibrium position.
It is known however that fast ships may develop a considerable hydrodynamic lift. This lift results in a change of the reference poition of the ship: its sinkage and trim. In addition the continous change of the hydrodynamic lift on the hull while performing its motions in waves appears to be a major contribution in the forces. The wave exciting- and the hydrodynamic reaction forces also have a considerable nonlinear character due to the change in instantenous submerged hull geometry of the ship while performing large relative motions with respect to the wave.

In the present study the nonlinear behaviour of the fast monohull in waves will be demonstrated using the results of model experiments. The possible causes of the nonlinear behaviour will be highlighted.

Then a computational model will be discribed in which special attention is been given to:
- the computation of the sinkage and the trim of the ship at speed.
- the computation of the hydrodynamic lift force and its distribution along the length of the ship.
- the influence of the large relative motion and the (bow) flare of these ships
- the vertical added mass and its distribution along the length of the ship at high forward speed.
- the wave exciting forces.

The aim of the computational model is to check whether the implementation of these effects has a positive effect on the prediction of the motions and accelera-

tions. Hereto the emphasis will be placed on a proper, more emperical discription of the effects rather than on an exact mathematical formulation (if at all possible).

The results of the computations, using this addapted model, will be validated with the results of model experiments. They will also be compared with the results obtained using linear computational models.

It will be demonstrated that the implementation of the discribed nonlinear effects improves the predictions considerably when compared with results obtained with the linear models. In particular the prediction of the peaks in the vertical accelerations is improved, which has a positive effect on the acurracy of the operability analyses carried out in a design stage for optimisation purposes. In particular the effects of the forward speed, the deadrise and the varying hull geometry are better predicted.

Summary

In deze studie wordt het bewegings gedrag van snelle enkelromps schepen in onregelmatige kop golven onderzocht. Het blijkt dat voor de inzetbaarheid van deze schepen het plotseling optreden van grote pieken in de verticale versnellingen de maatgevende beperking is. De huidige methoden welke gebruikt worden voor het berekenen van de bewegingen van deze schepen in golven blijkt niet in staat deze pieken voldoende nauwkeurig te voorspellen. Voor het beter bepalen van de inzetbaarheid van deze snelle schepen zal derhalve gezocht moeten worden naar een aangepaste methode. In deze aangepaste methode zal rekening gehouden worden met een aantal physische verschijnselen, welke bij snelle schepen een belangrijke rol spelen en welke in de huidige berekenings methode verwaarloosd worden.

Tot op heden worden de bewegingen van schepen tengevolge van de aanwezigheid van windgolven veelal uitgerekend door gebruik te maken van lineaire theorieen. Dit impliceert ondermeer dat ervan uit wordt gegaan dat het schip kleine bewegingen maakt ten opzichte van zijn evenwichts situatie, waarin het zich zou bevinden in vlak water en bij snelheid nul.
Het is evenwel bekend dat snelvarende schepen een aanzienlijke hydrodynamische lift kunnen ontwikkelen. Deze geeft ondermeer aanleiding tot een veranderende positie van het schip in het water : de inzinking en trim. De verandering van de hydrodynamische lift tengevolge van de bewegingen van het schip in golven blijkt bovendien een belangrijke component te zijn in het krachten spel op de romp.
Daarnaast blijken de exciterende- en hydromechanische reactie-krachten een significant niet lineair karakter te hebben tengevolge van een sterk veranderende geometrie van het schip zoals dat daadwerkelijk in contact is met het water in de situatie waarin het schip grote relatieve bewegingen maakt.

In deze studie wordt allereerst met behulp van modelproef resultaten het niet lineaire gedrag van een snelle monohull in golven onderzocht. Waar mogelijk wordt de oorzaak van het niet lineaire gedrag aangeduid..

Vervolgens wordt een berekenings model opgesteld voor de domp en stamp beweging van een snelle monohull in kopgolven, waarbij speciale aandacht besteed wordt aan:
- het berekenen van de trim en inzinking van het schip tengevolge van zijn voorwaartse snelheid
- het berekenen van de hydrodynamische lift en de verdeling hiervan over de lengte van de romp

- de invloed van de grote relatieve bewegingen en de sterk uitwaaierende geometrie van vele snelle schepen, vooral in het voorschip
- de berekening van de hydrodynamische massa bij deze hogesnelheden en de verdeling hiervan over de lengte van de romp
- de berekening van de golfexciterende krachten bij deze hogesnelheden.

Het doel van het opstellen van dit berekenings model is om te bezien of het mee in de berekeningen betrekken van deze niet lineaire effecten de resultaten van de voorspellingen verbetert. Hiertoe ligt het accent meer op het vinden van een verantwoorde empirische beschrijving van de effecten dan op het volstrekt zuiver mathematisch formuleren ervan (voorzover trouwens mogelijk).

De resultaten van de berekeningen met het hier gepresenteerde berekenings model worden geverifieerd met behulp van model proefresultaten. De uitkomsten van dit model worden vergeleken met resultaten, welke verkregen zijn door gebruik te maken van bestaande lineaire modellen. Het zal worden gedemonstreerd dat door het meenemen van de eerder genoemde phenomenen in het aangepaste berekenings model een aanzienlijke verbetering tenopzichte van de lineaire modellen is bereikt, vooral daar waar het betreft het voorspellen van de pieken in de vertikale versnellingen.
Het uitvoeren van ontwerp optimalisaties wint daardoor aan nauwkeurigheid, zoals met een voorbeeld zal worden geillustreerd, vooral omdat de invloed van een aantal parameters, zoals snelheid, deadrise en rompgeometrie , nu beter meegenomen kan worden.

Curriculum Vitae

De auteur werd op 6 mei 1950 te Enschede geboren.
De eerste jaren van de middelbare school werden doorgebracht op Het Enschedees Lyceum. In 1968 voltooide hij de Gymnasium-Beta opleiding aan Het West Fries Lyceum te Hoorn.
In 1968 begon hij zijn opleiding aan de Technische Universiteit Delft, alwaar hij in maart 1977 slaagde voor het doctoraal examen in de Scheepsbouw- en Scheepsvaartkunde met als afstudeer onderwerp het nietlineaire bewegingsgedrag van draagvleugelboten in golven. In deze periode werkte hij bovendien twee en een half jaar als student assistent op het Laboratorium voor Scheepshydromechanica.
In maart 1977 ging hij als project ingenieur werken bij het Waterloopkundig Laboratorium Delft te Delft op de Afdeling Maritieme Konstructies.
In december 1978 werd hij aangesteld als Universitair Docent bij de Vakgroep Scheepshydromechanica van de Afdeling der Maritieme Techniek van de Technische Universiteit Delft. Sinds november 1992 is hij bij dezelfde Vakgroep werkzaam als Universitair Hoofd Docent, met als speciale aandachtsgebieden de geavanceerde schepen en (zeil)jachten.

Acknowledgement

I like to express my sincere gratitude to my promotor prof ir J Gerritsma who guided and stimulated me throughout this entire study, also after his retirement as full time professor from the University. Already in the period, in which I carried out my student graduation work, he introduced me into the area of advanced naval vehicles (including sailing yachts) an area that has interessted me ever since.

Special thanks are also forwarded to Dr ir A E Mynett who allways quite willingly acted as an inspiring sparring partner in the many lengthy discussions we had about the topics dealt with in these studies.

I also gratefully acknowledge the considerable support given by the entire staff of the Shipshydromechanic Laboratory, both for their assistance given in carrying out all the different components of this study as well as in accepting my sometimes unbearable behaviour whilst doing it.

The dedicated work carried out by F Verkerk, R Kant and F H H M Quadvlieg whilst carrying out their student graduation work in the framework of this study is also explicitly acknowledged.

Finally the great effort put into the final drafting of this thesis by C Bom and in particular the final editing by P W de Heer is very gratefully acknowledged. Whithout their effort there probably would not have been a thesis in any readable format.